The hydrogeology of bromate contamination in the Hertfordshire Chalk: double-porosity effects on catchment-scale evolution

Ciara Marie Fitzpatrick

A dissertation submitted in partial fulfilment

of the requirements for the degree of

Doctor of Engineering

of

University College London.

Department of Earth Sciences

University College London

2010

I, Ciara M. Fitzpatrick, confirm that the work presented in this thesis is my own. Where information has been derived from other sources, I confirm that this has been indicated in the thesis.

_____

_____

Foreword

This Engineering Doctorate (EngD) was funded by an Engineering and Physical Sciences Research Council (EPSRC) Studentship in association with Veolia Water Three Valleys Ltd[1] (VWTV) and Thames Water Utilities Ltd (TWUL).

As part of the research project two EngD studentships were awarded: (1) to Ciara Fitzpatrick, originator of this document, and (2) to Simon Cook. The research project was intended to be collaborative between the water utilities and University College London, with neither individual student affiliated preferentially to either company.

The work documented within this thesis constitutes independent original research, however the research described is complementary to that by Simon Cook in:

> The hydrogeology of Bromate Contamination in the Hertfordshire Chalk Aquifer: Incorporating Karst in Predictive Models. EngD Thesis, University College London, 2010.

The views, opinions and conclusions expressed in the thesis are those of the researcher and do not necessarily reflect the views of Veolia Water Three Valleys Ltd or Thames Water Utilities Ltd (TWUL).

[1] formerly Three Valleys Water Ltd (TVW)

Abstract

Bromate contamination over an area of more than 40 km^2 in the Hertfordshire Chalk aquifer was first detected in 2000 and is the largest case of point-source groundwater contamination in the UK. Bromate is a possible human carcinogen, and a regulatory limit for drinking water of 10 $\mu\mathrm{g\ l}^{-1}$ had been implemented in the U.K. since 2003. Background concentrations of bromate in groundwater are believed to be effectively zero. In the affected area, bromate at concentrations of several 100 $\mu\mathrm{g\ l}^{-1}$ have forced the closure of a large public water supply source and restricted the use of seven other public supply boreholes up to 20 km from the contamination source.

The source has been identified as a former industrial site which operated between 1955 and 1983. Residual contamination at the site provides a continuing source of bromate to groundwater. A range of conceptual scenarios for bromate mobilisation and release to groundwater have been developed and quantified based on interpretation of the available data, and constrained by interpolation of the observed concentrations.

Analysis and interpretation of all available monitoring and investigation data throughout the catchment has revealed the influence of recharge, water level, and groundwater abstractions on bromate concentrations. These relationships, integrated with observations of the geology and hydrogeology of the area, support a conceptualisation of transport of bromate by dominantly double-porosity processes within the Vale of St. Albans area, which maintains a highly attenuated, stable contaminant distribution west of Hatfield. An extensive karst network related to the position of the Palaeogene overlap of the Chalk influences bromate transport to the east of Hatfield, dispersing bromate rapidly over large distances toward the Lea Valley. The revised conceptual understanding has enabled the development of a new interpretation of bromate transport within the catchment between 2000 and 2008.

A new analytical network modelling approach has been developed to predict the long-term, large-scale transport of bromate. The model simulates Fickian double-porosity diffusive exchange along interconnecting flow-lines, linked to rapid karst flow. The model is parameterised on the basis of single borehole dilution testing, catchment-scale natural gradient tracer testing, and literature derived values. The network model, combined with quantified bromate source terms, simulates bromate and bromide concentrations of the order of magnitude of those observed at locations within the Vale of St. Albans, and predicts bromate concentrations to remain above regulatory limits for around 200 years. This highlights the importance of double-porosity diffusion for the long-term evolution of contaminants at catchment-scale in the Chalk aquifer.

Acknowledgements

I am sincerely grateful to my supervisors, Dr Willy Burgess and Prof. John Barker for providing inspiration, support and guidance over the past four years, and above all, for believing in my capabilities. I am indebted to Willy for his constant enthusiasm, and ability to renew mine.

This Engineering Doctorate was funded by an EngD studentship at UCL and I am grateful to EPSRC, Veolia Water Three Valleys Ltd, and Thames Water Utilities Ltd for sponsoring the project. In particular, I would like to thank my supervisors Rob Sage, Lucy Lytton, and Philip Bishop for their insights and information.

I owe my gratitude to Jon Newton at the Environment Agency, firstly for introducing me to the Hertfordshire bromate problem, and subsequently for sharing his understanding, providing monitoring data and a wealth of other relevant information.

The single borehole dilution tests were undertaken with assistance from a number of people: many thanks to the Environment Agency for permission and funding, Adrian Sheriff for access to the Nashe's Farm borehole, Simon Cook and Gemma Russell for help with the fieldwork, Louise Maurice for guidance on the method and use of the equipment, and Jessica Randle for associated geophysical testing of the boreholes.

I am grateful to Simon Cook, for his contributions to understanding and progressing research into the bromate contamination. Thanks also to Rakia Meister, Simon Quinn, Mohammed Abdul Hoque, Qiong Li, Mike Davis, Bethan Hallett and Gemma Russell for putting up with sharing an office with me, and for some welcome conversation.

'Go raibh maith agat' to my fiancé, Neal O'Grady, for his love, understanding and patience. Finally, I thank my family; without their love and support over the last 29 years I would not be in a position to be submitting this thesis. I dedicate this thesis to my grandparents, Mona and Chris Fitzpatrick.

Abbreviations

BH Borehole

BGS British Geological Survey

EA Environment Agency

MDL Method Detection Limit

NNR Northern New River

OBH Observation Borehole

P.S. Pumping Station

PWS Public Water Supply

STW Sewage Treatment Works

SMD Soil Moisture Deficit

SLC St. Leonard's Court

TWUL Thames Water Utilities Limited

TVW Three Valleys Water Limited (renamed Veolia Water Three Valleys Limited in 2009)

Contents

List of Tables

List of Figures

Chapter 1

Introduction

1.1 Background

Changes to the Water Supply (Water Quality) Regulations (2000), effective from 2003, introduced bromate (BrO_3^-) as a new sampling parameter with a regulatory limit of 10 $\mu g\,l^{-1}$ in drinking water. Bromate is a possible human carcinogen based on extrapolation from rodent studies. Background concentrations of bromate in groundwater are believed to be effectively zero. In May 2000, during the course of preliminary sampling in advance of the regulations, Three Valleys Water Ltd[1] (TVW), detected bromate concentrations of 135-140 $\mu g\,l^{-1}$, well in excess of this standard, at the Hatfield Bishop's Rise Pumping Station. The Environment Agency (EA) and the Drinking Water Inspectorate (DWI) were informed and the Hatfield source was removed from public supply.

In June 2000 a joint water quality monitoring programme was initiated, involving the Environment Agency, the local authorities, and the water companies to identify the source and extent of the bromate contamination. The source has been identified as a former industrial site in Sandridge (Figure 1.1) which operated between 1955 and 1983. The site is now the St Leonard's Court residential development. This site has been determined as 'Contaminated Land' and designated a 'Special Site' as defined under Part IIA of the Environmental Protection Act 1990. The bromate contamination was found to extend up to 20 km to the east of the source site affecting an area of more than 40 km^2 of the Hertfordshire Chalk aquifer (Figure 1.1), and restricting the use of a further seven public water supply boreholes in the Lea Valley. Bromide (Br^-) concentrations were also found to be elevated above background concentrations across the catchment. The Environment Agency, TVW and TWUL have continued to monitor water quality and water levels at a number of locations throughout the area affected by the bromate plume. A chronology of key events is included in Appendix A.

The Chalk is one of the most important aquifers in the UK; according to the UK Groundwater Forum[2] it provides over half of all groundwater for public supply in the UK and, in the south-east of England, up to 70 % of all water in public supply. The area of Chalk aquifer affected by the bromate contamination has a licensed abstraction of approximately 200 $Ml\,d^{-1}$. Surface waters of the River Lea, and tributaries of the River Colne are also affected. The bromate contamination is therefore a significant

[1] renamed in 2009 as Veolia Water Three Valleys Limited

[2] www.groundwateruk.org/

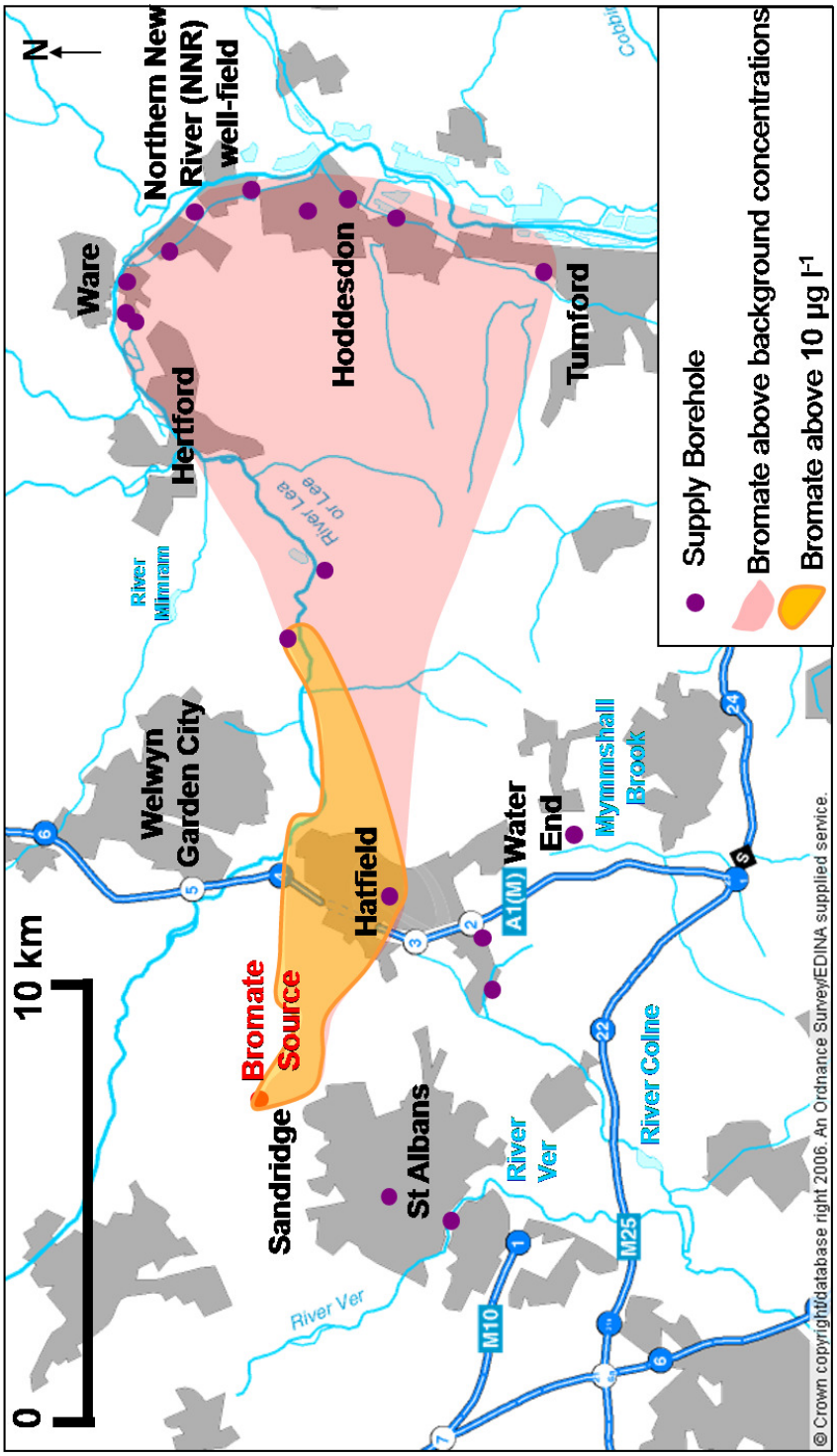

Figure 1.1: Extent of the bromate contamination in Hertfordshire. The regulatory limit for bromate in drinking water is 10 μg l^{-1}. Background concentrations are effectively zero.

threat to the long-term quality of a number of strategic public water supply sources, and also many private supply sources. The financial cost to the water companies, which include costs incurred for additional monitoring of sources, treatment of bromate and bromide contaminated water, operation of the interim scavange pumping at Hatfield PWS, and drilling and investigatory work for replacement supply wells, have been estimated to be of the order of in the region of £50,000,000 for TVW and TWUL (R. Sage & P. Bishop, *pers. comm.*) for the period 2000 to 2006. A Business Case for the reserach is included in Appendix B.

1.2 Bromate transport in the Hertfordshire Chalk aquifer

The behaviour of the Chalk as an aquifer is complex, and results from a combination of porosity and permeability components that are a consequence of the Chalk lithology, tectonic history and weathering and erosional processes. The Chalk is composed of very fine grained calcium carbonate micro-fossil fragments which form a a highly porous, yet essentially impermeable, matrix. More than 95 % of water in the Chalk is held in the interstices of the rock matrix, but the pore spaces are so small that this water is effectively immobile. The mobile water (the remaining 5 % or less) is held within the fractures that transect the chalk matrix. Some fractures have been enlarged by dissolution to become fissures or even karstic conduits. The fissures and conduits provide the permeable pathways for flow. These multiple components of porosity and permeability within the Chalk have long been recognised, and it has been described as a double-porosity (dual-porosity) aquifer (Foster, 1975; Price, 1987; Barker, 1991; Price et al., 1993), a double-permeability (dual-permeability) aquifer (Price et al., 1993), and a triple-porosity and/or triple-permeability aquifer (Worthington, 2003; White, 2003).

The double-porosity nature of the chalk has important consequences for contaminant transport: diffusive exchange of dissolved species can occur between mobile fissure water and the immobile matrix water. In the early stages of a contamination incident, this double-porosity diffusive exchange acts to retard the transport of contaminants relative to groundwater flow and attenuate contaminant concentrations due to diffusion into the (initially uncontaminated) matrix porewater. At a later stage, when the primary source of contamination input to the mobile fissure water has ceased, back-diffusion from the matrix porewater acts as a secondary source of contamination, significantly prolonging the duration of contamination. It is likely that the apparent stability of the bromate extent and concentrations over recent years is a result of the attenuating effects of double-porosity diffusion in the Hertfordshire Chalk.

Double-porosity diffusion between mobile fissure water and immobile matrix water can be described mathematically using Fick's Laws of diffusion (*e.g.* Barker and Foster, 1981; Barker, 1982, 1985b). Previous modelling representations of bromate transport in Hertfordshire (*e.g.* Buckle, 2003; Atkins, 2005) have used a first order mass-transfer coefficient (FOMT) to represent the effects of double-porosity attenuation. The FOMT approach is a mathematical simplification of the Fickian approach, and the approximation is likely to underestimate the mobile groundwater concentrations in the longer-term.

In the east of the study area, there is evidence (*e.g.* Harold, 1937; MacDonald et al., 1998) of rapid groundwater flow occurring between swallow holes and stream sinks in the Water End area (Figure 1.1) and springs and boreholes in the Lea Valley, which is indicative of a dispersive system of karstic conduits.

Such a system would allow rapid transport of bromate, with low-attenuation of concentrations, and is likely to be the cause of the wide distribution of bromate across the east of the catchment. Previous modelling exercises (*e.g.* Buckle, 2003; Atkins, 2005) have been unable to reproduce the migration of bromate to the Lea Valley due to deficiencies in the representation of the karst system.

Therefore, in order to represent the distribution and temporal evolution of bromate contamination in the Hertfordshire Chalk, predictive models of bromate transport must integrate the effects of double-porosity diffusive exchange between fissures and the chalk matrix with the effects of rapid, low-attenuation transport within karstic conduits. The complex nature of these processes, and quantifying their relative importance, presents particular difficulties for prediction of contaminant transport.

1.3 The bromate source

The site of a former chemical works in Sandridge, which is now a residential development, has been identified as the source of the bromate and bromide contamination. Limited site data are available from investigations undertaken during redevelopment of the site in the mid 1980s and subsequent to the discovery of the bromate contamination at Hatfield in 2000. To date, relatively little attention has been directed at quantifying the bromate source: models by Buckle (2003) and Atkins (2005) have used a constant concentration source term which is unrealistic over the longer term. During calibration, the bromate source term was shown to exert a significant control on the form and magnitude of the simulated contaminant breakthrough. Therefore, the magnitude and dynamics of bromate release to groundwater beneath the source site, and thus to locations down-gradient of the source site, have consequences for the magnitude and duration of bromate contamination within the catchment. Predictive models of bromate contamination within the catchment are dependent on a realistic and representative source term to quantify the input of bromate from the source site.

1.4 Research aims and objectives

The overall aim of the research presented in this thesis is to develop greater understanding of the processes controlling the spatial distribution and temporal evolution of bromate contamination within the Hertfordshire Chalk aquifer, including bromate release from the source zone, and to use this understanding as the basis for predictive models incorporating the effects of double-porosity diffusion on the long-term evolution of bromate.

The specific research objectives were:

Evolution of bromate contamination

- To develop a conceptual model for groundwater flow and contaminant transport in the Hertfordshire Chalk aquifer system by review of existing data and interpretation of additional tracer testing and geophysical testing;

- To use the available information and monitoring data to describe the spatial distribution and temporal evolution of bromate across the catchment, and to interpret this in association with the conceptual model of the flow and transport system.

The source

- To describe and quantify the distribution of bromate at the source site through collation and description of site investigation and monitoring data;
- To develop alternative conceptual scenarios for bromate release to groundwater and quantify these as 'source terms';
- To use the available monitoring data to constrain the potential source terms.

Catchment-scale modelling of bromate transport

- To develop analytical network modelling of contaminant transport to allow representation of Fickian double-porosity diffusion and to integrate karstic transport pathways within the network;
- To use this model to produce predictions for the likely bromate concentrations at key output locations over the long-term.

1.5 Approach

The objectives were approached by developing a conceptual model of groundwater flow within the Hertfordshire Chalk, which was informed by a new interpretation of the Hertfordshire karst system by Cook (2010) following catchment-scale tracer tests. All available monitoring and investigation data were analysed and interpreted to describe the evolution of the bromate contamination within the aquifer. The processes controlling bromate transport were investigated by examining relationships between bromate concentrations and variables including bromide and chloride concentrations, piezometry, catchment recharge, and groundwater abstraction rates.

The bromate pollution in Hertfordshire is of a similar scale to the extensive chloride pollution of the Chalk of the Tilmanstone valley in Kent (Watson, 2004) from coalfield brines. Watson (2004) developed an investigatory methodology - the 'Tilmanstone Methodology' - for characterising and parameterising catchment-scale double-porosity flow and transport in the Chalk. The investigatory methodology comprised geophysical testing, single borehole dilution tracer testing, borehole-to-borehole natural gradient tracer testing, and sampling of chalk porewater and chalk fissure water to produce vertical porewater and fracture water profiles at locations along the flow line. A one-dimensional semi-analytical model (DP1D), incorporating Fickian diffusion between matrix water and fracture water, was used to simulate chloride migration and was able to reproduce the observed porewater and fracture water profiles. Forward modelling indicated that the double porosity diffusion extends the duration of contamination in the catchment by several decades.

It was therefore considered that the 'Tilmanstone Methodology' could be adapted for application to the Hertfordshire bromate contamination. However, initial plans for a number of cored boreholes to provide porewater profiles in the catchment had to be reconsidered due to the financial constraints of the Water Companies. The scope of the field testing was reduced to a number of single borehole dilution tests to determine groundwater velocities in the Hertfordshire Chalk.

Representing Fickian double-porosity diffusion was still considered of great importance, despite the lack of data for porewater concentrations to fully validate predictions of fissure concentrations. Therefore, an analytical network model was developed which represents Fickian double-porosity diffusive exchange between fissure water and matrix porewater along interconnecting flow-lines, while allowing karstic branches to be incorporated into the network. The model was parameterised by a combination of values found within the literature, and the results of the single borehole dilution testing and catchment-scale natural gradient tracer testing. Results were compared to groundwater monitoring data at key locations within the catchment.

The bromate source term for the Hertfordshire network model was quantified through analysis and interpretation of site investigation data available for the source site to constrain a range of conceptual scenarios for bromate mobilisation and release to groundwater.

1.6 Structure of thesis

Following this introductory chapter, Chapter 2 presents a review of the mechanisms of groundwater flow and transport of solutes within the Chalk, and a summary of typical parameters related to flow and transport in the Hertfordshire Chalk. Chapter 3 develops a conceptual model for groundwater flow and contaminant transport in the Hertfordshire Chalk by review of existing data, interpretation of additional tracer testing, and statistical analysis of the effects of scavenge pumping at Hatfield on bromate occurrence. Chapter 4 describes and interprets the distribution and temporal evolution of bromate contamination in Hertfordshire in association with a new conceptual model developed in Chapter 3. Chapter 5 describes and quantifies the distribution of bromate and bromide at the source site, and uses the results to constrain a number of conceptual scenarios for bromate and bromide release to generate source terms to be used for predictive modelling. Chapter 6 critically reviews existing models that have been developed for bromate transport in the Chalk, and then develops a novel analytical network model to represent the Hertfordshire Chalk catchment which is used, along with the source terms developed within Chapter 5, to simulate bromate and bromide transport at a number of key locations, to compare the simulated results with observed data, and to predict bromate concentrations into the future. The importance of double-porosity diffusion between the matrix and the fissures for the long-term evolution of bromate is demonstrated and discussed. Chapter 7 discusses and summarises the finding of the work in the context of the objectives outlined in Section 1.4 and makes recommendations for further work.

1.7 Environmental Hydrochemistry of Bromate and Bromide

1.7.1 Occurrence of Bromate and Bromide in surface and groundwaters

Bromine is a naturally occurring trace element in groundwater. Inputs to natural waters include atmospheric aerosols, contact or mixing with saline environments, weathering of materials present within the aquifer, and pollution (*e.g.* burning of fossil fuels). Under the field conditions of most natural waters, bromine occurs almost exclusively as the unassociated bromide ion (Br^-) (Edmunds, 1996).

As such, bromide (Br^-) is found naturally in most water systems. The concentrations of Br in

potable groundwaters in the United Kingdom range from 60 to 340 $\mu g\,l^{-1}$. Concentrations in the Chalk are summarised in Table 1.1. Due to the similarity of the geochemical behaviour of Br and Cl, using the Br/Cl ratio is necessary to identify significant anomalies in the natural environment (Edmunds, 1996).

Table 1.1: Bromide in UK groundwaters, summarised from Edmunds et al. (1989). r^2 is the linear correlation coefficient squared for a regression of Br *vs.* Cl

Aquifer	Bromide ($mg\,l^{-1}$)			Chloride ($mg\,l^{-1}$)	Br/Cl	r^2
	Min	Median	Max	Median	$\times 10^{-3}$	(Br/Cl)
Chalk (Berkshire)	0.020	0.067	1.140	17.7	3.78	0.95
Chalk (London)	0.045	0.183	0.620	42.0	4.35	0.98

In a survey of baseline quality of the Chalk of the Colne and Lee River catchments, Shand et al. (2003) identified elevated concentrations of Br^-: samples from the vicinity of Hatfield had (Br)/(Cl) ratios which plotted above the background trend (Figure 1.2).

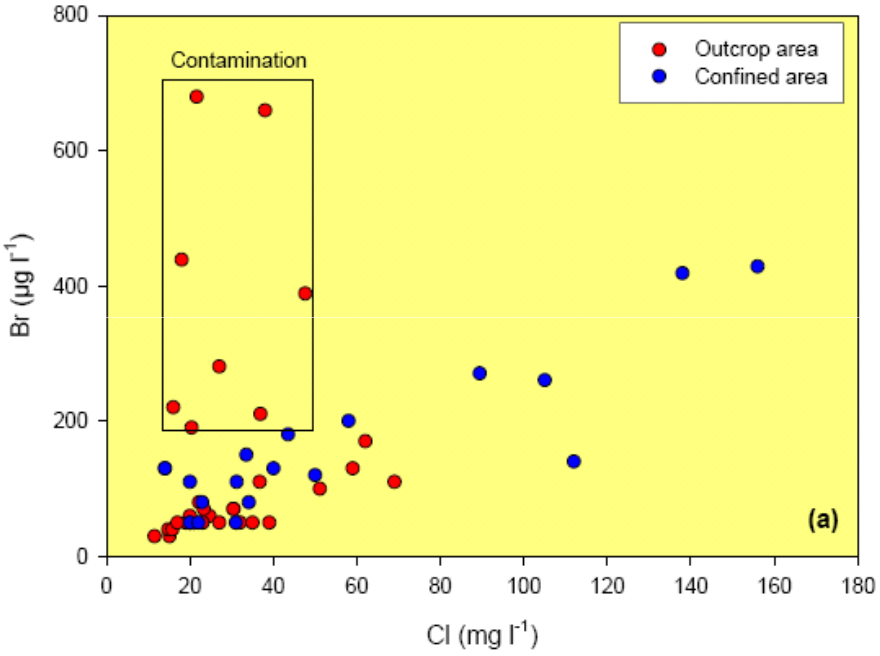

Figure 1.2: Plot of Br *vs.* Cl concentrations in groundwaters from the Chalk of the Colne and Lee River catchments. Points plotting in the 'contamination' box are from the Hatfield area. From Shand et al. (2003).

In contrast to bromide, bromate (BrO_3^-) is not reported as occurring naturally in surface waters and is not normally present in aquifers (Butler et al., 2005). However, bromate has been detected in the surface water environment as a result of industrial oxidation/disinfection processes (Butler et al 2005)

with one study of 36 river samples detecting bromate at levels from 4 to 8 $\mu g\,l^{-1}$ (Kruithof and Meijers, 1995). The occurrence of bromate within aquifers other than the Hertfordshire Chalk could not be found reported within the published literature.

1.7.2 Environmental Behaviour

The bromide ion (Br^-) is typically non-reactive under conditions typical of most groundwaters, it does not readily form complexes, participate in redox reactions, or sorb onto mineral or organic matter. Bromide has been used extensively as a tracer in aquifers due to it conservative nature (Ward et al., 1998).

The bromate ion (BrO_3^-) exists as a number of salts, including the industrially important potassium ($KBrO_3$) and sodium ($NaBrO_3$) bromates, which dissolve readily in water[3], and once in solution, bromate is highly stable (Butler et al., 2005). There is no direct evidence for a specific bromate reduction pathway, and it has been concluded by most authors that biological reduction of bromate to bromide is a side reaction of the nitrate reduction pathway (Hijnen et al., 1995). However, given that the Hertfordshire Chalk aquifer is largely unconfined, the reduction of bromate to bromide is likely to be negligible.

Bromate is therefore considered to behave conservatively under most conditions. The environmental behaviour of bromate is poorly understood, and there appears to have been little research to date into this area. However Butler et al. (2005) suggest that nitrate (NO_3^-) and perchlorate (ClO_4^-) may be considered potentially analogous oxyanions; both of which tend to behave conservatively within groundwater under the conditions encountered in natural, unconfined aquifers.

[3] $KBrO_3$ solubility at 25°C is 75 $g\,l^{-1}$

Chapter 2

Groundwater flow and transport in the Chalk

2.1 Introduction

The aim of this chapter is to describe the mechanisms of groundwater flow and transport of solutes within the Chalk, with particular reference to behaviour of the Hertfordshire Chalk aquifer, to review typical parameters related to flow and transport in the Hertfordshire Chalk, and to review approaches to representation and modelling of flow and transport in the Chalk.

2.2 The Chalk

2.2.1 Chalk stratigraphy

Three subdivisions were traditionally recognised in the Chalk Group: Lower, Middle and Upper Chalk. Over the last 20 years there has been much research into Chalk Group stratigraphy (*e.g.* Bristow et al. (1997); Gale et al. (1999); Woods (2006)) and the British Geological Survey has now adopted a revised classification that follows Rawson et al. (2001) (Figure 2.1).

2.2.2 Lithology

In general the Chalk is a very fine grained (less than 10 μm), pure (*circa* 98 % $CaCO_3$), soft, white limestone of high ($\sim$40 %) interstitial porosity, containing some marl bands and flint (Hancock, 1975), with pervasive fractures of a variety of styles. The Chalk matrix is composed of calcium carbonate micro-fossil fragments: the major, finer fraction comprising coccoliths and coccolith debris, and the minor, coarser fraction comprising foraminifera and other shell debris (Hancock, 1975).

The marl bands can be several centimetres thick, some of them being laterally continuous for several hundreds of kilometres. Many were deposited on erosional surfaces and are thought to be of volcanic origin as they contain Mg-rich smectite. Flint occurs predominantly in layers parallel to bedding, either in tabular layers or as scattered discrete nodules. Locally it forms cross-cutting veins and vertical cylinders with a burrow at the core. 'Hardgrounds' are horizons of hard, brittle chalk in which porosity is reduced to 10-20 %. The formation of hardgrounds is thought to be a result of sea floor cementation associated with a reduction or cessation in the supply of coccoliths.

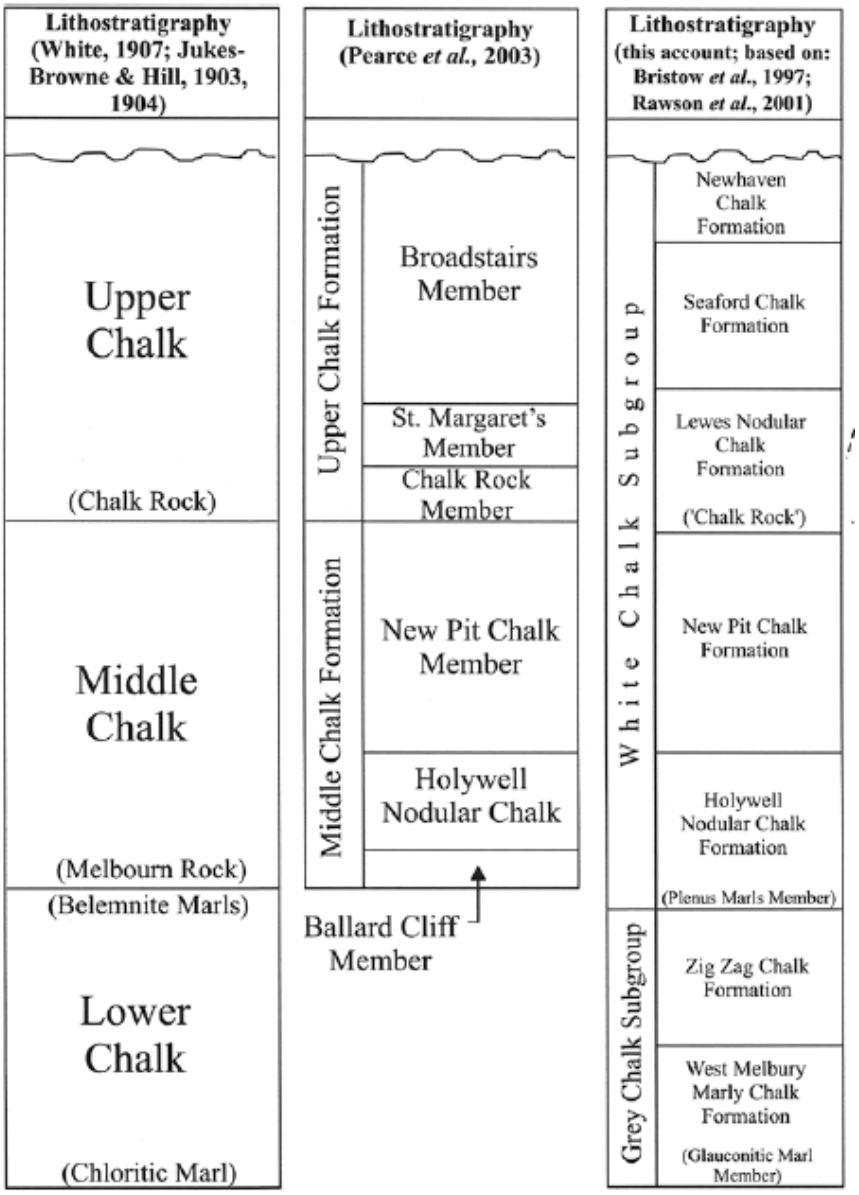

Figure 2.1: Relationship between the traditional and revised stratigraphy of the Chalk. After Woods and Aldiss (2004)

2.2.3 Tectonic History

Three basic types of fracture can be recognised in the Chalk (Bloomfield, 1996): faults, bedding plane fractures and joints. Tectonic movements were responsible for the formation of faults in the Chalk and controlled the orientation of joint sets. Joints generally form in three mutually perpendicular orientations: one parallel to bedding and two orthogonal set perpendicular to the bedding plane. The dominant regional fracture set in the Chalk of southern England trends NW-SE with a minor cross-cutting NE-SW trending set (Bloomfield, 1996), as a result of the stress regime initiated in the early Palaeogene. In addition, in southern England a series of E-W flexures and fractures developed in Oligocene-Miocene time.

2.2.4 Influence of periglaciation

The Chalk of southern England remained largely free of ice sheets throughout the Quaternary period, but was significantly affected by ground ice (periglaciation). In particular, the 'active' surface zone of the Chalk underwent cycles of freezing and thawing, which has produced a weathered mantle of broken rubbly chalk, frequently 1 m to 2.5 m thick (Williams, 1987). In some places, just below the sub-soil, the Chalk is highly pulverised to a 'putty chalk': structureless chalk with irregular sized blocks set in a soft to firm putty matrix. Much of this is absent from the interfluves but is present within wide sections of the valleys. In contrast, the permanently frozen sub-strata was probably not seriously affected by periglacial activity.

Putty Chalk has a low permeability and can therefore impede the flow of groundwater at the top of the Chalk, sometimes confining the aquifer below or restricting the flow of groundwater between the gravels and the Chalk. Putty Chalk has been detected in sections of the Thames and the Colne valleys, especially where the Chalk it is overlain by river gravels.

Periglacial activity is the most commonly invoked explanation for the origin of the dry valley network of the Chalk (Goudie, 1990). Infiltration was reduced during cold climatic conditions so that rapid melting of winter precipitation released a large volume of runoff which easily eroded chalk that had been already weakened by frost action. Periglacial activity is also thought to have contributed to the development of enhanced permeability in the Chalk, through the development and dissolution of fractures (Section 2.4.3).

2.3 The Chalk as an aquifer

The Chalk is one of the most important aquifers in the UK; according to the UK Groundwater Forum[1] it provides over half of all groundwater for public supply in the UK and, locally in the south-east of England, up to 70 % of all water in public supply.

The behaviour of the Chalk as an aquifer is complex, and results from a combination of porosity and permeability components that are a consequence of the Chalk lithology, tectonic history and weathering and erosional processes. The calcium-carbonate micro-fossil fragments that make up the chalk form a highly porous, yet essentially impermeable, matrix. More than 95 % of water in the Chalk is held in the

[1] www.groundwateruk.org/

interstices of the rock matrix, but the pore spaces are so fine that this water is effectively immobile. The mobile water (the remaining 5 % or less) is held within the fractures that transect the chalk matrix. Some fractures have been enlarged by dissolution to become fissures or even karstic conduits. The fractures, fissures and conduits provide the permeable pathways for flow.

Barker (1993) provided illustrative relative flow rates permitted by matrix, primary fissures (fractures) and secondary fissures (fractures enlarged by solution): rates of movement of groundwater through the Chalk's secondary fissure system[2] can often be several hundreds of metres per day, compared to rates of the order of a few *millimetres* per day in the primary fissure system[3], and the order of just a millimetres per *year* in the matrix[4]. The matrix water is therefore considered to be essentially immobile.

2.4 Karstic behaviour of the Chalk

It is increasingly recognised (*e.g.* Atkinson and Smith (1974); Price et al. (1992); Banks et al. (1995); MacDonald et al. (1998); Worthington (2003); Maurice et al. (2006)) that aspects of aquifer behaviour of the Chalk of southern England are indicative of karstic development. The term *karst* is a geomorphological term associated with terrain having distinctive landforms and hydrology (Ford and Williams, 2007). Karst characteristics (particularly surficial features) are more developed in some terrains (*e.g.* Carboniferous limestone) than others (*e.g.* Jurassic Limestone and Chalk). However, in hydrogeological terms, the importance of karst is that groundwater flows rapidly through, a network of fractures, conduits (significantly enlarged fractures) and caves (conduits that are large enough to be explored physically by man). Following MacDonald et al. (1998), the term *karst* is used within this thesis to describe features of any dimension that allow rapid groundwater flow and also, where appropriate, geomorphological dissolution features.

Worthington et al. (2000) examined matrix, fracture and channel (conduit) flow in four contrasting carbonate aquifers (including the Cretaceous Chalk) and found considerable similarities in hydraulic functioning between them: in all four cases, more than 90 % of the aquifer storage is in the matrix and more than 90 % of the flow is in the karst channels, with fractures playing an intermediate role. Worthington (2003) suggests that the similarity between the matrix, fracture and and channel flow and storage properites in the four contrasting carbonate aquifers points to a similarlity between all unconfined carbonate aquifers, which by their nature are subject to fracturing and then dissolution, resulting in channel networks which contribute minimally to enhancing aquifer porosity, but greatly enhance permeability. Worthington (2003) argues that differences reported in the literature are often largely attributable to sampling differences as a result of *a priori* assumptions on the behaviour of aquifers: tracer tests from sinkholes to springs characterise channel flow in the aquifer but do not provide information about non-channel flow, whereas studies using wells characterise fracture and matrix flow but give little of no indication of the rapid solute transport than may be occuring in the channel network located between the wells. Therefore, it has been suggested that carbonate aquifers should all be considered as possessing

[2]based on tracer tests

[3]assuming K of the order of 10^{-7} to 10^{-5} $\mathrm{m\ s^{-1}}$, a porosity of 1% and a hydraulic gradient of 10^{-3}

[4]assuming K of 10^{-8} $\mathrm{m\ s^{-1}}$, a porosity of 35% and a hydraulic gradient of 10^{-3}

varying degrees of karst, rather than being wholly karstic or wholly non-karstic (Atkinson and Smart, 1981), or that all carbonate aquifers should be considered as triple-porosity/permeability aquifers, with matrix, fissure and channel/conduit components (Worthington, 2003).

MacDonald et al. (1998) presented various strands of evidence which point to rapid groundwater flow being widespread throughout the Chalk of Southern England. This evidence was drawn from:

- Surface drainage patterns;
- Geomorphological features;
- The presence of explorable caves and cave systems;
- Rapid flow rates implied by tracer tests, including those associated with observed karstic features (such as swallow holes, stream sinks, springs etc) and those carried out without direct association to such features (such as boreholes, soakaways);
- Incidence of chalk boreholes pumping sand;
- Construction details and descriptions from adits;
- Water level response to pumping and recharge;
- Occurrence of indicator bacteria in abstraction boreholes.

The evidence suggests that rapid groundwater flow is generally more frequent close to Palaeogene cover and may also be associated with other forms of cover and valley bottoms (Section 2.4.3).

2.4.1 Geomorphological Evidence of Chalk Karst

Geomorphological evidence of karst characteristics, *e.g.* dolines, solution pipes and swallow holes, are widespread within the Chalk. The common features are defined below:

Swallow hole The point at which a stream sinks underground. A swallow hole generally implies nearly instantaneous water loss into an opening at the bottom of a sinkhole or karst valley, whereas a swallet may refer to gradual water loss into the gravel along a streambed, with no depression apparent.

Sinkhole A closed depression (circumscribed by a closed topographic contour) which drains to the subsurface.

Doline (dissolution sinkhole) A sinkhole resulting from gradual dissolution of the bedrock. A classic bowl-shaped contour (gently sloping depression that is wider than it is deep). Dolines can be considered as depressions that do not necessarily have water flowing into them.

Sinking stream any stream that disappears underground, typically into a swallow hole.

Spring Any natural discharge of water from rock or soil onto the surface of the land of into a body or surface water. Springs which occur on the dip slope of the Chalk are nearly always in the bottoms of valleys and reflect the emergence of the water table at the surface.

Bourne Seasonal streams arising from Chalk springs in response to seasonal water table fluctuations.

The relationship between surface karst features and hydrogeologically significant subsurface karstic features in the Chalk is unclear. MacDonald et al. (1998) point out that there is an inherent bias in the recorded solution features towards those that are easily visible from the ground surface such as swallow holes or dolines, and not necessarily those that are hydrogeologically significant. Relatively rare exposures of chalk faces at Quarries (*e.g.* Castle Lime Works Quarry, Hertfordshire) give some indication of potentially more laterally persistent features. Solution enlarged fractures are observed at Water End, Hertfordshire, which may indicate hydrogeolgical connections from the swallow holes and dolines. The high concentration of swallow holes and dolines in the region of Water End may be hydraulically significant as they are likely to provide a mechanism for directing a significant volume of recharge into the chalk aquifer. In particular they may direct recharge rapidly to a depth at which more laterally persistent solution features occur.

2.4.2 Evidence of rapid flow rates from tracer tests in the Chalk

Atkinson and Smith (1974) conducted a tracer test in the Hampshire Chalk, where swallow holes occur near to the northern margins of the Eocene outcrop. Rhodamine WT dye was pumped into a swallow hole for three days. The travel time to its emergence at the Bedhampton spring (a distance of 5.75 km) was 62.5 hours, corresponding to a velocity[5] of 2.2 $\mathrm{km\ day^{-1}}$ (peak concentration). Atkinson and Smith (1974) concluded that turbulent flow in an open system of fissures widened by solution, or conduits, is required to achieve the observed velocities.

Banks et al. (1995) conducted a tracer test in the Berkshire Chalk between the Holly Grove stream sink and the Blue Pool spring 4.7 km away. Both the spring and the stream sink were less than 1 km from the Chalk/Eocene boundary. The observed velocities were 5.8 $\mathrm{km\ day^{-1}}$ for peak concentration and 6.8 $\mathrm{km\ day^{-1}}$ for breakthrough. The authors suggest that little attenuation occurred as the tracer moved from the sinkhole to the spring. Maurice et al. (2006) carried out two injections of flourescein tracer from the Smithcroft Copse (nearby to Holly Grove) to the Blue Pool. Maurice et al. (2006) determined groundwater velocities of 5.12 and 4.71 $\mathrm{km\ day^{-1}}$ with tracer recoveries of 25.5 % and 21.7 % respectively.

In the Hertfordshire Chalk, there is abundant evidence of the existence of rapid preferential flow routes within the Chalk. Water End is a well known site of swallow hole activity (Section 3.2.5). The swallow holes are located close to boundary between the Chalk and Eocene cover. Three tracer tests, carried out in 1927, 1928 and 1932 using fluorescein dye showed that water recharging the swallow holes were detected in a series of springs and wells in the Lea Valley up to 16 km from the swallow holes (Harold, 1937). The breakthrough times gave flow velocities up to 5.5 $\mathrm{km\ day^{-1}}$, with tracers being detected over a $30\,^{\circ}$ arc from the swallow holes (Harold, 1937). The velocities between the swallow holes and a particular detection point in the Lea Valley varied by up to 37 % between tests, and the fastest route also varied between tests. A test carried out in 1935 in swallow holes at South Mimms (3.5 km to the sourthwest of Water End) also showed flows towards the Lea Valley over distances up to

[5] Velocities quoted are mimimum velocities calculated based on straight line distance between input and output locations

19 km, with velocities up to 3.5 $\mathrm{km\ day^{-1}}$.

In addition, bacteriological examination of groundwater samples taken from the Lea Valley in 1935-36 showed a strong correlation between rainfall and the level of bacteria (Harold, 1937). The increase in bacteria numbers coincided with periods when streamflows known to contain bacteria entered the swallow holes at North and South Mimms. Given the connection between the swallow holes and the sampling points in the Lea Valley, this suggested that particles of bacterial size could travel rapidly through fissures in this area of the Chalk.

Cook (2010) undertook an extensive programme of tracer testing to investigate the nature of karst connections in the Hertfordshire Chalk. The tracing was conducted using three species of bacteriophage (phage), injected at three locations in Hertfordshire:

- *MS2 Coliphage* were injected by borehole dilution in Harefield House Borehole, near Sandridge;
- *Phi X174* phage were injected by borehole dilution at Comet Way Borehole, near Hatfield;
- *Serratia Marcescens* phage were added to a sinking stream close to a large swallow hole complex at Water End near North Mymms.

Monitoring for the tracers was conducted at 21 locations throughout the study area, comprising abstraction wells, observation boreholes, springs and surface waters. The duration of the monitoring period was approximately two months.

The connections indicated by the tracer tests are further described in Section 3.2.6. Results indicated rapid groundwater flow between the Water End swallow holes and a wide spatial distribution of locations in the Lea Valley. Rapid flow connections were also indicated between locations to the west of the main karst system toward Hatfield, Sandridge and within the Vale of St. Albans.

Between Water End and the Lea Valley (*Serratia Marcescens* phage), travel times and distributions were broadly consistent with the 1920s and 1930s tracing results. However, better data resolution allowed for the observation of breakthrough curves and secondary tracer peaks suggesting multiple arrivals of tracer. First detections indicated groundwater velocities of between 1.8 $\mathrm{km\ day^{-1}}$ and 3.9 $\mathrm{km\ day^{-1}}$. Overall tracer recovery was estimated at approximately 15 % of the injected tracer mass.

Identification of tracer breakthrough for the *MS2 Coliphage* and *Phi X174* phage was complicated by measured concentrations being close to background. However, observations suggest groundwater velocities between Hatfield (*Phi X174* phage, Comet Way BH) and Essendon PWS, Arkley Hole Spring and Lynchmill Spring of between 0.8 $\mathrm{km\ day^{-1}}$ and 1.8 $\mathrm{km\ day^{-1}}$. Groundwater velocities between Sandridge (*MS2 Coliphage*, Harefield House BH) and Hatfield Quarry, Essendon PWS, Arkley Hole Spring and Lynchmill Spring indicated groundwater velocities between 0.05 $\mathrm{km\ day^{-1}}$ and 0.9 $\mathrm{km\ day^{-1}}$. In both cases, attenuation was high: overall tracer recovery was estimated at less than 1 % of the injected mass.

There are also examples of tracer tests indicative of karst flow in ares of the Chalk of Southern England that are unconnected with obvious karstic features. Price et al. (1992) reported a tracer experiment at the M1/M25 motorway intersection, an area close to the Chalk/Palaeogene boundary where karstic

features are common, but the studies were carried out in soakaways that were apparently unassociated with karstic features. Some tracer traveled rapidly to a pumping station a distance of 3 km away, with recorded velocities in excess of 2.4 $\mathrm{km\,day^{-1}}$. The tracer recovery was very low, and it was thought that a significant fraction of the flow was moving through fine fractures.

A number of borehole dilution tests and radial tests from an injection borehole to a pumped borehole, were carried out in East Anglia (Kachi, 1987; Ward, 1989). The main conclusion of the extensive testing and modelling was that flow was dominated by micro-fractures with a range of sizes rather than by a few discrete high-permeability conduits.

2.4.3 Development of permeability within the Chalk

A number of factors contribute to the pattern of occurrence and development of fractures within the Chalk, including the effects of periglaciation.

The lithology of the Chalk has an important effect on aquifer properties (Mortimore, 1993):

- Within the Newhaven, Lewes Nodular, New Pit, and Holywell Nodular Chalk members, conjugate fractures are common. At the intersection of the fractures, cavities can develop which could give rise to rapid groundwater flow and therefore high permeability.

- Marl horizons restrict vertical flow due to their high clay content. However, marl and flint bands may act to 'seed' the development of larger solution features, *e.g.* by forcing groundwater moving downwards from the Chalk above to dissipate horizontally.

- The presence of hardgrounds, where shallower than about 100 m below ground level, can significantly increase the permeability of the Chalk. Hardgrounds (such as the Chalk Rock and the Melbourne Rock) fracture more cleanly than other chalks due to their greater hardness (Price, 1987), and since the hardgrounds are better cemented, fractures within them tend to remain open at greater depths than in softer chalk. The open fractures allow groundwater to flow through them generating preferential flow paths which may then be enhanced by dissolution.

The structure of the Chalk can affect aquifer properties, although the relationship between structure and permeability is complex. Generally, folding tends to increase the fracturing of the Chalk along the axis of anticlines. Deep burial of the Chalk (e.g. beneath Palaeogene deposits of the London Basin) tends to reduce permeability and storage . Rapid, anisotropic, groundwater flow is often associated with fault zones in the Chalk (Allen et al., 1997): parallel to the fault groundwater flow is rapid, while it is impeded perpendicular to the fault.

Price et al. (1993) reviewed the factors that may have contributed to the development high transmissivity along valleys. There may be a higher frequency of open fractures within valleys since valleys often follow lines of structural weakness, and erosion along the valleys reduces effective stress, allowing horizontal fractures to open. However, a higher frequency of fractures in not necessarily a prerequisite to high permeability; it can develop by solution enhancement of a lower frequency of fractures. Price (1987) illustrated how the increased flux of groundwater along a valley could give rise to high permeability within the valleys and the development of a single zone of dissolution-enhanced fractures. The

concentration of groundwater flux, and hence increase in velocity, occurs as groundwater flows from recharge areas to discharge areas in the valleys. The mixing of groundwaters of different chemistry towards discharge points can also increase the dissolution potential of groundwater.

Periglaciation is believed to have played an important role in the enhancement of permeability along the valleys (Younger, 1989). Repeated freezing and thawing of the active layer would have broken down the top few metres to a weathered chalk that would have been easily eroded. Furthermore, in the valleys, the flow of surface water would have kept the ground unfrozen to a greater depth for large parts of the year, forming a talik within the Chalk of the valley floor. Chalk is dissolved more easily under cold conditions, therefore the concentrated flow of groundwater within these taliks and the low temperature of the groundwater would combine to dissolve Chalk within factures. Within valleys, an increase of fracturing is observed in the top 5–6 m of the Chalk. In some valleys, periglacial activity led to fractures opening up to a depth of 20–30 m.

Geomorphological karstic features, and rapid groundwater flow, are generally more frequent close to Tertiary cover (MacDonald et al., 1998). Based on a field survey of the Pang and Lambourn catchments in Berkshire, Maurice et al. (2006) identified three distinctive geomorphic Zones characterised by the density of surface karst features which was related to the proximity to the Palaeogene-Chalk contact. Soils associated with Palaeogene deposits tend to be quite acidic. The soils associated with Quaternary cover also tend to be clayey and therefore to concentrate runoff into discrete points. As recharge drains through the cover, it remains unsaturated with respect to calcite until it reaches the Chalk surface, thus allowing acidic recharge to be channelled to discrete points of the Chalk surface.

Solution pipes and swallow holes can allow acidic recharge to penetrate deep into the unsaturated zone (and even the saturated zone). Therefore the acidic recharge can link up with fracture systems within the aquifer and allow the enlargement of fractures to conduits. This is probably the mechanism for the observed rapid groundwater flow near Quaternary cover (Allen et al., 1997). It is likely that zones of slightly wider initial aperture occurring in fractures with asperities will be preferentially widened by dissolution until discrete ‘conduits’ are formed (Younger and Elliot, 1995). Even once the cover and geomorphological features have been moved by erosion, the deeper hydrogeological features will remain, providing rapid groundwater flow and preferential flow paths.

Rapid groundwater flow and swallow holes are also often observed on valley bottoms, associated with flowing streams. These ’karst’ type features may have a different origin to those observed on the Chalk interfluves (Allen et al., 1997). Surface water flowing within streams has different chemistry from the groundwater, therefore mixing can produce water that has a high dissolution potential. This aggressive water, coupled with the high flux through the valleys and the dynamic of surface water flow can produce sink holes and springs in stream beds, probably linked with conduits. Therefore, as in more classic ‘karst’ environments, surface water can flow in discrete channels underground within valleys.

2.5 Hierarchy in the Chalk aquifer

Cushman (1990) introduced the concept of natural hierarchy in porous media. He recognised that many, if not most, porous media, such as soil and geological formations, possess some sort of hierarchy: either

structural (relating to successively nested, interacting, physical subunits) or functional (relating to a hierarchy of transport processes). Furthermore, structural (functional) hierarchy may be *discrete* or *continuous*. In a discrete hierarchical medium there are a finite number of nested structural subunits or functional subprocesses, whereas in a continuous hierarchical medium there are an infinite number of subunits (subprocesses) that cannot be clearly decomposed.

The Chalk has long been recognised as having multiple components of porosity and permeability, being described as a double-porosity (dual-porosity) aquifer (Foster, 1975; Price, 1987; Barker, 1991; Price et al., 1993), a double-permeability (dual-permeability) aquifer (Price et al., 1993), and a triple-porosity and/or triple-permeability aquifer (Worthington, 2003; White, 2003).

A classic *double-porosity* (or *dual-porosity*) aquifer consists of a porous matrix divided into blocks by a well-developed (orthogonal) fracture set (Price et al., 1993). The matrix pores provide storage and the fractures/fissures provide the permeable pathways for flow. Dual-porosity aquifers are distinct from *double-permeability* (or *dual-permeability*) aquifers, which are heterogeneous formations with permeable intervals alternating with layers or lower permeability (Figure 2.2). The permeable intervals may have higher primary permeability than the others, or they may be beds displaying extensive fissuring.

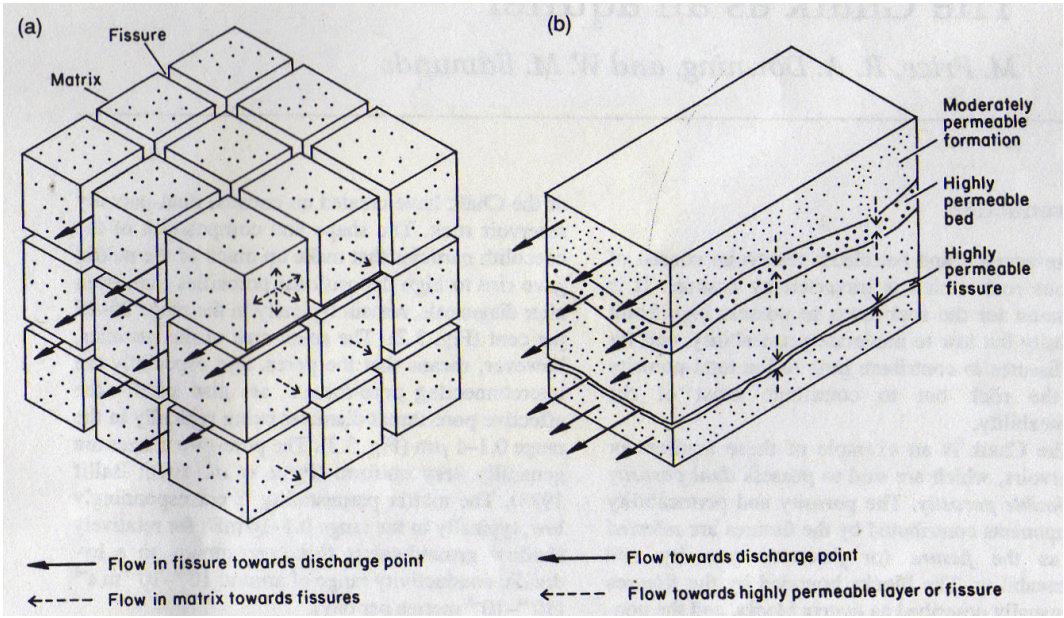

Figure 2.2: (a) An idealised double-porosity aquifer; (b) an idealised double-permeability aquifer. From Price et al. (1993)

The porosity and permeability components contributed by the fissures are referred to as the as the *fissure* (or *fracture*) porosity and permeability. The blocks bounded by the fissures are usually described as *matrix blocks*, and the non-fissured fraction of the porosity and permeability as the *matix* (or *matric*) porosity and permeability.

The behaviour of the Chalk is more complex than described in the classical double-porosity model. The majority of the water within the matrix pore space does not represent usable groundwater storage; effective groundwater storage is primarily within the fracture network and the larger pores (Section 2.6).

In terms of groundwater flow, there is a hierarchy in permeability components (Section 2.7) as a result of solution enhancement of primary fractures to form fissures and karstic conduits. The Chalk has therefore been described as exhibiting *dual-permeability behaviour* (Price et al., 1993).

The Chalk is increasingly recognised as possessing karstic characteristics in places (Section 2.4.2). This additional flow component is neglected by classic double-porosity models (Section 6.2.6). More recently, it has been proposed that carbonate aquifers, including the Chalk, be considered as *triple porosity* and *triple permeability* aquifers (Worthington, 2003; White, 2003), to account for flow and storage in three porosity and permeability elements:

- the three-dimensional matrix;
- two-dimensional, or planar, fracture (fissure) elements; and
- one-dimensional, or linear, channel (conduit) elements.

2.6 Porosity components of the Chalk aquifer

Chalk matrix porosity and pore size distributions show both regional and stratigraphic variations. Bloomfield et al. (1995) described regional trends in matrix porosity data, based on BGS Aquifer Properties Laboratory core analysis database. Within the Thames and Chilterns area, mean porosity is 38.8 % for the Upper Chalk, and 31.4 % for the Lower Chalk (standard deviations of 5.8 % and 6.6 % respectively). Watson (2004) recorded slightly higher values for the Chalk in the Tilmanstone and Eastry areas of Kent: 43 % for the Upper Chalk (44.5 % for samples from the Seaford Chalk and 40.0 % for samples from the Lewes Nodular Chalk) and 38 % for the Lower Chalk. Watson (2004) found a general decline in values from approximately 45 % at 8 m below ground level (BGL) to 40 % at 60 m BGL. Price et al. (1976) described regional and stratigraphical trends in pore size distributions in the Chalk. The median pore size was 0.65 $\mu\mathrm{m}$ for the Upper Chalk of the Southern Province, 0.53 $\mu\mathrm{m}$ for the Middle Chalk, and 0.22 $\mu\mathrm{m}$ for the Lower Chalk. Atkins (2002) obtained values from 30.8 % to 46.8 %, with an average of 38.0 % from chalk samples taken during the 2001 site investigation at St. Leonard's Court, Sandridge.

Although the matrix has high porosity, small pore throat diameters mean that the pores are not readily drained under gravity. It has been estimated that for the Upper Chalk, about 3 % of the total porosity (or 1 % of the bulk volume) of the Chalk represents useable storage (Price, 1987). Effective (accessible) groundwater storage is probably primarily within the fracture network and the larger pores (Price et al., 1993). The relative contribution to the storage coefficient from the matrix and fractures of various sizes is difficult to ascertain. The total specific yield is in the range 1 % to 3 % (Allen et al., 1997). Overlying deposits, where present, often make an important contribution to groundwater storage: groundwater stored in the overlying Palaeogene deposits of the London Basin can be drawn down into the Chalk facture system (Allen et al., 1997).

MacDonald and Allen (2001) collated data from pumping tests carried out on the Chalk (but see Section 2.7.2 below for discussion of inherent data bias). One thousand two hundred pumping tests had estimates of storage coefficient. The median value of storage coefficient from all the pumping tests

was 0.0023, and the 25^{th} and 75^{th} percentiles were 0.0004 and 0.01 respectively. Approximately one order of magnitude difference was recorded between estimates of storage coefficient from confined and unconfined tests: unconfined tests had a median of 0.008 and confined tests had a median of 0.0006. The authors suggest that the relatively small difference between unconfined and confined measurements may be explained by the limited gravity drainage of the Chalk matrix, and therefore the relative importance of elastic storage in both confined and unconfined conditions. However, MacDonald and Allen (2001) also found a direct relationship between transmissivity and the storage coefficient, which indicates that gravity drainage from the fracture network is still a significant component of storage.

In fissured rocks such as the Chalk, where nearly all groundwater movement occurs in the fissure network, the porosity that is of importance when groundwater flow velocities are being considered is the porosity that represents the saturated pore space which contributes to the flow. This porosity, which will be practically equivalent to the porosity of the fractures, is significantly lower than the total porosity: in general, the porosity of the fractures is around 0.01 % Price et al. (1993). De Marsily (1986) defines the ratio of the volume of water able to circulate to the total volume of rock as the *kinematic porosity*. The term *effective porosity* is also frequently used in this context. However, Ward et al. (1998) encourages the use of the term *kinematic porosity* over *effective porosity* for the purposes of solute transport to prevent association with the *specific yield*, which is sometimes taken to be representative of the effective porosity, and has been used for the purposes of solute transport in fractures (*e.g.* Bibby (1981)). However, it may not be appropriate to use values of specific yield in this context: specific yield values are usually derived during hydraulic testing and the fluid volumes released due to the stresses applied during testing may be unrepresentative of the volume of water through which solute transport occurs.

The effective porosity is related to the aperture of the active fractures and the frequency of occurrence of those fractures. Atkins (2004) estimate an effective porosity range of 0.05 % to 0.50 % for the Hertfordshire Chalk, assuming fracture apertures between 0.5 mm and 5.0 mm and an average of one fracture per metre of borehole. However, they note that this range does not take into account the contribution of the vertical fractures to the effective porosity (vertical boreholes only detect horizontal or sub-horizontal fractures) and therefore state a more 'reasonable' effective porosity range of 0.5 % to 2.0 %.

Values for effective porosity in a fractured rock can be determined if the Darcy velocity or flux q and average linear velocity v are known through the relationship

$$n_e = \frac{q}{v}. \tag{2.1}$$

Watson (2004) calculated effective porosity for the Chalk of the Tilmanstone-Eastry Valley in Kent based on the results of single borehole dilution tests and natural gradient tracer tests. Single borehole dilution tests were undertaken to obtain darcy velocity, q, for specific depth intervals. The groundwater (fissure) velocity, v, was estimated from the arrival times of the natural gradient tracer tests. The effective porosity was then calculated using equation 2.1. The calculated effective porosities were in the range 0.1 % to 0.3 %.

2.7 Permeability components of the Chalk aquifer

2.7.1 Terminology

There is no clear consensus within the hydrogeological literature on the definition relating to openings or partings in rock that carry water. Throughout this thesis, the term *fracture* is used to refer to any planar discontinuity in the Chalk which has a finite aperture, and is used where the intention is to avoid any generic or hydraulic inferences (*e.g.* Bloomfield (1996)). Fractures may originate as joints (tensional or shear) or small faults (Section 2.2.3). The term *fissure* is applied to fractures that have been enhanced by solution. By implication, fissures are hydraulically significant features of the rock.

Solution enhancement may take the form of small channels on the fracture surfaces or of a general widening over a substantial proportion of the fracture area. *Fissures* are distinguished from *conduits* by the fact that they retain the generally planar geometry of unmodified fractures. Following the terminology used by Maurice et al. (2006), *conduits* are tubular voids or channels formed by solution, and are distinguished from fissures by the aspect ratio they present in cross section: trace length to maximum aperture ratios for conduits is approximately one in contrast to greatly in excess of ten for fissures.

In relation to groundwater flow within the Chalk aquifer, the terms *primary fissures* and *secondary fissures* are often used (Price, 1987; Barker, 1993) to distinguish between fractures which are tectonic in origin, and fractures that have been significantly enlarged, respectively. Price et al. (1993) point out that in reality there is a more or less continuous range from tight fissures to greatly enlarged, karstic openings.

2.7.2 Bulk transmissivity

Hydraulic properties determined by well tests (pumping tests) on the Chalk provide an averaged value over the depth of the borehole. Similar aquifer properties might be estimated from two boreholes with radically different flow regimes: a borehole that intersects one highly permeable fracture can give the same transmissivity and storage coefficients as a network of small fractures with moderate permeability (*e.g.* Foster and Milton (1974)).

MacDonald and Allen (2001) collated and analysed data from pumping tests carried out on the Chalk, using both observation and production boreholes, at approximately 1300 locations throughout England. The filtered dataset comprise 2100 measurements of transmissivity and 1200 estimates of storage coefficient. Distributions give the appearance of log-normality, however are not truly log-normal. The median transmissivity value was 540 $\mathrm{m}^2\ \mathrm{day}^{-1}$; the 25^{th} and 75^{th} percentiles were 190 $\mathrm{m}^2\ \mathrm{day}^{-1}$ and 1500 $\mathrm{m}^2\ \mathrm{day}^{-1}$ respectively. However, MacDonald and Allen (2001) stress the inherent bias to this data which has predominantly been calculated from pumping tests undertaken in boreholes that have generally been drilled for production and are therefore in areas known to be high-yielding. Throughout the Chalk outcrop, data are clustered within valleys, where the transmissivity and storage tends to be high. The median value of 540 $\mathrm{m}^2\ \mathrm{day}^{-1}$ is therefore unreasonably high for large areas of Chalk (Allen et al., 1997).

It has long been observed that the transmissivity within the Chalk is greater in valleys than on the interfluves (*e.g.* Ineson (1962)). However, the existence of this pattern has lead to the majority of

boreholes being drilled within the valleys, and the consequent lack of data available across the interfluves hinders the understanding of the variations in transmissivity away from the valleys. However, Allen et al. (1997) report that flow logging from boreholes drilled on interfluves of the Berkshire Downs indicated a general thinning of the transmissive zone compared with valleys.

Transmissivity values were also found to be significantly higher in unconfined areas compared to confined areas: unconfined sites had a median transmissivity of 920 $\mathrm{m}^2\ \mathrm{day}^{-1}$ compared to a median of 220 $\mathrm{m}^2\ \mathrm{day}^{-1}$ at confined sites. It is thought that this reflects increased solution enhancement of fractures under unconfined conditions.

2.7.3 Permeability components

2.7.3.1 Matrix Permeability

The Chalk matrix is generally isotropic with respect to permeability, and matrix hydraulic conductivity is typically in the range of 10^{-4} to $10^{-2}\ \mathrm{m\ day}^{-1}$ (Price, 1987). The distribution of horizontal hydraulic conductivity values, derived from 977 gas permeability measurements on chalk core samples, was found to approximate to a lognormal distribution with geometric mean of $6.3 \times 10^{-4}\ \mathrm{m\ day}^{-1}$ (Allen et al., 1997). This low value indicates that the hydraulic conductivity of the Chalk matrix is negligible with respect to the hydraulic conductivity of Chalk fracture systems (Section 2.7.3.2). For the same data, a general correlation between bulk matrix porosity and hydraulic conductivity was observed and a linear regression (r^2 = 0.651) of the form:

$$\log_{10} \mathrm{K}\ (\mathrm{m\ day}^{-1}) = 0.0654 \times \Phi(\%) - 5.3378$$

Allen et al. (1997) speculated that a correlation between some function of the matrix pore size distribution and hydraulic conductivity is likely to be more significant, although such a correlation was not established for the Chalk matrix.

2.7.3.2 Fissure Permeability

If groundwater flow withn the Chalk is primarily through a system of fissures, the transmissivity is typically a function of the degree of fracturing. More specifically, the transmissivity of the Chalk is dependent on the aperture and spacing of the fissures and the interconnectedness of the fissure network.

A single, perfectly planar, smooth-sided fissure with uniform aperture, a, can be ascribed a transmissivity, T_f, by the so-called *cubic law* (Snow, 1968; Barker, 1993):

$$T_f = \frac{ga^3}{12\nu} \tag{2.2}$$

where g is the acceleration due to gravity and ν is the kinematic viscosity. The transmissivity of a fracture is therefore very sensitive to aperture size since the transmissivity is a function of the cube of the aperture. Barker (1993) highlights this by a simple example: equation 2.2 gives a transmissivity of about $10^{-3}\ \mathrm{m}^2\ \mathrm{s}^{-1}$ for a fissure with an aperture of only 1 mm, and an enormous $1\ \mathrm{m}^2\ \mathrm{s}^{-1}$ for a 1 cm aperture. Equation 2.2 is valid providing flow is laminar (Section 2.8).

2.7.3.3 Fracture aperture and spacing

Generally, there are three types of fractures (*primary fissures*) present in the Chalk: joints, bedding plane fractures and faults. A combination of factors such as dissolution, weathering, and release of overburden, can lead to significant enlargement of these initial fractures, either individually or in layers or zones, (forming *secondary fissures*). The primary fissures typically have apertures of much less than 1 mm; Solution enlarged secondary fissures typically have apertures of greater than 10 mm (Worthington, 2003). Price et al. (1993) calculated theoretical hydraulic conductivities for the Chalk related to aperture and spacing (Figure 2.3).

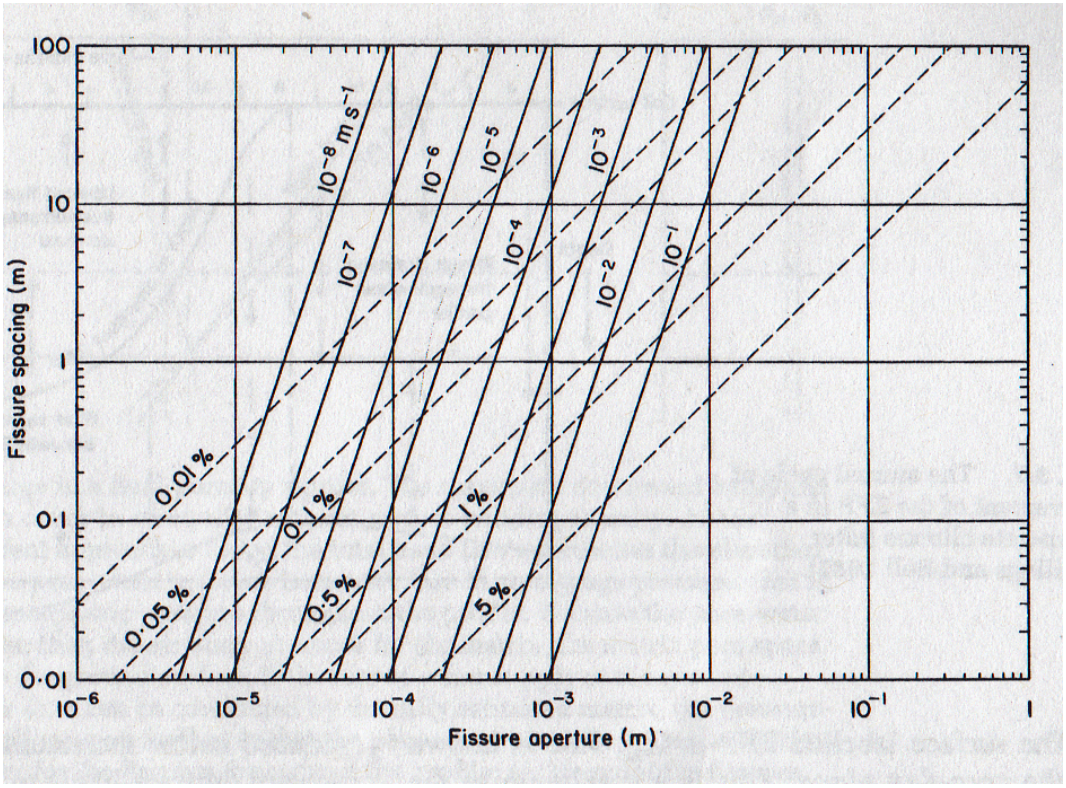

Figure 2.3: Relationsip between fissure spacing, aperture, porosity and hydraulic conductivity for a fissure system containing three plane, parallel, mutually perpendicular smooth-walled fissures filled with pure water at 10 degC and porosity relationship (Price et al., 1993).

Bloomfield (1996) measured fracture orientation, trace length, spacing and aperture using section and scan-line surveys on the Upper Chalk at Play Hatch Quarry, Berkshire. There were two dominant joint sets: a set parallel to bedding and a set at a high angle to bedding. The trace length and spacing distributions of the two joint sets approximated to log-normal distributions, with geometric mean trace lengths of 0.15 m and 0.30 m, and spacings of 0.10 m and 0.12 m, respectively. Calculated fracture interconnectivity indices suggest that the bedding parallel joint set is likely to be of greater hydraulic importance than the high-angle joint set. Bloomfield (1996) used the fracture interconnectivity index of Rouleau and Gale (1985) to demonstrate that the bedding parallel joint set fractures had a higher interconnectivity, suggesting that the are likely to be of greater hydraulic importance than the high-angle

joint set. Bloomfield (1996) proposed that the results of the Play Hatch Quarry support a visualisation of the Chalk consisting of "scale-invariant fault-bounded segments, where the internal fracture architecture of each segment is dominated by continuous bedding plane fractures, and subordinate, scale-dependent, arrays of joints". The scale of jointing within a given fault-bounded segment is a function of bedding thickness.

Aperture measurements obtained for a single bedding plane fracture ranged from less than 0.5 mm to 23.5 mm. Apertures approximated to a negative exponential distribution (with a mean of 1.2 mm) below 7 mm, and to a log-normal distribution (with a mean of 11.7 mm) above 7 mm. It was inferred that the larger apertures have been affected by solution processes and that flow through bedding plane fractures is channeled across 10–20 % of the fracture surface area.

Watson (2004) calculated block sizes (fracture spacing) for the Chalk of the Tilmanstone-Eastry valley in Kent corresponding to fracture density predicted by the relationship established for the area:

$$Log_{10}[\text{fracture density}] = -1.685 \times Log_{10}[\text{depth}] + 2.5365$$

This relationship was determined based on data from scanline surveys in the area and a fracture profiled produced with televiewer an optiviewer logging.

Watson (2004) used data for block sizes and effective porosity (Section 2.6) to calculate fracture aperture using the relationship

$$\text{fracture aperture} = \text{block width} \times \text{effective porosity}$$

In general, fracture apertures were found to increase with depth, and ranged from 0.44 mm to 3.83 mm. Watson (2004) also calculated fracture apertures from hydraulic conductivity data from packer testing using an approximation to the cubic law:

$$K_{effective} \approx 50a^3N$$

where N is the fracture density, a is the fracture aperture, and $K_{effective}$ is the effective hydraulic conductivity. Apertures determined by this method (*cubic law* or *hydraulic* apertures) ranged from 0.92 mm to 1.39 mm.

Figure 2.4 summarises the range of fracture spacing and fracture aperture measurements from a number of sources. It should be noted that fracture apertures are difficult to measure *in-situ*: at outcrop, weathering effects may produce enlarged apertures, and accurate down-hole measurement is only feasible for larger openings. As such, there are few direct observations for the Chalk, and apertures are usually determined from cubic law approximations or in relation to fracture density and fracture porosity measurements.

It has been shown that groundwater velocities measured from the tracer tests described in Section 2.4.2 could result from flow through either small channel conduits or more laterally extensive fissures. For the Hampshire study Atkinson and Smith (1974) calculated that, for the estimated head gradient, the volume indicated by the tracer time to peak was equivalent to flow in a single circular pipe

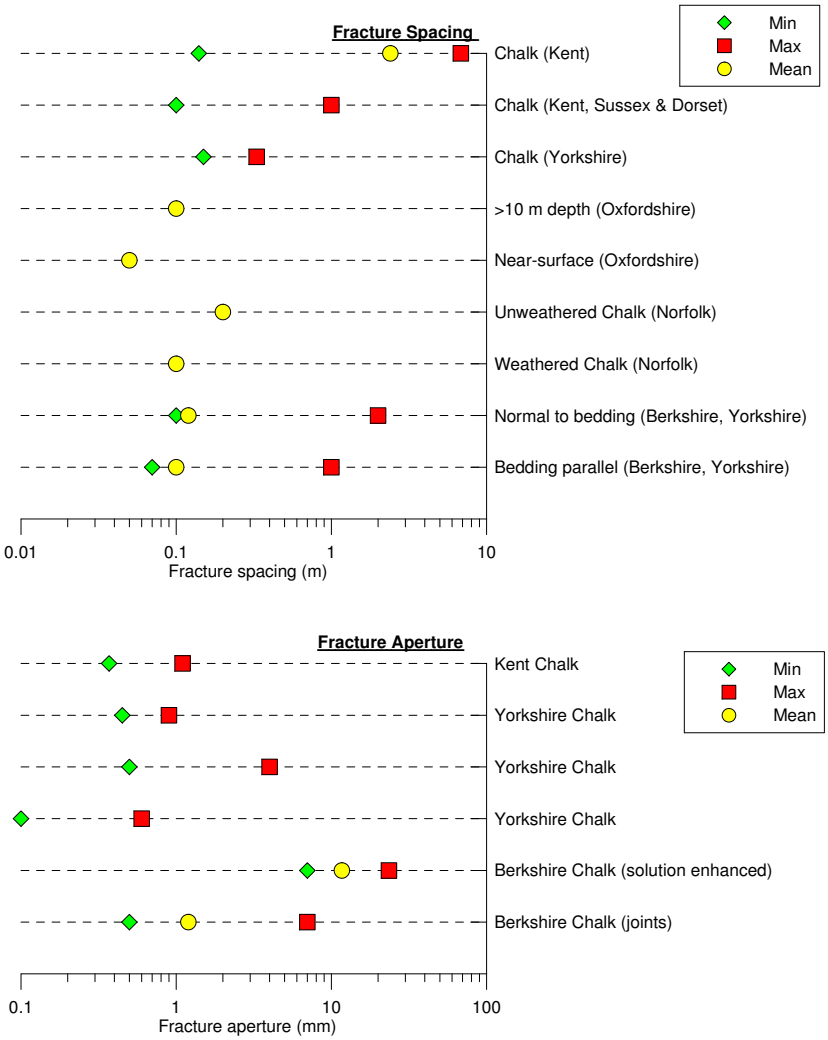

Figure 2.4: Ranges of fracture spacings and fracture apertures for the Chalk. Results as cited in Bloomfield (1996) and Watson (2004).

740 mm) in diameter (although in reality several features would probably be involved). Price (1987) suggested that in an ideal case (a plane parallel fracture with no roughness or chanelling) a fissure of only 4.5 mm width, with a transmissivity of 5000 $\mathrm{m^2\ day^{-1}}$, provides an alternative hydraulic explanation for the observed combination of displacement volume and velocity. By using the same method Banks et al. (1995) calculated that a single fissure 5.4 mm in width could theoretically be sufficient to represent the fracture system in Berkshire, and similarly, Maurice et al. (2006) calculated that the observed velocities would suggest a comparable aperture of 4.9 mm. However, they note that the hydraulic gradient (0.004) is calculated using the elevation difference between the sink and the spring, and since the water table is lower than the surface elevation of the stream sink, the actual hydraulic gradient must be smaller, and therefore the calculation must underestimate aperture. Cook (2010) determined apertures around 2 mm to 4 mm using the cubic law approach for the results of the tracer tests in Hertfordshire. These results were also interpreted as minimum equivalent conduit diameters between 0.6 m and 2.1 m, based on maximum recorded discharges and flow velocities at locations including Water End and Catherine Bourne swallow holes, and Arkley Hole and Lynchmill Springs.

2.7.3.4 Distribution of fractures

Small aperture fractures (primary fissures), present throughout the Chalk, are significant in increasing the transmissivity of the Chalk aquifer compared to the permeability of the Chalk matrix. In general, flow logs and packer tests indicate that permeability measured throughout the depth of a borehole is generally at least an order of magnitude higher than matrix permeability (Allen et al., 1997), and Price et al. (1982) found that packer test values for intervals in the Chalk are always higher than the intergranular measurements (in contrast to the good agreement found in the Penrith Sandstone).

However, Price (1987) estimated the transmissivity of the Chalk without secondary fissuring to be approximately 20 $\mathrm{m^2\ day^{-1}}$, which is much lower than the typical values of the order of 2000 $\mathrm{m^2\ day^{-1}}$ reported in the Chalk (Section 2.7.2). Solution enlarged fissures, with high individual transmissivities, are therefore necessary to account for the high (bulk) transmissivities that characterise the Chalk aquifer. For example, in areas of high transmissivity, there is evidence that most of the thickness of the Chalk may have relatively low hydraulic conductivities with the bulk of the water movement occurring at a few horizons where fissures have been enlarged by solution (Headworth, 1978; Headworth et al., 1982). Geophysical logging indicates that flow in the Chalk aquifer is often limited to discrete flow horizons, and TV-logging reveals that these are often macroscopic solution pipes up to several centimetres across. These conduits may be few in number, but will completely dominate the overall hydraulic conductivity of the aquifer (Younger and Elliot, 1995).

These hydraulically significant fissures are not present through the full thickness of the Chalk, but are concentrated in the upper sections of the Chalk, typically the upper few tens of metres, with little flow deeper than 50 m below groundwater levels (Allen et al., 1997). For example, packer testing at Trumpletts Farm on the Berkshire Chalk (Williams et al., 2006) indicated that hydraulic conductivity varied by three orders of magnitude (from $\sim$50 $\mathrm{m\ day^{-1}}$ to $\sim$0.05 $\mathrm{m\ day^{-1}}$) over the 70 m of chalk tested, with a strongly non-linear decrease with depth below ground level. Deeper within the Chalk the

frequency and aperture of fractures declines due to increasing overburden and a general reduction in circulating groundwater and hence dissolution. The greatest permeability in the Chalk is observed in the zone of water table fluctuation where the movement of groundwater can enhance the aperture of the fractures by dissolution. A similar pattern of permeability variation with depth is observed where the Chalk is confined by younger deposits within the London and the Hampshire Basin. In the London Basin, flow logging has illustrated that the majority of inflows to boreholes, shown by geophysical logging, occur within 20 m to 30 m of the upper surface of the Chalk.

Williams et al. (2006) compared the results of the packer testing at Trumpletts Farm with results from borehole imaging and geophysical testing; while some of the highly permeable zones appeared to be associated with obvious fractures, large fractures could be seen in zones which had much lower permeability, and some highly permeable zones appeared to be associated with poorly developed fractures. Therefore, not all fractures are hydraulically active. Furthermore, Williams et al. (2006) found differences in flow velocity depth profiles (from single borehole dilution tests) in the same borehole which was tested both before and during a pumping test at an abstraction borehole about 40 m from the site, indicating that different fractures become active when the aquifer is stressed. Therefore, field studies show that flow near individual boreholes is highly heterogeneous, and that there is uncertainty in the relationship between the characteristics of a fracture observed in a borehole and the amount of flow which that fracture contributes to the borehole.

Groundwater flow in the Chalk is highly heterogeneous and borehole yields may vary by orders of magnitude over distances of less that 100 m reflecting the complexity of flow in the aquifer. The single borehole dilution testing by Williams et al. (2006) showed differences in flow velocity depth profiles between boreholes located within a few tens of metres across the site. These are inferred because the different boreholes, although of similar depth and drilled in very close proximity, intersect slightly different parts of the fracture network an hence groundwater flow system. In particular, a flowing feature at the base of one borehole is not intersected by the second, which is drilled from a slightly higher elevation.

When considering flow observations in boreholes, it is important to note that the presence of the borehole connects flowing horizons and allows vertical flow. Therefore, the observed flow may not be representative of flow in the aquifer in the absence of the borehole.

2.7.3.5 Connectivity of fissures and conduits

Worthington (2003) described a triple porosity/permeability model of carbonate aquifers (including the Chalk). This visualises groundwater flow via an interconnected tributary network of channels, formed by dissolution, which discharges to springs. The smaller (upgradient) channels are in the millimeter to centimeter range (*i.e.* correspond to *fissures*). The larger (downgradient) correspond to conduits (diameter >1 cm) and caves (diameter >1 m).

The nature and connectivity of fissures and conduits, and their relationship with surface karst features is poorly understood. Fissures are the features most commonly encountered in boreholes and wells; conduits are rarely intersected. However, tracer tests using surface karst features will directly encounter

the conduit system. Connectivity between cave conduits and fissures intercepted by quarrying has been demonstrated in the highly karstic Carboniferous Limestone (Edwards et al., 1991). The occurrence of turbidity and bacteria in some Chalk boreholes suggest that there may also be interaction between fissures and larger scale conduits in the Chalk (MacDonald et al., 1998).

During the Water End tracer tests in Hertfordshire (Section 2.4.2), visible colouration demonstrated connections to seven spring and borehole abstraction sites up to 6 km apart. Visible colouration in the Blue Pool complex during the tracer tests in Berkshire by Maurice et al. (2006) demonstrated that tracer was discharged at a number of sites up to 100 m apart, suggesting flow through laterally extensive fissures in the vicinity of the springs. The results of both these tracer studies are consistent with the downstream sections of conduit systems being characterised by fissure flow resulting in lateral dispersion across a large scale three-dimensional network.

Significant loss of tracer mass is indicated by the recovery data from the Hampshire and Berkshire tracer tests: tracer recoveries were 70 % (Atkinson and Smith, 1974) and 25 % and 21 % (Maurice et al., 2006) respectively. The breakthrough curves displayed a steep falling limb after the main peak, followed by a long flat tail of low concentration. Such a pattern is indicative of exchange between mobile water and immobile water by the mechanism of double porosity diffusion (Section 2.9.4), but the rapid travel time implies that for a single conduit or fissure, tracer transport would be too rapid for double porosity diffusion to account for the tracer loss. Maurice et al. (2006) invokes a complex flowpath, with sections of the flowpath characterised by multiple pathways with dispersion from the main conduit into smaller fissures and fractures, as a possible explanation for the loss of tracer.

The tracer test from soakaways at Bricket Wood in Hertfordshire (Price et al., 1992) showed very low tracer recoveries of $<$0.01 % which the authors propose reflect a significant fraction of the flow occurring in fractures and fissures with relatively small apertures, allowing attenuation of the tracer by diffusion into the Chalk matrix.

2.8 Groundwater Flow in the Chalk

Conventional groundwater hydrogeology usually considers aquifers to be porous, granular media.

The quantity of water flowing through a granular medium is proportional to the hydraulic gradient, a relationship expressed in what is termed Darcy's Law:

$$q = -K\frac{dh}{dl} \tag{2.3}$$

where q is the flow per unit cross-sectional area of aquifer (the *specific discharge*), and K is the hydraulic conductivity. Darcy's Law is only valid if flow is laminar. Under laminar flow conditions individual 'particles' of water move in parallel paths in the direction of flow, with no mixing or transverse component to their motion. As flow velocity increases, fluctuating eddies develop and transverse mixing occurs, and the flow is termed turbulent.

The Reynold's number, R_e, identifies the critical velocity above which laminar flow gives way to turbulent flow, and is expressed as:

$$R_e = \frac{\rho\nu d}{\mu} \tag{2.4}$$

where ν is the mean velocity of a fluid with density ρ and dynamic viscosity μ passing through a pipe of diameter d. In a porous or fissured medium, d becomes a representative length dimension characterising interstitial pore-space diameter or fissure width (Ford and Williams, 2007). Laminar flow generally occurs for R_e<2300.

For flow in pipes, under laminar conditions, specific discharge can be evaluated by what is termed Poiseuille's law:

$$q = \frac{\pi d^4 \rho g}{128\mu} \cdot \frac{dh}{dl} \tag{2.5}$$

Increasing velocity, sinuosity and roughness may eventually result in flow through the tube becoming turbulent. For turbulent flow, the specific discharge can be calculated by the Darcy-Weisbach equation:

$$q^2 = \frac{2dg}{f} \cdot \frac{dh}{dl} \tag{2.6}$$

where f is a friction factor.

Turbulent flow conditions frequently arise in pipes and fissures in karst (Ford and Williams, 2007). In karst, the range of conditions under which Darcy's Law can be considered valid is very restricted: it only applies in conditions that permit velocities to be low, and this usually involves some combination of relatively small aperture and low hydraulic gradient (Ford and Williams, 2007).

For the range of karstic flow velocities observed in the Hertfordshire tracer tests (0.022–0.068 $\mathrm{m\ s^{-1}}$), turbulent flows (where R_e >2300) would occur above a conduit diameter of 0.04–0.13 m (Cook, 2010). Therefore, the majority of karst flows within the Hertfordshire karst conduits are expected to be turbulent.

2.9 Solute transport in the saturated zone of the Chalk

In a multiple-porosity aquifer such as the Chalk, solute transport is dominated by two processes: advection in fissures and diffusional exchange of solutes between fissures and matrix porewater. Adsorption may also affect the transport of some solutes. At larger scales, the effects of dispersion across the network of fissures may become important.

2.9.1 Advection

Advection is the term used to describe movement attributed to transport by the flowing groundwater: advecting solutes travel at the same rate as the average linear velocity of the groundwater.

The groundwater velocity, v, is given by the volumetric flux, q, divided by the kinematic porosity, n_e:

$$v = \frac{q}{n_e}$$

The volumetric flux, q, can be determined from Darcy's law (equation 2.3).

2.9.2 Adsorption

Solutes can be attenuated relative to advective transport by the process of adsorption. Most of the surface area of chalk onto which adsorption can take place is within the rock matrix. Mineral or organic deposits are quite often observed on the surfaces of fissures, and when present, must have a significant

impact on the amount of adsorption taking place, by providing adsorption sites and acting as a barrier for diffusion into the matrix (Barker, 1993). Some models include a *fracture skin* to take some account of the phenomenon.

2.9.3 Dispersion

Dispersion refers to the process of spreading (of solutes, particles or heat) during transportation. Matrix diffusion and adsorption both have dispersive effects. The term *mechanical dispersion* refers more specifically to the spreading caused by variations in groundwater flow velocity. Dispersion arises because of the detailed variations in flow velocity in pores and fractures mainly due to the complex splitting and joining of paths but also due to flow velocity variations in single paths. Strictly speaking, mechanical dispersion is not a process in its own right; it is rather an expression of the fine (often random) detail of the advection process. Therefore, if advective transport could be fully characterised throughout the system, there would be no additional dispersion phenomenon to consider. Dispersion must therefore be related to the advective model (conceptual or mathematical) in use, particularly to its scale of averaging (Ward et al., 1998).

The normal approach to describing transport in a dispersive medium is via the convection-dispersion equation (Equation 2.7 for flow in one-dimension), which contains a characteristic dispersion coefficient, D.

$$\frac{\partial C}{\partial t} = D\frac{\partial^2 C}{\partial x^2} - v\frac{\partial C}{\partial x} \tag{2.7}$$

The dispersion coefficient is normally considered to increase in proportion to the absolute value of the velocity, v, so $D = \alpha v$ where α is known as the *dispersivity*. Dispersion is sometimes separated into *longitudinal* and *transverse* dispersion to refer, respectively, to dispersion in the direction of flow and dispersion perpendicular to that direction. Transverse dispersivity is typically much less than longitudinal dispersivity. Dispersion coefficients for single fractures are more likely to show proportionality to the square of velocity rather than to the velocity (Ward et al., 1998).

In practice, the processes of molecular diffusion and mechanical dispersivity cannot be separated in flowing groundwater. Instead, a factor termed the coefficient of hydrodynamic dispersion is introduced which takes into account both mechanical mixing and diffusion:

$$D = \alpha v + D*$$

where D is the coefficient of hydrodynamic dispersion, $D*$ the effective molecular diffusion coefficient. An analytical solution to Equation 2.7 was provided by Ogata and Banks (1961).

Dispersion in individual fissures is likely to be small and dependent on the fissure aperture, roughness *etc.*, and at a larger scale dispersion depends on the interconnecivity of fractures (Grisak and Pickens, 1980, 1981). Barker (1993) demonstrated that dispersion, although not negligible, can normally be ignored, in relation to matrix diffusion, when modelling solute transport in the Chalk.

2.9.4 Diffusion

Molecular diffusion represents the net movement of solute under a concentration gradient and can be described by Fick's first and second laws. Molecular diffusion of contaminants is not normally of practical consideration where advection and mechanical dispersion are dominant. However, within the water in the chalk matrix, which is (effectively) immobile, transport of solutes can take place by molecular diffusion. For any diffusive process, a characteristic time for diffusion over a distance x can be defined as $\frac{x^2}{D}$, where D is the diffusivity (Diffusion coefficient divided by porosity) (Barker, 1993).

For the double-porosity Chalk, and other comparable fractured porous media, Foster (1975) proposed that a major component of solute movement was controlled by a mechanism involving solute exchange, through lateral molecular diffusion, between mobile fissure water and (relatively) immobile matrix water. This double-porosity diffusive exchange has been demonstrated to be of significance to the interpretation of thermonuclear tritium and pollutants, such as nitrate, in the unsaturated zone of the Chalk (Foster, 1975; Barker and Foster, 1981) and when predicting the rate of lateral migration of pollutants in the saturated zone of the aquifer (Watson, 2004; Burgess et al., 2005).

Double-porosity diffusive exchange acts to attenuate contaminants and significantly prolongs the duration of contamination (Figure 2.5). Considering an initially contaminated fracture water, and uncontaminated matrix water, there will be a diffusive flux of the dissolved contaminant from the fracture water into the matrix water. The movement of the contaminant down hydraulic gradient will therefore be retarded compared to transport by advection. At a later stage, when the primary source of contamination input to the fracture water has ceased, there will be a diffusive flux from the now contaminated matrix water to the fracture water. The matrix water therefore acts as a secondary source of contaminant input, which prolongs the duration of contamination detected down-gradient.

2.9.4.1 Diffusion Coefficients

Fick's first law can be expressed as:

$$J_m = -D_E \frac{\partial c}{\partial x} \tag{2.8}$$

where J_m is the mass flux (per unit area of water and rock) in the x direction in saturated rock, D_E is the *effective* diffusion coefficient, c is the mass per unit volume of water (not matrix and water), and t is time.

Fick's second law can be expressed as:

$$\frac{\partial c}{\partial t} = D_A \frac{\partial^2 c}{\partial x^2} \tag{2.9}$$

where D_A is the *apparent* diffusion coefficient.

The two diffusion coefficients are related through:

$$D_E = \phi_D D_A \tag{2.10}$$

where ϕ_D is the 'diffusion porosity' or 'fictitious porosity' (Section 2.12.2).

Oakes (1977) measured the effective diffusion coefficient for chloride in Chalk as $1.3 \times 10^{-10}\ \mathrm{m^2\ s^{-1}}$. Hill (1984) measured molecular diffusion coefficients of nitrate, chloride, sulphate and water (labelled

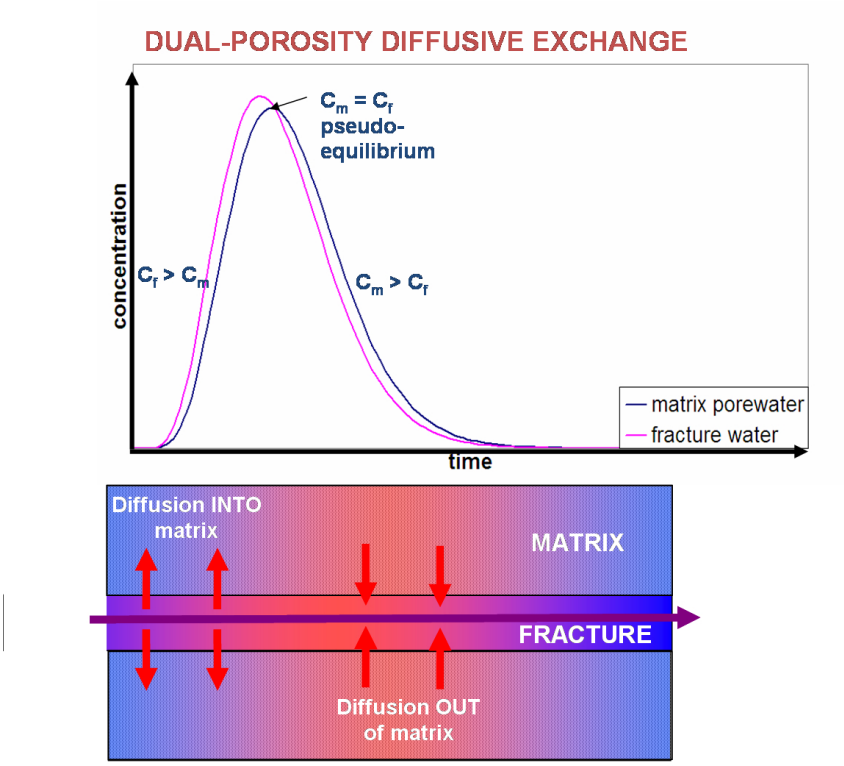

Figure 2.5: Double-porosity diffusive exchange of solutes. At an early stage, diffusion from the contaminated fracture water into the matrix water acts to retard the transport of contaminants down-gradient. At a later stage, contaminated porewater acts as a persistent secondary source of contamination.

using tritium) in samples of both fissured and unfissured chalk (Table 2.1). These values represent the mass flux through the saturated matrix per unit concentration gradient in the water. Hill's values are appropriate for use in Fick's first law of diffusion. In a critical discussion of Hill's results, Muller (1987 deduced that the ratio of the diffusion coefficient to the free water diffusion coefficients is about 0.25. So the diffusion coefficient in chalk can be estimated as one quarter of the free water value, if this value is known for a solute.

Table 2.1: Molecular diffusion coefficients in fissured and unfissured chalk. After Hill (1984). These values represent the mass flux through the saturated matrix per unit concentration gradient in the water.

solute	Diffusion coefficient range	$(\mathrm{m}^2\ \mathrm{s}^{-1})$
sulphate	0.28×10^{-10}	1.47×10^{-10}
nitrate	0.53×10^{-10}	3.2×10^{-10}
chloride	0.52×10^{-10}	3.23×10^{-10}
tritiated water	0.6×10^{-10}	3.51×10^{-10}

No values of diffusion coefficients for bromate or bromide have been reported in the literature. In the absence of a specific value for bromide and bromate, it seems reasonable to expect the bromide and bromate ions to behave similarly to chloride and nitrate ions.

2.10 Flow and transport in the unsaturated zone of the Chalk

A consequence of the small pore throat sizes of the Chalk matrix (Section 2.6) is that, even in the *unsaturated* zone, the intergrannular pore space will be almost fully saturated (Foster, 1975; Price, 1987). Thus the unsaturated matrix conductivity is very close to the saturated hydraulic conductivity. Within the literature, there has been much debate as to the significance of fissure flow versus intergranular matrix) flow in the unsaturated zone of the Chalk. The early consensus was that flow in the unsaturated zone of the Chalk was entirely through the fissure network, supported by observations of rapid response of the water table after high intensity rainfall events (Headworth, 1972). However, unsaturated zone porewater tritium profiles from the Berkshire Chalk (Smith et al., 1970) indicated distinct tritium peaks, believed to be associated with the high tritium levels found in rainfall during the periods 1963-1964 and 1958-1959, at depths of 4 m and 7-9 m respectively. Smith et al. (1970) suggested that these profiles indicated that 85 % of the total flow through the unsaturated zone was by intergranular seepage through the matrix at a mean rate of 0.88 m/yr , with some 'bypass flow' through fissures occurring to explain the presence of tritium at depth. A 'piston displacement' mechanism , whereby recharge at the top of the column of matrix displaces water at the bottom of the unsaturated zone , releasing it to the water table, was invoked to explain the rapid water table response to rainfall (Price et al., 1993). Foster (1975) noted that Chalk outcrop areas are characterised by an almost complete absence of surface runoff, which is incompatible with UK rainfall rates of up to 100 $\mathrm{mm\ d}^{-1}$, an order of magnitude greater than the unsaturated zone Chalk matrix hydraulic conductivity (Section 2.7.3.1), unless substantial fracture flow occurs to transport the excess during these rainfall events. Foster (1975) proposed a mechanism by which fracture-dominated

flow could be reconciled with a much slower observed downward movement of tritium: fissures within the Chalk would focus tritium input to the unsaturated zone and the concentration gradient between the contaminated fracture water and the matrix water would cause lateral diffusion of the solute into the matrix (*i.e.* double-porosity diffusive exchange discussed in Section 2.9.4), greatly retarding its downward movement. Simulations using a double porosity diffusion exchange model (Barker and Foster, 1981) indicated that this mechanism lead to preservation of the tritium profile in the unsaturated zone with only minor dispersion. However, Mathias et al. (2005) showed that double porosity models which assume matrix flow to be negligible (*e.g.* Barker and Foster 1981), require an unrealistically small fracture spacing (<25 cm) to preserve peaks without 'solute spreading' through the profile. Mathias et al. (2005) analysed the impact of flow in the matrix by comparing a double porosity model (based on Barker 1982) with an equivalent double-permeability model with a portion of flow in the matrix and demonstrated that solute spreading in such models can only be reduced (whilst using sensible estimates of fracture spacing and diffusion coefficients) by allowing for a portion of flow in the matrix. Thus, Mathias et al. (2005) argues that flow in the matrix of the Chalk of the unsaturated zone is significant.

However, Mathias et al. (2005) was not able to obtain a sensible estimate for the proportion of total infiltration that enters the matrix as the model assumed steady-state flow conditions necessitating the use of annual mean estimates of infiltration. The assumption of steady-state flow also forces fracture flow to be either negligible or persistent whereas in reality it is likely to be intermittent (Price et al., 2000). Subsequently, Mathias et al. (2006) developed a transient one-dimensional double permeability model for the unsaturated zone of the Chalk. This model indicated that infiltration (as calculated by simple two-store models) needs to be significantly attenuated to ensure that enough flow occurs in the matrix such that solute spreading is reduced to a reasonable level. The justification for the attenuation was the existence of soil and gravelly chalk layers. Mathias et al. (2006) demonstrated that such a model was compatible with a fast water table response: there was a time lag of only three days between effective precipitation input and water table flux.

2.11 Modelling flow and transport in fissured rocks

The Chalk is a fissured rock, and the interconnected fissures provide routes for water flow with the intervening blocks of rock essentially impermeable. Domenico and Schwartz (1998) suggested that at the scale of the field problem one of two approaches might be followed when trying to represent the flow of water in fissured and/or karstified rocks:

1. the *continuum* approach, which assumes that the fractures mass is hydraulically equivalent to a porous, granular medium, *i.e.* an equivalent porous medium (EPM) model; and

2. the *discontinuum* or *discrete* approach, which assumes that the rock cannot be characterised as a granular medium, and so considers that flow is best dealt with in individual fractures or fracture sets.

The appropriate model to simulate transport of water and/or solutes within fissured systems such as the Chalk depends on a consideration of how the behaviour of a fissured system is related to the time-

scales of the transport processes. For double-porosity systems, with advective transport in the fissures and diffusive transport in the matrix, the suitable model representation depends on the time-scale of the process under consideration in relation to the characteristic times for diffusion across a fissure or a matrix block (Barker, 1993).

2.11.1 Equivalent Porous Medium (EPM) models

An EPM model is a homogeneous model with parameters chosen to be characteristic of the fissured rock. Barker (1993) considers that an EPM model might be suitable under two regimes of double-porosity behaviour:

1. **When the fissures act independently of the matrix.** If the time-scale of interest is small with respect to the characteristic time for diffusion across the fissure width, then the effects of the porous matrix can be ignored (because of both the restricted diffusion out of the fissure and of the small volume of matrix accessed, in relation to fissure volume). Under these conditions (which rarely exist outside a laboratory), the chalk can be modelled with an EPM model with a porosity equal to the fissure porosity.

2. **When the fissures and matrix act in unison.** If the time taken for diffusive equilibrium between fissures and matrix is small in relation to the time for any significant change in the fissure system, then the chalk will behave as a (locally) homogeneous medium characterised by the total porosity. A *Quasi-steady-state (QSS) double-porosity model* might also be adequate (Section 2.11.2.2).

EPM models are commonly used for regional water resources models, where the fissured system is represented as homogeneous, with storage and permeability parameters characteristic of the matrix and fractures combined.

2.11.2 Double-porosity (DP) models

DP models comprise two overlapping continuous media (the fracture and matrix phases) coupled by an exchange mechanism. Such DP models can be divided into *diffusive type* and *quasi-steady-state (QSS) type* models depending on the physical and mathematical description of the exchange mechanism:

2.11.2.1 Diffusive type

Diffusive-type models are those for which the transport in the matrix blocks can be described by a flux law (*i.e* Darcy's, Fourier's or Fick's Laws for water, heat and solute transport respectively). The potential (head, temperature, or concentration) within a matrix block is controlled by the variations within the fissure system, and the two potentials are normally assumed equal at the surfaces of the matrix blocks (Barker, 1993). The shapes of the matrix blocks affect the behaviour (Barker, 1985a,b).

Diffusive-type double-porosity models, simplified by assuming an infinite matrix, are appropriate if the time-scale of interest is a small fraction of the time for diffusion across a matrix block. Under these conditions only the matrix/fissure surface area per unit volume of the rock is important, not the block size or shape. If the time-scale is similar to the time for diffusion across a matrix block, then the sixes of the matrix blocks become important, and the assumption of an infinite matrix is not valid. Under these

conditions, Barker (1993) considers that a general diffusive-type DP model should be used, (although a QSS-type DP model may be adequate over some periods).

2.11.2.2 Quasi-steady-state (QSS) type

In QSS models, the matrix is characterised by a single potential (*e.g.* concentration) and the diffusive flux between the matrix and the fissures is taken to be proportional to the difference between their (local) potentials. QSS type models are only valid alternatives to the diffusive-type model if the time for any significant change in the fissure system is slow in relation to the time for diffusive equilibrium across a matrix block. Under these conditions the chalk will behave as a (locally) homogeneous medium characterised by the total porosity (an EPM mode might also be suitable under these conditions).

2.11.2.3 Importance of matrix diffusion for water and solute transport in the Chalk

Characteristic times for hydraulic diffusion in the chalk matrix are around 5–500 *seconds* and for solute diffusion in the chalk matrix are 50–500 *years* (Barker, 1993). Therefore, for water transport, matrix diffusion will only be significant for very rapidly changing conditions, and it is reasonable to adopt a QSS model for all but the most rapid transient pumping tests. In contrast, matrix diffusion will have an important effect on solute transport over most time-scales of interest for contamination incidents, and diffusive-type double-porosity models should be adopted.

2.11.3 Double-permeability Models

In contrast to double-porosity models, the advective velocity in the matrix, although much less than in the fissures, is not regarded as negligible in double-permeability models. Barker (1993) considers double-permeability concepts to be more applicable to the interaction between the primary and secondary fissure systems in the Chalk than to the interaction between matrix and fissures, for which the permeability contrast is much larger.

2.11.4 Network Models

Network models have been used for the study of groundwater in 'hard rocks', generally in relation to radioactive waste disposal. Hard-rock systems generally have little intrinsic porosity, although they do often contain a dense network of micro-fissures concentrated near the fractures which can impart a double-porosity character. Barker (1993) considers that such models are valuable when considering flow in the Chalk under karstic conditions, when matrix porosity may not be significant.

2.12 Diffusion exchange model for solute transport in fissured porous rocks

In a series of papers, Barker (1982, 1985a,b) developed a general model of flow and transport in double-porosity media. Barker (1982) considered a simple 'slab geometry' model, with parallel fissures separated by finite slabs of matrix material (Figure 2.6). Fissured rocks have been represented in this way by others *e.g.* Grisak and Pickens (1980). Because of the periodicity of the model only a single, semi-infinite unit extending from the centre of a matrix slab to the centre of a neighbouring fissure need be considered. The solution of the transport equations was developed as as far as Laplace transforms of the

solute concentrations in the fissure and matrix water. Numerical inversion of the transforms was then used to investigate characteristic behaviour of the model for a number of special cases.

2.12.1 Block geometry

Barker (1985a) developed a Block Geometry Function (BGF) which characterises block shape based on the diffusion equation. For simple geometries, such as the sphere, this function is quite simple. For any well defined geometry, even mixtures of blocks of different shapes and sizes, this function can be determined.

2.12.1.1 Block sizes

Barker (1985b) characterises the size of a block by the parameter, in this thesis referred to as ℓ, which represents the volume to surface area ratio. More precisely, ℓ is the root-mean-square distance of diffusion[6] in time $\frac{\ell^2}{2D_A}$. For an infinite slab geometry, with slabs of thickness $2b$, $\ell = b$; for a spherical geometry with blocks of radius r, $\ell = \frac{r}{3}$.

2.12.2 Porosity Ratio

Barker (1985a) defines a parameter, σ, which represents the ratio of the matrix and fracture porosities, and which equals the porosity of the matrix void volume per unit volume of rock matrix divided by the fracture void volume per unit volume of total space within the rock. So the total porosity (matrix plus fractures) is 1+ σ times the fracture porosity. More precisely, sigma is the ratio of the matrix volume to fracture volume in a given total volume, times the ratio of D_E and D_A (diffusion coefficients defined in Section 2.9.4.1) which is the 'fictitious' porosity.

The porosity ratio is also related to the diffusion porosity ϕ_D, for example for a simple slab model:

$$\sigma = \frac{2b\phi_D}{a} \tag{2.11}$$

The diffusion porosity is defined as $\phi_D = \frac{D_E}{D_A}$, which is the ratio of the 'apparent diffusion coefficient', D_A, (as appears in Fick's second law) and the 'effective diffusion coefficient', D_E, (as appears in Fick's first law). This porosity has been referred to in the literature as a fictitious porosity and can be somewhat less than the total porosity (Barker et al., 2000).

2.12.3 Characteristic Times

Characteristic times for the simple slab model are given in Table 2.2.

2.12.3.1 Fracture advection time

The fracture advection time is normally determined from the hydraulic gradient, (bulk) hydraulic conductivity and kinematic porosity.

[6] In molecular diffusion, the mean-square distance traversed by a particle in time t is given by $2Dt$, where D is the diffusion coefficient.

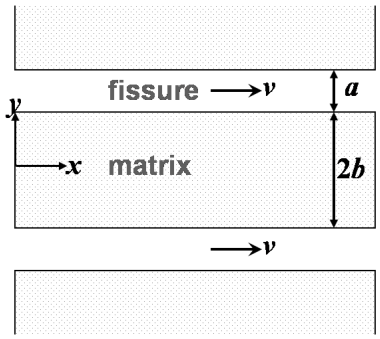

Assumptions:

- Identical slabs of matrix material separated by equally spaced planar fissures;
- The matrix is homogeneous and saturated with immobile water;
- Solute transfer between fissures and matrix and within the matrix occurs by molecular diffusion in the immobile water in a direction perpendicular to the plane of the fissures;
- There is no concentration gradient across the fissures;
- The flow velocity in the fissures is uniform;
- Longitudinal dispersion in the fissures is characterised by a constant dispersion coefficient;
- The solute concentration in water entering the system is a known function of time;
- Initially, the concentrations in the fissure and matrix water are known functions of distance in the flow direction.
- The solute is non-reactive and does not decay.

Let $f(X,T)$ be the solute concentration in the fissure water

and $c(X,Y,T)$ the concentration in the matrix water at time T

By consideration of conservation of mass in a fissure, the movement of solute in a fissure is described by:

$$\frac{\partial f}{\partial T} + V\frac{\partial f}{\partial X} - D_L\frac{\partial^2 f}{\partial X^2} + \frac{D\varphi}{b}\left(\frac{\partial c}{\partial Y}\right)_{Y=a} = 0 \qquad \text{Equation (1)}$$

V is the water flow velocity in the fissure,
D_L is the longitudinal dispersion coefficient in the fissure,
D is the molelcular diffusion coefiicient in the matrix,
φ is the matrix porosity.

By consideration of conservation of mass in the matrix, solute movement in the matrix is described by:

$$\frac{\partial c}{\partial T} - D\frac{\partial^2 c}{\partial Y^2} = 0 \qquad \text{Equation (2)}$$

As a result of symmetry of the model there will be no net movement of solute across a matrix slab, so:

$$\frac{\partial c}{\partial Y} = 0 \quad \text{at } Y = 0 \qquad \text{Equation (3)}$$

The concentrations of matrix and fissure water will be the same at the interface:

$$c(X,a,T) = f(X,T) \qquad \text{Equation (4)}$$

The input of the concentrations in the fissure is a known function, f_0 say:

$$f(0,T) = f_0(T) \qquad \text{Equation (5)}$$

The initial concentration distribution is a known function, $g(X)$say, of distance in the flow direction:

$$c(X,Y,0) = f(X,0) = g(X) \qquad \text{Equation (6)}$$

Figure 2.6: Governing equations and assumptions for a double-porosity mocel with slab geometry. After Barker (1982).

2.12.3.2 Block diffusion time

Barker (1985b) defines a characteristic time for diffusion across a matrix block, in this thesis referred to as t_{cb}, which is a related to the block size (via the parameter ℓ) and apparent diffusion coefficient D_A by:

$$t_{cb} = \frac{\ell^2}{D_A} \tag{2.12}$$

2.12.3.3 Fracture diffusion time

The behaviour of a double-porosity system can be fully described by σ, t_{cb}, ℓ and the BGF. However, Barker et al. (2000) introduces a further parameter which can be more characteristic of certain behaviour. This is the characteristic time for diffusive equilibrium between fractures and matrix, in this thesis referred to as t_{cf}, which is a defined as:

$$t_{cf} = \frac{t_{cb}}{\sigma^2} \tag{2.13}$$

The time t_{cf} can be thought of as the time for diffusion through a matrix volume equal to the fracture volume. This parameter tends to be important when the interaction time between the fracture water and the matrix water are less that the time for diffusion across a matrix block. Under those conditions the fracture water concentration is determined mainly by the surface available for diffusion in relation to the fracture size. The block size and geometry become unimportant.

2.12.3.4 Relative times

The relative values of the three times (t_{cb}, t_{cf} and t_a) can provide valuable insights into the behaviour of a double-porosity system. When times are much less than t_{cb}, then the only effective parameter is t_{cf}; physically this represents conditions where fracture water concentration is determined mainly by the surface area available for diffusion in relation to the fracture size.

Table 2.2: Characteristic times for infinite slab geometry, with slabs of thickness $2b$ separated by fractures of aperture a. For this model, the ratio of volume to area for a matrix block (ℓ) is represented by b.

t_a	$= \frac{x}{v}$	Advection time in mobile phase
t_{cb}	$= \frac{b^2}{D_{im}}$	Characteristic time for diffusion across a matrix block
t_{cf}	$= \frac{t_{cb}}{\sigma^2}$	Characteristic time for diffusion from a fracture into an equal volume of matrix water
σ	$= \frac{\theta_{im}}{\theta_m}$	The ratio of matrix to fracture porosity

2.13 Summary

The behaviour of the Chalk as an aquifer is complex, and results from a combination of porosity and permeability components that are a consequence of the Chalk lithology, tectonic history and weathering and erosional processes. The Chalk is composed of very fine grained calcium carbonate micro-fossil fragments which form a a highly porous, yet essentially impermeable, matrix. More than 95 % of water in the Chalk is held in the interstices of the rock matrix, but the pore spaces are so small that this water is effectively immobile. The mobile water (the remaining 5 % or less) is held within the

fractures that transect the chalk matrix. Some fractures have been enlarged by dissolution to become fissures or even karstic conduits. The fissures and conduits provide the permeable pathways for flow. Within the unsaturated zone of the Chalk, although the dominant flow pathways are via the fissures, a small but significinat portion of flow is thought to occur within the matrix (Mathias et al., 2005, 2006). These multiple components of porosity and permeability within the Chalk have long been recognised, and it has been described as a double-porosity (dual-porosity) aquifer (Foster, 1975; Price, 1987; Barker, 1991; Price et al., 1993), a double-permeability (dual-permeability) aquifer (Price et al., 1993), and a triple-porosity and/or triple-permeability aquifer (Worthington, 2003; White, 2003).

The Chalk is increasingly recognised as possessing karstic characteristics. In the Hertfordshire Chalk, there is abundant evidence of the existence of rapid preferential flow routes within the Chalk. Swallow holes and other dissolution features tend to be located close to boundary between the Chalk and Eocene cover, and are particularly concentrated in the Water End area. Tracer tests have shown that rapid groundwater flow occurs between swallow holes and stream sinks in the Water End area and springs and boreholes in the Lea Valley, which is indicative of a dispersive system of karstic conduits.

In a multiple-porosity aquifer such as the Chalk, solute transport is dominated by two processes: advection in fissures and diffusional exchange of solutes between fissures and matrix porewater. Adsorption may also affect the transport of some solutes. At larger scales, the effects of dispersion across the network of fissures may become important.

Double-porosity diffusive exchange of of solutes between fissures and matrix porewater acts to attenuate contaminants and significantly prolongs the duration of contamination. Considering an initially contaminated fracture water, and uncontaminated matrix water, there will be a diffusive flux of the dissolved contaminant from the fracture water into the matrix water. The movement of the contaminant down hydraulic gradient will therefore be retarded compared to transport by advection. At a later stage, when the primary source of contamination input to the fracture water has ceased, there will be a diffusive flux from the now contaminated matrix water to the fracture water. The matrix water therefore acts as a secondary source of contaminant input, which prolongs the duration of contamination detected down-gradient. Double-porosity diffusion between mobile fissure water and immobile matrix water can be described mathematically using Fick's Laws of diffusion (*e.g.* Barker and Foster, 1981; Barker, 1982, 1985b), and has been demonstrated to be of significance when predicting the rate of lateral migration of pollutants in the saturated zone of the aquifer (Watson, 2004; Burgess et al., 2005).

Chapter 3

A conceptual model for flow and transport of bromate in the Hertfordshire Chalk

3.1 Chapter Objective

The objective of this chapter is to develop a conceptual model for groundwater flow and contaminant transport in the Hertfordshire Chalk aquifer system by review of existing data, interpretation of additional tracer testing, and statistical analysis of the effects of scavenge pumping at Hatfield on bromate occurrence.

3.2 Geology and Hydrogeology of Hertfordshire

3.2.1 Topography

The study area is located in Hertfordshire, south-east England, and covers an area of approximately 600 km^2 bounded by eastings TL511000 and TL540000 and by northings TL200000 and TL219000 (Figure 3.1).

The highest elevations (+150 m OD) are found on the dip slope of the Chiltern Hills in the north-west of the study area. The land slopes gently to the southeast towards the relatively flat lying Vale of St Albans (elevations +60 to +75 m OD), which forms a broad valley trending northeast-southwest between Colney Street and Hertford. To the east of Hatfield, the Vale of St Albans joins the Middle Lee Valley (elevations +60 to +65 m OD). The land rises to the south-east of the Vale of St Albans to elevations of approximately +100 m OD) over the Palaeogene escarpment (Tertiary Escapement), before falling to the east and south-east towards the Lee Valley (elevations less than +50 m OD).

Superimposed on this overall topographic pattern are smaller river valleys. River Valleys (both dry and flowing valleys) tend to be deep, incised valleys, which extend far up the dip slope. There are a number of dry valleys in the Chalk uplands of the Chiltern Hills, including two dry valleys which converge at Sandridge.

3.2.2 Hydrology

River flows, rainfall and potential evapotranspiration data are reviewed and analysed in Buckle (2002) and Atkins (2004). Much of the data were collated in work by Entec (2000) in connection with the Upper

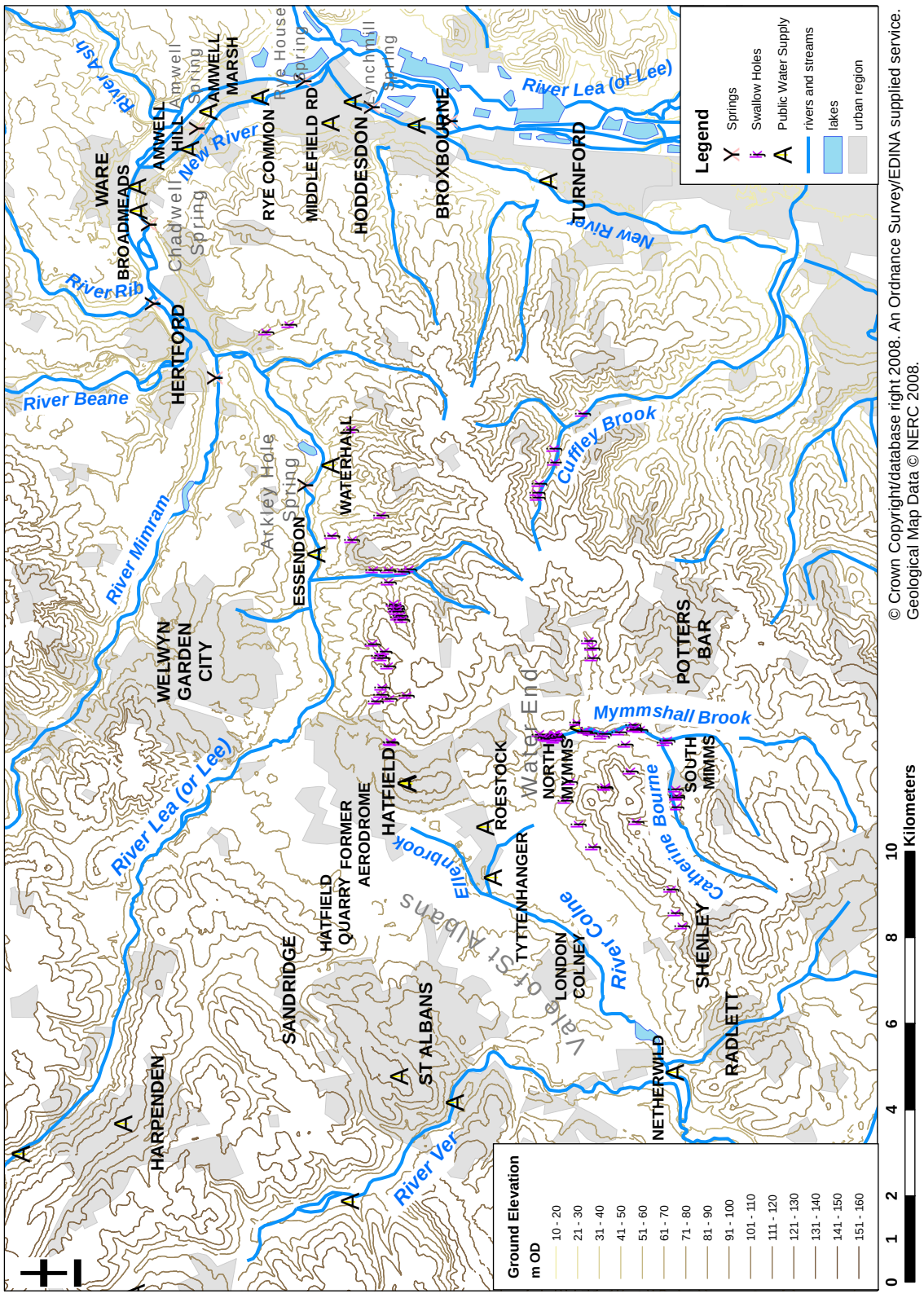

Figure 3.1: Location of study area, including topography and hydrology

Mimram study, and along with additional data available from the Environment Agency.

In the east of the area, the upper River Lea and the River Ver flow south-east from the Chiltern Hills. The surface water divide between the Lee and the Ver catchments is not well defined in terms of topography, but it runs approximately south-east through Harpenden and Hatfield and also forms the surface water divide between the catchments of the River Lee and the River Colne (Figure 3.1). The River Colne flows southwest along the foot of the Palaeogene escarpment in the Vale of St Albans to join the River Ver in the south-west of the study area. Significant groundwater–surface water interactions occur in both the River Lee and River Colne catchments (Section 3.2.7).

The middle River Lee flows east through the central part of the study area along the northern foot of the Palaeogene escarpment. Downstream of Hatfield, the Lee swings north-east and is joined near Hertford by the Rivers Mimram, Beane and Rib flowing from the Chalk upland to the north, and further downstream by the Rivers Ash and Stort. The River Lee then swings to flow south towards the River Thames. Along this southerly flowing section, the middle and lower Lee is joined by a number of rivers draining the Palaeogene escarpment. South of Hertford, the New River (an aqueduct constructed in the 17^{th} Century) runs to the west of, and parallel to, the River Lea. The New River is fed from the River Lee upstream of Ware and also accepts discharge from the Chadwell Spring when the spring is flowing. The New River also takes pumped discharge from pumping stations of the Northern New River well field.

In the west of the study area, the Catherine Bourne and the Mimmshall Brook drain to the River Colne from the west of the Palaeogene escarpment. For most of the year, the Mimmshall Brook and Catherine Bourne drain to a series of stream sinks and swallow holes near Water End. At times of overflow, a spillway carries water north-west to the River Colne.

3.2.3 Geology

3.2.3.1 Regional geological context

The solid and drift geology of the study area is summarised in Figure 3.2 and Figure 3.3.

The study area lies on the north-western margin of the Thames Basin. The Chalk outcrops in the north-west on the study area, where it forms part of the dip slope of the Chiltern Hills. The Chalk dips gently (at $<$1 degree) south-east towards the main axis of London Basin syncline.

To the south and south-east of the area, the Chalk within the London Basin is overlain by Palaeogene Deposits (Reading Beds, the London Clay and the Claygate Beds) which form the Tertiary escarpment. There are Palaeogene outliers on the dip slope of the Chalk near St Albans and Welwyn Garden City.

In the Chiltern Hills, drift deposits overly the Chalk in the valleys (Alluvium and Valley Gravels) and on the higher interfluves (Clay-with-Flints and associated Pebbly Clay and Sand). A band of Boulder Clay and Glacial Gravel overly the Chalk in the Vale of St Albans and the Middle Lee Valley. Pebble Gravel caps the Tertiary strata in places.

3.2.3.2 Lithostratigraphy

The generalised lithostratigraphy of the Hertford district is summarised in Table 3.1.

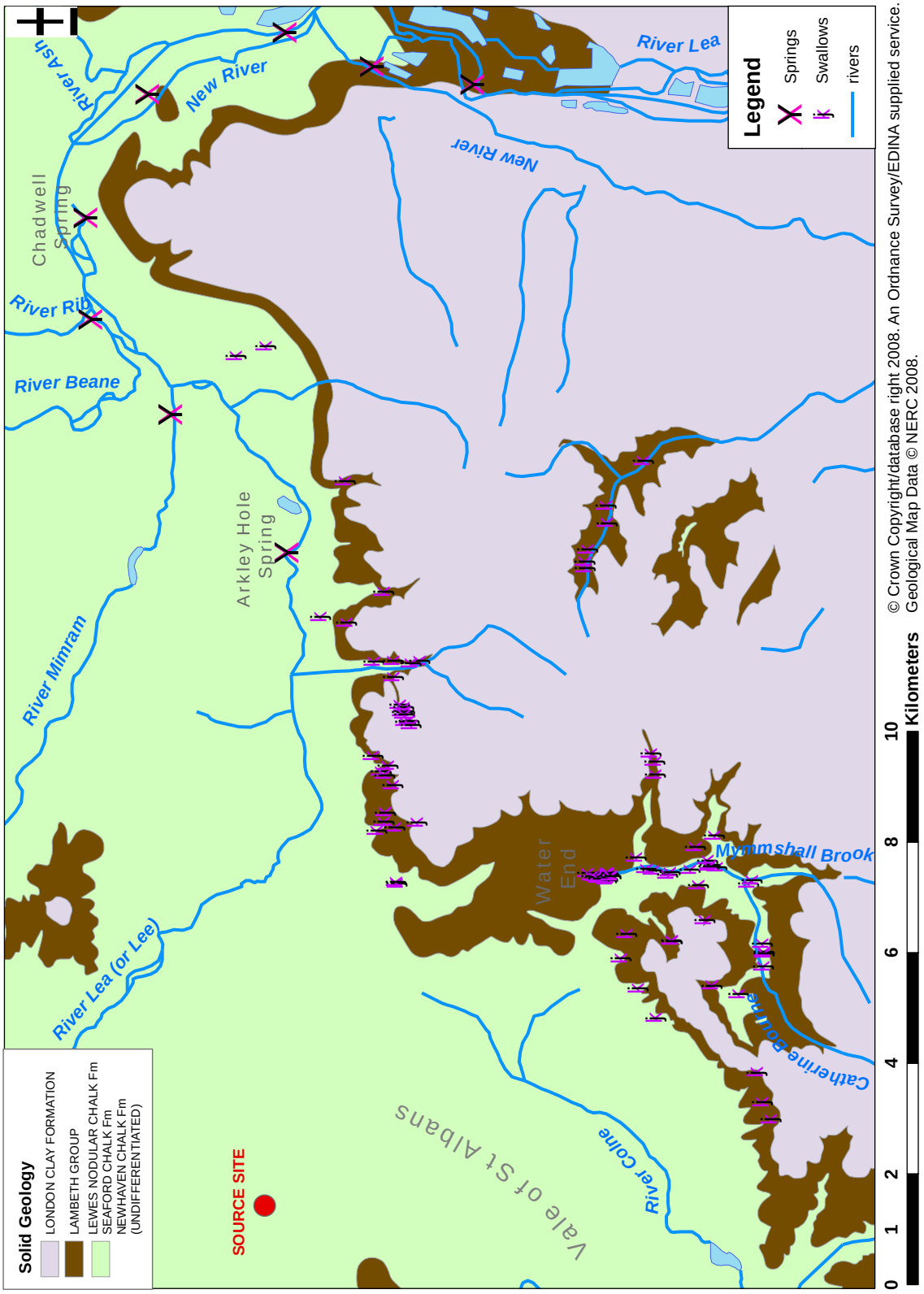

Figure 3.2: Solid Geology of the Study Area

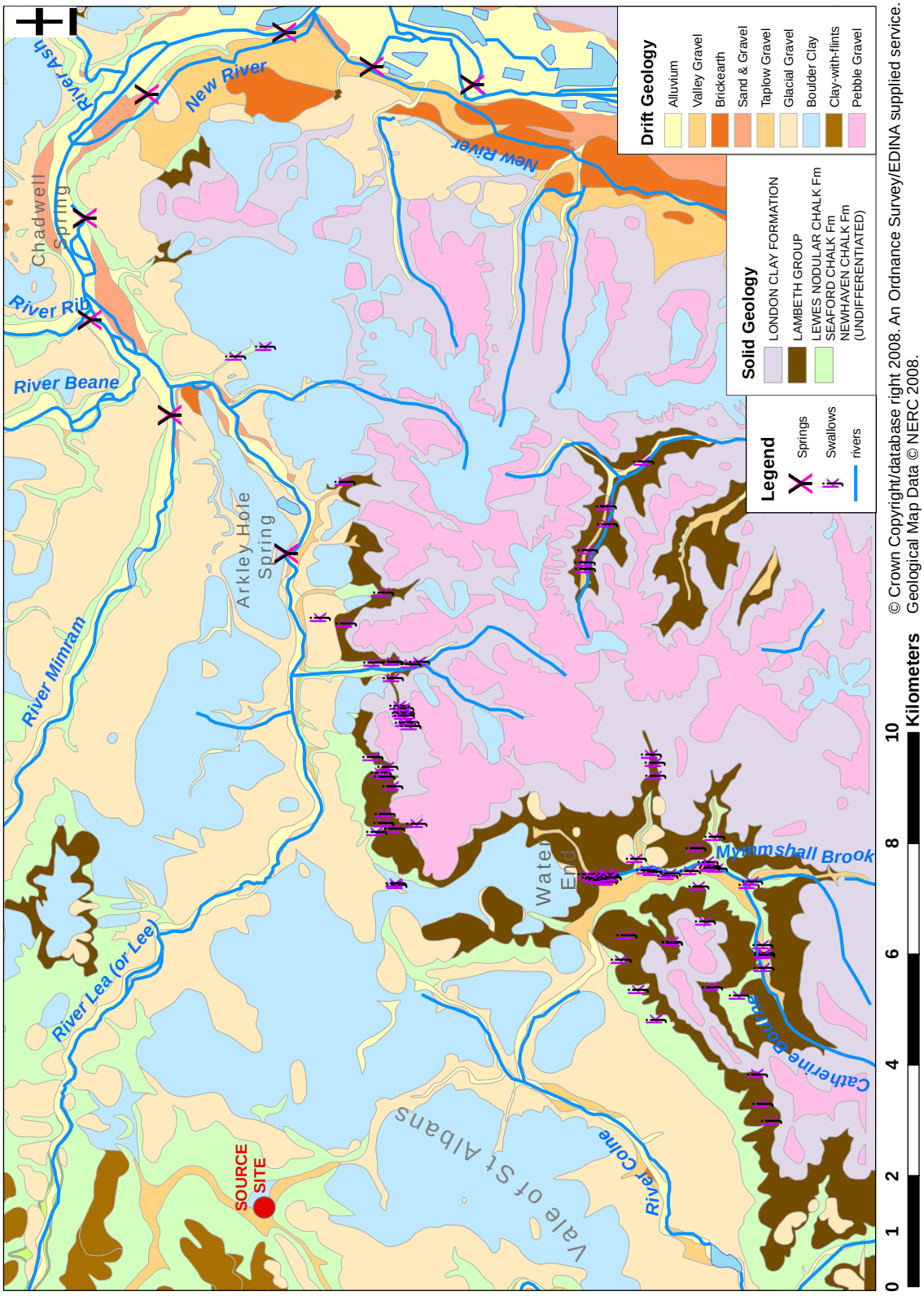

Figure 3.3: Solid and Drift Geology of the Study Area

Table 3.1: Lithostratigraphy of the Hertford district. After Bloomfield et al. (2004).

Period	Epoch	Formation	Lithology	Approx thickness
Quaternary	Recent and Pleistocene	Alluvium	Silty, fine sandy clay	-
		Valley Gravels	Fine to coarse subangular sands and gravels	-
		Brickearth	Silt, clay and fine sand. Often interlaminated	-
		Clay-with-Flints (and Pebbly Clay and Sand)	Brown to reddish brown clay, containing flints and pebbles	< 8m
		Boulder Clay (Upper Glacial Drift & Anglian Till)	Dark blue-grey silty/fine sandy clay with chalk and flint pebbles	< 10m
		Glacial Sand and Gravel (Proto-Thames Gravels)	Generally 'clayey' sandy gravel	< 15m
		Pebble Gravel	Orange-brown 'clayey' gravel	-
Palaeogene	Eocene	Claygate Beds	Glauconitic interbedded sand and loam.	-
		London Clay	Dark grey, silty clay. Stiff clay with some fine sand, dark bluish grey.	< 80m
	Palaeocene	Lower London Tertiaries (including Reading Beds)	Stiff waxy variegated clays overlying clayey fine sands.	< 15m
UNCONFORMITY				
Cretaceous	Upper Cretaceous	Chalk Group Formations (see Chalk lithostratigraphy)		

Table 3.2: Lithostratigraphy of the Chalk of the Hertford district. Based on Woods (2003).

Period	Subgroup	Formation	Characteristic features	Approx thickness
Upper Cretaceous	White Chalk	Newhaven Chalk	May be locally preserved below the Palaeogene cover towards Beaconsfield, although no definite evidence. Soft chalk, with marl and flint horizons.	<5 ?
		Seaford Chalk	Soft, flinty chalk with common marl seams and shell remains in the lower part. Shoreham Marl 2 located at base of this formation. Youngest Chalk at outcrop and subcrop.	50-60
		Lewes Nodular Chalk	A hard, nodular, flinty chalk with common marls and hardgrounds: Top Rock, Chalk Rock and Southerham Marl 1. Exposed extensively at outcrop in the region.	34-40
		New Pit Chalk	Massively bedded, firm, smooth textured Chalk with few flints and regular thin marl horizons. Glynde Marls and New Pit Marl 1 present in this formation. Slight thinning of this formation to the northeast around Thundridge and Ware and perhaps southeast towards Cheshunt. Outcrops in the northwest of the region.	55-63
		Holywell Nodular Chalk	A hard nodular chalk with little flint except the presence of the Morden Flint. Well developed marl sequence, Plenus Marls member is at the base of the formation. Not present at outcrop in the region.	16-18
	Grey Chalk	Undivided	Marl/limestone rhythms passing up into smooth textured creamy grey chalk.	50-77m

Woods (2003) provided a detailed description of the various Chalk formations in the Hertford District (BGS Sheet 239), subdividing the Chalk Group into 5 lithostratigraphical units on the basis of borehole resistivity and gamma log interpretations (Table 3.2). The lithostratigraphical units correspond to the revised Chalk Group stratigraphy following Rawson et al. (2001) (Section 2.2.1). Cross-sections produced from the resistivity log interpretations show the general southeasterly dip of the individual Chalk subgroups. The New Pit Chalk outcrops in the far west of the study area. Moving east, the Lewes Nodular Chalk is at outcrop up to Hatfield, and then the Seaford Chalk outcrops to the east of Hatfield. Borehole correlations suggest that there are no major lateral changes in the development of Chalk Group lithostratigraphical units across the district, except for slight thinning of the New Pit Chalk and a slight expansion of the Lewes Nodular Chalk (Woods, 2003).

3.2.3.3 Geological Structure

Bloomfield et al. (2004) present a structural interpretation of the Chalk in the study area based on slope aspect mapping. Land surface aspect mapping of a digital terrain model (DTM) was used to identify lineaments that may reflect structures within the Chalk aquifer in the Hertford District. These lineaments were then used in conjunction with additional information to develop a model of the geological structure of the Chalk in the study area (the area between St Albans in the west and the Lee Valley in the east).

A number of cross-sections across the study area have been produced by BGS, VWP and TWUL which show the Chalk and Palaeogene formations dip gently southeast towards the centre of the London Basin (forming the northern limb of the London Basin syncline). Superimposed on this surface are a series of inferred buckles and/or faulted folds, and a number of faults, typically downthrown to the west.

The BGS slope aspect mapping study (Bloomfield et al., 2004) identified 78 lineaments within the area of the Hertford district (BGS Sheet 239), which were distinguishable as four distinct sets (Table 3.3). Sets L1 to L3 are consistent with the limited field observations on Chalk fracturing available and with previous published regional and generic model of fracturing in the Chalk. Due to their presence in Palaeogene outcrop areas only, Bloomfield et al. (2004) infer that the east-west lineaments may not be associated with structures in the underlying Chalk.

3.2.4 Hydrogeology

3.2.4.1 The Aquifer System

The Chalk, which underlies the whole of the study area, forms the principal aquifer in the region and the main source of public water supply. In the Chalk upland of the northern and western parts of the study area the Chalk is mostly unconfined. In places, the Chalk is overlain by Clay-with-Flints, although this unit is not considered to limit recharge to the Chalk (Klinck et al., 1998). In the valley areas, the Chalk is in hydraulic continuity with gravels, where present, and elsewhere semi-confined by alluvium (Buckle, 2002).

Within the Vale of St Albans and Middle Lee Valley, the Chalk is overlain by an interbedded sequence of Boulder Clay and Glacial Sands and Gravels which forms a multi-layered hydrogeological unit (Buckle, 2002). In general this unit comprises a lower sand and gravel aquifer (the Proto-Thames

Table 3.3: Interpretation of lineaments. Based on Bloomfield et al. (2004).

Set	Trend	Location/association	Interpretation
L1	northwest-southeast	Restricted to the Chalk outcrop in the northwest of the study area	Fracture zones, probably consisting of a mixture of single layer and multi-layer joints and small en-echelon faults. Denoting zones of more intense sub-vertical fracturing in the Chalk.
L2	northeast-southwest	Associated with either Chalk outcrop or the contact between the Chalk and Palaeogene cover. Form two broad sub-parallel NE-SW zones belts across the study area.	Zones of extensional en-echelon faulting and folding, parallel the regional strike of the Chalk bedding, with predominant downthrow to NW. Possibly reflecting both lithological changes and strike-parallel fractures and fault controlled fold structures
L3	north-south	N-S trending zones up to 1km wide found throughout the study area regardless of geology.	Zones of distributed faulting and faulted folds.
L4	east-west	restricted to the Palaeogene cover	Not associated with structures in the underlying Chalk.

Gravels) in hydraulic continuity with the Chalk, and an upper perched sand and gravel aquifer above the Boulder Clay. The degree of continuity between the upper sand and gravel aquifer and the Chalk aquifer system is dependent on the extent and thickness of clay layers, which impede vertical flow. In places, the Chalk-PTG aquifer system is only partially saturated and unconfined, elsewhere it is semi-confined to confined by Boulder Clay.

In the southeast of the study area the Chalk is overlain by the Palaeogene Deposits, comprising the Reading Formation of the Lambeth Group (formerly Woolwich and Reading Beds) and the London Clay. The Thanet Sands are absent in the area. The Reading Fm sediments are unsaturated over the majority of the study area, although in the far southeast of the study area they become saturated, and together with the Chalk are confined by the London Clay aquiclude.

From a hydrogeological point of view, a unit known as the 'Basal Sands' is used to describe the Palaeogene sediments that are in hydraulic continuity with the Chalk aquifer of the London Basin. In general the 'Basal Sands' comprises the Thanet Sand and the lower part of the Lambeth Group. The top of this unit is defined non-stratigraphically as the lowest clay greater than 3 m thick in the Palaeogene succession (Board, 1972). In the study area, the London Clay aquiclude acts as the confining layer to the Chalk-Basal Sands aquifer unit (Buckle, 2002).

3.2.4.2 Geomorphological controls

Geomorphology appears to be an important control on aquifer properties of the Chalk (Section 2.7.2): transmissivity values appear to differ considerably between the valleys (dry and flowing) and the interfluves (Allen et al., 1997). The origin of this pattern is discussed in Section 2.4.3.

Within the major valleys (Thames and Colne), high yields are gained from boreholes close to the rivers. The high transmissivities recorded, (e.g. 25 000 $\mathrm{m^2\ day^{-1}}$ for the Chalk at Medmenham) are in part attributable to high degree of leakage to from the River Thames (either directly or via the Gravels). Nevertheless, the high flux of groundwater flowing through the major valleys is likely to enhance the aperture of existing fractures, and thus high transmissivity values are expected within the Chalk in these areas. From the available data, Allen et al. (1997) state typical values in the range 1500 to 3000 $\mathrm{m^2\ day^{-1}}$. Little quantitative data are available for dry valleys, although it is generally assumed that the dry valleys show similar transmissivity values to flowing valleys. Allen et al. (1997) report that transmissivity values of between 400 and 1000 $\mathrm{m^2\ day^{-1}}$, and storage coefficient values of 10^{-3} to 10^{-2} were recorded for dry valleys near Chesham and High Wycombe. Within the valleys, putty chalk can reduce the permeability of the aquifer. Putty Chalk is present beneath the wider sections of valley, and has been detected in sections of the Thames and the Colne valleys. The formation and properties of putty chalk are discussed further in Section 2.2.4.

Within the interfluve areas, in high ground away from flowing or dry valleys, transmissivities are generally considered to be low. Although Allen et al. (1997) could not obtain any pumping test data for the interfluve areas within the Chilterns, low transmissivities ($<$50 $\mathrm{m^2\ day^{-1}}$) and storage coefficients (0.01) were obtained in interfluve area of the Kennet Valley in Berkshire.

Pumping tests conducted at the Northern New River wells indicate transmissivities in the range

1000 $\mathrm{m}^2\ \mathrm{day}^{-1}$ to 4000 $\mathrm{m}^2\ \mathrm{day}^{-1}$. This equates to a hydraulic conductivity values between 3 $\mathrm{m\ day}^{-1}$ and 30 $\mathrm{m\ day}^{-1}$.

3.2.4.3 Lithological controls

The individual Chalk formations vary in their fracture characteristics and hydraulic properties (Table 3.4). It is likely that lithostratigraphic variation will affect the hydrogeology in the area. Indeed, Atkins (2004) suggest that the change from New Pit Chalk to Seaford Chalk at outcrop/subcrop in the Hatfield area may explain the observed difference in flow behaviour between the areas east of Hatfield and the area to the west.

In general, the Seaford Chalk is thought to show the highest hydraulic conductivity (Table 3.4), although there is little published information available on the variation between formations. Hardgrounds are typically associated with higher flows. Marls are relatively impermeable and represent barriers to vertical flow. However, preferential flow paths may develop above marl layers (Section 2.4.3). The degree of hydraulic continuity between Chalk formations can be variable, with the potential for significant head gradients.

Table 3.4: Chalk Group Aquifer Potential. After Mortimore et al. (1990).

Chalk Group Bed/Member	Hardness	Fracture Characteristics	Aquifer Potential
Seaford Chalk	Very soft to medium hard	Medium spaced regular joints	High
Lewes Nodular Chalk	Alternating very soft to very hard, some massive bands	Nodular chalk fracturing and widely spaced conjugate joints	Mixed; low except on faults
Holywell Nodular Chalk	Very soft to medium hard	Medium spaced conjugate joints	Locally good where well fractured
New Pit Chalk Beds	Very soft to medium hard	Intense steeply inclined fractures dissipating along marls seams	Solution widened features along marl seams
Melbourn Rock	Hard	Medium spaced conjugate sets	High
Plenus Marls	Medium hard	Poorly fractured	Low

3.2.5 Karstic Features

Evidence for geomorphological karstic features in the Chalk of Hertfordshire is abundant, and has been well documented (e.g. Whittaker, 1921; Harold, 1937; Walsh and Ockenden, 1982. The distribution of karstic features is related to the geology and hydrology of the area (Section 2.4.3), most notably the Chalk-Palaeogene contact. The distribution of the karstic features in shown in Figures 3.2 and 3.3.

A number of stream sinks occur along the Chalk-Palaeogene contact between Radlett and Hertford, and within the Lambeth Group inlier at Cuffley Brook. Bloomfield et al. (2004) report that the density of stream sinks is highest where the Palaeogene is dominated by clay facies; where the strata

are more sandy, recharge may occur directly into the Chalk without the generation of surface streams (although the density and size of dissolution pipes developed beneath the cover may be greater). Most stream sinks are fed by small, usually ephemeral, streams, although larger perennial streams occur. The sinkholes/swallow holes allow rapid percolation of surface water to the Chalk water table.

The greatest concentration of stream sinks is in the North Mimms–Water End area. The behaviour of the swallow holes in the North Mimms/Water End area has been described by Whittaker (1921), Walsh and Ockenden (1982), Harold (1937). The area is part of the surface water catchment of the Colne, and includes the Mymmshall Brook, its tributary the Catherine Bourne, and the Welham Green Brook, which meet at Water End. The upper streams rise in the Palaegene escarpment, where they are underlain by London Clay, and flow northwards. The streams disappear underground in a number of sinks within the lower parts of the main valley and tributary valleys, which are underlain by Lambeth Group deposits (Reading Fm) and/or Chalk. The swallow holes that appear to receive the greatest volume of water are located at Water End (Walsh and Ockenden, 1982). The actual sinks used by the streams depend on the flow (Walsh and Ockenden, 1982). During dry periods, the feeder stream sinks at several points before reaching the main sinkhole complex. During periods of wet weather, flows reach the Water End swallow holes and a lake forms in the depression occupied by the swallow holes. When the capacity is exceeded, the area overflows to the upper reaches of the River Colne via a (normally dry) channel which flows beneath the A1(M) which runs north-south through Hatfield (Figure 1.1).

A second major set of swallow holes occurs in the Hatfield area (Whittaker, 1921). It is thought that that it drains east to the large springs at Arkley Hole, and may be linked to the conduit system draining the Water End sinks. Also, numerous swallow holes (sinks or dolines) were mapped by Price et al. (1989) near the M25/M1 junction (Figure 1.1) at Bricket Wood in the far west of the study area . Many of the sinks are associated with the margins of dry valleys and were interpreted by Price et al. (1989) as having been caused by groundwater issuing from the Chalk during the Pleistocene period under periglacial conditions.

The major springs, which may be fed by karstic conduits, are the Chadwell Spring, and the Arkley Hole Spring. Whittaker (1921) described several other springs between Amwell and Rye House, and between Hoddesdon and Broxbourne. Chadwell Spring, a large spring just west of Hertford, is thought to act as an estavelle (Whittaker, 1921): it runs turbid after heavy rain indicating conduit flow, but in drier weather, it ceases to flow and takes water from the New River. Bloomfield et al. (2004) report that it is suspected that the Arkley Hole springs are fed by the sinks in the Hatfield area and possibly the Palaeogene outliers to the north, although it is not clear what evidence this is based on.

3.2.6 Karst Flow

Section 2.4.2 described the tracer tests that have been undertaken in the Hertfordshire Chalk. The karstic connections established by Harold (1937) and Cook (2010) are summarised in Figure 3.4. The Hertfordshire tracer tests indicated rapid (several kilometres per day) flows from the Water End area to locations in the Lea Valley 15 km to 20 km away. The dispersion of the detected tracer along a Section of the Lea Valley several kilometres in length indictes that the system of conduits through which which the

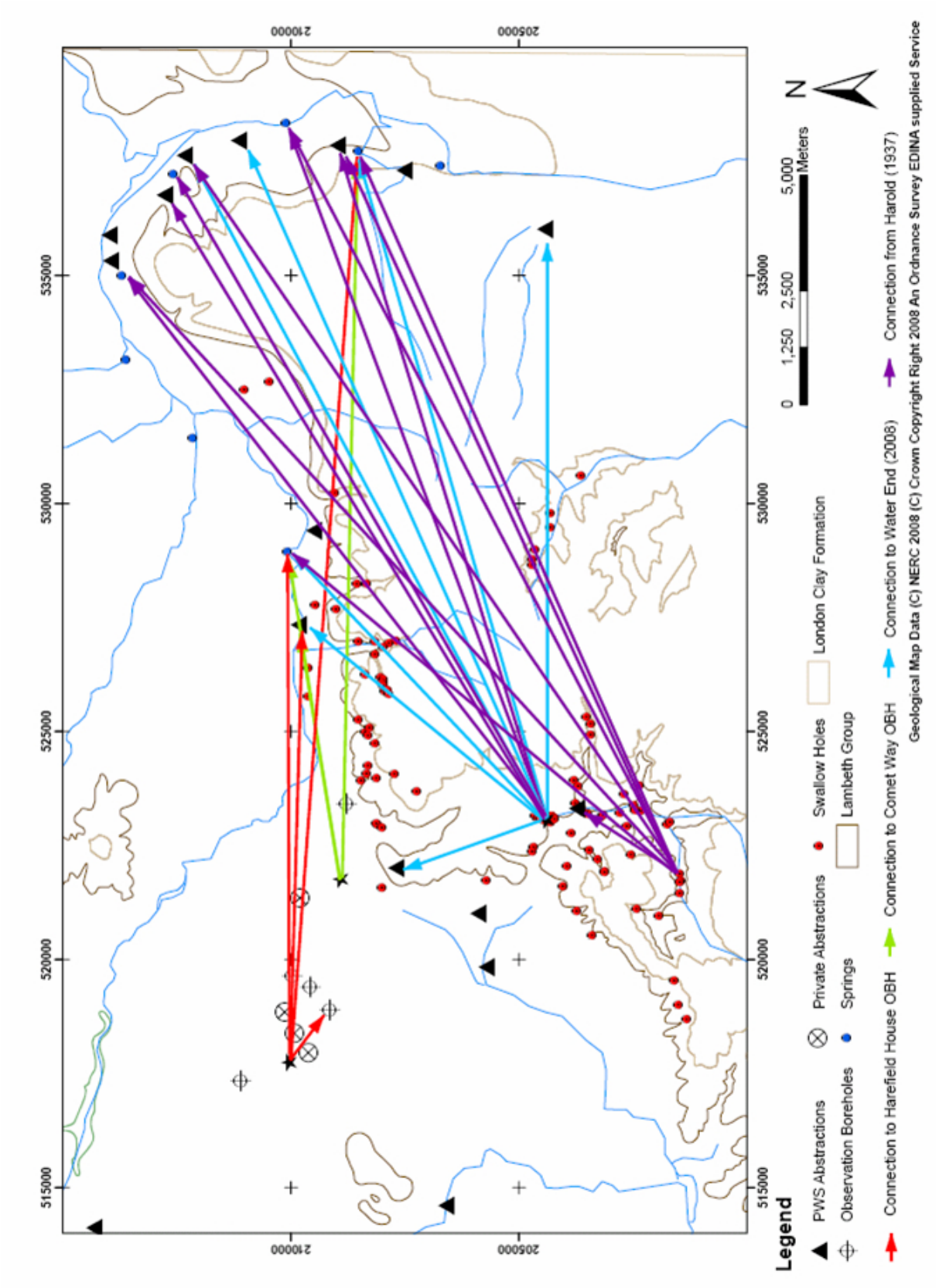

Figure 3.4: Established tracer connections in Hertfordshire. After Cook (2010)

flow occurs is widespread. Furthermore, the series of tests show that the individual pathlines followed by flow are not constant and may vary with water level. Cook (2010) considers that the major conduits in Hertfordshire are most likely to be developed at or just below the zone of water table fluctuation. This interpretation is supported by relatively stable groundwater elevations east of Hatfield (Section 3.3): the water table may be controlled by the high transmissivity of such features.

Cook (2010) integrated the information from the historic and recent tracer tests, in combination with a consideration of structural controls on groundwater flow, to form a new quantitative conceptual understanding of the function of the karstic flow system in Hertfordshire. The tracer tests undertaken in the study area suggest that there is a distributive karst flow system in Hertfordshire developed in a broadly north-east direction between North Mymms and the Lee Valley (Figure 3.28). Tracing from Water End and the Catherine Bourne has provided evidence that connectivity to the karstic features of the Mymmshall Brook system extends along the entire Palaeocene feather edge between the Lee Valley as far south as Turnford PS and at least as far west as south east Hatfield and also possibly to north-western Hatfield. The overall system appears to comprise a recharge area comprising a convergent network of conduits centered around the Mymmshall Brook Catchment and the North Mymms water table mound. This then drains via a solution-enhanced pathway adjacent to the Chalk-Palaeocene boundary and via a distributive network to springs in the Lee valley.

This distributive karst flow system is characterised by rapid, low attenuation transport. Cook (2010) interprets the progression of tracer arrivals to suggest that flow paths could be coincident with the pattern of surface karst and swallow holes between the feather edge of the Palaeocene outcrop and the River Lee. This provides an alternative interpretation to earlier conceptual models, *e.g.* Buckle (2002), which suggested a fan like series of major flow routes between Water End and the Lee Valley. Cook (2010) proposes that the pattern of tracer breakthroughs could suggest that the Northern Loop of the Palaeocene Feather Edge and River Lee is short-cut by the subsurface karst system, with a more direct karst component to the central Lee Valley, and a dispersive component beyond Arkley Hole to the northern Lee Valley.

Cook (2010) takes the consistency of connections for all three tracers to major springs at Arkley Hole and Lynchmill Spring to suggest that these springs terminate karstic flow routes established prior to the more recent development of abstraction wells. Furthermore, recovery of all three tracer species at Essendon PWS as well as similarities with both bromate concentrations and turbidity at Arkley Hole implies that this groundwater source is also probably directly connected to the same system. Therefore, the implication is that a rapid approximately east-west aligned major flow pathway exists between Essendon and the Southern Lee Valley, principally to the Lynchmill Spring, but also a likely distributary connection to Amwell Marsh, the Rye House/Rye Common Area, Hoddesdon and further south to Turnford. Cook (2010) notes that this flow pathway is approximately sub-parallel to the Hoddesdon Syncline which points to a structural influence on the flow regime.

A number of public supply abstraction wells show connections to the karst network. These are generally located relatively close to known springs (*i.e.* Broadmeads PWS and Chadwell Spring, Amwell

Marsh PWS and Emma's Well, Rye Common and Rye House Spring, and Hoddesdon/Middlefield Road and Lynchmill Spring) and the majority have extensive adit systems. It is likely that long-term operation and aquifer development around the abstraction wells has encouraged the convergence of rapid flow paths to these discharge points.

The tracing by Cook (2010) also indicated that rapid flow paths appear to extend further west beyond the zone of main karst development into the Vale of St. Albans. Surface karst features are not apparent within the Vale of St. Albans due to the extensive glacial deposits covering the Chalk. The karst system in the Vale of St. Albans appears to be less continuous and less well developed than the main karst network along the Palaeocene feather edge, perhaps restricted as a result of infilling, weathering and/or erosion of karst features with increasing distance from the Palaeocene feather edge (or within 'Geomorphic Zone 2' of Maurice et al. (2006)). Flow velocities in this area are more variable, and generally lower. The breakthroughs suggest a general decline in velocity and mass recovery with distance from the Palaeocene outcrop. Transport is significantly attenuated, perhaps suggesting multiple flow paths reflecting a range of dissolution enhanced fissure sizes. This higher attenuation may also, at least partly, be a consequence of the tracer injection locations being boreholes, and therefore not directly connected to the conduit system, resulting in dilution and dispersion before the karst system is reached (Worthington, 2003; White, 2003). In addition to the tracer evidence, small conduits have been observed in boreholes in the northern part of St. Albans CL:AIRE (2002).

3.2.6.1 Karst flow in relation to bromate contamination

The injection locations used by Cook (2010) were approximately 1 km south east of the Bromate Contaminant Source (*MS2 Coliphage*, Harefield House Borehole), approximately 9 km from the source of contamination (*Phi X174* phage, Comet Way Borehole) and within a sinking stream close to the Water End swallow hole complex (*Serratia Marcescens* phage, North Mymms) which was located south of the bromate occurrence in the Chalk aquifer, but had been shown by the 1920s and 1930s tracer tests to be connected to locations currently affected by bromate.

The interpretation of Cook (2010) is consistent with karst flow paths intersecting bromate affected groundwater in the Hatfield area. However, tracers from Comet Way borehole suggest a by-pass of Hatfield PWS by karst flow paths in this area. Bromate may be entering the karst flow system to the North and East of the Comet Way borehole. In the area west of Hatfield, whilst some rapid flow pathways exist, they are weathered and probably poorly connected and so do not dominate bromate transport as they do east of Hatfield.

The observed spread of tracer from Water End matches closely the pattern of groundwater sources affected by bromate contamination between Hatfield and Turnford and the inferred travel times show close agreement with interpretation of the effects of abstraction at Hatfield PWS (Section 3.5) on bromate concentrations at the Lee Valley sources. Therefore, between Hatfield and the Lee valley, bromate transport appears to be in large part controlled by groundwater flow in Chalk karst which is influenced to some extent by abstraction at Hatfield PWS which has been shown to be connected to the karst flow system.

Tracer was not detected at Chadwell Spring in the recent tracer tests (Cook, 2010), despite being detected in the 1920s and 1930s tests. Cook (2010) suggests that flow to this spring has been affected by recent changes in abstraction patterns and it now derives water from further north, outside the catchment area of the tracer. This is supported by evidence from water chemistry (Section 3.4). This could also explain why bromate concentrations are typically lower at Chadwell Spring than at other locations to the south along the Lea Valley.

Cook (2010) proposes that the pattern of tracer breakthroughs could suggest that the Northern Loop of the Palaeocene Feather Edge and River Lee is short-cut by the subsurface karst system, with a more direct karst component to the central Lea Valley, and a dispersive component beyond Arkley Hole to the northern Lea Valley. This could provide the mechanism by which the bromate concentrations tend to be higher in the more southerly Wells than the NNR Wells since they receive a more direct and a less diluted karst component.

3.2.7 Groundwater–surface water interactions

Buckle (2002), Entec (2000) and Atkins (2004) describe the groundwater-surface water interactions in more detail. A summary is provided below:

3.2.7.1 River Colne and Tributaries

As described in Section 3.2.6, the Mimmshall Brook swallow hole system allows rapid transfer of surface water to the Chalk water table. Also, during wet periods, surface water overflow from the Water End swallow holes flows to the River Colne (Section 3.2.2). The section of the Colne around the North Mymms area, immediately downstream Water End overflow, is underlain by alluvial sediments over sand and gravels which are in hydraulic continuity with the Chalk, and leakage from the river to the surface water system is thought to occur.

In the area between North Mimms and Tyttenhanger Park, and the Ellenbrook, the Chalk-PTG groundwater aquifer is separated from the river by a continuous (although <3 m in places) layer of Boulder Clay. The shallow perched sand and gravel aquifer overlying the boulder clay is considered to be in hydraulic continuity with the surface water system. This system is likely to have been influenced by gravel extraction activities, which may have locally increased the connectivity between the Chalk aquifer and the river.

Boulder Clay is absent in some areas over the section downstream of Tyttenhanger Park to the confluence with the River Ver, which suggests potential for greater connection between the river and the Chalk-PTG groundwater system. The river may be influent during periods of high groundwater levels and effluent over some sections during periods of low water levels.

3.2.7.2 River Ver

Along most of its length the River Ver is underlain by shallow alluvium and valley gravels. The Ver has high baseflow fed by the Chalk. However, locally near to abstractions there is leakage of river water to the ground, especially in the vicinity of St Albans.

3.2.7.3 River Lee

The Upper Lee, like the Ver, flows within an incised valley underlain by shallow alluvium over Chalk. It is a Chalk-fed stream, but has a lower base flow than the Ver. Downstream of Welwyn Garden City the river is underlain by shallow alluvium and drift, which includes a layer of Boulder Clay that separates the Lee from the Chalk-PTG aquifer system. Further downstream to Water Hall, there appears to be more surface water–groundwater interaction, and at Water Hall the river is underlain by sands and gravels in continuity with the Chalk.

Further downstream of Water Hall, the Lee is underlain by alluvium and drift. In some places the alluvium lies directly over valley gravels and/or Chalk. It is expected that in this section the river is in hydraulic continuity with the Chalk aquifer system, but the degree of hydraulic interaction may be impeded by the vertical permeability of streambed sediments.

3.2.8 Chalk–Drift Groundwater interactions

3.2.8.1 Hatfield Quarry and Former British Aerodrome Site

A detailed review of water level data and borehole information from the RMC Hatfield quarry site was undertaken by Buckle (2002) to assess the hydraulic relationships between the Chalk-lower sand and gravel (PTG) aquifer and the upper shallow sand and gravel aquifer (UGD). The data indicated that the Chalk-PTG aquifer experiences a range of conditions both seasonally and spatially across the site. In some boreholes water levels vary from being below the top of the chalk, or within the PTG, to being above the Boulder Clay; in others the lower aquifer is always confined with water levels observed to be above the top of the PTG.

Water levels in the UGD aquifer are between 3 m and 7 m above those in the Chalk-PTG aquifer. It appears therefore that under normal water level conditions there may be the potential for downward movement of groundwater from the upper perched UGD to the Chalk-PTG, but not vice versa.

A similar situation is observed, with a difference in water levels of 6 m to 8 m at the former British Aerodrome site. The degree of downward movement is dependent on the permeability of the Boulder Clay and its lateral continuity (Buckle, 2002).

3.3 Piezometry

Long-term water level data is available for a number of observation boreholes across the catchment (Figure 3.5). These boreholes form part of the Environment Agency monitoring network. The long-term rainfall and water level variations are shown in Figure 3.6, and a detailed time series for Orchard Garage monitoring well, located close to the source site in Sandridge is shown in Figure 3.7.

Details of the Chalk piezometry, groundwater movement and water level fluctuations in the area have been collated and described by Entec (2000), Buckle (2002) and Atkins (2004). In general, water levels in the Chalk respond to variations in rainfall. Locations in the western part of the study area, on the upland interfluve between the River Lea and River Ver show the largest fluctuations (approximately 5 m to 8 m), and locations nearer to the river valleys (*e.g.* in the west of the study area near the River Colne, or in the east of the study area, close to the River Lea and River Mimram) show less pronounced

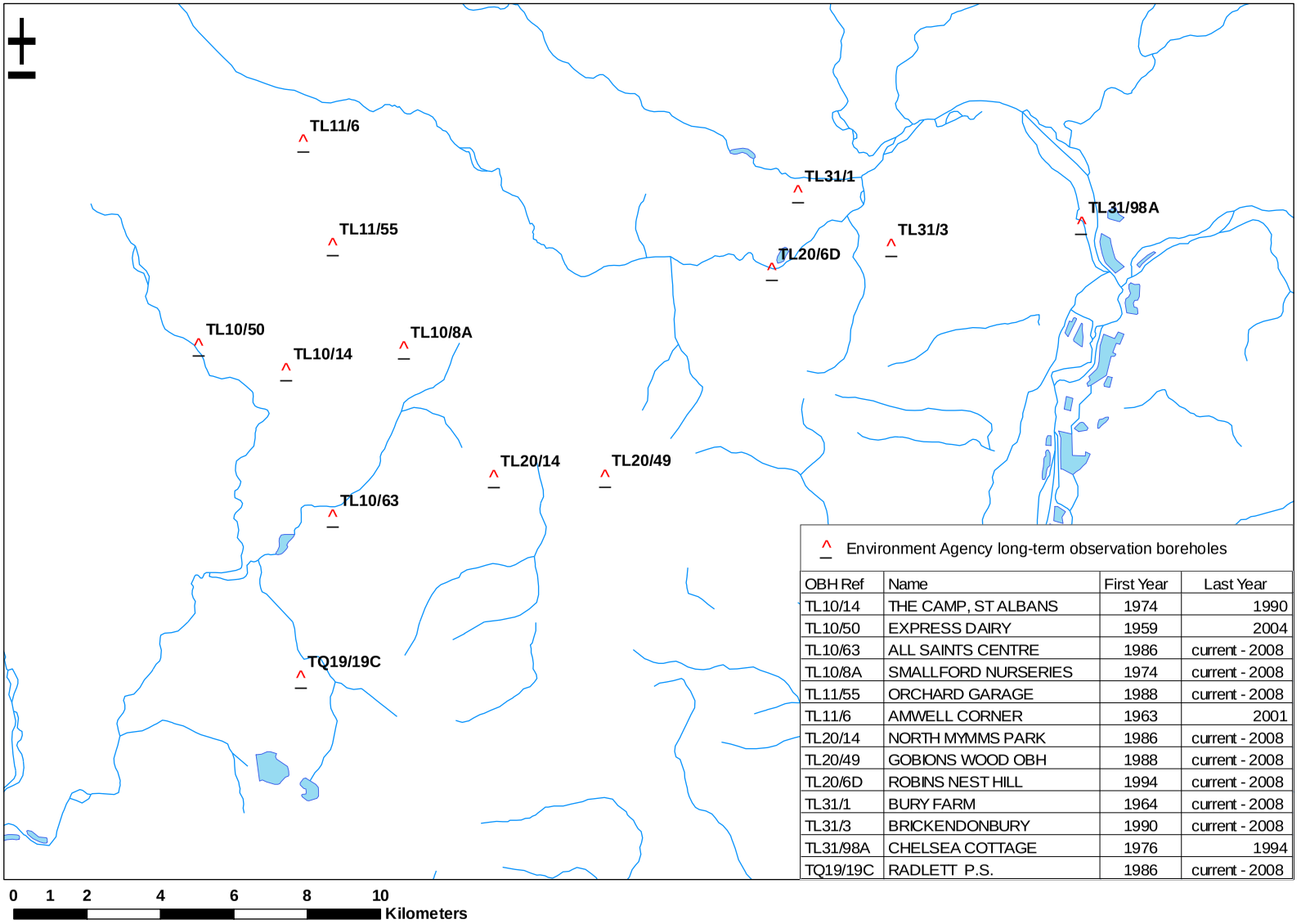

Environment Agency long-term observation boreholes

OBH Ref	Name	First Year	Last Year
TL10/14	THE CAMP, ST ALBANS	1974	1990
TL10/50	EXPRESS DAIRY	1959	2004
TL10/63	ALL SAINTS CENTRE	1986	current - 2008
TL10/8A	SMALLFORD NURSERIES	1974	current - 2008
TL11/55	ORCHARD GARAGE	1988	current - 2008
TL11/6	AMWELL CORNER	1963	2001
TL20/14	NORTH MYMMS PARK	1986	current - 2008
TL20/49	GOBIONS WOOD OBH	1988	current - 2008
TL20/6D	ROBINS NEST HILL	1994	current - 2008
TL31/1	BURY FARM	1964	current - 2008
TL31/3	BRICKENDONBURY	1990	current - 2008
TL31/98A	CHELSEA COTTAGE	1976	1994
TQ19/19C	RADLETT P.S.	1986	current - 2008

Figure 3.5: Environment Agency monitoring network long-term water level monitoring locations

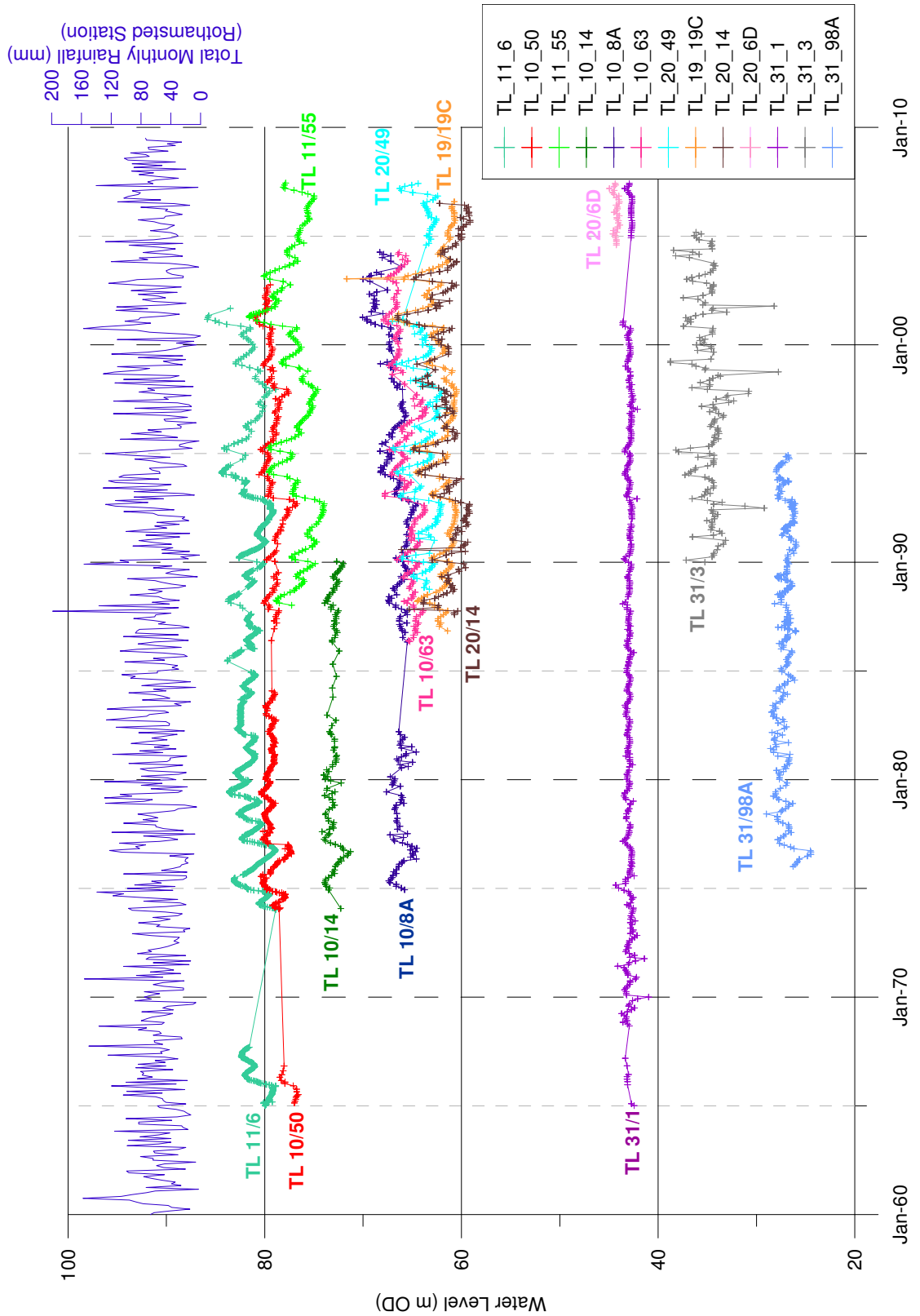

Figure 3.6: Rainfall and Environment Agency monitoring network water level variations. Locations of monitoring wells are shown in Figure 3.5

fluctuations (typically less than 3 m). The presence of sand and gravel drift deposits above the chalk is also likely to reduce water level fluctuations as a result of greater storage capacity.

Notable fluctuations in water levels are summarised below:

- Between 1990 and 1992, water levels fell to some of their lowest recorded levels, following a period of relatively high water levels between 1981 and 1988.
- Between 2000 and 2003 (particularly 2001), water levels rose to the maximum recorded levels.
- Between 2003 and 2006, water levels declined but started to rise again over 2007.

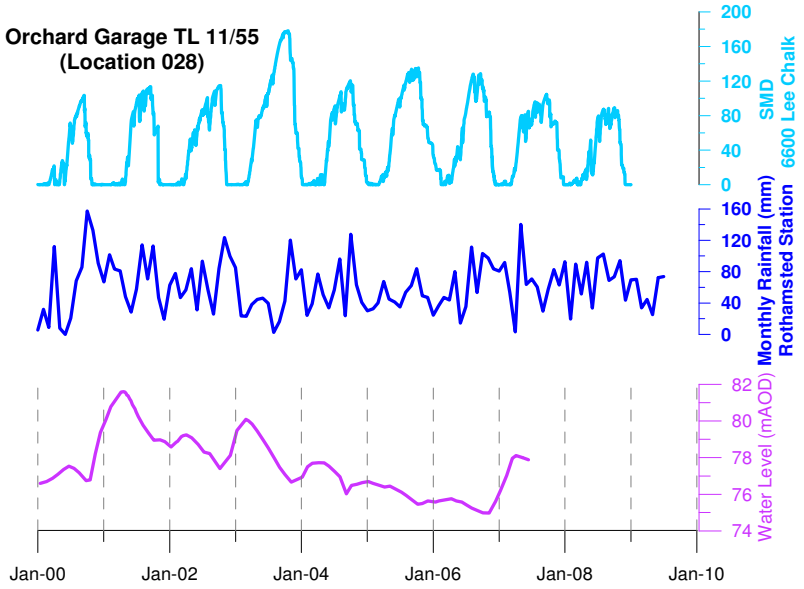

Figure 3.7: Water Level, Soil Moisture Deficit and rainfall at Orchard Garage Monitoring Well

A series of piezometric contour maps have been produced by Entec (2000), Buckle (2002) and Atkins (2004). The maps show that the overall pattern of piezometry has remained reasonably constant over the 1990s and early 2000s (although data up until 1997 is less extensive than later dates, particularly in the areas between Sandridge and Hatfield). There is some uncertainty in delineating contour lines where insufficient data points were available, notably between Tyttenhanger PS and Netherwild PS. It is thought likely that the most significant water balance shifts in the Upper Lea area probably occurred prior to 1970 as a result of significant changes in abstraction regimes. The long-term average piezometry is shown in Figure 3.8.

On the basis of the piezometric data, groundwater flow tends to follow topography away from the Chalk upland in the north and north-west, where groundwater elevations can exceed +100 m OD, towards the confined Chalk in the south and south-east, where groundwater elevations are less than +20 m OD. Within the Lee Valley in the vicinity of the NNR sources, flow directions tend to follow the course of the river such that groundwater generally flows from north to south (Atkins, 2004). Groundwater elevations continue to fall south-east towards the Lee Valley and ultimately south towards Central

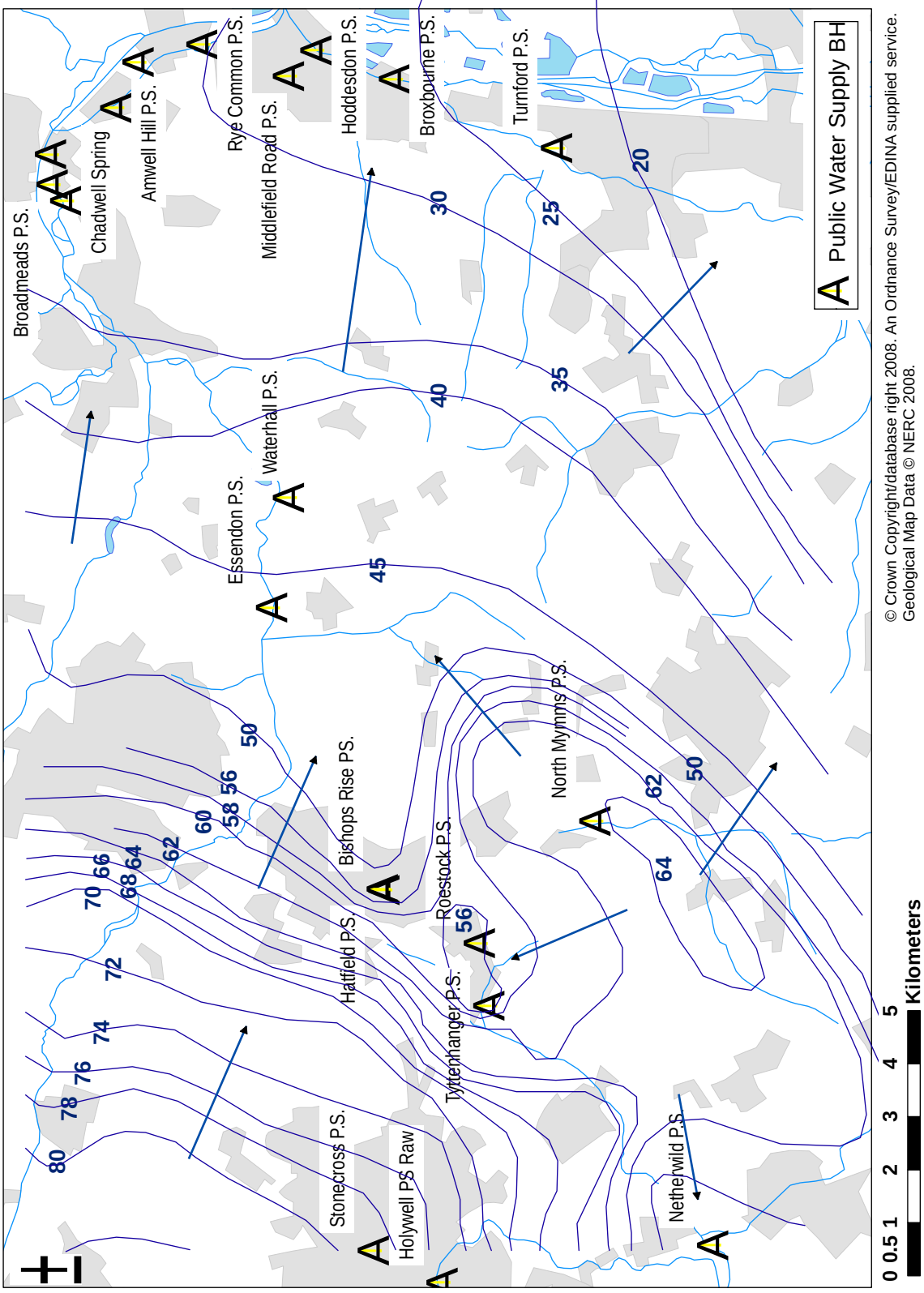

Figure 3.8: Average piezometry 1998 to 2008. Contour levels are in m AOD. Arrows indicate groundwater flow direction

London. There is a groundwater divide between units contributing to the River Lee and those contributing to the River Colne. This divide runs through the central part of the study area between Sandridge and North Mymms.

Superimposed on the general north-west to south-east pattern of groundwater movement, Buckle (2002) note a number of features, in addition to anthropogenic abstractions and discharges, which exert a significant local influence on groundwater flow. These features include the Radlett–North Mymms area recharge mound, the Mimmshall Brook and the Water End swallow holes, the Colney Heath-Hoddesdon syncline, and groundwater-surface water interactions.

The Radlett–North Mymms area recharge mound can be seen on piezometric maps as a groundwater high aligned along the Palaeogene escarpment. The London Clay cover is absent in places, exposing the Chalk and the sands and clays of the Reading Formation, thus allowing recharge to the Chalk aquifer to occur more readily in this area compared to the surrounding areas. Recharge is also contributed to by the presence of swallow holes in this area, notably the Water End complex. This feature is seen to be present even during extended periods of low rainfall. Groundwater moves in all directions away from the mound, although the greatest flow is towards the north-east. Piezometry and groundwater flow in this area is not well defined, and is considered to be sensitive to changes in recharge Buckle (2002). Water flow in this area is also influenced by the abstractions to the northwest and west of the recharge mound.

The swallow holes in the North Mymms-Water End area are discussed further in Section 3.2.5. Walsh and Ockenden (1982) note that the there is an apparent barrier to flow coincident with the Shenley-Broxbourne anticline, and a preferential flow direction along the line of the Colney Heath-Hoddesdon syncline. This may indicate a high permeability conduit or zone linking the mound and the River Lee. Buckle (2002) invokes the presence of such a zone, straddling the zone of water table fluctuation and underlain by a lower permeability main body of Chalk, to explain the persistence of the mound. When operative under high flow conditions, the zone allows removal of the groundwater from the recharge area. However, under low recharge conditions, the recharge mound is maintained by the lower transmissivity of the main body of Chalk in which flows are much reduced.

3.3.1 Groundwater flow in the Sandridge-St Leonard's Court Area

Sandridge is situated at the confluence of two dry valleys, and the St Leonard's Court (SLC) source site itself is situated on the northern edge of the valley down from the confluence. The dry valley trends south-east from Sandridge, following the general trend of a major joint/fracture set. Roberts (2001) suggests that preferential flow paths may have developed within the upper levels of the Chalk in the Sandridge area as the dry valley represents a local discharge area for the Chalk aquifer, and it was probably also a tributary of the former course of the Thames through the Vale of St Albans. Piezometric maps show that in the Sandridge area groundwater movement is in general from west-north-west to east-south-east. However, information is not available in sufficient detail to allow more precise delineation of flow direction along the line of the dry valley. The groundwater flow in the vicinity of the SLC site is discussed further in the Chapter 5.

3.3.2 Abstractions and Discharges

Abstractions within the central part of the study area exert a significant local effect on the piezometry, causing a depression of water levels in immediate vicinity of the pumping borehole. The main TVW abstractions are grouped at Roestock, Tyttenhanger and Hatfield and Netherwild PWS. TWUL groundwater abstractions are concentrated along the River Lee and New River, including Amwell Marsh, Rye Common, Hoddesdon, Broxbourne and Turnford PWS.

It is likely that groundwater pumping in the North Mymms area and the Lee valley influences the natural flow of the karstic conduit system between and is likely to have a significant influence on the natural flow regime. A reduction in springflows from Chadwell Spring can be directly correlated with an increase in groundwater abstractions within the catchment (Hydrotechnica, 1988).

Significant dewatering activities are undertaken by Lafarge Aggregates at Tyttenhanger Quarry, and subsequent discharges made to the River Colne. Additionally, gravel extraction activated in other areas (*e.g.* Hatfield Quarry) may result in changes to the natural piezometry. Removal of superficial deposits may in some instances lead to increased recharge to the Chalk aquifer system. Dewatering of working areas may also be required during quarrying.

3.4 Regional hydrochemisty

The regional hydrochemistry, in relation to the NNR sources, was assessed by Hydrotechnica (1988), and is summarised in Atkins (2004). On the basis of major ion chemistry, five major water types were identified:

Type IA Background regional waters, characterised by calcium bicarbonate waters with low potassium and magnesium concentrations. Occur extensively to the north of the River Lee and to the north and west of Ware.

Type II Recharge/surface waters, with low alkalinity and high pH, nitrate, suplphate, chloride and sodium concentrations. Grouped around the North Mimms area swallow holes and represent rapid recharge waters.

Type III Mature groundwaters. Typically present in the confined section of the aquifer and have characteristically very low to negligible nitrate. Found in the confined section of the Chalk.

Type IV Polluted groundwaters.

Type V Mixed groundwaters. These have characteristics intermediate between Type IA and Type II waters. Wide spatial scatter and occur throughout the region, but found mainly at locations south and west of the River Lee in the areas known to be affected by rapid recharge mechanisms.

The groundwater abstracted from the NNR sources appears to contain varying proportions of Type IA and Type II groundwaters. Furthermore, the Type IA groundwaters can be further distinguished as those derived from the north of the River Lee towards Ware and Stevenage (Type IA-N), and those derived from the west of the area around Sandridge (Type IA-W). Atkins (2004) point out that determining

the proportion of Type 1A-W water (which contains bromate) contributing to each of the sources would be an effective way of estimating likely bromate concentrations. To do this would require that Type IA-N waters could be more readily distinguished from Type IA-W waters, for example on the basis of a contaminant (other than bromate) present in one body of water but not the other.

The data were interpreted as suggesting that there is seasonal variation in dominant flow directions between the Water End swallow holes, the Essendon area and the Lee valley in the vicinity of the NNR wellfield. During the winter months flow directions away from the Essendon area appear to be predominantly northeast or east, whilst in the summer months they have less of a north-easterly component.

3.5 Scavenge Pumping at Hatfield Pumping Station

3.5.1 Introduction

In July 2005 Three Valleys Water (TVW) and Thames Water Utilities Limited (TWUL) began a scavenge pumping trial at the TVW disused Public Water Supply (PWS) source at Hatfield. The source site of the bromate contamination in Sandridge is hydraulically up-gradient of Hatfield PWS. The purpose of the trial was to determine the influence of pumping Hatfield on bromate values elsewhere in the contamination plume.

The Hatfield PWS source was taken out of supply in May 2000 due to bromate contamination. Prior to this, the PWS source was used fairly continuously and on average abstracted close to its licence value of 9 $\mathrm{Ml\,day^{-1}}$. Between the cessation of pumping at Hatfield in 2000 and the start of the pumping trial in 2005, there was an increase in bromate concentrations recorded at Essendon. Also, the TWUL Northern New River (NNR) sources, which have been monitored since mid-2001, appeared to be increasingly affected by bromate contamination. It was therefore thought possible that pumping at Hatfield originally acted to intercept some of the bromate released into the aquifer from the source site. Since cessation of pumping, the sources down-gradient of Hatfield have been detrimentally affected by increased bromate contamination. However, this hypothesis could not be verified owing to a lack of bromate data for all sources prior to Hatfield ceasing abstraction.

The Hatfield Scavenge Pumping has provided the opportunity to make a quantitative statistical analysis of connections between Hatfield and sites across the catchment to the Lea Valley. The objectives of the statistical analysis are:

- to assess whether there is a statistically significant relationship between Hatfield abstraction rate and bromate concentration at Essendon and the NNR sources;
- to assess if the relationship differs between sources.

The Hatfield source has been pumped at rates up to 9 $\mathrm{Ml\,day^{-1}}$ while bromate, bromide, sulphate and chloride concentrations have been monitored at the TVW Hatfield and Essendon sources and the TWUL Northern New River Sources (see Figure 3.1 for locations). Pumping has continued into 2009. Initial analysis as an internal report to TWUL and TVW (Fitzpatrick, 2007) considered data up until the end of December 2006 only. This thesis considers the data up until the end of December 2008.

3.5.2 Data sources

Data for bromate and bromide concentrations at the twelve monitored sources were provided by Three Valleys Water (TVW) and Thames Water Utilities (TWUL), along with daily abstraction rates and water level data. Water levels at a selection of Observation Boreholes (OBH) were provided by TVW.

Daily and monthly soil moisture deficit (SMD) data (MORECS) were obtained from the Environment Agency for the Chilterns E-Colne and the Lee-Chalk areas. Daily rainfall was obtained for four locations in the area: Mill Green, Darnicle Hill, Broadmeads and North Mymms. The Environment Agency also provided stage-discharge relationships and monitoring data for the Mymmshall Brook catchment which had been derived from flow gauging work undertaken by Atkins.

3.5.3 Data handling

Raw data were managed using a Microsoft Access database (Section 4.2). Queries were used to select data for statistical analysis and graphing. Where concentration results were recorded as below detection limits, the value at the detection limit was used for data analysis purposes. Minitab software was used to perform the statistical analysis (correlation and regression).

3.5.4 Abstraction rates at Hatfield

The pumping test of the Hatfield source commenced on 29 July 2005. This analysis considers data up until the 31 December 2008. In general, continued periods of abstraction range from 3 $\mathrm{Ml\,day^{-1}}$ to 8 $\mathrm{Ml\,day^{-1}}$, with brief periods up to 9 $\mathrm{Ml\,day^{-1}}$ (Figure 3.9). Abstraction has been intermittently halted due to surcharging events after periods of heavy rainfall. The test was halted for prolonged periods of time between January and May 2006, and October 2006.

In order to prevent surcharging events, abstraction rates have generally needed to be maintained at lower rates during the winter and spring months. However, between November 2007 and June 2008 abstraction rates were maintained at relatively consistent high values of $\sim 6\ \mathrm{Ml\,day^{-1}}$ to $\sim 8\ \mathrm{Ml\,day^{-1}}$.

3.5.5 Bromate and Bromide time series trends

Figures 3.10 to 3.19 show the time series for bromate and bromide concentrations at the monitoring locations, including raw data, monthly average data, and a 'deseasonalised' average trend (Section 3.5.5.1).

3.5.5.1 Data processing and Statistical Methodology

Bromate and bromide concentration data are available from May 2000 for the Hatfield and Essendon sources, and from May 2001 or September 2001 for the Northern New River sources. Sampling intervals are approximately weekly for Hatfield and Essendon. The sampling frequencies for the NNR wells progressively increase from quarterly between May 2001 and July 2002, to monthly between July 2002 and January 2003, fortnightly between the end of January 2003 and the end of Aug 2003, and subsequently weekly. During the scavenge pumping trial, sampling frequencies increase to daily for all twelve sources.

Monthly average concentrations were calculated from the raw concentration data. Where data were not available, the monthly time series was completed by taking the mean of data for the previous and

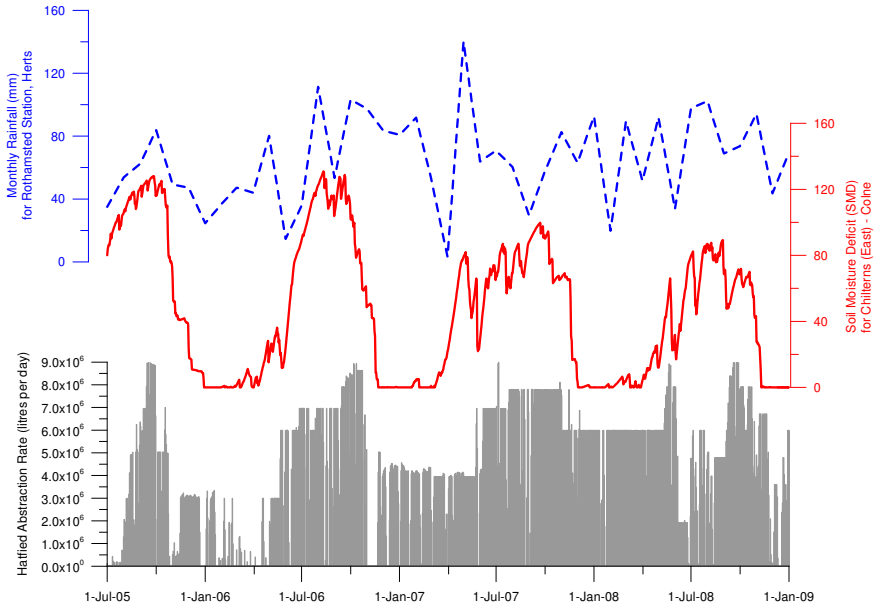

Figure 3.9: Abstraction rates at Hatfield PS between 31 June 2005 and 31 December 2008

following months. A 'deseasonalised' trend was estimated separately for data before and after the start of the pumping trial. This was estimated following the method outlined in Chatfield (2004.):

$$S_m(x_t) = \frac{\frac{1}{2}x_{(t-6)} + x_{(t-5)} + \ldots + x_{(t+5)} + \frac{1}{2}x_{(t+6)}}{12} \tag{3.1}$$

where x_t is the average monthly concentration at time t and $S_m(x_t)$ is the deseasonalised component of x_t.

3.5.5.2 Seasonal Variations

The time series for Essendon bromate (Figure 3.11) exhibits distinct seasonal variation, with the lowest concentrations on the cycle corresponding to the winter months (December, January, February) followed by a gradual build up through Spring and Summer to concentration peaks in the early autumn months (September/October) followed by a fall through November and December to winter concentration lows. Annual differences between winter minimum and autumn maximum appears to be relatively constant at approximately 10 μg l^{-1}. Seasonal variation is not as consistent in the Hatfield time series. However, minimum seasonal bromate concentrations tend to occur between January and April after which concentrations peak in October and then fall back to lower concentrations during the winter/spring. Differences in bromate concentrations are approximately 70 μg l^{-1}. The Hatfield pumping trial begins on 29 July 2005 when bromate concentrations are reaching their peak of the seasonal cycle. Concentrations are rapidly decreased during pumping, rising in the spring of 2005 when continued abstraction was halted at Hatfield between February and May 2006. Concentrations then generally decline through to October once pumping is resumed. Distinct seasonality is not evident after the start of the pumping trial; peaks appear to coincide with periods of Hatfield switch-off rather than regular seasonal variation.

Seasonality in bromate concentrations is also evident in the NNR time series. Amwell Hill (Fig-

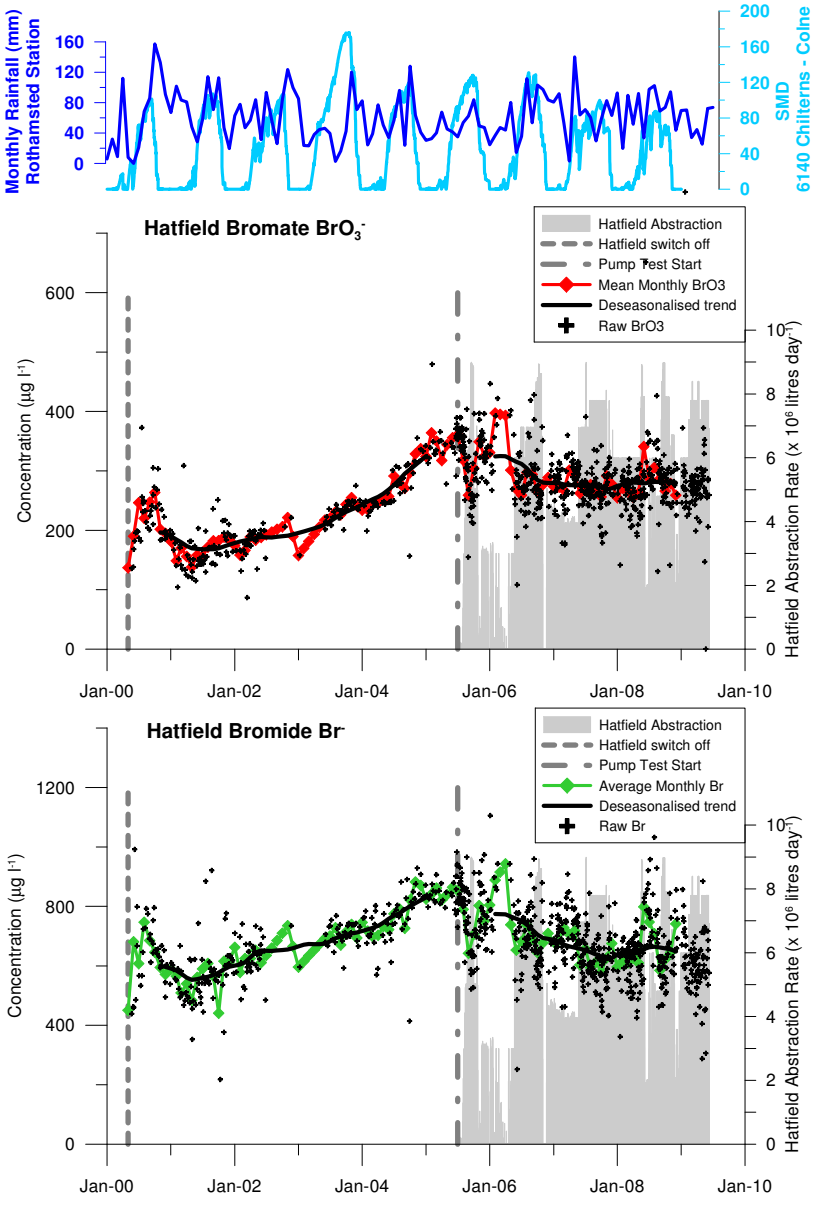

Figure 3.10: Time series of bromate and bromide concentrations at Hatfield PS, soil moisture deficit, and monthly rainfall.

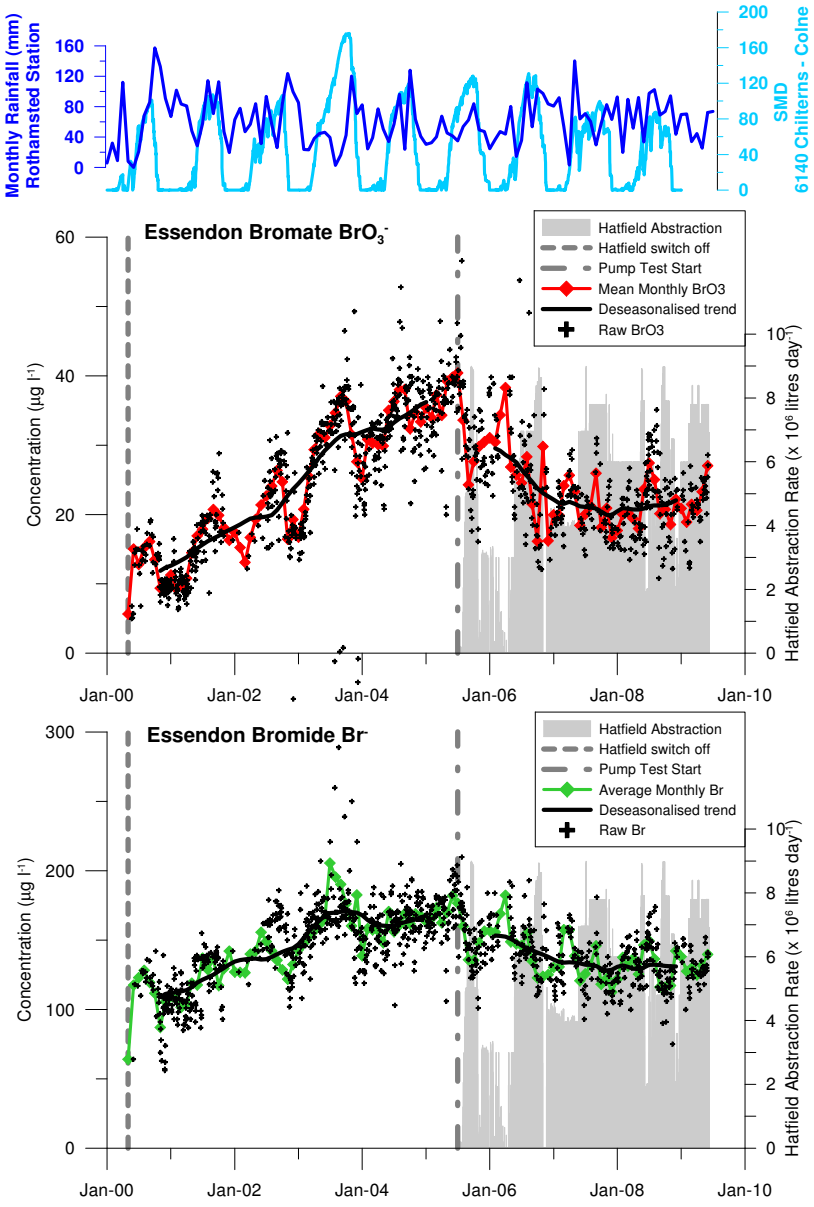

Figure 3.11: Time series of bromate and bromide concentrations at Essendon PS, soil moisture deficit, and monthly rainfall.

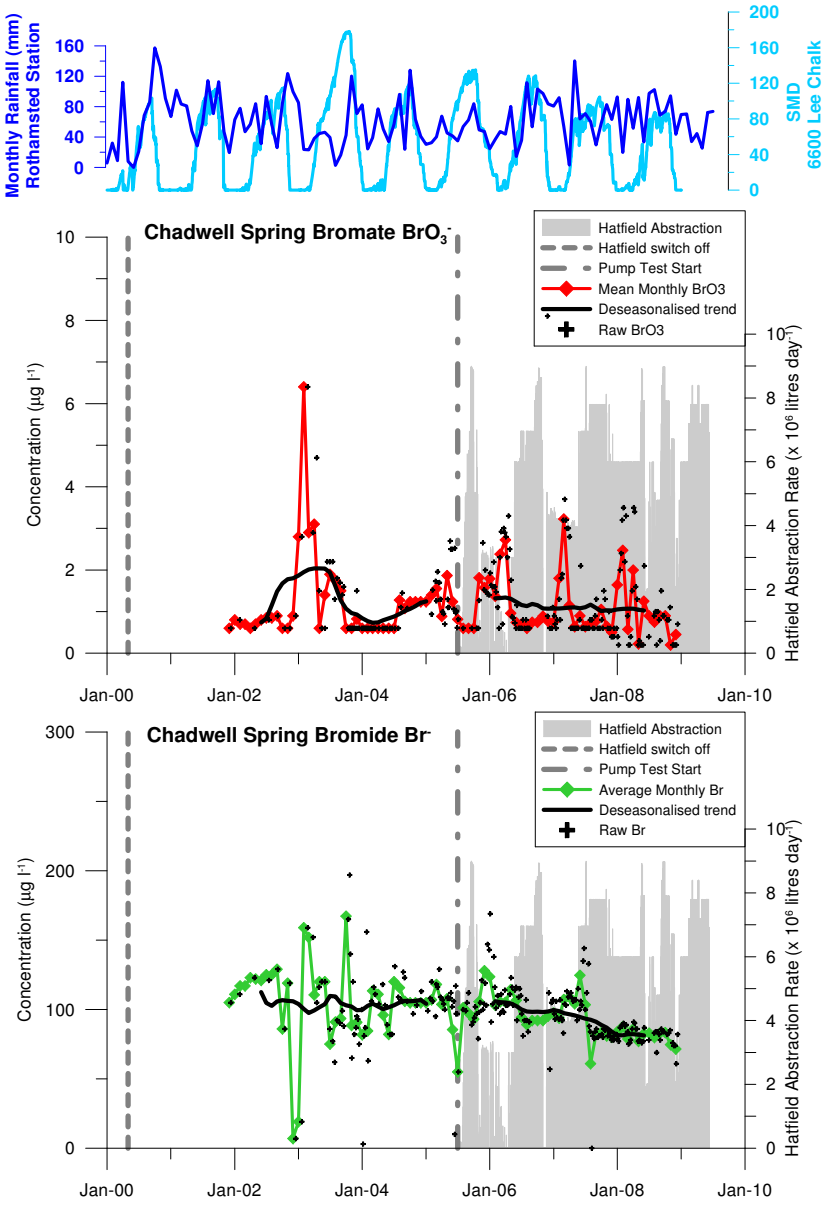

Figure 3.12: Time series of bromate and bromide concentrations at Chadwell Spring, soil moisture deficit, and monthly rainfall.

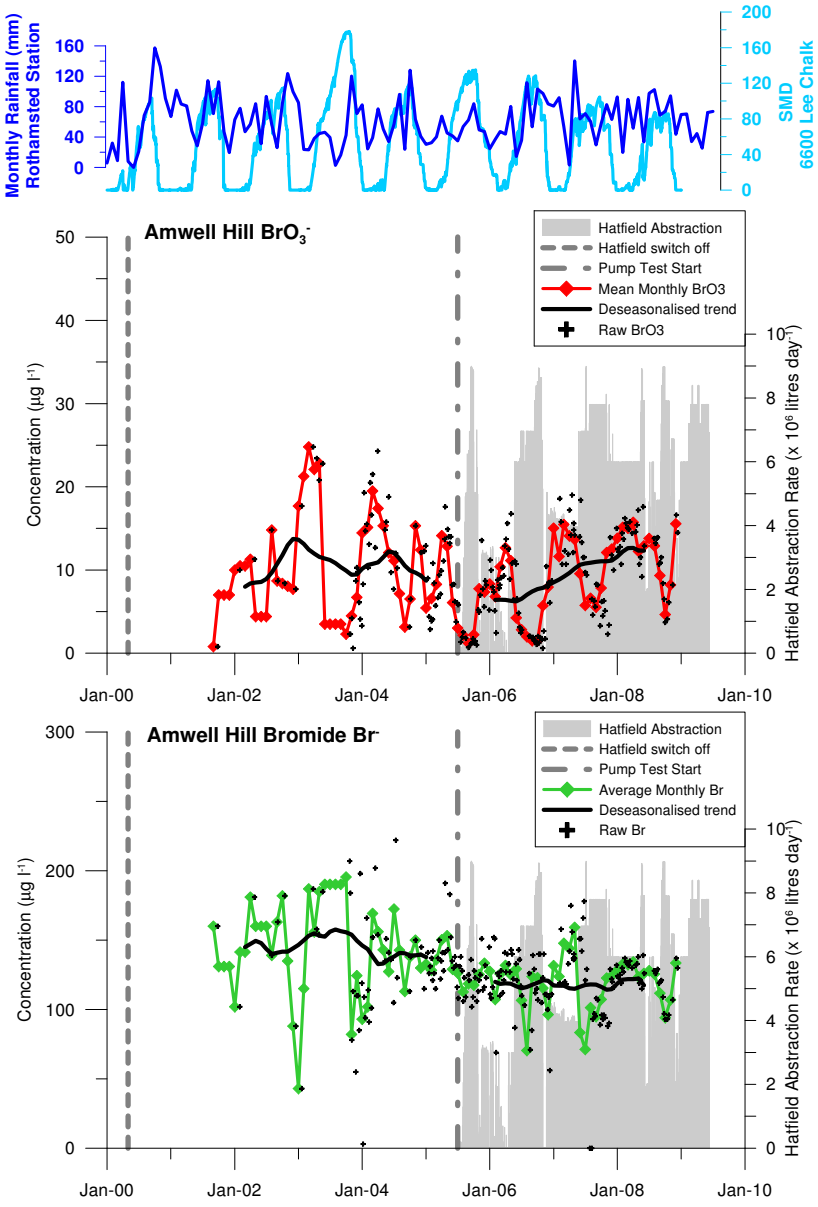

Figure 3.13: Time series of bromate and bromide concentrations at Amwell Hill PS, soil moisture deficit, and monthly rainfall.

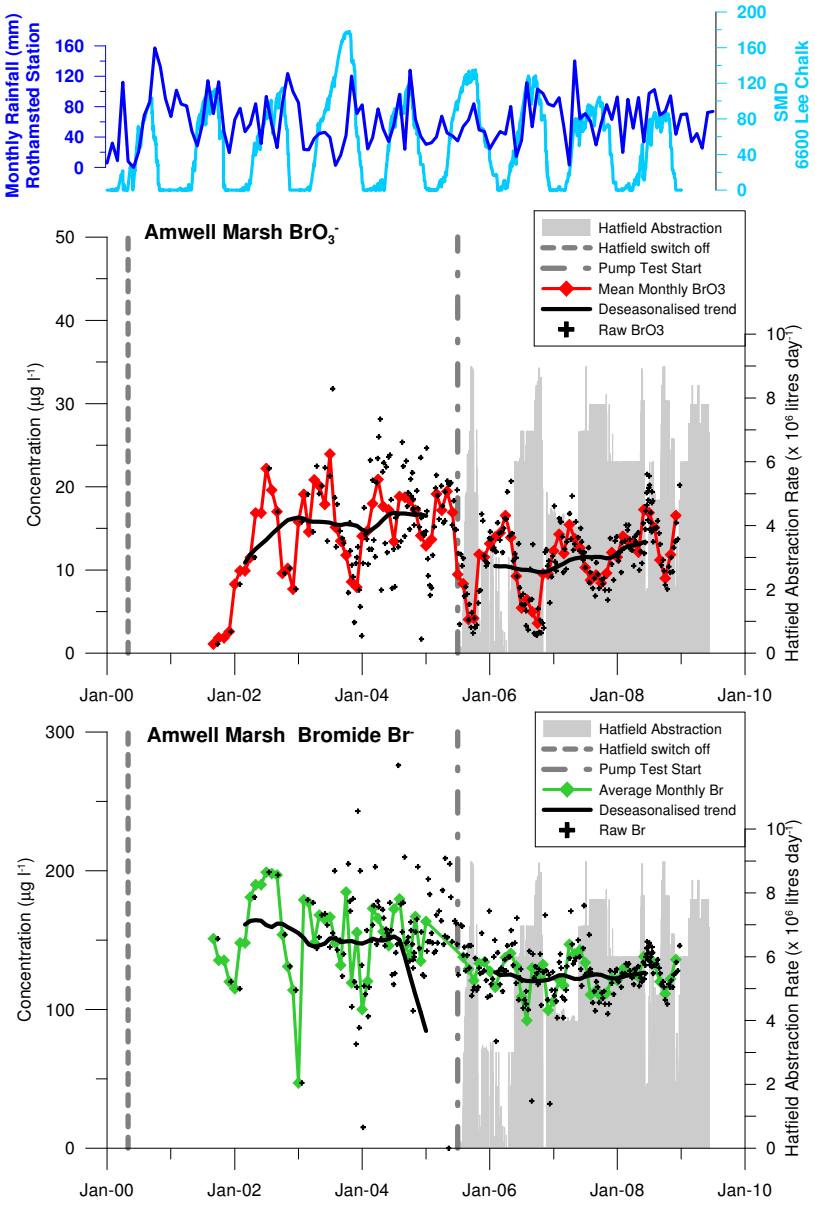

Figure 3.14: Time series of bromate and bromide concentrations at Amwell Marsh PS, soil moisture deficit, and monthly rainfall.

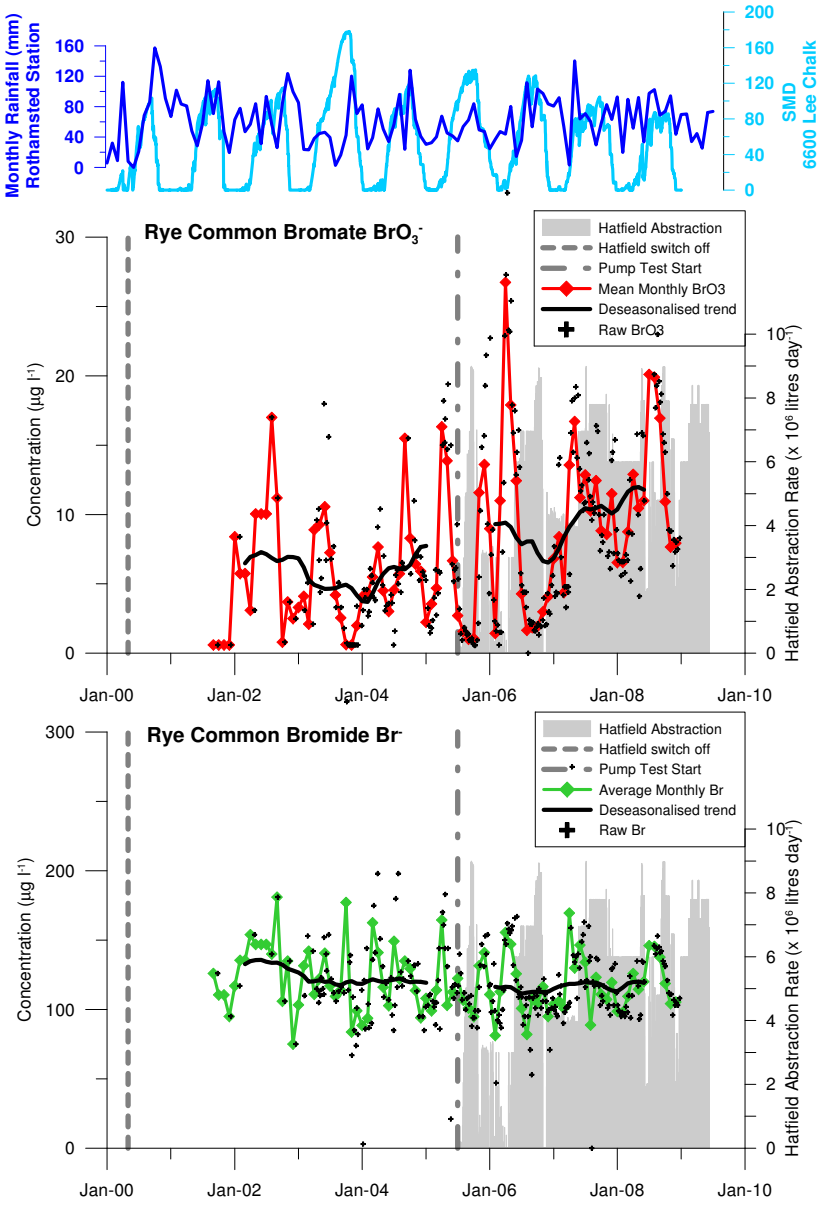

Figure 3.15: Time series of bromate and bromide concentrations at Rye Common PS, soil moisture deficit, and monthly rainfall.

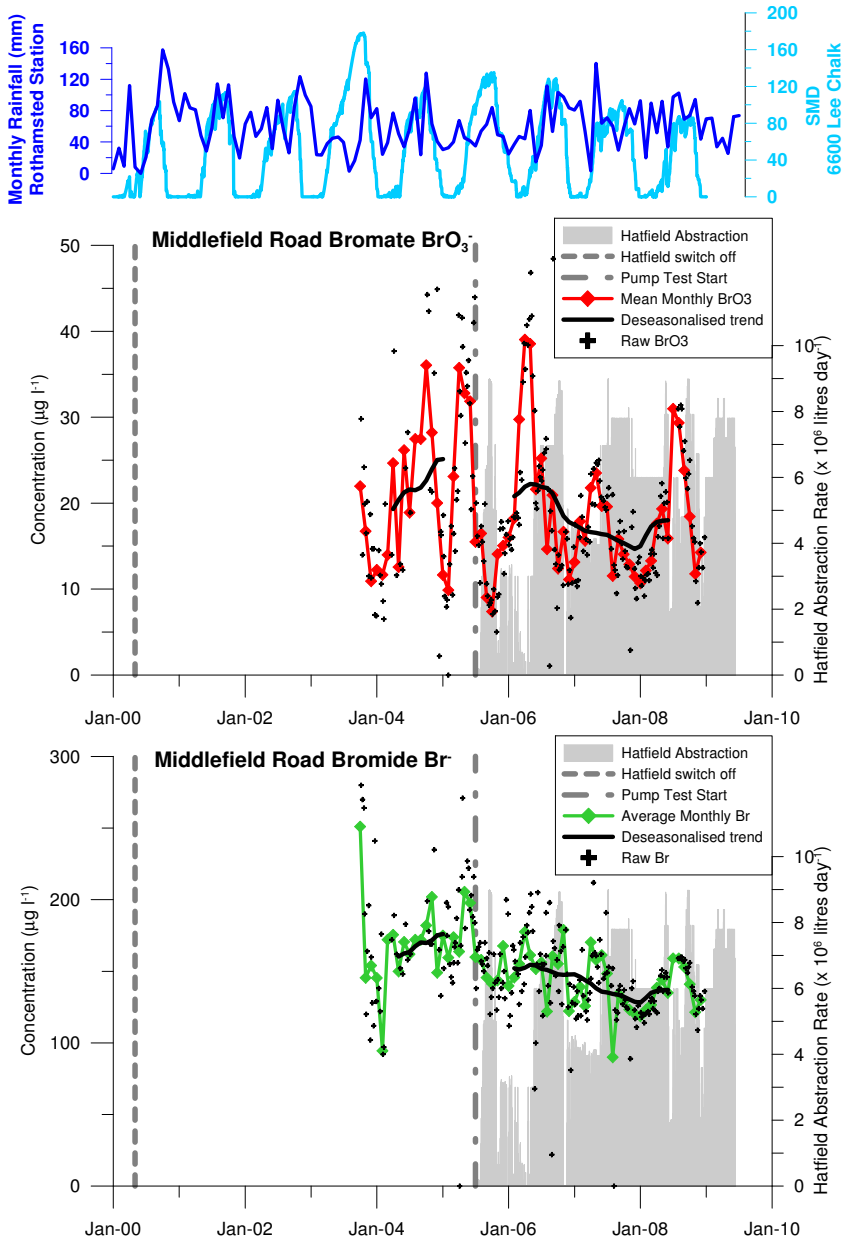

Figure 3.16: Time series of bromate and bromide concentrations at Middlefield Road PS, soil moisture deficit, and monthly rainfall.

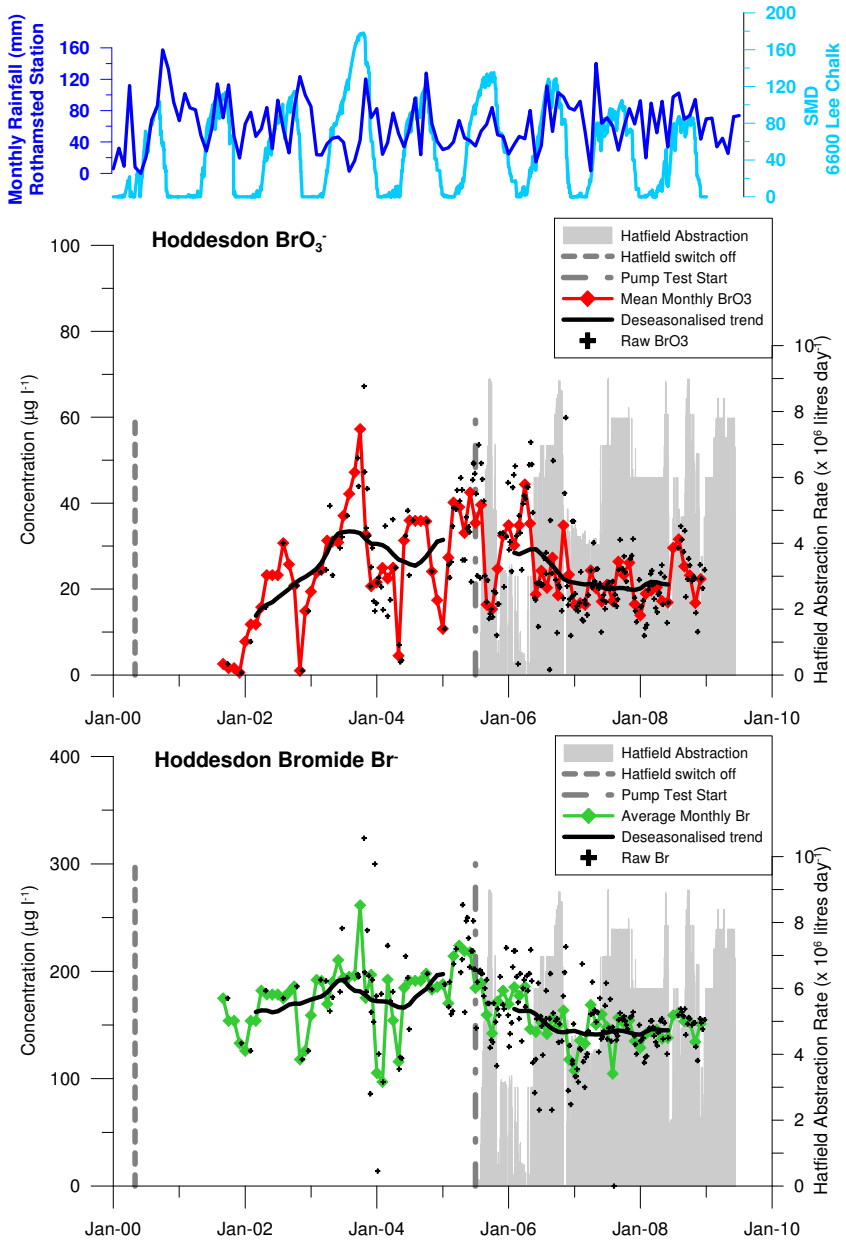

Figure 3.17: Time series of bromate and bromide concentrations at Hoddesdon PS, soil moisture deficit, and monthly rainfall.

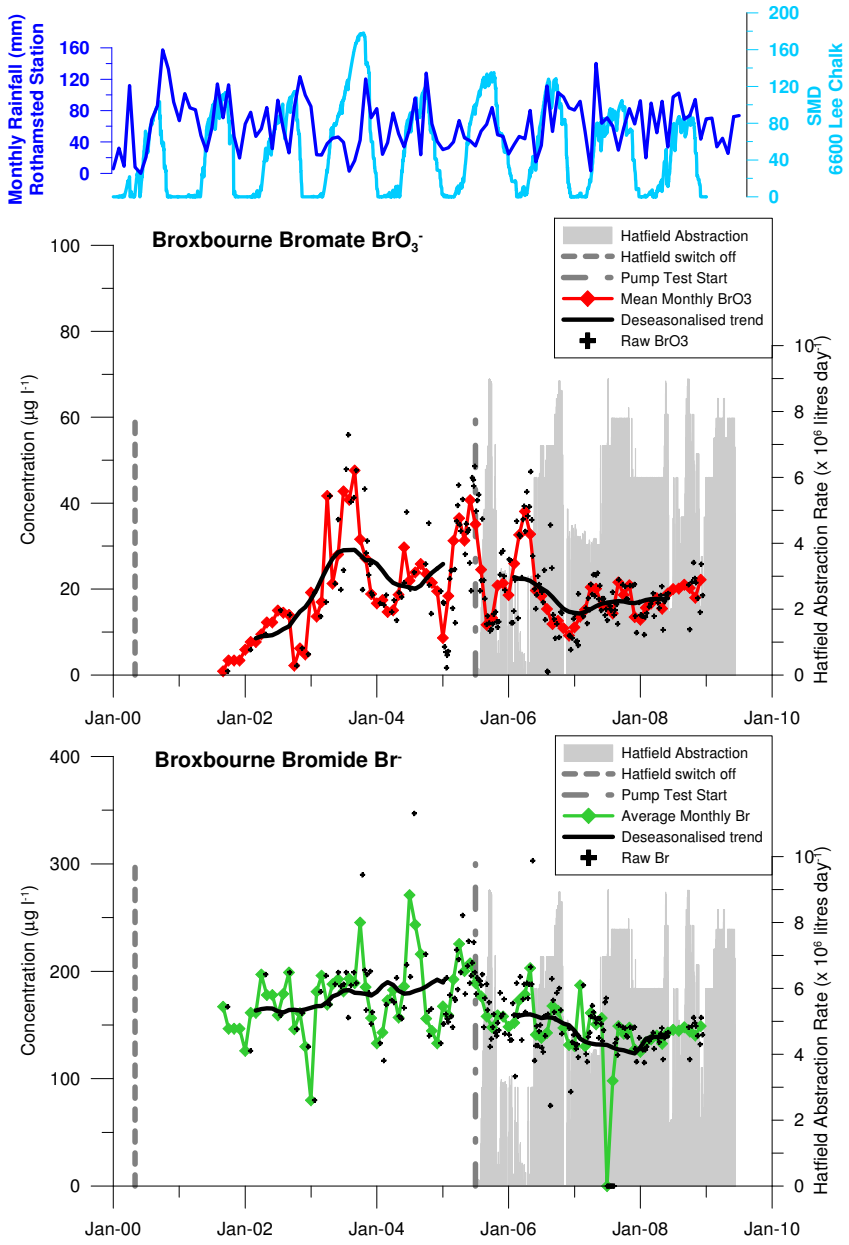

Figure 3.18: Time series of bromate and bromide concentrations at Broxbourne PS, soil moisture deficit, and monthly rainfall.

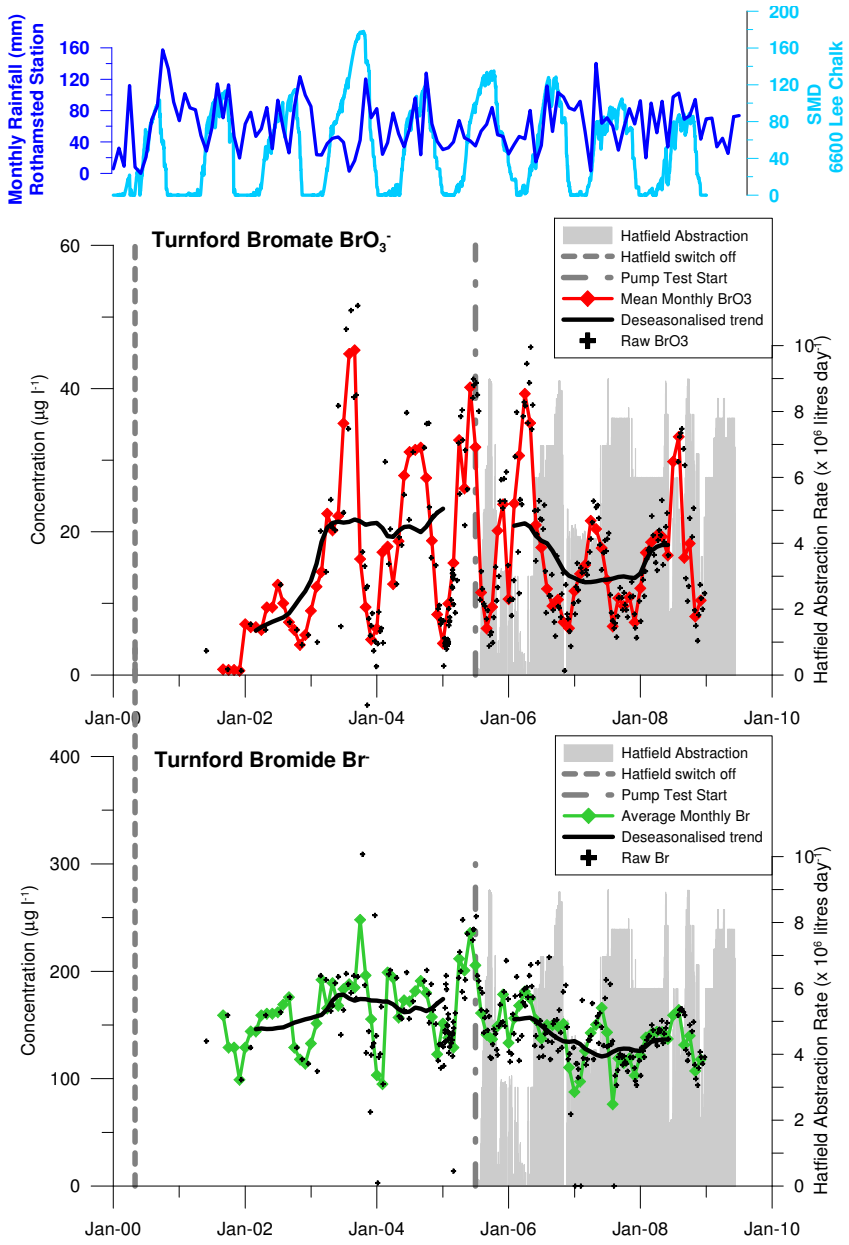

Figure 3.19: Time series of bromate and bromide concentrations at Turnford PS, soil moisture deficit, and monthly rainfall.

ure 3.13), Amwell Marsh (Figure 3.14) and Rye Common (Figure 3.15) sources follow a similar pattern. Maximum concentrations for each cycle occur in the spring months (March, April, May) and lowest concentrations occur in the autumn months between September and December. However, a second peak occurs in 2004 during September, October and November followed by a trough in December or January. The Hatfield pumping trial begins at the end of July when bromate concentrations are on the downward limb of the seasonal cycle. The seasonal cycle appears to continue, with peak concentrations occurring in April and concentrations declining to a trough in October, and appears to continue through 2007 and 2008.

The Hoddesdon (Figure 3.17), Broxbourne (Figure 3.18) and Turnford (Figure 3.19) sources show a slightly different seasonal trend. Maximum concentrations occur slightly later in summer and early autumn (June, July, August, September) with a more rapid decline to minimum concentrations in winter (November, December, January). The Hatfield pumping trial begins at the end of July when bromate concentrations are at their peaks. Concentrations appear to be rapidly decreased during pumping. The seasonal cycle appears to be perturbed, with peaks occurring in April, earlier than expected and during the period that pumping at Hatfield was suspended, and the falling limb occurring earlier over May and June when pumping was resumed. However, the seasonal cycle is resumed during the prolonged periods of pumping in 2007 and 2008.

3.5.5.3 General Trends

For Hatfield the deseasonalised trend indicates an overall increasing trend in bromate concentrations between 2000 and July 2005, although mean concentrations appear to level off in 2006, and there is an indication of an overall decrease in concentrations by December 2006. Since then the variation in bromate concentrations about the average trend has increased dramatically. For Essendon, the seasonal variation is superimposed on an overall rise in bromate concentration, which is clearly indicated by the 'deseasonalised' trend line. Between July 2005 and October 2007 there is a general decline in bromate concentrations with a few peaks, corresponding to periods of non-pumping from Hatfield. Between October 2007 and December 2008 concentrations appear to level off, with an indication of a slight rise in bromate concentrations from January 2008.

For the NNR wells the overall trends in bromate concentrations since the beginning of 2002 indicate a general increase from 2002 until mid 2003. Subsequently, concentrations appear to level off, albeit with fluctuations. The trend lines then show an increasing trend through the late 2004 and into 2005 (with the exception of Amwell Marsh where concentrations continue to decline into 2005). Concentrations generally fall with the start of pumping from Hatfield at the end of July 2006. In February and March 2006 all NNR sources show a significant rise corresponding to the period when pumping was suspended at Hatfield. Concentrations fall once again in May 2006 following the Hatfield switch on. The trend lines for bromate concentrations show a general increase from late 2006-early 2007 until the end of 2008, with concentrations approaching those seen prior to the start of the pumping trial (and higher in the case of Middlefield Road).

3.5.5.4 Relationship to Soil Moisture Deficit (SMD)

Figures 3.10 to 3.19 indicate that prior to the start of the Hatfield pumping trial (29 July 2005) the seasonal cycle of bromate concentrations follows the seasonal cycle of soil moisture deficit (SMD). For Essendon the relationship is particularly apparent (L. Lytton, *pers. comm.*) . Seasonal peaks in bromate concentrations correspond to peaks in SMD, i.e. higher bromate concentrations at Essendon correspond to dry conditions (high SMD). Prior to the start of Hatfield pumping, the time series for Turnford, Broxbourne, Hoddesdon, Rye Common and Middlefield Road show a similar trend, although generally the peaks in SMD are offset slightly from the peaks in bromate concentrations and occur approximately 2 months later. For the more northerly NNR wells Amwell Marsh and Amwell Hill, SMD peaks generally occur 3-4 and 4-6 months later than bromate concentration peaks.

The strength of the correlations between seasonal bromate concentrations and SMD before the start of the Hatfield Pumping trial were assessed by comparing departures from the 'deseasonalised' trend lines with monthly SMD data. Time lags were assessed by comparing monthly concentrations with SMD for the previous month, two months previously etc. The correlation coefficients are summarised in Table 3.5. Essendon and the southern NNR wells (Hoddesdon, Broxbourne, Turnford) show a similar relationship to SMD. The northern NNR wells (Amwell Hill, Amwell Marsh, Rye Common) show a more delayed response to SMD.

Table 3.5: Pearson correlation coefficients for Bromate concentration and Soil Moisture Deficit (SMD) before the start of the Hatfield pumping trial on 29th July 2005. SMD-X corresponds to the SMD value X months previously. Shaded cells indicate the strongest relationship.

	SMD	**SMD-1**	**SMD-2**	**SMD-3**	**SMD-4**	**SMD-5**	**SMD-6**
Hatfield	0.270 *0.055*	0.529 *0.000*	0.613 *0.000*	0.501 *0.000*	0.290 *0.039*	0.008 *0.956*	-0.255 *0.070*
Essendon	0.818 *0.000*	0.607 *0.000*	0.246 *0.082*	-0.097 *0.500*	-0.353 *0.011*	-0.531 *0.000*	-0.618 *0.000*
Amwell Hill	-0.460 *0.005*	-0.642 *0.000*	-0.677 *0.000*	-0.514 *0.002*	-0.199 *0.253*	0.118 *0.499*	0.336 *0.048*
Amwell Marsh	0.119 *0.497*	-0.207 *0.233*	-0.471 *0.004*	-0.567 *0.000*	-0.513 *0.002*	-0.380 *0.024*	-0.199 *0.253*
Middlefield Rd	0.569 *0.086*	0.682 *0.030*	0.456 *0.186*	-0.002 *0.995*	-0.254 *0.479*	-0.352 *0.319*	-0.431 *0.214*
Rye Common	0.225 *0.195*	0.054 *0.759*	-0.110 *0.530*	-0.273 *0.112*	-0.353 *0.037*	-0.368 *0.030*	-0.315 *0.065*
Hoddesdon	0.787 *0.000*	0.547 *0.001*	0.171 *0.326*	-0.136 *0.437*	-0.321 *0.060*	-0.449 *0.007*	-0.557 *0.001*
Broxbourne	0.700 *0.000*	0.396 *0.018*	0.070 *0.691*	-0.213 *0.219*	-0.445 *0.007*	-0.595 *0.000*	-0.536 *0.001*
Turnford	0.672 *0.000*	0.341 *0.045*	-0.056 *0.749*	-0.350 *0.039*	-0.505 *0.002*	-0.610 *0.000*	-0.595 *0.000*
key	Pearson correlation *P-value*						

After the start of pumping at Hatfield, for the majority of the monitored source wells, the relationship between bromate concentration and SMD is not as strong, and in many cases appears contrary to previous years. This is especially noticeable at Essendon, Hoddesdon, Broxbourne and Turnford where a peak in bromate concentration between March and May 2006 is associated with low SMDs. However, as discussed further in Section 3.5.6.5, this is also associated with the period when Hatfield was switched off and therefore likely to indicate a rebound in bromate concentrations which were lowered by pumping at Hatfield.

3.5.6 Bromate and Bromide: Relationship to Hatfield abstraction rates

3.5.6.1 General Trends

Bromate (as BrO_3^-) and bromide (as Br^-) concentrations for the Hatfield, Essendon and the NNR sources are shown alongside abstraction rates from the Hatfield source in Figures 3.10 to 3.19. Examination of the bromate concentrations at Hatfield over the period of the pumping trial indicates that the abstraction rate from Hatfield influences the concentration at the Hatfield source. In general, the highest rates of pumping correspond to the lowest concentrations of bromate recorded. Following periods of non-pumping, there are considerable rises in concentration to pre-pumping levels. Concentrations fall as pumping is resumed. Bromide concentrations follow a similar pattern as bromate concentrations.

Concentrations of bromate and bromide at Essendon appear to be influenced by changes in Hatfield abstraction rate in a similar way to concentrations at Hatfield. The pump test begins in July 2005, on the rising limb of the usual seasonal trend. The expected rise to September/October is not seen and concentrations are rapidly decreased. The seasonal component is much less consistent after the start of the pumping test. A peak in bromate concentrations occurs between March and May 2006 associated with the period that pumping at Hatfield was suspended, and contrary to the trend before the Hatfield pumping trial (Sections 3.5.5.2 and 3.5.5.4). Therefore, variations in pumping rate appear to be the dominant influence on bromate concentration. The relationship between pumping rates and bromate concentrations is discussed further in Section 3.5.6.5. The rising trend appears to be curtailed by the pumping test. There is an indication of an overall decreasing trend between August 2005 and December 2006. Maximum concentrations (which occur during times of non-pumping) have not risen to the projected trend line if it is projected until December 2006. However, the general trend appears to level off in January 2007, and even increase slightly from December 2007 through until the end of 2008, despite relatively consistent high rates of abstraction from Hatfield during this period.

Concentrations of bromate measured at the Northern New River (NNR) sources appear to follow a similar pattern to Hatfield bromate concentrations, and show a general decrease in response to increased abstraction rates from Hatfield. There appears to be a time lag of 3-5 days between turning off of Hatfield abstraction and a noticeable rise in bromate concentration, or between resuming abstraction at Hatfield and a noticeable fall in bromate concentration. For a number of NNR sources, bromate concentrations show a more marked decline during the second phase of the test from May to October 2006. This may be attributable to the heavy rainfall in May 2006.

The highest bromate concentrations at the NNR wells are recorded at Hoddesdon, Turnford and

Broxbourne which show concentrations between 10 μg l^{-1} and 50 μg l^{-1}. Rye Common, Amwell Hill and Amwell Marsh show concentrations between 5 μg l^{-1} and 20 μg l^{-1}. Amwell End, Broadmeads, and Chadwell Spring show bromate concentrations less than 0.6 μg l^{-1} for much of the test. These three sources are the most northerly of the NNR sources. Bromate concentrations at Amwell End remain less than 0.6 μg l^{-1} throughout the period of the test. Bromate concentrations at Broadmeads rise above 0.6 μg l^{-1} on three occasions throughout the test to 1.1, 1.3 and 1.5 μg l^{-1}, although these rises occur at separate times which do not appear to be associated with changes in pumping rates. Bromate concentrations at Chadwell Spring drop below detection limits during the periods of high pumping rates, and rise to maximum of 3.3 μg l^{-1} in March and April 2006. For these three sources bromide concentrations do not appear to show a response to the changes in Hatfield abstraction rate.

As with Essendon, the seasonal relationship between bromate concentration and SMD at Hoddesdon, Broxbourne and Turnford appears to be perturbed by the effect of abstraction at Hatfield. Peaks in bromate concentration occur in April, earlier than in previous years and during the period when pumping at Hatfield was suspended, and the falling limb occurs over May and June, earlier than in previous years and when pumping was resumed. For Amwell Hill, Amwell Marsh and Rye Common, the expected peak concentration occurs during the spring months (March, April, May) which coincides with the period when Hatfield was switched off.

3.5.6.2 Data processing and Statistical Methodology

The abstraction rate at Hatfield for the day corresponding to the bromate and bromide sample was selected. Bromate and bromide concentrations for each source well were compared to abstraction rates from Hatfield and also abstraction rates from that particular source. Linear regression was undertaken using Hatfield abstraction rate as a predictor. Statistical summary tables are included in Appendix C.

For the regression analysis, bromate concentrations for the each of the source wells were first compared to Hatfield abstraction rate for the same day as the sample was taken (day T), and then sequentially to abstraction rates for the previous days (day $T-1$, $T-2$, $T-3$ *etc.*). At each stage the strength of the relationship was assessed by examining the fitted line scatter plot, the F-statistic and associated P-value to determine the significance of the relationship, the standard error of the regression as a measure of the dispersion of the data around the regression line, and the R^2 value as a measure of the proportion of the variation in the response (y) variable that is accounted for the variation in the explanatory variable (x). The combination of these parameters was used to select the time lag for Hatfield pumping rate that produced the best predictor variable for bromate concentration at each source well. The residuals for this 'best fit' regression relationship were examined to assess whether the assumptions of linear regression (Section 3.5.6.3) were adhered to and therefore if the regression relationship could be used for further hypothesis testing.

Where the regression relationship was deemed to conform to the assumptions, the hypothesis that the coefficient of the regression line was significantly different from zero was tested by examining the t-statistic and associated P-value from the Minitab output.

3.5.6.3 Assumptions of linear regression

R^2 is a measure of the percent of the variation in the response (y) variable that is accounted for by the variation in the explanatory variables. The F-statistic determines if the regression relationship is statistically significant, *i.e.* that the apparent relationship between y and x is not likely to arise due to chance alone. However, a large R^2 or a significant F-statistic does not guarantee that data have been fitted well.

In order to predict y (and a variance for the prediction) for a given x, it is assumed that the y variable is linearly related to x and that data used to fit the model are representative of data of interest. However, in order to test hypotheses (such as whether the slope significantly differs from zero, or estimate confidence or prediction intervals from the linear regression, the following assumptions are also necessary (Helsel and Hirsch, 1993):

- the variance of the residuals is constant (homoscedastic), *i.e.* it does not depend on the x or on anything else (*e.g.* on time);
- the residuals are independent;
- the residuals are normally distributed.

Plots of residuals versus predicted values can indicate heteroscedasticity of the residuals, and the normality of residuals can be checked by a normal probability plot. A plot of residuals against time can indicate correlations between residuals over time.

3.5.6.4 Source Abstraction Rate

Fitted line plots for bromate concentration at each source well versus abstraction rate at the same source for the period of the pumping test are shown in Appendix C. Plots are not shown for Amwell End and Broadmeads because concentrations remained below detection limits throughout the period of the pumping trial. A number of the NNR wells showed apparently statistically significant regression relationships. However, inspection of the fitted line plots indicate that the lines are strongly influenced by the uneven spread of the data points, with points available for a limited range of abstraction rates. It is therefore difficult to be confident in these apparent relationships. Data are available over a much wider range of abstraction rates at the Essendon source. At Essendon the data points show large variability, and there is no clear relationship between bromate concentrations and Essendon abstraction rates. Source abstraction rate was not considered as a predictor in further regression analysis because of the likely influence of uneven distribution of data points on the correlation.

3.5.6.5 Hatfield Abstraction Rate

Fitted line plots for the 'best-fit' relationship (Section 3.5.6.2) and plots of residuals are included in Appendix C. The regression parameters are summarised in Table 3.6.

Analysis of the residuals of the regression lines (Figure 3.5.6.5 and 3.5.6.5) indicates that the regression lines do not conform to the assumptions of linear regression for two main reasons:

1. variation in the residuals is larger for larger fitted values (lower pumping rates);

Source	Time Lag	Linearity of relationship[1]	Residuals			Adherence to Assumptions of Linear Regression?
			Homoscedasticity[2]	Independence[3]	Normality[4]	
For equation Bromate = A + B(Hat abst)						
Hatfield	0 days	Although there is a lot of scatter about the line, a linear relationship describes the 'average' data trend reasonably well.	The variation of the residuals is reasonably constant.	Seasonality is not evident in the residuals.	Residuals follow the normal line well.	✓
Including SMD						✓
Essendon	2 days	Although there is a lot of scatter about the line, a linear relationship describes the 'average' data trend reasonably well.	Reasonably constant, although slightly less for smaller fitted values.	Weak seasonality may be present in the residuals: the most positive residuals are generally associated with higher SMD and vice versa.	Residuals follow the normal line well.	✓ Reasonable, but may need to add seasonal term to equation
Including SMD				Residuals are still correlated with date. The most positive residuals tend to occur between July 2005 and June 2006.		✓ Reasonable, but still dependent on date.
Amwell Marsh	6 days	Although there is a lot of scatter about the line, a linear relationship describes the 'average' data trend reasonably well.	The variation of the residuals is reasonably constant, although slightly less for smaller fitted values and more variation between July 2005 and June 2006.	Seasonality is evident with positive residuals in the winter/spring and negative residuals in the summer/autumn.	Residuals show slight departure from normality.	× May need to add seasonal term
Including SMD				Residuals are still associated with date.		× Still correlation with date
Hoddesdon	4 days	Although there is a lot of scatter about the line, a linear relationship describes the 'average' data trend reasonably well.	The variation of the residuals is reasonably constant, although slightly less for smaller fitted values and more variation between July 2005 and June 2006.	Slight seasonality present.	Residuals follow the normal line well.	✓ Reasonable, but may need to add seasonal term to equation
Including SMD				Seasonality is not evident in the residuals.		✓ Reasonable, but still dependent on date.
Broxbourne	5 days	Although there is a lot of scatter about the line, a linear relationship describes the 'average' data trend reasonably well.	The variation of the residuals is reasonably constant, although slightly less for smaller fitted values and more variation between July 2005 and June 2006.	Slight seasonality present.	Residuals follow the normal line well.	✓ Reasonable, but may need to add seasonal term to equation
Including SMD				Residuals are still associated with date.		✓ Reasonable, but still dependent on date.
Turnford	4 days	Although there is a lot of scatter about the line, a linear relationship describes the 'average' data trend reasonably well.	The variation of the residuals is reasonably constant, although slightly less for smaller fitted values.	Seasonality is evident with positive residuals in the winter/spring and negative residuals in the summer/autumn.	Residuals show slight departure from normality.	× May need to add seasonal term
Including SMD			The variation of the residuals is reasonably constant.	Residuals are still associated with date.		× Still correlation with date

[1] Inspection of fitted line scatter plots
[2] Inspection of residuals versus fits plots
[3] Inspection of residuals versus order plot
[4] Inspection of normal probability plot

Figure 3.20: Assessment of residuals for each 'best-fit' regression for the response of bromate concentration to Hatfield abstraction rate. (1)

Source	Time Lag	Linearity of relationship[1]	Residuals			Adherence to Assumptions of Linear Regression?
			Homoscedasticity[2]	Independence[3]	Normality[4]	
For equation Log(Bromate) = *A* + *B*(Hat abst)						
Chadwell Spring	6 days	There is more variation at low pumping rates, however the position of the line looks reasonable.	Variation is less for smaller fitted values and less variation between July 2005 and June 2006.	Seasonality is evident with positive residuals in the winter/spring and negative residuals in the summer/autumn.	Residuals follow the normal line well.	× May need to add seasonal term
Including SMD				Residuals are still associated with date.	Residuals show slight departure from normality.	× Still correlation with date
Amwell Hill	5 days	There is more variation at low pumping rates, however the position of the line looks reasonable.	The variation of the residuals is reasonably constant, although more for positive residuals.	Seasonality is evident with positive residuals in the winter/spring and negative residuals in the summer/autumn.	Residuals show departure from normality.	× May need to add seasonal term
Including SMD			The variation of the residuals is reasonably constant.	Residuals are still associated with date.	Residuals follow the normal line well.	× Still correlation with date
Middlefield Road	8 days	Although there is a lot of scatter about the line, a linear relationship describes the 'average' data trend reasonably well.	The variation of the residuals is reasonably constant, although slightly less for smaller fitted values.	Slight seasonality present.	Residuals show slight departure from normality.	✓ Reasonable, but may need to add seasonal term to equation
Including SMD				Residuals are still associated with date.		✓ Reasonable, but still dependent on date.

[1] Inspection of fitted line scatter plots
[2] Inspection of residuals versus fits plots
[3] Inspection of residuals versus order plot
[4] Inspection of normal probability plot

Figure 3.21: Assessment of residuals for each 'best-fit' regression for the response of bromate concentration to Hatfield abstraction rate. (2)

Table 3.6: Summary of regression parameters for the 'best-fit' regressions for the response of bromate concentration to Hatfield abstraction rate.

Source	Time lag[a]	R^2	Standard error	P-value[b]	R^2 Hat abst	R^2 SMD
For equation Bromate = A + B(Hat abst) + C(SMD)						
Hatfield	0 days	33.3%	39.44	0.000	29.0%	4.3%
Essendon	2 days	49.0%	5.00	0.000	38.1%	10.9%
Amwell Marsh	5 days	39.5%	3.45	0.000	21.7%	17.8%
Rye Common	7 days	4.9%	6.52	0.020	3.2%	1.7%
Hoddesdon	4 days	30.2%	9.17	0.000	24.6%	5.6%
Broxbourne	5 days	27.1%	7.20	0.000	26.1%	1.0%
Turnford	4 days	14.0%	8.71	0.000	13.8%	0.2%
For equation Log(Bromate) = *A* + *B*(Hat abst)						
Chadwell Spring	6 days	14.0%	0.311	0.000	11.9%	2.1%
Amwell Hill	5 days	55.1%	0.228	0.000	4.6%	50.5%
Middlefield Rd	8 days	7.5%	0.200	0.002	7.1%	0.4%

[a] time lag refers to the number of days between the Hatfield abstraction rate and the strongest response in source bromate concentration.
[b] The P-value refers to the hypothesis that the regression relationship is statistically significant, i.e. that the apparent relationship between y and x is not likely to arise due to chance alone.

2. seasonality is evident in the residuals.

Heteroscedasticity in the residuals was improved in the majority of cases by transforming the data by taking logarithms of bromate concentrations (as recommended in Helsel and Hirsch 1993).

Seasonality was apparent in the majority of the NNR wells, and at Essendon. Therefore, SMD was included as a predictor in the regression relationship. In general, including SMD as a predictor in the regression increased the amount of variation explained by the regression (increased the value of R^2).

The residuals showed correlation to SMD. Positive residuals, indicating that observed bromate concentrations are above the fitted regression line, generally occur when SMD is low (winter and spring), and negative residuals, indicating that observed bromate concentrations are below the fitted regression line, generally occur when SMD is high (summer and autumn). This appears to be contrary to the relationship observed between bromate concentration and SMD prior to the start of the Hatfield pumping test (Section 3.5.5.2). Positive residuals occur earlier than the expected seasonal peak in bromate concentrations. For Essendon, the normal relationship of positive residuals with low SMD and negative residuals with high SMD occurred.

However, the residuals are also dependent on date, even after the inclusion of SMD. It is apparent that the most positive residuals occur mainly during the period between January 2005 and May 2006 and the period over November 2006 when the Hatfield pumping test was suspended for prolonged periods and only sporadic abstraction at rates less than 3 $\mathrm{Ml\ day^{-1}}$ occurred for sampling purposes. The positive residuals may therefore reflect a rebound in bromate concentrations after a reduction due to the effects

of pumping. The fact that the positive residuals become less positive and more negative when pumping was resumed in May 2006, and are negative between August 2005 and December 2005 and between May 2006 and December 2006 when prolonged periods of higher abstraction rates occurred, indicates that the effect of Hatfield abstraction rate on bromate concentration appears to dominate the seasonal relationship between SMD and bromate concentration. The apparently contrary relationship between bromate concentrations and SMD may therefore be an artefact of the timing of the abstraction rate variations at Hatfield.

The relative effect of SMD and Hatfield abstraction rate is difficult to measure due to the timing of the abstraction rate variations at Hatfield. The SMD curves reach their seasonal trough between January and April 2006. The Hatfield pumping test was suspended between January 2005 and May 2006 and only sporadic abstraction at rates less than 3 $\mathrm{Ml\ day^{-1}}$ occurred for sampling purposes. The higher abstraction rates occurred from August 2005 to December 2005 and May 2006 to December 2006 when SMD was in the higher part of its seasonal cycle. This results in an apparent positive correlation between Hatfield abstraction rate and SMD. In order to separate these two effects it would be necessary to maintain more constant abstraction rates at Hatfield over the full cycle of SMD variations.

A more constant period of abstraction occurred between November 2007 and June 2008, when abstratction rates were maintained at relatively consistent high values of $\sim 6\ \mathrm{Ml\ day^{-1}}$to $\sim 8\ \mathrm{Ml\ day^{-1}}$. Residuals still tend to show seasonal variations, which suggests that other seasonal variables are important in controlling bromate concentrations.

The effect of rainfall is also complicated as a result of its relationship to abstraction rate at Hatfield. Sewer surcharging events in response to heavy rainfall caused Hatfield abstraction to cease. As a result, the abstraction rate at Hatfield is heavily influenced by rainfall in the catchment.

3.5.6.6 Testing the hypothesis of direct control by pumping at Hatfield

On the basis of the analysis of residuals and the discussion of seasonal variables, Hatfield, Essendon, Broxbourne, Hoddesdon, Turnford, Middlefield Road and Rye Common were considered to adhere to the assumptions of linear regression reasonably well to allow an estimation of confidence intervals and hypothesis testing. In this way, the statistical analysis was applied to test the controlling effect of Hatfield pumping on bromate occurrence at particular sites, to quantify the time lag before the effect is observed, and to assess if the gradient of the regression relationship differs between sources.

Mean coefficients along with upper and lower 95% confidence intervals are given in Table 3.7. For the response of bromate concentration to Hatfield abstraction rate, the null hypothesis that the coefficient of the regression is equal to zero can be rejected at a significance level of 0.001 for Hatfield, Essendon, Hoddessdon, Broxbourne and Turnford. Therefore a significant linear correlation exists between bromate concentration and Hatfield abstraction rate for these source wells. The regression equations indicate that an increase in Hatfield pumping rate of 1 $\mathrm{Ml\ day^{-1}}$ would result in a predicted decrease in bromate concentration of 1.2 $\mu\mathrm{g\ l^{-1}}$ to 2.2 $\mu\mathrm{g\ l^{-1}}$ at the abstracting sources (with the specified time lag). For the response of bromate concentration to soil moisture deficit (SMD), the null hypothesis that the coefficient of the regression is equal to zero can be rejected at a significance level of 0.001 for Hatfield, Essendon,

and Hoddessdon only. Therefore a significant linear correlation exists between bromate concentration and SMD for these source wells.

Table 3.7: Coefficients determined by the 'best-fit' regressions for the response of bromate concentration to Hatfield abstraction rate.

Source	Time lag[a]	Mean Coefficient B	P-value[b]	Upper 95.0% CI	Lower 95.0% CI	Mean Coefficient C	P-value[b]	Upper 95.0% CI	Lower 95.0% CI
For equation	**Bromate = A + B(Hat abst) + C(SMD)**								
Hatfield	0 days	-12.50	**0.000**	-14.06	-10.94	0.245	**0.000**	0.161	0.329
Essendon	2 days	-1.66	**0.000**	-1.86	-1.46	0.054	**0.000**	0.042	0.067
Rye Common	7 days	-0.35	0.076	-0.73	0.03	-0.021	0.098	-0.045	0.004
Hoddesdon	4 days	-2.19	**0.000**	-2.72	-1.65	0.060	**0.001**	0.027	0.094
Broxbourne	5 days	-1.65	**0.000**	-2.11	-1.19	0.020	0.170	-0.009	0.049
Turnford	4 days	-1.19	**0.000**	-1.69	-0.68	-0.009	0.576	-0.042	0.023

[a] time lag refers to the number of days between the Hatfield abstraction rate and the strongest response in source bromate concentration

[b] The P-value refers to the hypothesis that the slope of the regression line is significantly different from zero. [The p-value is the probability of obtaining a result at least as extreme as that obtained by chance alone, assuming the truth of the null hypothesis (coefficient = 0).] Values in **bold type** indicate that the null hypothesis can be rejected at a significance level of 0.05 or less.

Figure 3.22 compares the mean and 95% confidence intervals for the coefficients determined by the linear regression for Essendon, Broxbourne and Hoddesdon. The confidence interval for Essendon is smaller than for Broxbourne and Hoddesdon and Turnford. The confidence intervals all overlap, indicating that the differences in mean coefficients are not statistically significant at a 95% confidence level. Therefore, the gradient of the relationships between bromate concentration and Hatfield abstraction rate for the monitored sources apart from Hatfield do not appear to differ significantly between each source.

3.5.7 Statistical relationships and bromate transport in Hertfordshire

Statistical analysis of the time lag between a change in abstraction rate at Hatfield PWS and the observed change in bromate concentrations at down-gradient locations (Section 3.5.6.5) indicates comparable times to the peak response times determined by Cook (2010) from the tracer test travel times from the Mymmshall Brook catchment (Figure 3.23).

The inferred arrangement of the conduit system (Section 3.2.6) connects the three regions Hatfield PWS, Water End and the major abstraction wells and springs in the Lee Valley along the main route of karst flows. Therefore, 'scavenge pumping' at Hatfield PWS appears to influence flows within the karst system via a direct connection, which in turn influences the observed concentration of bromate observed at the Lee Valley wells and springs. Karst flow paths are likely to be intersecting bromate affected groundwater in the Hatfield area. Tracers from Comet Way borehole suggest a by-pass of Hatfield PWS by karst flow paths in this area (Section 3.2.6). If, as seems likely, bromate is entering the karst flow system to the North and East of the Comet Way borehole, the by-pass of Hatfield PWS by karst flow paths implies that scavenge pumping at Hatfield PWS may only be having a partial influence on down-gradient

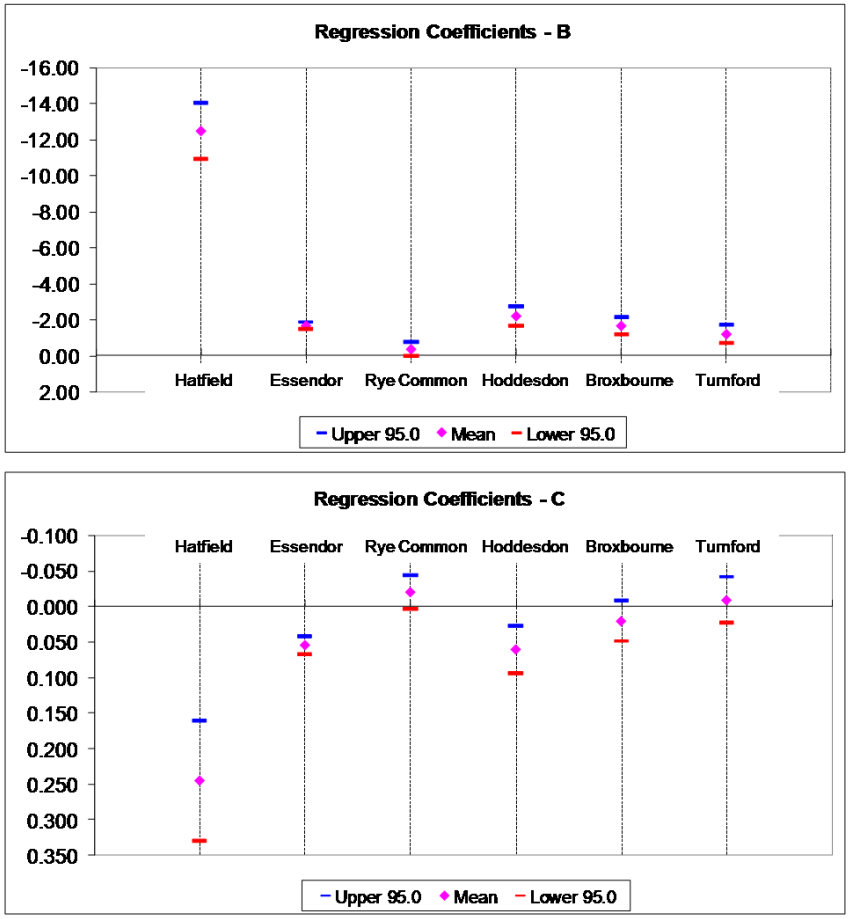

Figure 3.22: Regression coefficients: means and 95% confidence intervals

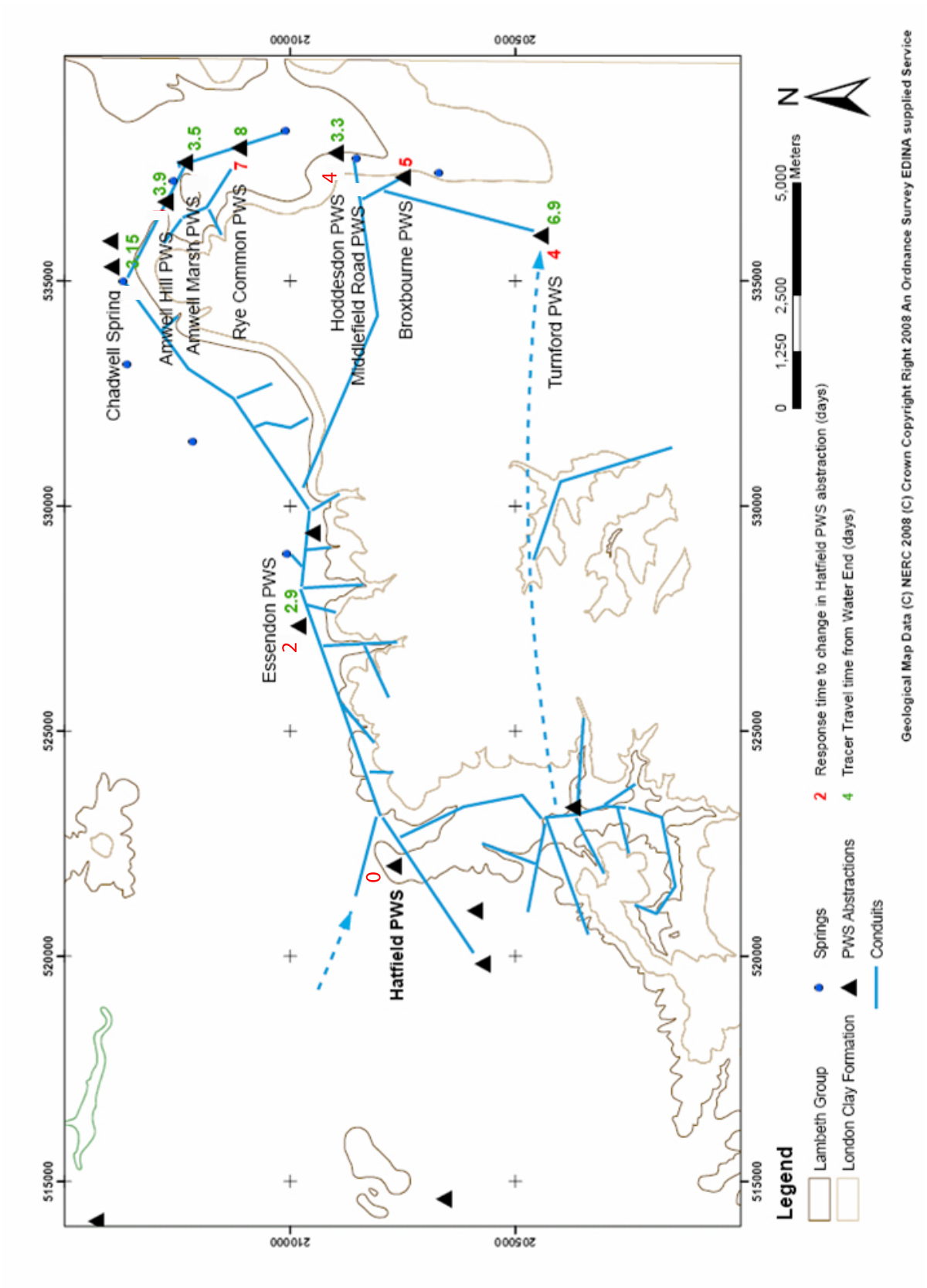

Figure 3.23: Comparison of statistical response times for bromate concentration response to hatfield abstraction and tracer travel times from Water End. Based on Cook (2010)

concentrations (Cook, 2010).

Essendon PWS responds fastest to both abstraction at Hatfield PWS and tracer arrival as might be expected given its closest proximity. Next to respond after four days are Amwell Hill PWS and Turnford PWS, situated at the apparent northern and southern boundaries of the bromate affected area. Changes in concentration then propagate towards the central part of the Lee Valley, the area around Rye Common responding slowest. Cook (2010) suggests that the spatial pattern of response could reflect a partial de-watering of minor conduits and flow paths which diverge from the main transport routes. The more marginally affected areas in the Lee valley respond fastest whilst the major flow paths, carrying the most water and therefore greatest bromate load being least and slowest affected.

3.6 Single borehole dilution testing

A series of single borehole dilution tests (SBDT) within existing boreholes in the Hertfordshire Chalk were undertaken during 2008. These single borehole dilution tests were undertaken in conjunction with the programme of point-to-point Natural Gradient Tracer Testing using Bacteriophage which are described by Cook (2010).

The objectives of the SBDTs were:

- To determine the hydraulically active horizons within the selected boreholes in order to guide injection strategies for the natural gradient point-to-point tracer testing;
- To use uniform injection SBDTs to obtain a direct measurement of horizontal specific discharge (Darcy velocity);

Detailed methodology and interpretation of the results is included in Appendix D. The determination of horizontal darcy velocities is described within this Section.

Horizontal specific discharge (Darcy Velocity) was determined (according the the methodology outlined in Figure 3.24) for three locations within the study area (location numbers refer to Figure 4.1):

- Nashe's Farm BH (location **019**)
- Harefield House BH (location **226**)
- Comet Way BH (location **402**)

3.6.1 Calculation of horizontal specific discharge (Darcy Velocity)

3.6.2 Methodology

3.6.2.1 Nashe's Farm BH

The estimated horizontal specific discharge (Darcy velocity) at each 0.5 m depth section ranges from 3.0 $\mathrm{m\ d^{-1}}$ to 0.3 $\mathrm{m\ d^{-1}}$ (Figure 3.25). The highest values occur in the top 1.0 m below the water table (between 20.5 and 21.50 m bD). This corresponds to the horizon of increased borehole diameter (Appendix D). The high darcy velocities indicate that more rapid flow occurs in this area and the widening is indicative of a fissure. The inferred outflow horizon at 24.5 to 26.0 m bD corresponds to velocities of $\sim$0.5 to 0.6 $\mathrm{m\ d^{-1}}$, whereas the intervening sections show velocities of $\sim$0.4 to 0.5 $\mathrm{m\ d^{-1}}$.

Assumptions:

- The concentrations within the borehole remains uniform and equal to the concentration leaving the borehole;
- The concentration at time zero is instantaneously raised to ci;
- Water enters the borehole from an aquifer thickness equal to the screened or open length of the borehole - i.e. there is not vertical flow in the aquifer
- Water upstream of the borehole is at a uniform background concentration of cb; and
- The flow is steady state.

If these assumptions above are met, then the change in tracer mass in the borehole over a time interval Δt will be equal to the mass fluxes into and out of the borehole(Ward et al., 1998):

$$\pi R^2 L_{sat} \Delta C = q L_{scrn} \alpha D (c_b - c) \Delta t \tag{1}$$

where:

R	borehole radius
L_{sat}	saturated depth of borehole
ΔC	change in borehole concentration
q	Darcy velocity in the aquifer
L_{scrn}	open length of the borehole
α	ratio of the width of the aquifer contributing flow to the borehole to the borehole diameter (see figure)
D	borehole diameter ($2R$)
c_b	background aquifer concentration of tracer (often zero)

The above equation can be integrated from time zero (borehole concentration c_i) to any given time t (borehole concentration $c(t)$):

$$\pi R^2 L_{sat} \int_{c_i}^{c} \frac{dc'}{c_b - c'} = q L_{scrn} \alpha D \int_0^t dt' \tag{2}$$

which becomes

$$\pi R^2 L_{sat} \ln\left(\frac{c_b - c}{c_b - c_i}\right) = q L_{scrn} \alpha D t \tag{3}$$

Rearranging to make q the subject

$$q = \frac{\pi R^2 L_{sat}}{\alpha D t L_{scrn}} \ln\left(\frac{c_b - c}{c_b - c_i}\right) \tag{4}$$

The value of α can be anywhere in the range 0 to 8 (Klotz er al 1972), although where there is no gravel pack,

$$\alpha = 2$$

is usually sufficient.

Assuming $L_{sat} = L_{scrn}$, and since $D = 2R$, then

$$q = \frac{\pi R}{4t} \ln\left(\frac{c_b - c}{c_b - c_i}\right) \tag{5}$$

which can be arranged as

$$\ln\left(\frac{c - c_b}{c_i - c_b}\right) = -\frac{4qt}{\pi R} \tag{6}$$

Therfore, if field results are ploted as $\ln\left(\frac{c-c_b}{c_i-c_b}\right)$ against t, then the gradient m of the straight line graph $y = mx + c$ is given by $\frac{4q}{\pi R}$, and hence

$$q = \frac{\pi R m}{4} \tag{7}$$

Once the darcy velocity is determined from equation above, further parameters can be obtained from the following relationships:

$$q = -Ki \tag{8}$$

$$v = q/n_e \tag{9}$$

Figure 3.24: Methodology for determination of specific discharge (darcy velocity) from the results of the Single Borehole Dilution Tests. Based on Ward et al. (1998)

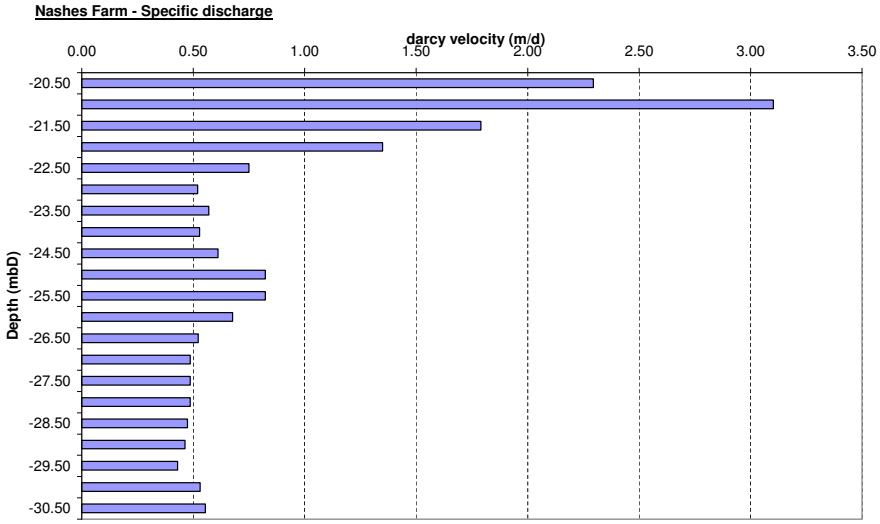

Figure 3.25: Specific discharge (darcy velocity) for each 0.5 m depth section at Nashes Farm. Estimated using the methodology in Figure 3.24. Plots of $\ln \frac{C_t - C_b}{C_0 - C_b}$ are included in Appendix D. The value at each section is estimated based on Based on Single Borehole Dilution test carried out at Nashes Farm 29 January 2008.

3.6.2.2 Comet Way BH

The estimated horizontal specific discharge (Darcy velocity) at each 0.5 m depth section ranges from 4.4 $\mathrm{m\ d^{-1}}$ to 14.7 $\mathrm{m\ d^{-1}}$ (Figure 3.26).

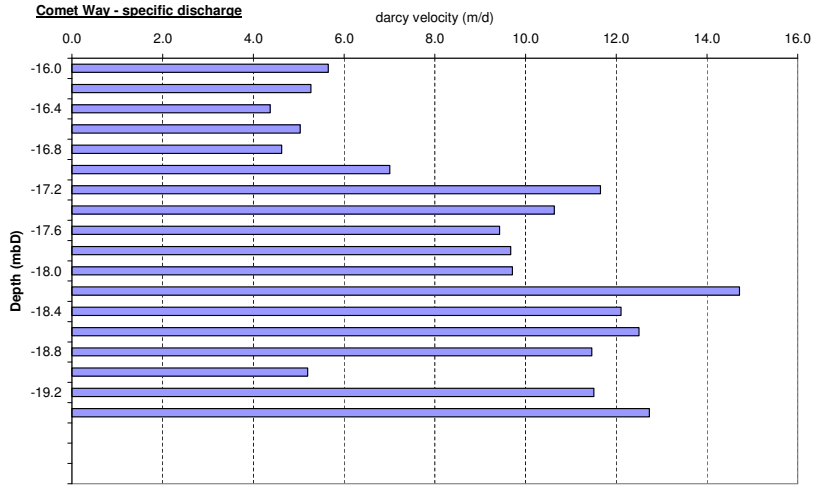

Figure 3.26: Specific discharge (darcy velocity) for each 0.5 m depth section at Comet Way BH. Estimated using the methodology in Figure 3.24. Plots of $\ln \frac{C_t - C_b}{C_0 - C_b}$ are included in Appendix D. The value at each section is estimated based on Based on Single Borehole Dilution test carried out at Comet Way BH 4 February 2008.

3.6.2.3 Harefield House BH

The estimated horizontal specific discharge (Darcy velocity) at each 0.5 m depth section ranges from 0.3 $\mathrm{m\ d^{-1}}$ to 1.3 $\mathrm{m\ d^{-1}}$ (Figure 3.27).

3.7 Conceptual Model for groundwater flow in Hertfordshire

The information and data reviewed, interpreted and analysed in this chapter have been used to develop a conceptual model for groundwater flow and bromate transport in the Hertfordshire Chalk aquifer (Figure 3.28). Between the source site in Sandridge and Hatfield, the flow of bromate contaminated water is in an east-south-easterly to south-easterly direction, following the hydraulic gradient. The nature of the Chalk in this area indicates a dominance of double-porosity characteristics, and consequently, bromate will be highly attenuated. There are some karstic rapid flow sections to the west of Hatfield, although these appear to be less well developed and/or connected than those along the Palaeogene boundary to the east of Hatfield, and consequently, flow rates are slower and attenuation of solutes is greater. To the east of Hatfield, there is a well developed main karst network, which follows the Palaeogene boundary. Flow in the karst network is likely to cause dispersion of the bromate contamination along the Lee Valley, approximately following the path of the conduit network, as far east as the northern New River

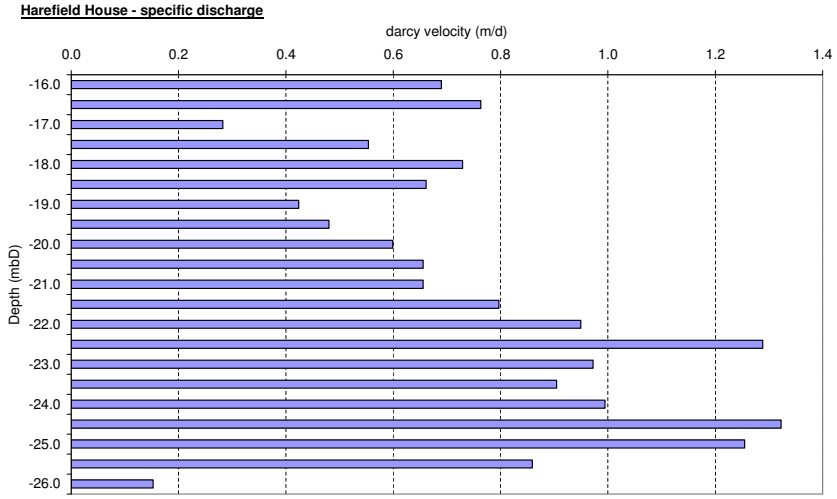

Figure 3.27: Specific discharge (darcy velocity) for each 0.5 m depth section at Harefield House BH. Estimated using the methodology in Figure 3.24. Plots of $\ln \frac{C_t - C_b}{C_0 - C_b}$ are included in Appendix D. The value at each section is estimated based on Based on Single Borehole Dilution test carried out at Harefield House BH on 22 January 2008.

wellfield. Transport in the karst conduits is characterised by low attenuation and high flow rates. There is also likely to be a background flow of bromate contaminated water east of Hatfield that is influenced by double-porosity characteristics.

3.8 Summary and conclusions

The topography, geology and hydrology of the study area result in a predominantly south-easterly groundwater flow direction within the Chalk from upland areas in the north and west, where the Chalk aquifer is largely unconfined, toward the south and east where the Chalk is overlain by Palaeogene Deposits. Within the Vale of St Albans and Middle Lee Valley, the Chalk aquifer is overlain by an interbedded sequence of Boulder Clay and Glacial Sands and Gravels; the degree of continuity between the upper sand and gravel aquifer and the Chalk aquifer system is dependent on the extent and thickness of clay layers. A number of abstractions in the Vale of St Albans, Hatfield, and Lea Valley areas influence local hydraulic gradients. A series of single borehole dilution tests were undertaken in the area between the source site at Sandridge, and the Hatfield area, which Darcy velocities of the order of 10 $\mathrm{m\ day^{-1}}$.

Superimposed on the south-easterly groundwater flow, an extensive karst network associated with the Palaoecene boundary allows rapid flow from the Water End area to the northern Lea Valley to the north east. Within this chapter, rigorous statistical analysis of the time lag between the relationships between a change in abstraction rate at Hatfield PWS and the observed change in bromate concentrations at down-gradient locations was undertaken, and the relationships indicate direct connections between

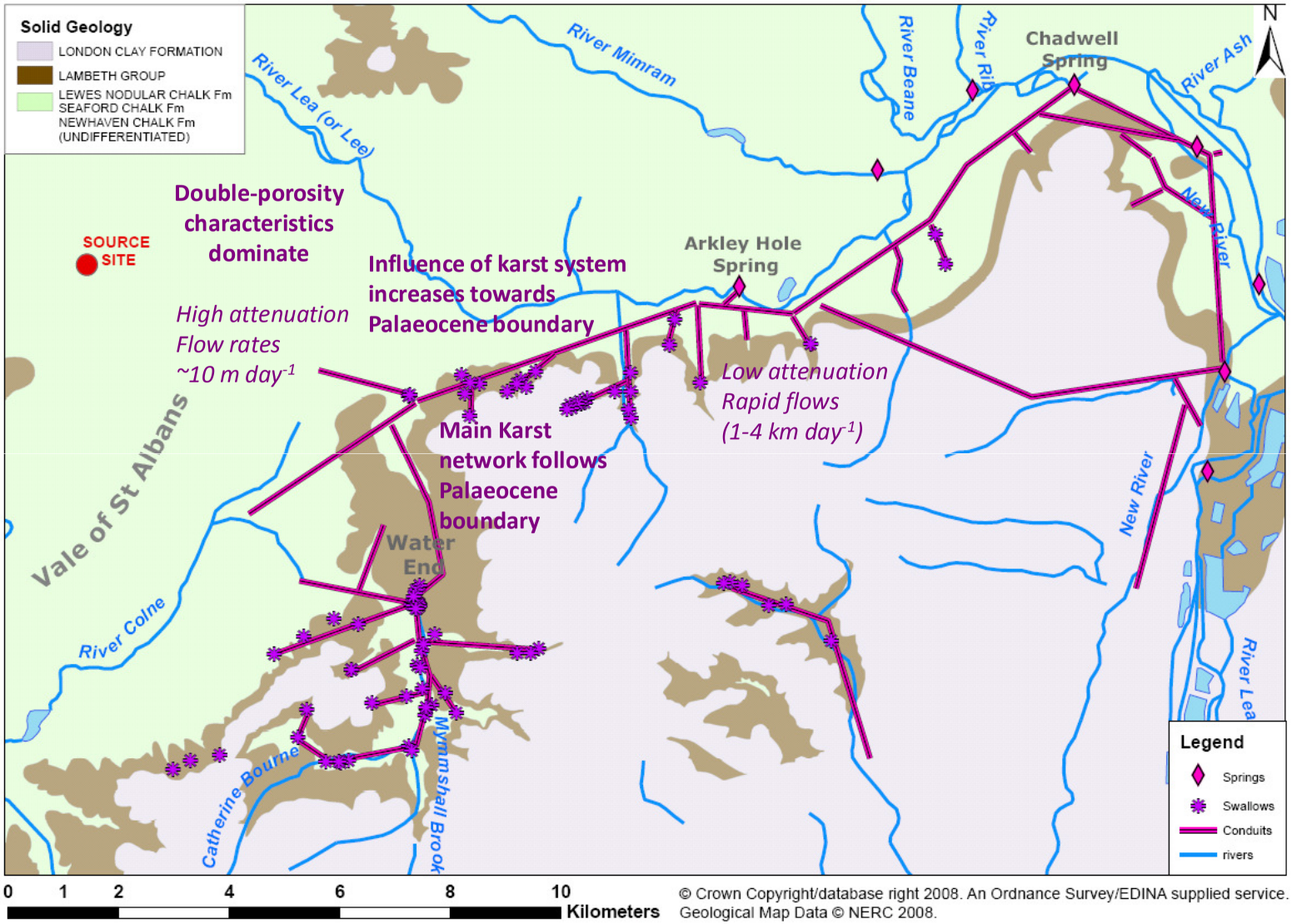

Figure 3.28: Conceptual model for groundwater flow in the bromate affected area of Hertfordshire. Position of conduits are based on the conceptual model developed by Cook (2010). Flow rates and attenuation characteristics are inferred from the results of the single borehole dilution testing presented in Section 3.6 and tracer tests undertaken by Cook (2010).

the Hatfield area and springs and abstraction wells in the Lea Valley. In combination with tracer testing undertaken by Cook (2010), this suggests a conduit system which connects three regions Water End, Hatfield, and the northern and middle Lea Valley. The results of the tracer testing from Water End indicate rapid flows of the order of 1000 $\mathrm{m\ day^{-1}}$ along the Palaeocene boundary.

The information assessed and interpreted in this chapter has been used to develop a conceptual model for flow and transport within the Hertfordshire Chalk aquifer which considers that double-porosity characteristics dominate close to the source site in Sandridge and within the Vale of St Albans, resulting in high attenuation of bromate. The main karst network is developed along the Palaeocene boundary and allows rapid transport of bromate, with low attenutation, toward the Lea Valley.

Chapter 4

The evolution of bromate contamination in the Hertfordshire Chalk

4.1 Chapter Objectives

The objective of this chapter is to use the available monitoring data to describe the spatial distribution and temporal evolution of bromate across the catchment, and to interpret the distribution and evolution of bromate in association with the conceptual model of the flow and transport system developed in Chapter 3.

4.2 Bromate Water Quality Monitoring Programme

New Drinking Water Regulations came into force in December 2003, which introduced a new standard for bromate (BrO_3^-) of 10 $\mu g\,l^{-1}$. In May 2000, during the course of preliminary sampling, Three Valleys Water (TVW) detected bromate concentrations of 135-140 $\mu g\,l^{-1}$, well in excess of this standard, at the Hatfield Bishop's Rise Pumping Station. As a precaution the source was removed from public supply.

In June 2000 a joint water quality monitoring programme was initiated, involving the Environment Agency, the local authorities, and TVW to identify the extent and source of the bromate contamination. Bromate contamination was found to extend across the catchment from Sandridge in the west to the Lee Valley in east where low levels were detected at an Thames Water Utilities (TWUL) Northern New River (NNR) sources between Ware and Turnford. Following the initial phase of water quality monitoring, management of the monitoring programme was essentially assumed by the Environment Agency (EA), with TVW and TWUL undertaking monitoring of their own sources.

The EA, TVW and TWUL continue to monitor water quality and water levels at a number of locations throughout the bromate impacted area. A total of approximately 370 locations have been monitored at some stage over the period 2000 to 2007 at various frequencies, although only approximately 50 locations continue to be monitored on a routine basis. Protection of the public water supply boreholes has been the main objective of the monitoring programme, which pays particular attention to key 'indicator' boreholes located within the main body and at the margins of the bromate affected area (the 'plume') to assess plume boundary movement.

The role of collating the monitoring data was initially undertaken by VWP within an Excel spread-

sheet. (Initially the monitoring data was held by a number of different organisations undertaking separate monitoring.) The Environment Agency assumed the role of data management and transfer of the data occurred in September/October 2001. The data was entered in the Agency's WIMS database, and from this the data was subsequently exported into an Access database (the 'Bromate Monitoring Database'). Although at the time, the majority of samples taken were being analysed at the VWP laboratory it was always the intention to eventually transfer sample analysis to the Agency laboratory (this occurred in October 2002). Automatic transfer of data occurs from the laboratory to the WIMS database. The EA continues to manage all publically available monitoring data (some public water supply data are excluded) within the database, including both water quality results and water levels. The database also includes a variety of other information including monitoring location reference information (e.g. NGR, owner, borehole depth, topographic elevation etc) and sample schedules ('runs').

In September 2005, the Environment Agency commissioned Atkins Limited to produce a factual and interpretative report (Atkins, 2006) of the data and associated information obtained through the five years of monitoring. In addition, Atkins amended/upgraded the monitoring database. In order to form the basis of the data presented in this thesis chapter, the Bromate Monitoring Database (including all data up to the end of December 2008) was provided by the Environment Agency. Monitoring data (up to the end of December 2008) provided by TVW and TWUL was included within a modified version of the database, the 'UCL Bromate Monitoring Database'. The UCL database was linked to a GIS database.

4.3 Monitoring Data Quality

The quality of data available within the UCL Bromate Database is reviewed in sections 4.3.1 to 4.3.4

4.3.1 Sampling Locations

The total number of locations monitored for bromate across the catchment is ∼380 locations (Figure 4.1). The core 'plume' was found to extend from Sandridge to Hatfield and therefore the majority of the sampling points were located in this area. Of these, ∼235 are are chalk groundwater locations (including 31 public water supply borehole locations), ∼15 are gravel groundwater locations (mainly abstraction boreholes for quarrying operations), ∼90 are surface water locations and an additional 11 are floodwater sampling locations (associated with the 2001 flooding in the area of House Lane, Sandridge). Approximately 30 additional monitoring locations were also introduced in response to circumstances such as groundwater flooding in Sandridge, discharge of bromate contaminated water at Hatfield Quarry as part of the quarrying operations, the discovery of low concentrations of bromate in boreholes drilled at Ashley Road, St Albans to investigate a hydrocarbon spillage. The chalk groundwater locations comprise public and private supply boreholes, observation boreholes (mainly pre-exisitng, but some purpose-drilled), site investigation boreholes, and landfill monitoring boreholes. The diameter, depth, construction (e.g. open hole, screen, lithology sampled) therefore varies considerably between locations.

4.3.2 Sampling Methodology

The Environment Agency's standard sampling protocol specifies purging of three well volumes where possible prior to sampling. Where purging of three well volumes is not possible, purging should be

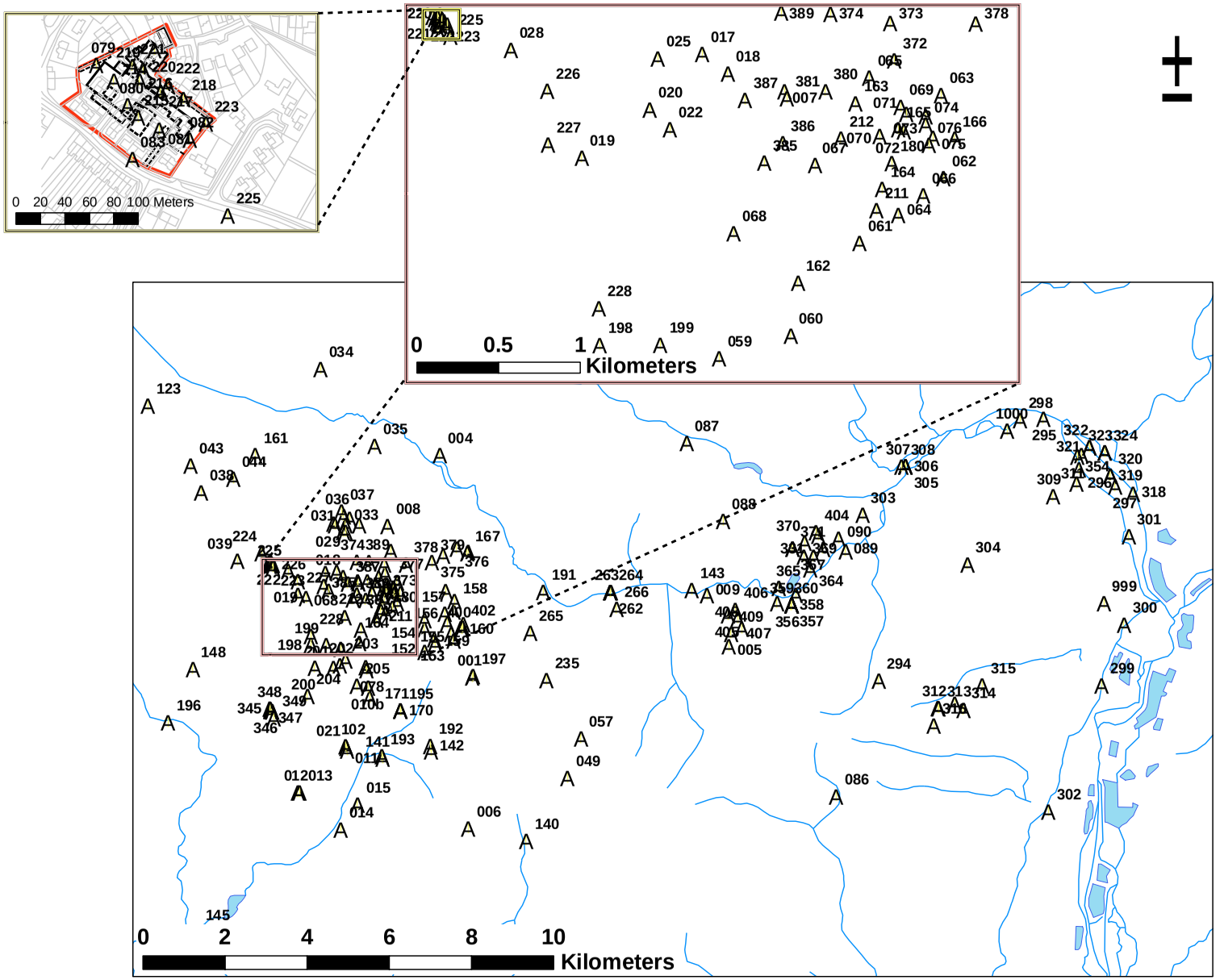

Figure 4.1: All bromate monitoring locations 2000-2008.

undertaken until stablilisation of physicochemical parameters is achieved. In general, for groundwater monitoring undertaken by the Environment Agency (EA), or by their appointed subcontractors, the EA's standard sampling protocol was followed to ensure, as far as possible, consistency of results. Instances when the standard sampling protocol could not be applied (*e.g.* due to wellhead restrictions) have generally been noted as comments within the database.

4.3.3 Analytical methods and detection limits

The typical analytical determinands are summarised in Table 4.1. Analytical methodology and method detection limits (MDL) for bromate and bromide are summarised in Table 4.2.

Table 4.1: Typical analytical suite for water samples May 2000 to December 2008

Early sampling (2000-2001)	Routine sampling	Physical parameters
Bromate	Bromate	pH
Bromide	Bromide	Temperature
cations and anions	Chloride	Electrical conductivity
Ammonium	Sodium	Total dissolved oxygen
Total oxidised nitrogen	Total oxidised nitrogen	
Organic compounds by GCMS	phosphorous$*$	
	total organic carbon$*$	
$*$Determinand excluded from approx 2001 when it was concluded that no significant down-gradient migration was occurring		

Table 4.2: Analytical methodology and detection limits for bromate analyses.

	Laboratory	Method	Method Detection Limit (μg l^{-1})
Up to end of Dec 2001	VWP	?	1.0
Jan 2002 end of Sep 2002	VWP	ion-chromatography	0.5
Oct 2002 to end of dec 2009	EA (Starcross)	ion-chromatography	0.5
	VWP	ion-chromatography	0.5
	TWUL	ion-chromatography	0.6

For the period May 2000 to late October 2002, all samples were analysed by the VWP laboratory. During this time, from January 2001, new analytical methods for bromate and bromide were introduced. A duplicate analysis was undertaken to compare the old and new analytical method. This involved the collection and analysis of approximately 20 field samples. Initial testing showed that bromate results were 20 % lower for concentrations above 150 μg l^{-1}.

According to Buckle (2002), the laboratory uses an ion-chromatographic technique, and has NAMAS accreditation for the parameters analysed. The occurrence of 'isolated and unexpected' bromate

sample results, particularly for TVW operated sources (e.g. Roestock and North Mymms), recorded above the detection limit of 1 μg l^{-1}, but generally less than 5 μg l^{-1}, has shown that the technique is not completely reliable at low concentrations. Under normal circumstances, bromate and bromide concentrations over the detection limit are subject to an estimated measurement error of ± 10 %.

From October 2002, all samples were collected by the EA were analysed by the Environment Agency's Starcross Laboratory in Exeter. During the period of changeover, duplicates (comprising some 20 field samples) were analysed by both the Starcross laboratory and VWP to check for consistency. According to the EA, the results of these comparisons indicated that discrepancies resulting from different methods or laboratories were unlikely to exceed 20 % for bromate and bromide concentrations greater than about 5 μg l^{-1}. (It should be noted that the comparisons were not intended to be rigorous statistical exercises, but to provide reassurance that discrepancies resulting from different laboratories or methods would not significantly distort the broad picture of the distribution of bromate and bromide, whose concentrations ranged over there orders of magnitude within the plume.)

Further to the above, in June 2005 an inter-laboratory comparison exercise was undertaken to check the consistency of results. Triplicate samples were analysed by VWP, TWUL and EA laboratories. Eleven samples were taken for the NNR wells and from TVW sources at Hatfield, Bishops Rise and Essendon. A comparison exercise was undertaken for the three laboratories, similar to that described above. Over the concentration range 10 μg l^{-1} to 350 μg l^{-1} the maximum deviation of an individual sample from the mean of three samples was 23 %. For one sample close to the MDL results varied from $<$0.5 μg l^{-1} to 2.3 μg l^{-1}. Results for bromide showed less variation.

4.3.4 Sampling frequency and completeness

Broadly, the monitoring programme had two main phases, and the frequency of sampling at each location (Figure 4.2 to Figure 4.10) has varied according to the main objectives:

- Phase 1 – An initial phase with the primary objective of identifying the source of contamination and the extent of the affected area. This phase was effectively achieved by the end of 2000;
- Phase 2 – A subsequent on-going phase to monitor concentrations and assess boundary migration.

In addition, a number of 'specialised investigations', involving sampling at additional/alternative locations and/or more detailed and/or more intense sampling, have occurred in response to specific issues such as monitoring of bromate in groundwater floodwaters, investigation of the source site (St Leonard's Court) in relation to Part IIA assessment, investigation of a petrol spillage at Ashley Road, investigation of the effects on dewatering at Hatfield quarry on bromate and bromide, depth sampling at Hatfield Business Park, investigation of bromate in the River Lee and Ellenbrook/Colne system. Resolution of anamolies in the results, suspected to have been related to sampling or laboratory analysis have also generated specific additional sampling aside from the main sampling programme.

The main phase of monitoring underwent significant 'rationalisation' in early 2002. Locations which provided no additional information were omitted, and additional boreholes specifically drilled by the EA and TVW to assist in the delineation of the contamination distribution and extent were in-

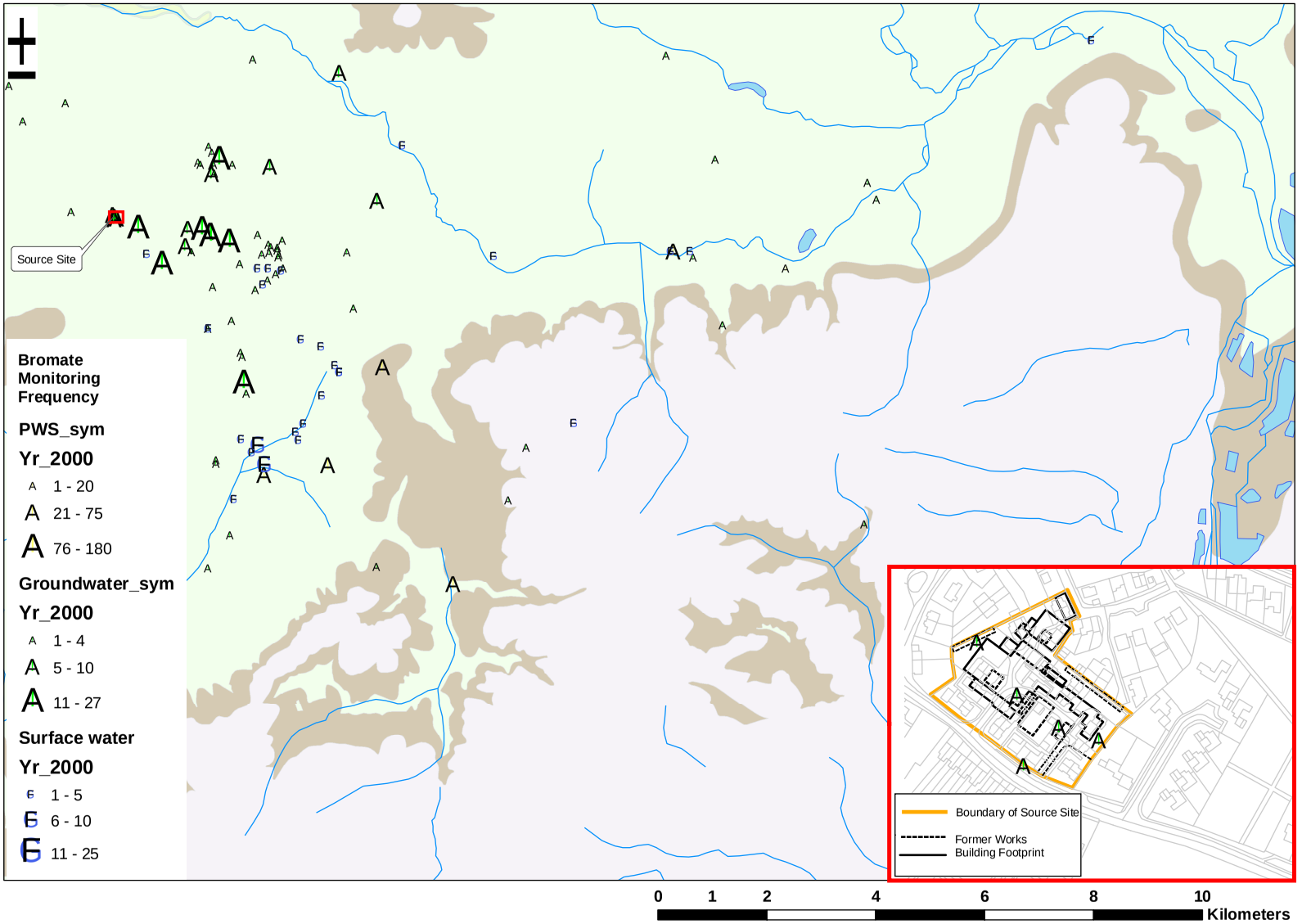

Figure 4.2: Sampling frequency for bromate at each monitoring location in 2000

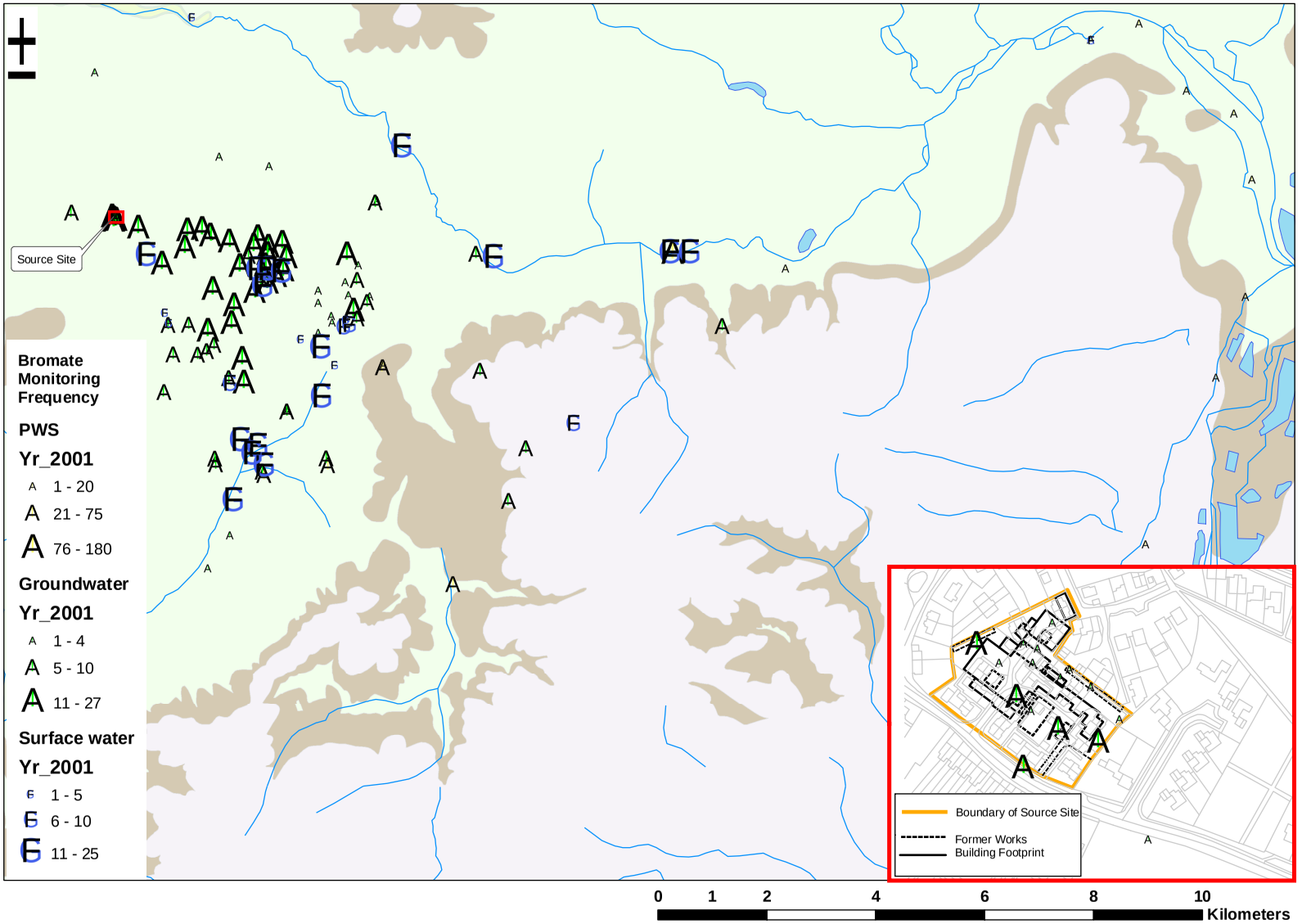

Figure 4.3: Sampling frequency for bromate at each monitoring location in 2001

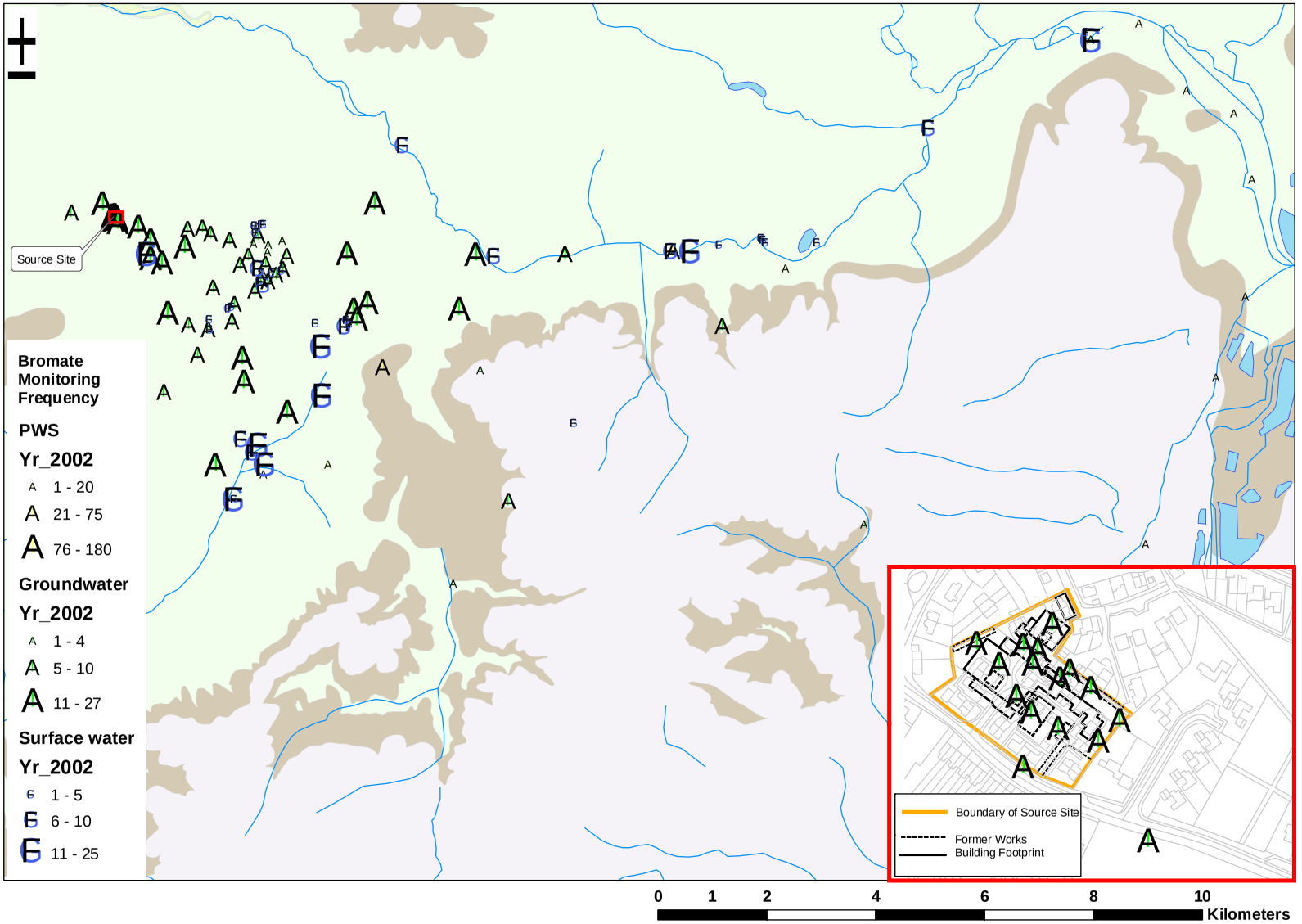

Figure 4.4: Sampling frequency for bromate at each monitoring location in 2002

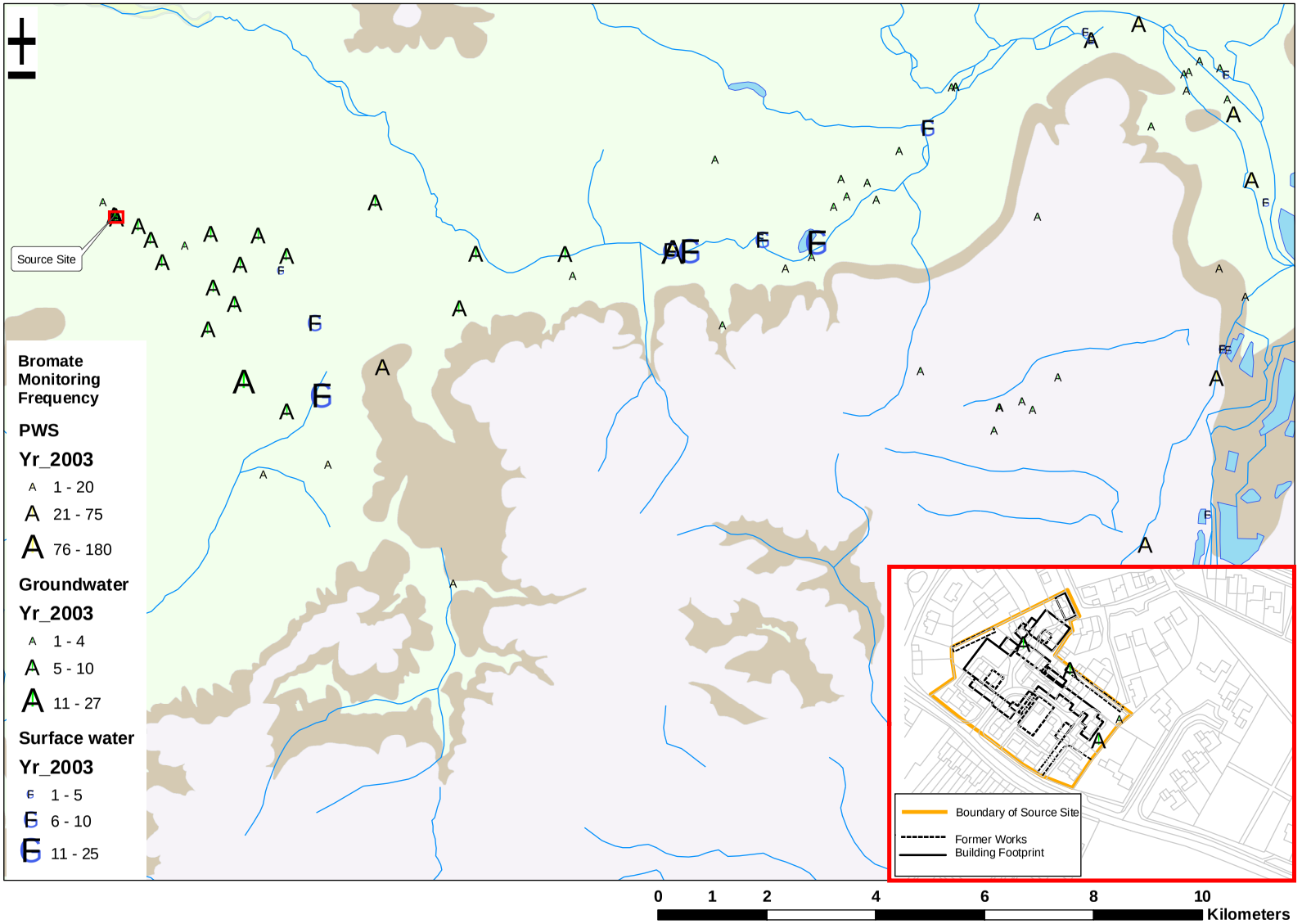

Figure 4.5: Sampling frequency for bromate at each monitoring location in 2003

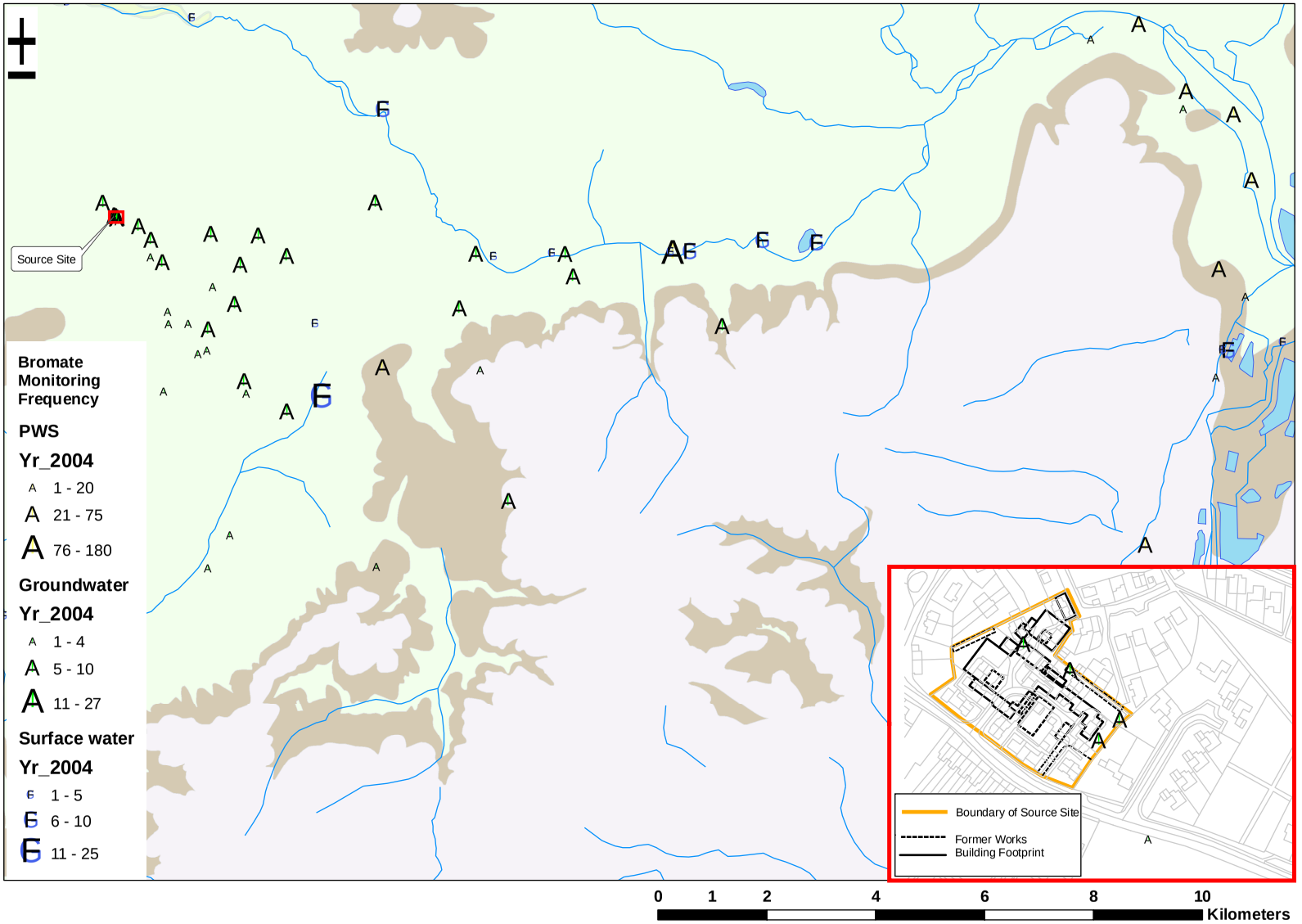

Figure 4.6: Sampling frequency for bromate at each monitoring location in 2004

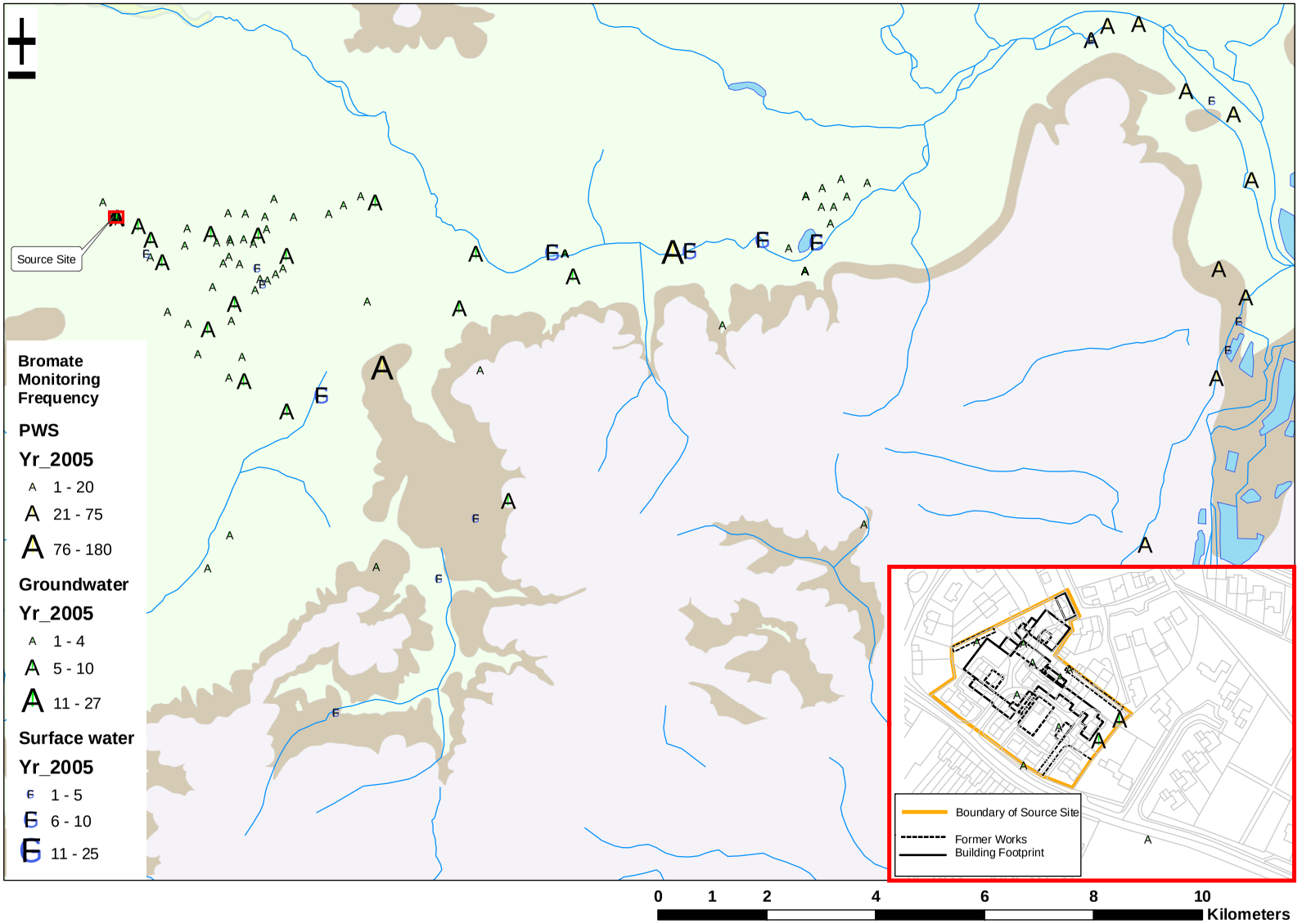

Figure 4.7: Sampling frequency for bromate at each monitoring location in 2005

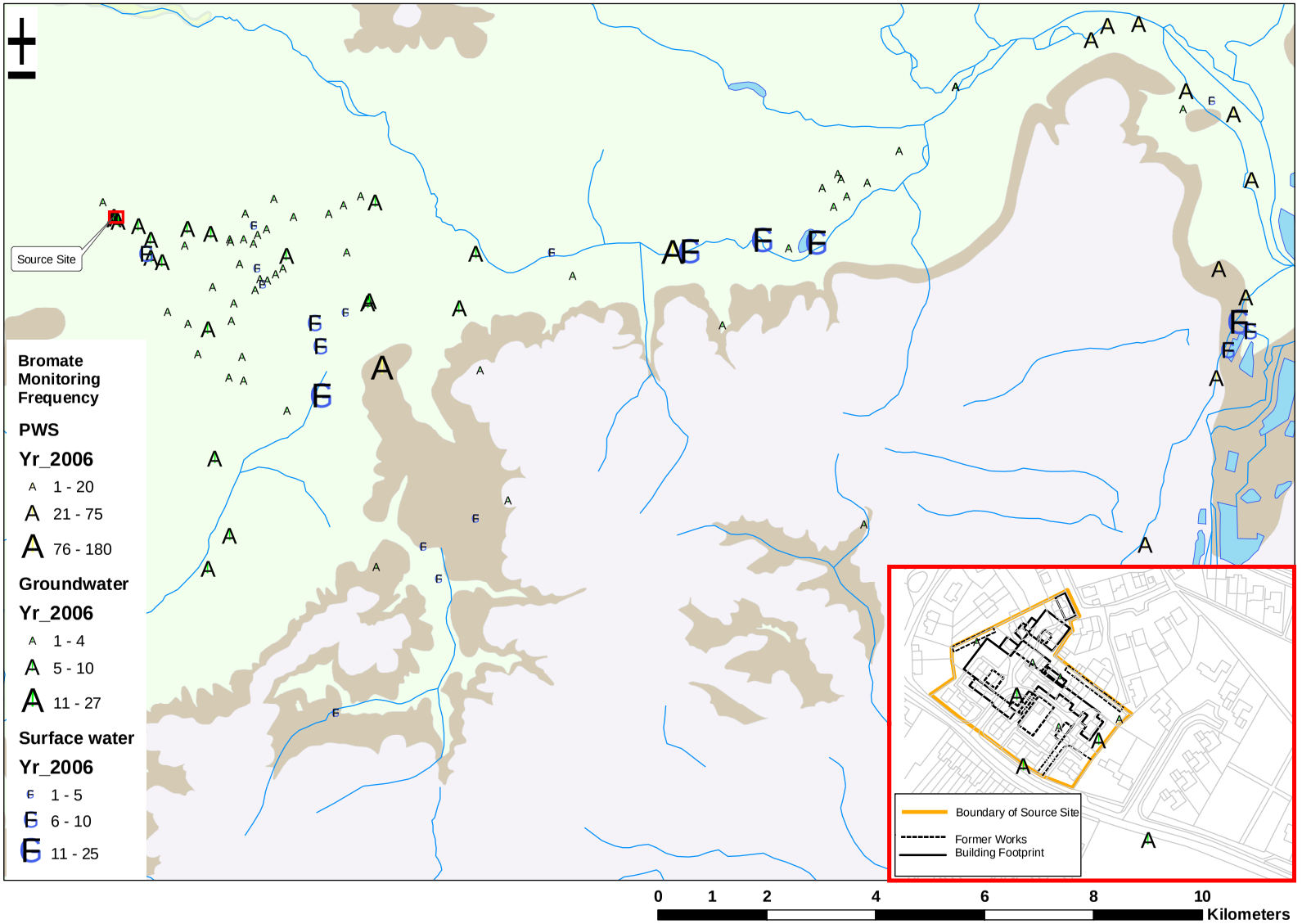

Figure 4.8: Sampling frequency for bromate at each monitoring location in 2006

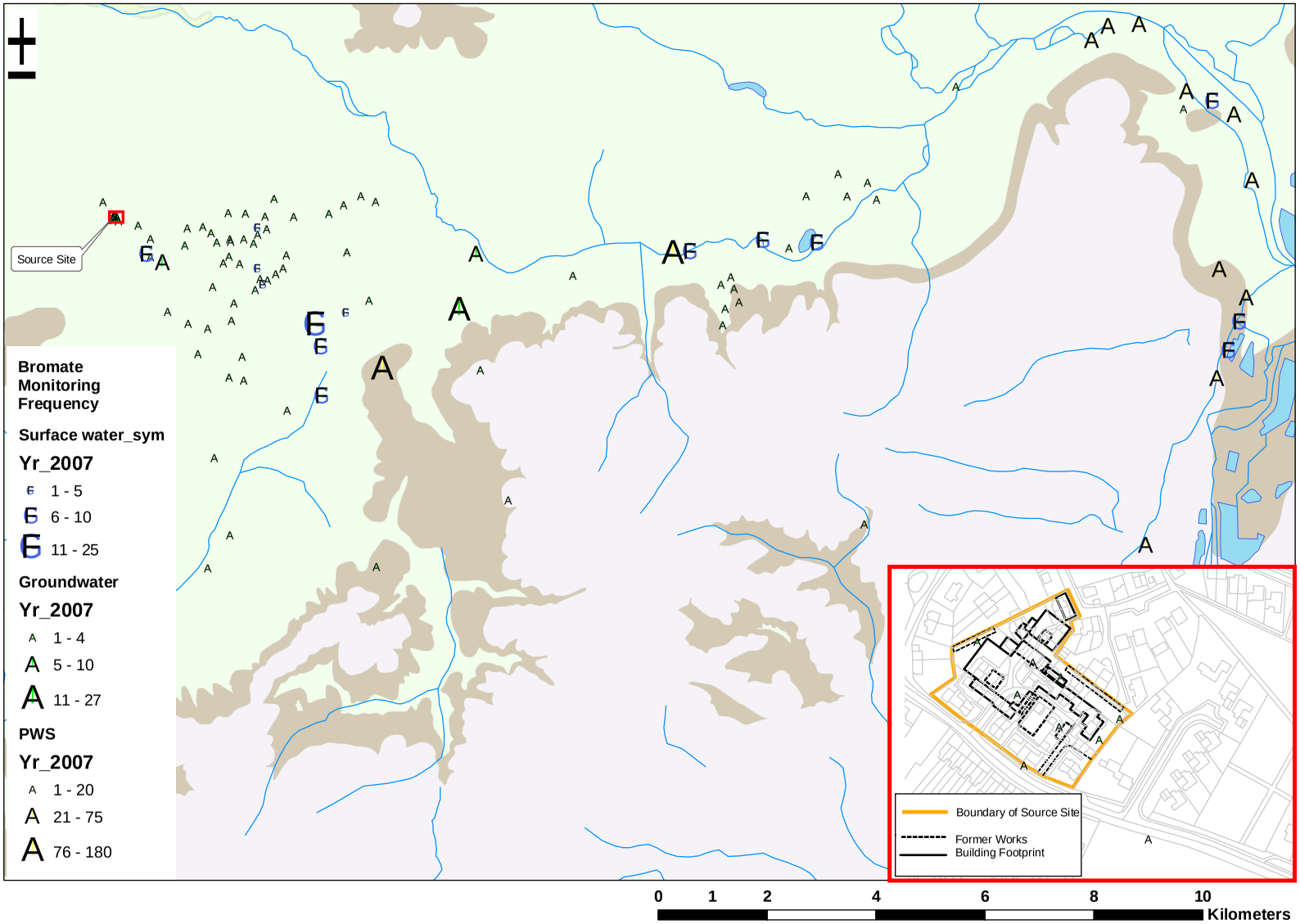

Figure 4.9: Sampling frequency for bromate at each monitoring location in 2007

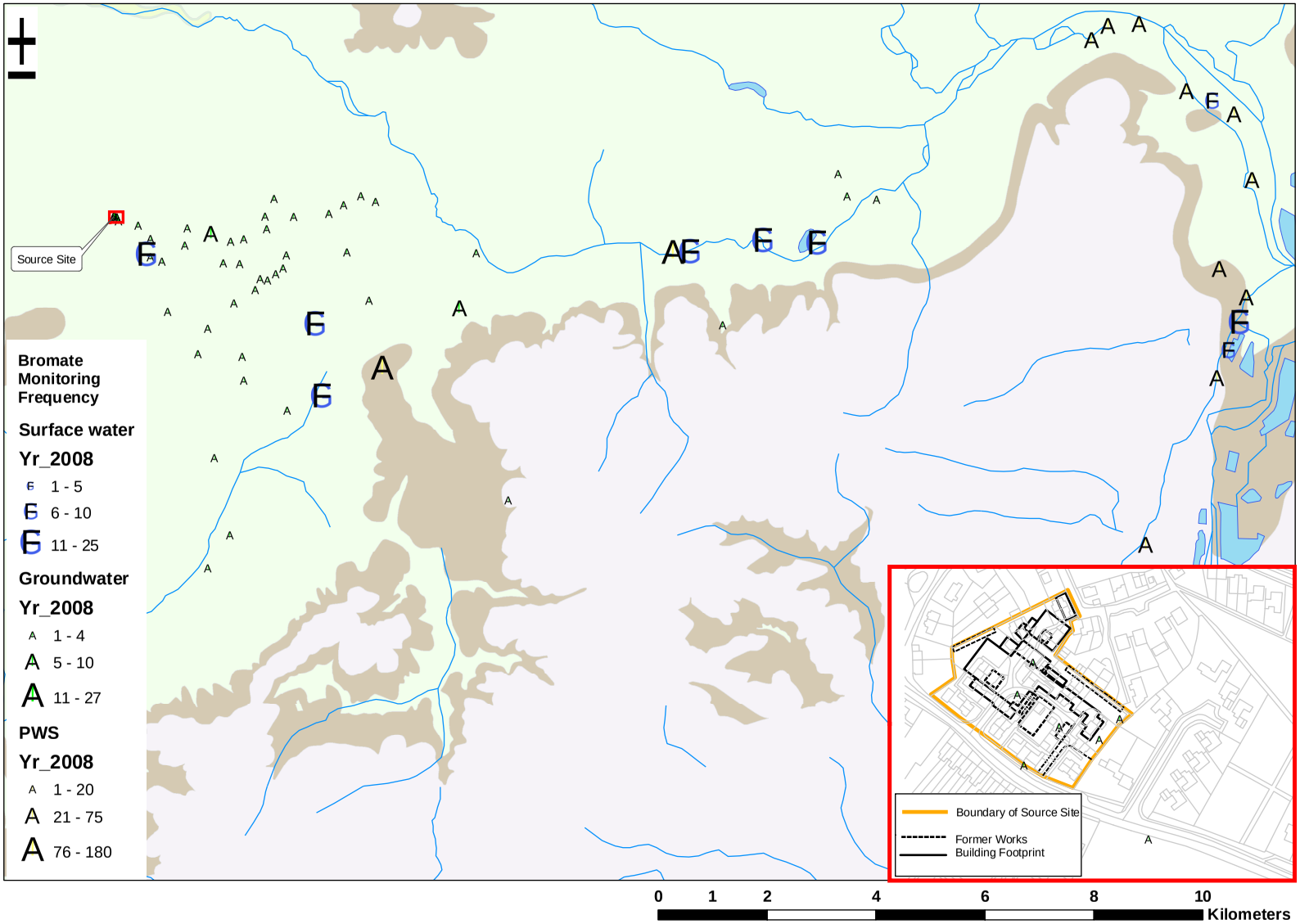

Figure 4.10: Sampling frequency for bromate at each monitoring location in 2008

cluded. Sampling frequencies were also reduced at most locations, although the aim was not to reduce the frequencies until a full year of data at regular intervals had been obtained.

In June 2002, sampling frequencies were further amended with the aim to monitor at a frequency of two-monthly or less with the exception of a small number of locations retained at monthly frequency due to their strategic role in providing an early warning of change. Furthermore, in November 2002 the sampling schedule was rationalised again due to funding constraints. Approximately 47 locations have been retained for on-going and regular monitoring.

4.4 Delineating the Bromate 'Plume'

The areal extent of the bromate contaminated groundwater is defined by a margin encompassing a number of locations that are typically, but not always, below the method detection limit (MDL). Beyond this margin, no bromate has been detected at monitoring locations. The margins are defined by results from a number of locations in mid-to-late 2000 and early 2001; during this time the emphasis of the monitoring programme was to identify the source of the bromate contamination and its extent. Many of these locations have been sampled just a few times (Figure 4.2 and 4.3), although some key locations have been sampled routinely as 'indicator boreholes' to monitor the potential migration of the contamination.

Broadly, the distribution of bromate contamination based on monitoring data from 2000 to 2008 (Figure 4.11) to 4.19, is a core 'plume' of concentrations in excess of 50 $\mu g\ l^{-1}$ extending from the St Leonard's Court source site in Sandridge down-hydraulic gradient as far as Hatfield, some 5 km to the south-east. To the east of the core 'plume', the bromate contamination extends as far as the Northern New River wellfield, with concentrations between 1 and 50 $\mu g\ l^{-1}$ affecting locations distributed along the path of the karst system.

The extent of the contamination (the 'plume' margin), the distribution of contamination within the core 'plume', and temporal variations between 2000 and 2008 are described in the sections 4.4.1 to 4.4.5. Integration of the new conceptual model of bromate flow and transport in the Hertfordshire Chalk (Section 3.7) has allowed an alternative interpretation of the distribution of bromate contamination across the catchment. Previous interpretations have been a broad 'envelope' of bromate contamination extending east of Hatfield to the northern New River. However, this distribution is not justified by the monitoring data available.

4.4.1 Up-gradient of the source site

In 2000, a number of samples of Chalk groundwater locations up-gradient of Sandridge gave results below the MDL. In 2002, a purpose-drilled monitoring borehole was installed at Location **224** (Pound Farm, Sandridge). This location has been monitored regularly between 2000 and 2008. The time series indicates that bromate concentrations are below the MDL, with the exception of two occurrences of low bromate concentrations in 2002 (30-35 $\mu g\ l^{-1}$). Bromide concentrations are detected within the normal background range (50-80 $\mu g\ l^{-1}$), with a few samples at around 100 $\mu g\ l^{-1}$ corresponding to the occurrences of bromate concentrations above MDL. Location **224** therefore defines the maximum bromate extent margin up-gradient of the source site.

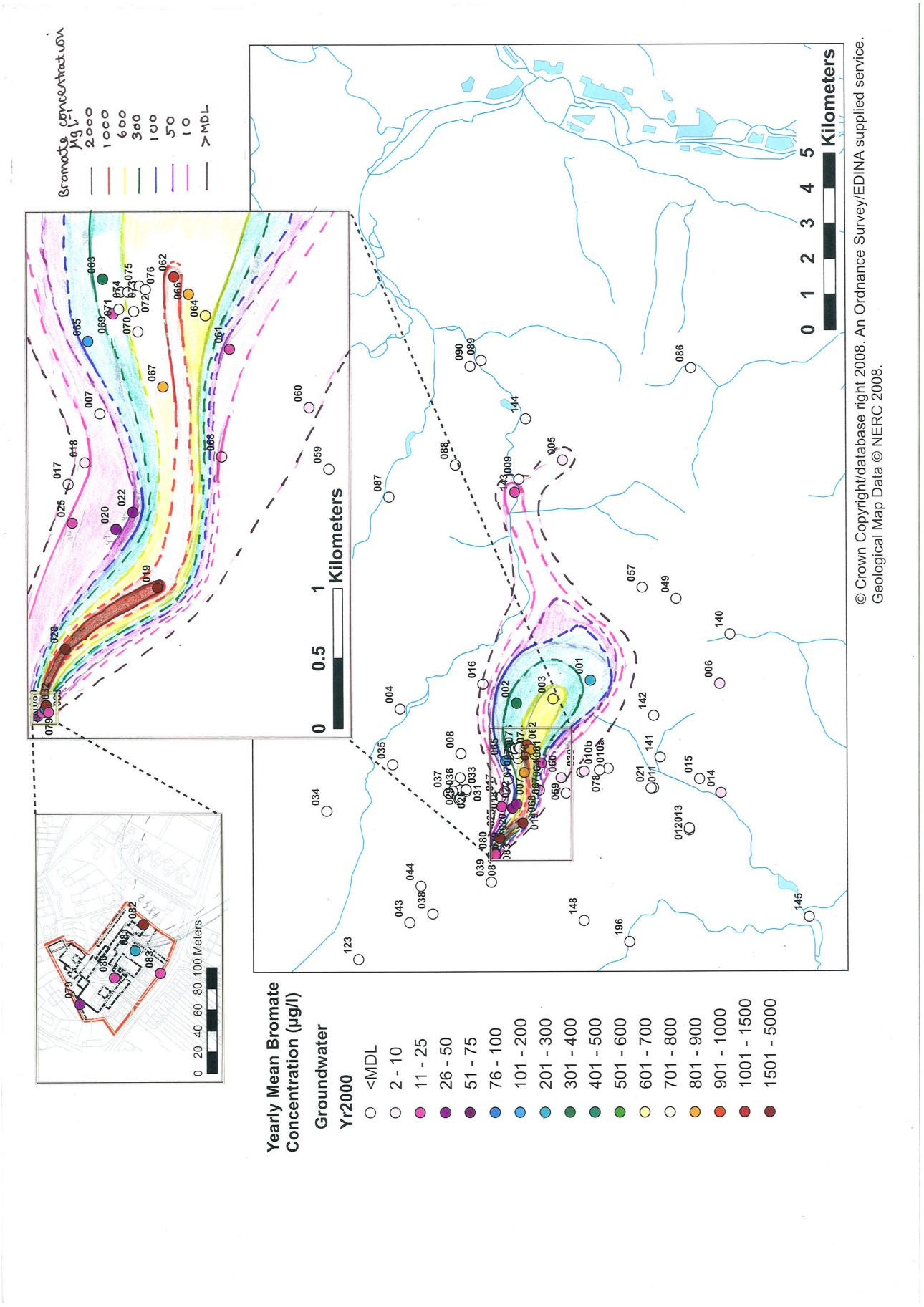

Figure 4.11: Annual average bromate concentrations at groundwater sampling locations in 2000.

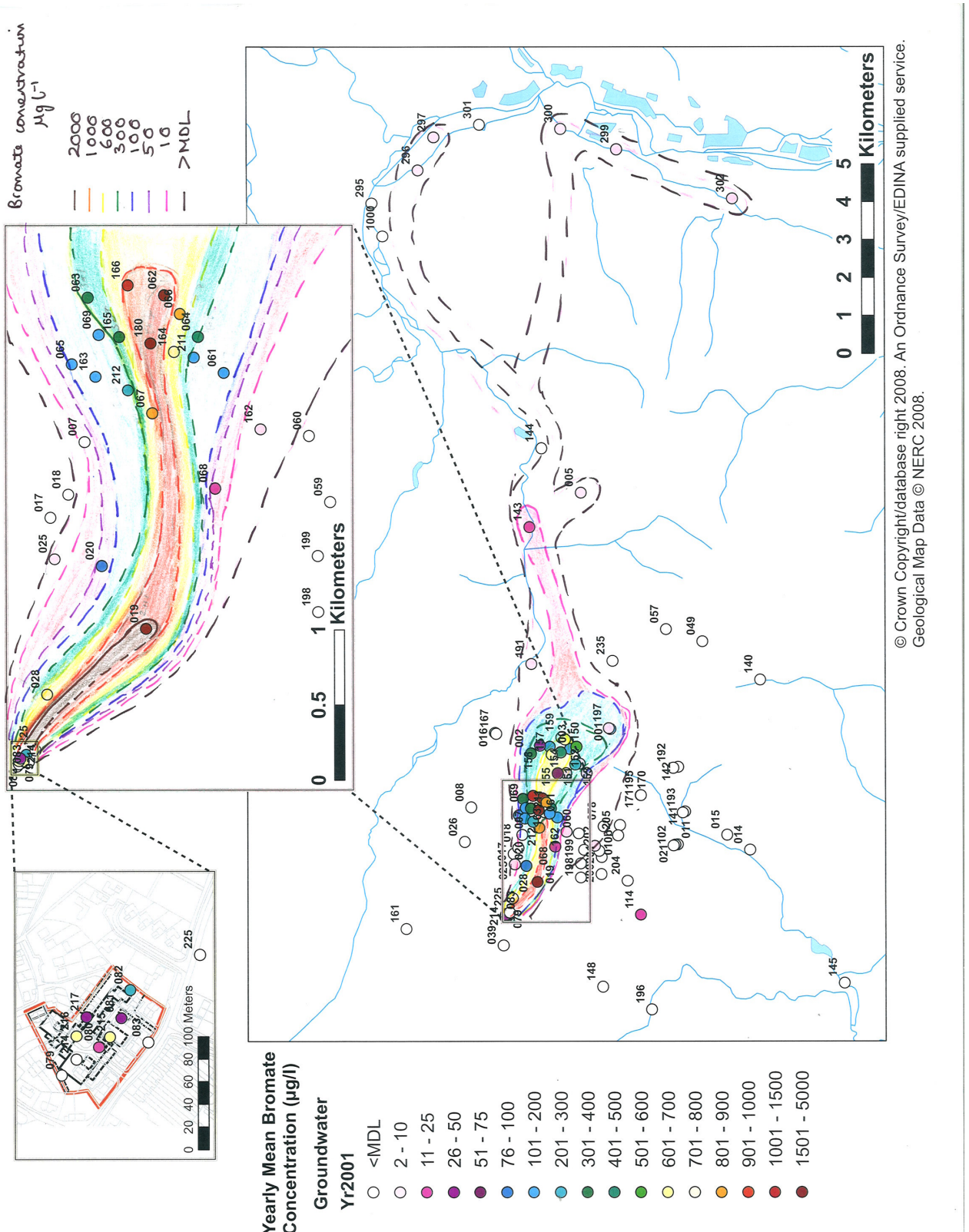

Figure 4.12: Annual average bromate concentrations at groundwater sampling locations in 2001.

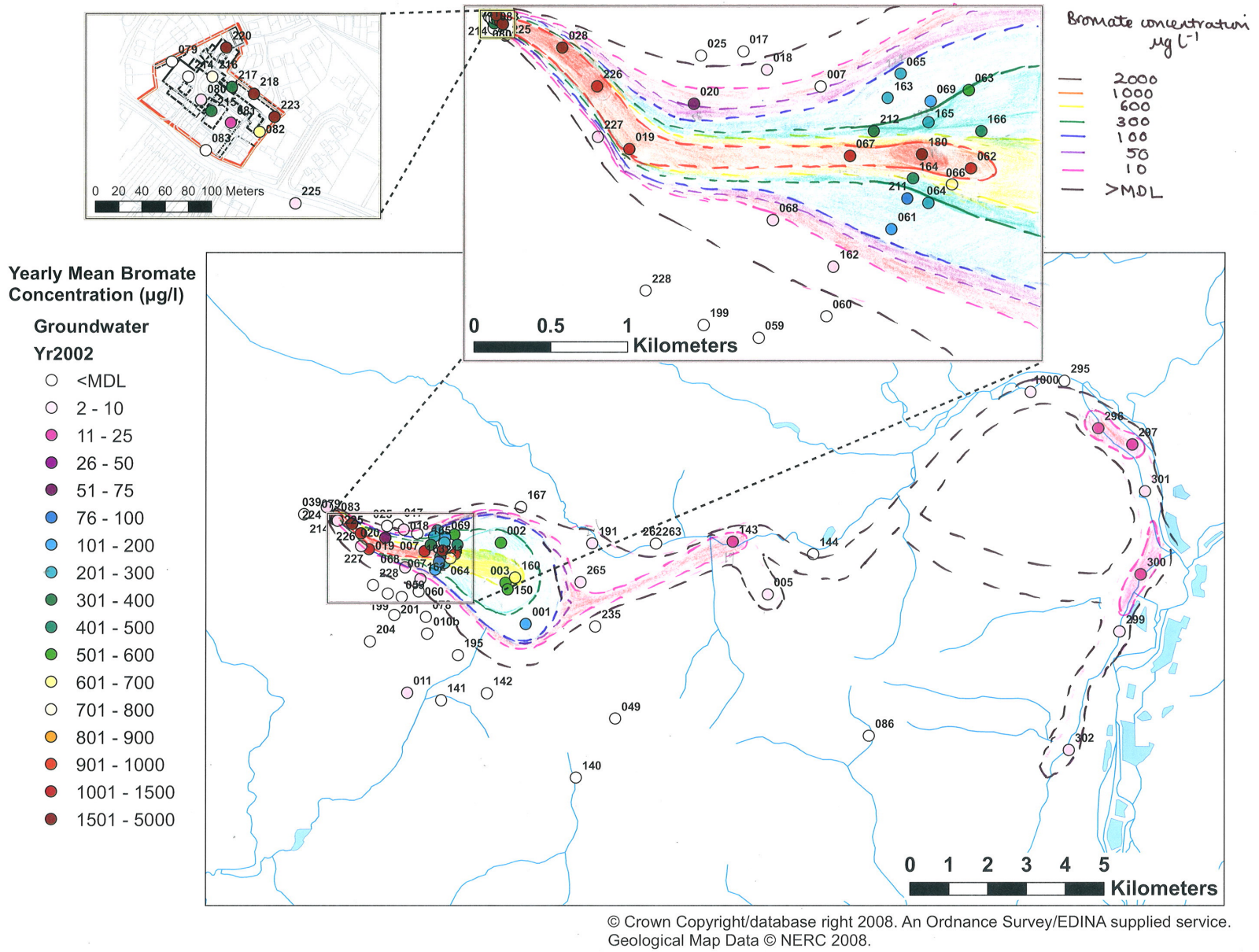

Figure 4.13: Annual average bromate concentrations at groundwater sampling locations in 2002.

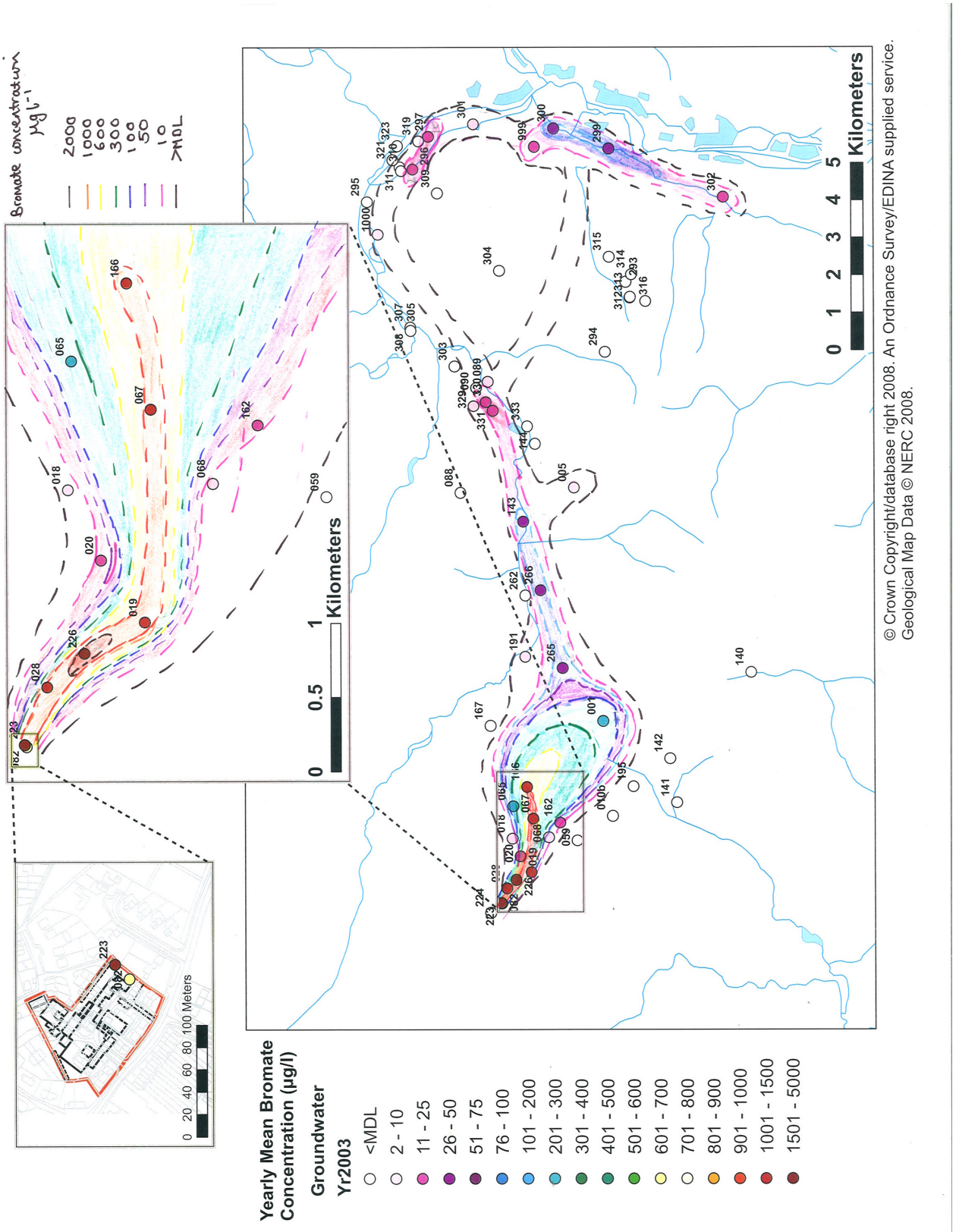

Figure 4.14: Annual average bromate concentrations at groundwater sampling locations in 2003.

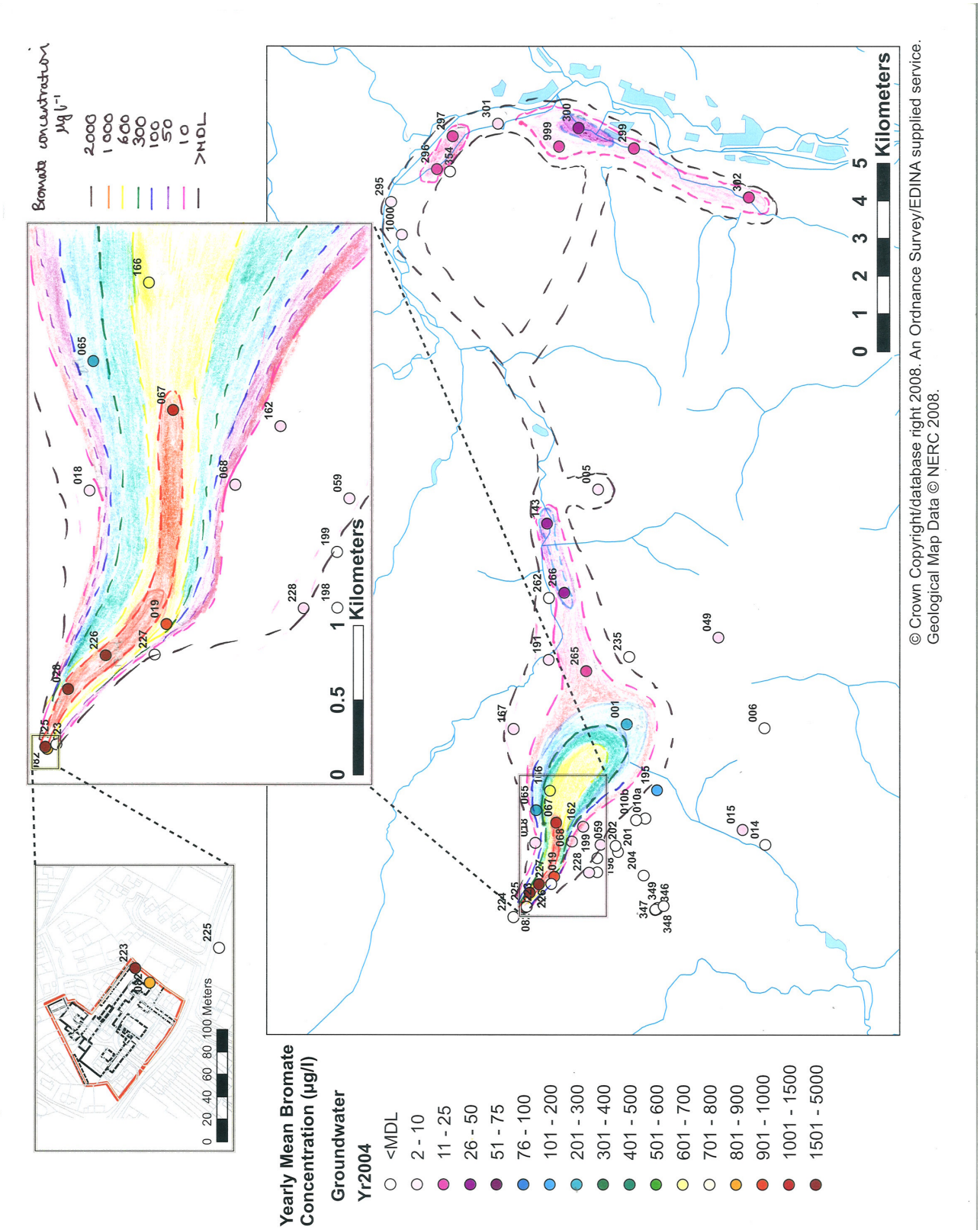

Figure 4.15: Annual average bromate concentrations at groundwater sampling locations in 2004.

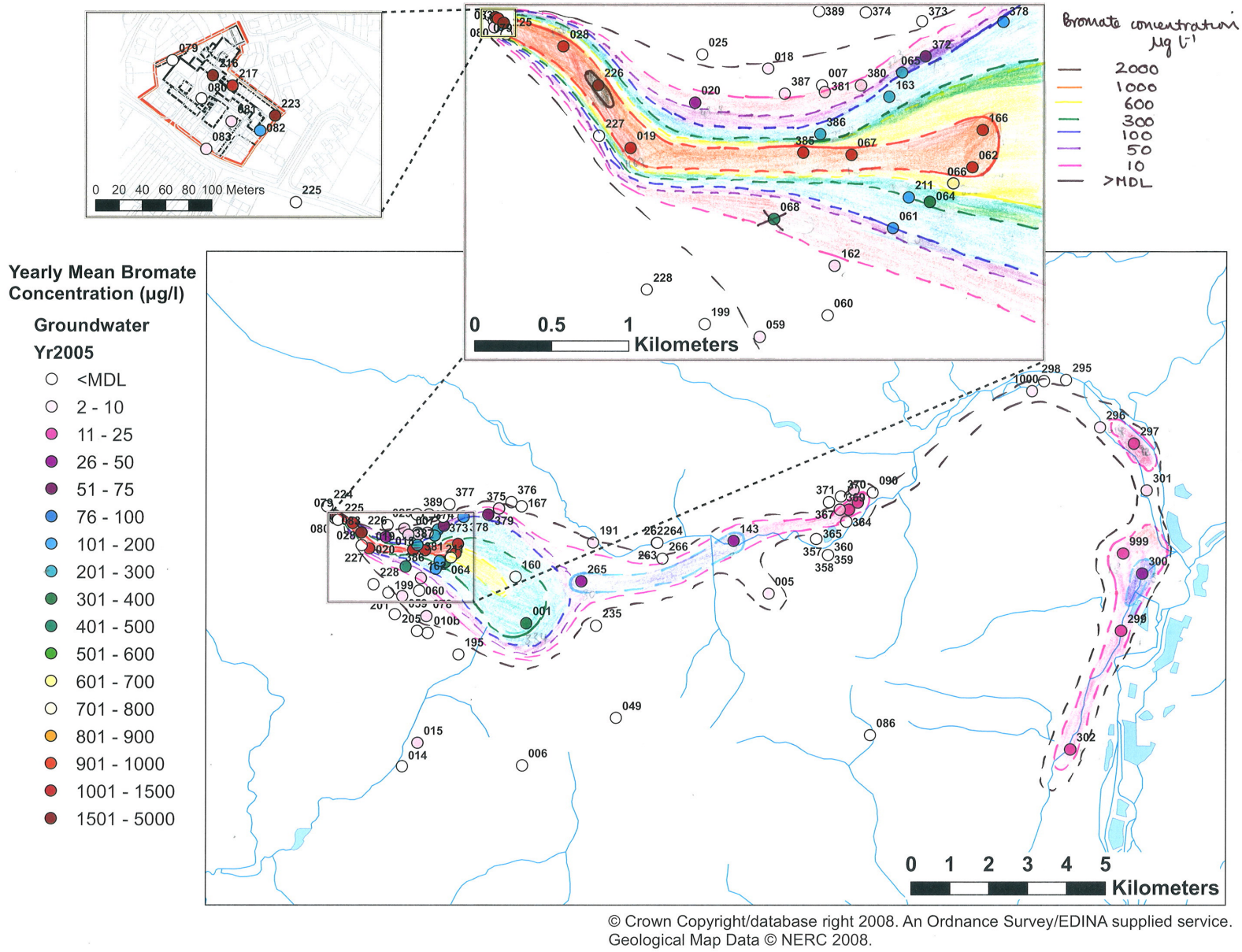

Figure 4.16: Annual average bromate concentrations at groundwater sampling locations in 2005.

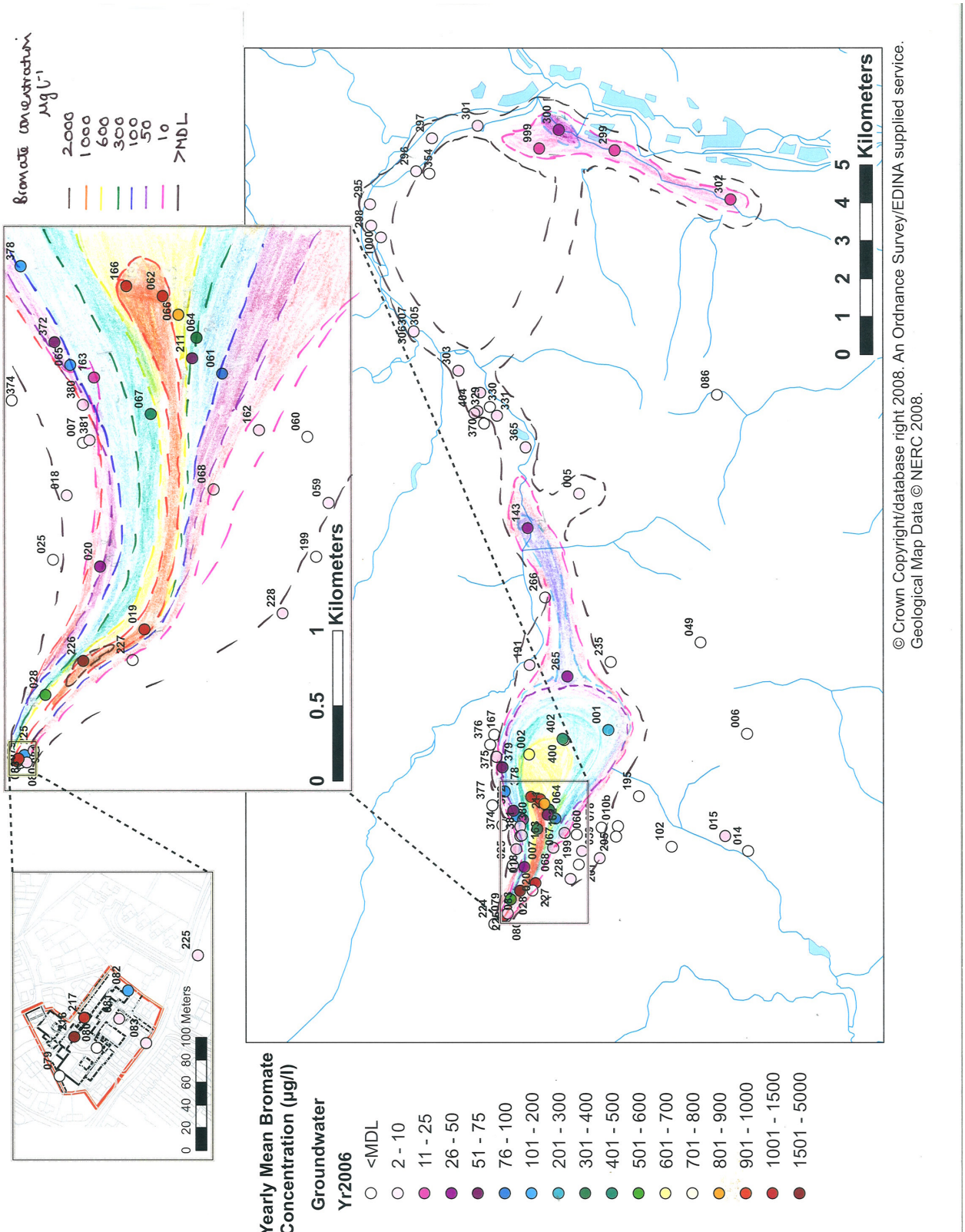

Figure 4.17: Annual average bromate concentrations at groundwater sampling locations in 2006.

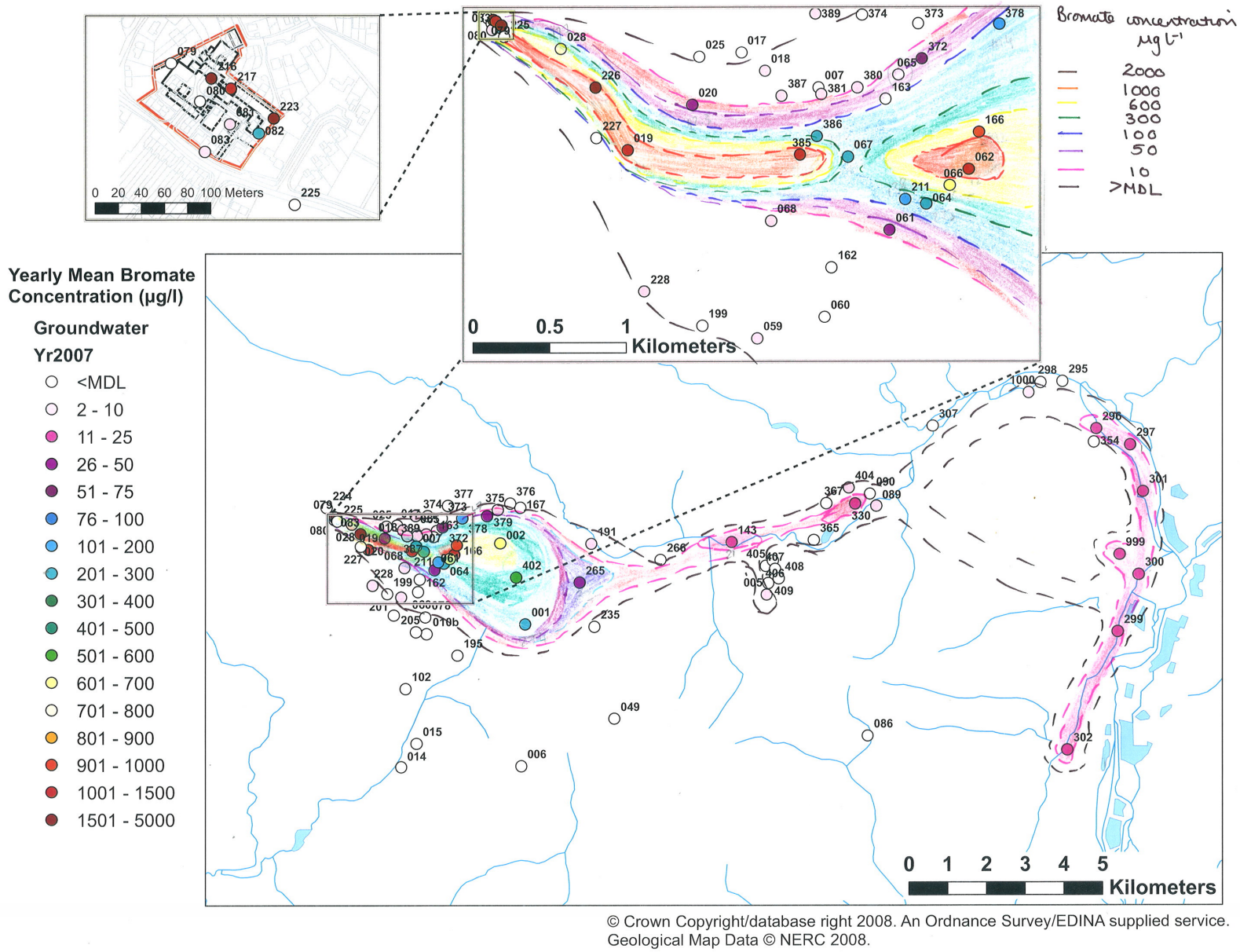

Figure 4.18: Annual average bromate concentrations at groundwater sampling locations in 2007.

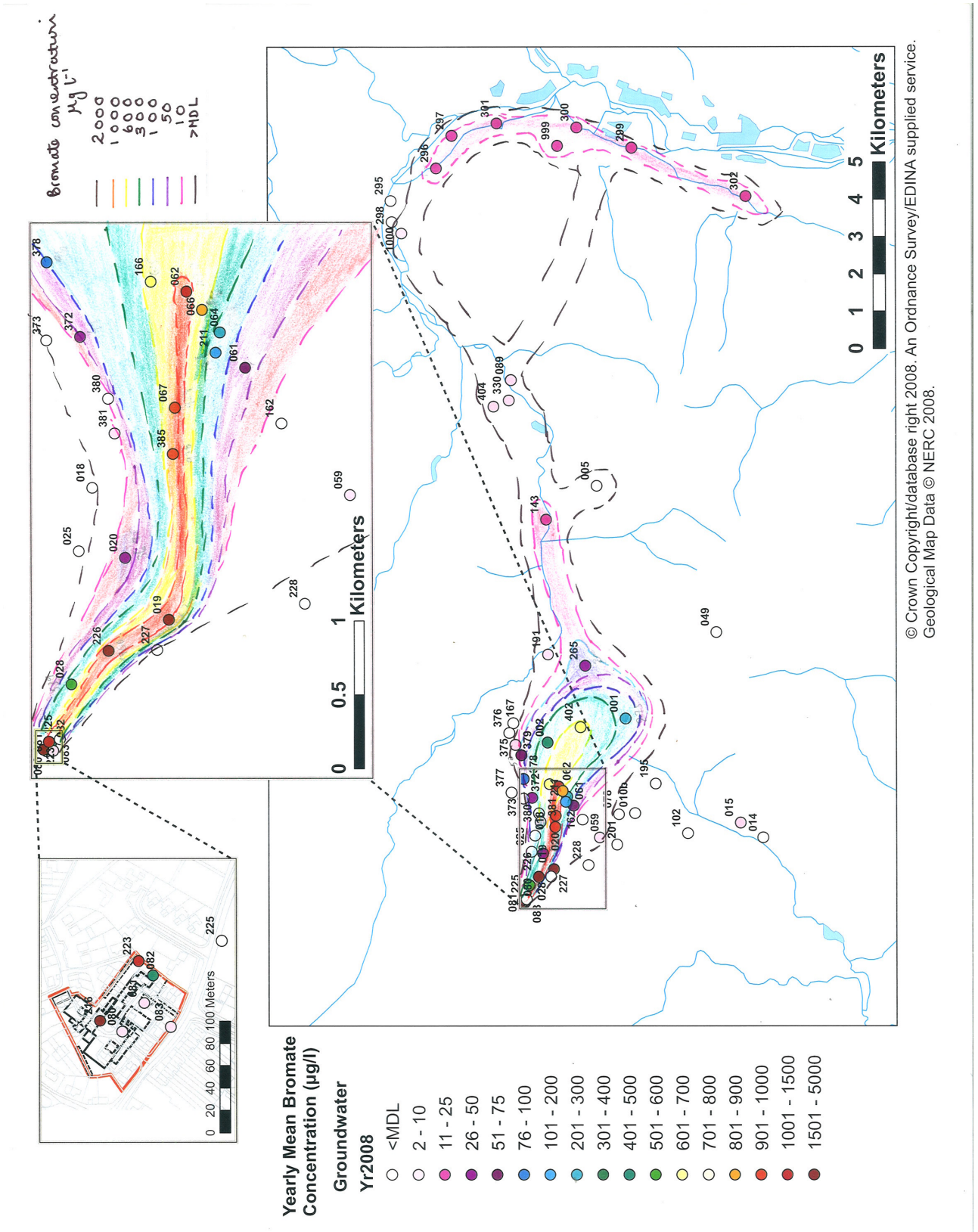

Figure 4.19: Annual average bromate concentrations at groundwater sampling locations in 2008.

4.4.2 Source site and Sandridge area

Groundwater bromate distribution beneath the source site is discussed in detail in Chapter 5, Section 5.6.2.

Down-gradient of the source site, in 2000, the 1000 $\mu g\,l^{-1}$ contour encloses locations **028**, and **019** and **062**. This zone remains relatively stable. From 2001, location **166**, from 2002 location **226**, and from 2004 location **385** are included in this zone. Location **067** shows variable concentrations and in some years shows average concentrations above 1000 $\mu g\,l^{-1}$, and other years below this.

The locations **028**, **019**, **020** and **226** provide good time series data over the period 2000 to 2008 (Figures 4.20 to 4.22). In general, the highest bromate (and bromide) concentration peaks for **028** and **019** were seen in 2000, after which concentrations declined significantly in early and mid 2001. At **028**, concentrations rose again over 2002 and 2003, but since 2004 concentrations have generally shown a declining trend, albeit with a slight increase in mid 2007. As a consequence, **028** falls outside the 1000 $\mu g\,l^{-1}$ contour in 2006 and 2008 (within 300-600 $\mu g\,l^{-1}$ contour interval), and in 2007 (within 600-1000 $\mu g\,l^{-1}$ contour interval). At **019**, concentrations remain relatively stable from 2002 to 2008. At **226**, bromate concentrations show a rising trend between early 2002 and mid 2005; between mid 2005 and 2008, concentrations are relatively constant, with a slight decreasing trend. Interestingly, the start of this declining trend coincides with the start of the Hatfield Scavenge Pumping Trial (Section 3.5). However, a decline is not seen at **019**, and at **028** concentrations had already started to decline over 2004 and 2005.

With the exception of the very low concentrations seen over 2001, the concentration trend at **028** and **019** broadly matches the water level trend (water levels decline from highs in 2001 to lows in late 2006, rising slightly over 2007. However, at location **226**, bromate concentrations only start to follow the water level trend from early 2005. For all three locations, fluctuations in concentration also appear to follow fluctuations in rainfall. The relationship between bromate concentrations and water level is discussed further in Section 4.6.

To the north, between the 1000 $\mu g\,l^{-1}$ contour and the northern margin, locations **020** and **022** show bromate concentrations between 30 $\mu g\,l^{-1}$ and 50 $\mu g\,l^{-1}$, although **020** does show annual average concentrations below this (2003) and above this (2001 and 2002).

4.4.2.1 Northern Margin (west of Hatfield area)

The northern extent of the bromate contamination is defined by locations **016** and **167** (old and new borehole at Old Cottage, Green Lane, Hatfield), location **017**, location **025** and location **007**. These locations have been monitored fairly regularly between 2000 and 2008 and time series for these locations show bromate concentrations below the MDL, with the exception of sporadic occurrences of low bromate concentrations ($<$10 $\mu g\,l^{-1}$). Location **025** does show bromate concentrations up to 45 $\mu g\,l^{-1}$. In 2000, a number of locations were monitored to the north of the aforementioned locations, and these all returned concentrations below the MDL.

Location **007**, which has consistently yielded bromate concentrations below the MDL, causes the maximum extent contour to deviate from an apparently smooth curve between **017** and **016**. This

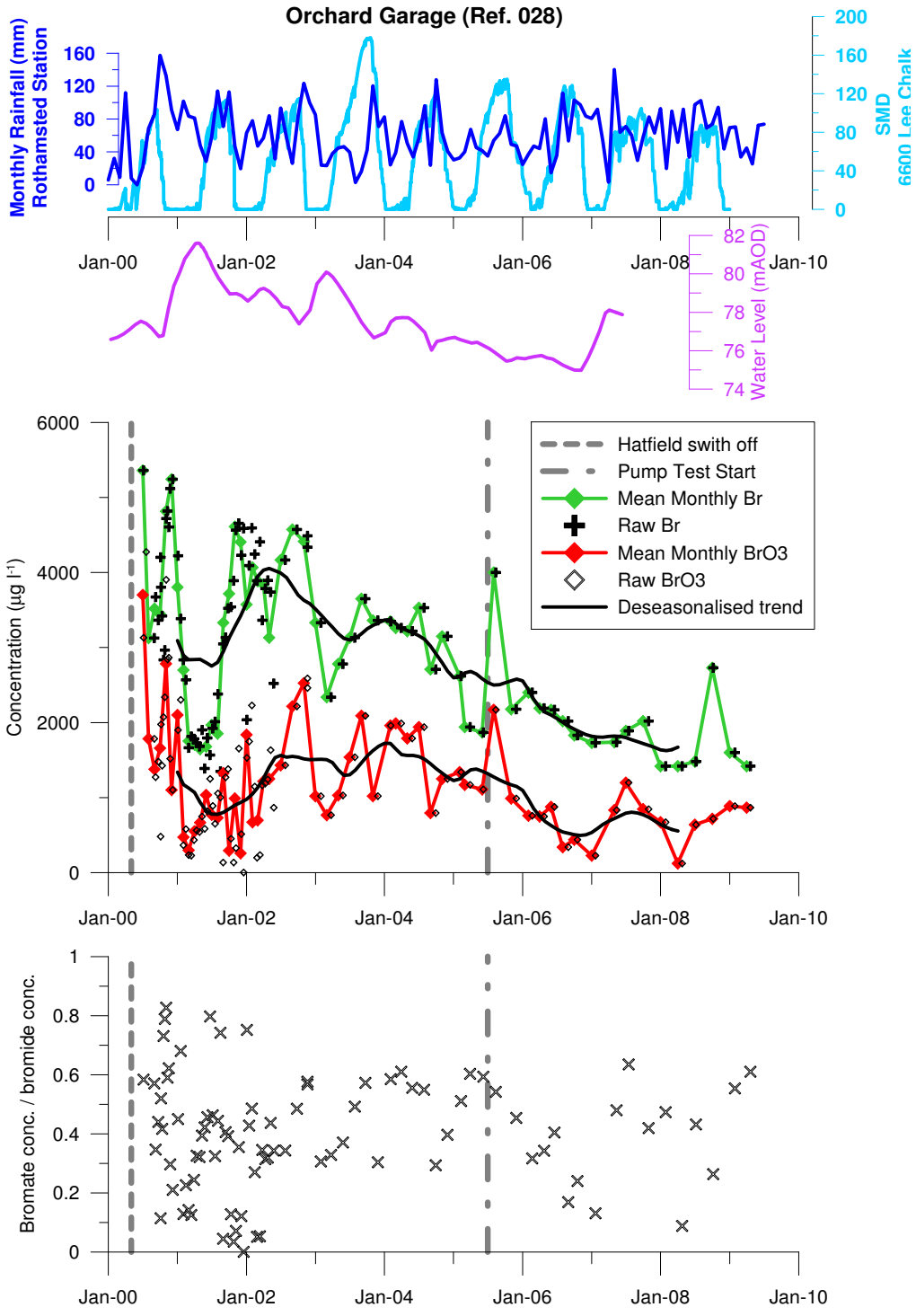

Figure 4.20: Time series of bromate and bromide concentrations at selected locations between Sandridge and Hatfield, soil moisture deficit, and monthly rainfall.

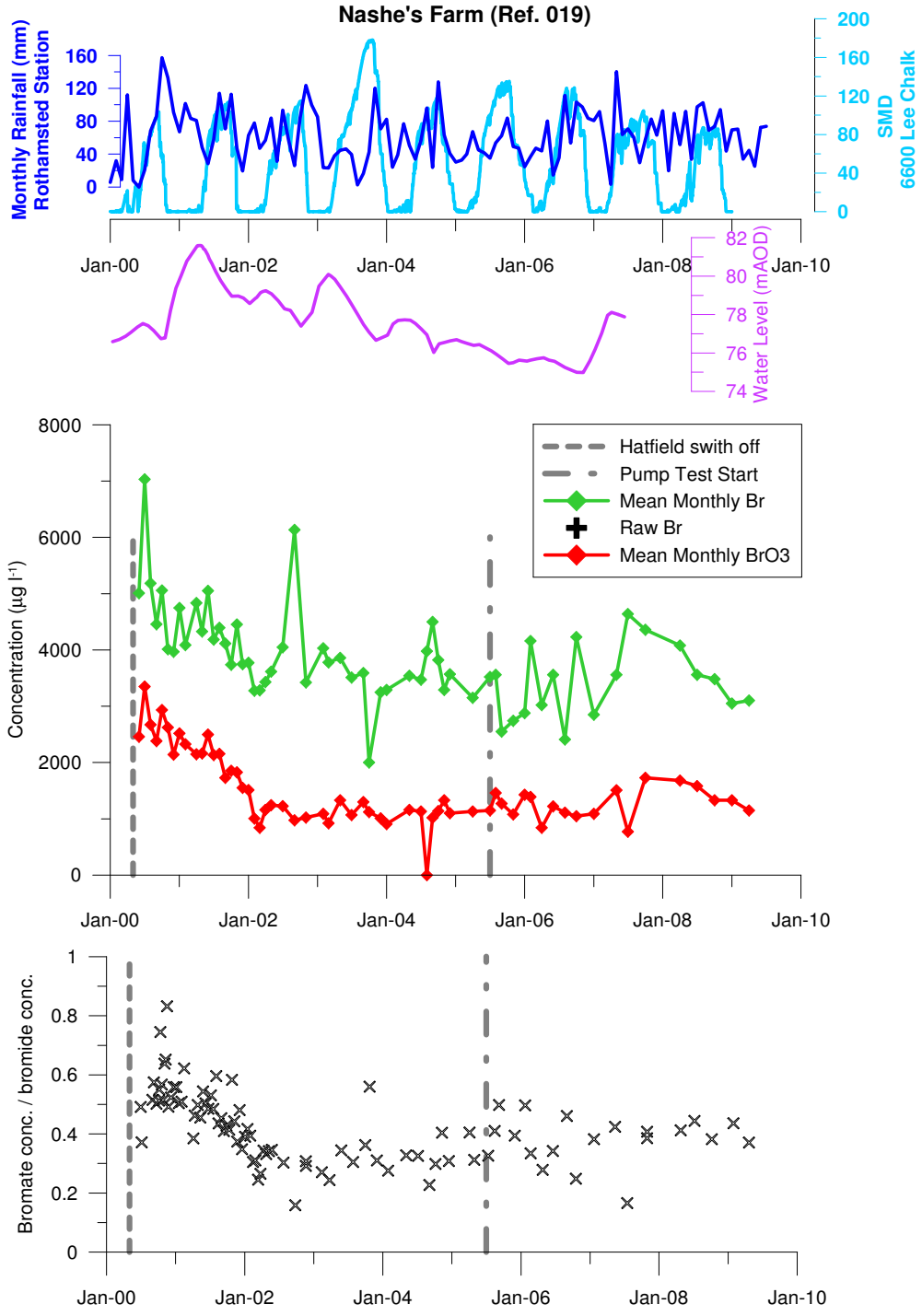

Figure 4.21: Time series of bromate and bromide concentrations at selected locations between Sandridge and Hatfield, soil moisture deficit, and monthly rainfall.

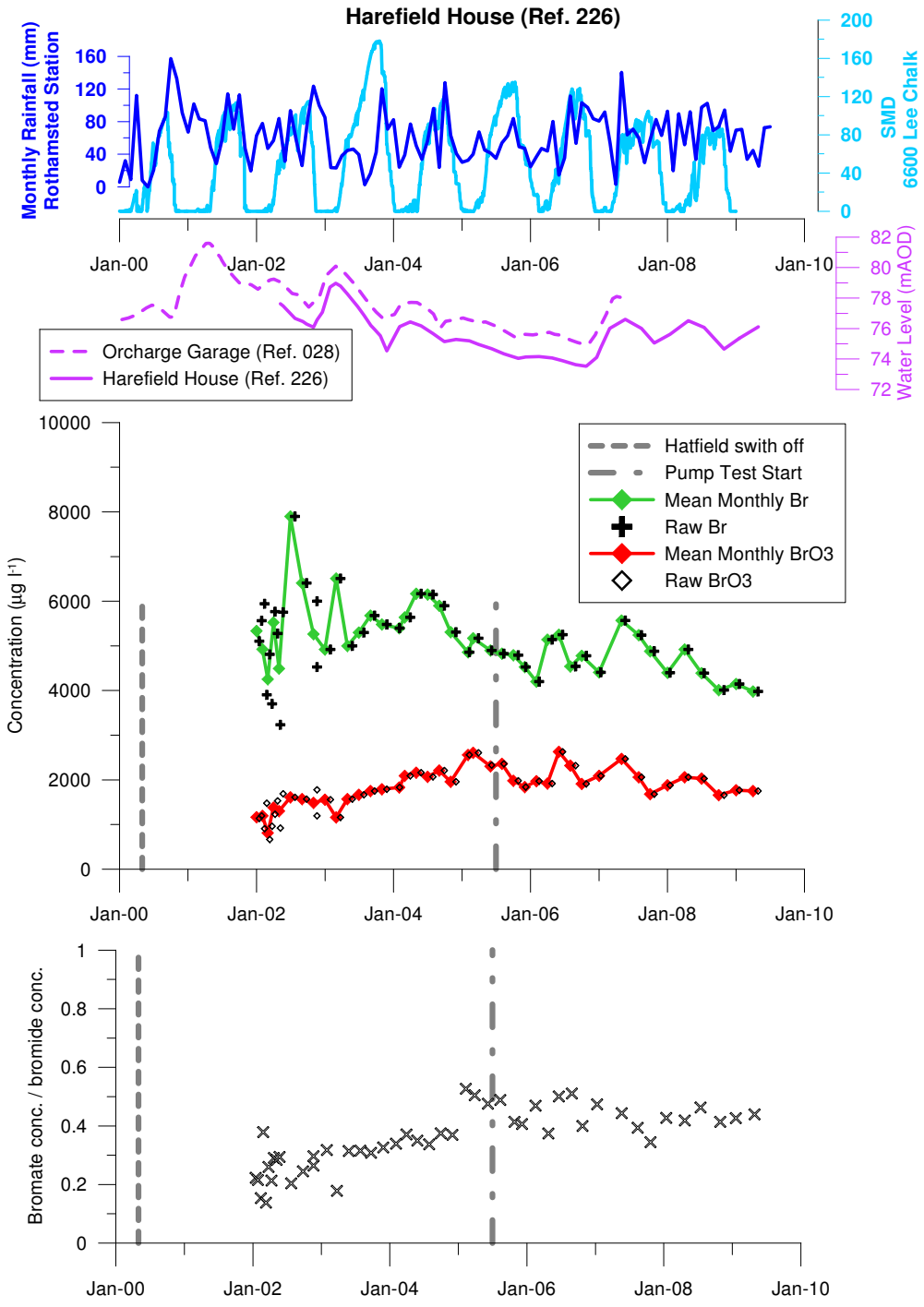

Figure 4.22: Time series of bromate and bromide concentrations at selected locations between Sandridge and Hatfield, soil moisture deficit, and monthly rainfall.

deviation is not supported by concentrations above 50 μg l^{-1} which are consistently monitored at location **065**, location **372** and location **378**.

4.4.2.2 Southern Margin (west of Hatfield area)

The southern margin is less clearly defined by the monitoring data. Close to the source site, location **227** (BH beside Jersey Farm Pond), drilled in 2002, shows concentrations below the MDL, except for low concentrations in 2002. Locations **059**, **060**, and **199** to the south of Hatfield Quarry show bromate concentrations generally below MDL, with some intermittent low bromate concentrations. Location **162** generally shows low concentrations of bromate (<10 μg l^{-1}) but concentrations fall below the MDL in 2007 and 2008. Additionally, location **228**, drilled in 2002, yields bromate concentrations below, and occasionally just above, the MDL. Location **010b** (Glinwell's Nursery) similarly shows isolated incidences above the MDL (these occur in late 2001 and early 2002). Generally, it is not possible to discern trends from the time series. Further south/southwest towards St Albans, there are groundwater monitoring locations that have shown bromate concentrations above the MDL, although these appear to be relatively isolated.

4.4.3 Hatfield Quarry

Further down-gradient, around the Hatfield Quarry area, the spatial distribution is defined by locations **067**, **068**, **061**, **064** **066**, **062**, **166**, **063**, **069**, **065** and **163**, and more recently (since 2005) locations **385**, **386**, **372** and **378**. In general, the bromate distribution is indicated by concentrations of approximately 500 μg l^{-1} to 1500 μg l^{-1} in the central part of the quarry, and lower concentrations in the range 100 to 500 μg l^{-1} in the northern part of the Quarry (Sutton's Farm area). A number of boreholes within the quarry (locations **070** to **076**) were sampled once in 2000 and all yielded bromate concentrations below the MDL. There is no information in the database on the construction of these boreholes, and it is therefore not clear whether they represent groundwater from the Chalk or from the superficial deposits.

The locations **067**, **065** and **166** provide good time series data over the period 2000 to 2008 (Figure 4.23 to 4.23). Locations **067** and **065** both show a rise in bromate (and bromide) concentrations in 2002 compared to 2000 and 2001 concentrations. Bromate concentrations then remain fairly stable until the end of 2005, after which concentrations at location **067** fall to levels comparable to 2000 and 2001 (with a particularly low concentration in October 2007). Locations **166** shows large fluctuations in its time series, However maximum concentrations remain at similar levels between 2000 and 2008, and no clear trend is discernible.

At location **068**, bromate concentrations have decreased from between 10 and 25 μg l^{-1} over 2001, to around 5 μg l^{-1} from 2002 to 2008. Although there is a gap in sample results between October 2002 and October 2005, the following observations can be made regarding trends in bromate concentrations at locations around the Quarry area:

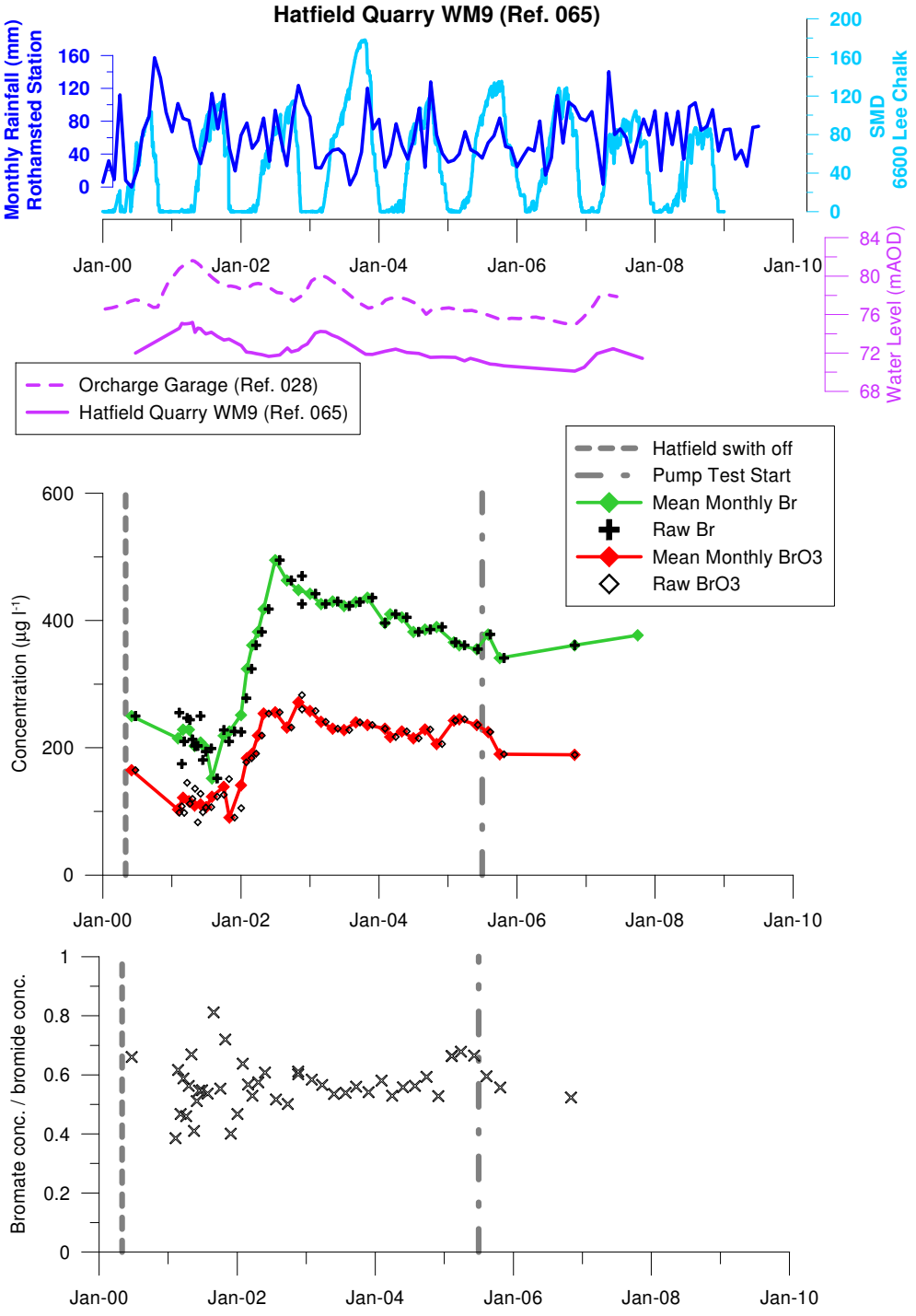

Figure 4.23: Time series of bromate and bromide concentrations at selected locations in the Hatfield Quarry area, soil moisture deficit, and monthly rainfall.

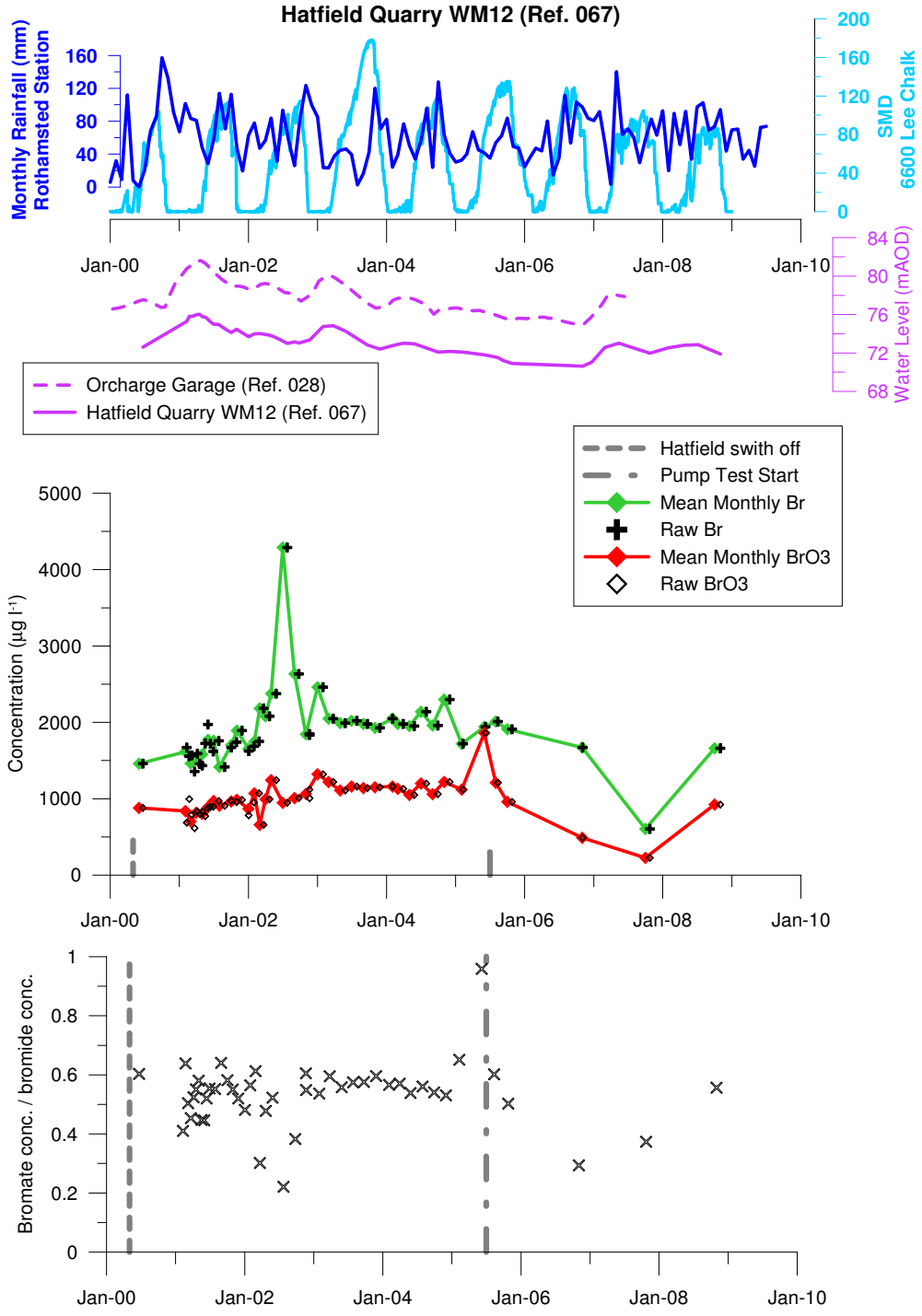

Figure 4.24: Time series of bromate and bromide concentrations at selected locations in the Hatfield Quarry area, soil moisture deficit, and monthly rainfall.

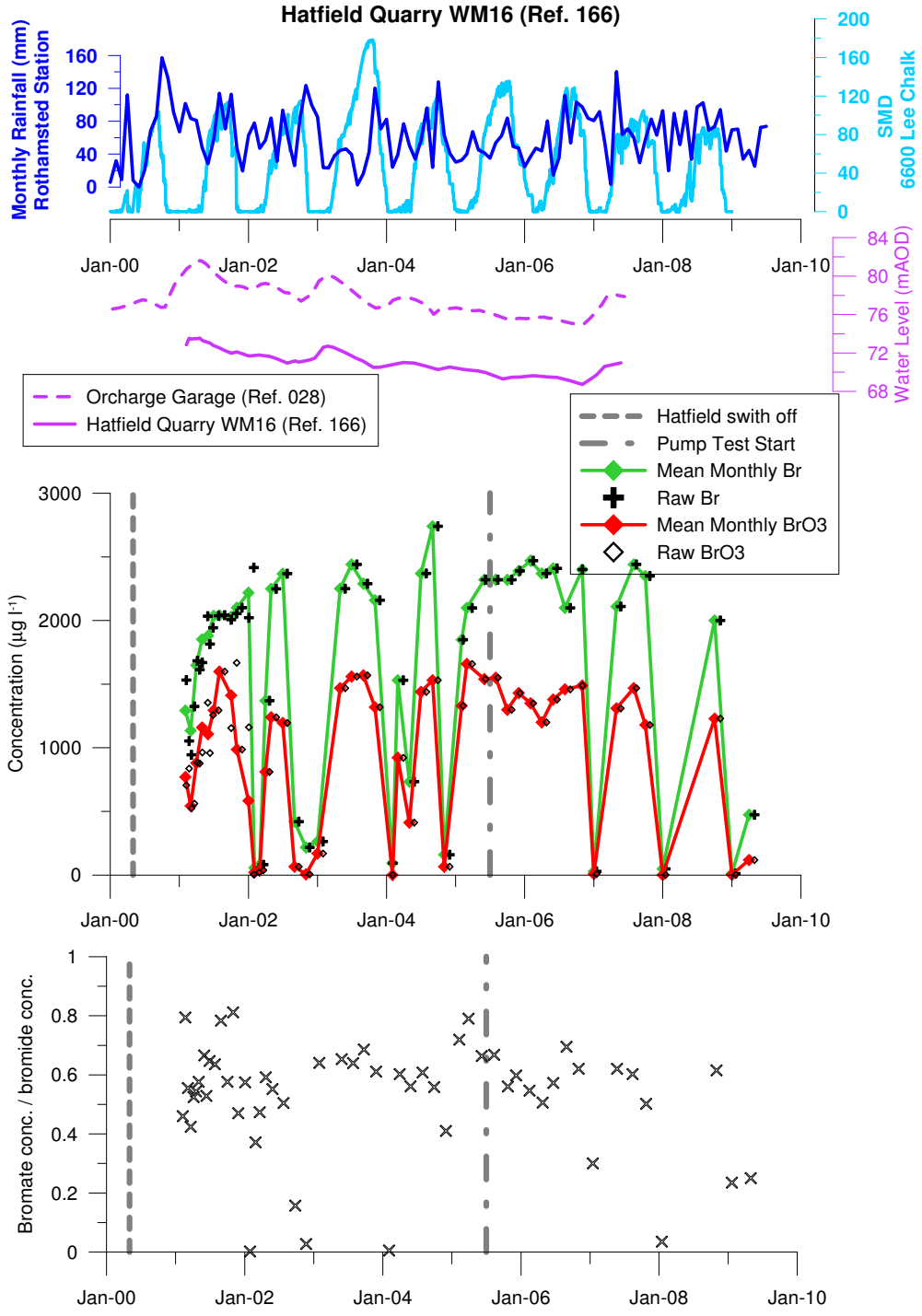

Figure 4.25: Time series of bromate and bromide concentrations at selected locations in the Hatfield Quarry area, soil moisture deficit, and monthly rainfall.

- Locations **061** and **064** show an apparent decreasing trend in bromate concentrations
- Locations **062** and **066** show generally stable trend in bromate concentrations
- Locations **211**shows a general increase (although concentrations are quite variable).

Since 2005:

- Locations **381** and **372** show stable concentrations
- Locations **385** and **386** show stable, or slight decline.
- Location **378** shows a decline in concentrations.

Additionally, locations **059**, **060**, **162** and **199** to the south of Hatfield Quarry define the southern margin of the bromate contamination, and locations **007**, **380**, **381** and **373** to the north of Hatfield Quarry define the northern margin of the bromate contamination. Locations **060** and **199** show only sporadic occurrences of bromate above the MDL. Location **059** shows concentrations below MDL or just above (<1 μg l^{-1}): the incidences of concentrations above the MDL become more frequent after June 2003, and three successive results between 2 and 5 μg l^{-1} occur in the latter half of 2006. Bromide concentrations show no obvious trend between 2001 and 2008. In contrast, location **162** shows variable concentrations up to $\sim$ 12 μg l^{-1}, with slight rising trend observable until the end of 2006. Subsequent concentrations have been below the MDL. Bromide concentrations have also decreased over 2007 and 2008.

Around the northern margin, at location **380**, bromate concentrations have decreased from between 1 and 3 μg l^{-1} between late 2005 and early 2007, to below the MDL over 2007 and 2008. Bromate concentrations are much more variable at location **381**, fluctuating between 1 and 5 μg l^{-1} (although one concentration of 9.3 μg l^{-1} in July 2008) with no discernible trend in bromate (or bromide) concentrations.

4.4.4 Hatfield area

In the Hatfield area, the spatial distribution of bromate is defined by locations **001**, **002**, **003**, **191**, **265**, **160**, **378**, **379** and **402**. Times series are given in Figure 4.26 to 4.30.

Location **001** (Hatfield P.S.) has a very good time series from 2000 to 2008. The trend had been described in Section 3.5. Location **002** (Hatfield Business Park BH) shows a slight rising trend. There is a gap between late 2002 and early 2006 when no samples were taken, and after this bromate concentrations remain relatively stable at around 300 to 500 μg l^{-1} over 2006, 2007 and 2008. The slight rising trend over 2000 and 2001 coincides with a decline in water levels. Also, Hatfield switch-off in May 2000 may have some influence on concentration trends, particularly as concentrations appear to level off after the start of the Hatfield scavenge pumping trial. The times series for location **003** (Hatfield Bus Garage BH) shows bromate concentrations around 600 μg l^{-1} from June 2000 until May 2001, and between about 400 and 800 μg l^{-1} from May 2002 until July 2002. These elevated concentrations are separated by an extended period of low bromate (and bromide) concentrations between June and

December 2001. The observations have been the subject of much discussion, and the Environment Agency concluded that leakage from shallow depth (via the borehole annulus) was impacting on borehole water quality (Atkins, 2006). Location **402** (Comet Way BH5) shows a rising trend of bromate (and bromide) concentrations from January 2006 and December 2008, with concentrations increasing from $\sim$ 400 μg l^{-1} to $\sim$700 μg l^{-1}. Location **160** shows a declining trend in bromate concentrations, from $\sim$ 800 μg l^{-1} in September 2001 to $\sim$ 500 μg l^{-1} in July and August 2002, although concentrations then increase to $\sim$700 μg l^{-1} in September and October 2002. No samples were taken again until May 2005, when concentrations were recorded below MDL until September 2005.

To the north, at location **378** bromate concentrations show a declining trend from $\sim$ 140 μg l^{-1} at the end of 2005 to $\sim$90 μg l^{-1} at the end of 2008. At location **379** bromate concentrations are generally around 40 to 60 μg l^{-1}, although a slight declining trend appears to occur over 2006, 2007 and 2008. Bromide concentrations mirror bromate concentration trends for both of these boreholes. The northern margin is defined by locations **016**/**162** (Old Cottage, Green Lane, Old BH/New BH), **375** and **376**. Location **016**/**162** shows only a few isolated results above the MDL. Location **375** yields concentrations around 1 μg l^{-1}, with a peak of 3 to 4 μg l^{-1} in Autumn 2006.

The southern margin is defined by location **235** (Carter's Pond BH), location **142** and location **195**. Locations **142** and **195** are almost always below the MDL. Time series for location **235** (Carter's Pond) shows bromate below the MDL, with the exception of intermittent concentrations of 1 to 2 μg l^{-1} in late 2001 and early 2002. Further south, locations **049** (Brand's Nursery BH), location **006**, **014** and **015** are typically below MDL, but show intermittent concentrations above the MDL.

Slight rising trends in bromate concentrations are observed at locations **191** (Mill Green BH) and **265** (Park Street BH) to the east towards the Lea Valley. Bromate concentrations rise from $\sim$2 to 4 μg l^{-1} in 2001 and 2002 to $\sim$8 to 10 μg l^{-1} in 2004 to 2008 (with lower concentrations of $\sim$ 2 to 4 μg l^{-1} in late 2006 and early 2008) for **191**. However, there are a number of results below MDL at **191**. The time series for **265** is very variable, with concentrations fluctuating considerably. However, there appear to be two parallel trend lines: one from $\sim$2 to 4 μg l^{-1} in 2002 to $\sim$18 to 22 μg l^{-1} in 2008, and another from $\sim$40 to 45 μg l^{-1} in 2002 to $\sim$50 to 60 μg l^{-1} in 2007, and a fall in concentrations to $\sim$45 μg l^{-1} in 2008.

4.4.5 Lea Valley (east of Hatfield area)

The density of the monitoring locations decreases east of Hatfield. The lower density of monitoring boreholes is at least partly due to the depths to groundwater being much greater where the chalk is overlain by London Clay south-east of the Tertiary Escarpment. In general, locations are clustered along the River Lea and New River. Consequently, it is difficult to define the full spatial extent of the bromate contamination. The bromate contamination east of Hatfield is therefore interpreted as extending in an arc following the main karst conduits (Section 3.7) along the River Lee and New River.

The bromate contamination continues from the Hatfield area along the course of the River Lea to location **143** (Essendon P.S.). Arkley Hole Spring (location **287**), located $\sim$1.1 km east of Essendon, shows concentrations comparable to Essendon (**143**) (Figure 4.31).

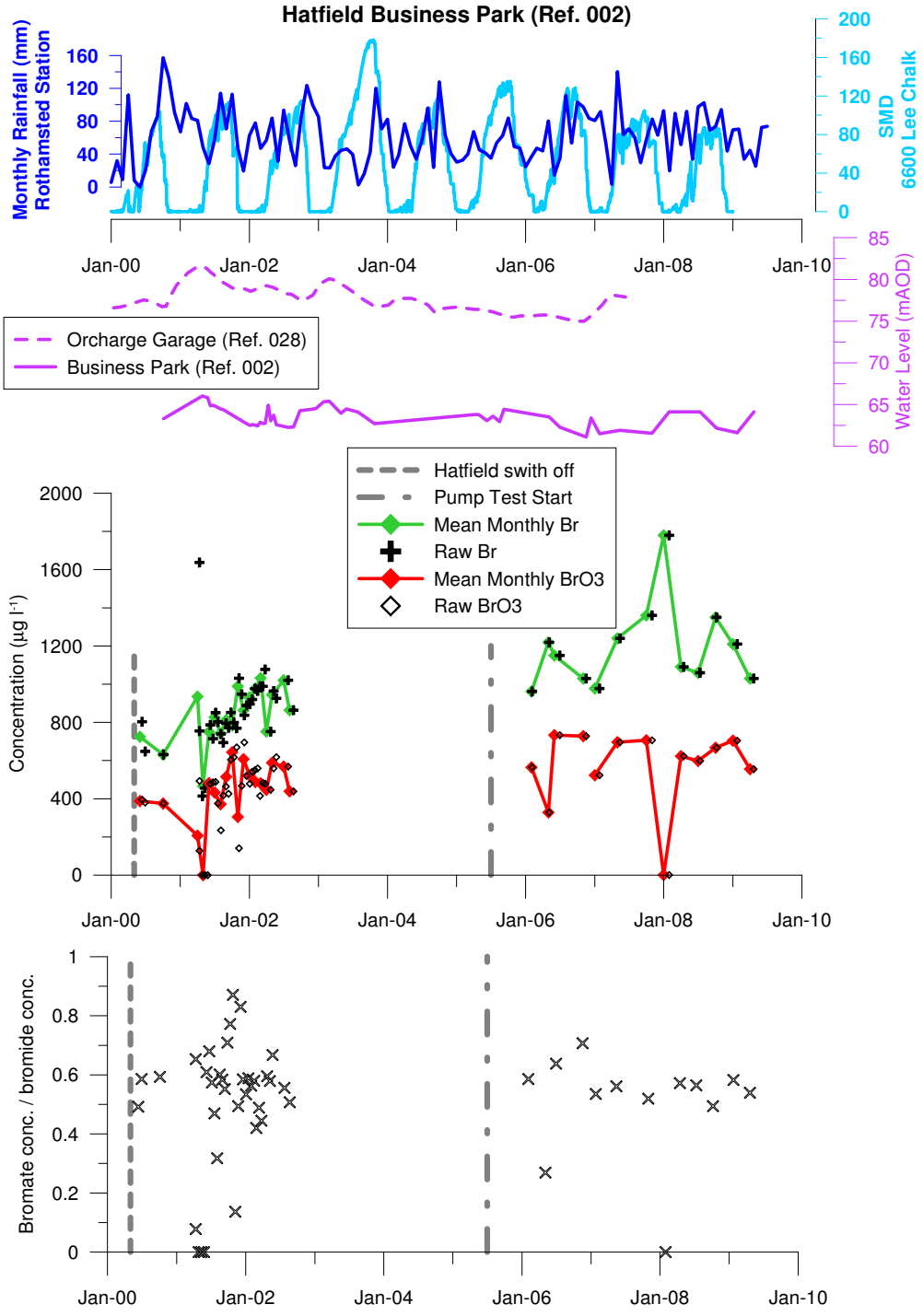

Figure 4.26: Time series of bromate and bromide concentrations at selected locations in the Hatfield area, soil moisture deficit, and monthly rainfall.

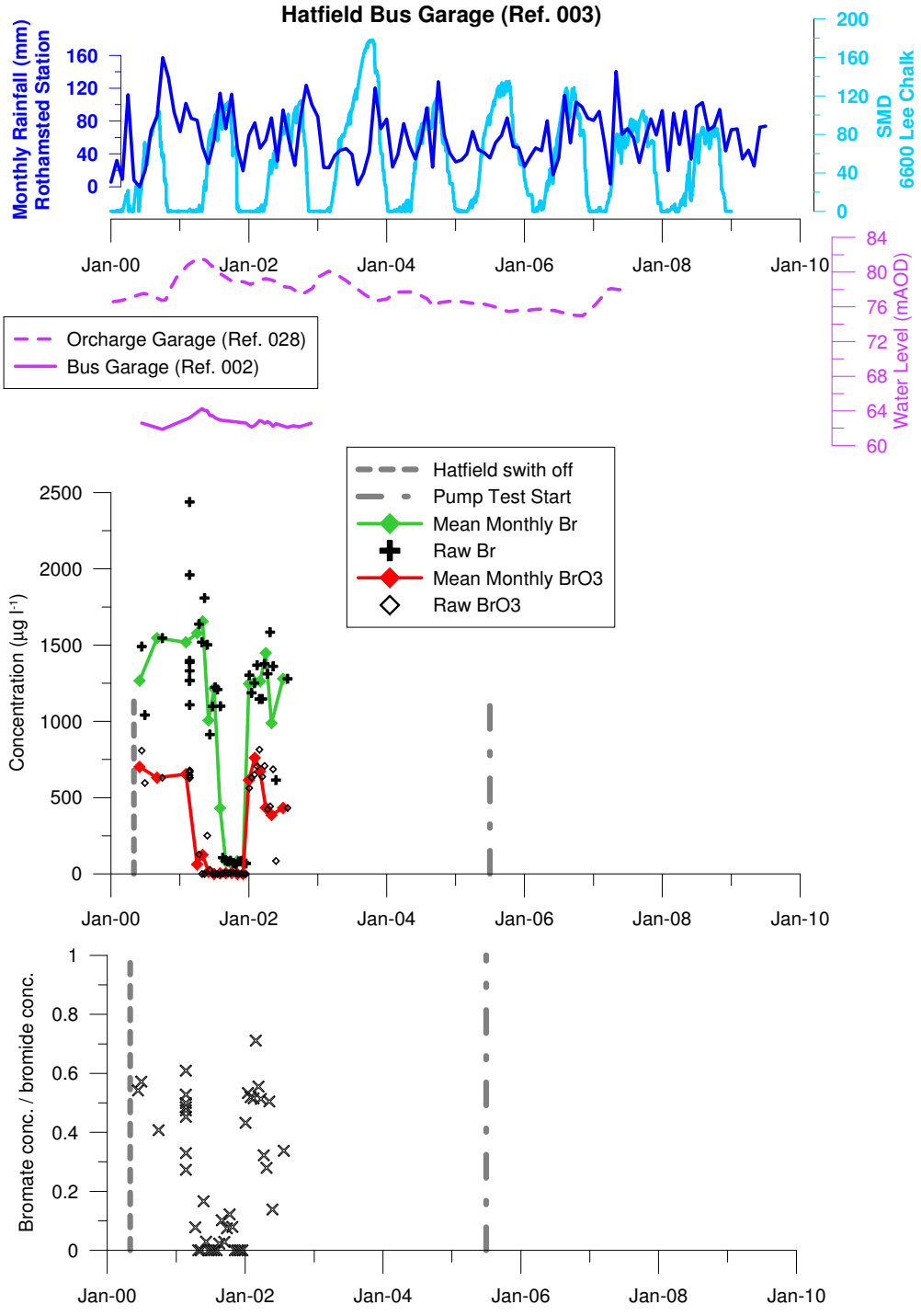

Figure 4.27: Time series of bromate and bromide concentrations at selected locations in the Hatfield area, soil moisture deficit, and monthly rainfall.

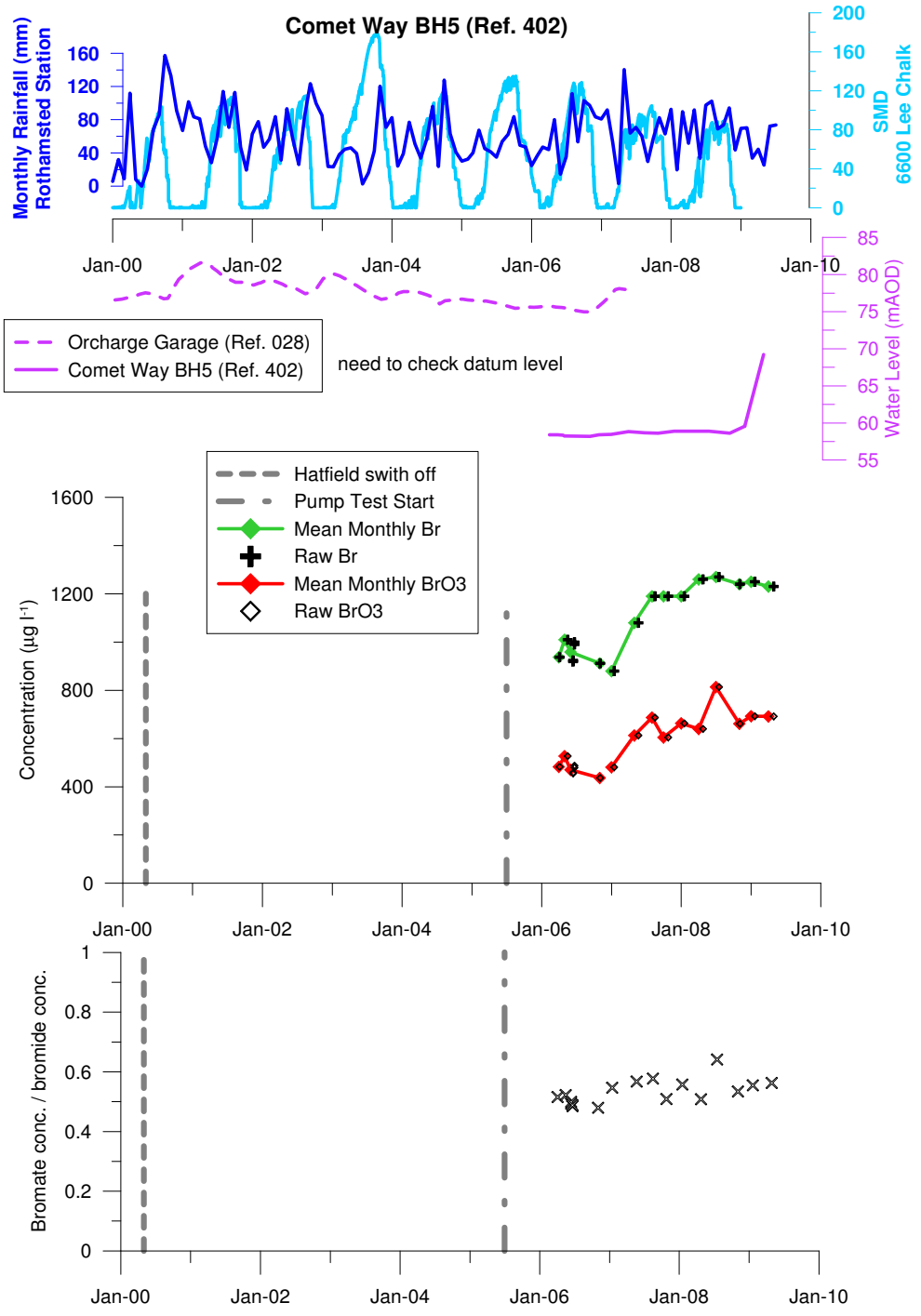

Figure 4.28: Time series of bromate and bromide concentrations at selected locations in the Hatfield area, soil moisture deficit, and monthly rainfall.

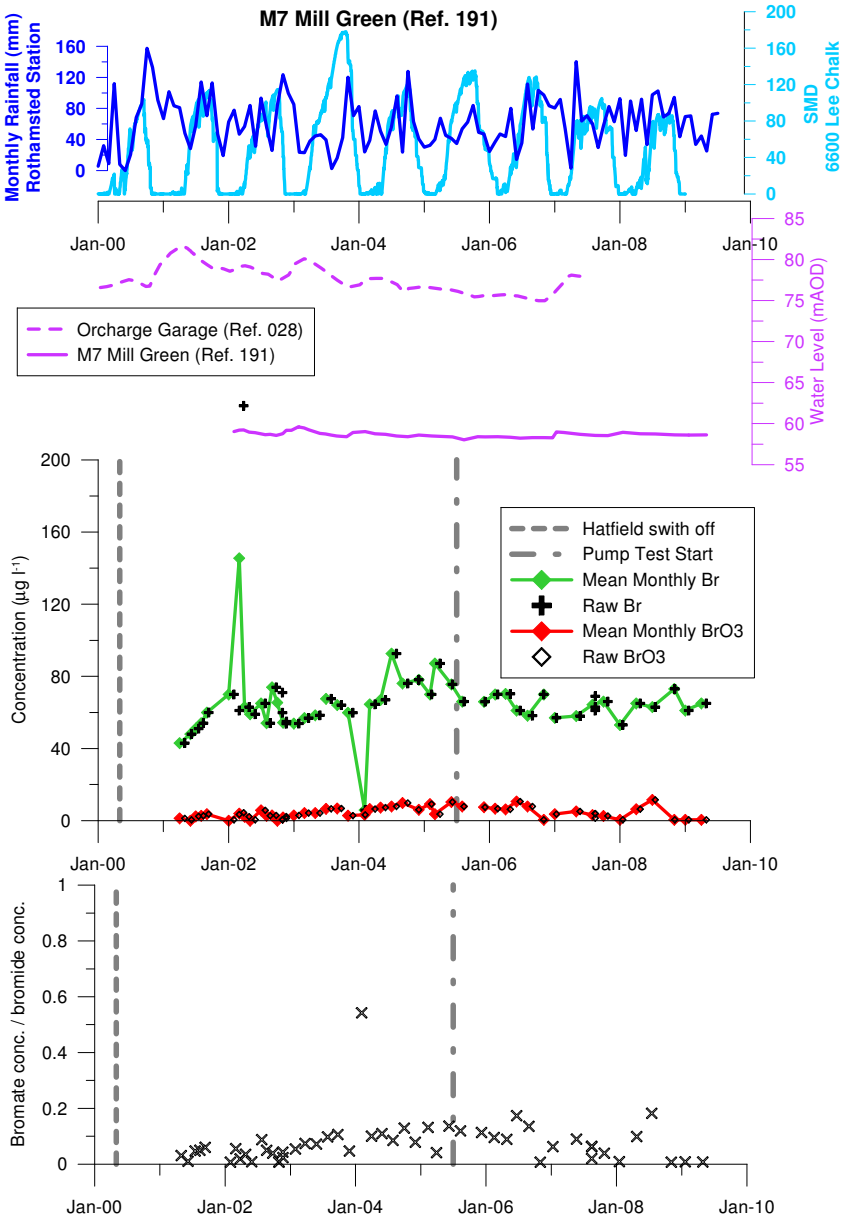

Figure 4.29: Time series of bromate and bromide concentrations at selected locations in the Hatfield area, soil moisture deficit, and monthly rainfall.

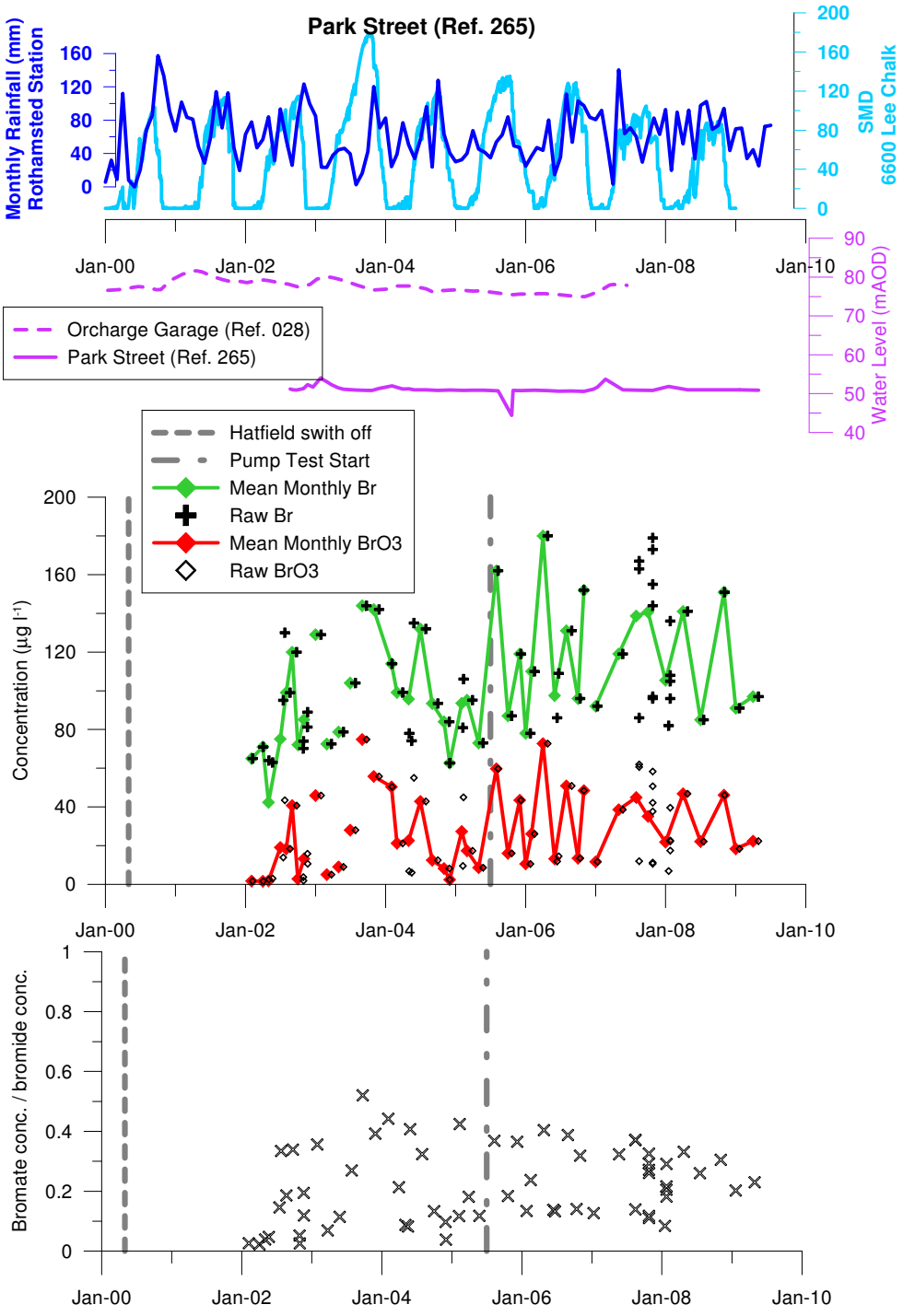

Figure 4.30: Time series of bromate and bromide concentrations at selected locations in the Hatfield area, soil moisture deficit, and monthly rainfall.

Between the Hatfield area and Essendon, at location **266** (Hill End Farm BH), there have been two occurrences of bromate concentrations around 75 $\mu g\ l^{-1}$, but all other concentrations have been below the MDL. These two high results lead to mean annual concentrations between 30 and 40 $\mu g\ l^{-1}$ in 2003 and 2004. These results may be anomalous. In support of this, locations **262**, **263** and **364**, in close proximity to **266**, all show concentrations below MDL. This is despite these locations being directly between bromate in the Hatfield area and Location **143** (Essendon P.S.) where bromate concentrations have consistently been above 10 $\mu g\ l^{-1}$. Interestingly, bromate is also not observed at **144** (Water Hall P.S.), on the southern side of the River Lea, but is recorded at certain locations to the north-east on the northern side of the River Lea at Southfield Wood Landfill boreholes (locations **329** to **331**, **364** to **367** and **369** to **370**). Bromate concentrations around 10 to 20 $\mu g\ l^{-1}$ are recorded at selected locations, generally in the central to north-eastern parts of this area. Additionally, location **404** shows annual average bromate concentrations around 2 to 5 $\mu g\ l^{-1}$, although approximately half of the samples are below MDL.

Bromate concentrations appear to have increased at location **089** (Holly Cottage BH), situated to the north-east of Southfield Wood Landfill, but on the southern side of the River Lea. Bromate concentrations generally rise from below MDL in 2000, to between 5 and 7 $\mu g\ l^{-1}$ between October 2007 and July 2008. This increase is accompanied by an increase in bromide concentrations. A bromate sample in October 2008 shows bromate concentrations return to 2 $\mu g\ l^{-1}$; bromide concentrations remained on a rising trend. Continuing on east along the Lea, locations **305** to **307** are generally below MDL, and always less than 1 $\mu g\ l^{-1}$.

Location **005** (Hatfield London Country Club BH) appears to mark the southern margin; bromate has been recorded on an intermittent basis (in approx two-thirds of the samples taken) throughout the monitoring period, up to a maximum of 13.0 $\mu g\ l^{-1}$. There are a number of locations between **005** and the River Lee that show concentrations below the MDL (Locations **405** to **409**). These were monitored once in 2007. Location **005** is at the end of an inferred conduit route, and locations **405** to **409** are to the east of this.

The locations along the Northern New River define the easterly extent of the bromate contamination. Chadwell Spring shows bromate concentrations intermittently above MDL. Chadwell Spring feeds into the New River. In general, the most northerly of the Northern New River wells, locations **295** (Amwell End P.S.) and **298** (Broadmeads P.S.), show bromate concentrations below the MDL, although sporadic occurrences of bromate above the MDL have occurred, particularly since 2004. Annual average concentrations tend to be highest in the central and southern parts of the wellfield: Hoddesdon, Broxbourne, Turnford and Amwell Marsh.

There are relatively few additional sampling locations to the west of the the River Lee - New River Loop. Location **354** (Van Hage Nurseries BH) shows bromate concentrations below MDL. In 2003, locations **304** and **309**, and locations **293** and **394** and locations **312** to **316** were sampled once, and showed bromate concentrations below MDL.

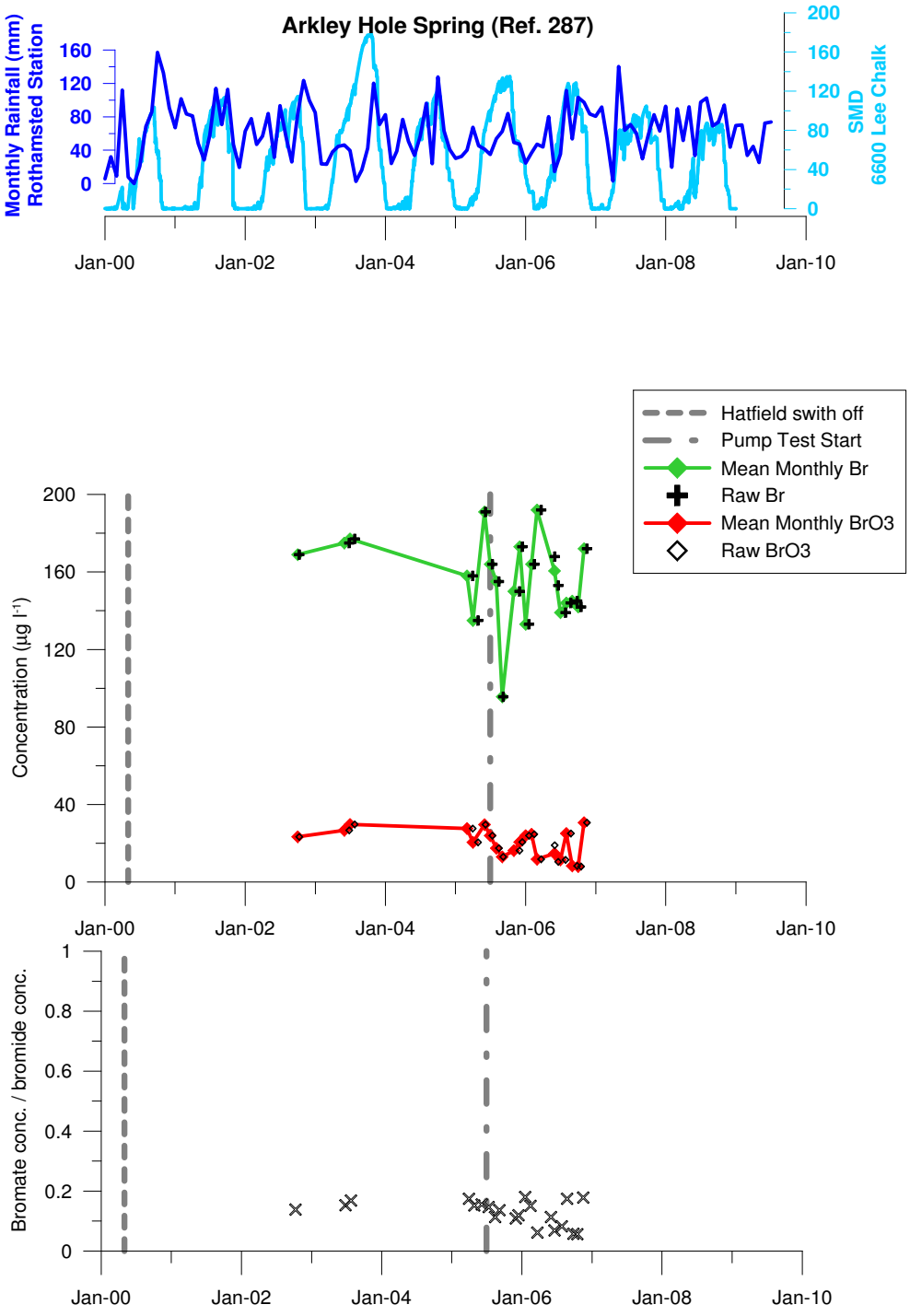

Figure 4.31: Time series of bromate and bromide concentrations at selected locations in the Lea Valley, soil moisture deficit, and monthly rainfall.

4.4.6 Bromide spatial distribution in groundwaters

The distribution of elevated bromide concentrations in groundwater (Figure 4.32) is broadly similar to the distribution of bromate contamination. It is more difficult to identify evidence of spatial variations or to discern evidence of increasing time series trends above background levels owing to the natural occurrence of bromide in groundwaters (typically in the range 50 to 150 $\mu g\, l^{-1}$) (Section 1.7).

In order to assess the background concentration of bromide in the catchment using the data in the UCL monitoring database, all samples from locations where bromate concentrations were consistently below MDL were selected (Figure 4.33). There are a number of locations where bromide is elevated above background concentrations despite these locations showing bromate concentrations below the MDL: location **214** at the source site, locations **070** to **076** around the central part of Hatfield Quarry, location **227** at the southern 'plume' margin between Sandridge and Hatfield Quarry. The background concentration of bromide was estimated using the available samples from location up-gradient of SLC and well beyond the bromate and bromide contamination extent (Figure 4.33). The mean bromide concentration was 65.8 $\mu g\, l^{-1}$.

The spatial distribution of elevated bromide concentrations is indicated in Figure 4.32. In general, the distribution of bromide mirrors that of bromate. However, Atkins (2005) suggest that the bromide 'plume' appears to extend slightly further south than the bromate 'plume' with slightly higher bromide to bromate ratio values in the southern section of Hatfield Quarry and in the Jersey Farm area. Interestingly at the source site, highest bromate concentrations are in the north and bromide concentrations in the south; it is possible that this variation in distributions is reflected at down-gradient locations.

Edmunds (1996) found that the bromide occurrence is best described in terms of the Br^-/Cl^- ratio. Unfortunately all samples that were tested for bromide concentration do not have corresponding chloride concentrations: approximately 22 % of samples have results for both chloride and bromide. Analysis of the regression of bromide concentrations against bromate concentration and chloride concentration indicate that more of the variation in bromide concentrations can be explained by a combination of bromate and chloride concentration than either bromate or chloride independently (Table 4.3).

4.5 Bromate-bromide ratios

Bromate/bromide ratios vary from 0.00 to 1.60 (Figure 4.34). Ratios above 0.80 are associated with Chalk groundwaters with bromate concentrations greater than 4000 $\mu g\, l^{-1}$. For samples with bromate concentrations between 200 $\mu g\, l^{-1}$ and 2000 $\mu g\, l^{-1}$, the bromate/bromide ratio is relatively consistent at around 0.30 to 0.60 for both surface waters and groundwaters. For samples with bromate concentrations between 40 $\mu g\, l^{-1}$ and 200 $\mu g\, l^{-1}$, the bromate/bromide ratio is relatively consistent at around 0.20 to 0.40 for both surface waters and groundwaters. The ratio appears to increase approximately linearly from 0.0 to around 0.20 with increasing bromate concentration for samples with bromate concentrations below 40 $\mu g\, l^{-1}$. There does not appear to be a discernible difference in ratios between surface water and groundwater ratio trends, or between chalk groundwater, gravel groundwater and groundwater from public water supply (PWS).

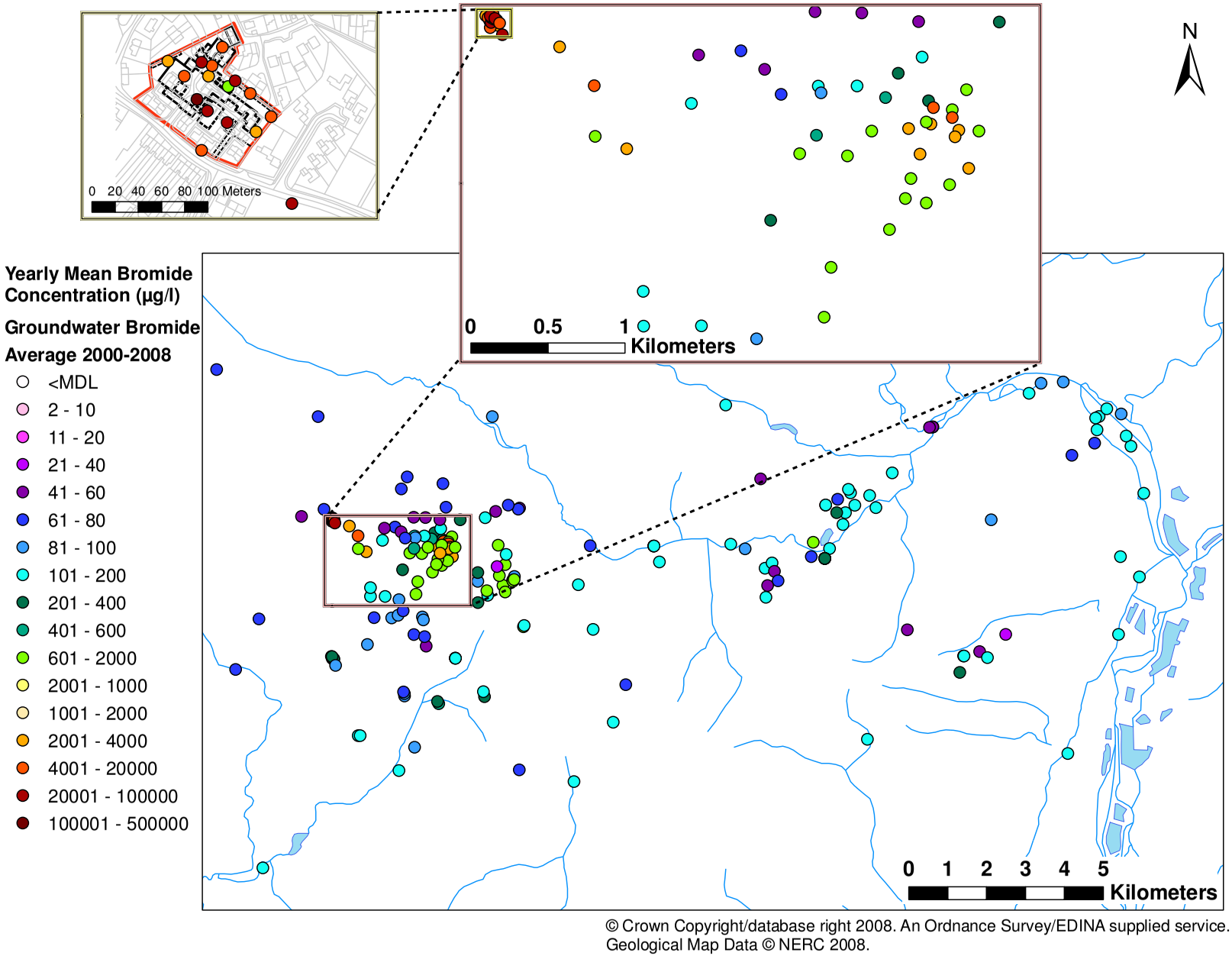

Figure 4.32: Annual average Bromide concentrations in groundwater 2000 to 2008.

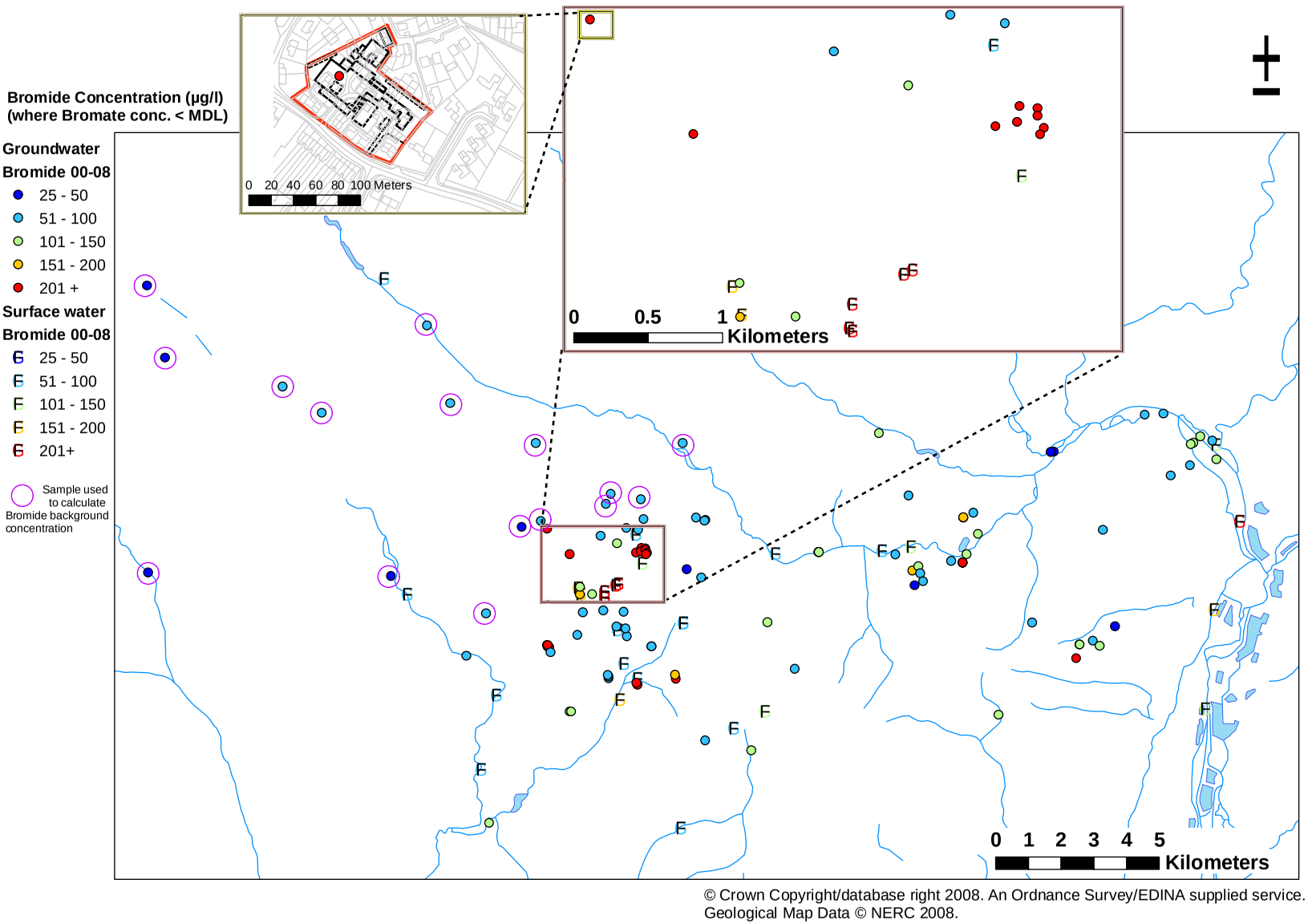

Figure 4.33: Bromide concentrations at locations where bromate concentrations are less than MDL.

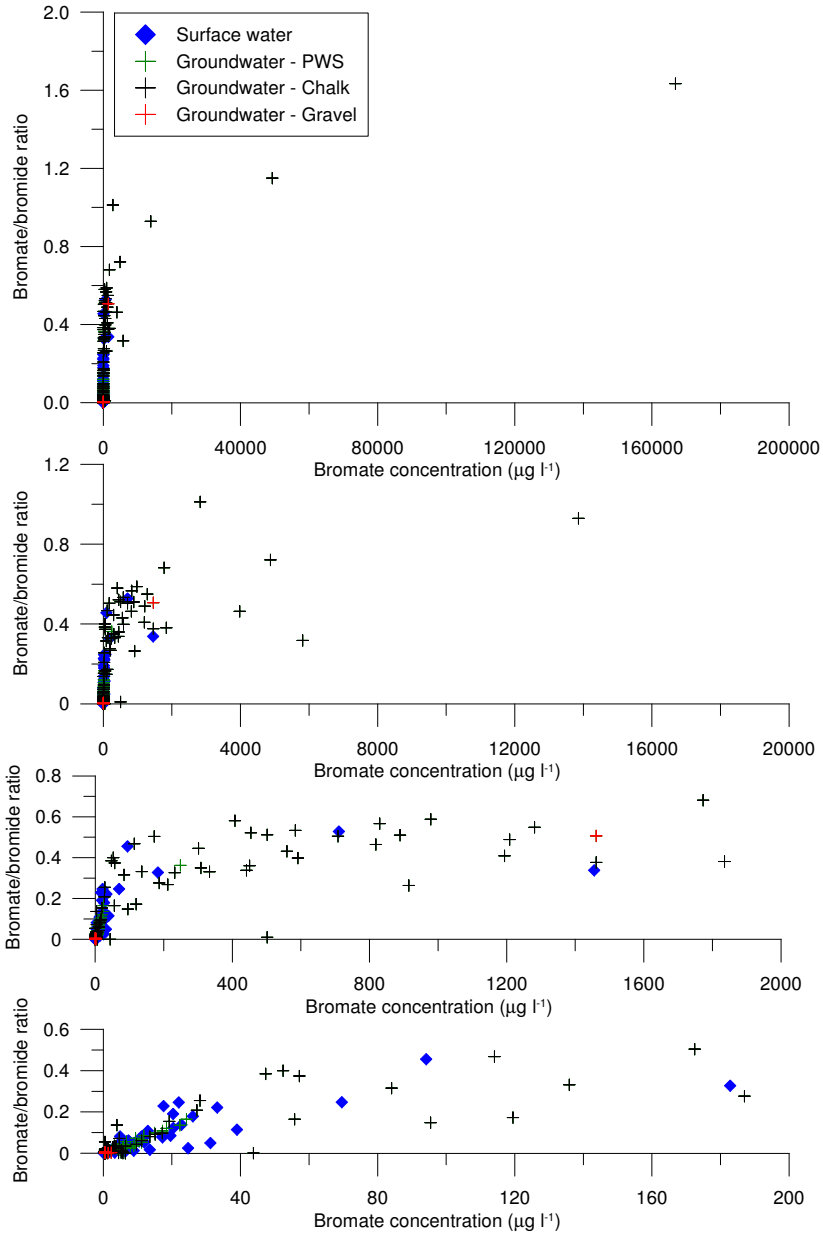

Figure 4.34: Bromate/Bromide ratio variation with bromate concentration for groundwater and surface water samples

Table 4.3: Regression statistics for the response of bromide concentration to bromate concentration and chloride concentration.

For equation Bromide = A + B(Bromate) + C(Chloride)		
N = 557	**R^2**	**P-value[a]**
R^2 overall	37.2%	0.000
R^2 Bromate	31.5%	0.000
R^2 Chloride	5.7%	0.000
[a] The P-value refers to the hypothesis that the regression relationship is statistically significant, i.e. that the apparent relationship between y and x is not likely to arise due to chance alone.		

The spatial distribution of bromate-bromide ratio is shown in Figure 4.35. In general, the higher ratios follow the distribution of bromate contamination. If locations with bromate concentrations less than 1 $\mu g\, l^{-1}$) are excluded from the plot, there is a noticeable cluster of locations with high ratios in the northern part of the St Leonard's Court source site, and following the path of the core bromate 'plume' to Hatfield Quarry and the Hatfield area.

4.6 Bromate concentrations and water levels

Figure 4.36 shows the percentage of samples of bromate concentrations for which there are accompanying water level measurements for each location.

Fluctuations in bromate concentrations are dependent on water level at a number of locations. The regression relationship for the response of bromate concentration to water level (m OD) was analysed for all locations for which there were sufficient time series data with bromate concentrations above MDL and associated water level measurements. Both positive and negative correlations were observed to be statistically significant ($p<0.05$), and water level explains between 10 % and 90 % of the variation in bromate concentration (Figure 4.37). Full statistical results are given in Appendix C. There does not appear to be a pattern in the spatial distribution of negative and positive correlations, or any obvious spatial pattern in those locations that show a statistically significant relationship and those that show no relationship.

4.7 Summary and Conclusions

Detailed analysis of bromate and bromide monitoring data has been undertaken, which has revealed that bromate concentrations are affected by influences including recharge (soil moisture deficit, rainfall), water level, and abstractions. The distribution of these relationships supports the conceptual understanding of an increasing influence of a karst system to the east of the Vale of St Albans area. The seasonal influences are superimposed on a generally stable distribution of bromate and bromide concentrations, which is likely to indicate the importance of the attenuating effect of the double-porosity Chalk. The

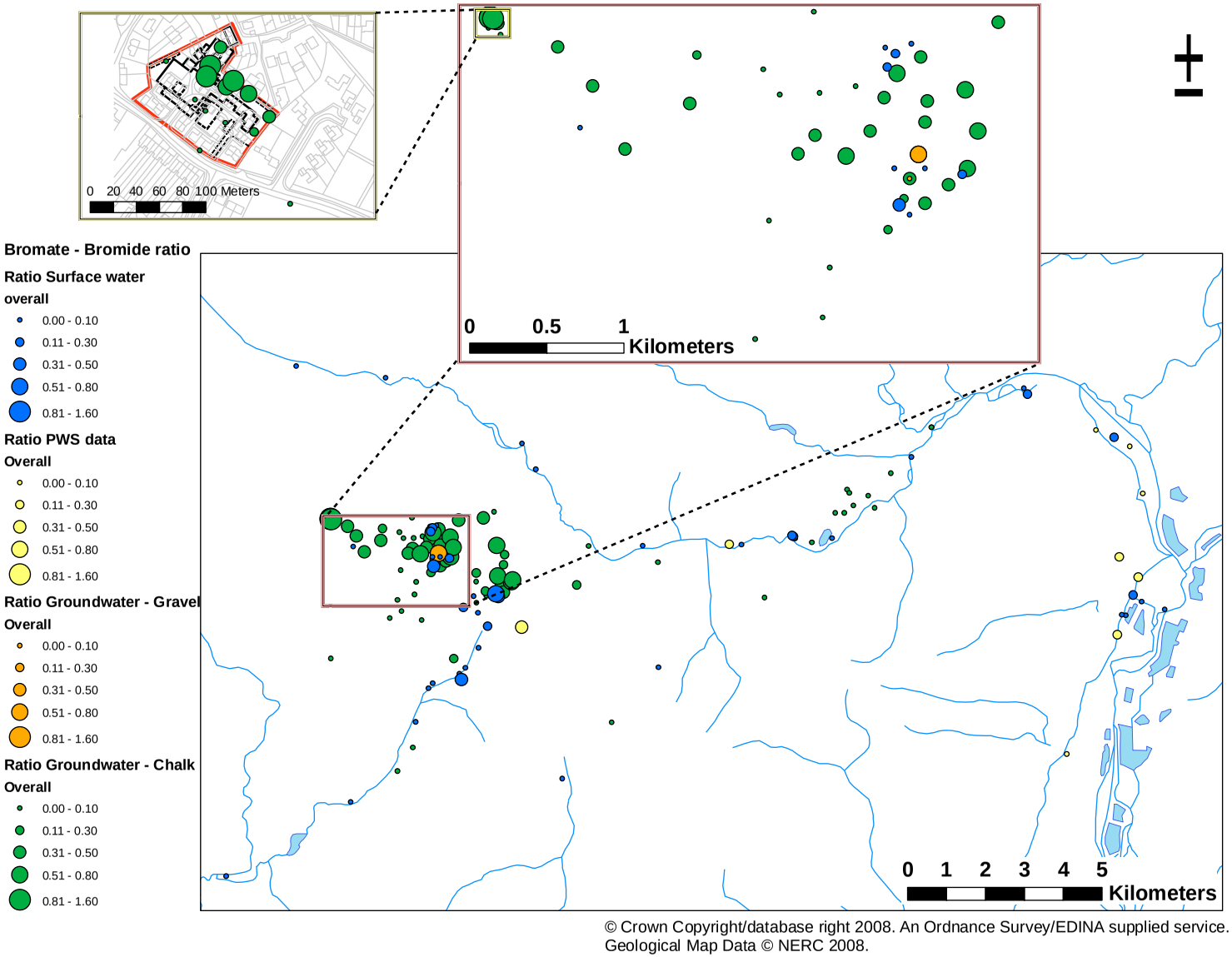

Figure 4.35: Spatial distribution of mean annual bromate/bromide ratio 2000 to 2008.

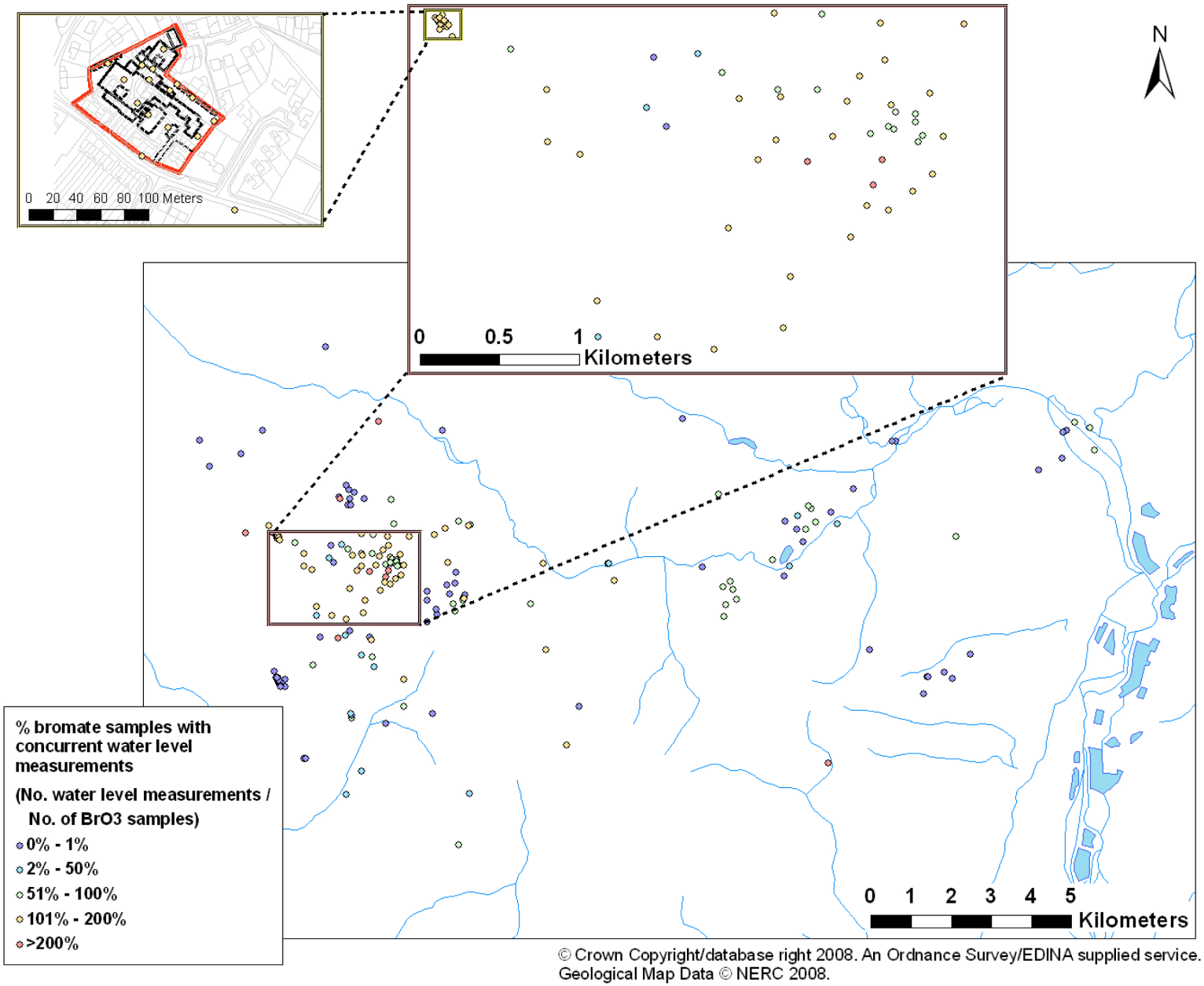

Figure 4.36: Percentage of samples of bromate concentrations for which there are accompanying water level measurements for each location

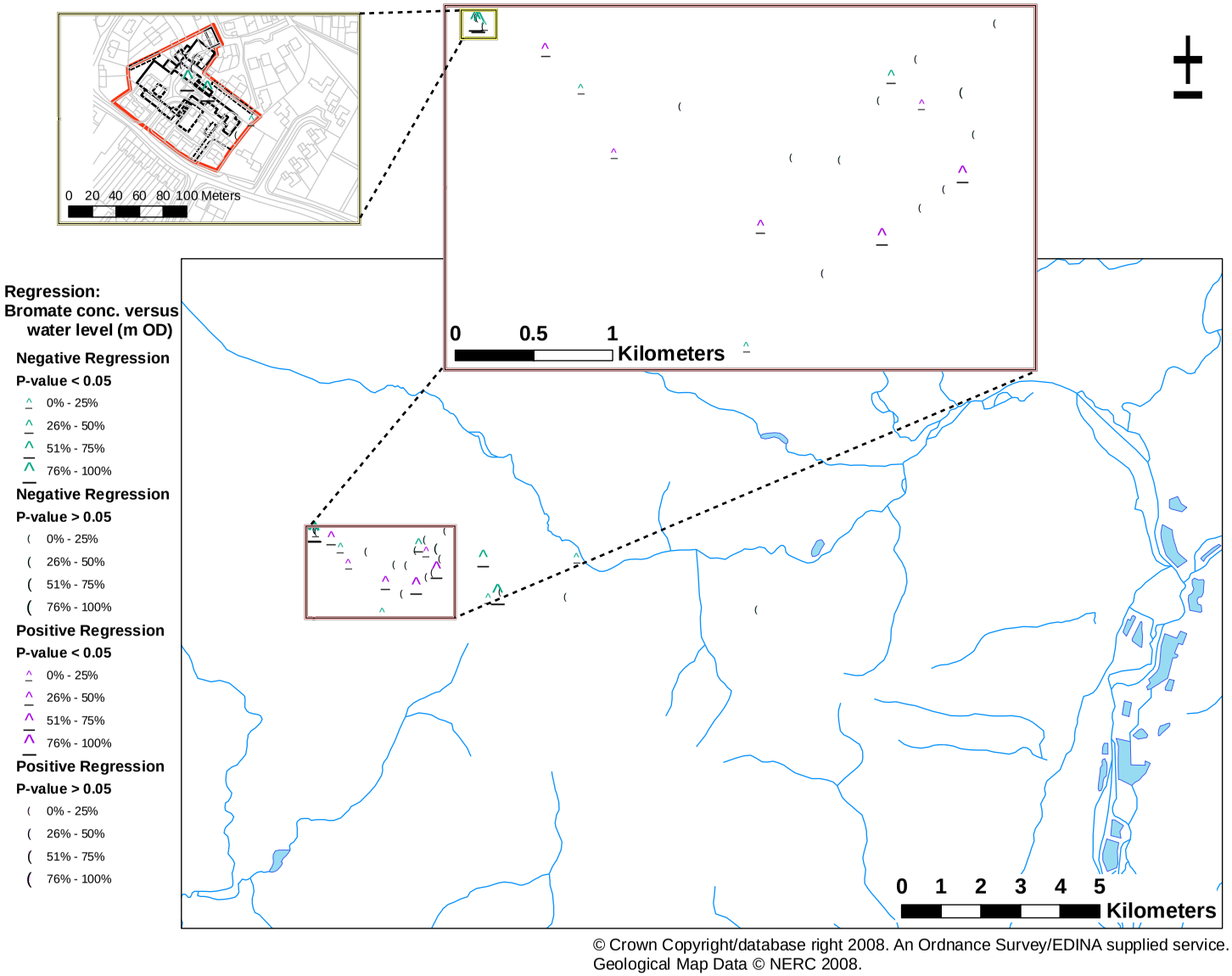

Figure 4.37: Regression relationship for the response of bromate concentration to water level. Percentages refer to the amount of variation explained by the regression (R^2 value)

revised conceptual understanding of flow and transport in the Hertfordshire Chalk has allowed a new interpretation of the spatial distribution and evolution of bromate and bromide within the catchment to be developed between 2000 and 2008. However, the interpretation of the spatial and temporal evolution of bromate and bromide within the catchment is hampered by a number of inadequacies in the available monitoring data:

- Monitoring data are available for a relatively short period of time (a maximum of 8 years continuous data) in relation to the likely timescale of bromate contamination within the catchment;
- Monitoring frequency varies considerably between locations, and varies over time at individual locations, which makes trends difficult to identify with confidence;
- The strong seasonal influences within the time series make trends difficult to discern;
- The data available are generally not depth-specific so that vertical distribution of bromate contamination cannot be investigated;
- The sampling results refer to (mobile) fissure water and there are no data available for (immobile) matrix porewater which is required to characterise the double-porosity behaviour and determine the long-term evolution of bromate contamination within the catchment.

Chapter 5

The Bromate Source

5.1 Chapter objectives

The source of the bromate contamination has been identified as the site of a former chemical works located in Sandridge, Hertfordshire. The site is now the St. Leonard's Court residential development (Figure 5.1). Limited site investigation and groundwater monitoring data are available for the source site and the vicinity. The magnitude and dynamics of bromate release to groundwater beneath the source site, and thus to locations down-gradient of the source site, has consequences for the magnitude and duration of bromate contamination within the catchment. Predictive models of bromate contamination within the catchment are dependent on a realistic and representative source term to quantify the input of bromate from the source site. Uncertainty in the history of the source may be incorporated by development of a range of source term scenarios which are constrained with the limited investigation data at the site.

The objectives of this chapter are:

- To describe and quantify the distribution of bromate at the source site through collation and description of site investigation and monitoring data;
- To develop alternative conceptual scenarios for bromate release to groundwater and quantify these as 'source terms';
- To use the available monitoring data to constrain the potential source terms.

5.2 Chapter structure

The chapter begins by describing the history of the site, then the distribution of bromate and bromide at the source site. A number of conceptual scenarios for bromate release are developed, and the data are used as a basis to constrain the source terms.

5.3 Site History

5.3.1 Sources of information

Information on the site history has been obtained from information and records held by the Environment Agency comprising:

Figure 5.1: Location of the source site in Sandridge, Hertfordshire. Formerly the Steetly chemical works, now the St Leonard's Court residential development.

- Original records from St Albans District Council (the local authority); and
- Additional information collected by the Environment Agency in response to a public request for information conducted in 2001.

An interview with a former worker at the chemical works, conducted by the Environment Agency in August 2001, provided details on the operational activities (EA, 2005). Aerial photograph taken in 1971.

5.3.2 General overview

The Steetly Chemical Works occupied the site from 1955, and is thought to have remained operational until around 1980. The buildings were demolished and the site cleared for redevelopment between 1983 and 1986. During this period the site was left uncovered, and free draining. The residential development, St Leonard's Court, has been present at the site since the end of 1987.

5.3.3 Site investigation and remediation history

A series of site investigations and assessments were undertaken during demolition and redevelopment between 1983 and 1986 (Section 5.4). Some groundwater monitoring data are available from existing boreholes in the vicinity of the site between 1983 and 1987.

Based on recommendations of the site investigations and assessments, the top layer of soil was excavated and removed from selected areas where high levels of contamination had been identified. It is understood this occurred between August 1986 and September 1986 (Roberts, 2001).

Subsequent to discovery of the bromate contamination at Hatfield, site investigations were undertaken in 2000 and 2001 (Section 5.4), alongside sampling from boreholes in the vicinity of the site as part of the bromate groundwater monitoring programme (Section 4.2).

5.3.4 Operational activities of the chemical works

The Steetly Chemical Works was a chemical manufacturing plant which specialised in the manufacture of industrial and pharmaceutical intermediates including potassium bromate and organobromine compounds. Raw materials including bromine, red and yellow phosphorus, and caustic soda were processed into products including ceta-stearyl bromide, sodium and potassium bromate, and zinc bromide.

The former locations of the process areas, based on historical plans, aerial photographs, and the interview are indictated in Figure 5.2. Bromine was stored as a raw material in two main areas of the site: small glass bottles were stored in an open area in the centre of the site, and bulk storage was in the north of the site, to the rear of the main building. Liquid bromate production and solid bromate handling took place in a process room in the northern corner of the site. This building included a sump, which was reported to be for collection of condensate from heating coils of reaction vessels, and spills of materials. The sump is reported to have discharged to foul sewer.

5.4 Chronology and scope of investigations

The scope of the site investigations that have been undertaken at the source site is summarised in Table 5.1 and Figures 5.3 and 5.4.

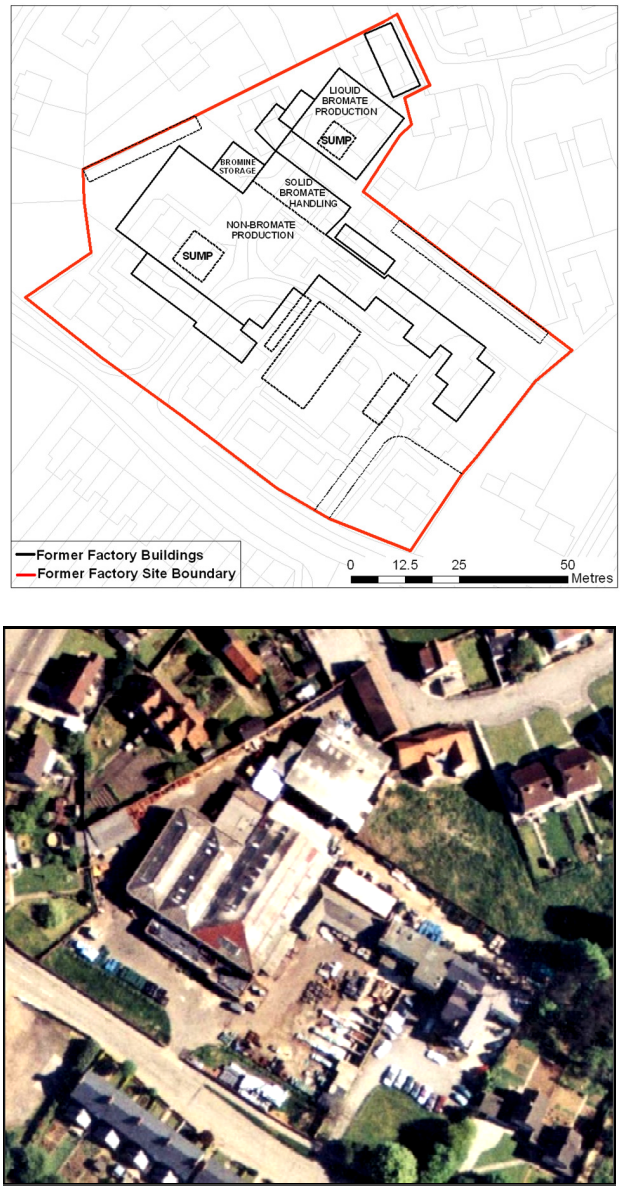

Figure 5.2: Location of former process areas of the Steetly Chemical Works. Based on Atkins (2002) interpretation of historical plans, aerial photographs, and the interview with a former employee of the works. Aerial photograph taken in 1971.

Table 5.1: Chronology and scope of site investigations and monitoring at the source site

Date of site work	Company	Scope of investigation	Associated Reports	Date of report	Client
Aug 1983	STATS	5 boreholes. Soil samples at depths of 0.5, 1.0 & 1.5m. Analysis for bromide and bromate.	Interim report on site investigation, ref 83/3105.	Aug 1983	Crest
None	STATS	Further tests on samples taken in August 1983. Analysis for total bromine and water-extractable bromide.	Second report on site investigation, ref 83/3105A	Sep 1983	Crest
Oct 1983	STATS	Soil samples taken on grid pattern at depths of 0.75 and 1.5m. Tested for Bromide only	Third report on site investigation, ref 83/3105C	Dec 1983	Crest
Mar 1984	STATS	3 boreholes. 6-8m deep into putty chalk. Soil and groundwater samples. Analysis for bromide only. Site was in process of being cleared by demolition contractors.	Report on further site investigations. ref AM/3554	May 1984	Crest
Jan 1985	Chemfix	Borehole C1 drilled to 5.4m deep. Core samples tested for moisture content and bromide.	Field report for drilling of borehole C1 at House Lane, Sandridge on 21/22 January 1985	Mar 1985	Crest
Mar 1985	Southern Testing	51 shallow boreholes, depth generally approx 1.5m. Analysis for bromide.	Hand-augered borehole logs at Sandridge, Herts for Chemfix International Ltd	Mar 1985	Chemfix
-	Chemfix	Report on Southern Testing trial holes from Mar 1985.	Report of the second phase of the field investigation at the Sandridge site	Mar 1985	Crest
May 1985	Chemfix	1 Borehole drilled 40m down-gradient of nearest part of site. Soil and groundwater samples. Analysis for bromide.	Evaluation of the results from the borehole situated 120m down dip from the Sandridge site	Jun 1985	Crest
Aug 2000	Komex	5 boreholes to depths of approx 12m. Soil and groundwater samples. Analysis for bromide and bromate.	Site Investigation at St Leonards Court, Sandridge, St Albans.	Oct 2000	St Albans City and District Council
Nov 2001	Atkins	12 boreholes to depths between 6m and 20m. Soil and groundwater samples. Analysis for bromide and bromate.	St. Leonard's Court, Sandridge, St. Albans. Environmental Site Investigation and Quantitative Pollutant Linkage Assessment.	Dec 2002	Environment Agency

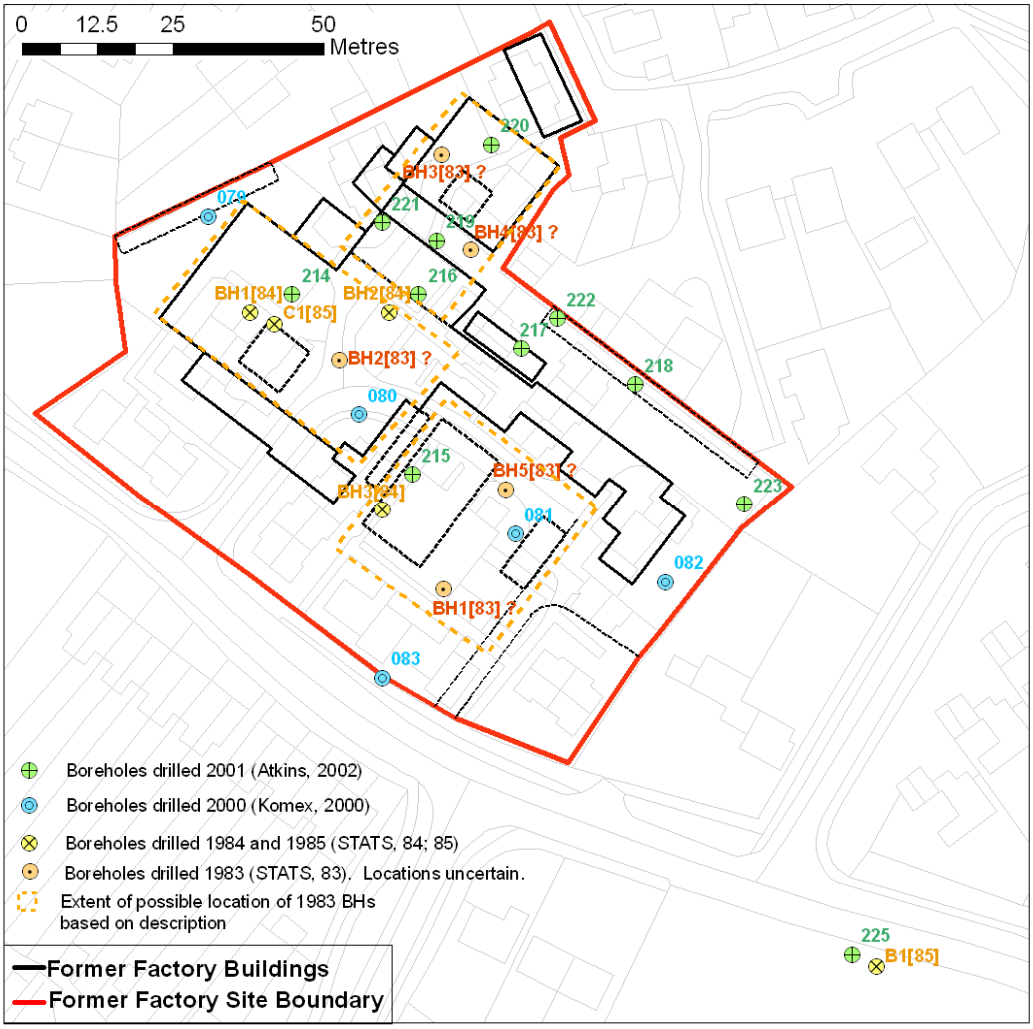

Figure 5.3: Borehole locations from investigations 1983-1985 (STATS, 1983a,b,c, 1984; Chemfix, 1985c) and 2000-2001 (Komex, 2000; Atkins, 2002). For locations from 1983-1985, numbers in square brackets indicate date of drilling.

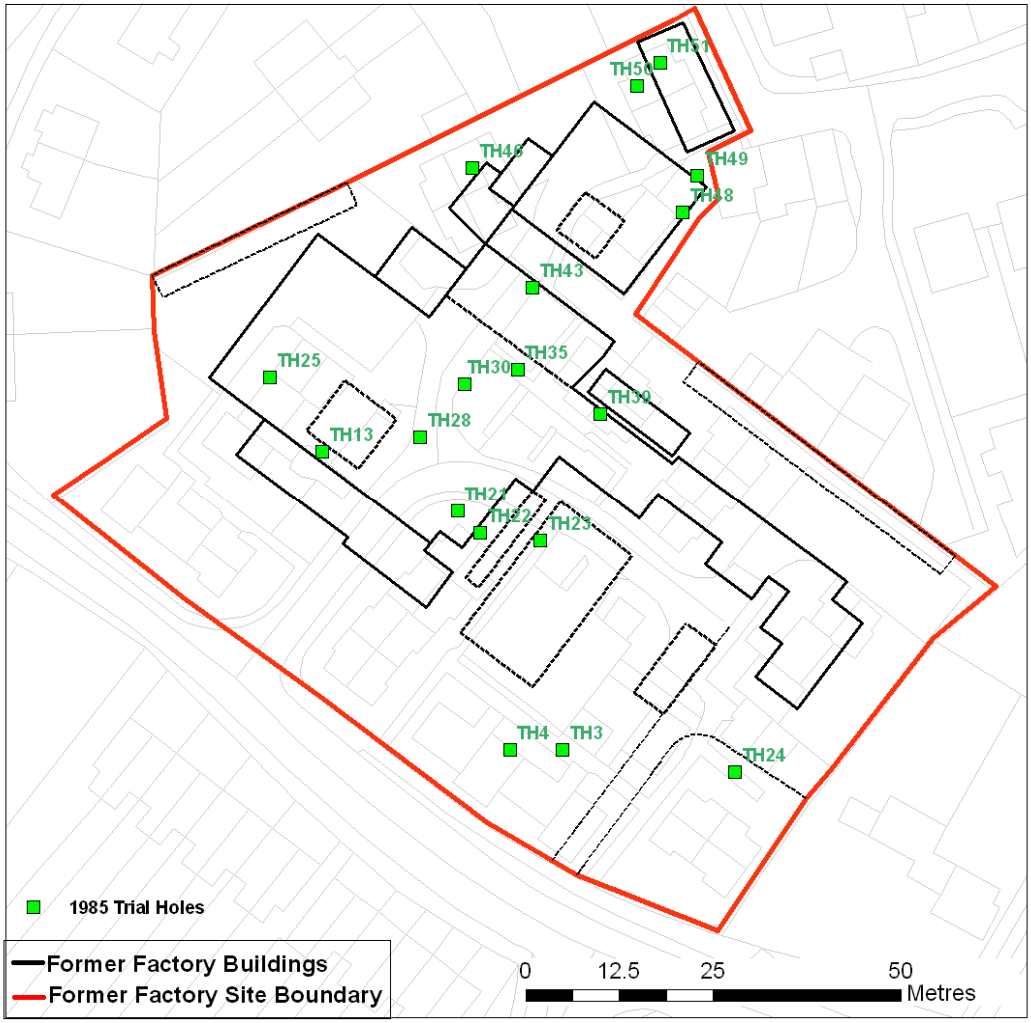

Figure 5.4: Trial hole locations from investigations in 1985 (Chemfix, 1985c)

5.5 Site Geology and Hydrogeology

The geology and hydrogeology of the site have been described in detail by Atkins (2002). The geology is summarised in Table 5.2.

Table 5.2: Geological strata encountered at the source site. Based on Komex (2000) and Atkins (2002)

Stratum	Thickness	Typical Description
Made Ground	Average 1.4m (absent in places)	Yellow to red brown clayey sandy gravely fill. In places containing brick fragments, asbestos roofing fragments, granite chippings, builders' rubble, breeze blocks, ash, some putty chalk and flint. Mixed silt/sand/clay with flint gravel with brick fragments. Occasional fly ash, clinker and metal fragments.
Fluvio-glacial sand and gravel deposits	4.25 to 1.35m Average 2.79	Lenses of orange to brown, medium dense silty clay to sandy gravel. Orange silt and sand with flint gravel. Some silty clay and clay interbeds.
'Putty' Chalk (Upper Chalk)	variable	Structureless, weathered Chalk with occasional flints.
'Blocky' Chalk (Upper Chalk)	>10 m	Chalk with horizontal and vertical fractures.

Groundwater levels varied between +78.78 m OD and 81.15 m OD during the 2001 investigation (Atkins, 2002). Borehole logs show that groundwater appears to be semi-confined by the low permeability 'putty chalk': there is generally a rise in groundwater rest levels compared to strike levels. Piezometric contours (Figure 5.5) indicate a south-easterly flow direction, with a hydraulic gradient across site of 0.0042 (Atkins, 2002). The local hydraulic gradient is lower: 0.0028 in south-easterly direction (Atkins, 2002). Vertical groundwater elevation contours on section along flow direction indicate flow is principally horizontal (Figure 5.6).

5.6 Contaminant Distribution

5.6.1 Spatial distribution of bromate and bromide within soil and soil porewater

The bromide and bromate soil concentration results are reported as $\mathrm{mg\,kg^{-1}}$ on a dry weight basis. Assuming bromide and bromate to be completely soluble in the soil moisture (porewater) at the observed concentrations, equivalent porewater concentrations for the unsaturated zone can be estimated by converting the results from the soil analyses in $\mathrm{mg\,kg^{-1}}$ (dry weight) to a concentration in $\mu\mathrm{g\,l^{-1}}$ using the soil moisture content[1].

Porewater analysis from the saturated zone was undertaken as part of the Atkins (2002) investigation. This is discussed in Section 5.6.2.

[1] Soil moisture contents ranged from approximately 10 % to 15 % in the unsaturated zone (Atkins, 2002)

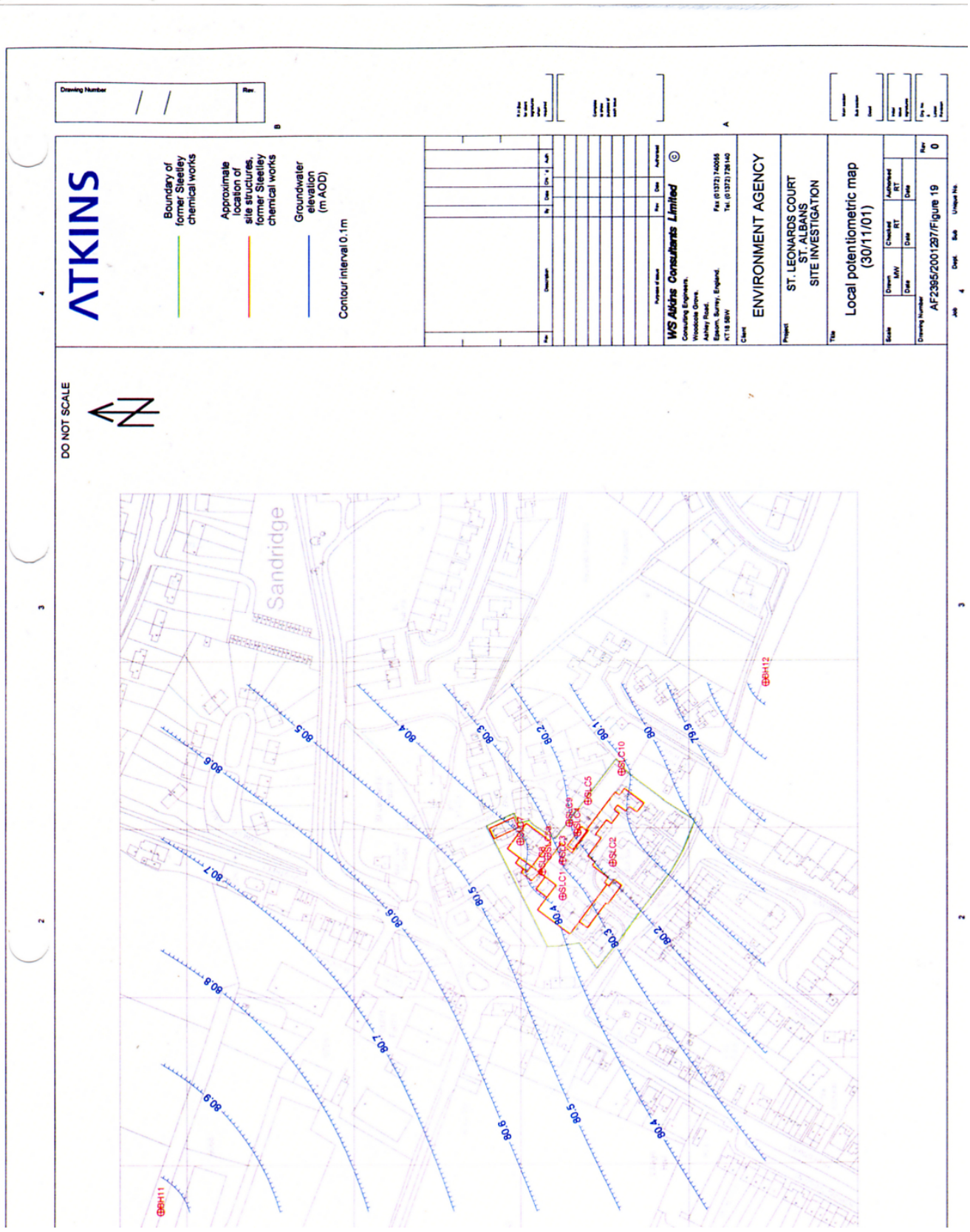

Figure 5.5: Piezometry at the St Leonard's Court site November 2001. From Atkins (2002)

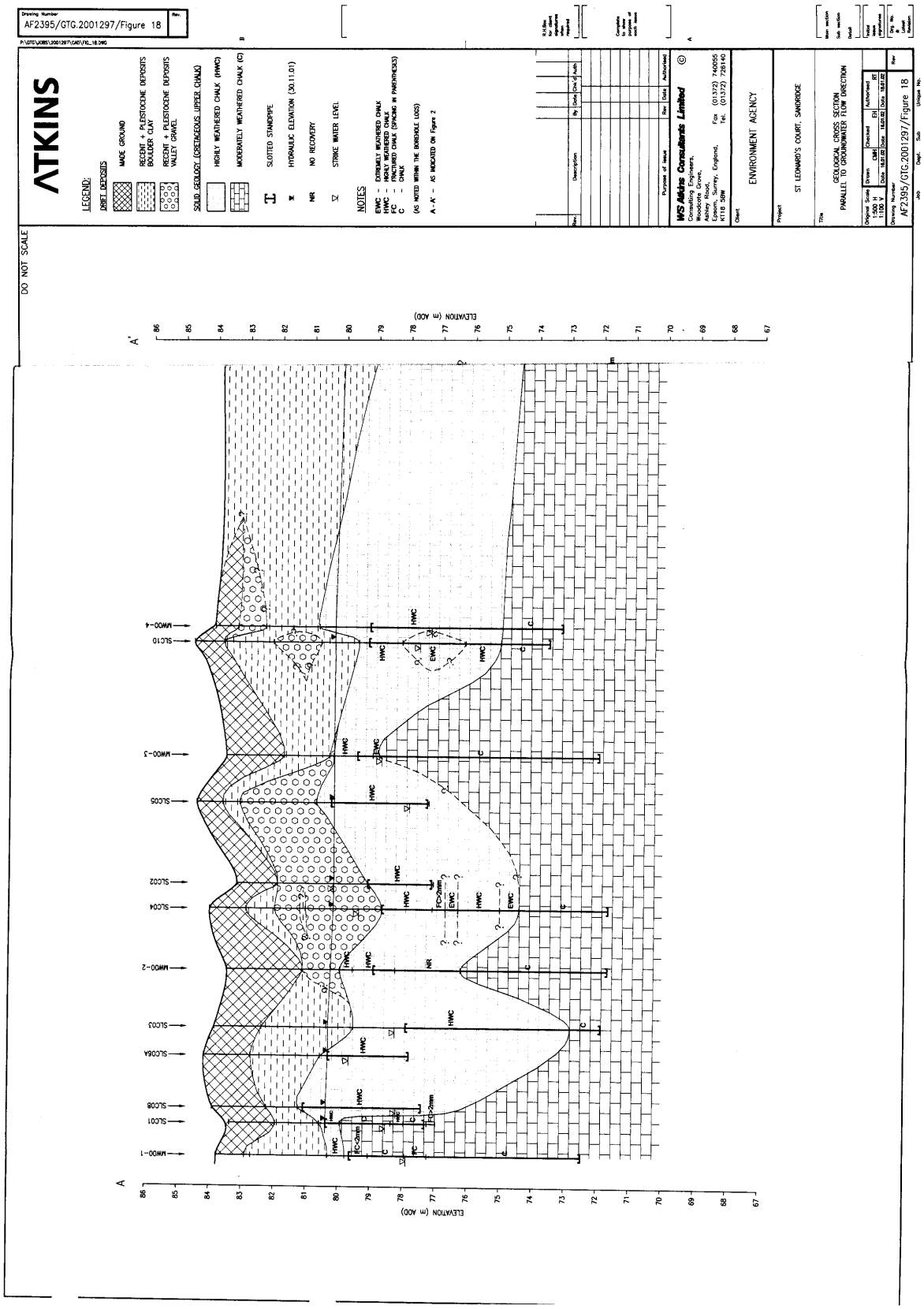

Figure 5.6: Cross-section parallel to groundwater flow direction. From Atkins (2002)

5.6.1.1 Pre-redevelopment as SLC: 1983 – 1985

The site investigations undertaken between 1983 and 1985 indicate that considerable bromide contamination was present in soils beneath the site (Figure 5.7). Soil samples were not tested for bromate after the initial investigation (STATS, 1983a) showed all samples to be below the detection limit of 20 $\mathrm{mg\ kg^{-1}}$. The exact locations of the boreholes from the STATS 1983 investigation is not known (the location plan is missing from the available report). However, the approximate locations have be estimated based on description within the text of the report and are shown in Figure 5.3 and Figure 5.7. Based on the occurrence of bromate contamination in the recent (2000 and 2001) investigations (Section 5.6.1.2), it is surprising that bromate was not detected in some of these locations, particularly around BH-3[83] & BH-4[83], which were reported to be located in the vicinity of the former bromate production area. The samples tested were from relatively shallow depths (0.5 m to 1.5 m); it is possible that bromate was not present in the shallower soils, but would have been encountered in the deeper strata.

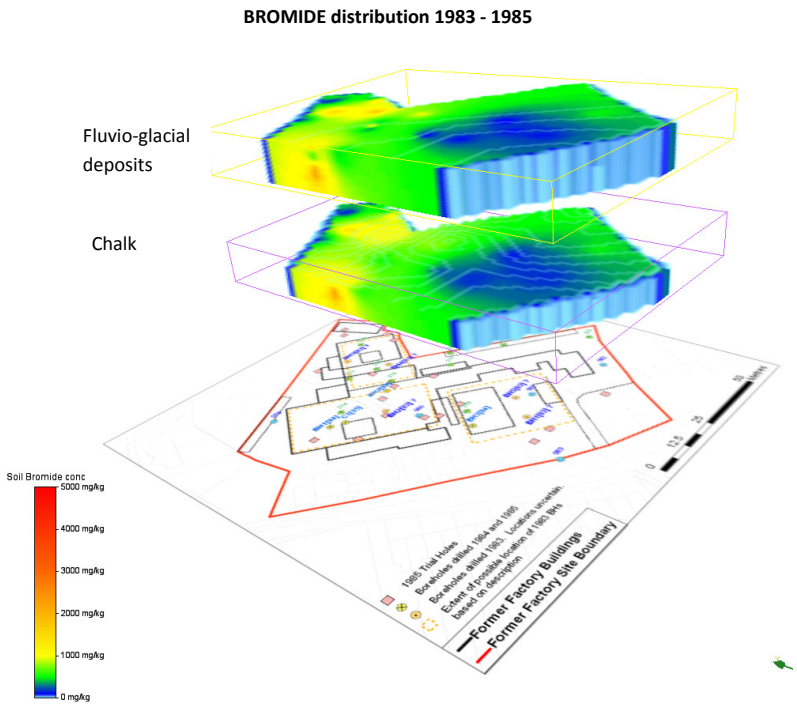

Figure 5.7: Spatial distribution of the bromide contamination based on investigations undertaken between 1983-1985.

The highest bromide concentrations (>1000 $\mathrm{mg\ kg^{-1}}$) occur in soil samples from boreholes in the vicinity of the former 'solid bromate handling' and 'bulk bromine storage' areas, and close to the sump in the 'non-bromate production' area (Figure 5.7). Locations in the southern and eastern areas of the site, corresponding to the non-process areas of the site showed much lower bromide concentrations (<200 $\mathrm{mg\ kg^{-1}}$).

Concentration-depth profiles for these boreholes (Figure 5.8) indicate highest bromide concentrations in the Made Ground and in the Putty Chalk, with generally lower concentrations in the fluvio-glacial deposits (clayey gravels).

The results of this sampling was used as a basis for the excavation of between 0.75 m and 1.5 m of the top layer of soil over much of the site as part of remediation carried out between 1985 and 1986 (Roberts, 2001). It is unclear whether any verification samples were submitted, or whether there were significant alterations to these proposals.

5.6.1.2 Post-redevelopment as SLC: 2000 – 2001

Figure 5.9 and Figure 5.10 illustrate the spatial distribution of the bromide and bromate contamination based on the 2000 and 2001 site investigations.

The pattern of bromide contamination within soil is generally in agreement with the 1983-1987 distribution, although concentrations are considerably lower in 2000 and 2001. The site investigations undertaken during 2000 and 2001 indicated generally low bromide concentrations ($<$0.01 to 8.0 $\mathrm{mg\ kg^{-1}}$) within the Made Ground and shallow soils ($<$1.5 m depth). This is presumably as a result of removal of the contaminated top layer of soil during redevelopment. The highest bromide concentrations (100 to 300 $\mathrm{mg\ kg^{-1}}$) were encountered within the Chalk and fluvio-glacial deposits in soil samples from boreholes in the vicinity of the former 'solid bromate handling' and 'bulk bromine storage' areas, and close to the sump in the 'non-bromate production' area. Bromide concentrations between 10 $\mathrm{mg\ kg^{-1}}$ and 60 $\mathrm{mg\ kg^{-1}}$ were encountered in the fluvio-glacial deposits and Chalk in locations down-gradient of the sump in the production areas. Many of the boreholes in the southern and eastern part of the site, corresponding to the non-process areas, showed low concentrations of bromide ($<$10 $\mathrm{mg\ kg^{-1}}$) within the fluvio-glacial deposits and (putty) Chalk.

It is difficult to discern a pattern from the bromide concentration-depth profiles (Figure 5.11 to Figure 5.21) as fewer depths were tested at each location than in the 1984 and 1985 investigations. However, profiles from the Komex (2000) investigation indicate that the highest concentrations were found in the top section of the putty chalk with lower concentrations in the fluvio-glacial deposits (including gravels, silty sands and silty clays). In the Atkins (2002) investigation, boreholes **219** and **222** showed this pattern, boreholes **217** and **223** show higher concentrations within the fluvio-glacial deposits (gravelly CLAY) than the Chalk, and borehole **218** shows relatively consistent concentrations.

The pattern of bromate contamination was found to be relatively similar to the pattern of bromide contamination. The site investigations undertaken during 2000 (Komex, 2000) and 2001 (Atkins, 2002) indicated generally low bromate concentrations ($<$0.010 $\mathrm{mg\ kg^{-1}}$ to 0.090 $\mathrm{mg\ kg^{-1}}$) within the Made Ground and shallow soils ($<$1.5 m to $<$2.0 m depth). This is presumably as a result of removal of the contaminated top layer of soil during redevelopment. Elevated bromate concentrations (195 $\mathrm{mg\ kg^{-1}}$ to 273 $\mathrm{mg\ kg^{-1}}$) were encountered within the Chalk (putty chalk) and bromate concentrations of 35 to 62 $\mathrm{mg\ kg^{-1}}$ in lower fluvio-glacial deposits (clay) from boreholes in the vicinity of the former bromate production area (down-gradient of the sump) and bromate handling area, and bulk bromine storage. The density of sampling locations around the former bromate production area is relatively sparse. It is

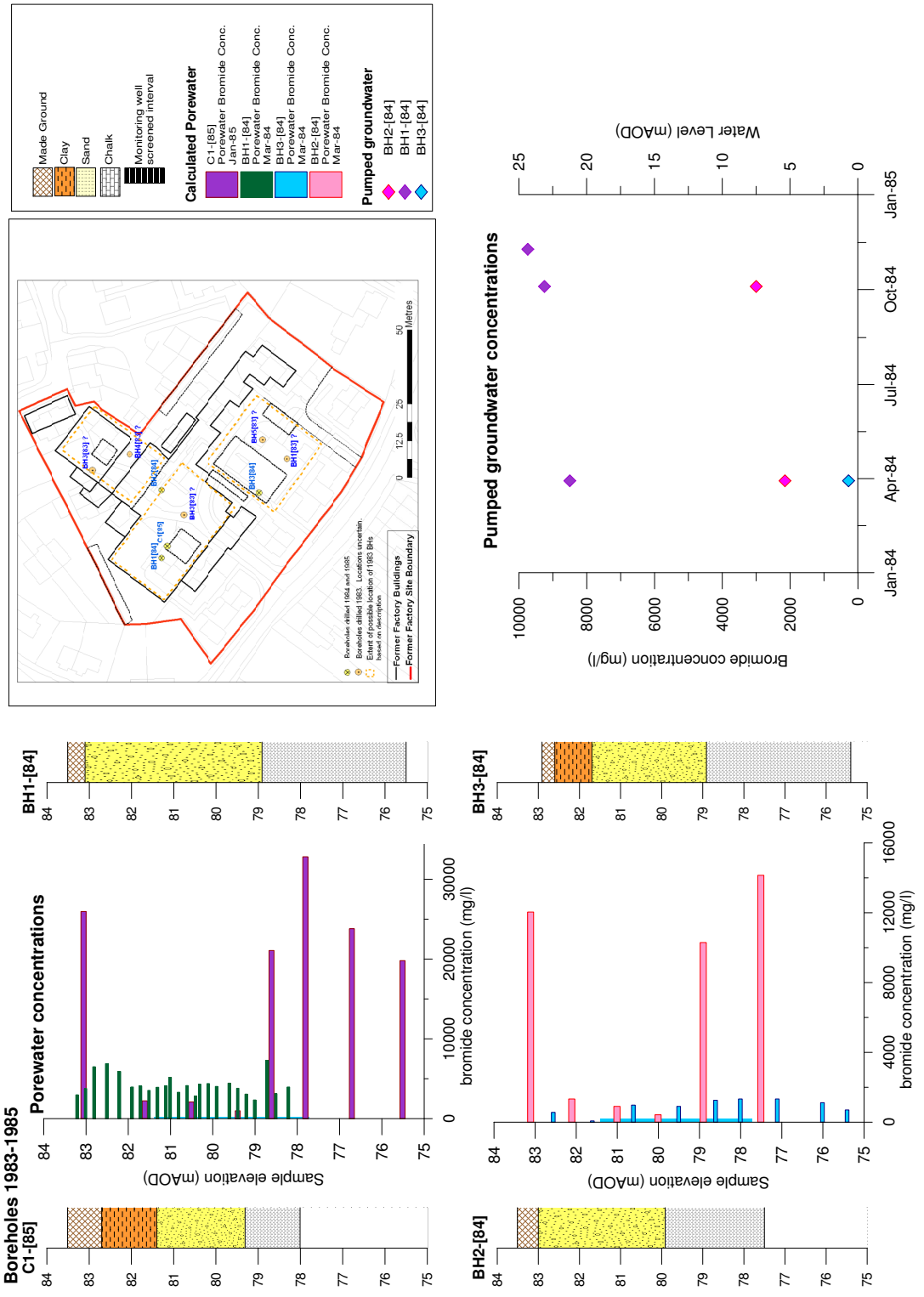

Figure 5.8: Depth profiles of porewater bromide compared to pumped groundwater concentrations for boreholes from investigations 1983-1985.

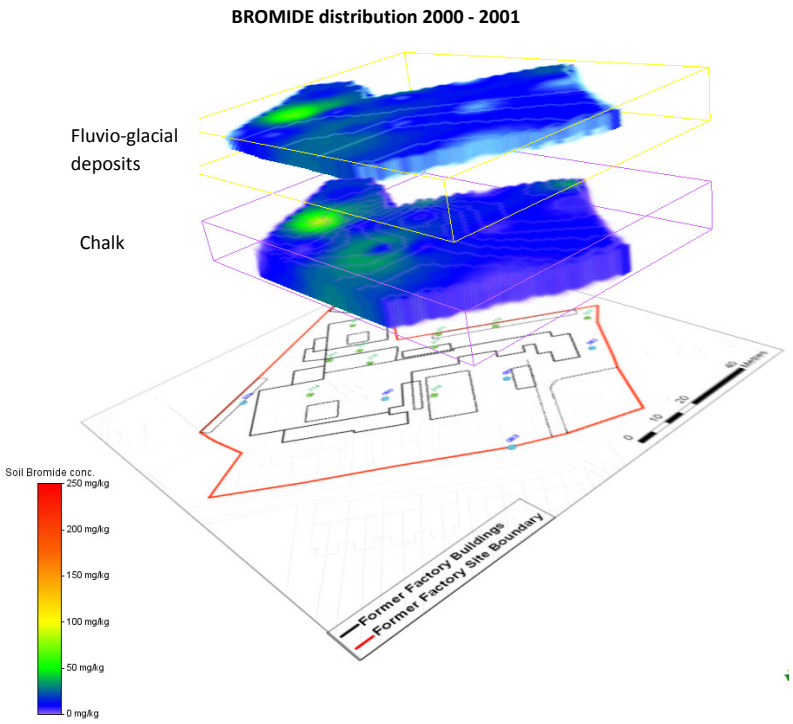

Figure 5.9: spatial distribution of bromide (as $\mathrm{mg\ kg^{-1}}$) based on investigations undertaken between 2000 and 2001.

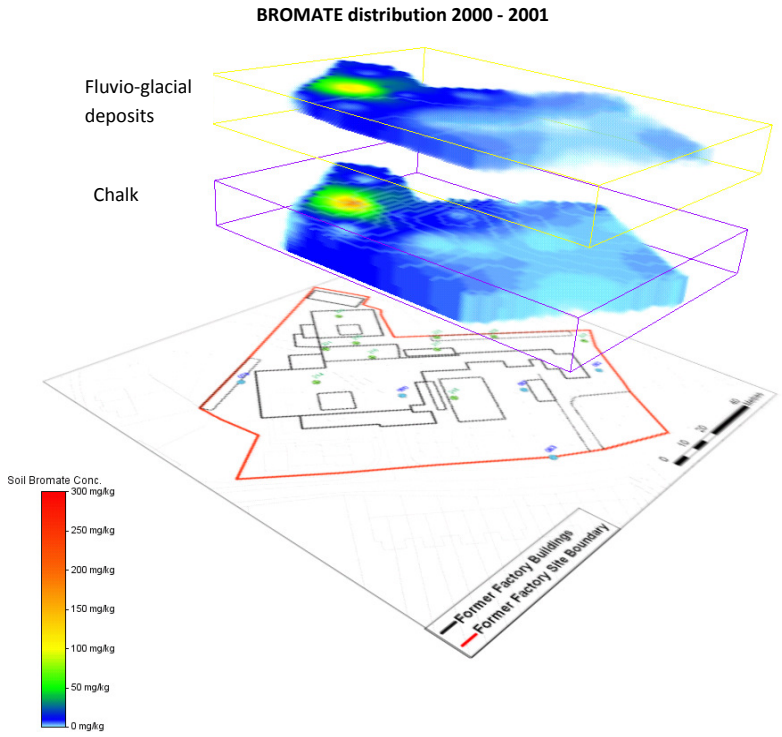

Figure 5.10: spatial distribution of bromate (as $\mathrm{mg\ kg^{-1}}$) based on investigations undertaken between 2000 and 2001.

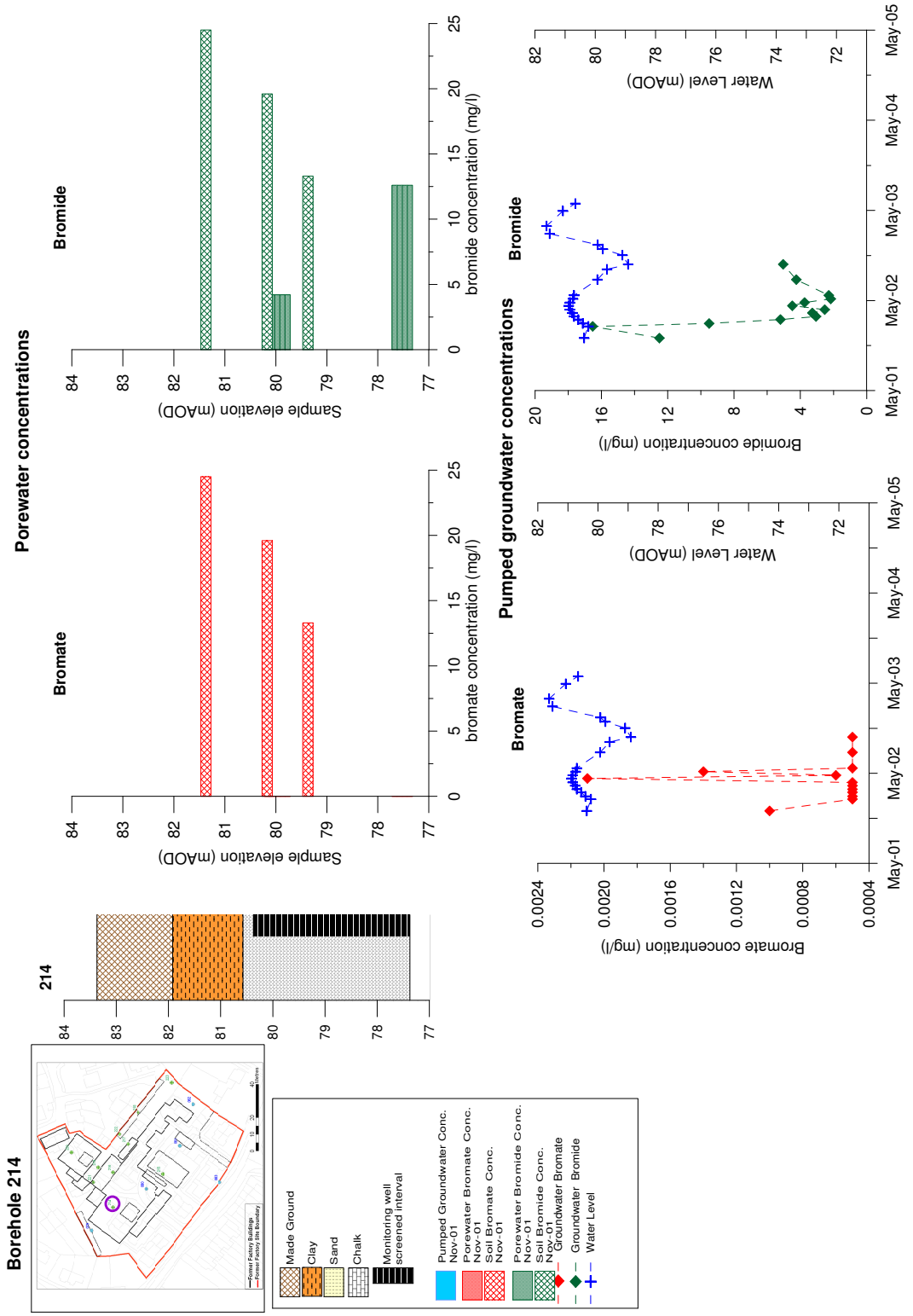

Figure 5.11: Depth profiles of porewater bromate and bromide compared to pumped groundwater concentrations for Borehole 214 from 2001 investigation (Atkins, 2002).

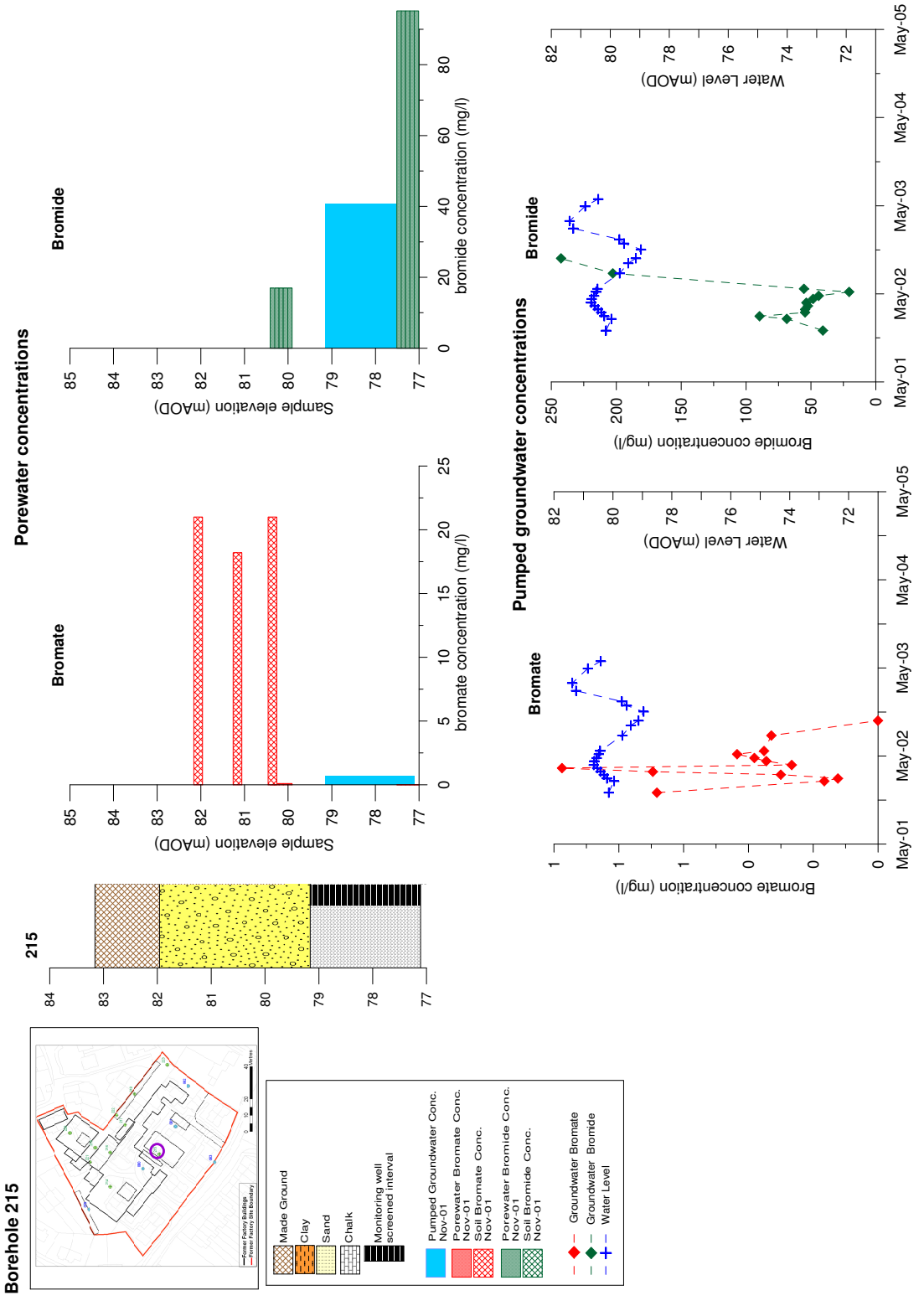

Figure 5.12: Depth profiles of porewater bromate and bromide compared to pumped groundwater concentrations for Borehole 215 from 2001 investigation (Atkins, 2002).

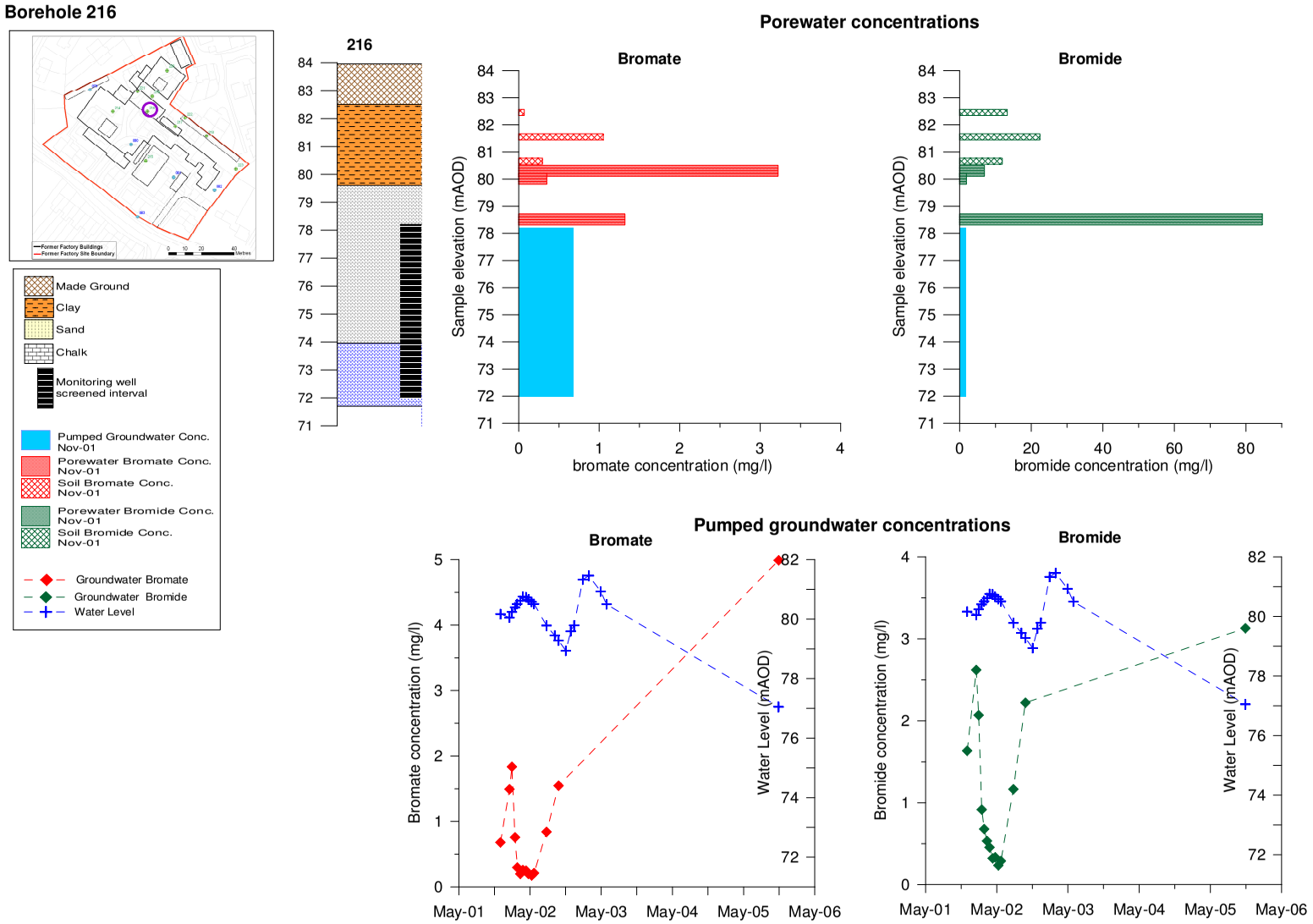

Figure 5.13: Depth profiles of porewater bromate and bromide compared to pumped groundwater concentrations for Borehole 216 from 2001 investigation (Atkins, 2002).

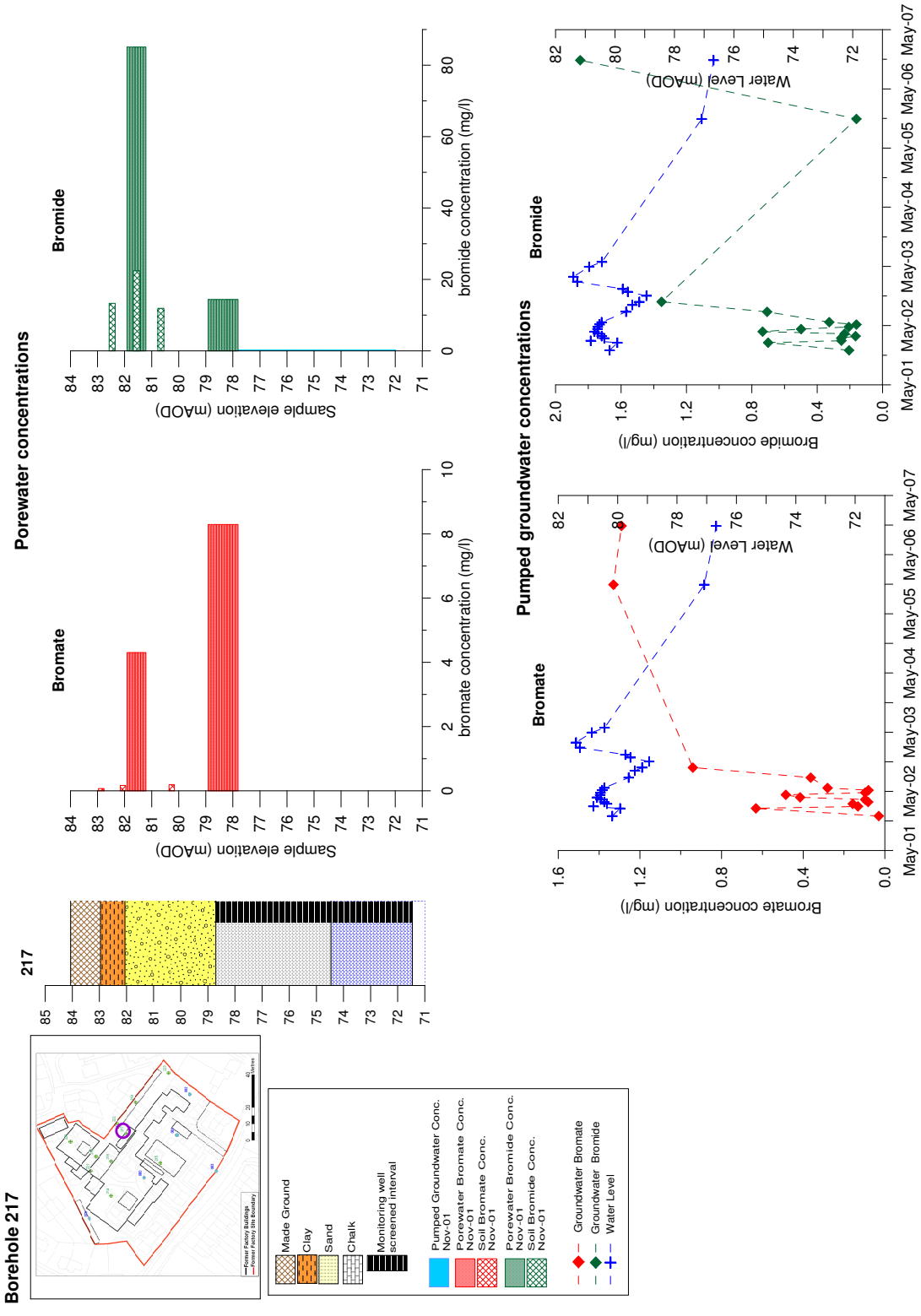

Figure 5.14: Depth profiles of porewater bromate and bromide compared to pumped groundwater concentrations for Borehole 217 from 2001 investigation (Atkins, 2002).

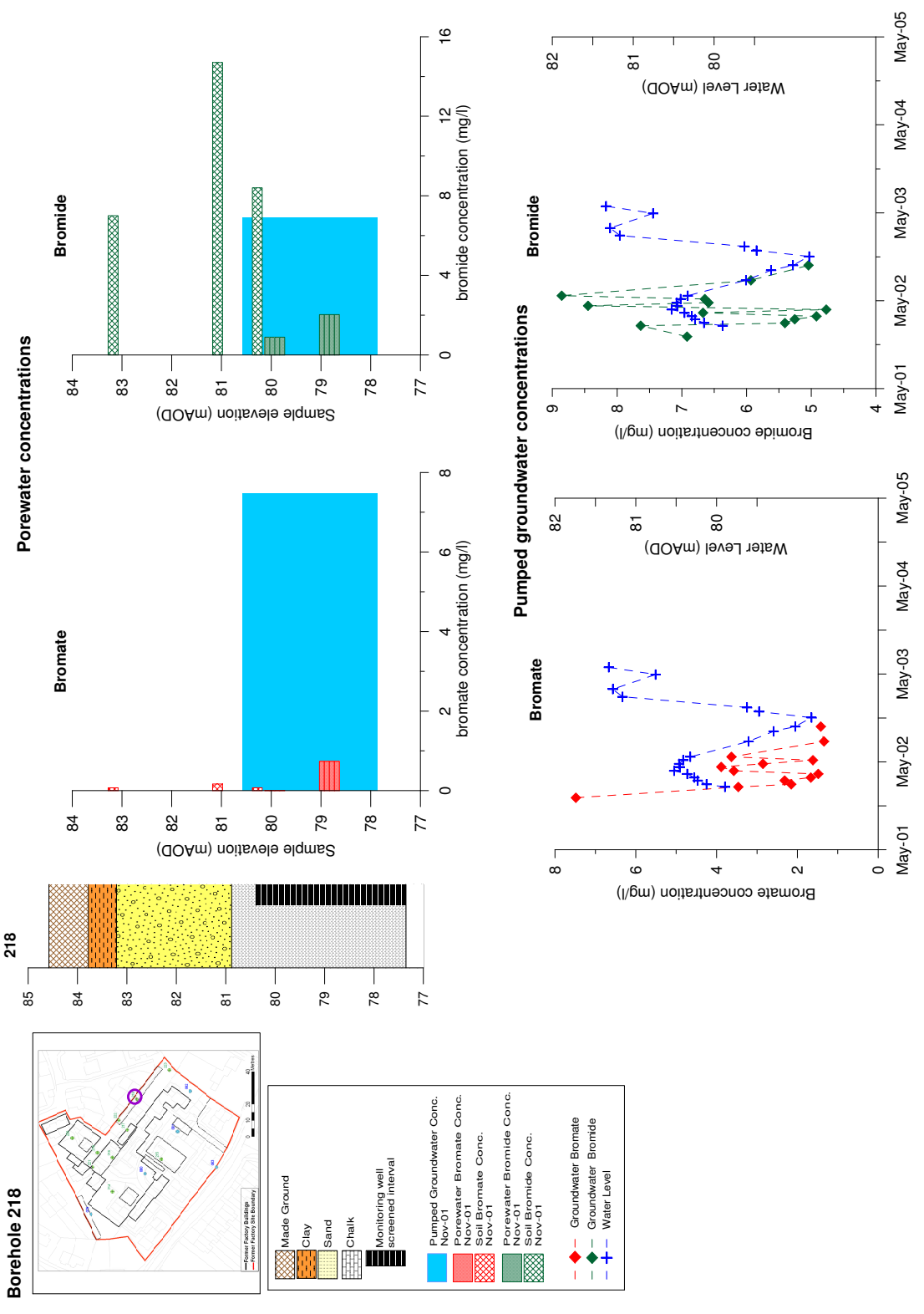

Figure 5.15: Depth profiles of porewater bromate and bromide compared to pumped groundwater concentrations for Borehole 218 from 2001 investigation (Atkins, 2002).

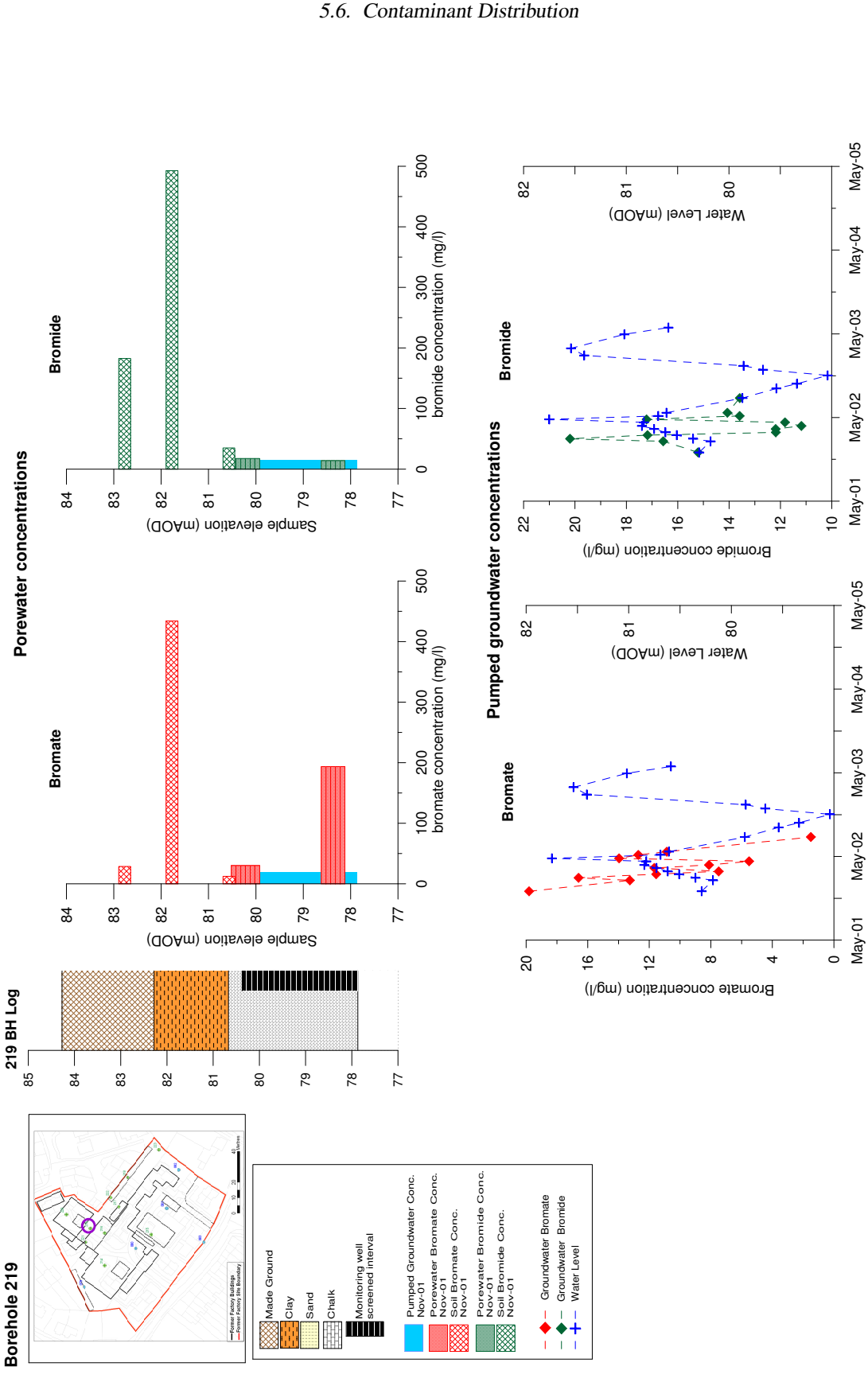

Figure 5.16: Depth profiles of porewater bromate and bromide compared to pumped groundwater concentrations for Borehole 219 from 2001 investigation (Atkins, 2002).

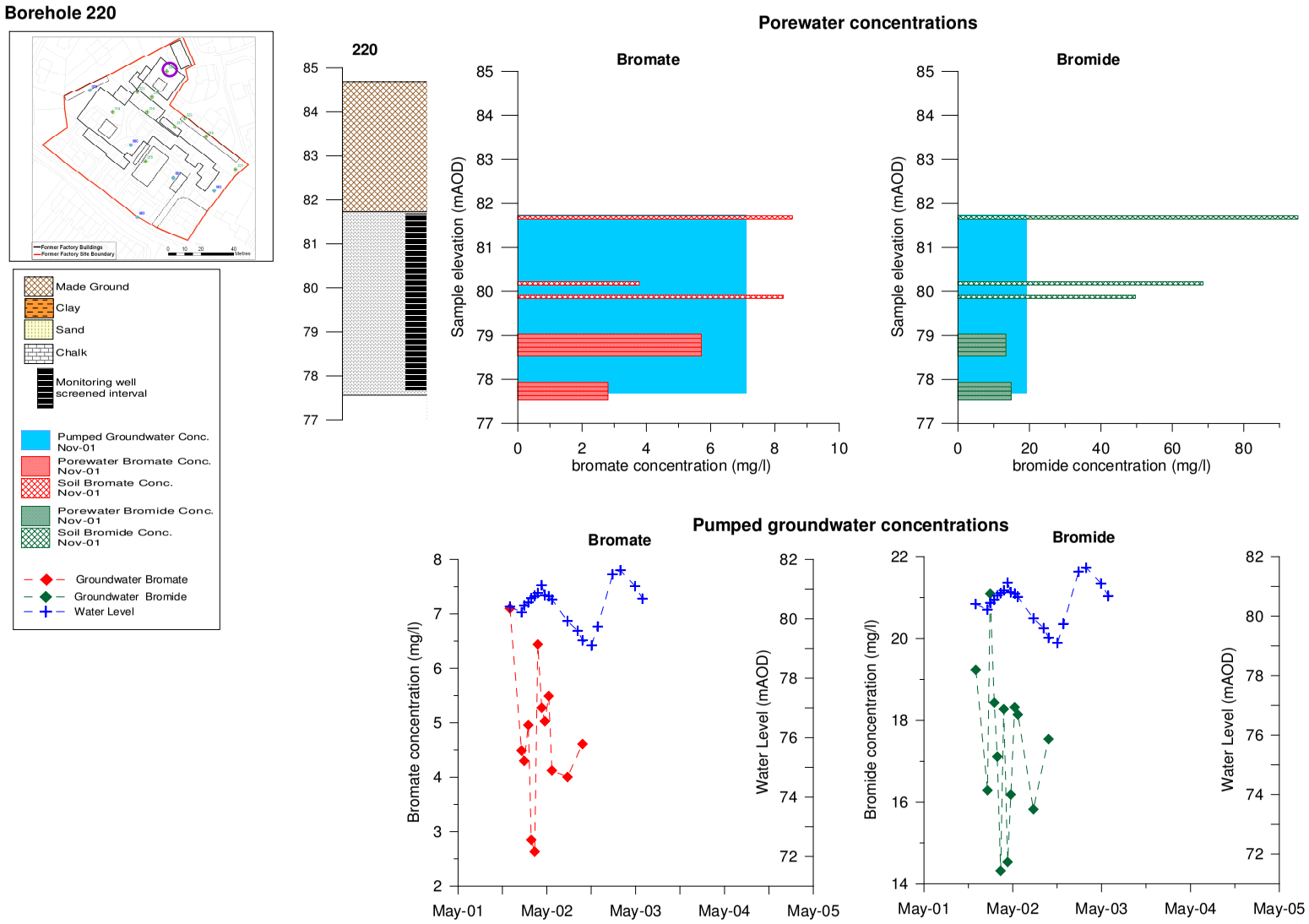

Figure 5.17: Depth profiles of porewater bromate and bromide compared to pumped groundwater concentrations for Borehole 220 from 2001 investigation (Atkins, 2002).

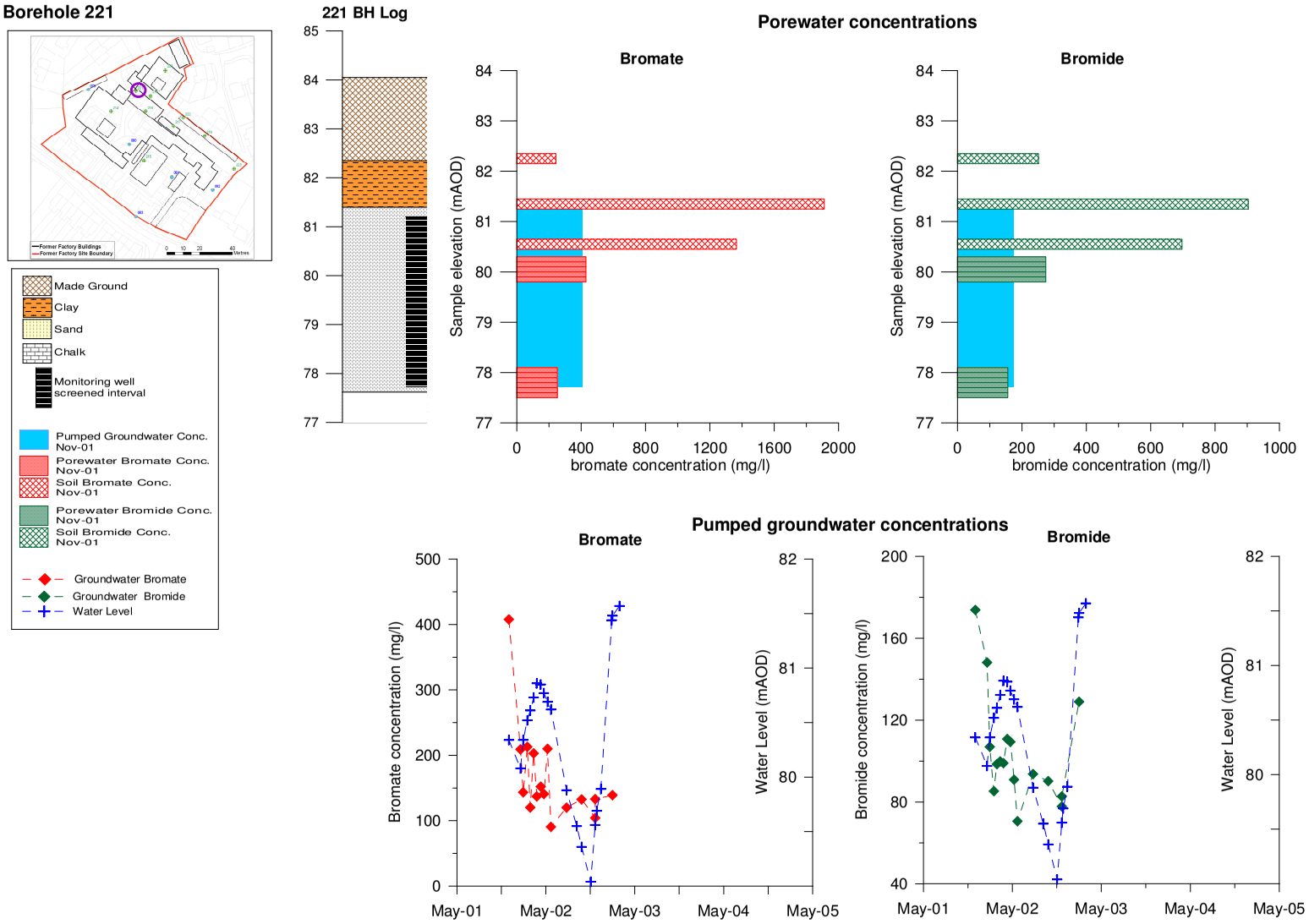

Figure 5.18: Depth profiles of porewater bromate and bromide compared to pumped groundwater concentrations for Borehole 221 from 2001 investigation (Atkins, 2002).

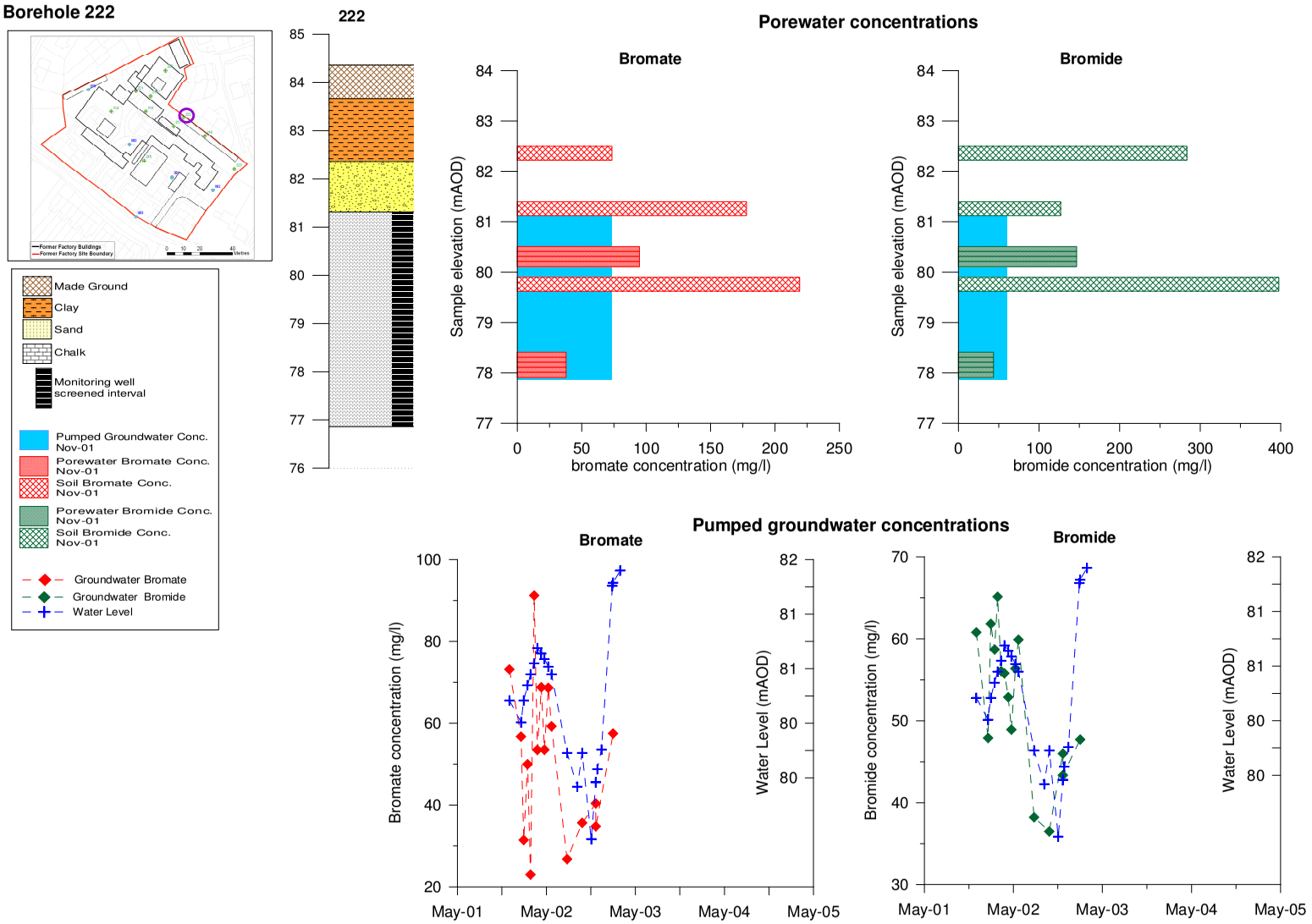

Figure 5.19: Depth profiles of porewater bromate and bromide compared to pumped groundwater concentrations for Borehole 222 from 2001 investigation (Atkins, 2002).

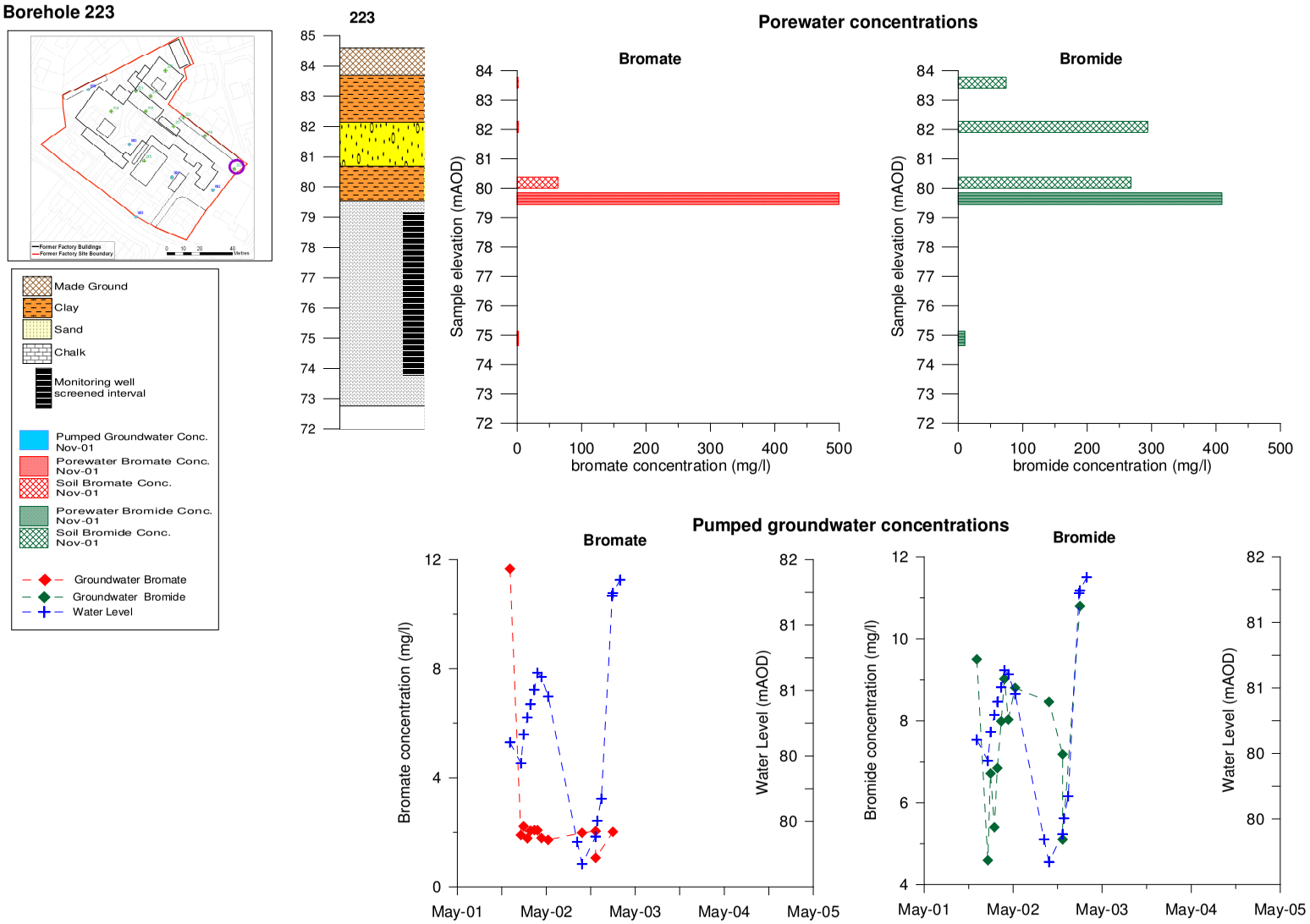

Figure 5.20: Depth profiles of porewater bromate and bromide compared to pumped groundwater concentrations for Borehole 223 from 2001 investigation (Atkins, 2002).

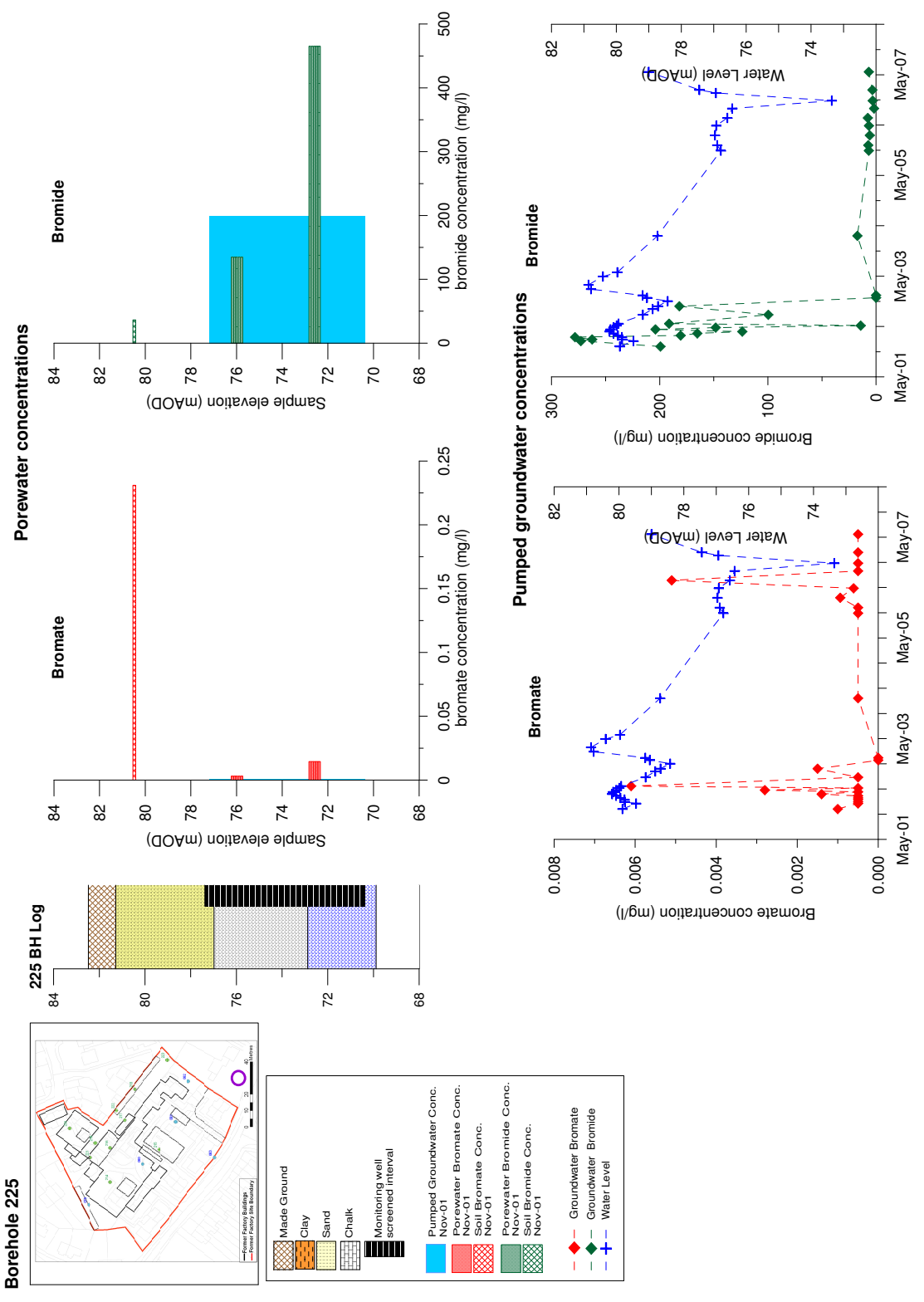

Figure 5.21: Depth profiles of porewater bromate and bromide compared to pumped groundwater concentrations for Borehole 225 from 2001 investigation (Atkins, 2002).

therefore possible that bromate and/or bromide contamination could extend further to the northern part of the site. Low bromate concentrations (<0.5 $\mathrm{mg\ kg^{-1}}$) were encountered in the southern and eastern part of the site. Bromate concentrations were below detection limits of 0.10 $\mathrm{mg\ kg^{-1}}$ in all but one of the samples tested during the August 2000 investigation (Komex, 2000). The samples included the fluvio-glacial deposits and Chalk strata, at a range of depths up to 11.7 m bgl. It is possible that bromate was not detected because the locations were sited away from the bromate production and handling areas. Clear concentration-depth patterns are difficult to discern for the bromate depth profiles. However, in a number of boreholes where elevated bromate concentrations are encountered, higher concentrations occur in the Chalk (putty chalk) compared to concentrations in the shallower fluvio-glacial deposits (clays and gravels).

5.6.1.3 Water table elevations in relation to contamination profiles

The zone of water table fluctuation is within the top of the putty chalk and bottom of the fluvial-glacial deposits, and incorporates the peak porewater concentrations (Figure 5.8 and Figures 5.11 to 5.21).

5.6.1.4 Bromide and Bromate relationships

Results of the 2000 and 2001 investigations indicate a statistically significant relationship between soil bromate concentrations and soil bromide concentrations (Figure 5.22). The relationship indicated by the regression is:

$$\text{Bromate conc. } (\mathrm{mg\ kg^{-1}}) = 0.36 \times \text{Bromide conc. } (\mathrm{mg\ kg^{-1}}) + 32.1\ (\mathrm{mg\ kg^{-1}})$$

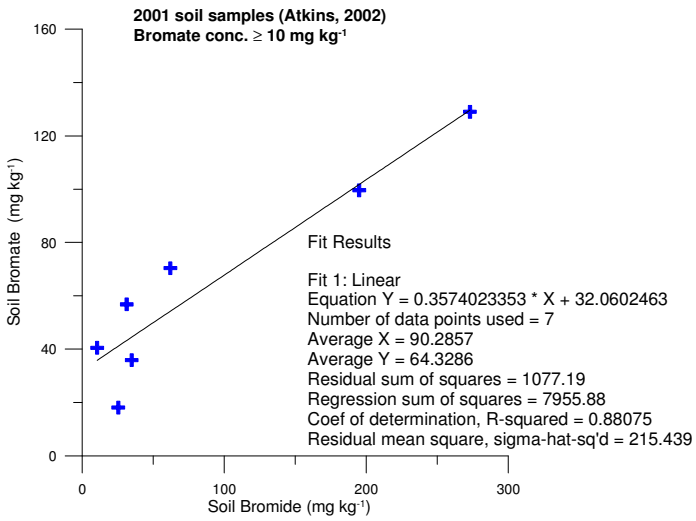

Figure 5.22: Relationship between soil bromate and soil bromide concentrations based on soil samples from the 2001 site investigation (Atkins, 2002).

5.6.2 Spatial distribution of bromate and bromide within groundwater

Bromate and bromide concentrations in groundwater are shown in Figure 5.23. The distribution of groundwater concentrations broadly reflects the pattern of soil concentrations, *i.e.* concentrations generally highest around the bromate and bromide production and handling areas, particularly around the sumps, and the bromine bulk storage areas.

Porewater analysis from the saturated zone was undertaken as part of the Atkins (2002) investigation, and the results are included in Figure 5.11 to Figure 5.21. Porewater bromate (and bromide) concentrations measured in November 2001 for location **221**, which had a maximum groundwater bromate concentration of 400 $\mathrm{mg\ l^{-1}}$, are approximately the same concentration as (mobile) groundwater concentrations sampled at that time (Figure 5.18). However, for **219**, also around the sump of the bromate production area, and showing high bromate concentrations, porewater bromate from the saturated zone was up to eight times higher than bromate concentrations in groundwater measured in November 2001, although bromide concentrations were similar in porewater and groundwater (Figure 5.16). At location **220**, **222** and **215** bromate and bromide porewater concentrations are approximately the same concentrations as bromate and bromide in groundwater sampled in November 2001. At the remaining locations, porewater samples were not available from the saturated zone.

Relatively high (135 $\mathrm{mg\ kg^{-1}}$ and 465 $\mathrm{mg\ kg^{-1}}$) porewater bromide concentrations were encountered in location **225**, which is located approximately 150 m down hydraulic gradient of the SLC site. However, concentrations of bromate in porewater were low (3 $\mu\mathrm{g\ l^{-1}}$ to 14 $\mu\mathrm{g\ l^{-1}}$). This is consistent with groundwater concentrations at location **225**: Relatively high bromide groundwater concentrations were encountered (192 $\mathrm{mg\ l^{-1}}$) but concentrations of bromate were low (0.002 $\mathrm{mg\ l^{-1}}$).

5.6.2.1 Trends in groundwater concentrations 2000 to 2008

The groundwater monitoring wells installed in 2000 by Komex and in 2001 by Atkins have been monitored for bromate and bromide as part of the bromate monitoring programme (Section 4.2).

Time series of groundwater monitoring data for these locations are included in Figure 5.11 to Figure 5.21. Overall, since 2000, groundwater bromide concentrations at the SLC site typically show a decline between 2000 and 2003 and where monitoring data are available, values decline or remain stable up until 2007. Overall since 2000, bromate concentrations have shown a reduction at monitoring locations within the site area, although recently on the basis of the data from the five locations still sampled, there is evidence of some slight increases in some of the locations (221 and 223).

5.6.2.2 Trends in groundwater bromide concentrations 1984 to 2008

Comparison of bromide concentrations in boreholes from the monitoring between 1983 and 1987 (Figure 5.8) with monitoring data between 2000 and 2008 (Figure 5.11 to Figure 5.21) indicate a decline in bromide concentrations within groundwater: a range of 25 $\mathrm{mg\ l^{-1}}$ to 10000 $\mathrm{mg\ l^{-1}}$ in 1984/1985 to a range of 10 $\mathrm{mg\ l^{-1}}$ to 1000 $\mathrm{mg\ l^{-1}}$ in 2000/2001 at similar locations.

Bromide concentrations in saturated zone porewater also appear to have decreased significantly from 10000 to 15000 $\mathrm{mg\ l^{-1}}$ at **BH2-[84]** (based on soil samples from the 1984 investigation (STATS, 1984)) to approximately 200 $\mathrm{mg\ l^{-1}}$ at location **221**. Estimated porewater concentrations in 1984

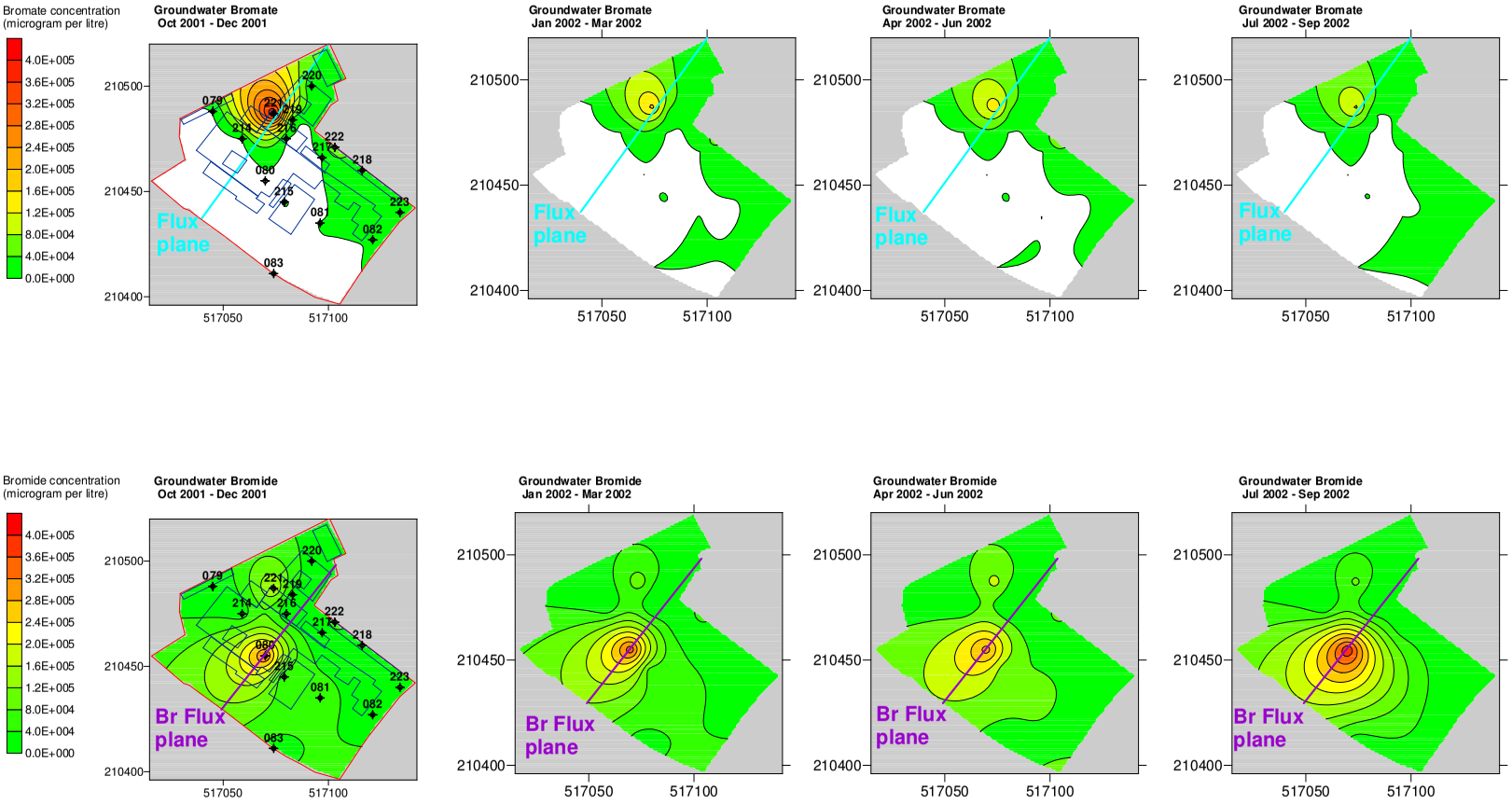

Figure 5.23: Groundwater bromate and bromide contours at the ‘source zone’ based on samples taken in 2001 and 2002.

were approximately five times greater than sampled groundwater concentrations at the same location in **BH2-[84]** and **BH3-[84]**, but they were similar in **BH1-[84]**.

Bromide concentrations at borehole **225** compared to borehole **B1-[85]** (Figure 5.24) which was located in approximately the same location, indicate slightly higher concentrations in 2002 compared to 1985/1986. However, concentrations decline substantially into 2004 and remain low into 2007.

5.6.2.3 Relationships Bromide and Bromate in groundwater

Bromide concentration in groundwater samples from the source site shows a strong positive correlation to bromate concentration (Figure 5.25).

5.6.3 Groundwater monitoring in the vicinity of the source site

In connection with the on-site investigations, some regional monitoring of groundwater quality (including analysis for *bromide*, but not *bromate*) was undertaken between 1983 and 1987 from existing boreholes in the vicinity of the source site (Figure 5.27). These boreholes were incorporated into the bromate monitoring programme which commenced in 2000 (Section 4.2).

Figure 5.27 shows the time series of bromide in groundwater between 1983 and 1987 and between 2000 and 2001. Borehole locations **028** (Orchard Garage) and **019** (Nashe's Farm) show potential increases from concentrations between 1983 and 1987 to concentrations between 2000 and 2008. However, a particularly high concentration at Orchard Garage confuses this pattern. A potentially anomalous high concentration is also seen at location **020** (Capp's Cottage). Boreholes **017**, **018**, **020** and **025** show small decreases from concentrations between 1983 and 1987 to concentrations between 2000 and 2008. Between 2000 and 2007 concentrations tend to show relatively constant concentrations, although a slight decline is noticeable at locations **028** and **019**.

Porewater analysis was also undertaken at the borehole locations **227** and **228**. At locations **227** and **228**, at distance of approximately $1\ \mathrm{km}$ and $2\ \mathrm{km}$ respectively down-gradient of the site along House Lane, Chalk porewater bromate concentrations were low ($<5\ \mu\mathrm{g\,l^{-1}}$) in both locations. Bromide concentrations were relatively high in borehole **227** (1-4 $\mathrm{mg\ kg^{-1}}$) but low ($<0.5\ \mathrm{mg\ kg^{-1}}$) in **228**. In each case, concentrations appear to be highest in the top of the Chalk and decrease with depth.

5.6.4 Relationships between contaminant concentrations and water levels

As described in Chapter 4, water levels were exceptionally high in 2001 (a very wet year in which localised groundwater flooding occurred). Peak groundwater levels at Orchard Garage (location **028**) occurred in April 2001. Groundwater levels then declined into January 2002 before rising again to follow the normal seasonal trends and amplitude.

Most locations at the source site show a substantial decrease in bromate and bromide concentration from November/December 2001 to January 2002. It is possible that high groundwater levels in 2001 contributed to the high bromate concentrations recorded in November/December 2001: high groundwater levels are likely to have led to increased mobilisation of bromate and bromide (leaching from soil and diffusion out of porewater held in matrix of the unsaturated zone). Higher groundwater levels may also have activated different flow paths, transferring bromate to a wider area, which may explain why

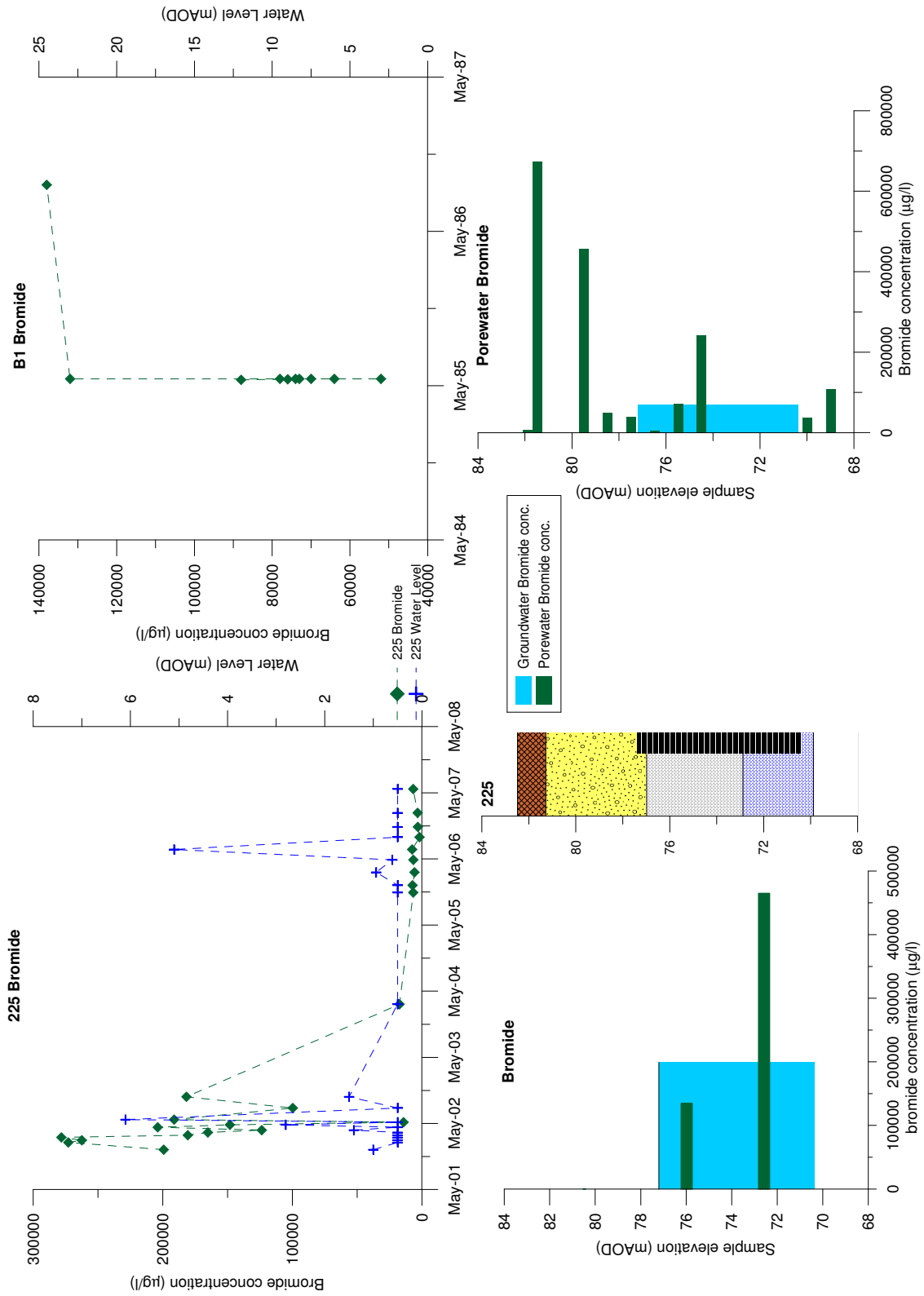

Figure 5.24: Depth profiles of porewater bromide compared to pumped groundwater concentrations for Borehole B1 from the 1985 investigation (Chemfix, 1985a) and Borehole 225 from 2001 investigation (Atkins, 2002) which are believed to have been located in similar positions.

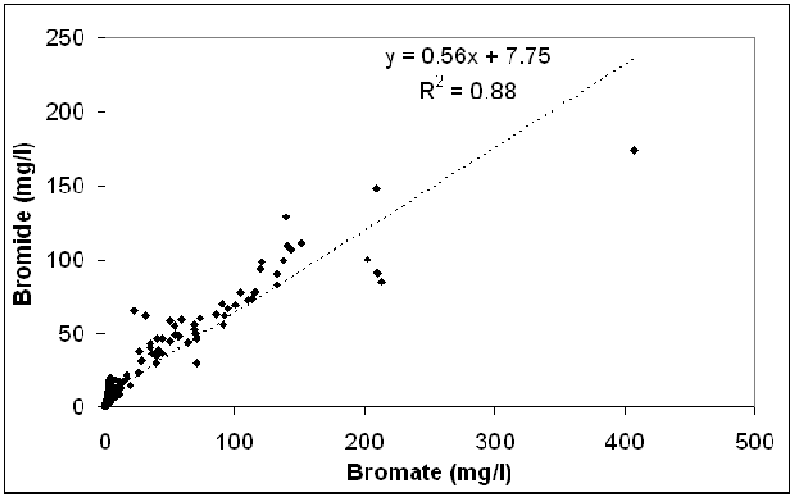

Figure 5.25: Relationship between bromide and bromate concentration in groundwater samples from the monitoring data between 2000 and 2008 for locations **079** to **083** and locations **214** to **223**.

bromate and bromide is seen over a wider area in 2001, followed by a rapid decline. Bromate relationship to water levels have been assessed in Section 4.6. At the source site, the regression relationships for the response of bromate concentration to water level are only statistically significant ($P<0.05$) for three locations out of the six locations with sufficient data to undergo statistical analysis (Figure 4.37).

5.6.5 Leachate results

Leachate tests measure the amount of contaminant mass associated with the solid (soil) phase that is mobile in the liquid (water) phase passing through the soil. Samples from the 2001 investigation (Atkins, 2002) were submitted for leachate analysis using Environment Agency recommended methodology (Lewin et al., 1994). Concentrations of bromate and bromide in leachate samples from the 2001 investigation are strongly correlated with bromate and bromide concentration in the corresponding soil sample (Figure 5.28). For bromide, there are no obvious differences in the regression relationships between samples from putty Chalk, clayey GRAVEL and gravelly CLAY samples. For bromate, samples from the fluvio-glacial deposits appear to leach slightly more (steeper regression line) than samples from the putty Chalk. As there is only one sample from clayey GRAVEL, it not possible to discern any differences between leaching behaviour between the clayey GRAVEL and gravelly CLAY samples.

5.6.5.1 Partition coefficients, K_d

A partition (or distribution) coefficient, K_d, describes the distribution of a species between a solid and aqueous matrix after equilibration. Sorption mechanisms include ion exchange (in particular cation exchange) and surface complexation. In groundwater risk assessments, the K_d value describes the degree of sorption of a particular species in the leachate and/or groundwater to the soil or rock that is in contact with that liquid. Partition coefficients are expressed in units of $\mathrm{L^3M^{-1}}$ (*e.g.* $\mathrm{l\,kg^{-1}}$ or $\mathrm{ml\,g^{-1}}$).

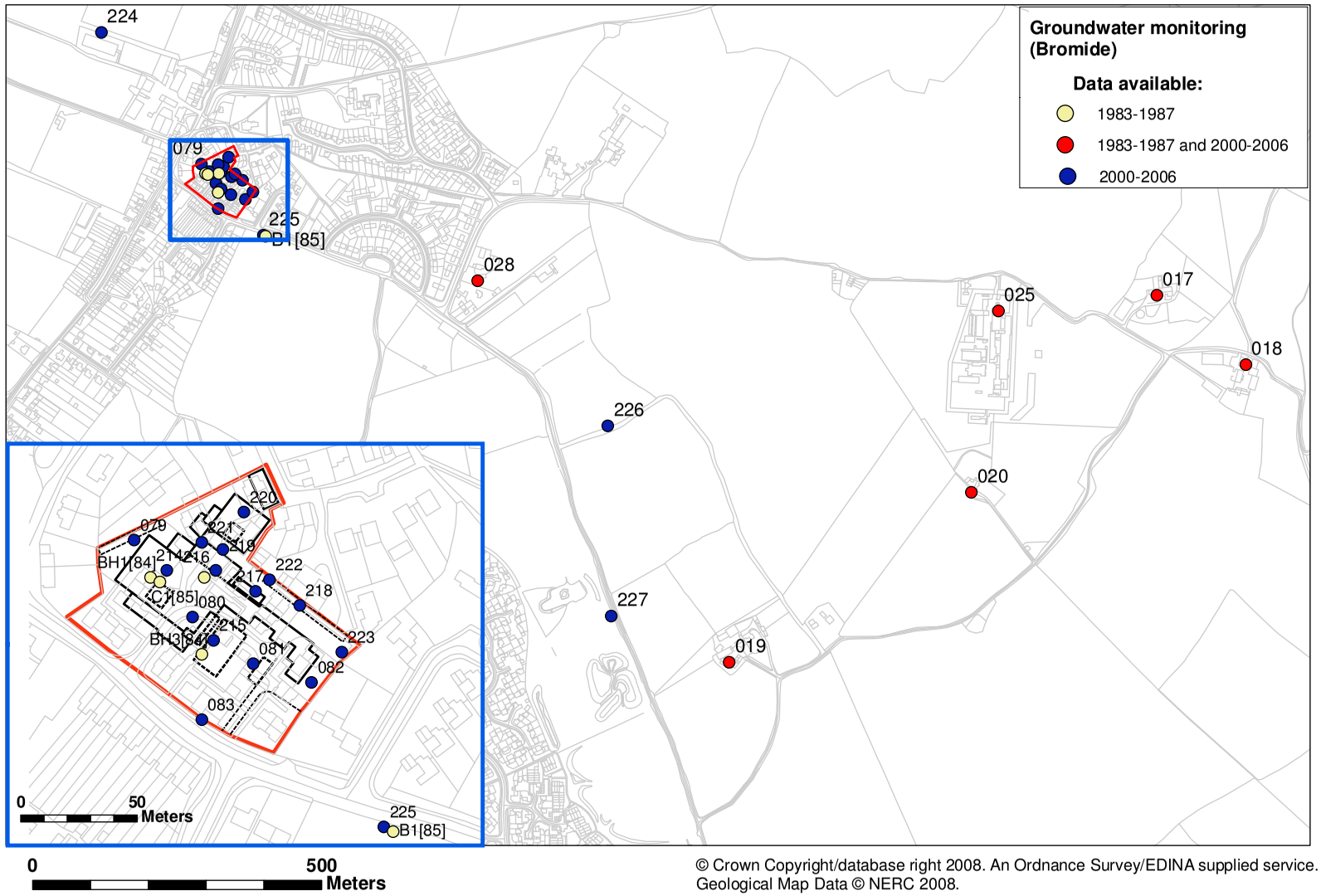

Figure 5.26: Groundwater monitoring locations in the vicinity of the source site that have been sampled for bromide concentrations between 1983 and 1987 and between 2000 and 2008.

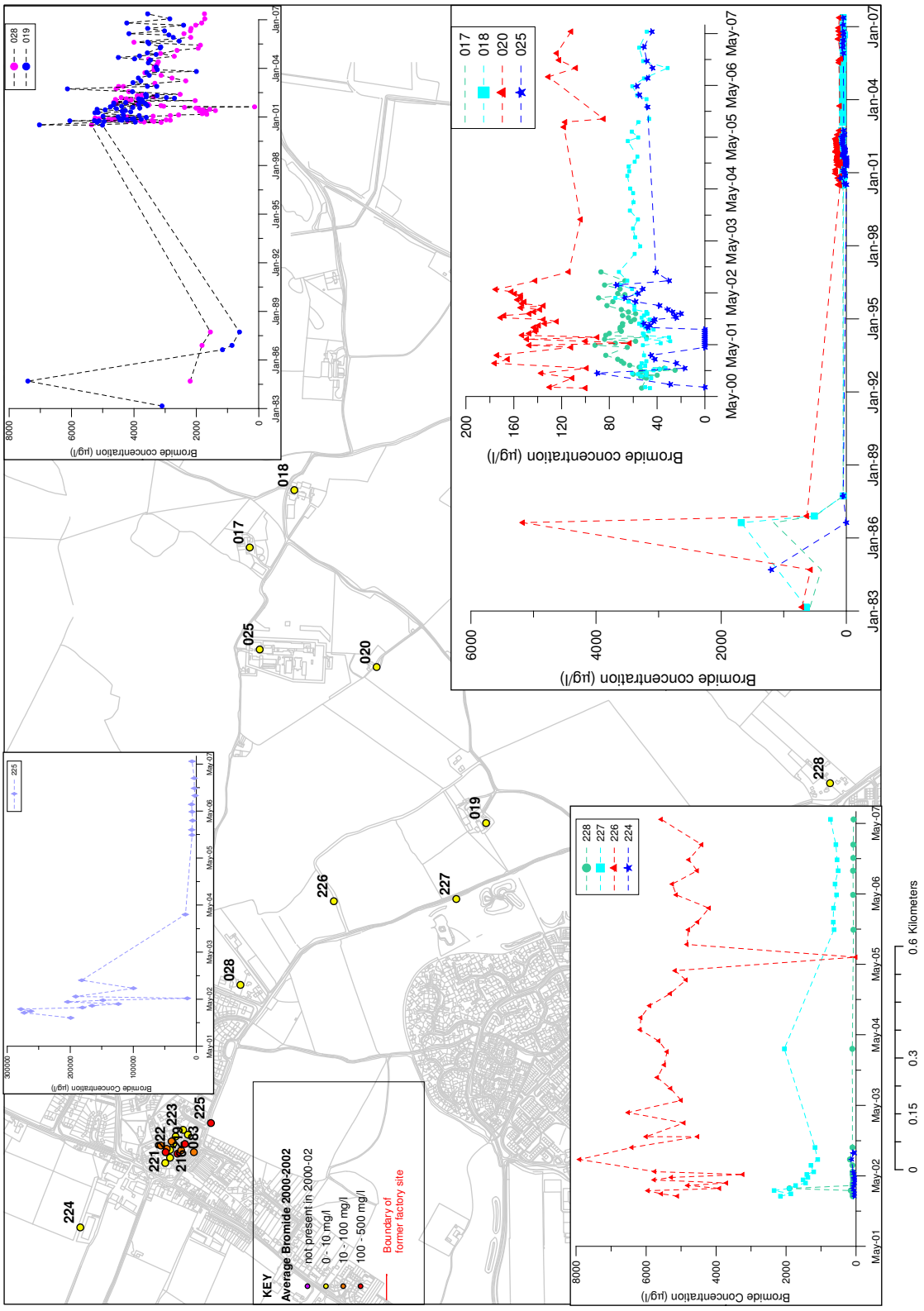

Figure 5.27: Groundwater bromide concentrations at monitoring locations in the vicinity of the source site 1983 to 2008.

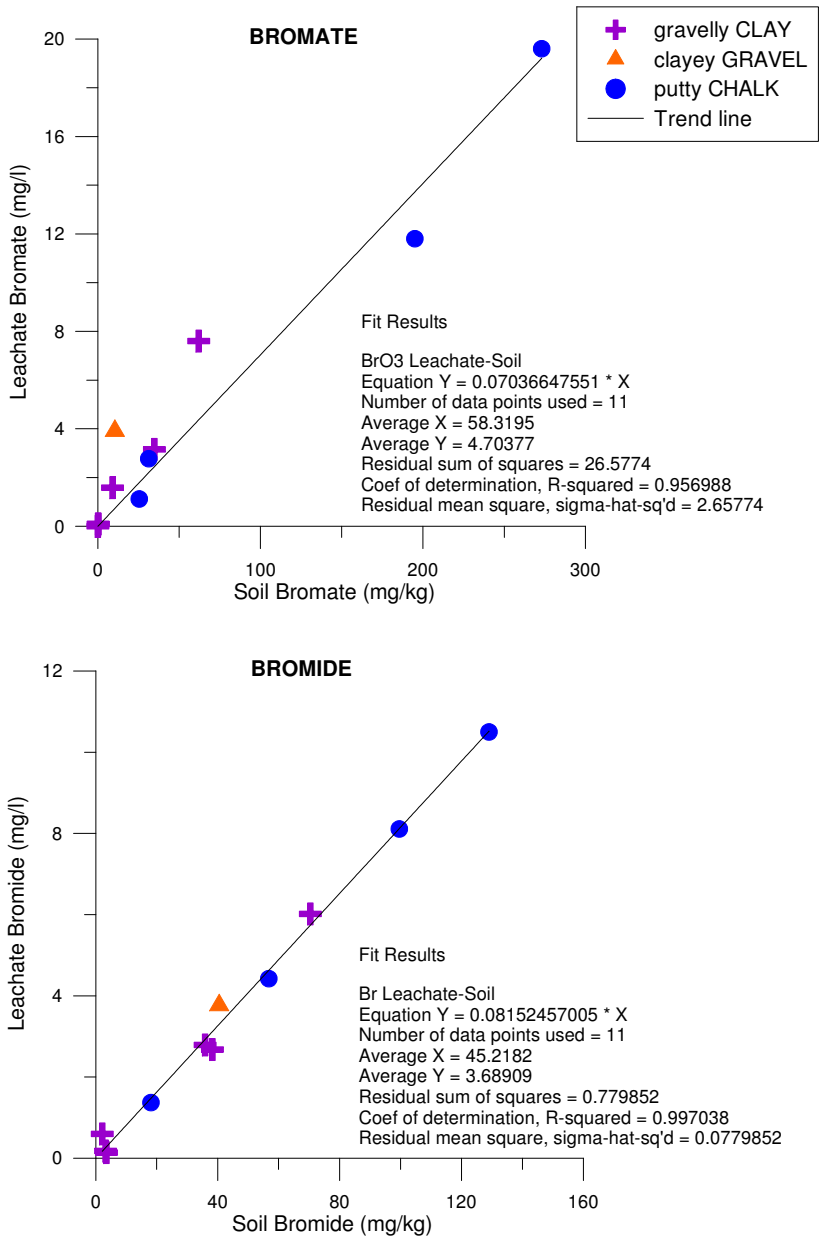

Figure 5.28: Relationships between leachate concentration ($\mathrm{mg\ l^{-1}}$) and soil concentration ($\mathrm{mg\ kg^{-1}}$) for samples from the 2001 investigation (Atkins, 2002).

The partition (or distribution) coefficient, K_d, was calculated as described in Lewin et al. (1994) as

$$K_d = \frac{C_{sorbed}}{C_{dissolved}}$$

Where C_{sorbed} is the sorbed contaminant concentration (mass of contaminant in $\mathrm{mg} \div$ mass of soil in kg) and $C_{dissolved}$ is the dissolved contaminant concentration (mass of contaminant in $\mathrm{mg} \div$ volume of solution in litres).

The soil concentration ($\mathrm{mg\ kg^{-1}}$) C_{soil} was assumed to represent the total mass of contaminant (sorbed plus dissolved). The dissolved contaminant concentration $C_{dissolved}$ was assumed to be the leachate concentration ($\mathrm{mg\ l^{-1}}$). C_{sorbed} was calculated as the total soil concentration, C_{soil}, minus the dissolved mass per kg of soil ($C_{leachate} \times$ L/S ratio[2]). Performing these calculations on the samples from the the 2001 investigation (Atkins, 2002), gave a mean K_d of 11.8 $\mathrm{l\ kg^{-1}}$ for bromate and 12.7 $\mathrm{l\ kg^{-1}}$ for bromide.

5.7 Mass of bromide and bromate at the source site

5.7.1 Previous estimates

A review of available data by the Environment Agency (Roberts, 2001) estimated that between 7,535 kg and 14,135 kg of bromide was present in the unsaturated zone (assumed to be 4 m thick); the estimated mass in the unsaturated zone after excavation of 2,406 kg bromide in the top layer of soil in 1986 was between 5,129 and 11,729 kg.

These estimates were based on the soil bromide distribution indicated by the results of the 1985 investigation (Chemfix, 1985c). The estimates were calculated by Roberts (2001) as follows:

- The site was divided up based on a 10 $\mathrm{m} \times 10\ \mathrm{m}$ grid. Assuming a thickness of unsaturated zone of 4 m, and a bulk density of 2000 $\mathrm{kg\ m^{-3}}$, there is 8×10^5 kg of material in each block. The mass of bromide in each block was then calculated as:

  $$M_{Br} = C_{Br} \times 10^{-6} \times M_s$$

  where M_{Br} is the mass (in kg) of bromide in a block, C_{Br} is the concentration (in $\mathrm{mg\ kg^{-1}}$) of bromide in the block and M_s is the mass (in kg) of soil in block. Calculating this for each block and summing the answers gives a total amount of bromide on site in the unsaturated zone.

- Two estimates were undertaken:

  1. Using just the squares where samples were taken (a total of 20 squares) gave a total amount of 7,535.2 kg bromide on site.
  2. Assuming that the squares with no analysis had concentrations the average of those squares surrounding them, and the contamination at the boundary is zero, gave a total of 14,135 kg bromide on site.

[2]Liquid to Solid ratio. For NRA leachate analyses (Lewin et al., 1994), the Liquid to Solid ratio is 10:1 ($\mathrm{l\ kg^{-1}}$)

- The mass of bromide removed as part of the top layer was estimated by assuming that based on the grid pattern, the remediation proposals encompassed the excavation of a total of 17 blocks to a depth of 0.75 m, and 23.5 blocks to a depth of 1.5 m. Calculating the mass of bromide for each block and summing the results, gave a total of 2406 kg (566 kg + 1840 kg). Subtracting this amount from the estimates of mass above gave a residue of 5129 kg and 11729 kg of bromide present in the unsaturated zone after contaminated soil removal.

5.7.2 New estimates

Additional estimates of bromide and bromate mass (Table 5.3) using additional data and a method of 3-D interpolation, were made as part of this thesis.

The *Voxler* software package (Golden Software) was used to plot data as (**X,Y,Z**) data points, with bromate/bromide concentration as a fourth variable. *Voxler* was used to interpolate bromate/bromide concentrations as a 3-D lattice (**X,Y,Z,C**). This provided a visualisation of the three-dimensional distribution of bromate and bromide contamination (Figure 5.7, Figure 5.9 and Figure 5.10). In order to estimate the mass of bromate/bromide present in the soil, bromate/bromide concentration contours were exported to *Surfer* as lattice slices of specified **Z** thickness (Figure 5.30 and Figure 5.29). The contours were 'blanked' at the site boundary so that only bromide/bromate within the site boundary was included in the mass estimates. *Surfer* was then used to calculate the 'volume' enclosed by each contoured surface. This 'volume' (area $\times$ concentration), when multiplied by the thickness of the slice and the bulk density of soil, represents the mass of bromate/bromide within the soil. The results from each slice (Figure 5.30 and Figure 5.29) were summed to calculate a total mass of bromate/bromide within the total thickness of unsaturated zone.

Maximum, mean and minimum unsaturated and saturated zone thicknesses are defined as follows (Figure 5.31):

- Based on the available samples in the vicinity of the source zone (*i.e.* from Boreholes **221** and **219**), bromate and bromide is present (above background concentrations) in porewater to a maximum depth of approximately +77.5 m OD. The maximum depth of sampling was at +75 m OD in Borehole **223**, and samples indicated very low concentrations (below or close to the MDL). It is therefore assumed that the depth of contamination extends to between approximately +75.5 m OD and +77.5 m OD beneath the source site.

- Ground level in the vicinity of the source zone is approximately +83.5 m OD.

- Water levels in the source zone range from +81.5 m OD to +79.0 m OD.

- Therefore, the thickness of *unsaturated* zone ranges from 2.0 m to 4.5 m thick and the thickness of *saturated* zone ranges from 1.5 m to 6.0 m thick. The mean unsaturated zone thickness (based on 2001-2008 data) is 4.1 m, and the mean saturated zone thickness is 3.4 m.

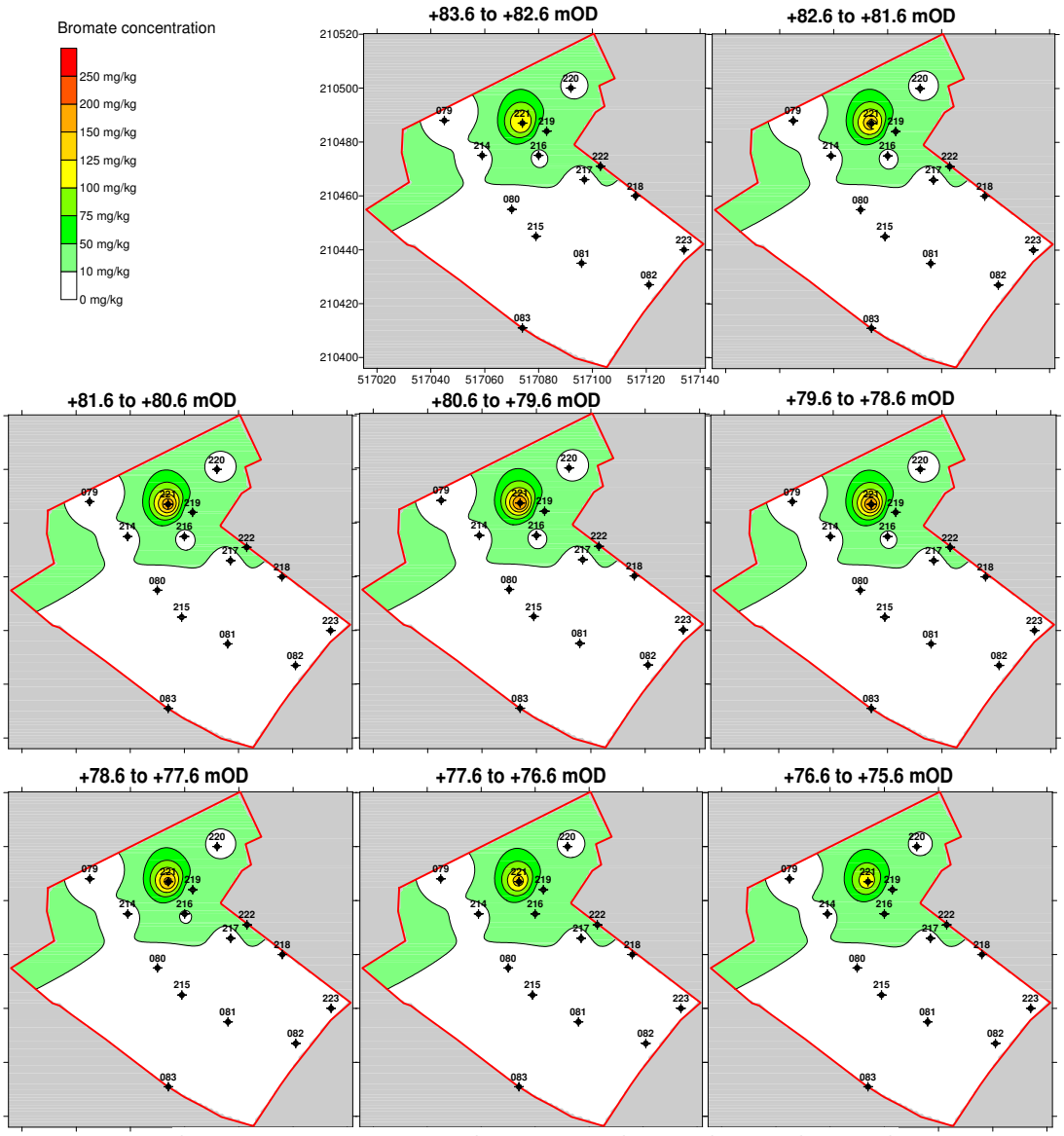

Elevation range of lattice slice				Calculated Mass of Bromate	Min. unsat. Max. sat.	Mean unsat. Mean sat.	Max. unsat. Min. sat.
83.6	to	83.1	mAOD	62.9kg			
83.1	to	82.6	mAOD	62.9kg			
82.6	to	82.1	mAOD	63.0kg			
82.1	to	81.6	mAOD	63.3kg	252kg		
81.6	to	81.1	mAOD	63.8kg			
81.1	to	80.6	mAOD	64.0kg			
80.6	to	80.1	mAOD	64.0kg			
80.1	to	79.6	mAOD	64.0kg		508kg	
79.6	to	79.1	mAOD	64.0kg			572kg
79.1	to	78.6	mAOD	63.9kg			
78.6	to	78.1	mAOD	63.7kg			
78.1	to	77.6	mAOD	63.6kg			191kg
77.6	to	77.1	mAOD	63.4kg			
77.1	to	76.6	mAOD	63.3kg			
76.6	to	76.1	mAOD	63.1kg		445kg	
76.1	to	75.6	mAOD	63.0kg	764kg		

Figure 5.29: Bromate soil concentration contours for 1.0 m thick grid slices based on investigation data from 2000 and 2001 (Komex, 2000; Atkins, 2002). Estimates for total mass in the unsaturated and saturated zones refer to minimum, mean and maximum thicknesses defined in Figure 5.31.

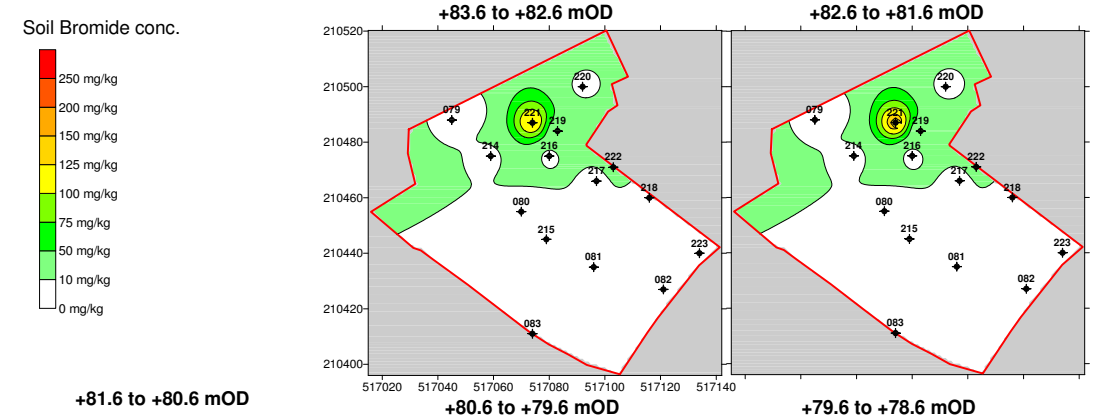

Elevation range of lattice slice				Calculated Mass of Bromide	Min. unsat. Max. sat.	Mean unsat. Mean sat.	Max. unsat. Min. sat.
83.6	to	83.1	mAOD	100.1kg			
83.1	to	82.6	mAOD	100.3kg			
82.6	to	82.1	mAOD	100.6kg			
82.1	to	81.6	mAOD	101.1kg	402kg		
81.6	to	81.1	mAOD	101.7kg			
81.1	to	80.6	mAOD	102.2kg			
80.6	to	80.1	mAOD	102.8kg			
80.1	to	79.6	mAOD	103.5kg		812kg	
79.6	to	79.1	mAOD	104.4kg			917kg
79.1	to	78.6	mAOD	105.3kg			
78.6	to	78.1	mAOD	106.5kg			
78.1	to	77.6	mAOD	107.8kg			320kg
77.6	to	77.1	mAOD	109.4kg			
77.1	to	76.6	mAOD	111.2kg			
76.6	to	76.1	mAOD	113.2kg		758kg	
76.1	to	75.6	mAOD	115.3kg	1283kg		

Figure 5.30: Bromide soil concentration contours for 1.0 m thick grid slices based on investigation data from 2000 and 2001 (Komex, 2000; Atkins, 2002). Estimates for total mass in the unsaturated and saturated zones refer to minimum, mean and maximum thicknesses defined in Figure 5.31.

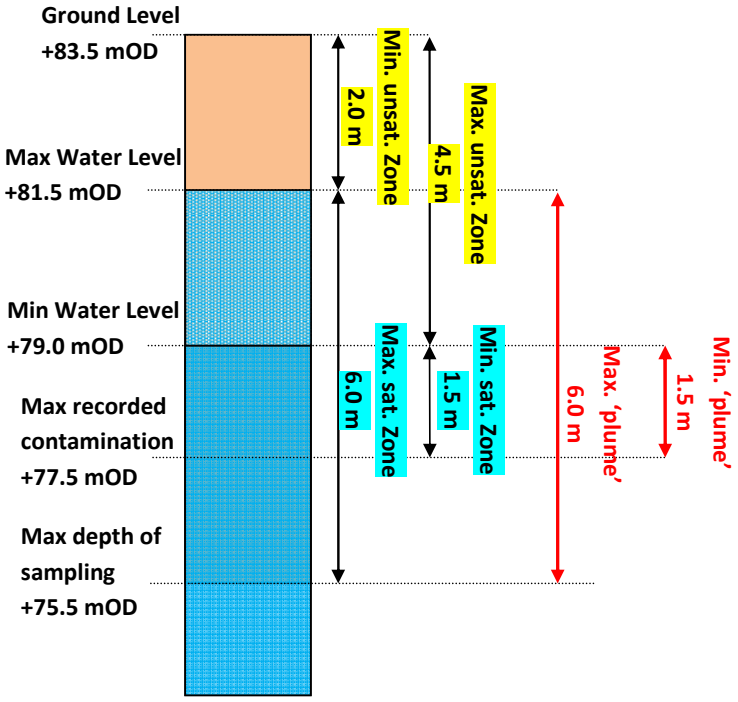

Figure 5.31: Minimum and maximum saturated and unsaturated zone thicknesses.

Table 5.3: Summary of mass estimates. Estimates for total mass in the unsaturated and saturated zones refer to minimum, mean and maximum thicknesses defined in Figure 5.31.

		1984-1985			1986	2000-2001		
		MIN	**MEAN**	MAX	*mass excavated*	MIN	**MEAN**	MAX
BROMIDE	unsat. zone (kg)	12745	**24907**	27617	*-2800*	402	**812**	916
BROMIDE	sat. zone (kg)	7672	**17936**	32645	0	320	**758**	1283
TOTAL BROMIDE	(kg)	–	**–**	–	–	–	**1570**	–
BROMATE	unsat. zone (kg)	–	**–**	–	–	252	**508**	572
BROMATE	sat. zone (kg)	–	**–**	–	–	191	**445**	764
TOTAL BROMATE	(kg)	–	–	**–**	–	–	**953**	–

5.8 Mass flux of bromate in groundwater migrating from the source site

The groundwater flux, F, across a plane perpendicular to groundwater flow direction taken directly through the source area (Figure 5.23), is given by the equation:

$$F = Dvn_e \int_{x=A}^{x=B} C\,dx \tag{5.1}$$

where D is the depth of the contaminated 'plume', v is the groundwater velocity and n_e is the effective porosity

The linear velocity, v, is related to the darcy velocity, q, by $q = vn_e$, so equation 5.1 can be written as:

$$F = Dq \int_{x=A}^{x=B} C\,dx \tag{5.2}$$

The integral $\int_{x=A}^{x=B} C\,dx$ is the area under a graph of concentration C against distance x along the section line from A to B (Figure 5.32).

As described in Section 5.7.2, the bromate contamination is estimated to extend to depths of between +75.5 m OD and +77.5 m OD beneath the source site. Water levels in the source zone range from +81.5 m OD to +79.0 m OD. Therefore, if the depth of the contaminated 'plume' is taken as the distance between the top of the water column and the estimated deepest recored contaminated porewater sample, then the thickness of of 'plume' could range from 1.5 m to 6.0 m (Figure 5.31).

Using a range of 1.5 m to 6.0 m for D, and a darcy velocity q of 0.9 $\mathrm{m\ d^{-1}}$ based on the results of the single borehole dilution tests (Section 3.6.1) at the nearby Harefield House (location **226**) and Nashe's Farm (location **019**) boreholes, groundwater flux estimates for bromate (Figure 5.32 range from

6.3 $\mathrm{kg\ d^{-1}}$ to 41 $\mathrm{kg\ d^{-1}}$ (572 to 3770 $\mathrm{kg\ y^{-1}}$) for a 'thick plume' and 1.6 $\mathrm{kg\ d^{-1}}$ to 10 $\mathrm{kg\ d^{-1}}$ (2289 to 15080 $\mathrm{kg\ y^{-1}}$) for a 'thin plume'. Flux estimates for bromate apparently decrease with time between 2001 and 2003.

These flux estimates seem extremely high in relation to the amount of bromate present at source site in the unsaturated and saturated zone (Section 5.7.2). This suggests that the dominant contributor to the groundwater concentrations is bromide/bromate in the saturated zone porewater, and that the mass of bromide/bromate in the porewater has not been fully accounted for in the mass calculations. Also, the 'plume' may extend deeper than accounted for in the mass calculations and/or concentrations may be higher in locations where samples were not taken.

5.9 Previous representations of the 'Source Term'

The representation of bromate (and bromide) release from the source site has received relatively little attention in previous assessments of the Hertfordshire bromate contamination. The assessments which have considered and quantified the 'source term' are discussed in the sections below.

5.9.1 Early assessments: 1984 and 1985

(Chemfix, 1984, 1985d) assumed an average porewater concentration of bromide of 5000 $\mathrm{mg\ l^{-1}}$ in 1984 over an area of 1200 $\mathrm{m^2}$ to a depth of 5 m, resulting in a total mass of bromide of 9400 kg. The conceptualisation assumed that the contaminated porewater was replaced by infiltration. Therefore, assuming an infiltration rate of 30 $\mathrm{mm\ y^{-1}}$ for the developed site, and 250 $\mathrm{mm\ y^{-1}}$ for the fallow site, this results in a bromate loading to the aquifer beneath the site of 180 $\mathrm{kg\ y^{-1}}$ and 1500 $\mathrm{kg\ y^{-1}}$ respectively. This would have resulted in a source lifetime of 52 years and 584 years respectively.

The modelling studies of (Chemfix, 1984, 1985d) assumed that leaching of the contamination from the soil from 1984 was the sole source of bromide into the aquifer. However, bromide concentrations in groundwater of around 9000 $\mathrm{mg\ l^{-1}}$ at the time indicate that there was already a considerable 'plume' of contamination present at the site which may have represented the effects of up to 30 years of contamination prior to 1984. The mass input to the aquifer is therefore likely to have been considerably underestimated by the Chemfix modelling.

5.9.2 Recent assessments: 2002 to 2008

5.9.3 CONSIM modelling

Atkins (2002) formed a conceptual model for the source site comprising a bromate source zone within the unsaturated zone soils. The pathway to the saturated zone was by leaching of bromate by infiltrating recharge through the contaminated unsaturated zone.

The soil source was modelled based on the presence of two 'hotspots' located in the north-eastern area of the site around locations **219** and**221**, where the highest soil concentrations were encountered. The source was modelled by a 10 m by 10 m block around each location, corresponding to a 20 m long by 10 m wide source zone. The source zone thickness was 2.0 m to 2.5 m based on the distance from the base of the made ground to the rest groundwater levels (November 2001). The soil source bromate

	Area under graph (ug/l * m)	1.5 m thick plume	
		Flux (kg/d)	Flux (kg/y)
Oct-Dec 2001	7645509	10.3	3770
Jan-Mar 2002	3253520	4.4	1604
Apr-Jun 2002	2863282	3.9	1412
Jul-Sep 2002	2404950	3.2	1186
Oct-Dec 2002	2143395	2.9	1057
Jan-Mar 2003	1263853	1.7	623
Apr-Jun 2003	1735090	2.3	856
Jul-Sep 2003	1908070	2.6	941
Oct-Dec 2003	1160306	1.6	572

	Area under graph (ug/l * m)	6.0 m thick plume	
		Flux (kg/d)	Flux (kg/y)
Oct-Dec 2001	7645509	41.3	15080
Jan-Mar 2002	3253520	17.6	6417
Apr-Jun 2002	2863282	15.5	5647
Jul-Sep 2002	2404950	13.0	4743
Oct-Dec 2002	2143395	11.6	4228
Jan-Mar 2003	1263853	6.8	2493
Apr-Jun 2003	1735090	9.4	3422
Jul-Sep 2003	1908070	10.3	3763
Oct-Dec 2003	1160306	6.3	2289

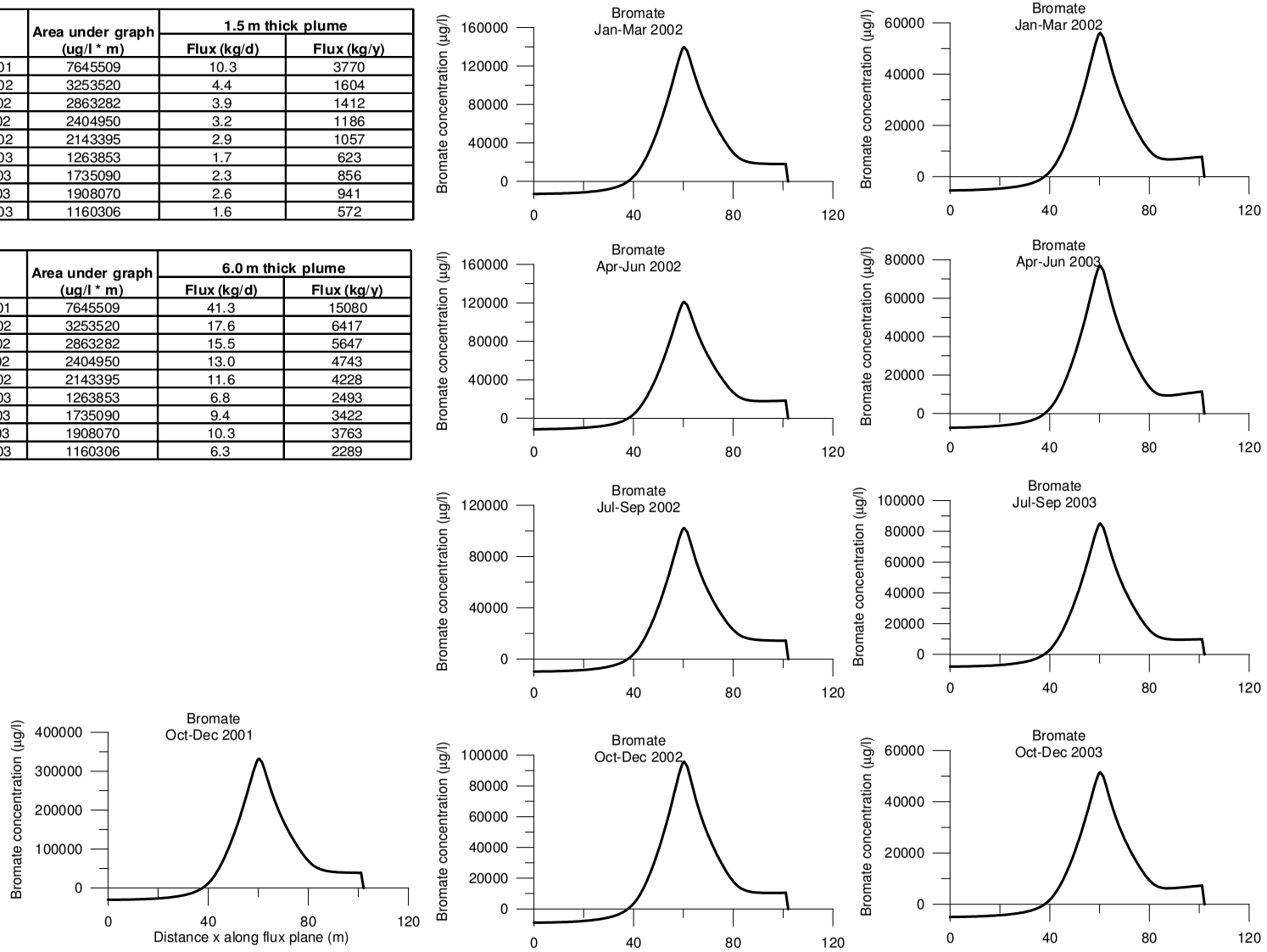

Figure 5.32: Estimates of bromate groundwater flux from the 'source zone' using equation 5.2 and the area under a concentration profile taken across a flux plane through the source zone. The area under a graph represents the integral $\int_{x=A}^{x=B} C\,dx$. The flux plane is shown in Figure 5.23.

concentration was assigned a range of 1.7 $\mathrm{mg\ kg^{-1}}$ to 273 $\mathrm{mg\ kg^{-1}}$ based on the analytical results of samples collected from the unsaturated soil zone at these locations.

The probabilistic CONSIM modelling package was then applied to predict leaching of soil contaminants through the unsaturated zone and to predict concentrations arising in the Putty Chalk aquifer. The subsequent dilution within the saturated Chalk aquifer (a 10 m thick mixing zone comprising saturated Putty Chalk and Blocky Chalk) was also simulated. The results of the simulations indicated bromate concentrations close to observed groundwater concentrations at monitoring locations **219** and**221**. Atkins (2002) concluded that this indicated that there was a 'significant pollutant linkage' (SOURCE → PATHWAY → RECEPTOR) between the bromate contamination **source** within the unsaturated zone soils and groundwater within the Chalk aquifer **receptor** beneath the site, via a **pathway** of leaching through the unsaturated zone.

5.9.4 MT3D modelling

Atkins (2005) used a constant source term of 5000 $\mu\mathrm{g\ l^{-1}}$ bromate at the source site from 1970 for the duration of the modelling period until 2050. A justification for this source term was not given explicitly. The 5000 $\mu\mathrm{g\ l^{-1}}$ concentration is equivalent to a constant input to the saturated zone of approximately 10 $\mathrm{kg\ d^{-1}}$ or 3650 $\mathrm{kg\ y^{-1}}$. This corresponds well to the bromate flux estimated from the source site (Section 5.8).

A constant source term is not realistic for the site: the bromate source will be depleted as mass is transported down-gradient and a steady concentration would not be expected to be maintained into the future. Also, monitoring data for *bromide* in groundwater at the site show that concentrations have decreased considerably between 1984/1985 and 2000/2001 (Section 5.6.2.2). There is also some indication that concentrations have declined at locations in the vicinity of the source site (Section 5.6.3). If bromate contamination has followed a similar history to bromide contamination, then it would be expected that bromate concentrations at the source site would have also shown some decline.

5.10 New Conceptual Models for Contaminant Release

Based on the groundwater distribution outlined in Section 5.6.2, the 'source zone' can be taken as the broad area encompassing the highest bromate and bromide concentrations, corresponding to the area around the former bromine storage, solid bromate handling and liquid bromate production areas, and also immediately downgradient of the sump for the non-bromate production area (Figure 5.33).

Based on the distribution of bromide from investigations in 1983, 1984 and 1985, it is apparent that by the end of the operational lifetime of the chemical works, considerable bromide (and most likely bromate), had accumulated in the unsaturated and saturated zone beneath the source area. Figure 5.34 presents a conceptual model for the release of bromate and bromide to groundwater beneath the source zone. The mechanism by which the contamination was released and accumulated between 1955 and 1983 is unknown. The main areas of uncertainty in the history of bromate and bromide release to groundwater beneath the site are summarised in Table 5.4.

Table 5.4: Main areas of uncertainty in the history of bromide and bromate release to groundwater beneath the source site.

Area of uncertainty	**Observations and constraints**
Timing of input Release of contaminants could have begun at an early stage of the operational lifetime of the chemical works (c. 1955 - 1980), or could have occurred towards the end of operation, or during decommissioning and demolition of the works (c. 1985-1987).	The presence of high concentrations of bromide in saturated and unsaturated zone porewater and groundwater in locations beneath the source site, and at a distance of approximately 150 m down-gradient (borehole B1-[85]), indicate that bromide input must have commenced prior to 1983 (shallow porewater), 1984 (porewater and groundwater at the site) and 1985 (porewater and groundwater 150 m down-gradient of the source zone).
Form of input The form of release could range from a relatively constant input through continuous leak/discharge, to an input over a short period of time as a result of a catastrophic leak/discharge or a recharge pulse. Release may have occurred as a focused input over a small area of the site (*e.g.* via sumps) or may have occurred as a more diffuse input over a larger area.	The bromide concentrations in soil porewater and groundwater recorded at the source site between 1983 and 1987 are significantly higher than concentrations recorded in 2000 and 2001. The buildings were cleared and the site was left to free-drain in 1984. The site clearance is likely to have coincided with a substantial increase in infiltration rate, and therefore a pulse of recharge. This recharge pulse may have been important in transporting bromide (and bromate) from unsaturated zone to the saturated zone.
Similarity of bromide and bromate release history The release history of bromate and bromide may or may not be related and show similarities in the form and timing of bromate input. If the predominant mobilisation of contamination occurred via a pulsed recharge event, the form of bromide and bromate release from 1984 is likely to be similar. However, if releases prior to 1983 have been more important in the mobilisation of bromide to groundwater, then due to lateral separation of bromide and bromate production areas, the relative magnitudes and timing of release may differ considerably.	Based on the site investigation data for 2000 and 2001, the spatial distribution of elevated bromide and bromate in porewater and groundwater shows similarities. Also, bromate and bromide concentrations are positively correlated based on groundwater monitoring data from 2000 to 2007. However, the lack of data for bromate concentrations prior to 2000 means that it is uncertain whether or not bromate concentrations were similarly elevated in the early 1980s. The only concentrations of bromate available are for shallow soil in 1983, and all samples were below detection limits. Therefore, it is possible that bromate contamination release occurred later than bromide contamination (hence bromate not as widespread in 1983), and/or at lower relative quantities. It is also possible that bromate was elevated in 1983 but was not detected because release mechanism meant that its distribution was deeper than 1.5 m (*e.g.* a more focused input into drainage via sumps).

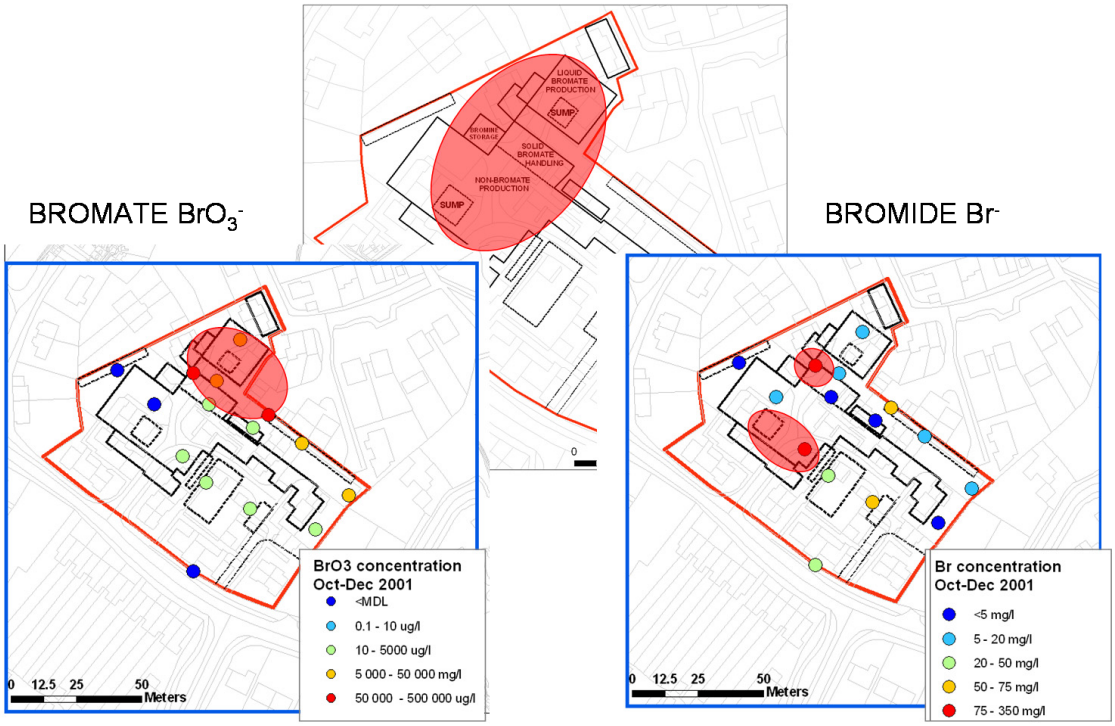

Figure 5.33: The combined 'source zone' (centre figure) based on the locations of high concentrations of bromate (left hand figure) and bromide (right hand figure) in groundwater

5.10.1 Mechanisms of bromide and bromate release

It is likely that the original bromate and bromide contamination accumulated from spills or leaks of substances containing bromide and/or bromate (and/or bromine) during the operation of the chemical works. It is possible that bromide and bromate were discharged to groundwater via the drainage system, allowing rapid introduction of these contaminants to deeper strata or direct to groundwater.

Due to the high solubility of bromide and bromate, it is assumed that bromide and bromate present within the unsaturated zone soils are present as dissolved ions in porewater rather than associated with the solid phase. The conceptual model considers that bromide and bromate ions are leached by infiltrating water and transported through the unsaturated zone to groundwater within the saturated 'putty chalk'. Groundwater transports contaminants (vertically) through the 'putty chalk' to the underlying 'blocky chalk', where contaminants are transported laterally with groundwater flowing through the fissures. Double-porosity diffusive exchange of contaminants occurs between groundwater within the fissures and porewater within the saturated chalk. These processes and mechanisms are described in more detail in the following sections.

5.10.1.1 Leaching of contaminants from unsaturated zone

The conceptual model considers that bromide and bromate ions are leached by infiltrating water and transported through the unsaturated zone to groundwater within the saturated putty chalk. Before the contaminated shallow soils were removed, there would have existed a plentiful source of bromide (and possibly bromate) contamination which would have been readily leached by infiltrating water. During the

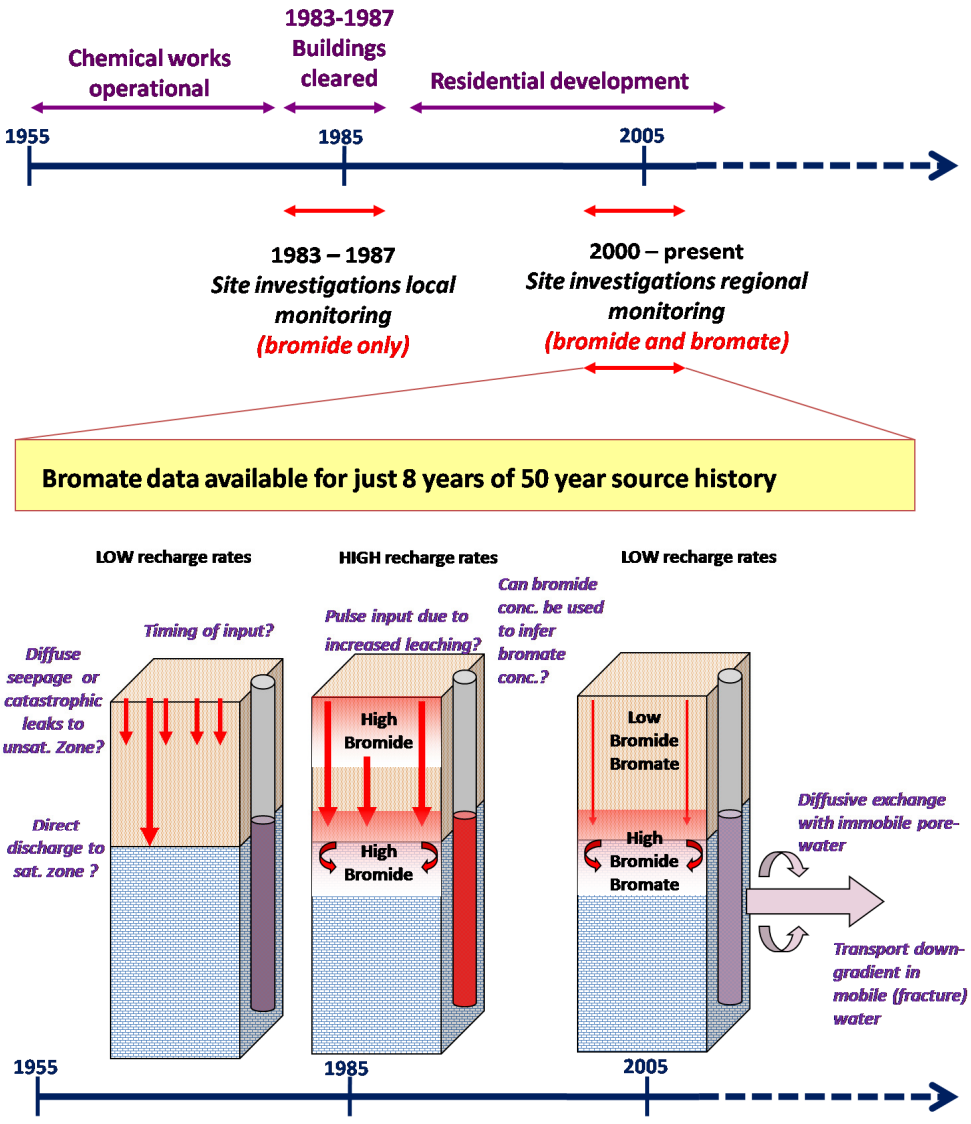

Figure 5.34: Conceptual Model for bromate and bromide release from the source zone.

operation of the factory, much of the site was covered with buildings or hard-surfaces which would have restricted the amount of recharge. However, a much higher rate of recharge would have been possible when the site was cleared and left to free-drain (end of 1983 to beginning of 1987). Leaching would have the effect of transporting bromate and bromide ions through the unsaturated zone to groundwater within the saturated putty chalk. The large decrease in bromide concentrations encountered in 2000 and 2001 compared to those recorded between 1983 and 1985 in comparable locations and depths, suggests that high recharge rates during 1984 to 1987 may have played an important role in leaching out contamination from the unsaturated zone profile.

Assuming recharge to occur via 'piston flow' (downward movement of water that has infiltrated at the surface occurs via vertical drainage through unsaturated matrix porewater), a minimum time for the complete leaching of the contaminant from the soil profile can be estimated by calculating the length of time it would take to replace the water contained within the unsaturated zone soil profile:

Time for replacement of water in unsat. zone = $\frac{V_U}{V_R}$

Where

V_U **= Volume of water in unsaturated zone = Area x moisture content**

V_R **= Volume of water recharged per year = Area x recharge rate**

Following the estimates of Roberts (2001), assuming a 4 m unsaturated zone with moisture content ranging from 11 % to 13 % and recharge rate 150 $\mathrm{mm\ y^{-1}}$ to 350 $\mathrm{mm\ y^{-1}}$, the minimum time for replacement is between 3.6 years and 1.3 years, with average values of approximately 2 years. These estimates predict that all the water present in the unsaturated zone could be replaced over a period of approximately 2 years, which implies that if the site was cleared at the end of 1983, and development took place at the beginning of 1987, all the water present in the unsaturated zone at the time of site clearance would have been replaced by infiltrated rainwater. Therefore, if the bromate and bromide ions behave conservatively (*i.e.* they are transported at the same rate as the water in which they are dissolved), then the 'free' bromide and bromate would have been almost completely removed from the unsaturated zone over this period.

However, it is clear that although bromate concentrations are generally low in the upper part of the unsaturated zone, relatively high concentrations still remain in the lower unsaturated zone (SUZ). The presence of discontinuous clay horizons within the fluvial-glacial deposits may have the effect of restricting recharge in some areas whilst concentrating recharge through other 'windows' in the clay. Where clay horizons restrict recharge, this may account for the continued presence of bromide and bromate within the unsaturated zone (present either as a result of transport from above, or introduction during high groundwater levels), despite high potential rates of leaching.

The bromide ion is generally thought to be conservative (Section 1.7) and so is transported at the same rate as the water in which it is dissolved. If the bromate ion behaves like the bromide ion, *i.e.* conservatively, then bromate will also be transported at the same rate as the water in which it is dissolved. However, the results of leachate tests carried out in 2001 (Section 5.6.5) at the site indicates that some

partitoning of bromate and bromide occurs between the soil phase and dissolved phase. The downward movement of bromate and bromide is therefore inhibited by soil interaction, and the time needed for complete removal from the soil is likely to be somewhat increased compared to the movement of soil porewater.

5.10.1.2 Evidence for pulse release

The bromide concentrations in soil porewater and groundwater recorded at the source site between 1983 and 1987 are significantly higher than concentrations recorded in 2000 and 2001. The buildings were cleared and the site was left to free-drain in 1984. The site clearance is likely to have coincided with a substantial increase in infiltration rate [3] and therefore a pulse of recharge. This recharge pulse may have been important in transporting bromide (and bromate) from unsaturated zone to the saturated zone. If this was the case, a sudden rise in groundwater concentrations at the source site, and/or a decrease in unsaturated zone concentrations between investigations in 1984 and 1985 might be expected.

The site was being cleared during the investigation in May 1984 (STATS, 1984). There are no reported groundwater samples from locations at the source site prior to this. The time series of groundwater concentrations from the three boreholes sampled in 1984 does indicate a rise in bromide concentrations from May 1984 to September 1984. Comparing concentration-depth profiles from BH1-[84] and C1-[85] which are reported to have been in approximately the same locations, bromide concentrations at similar depths appear to be less (about 25 % to 30 %) in 1985 compared to 1984. However, the profile has not clearly moved down as might be expected for piston-flow recharge, although it is difficult to be conclusive on this matter since fewer depths were sampled in 1984.

5.10.1.3 Migration down-hydraulic gradient in mobile groundwater

Due to the low permeability of the 'putty chalk' layer, groundwater transport through the saturated putty chalk is likely to occur predominantly in the form of vertical drainage. Diffusion into the matrix will result in retardation of bromide and bromate contamination compared to advective transport. Within the 'blocky chalk' bromate and bromide contamination will be transported down hydraulic gradient by advection, with dispersion and double-porosity diffusive exchange acting to retard the transport of contamination relative to groundwater flow.

5.10.1.4 Diffusive exchange with immobile porewater within the saturated zone

The (blocky) Chalk is considered to behave as a double-porosity aquifer with groundwater flow occurring predominantly through fissures, and the high porosity, low permeability matrix providing storage (Section 2.5). Diffusive exchange between the mobile fissure water and the immobile matrix water will occur during groundwater flow (Section 2.9.4).

Assuming initially contaminated fracture water and uncontaminated matrix water, bromate diffusion into the matrix water would have acted to retard the transport of bromate down-gradient. At a later stage, which may or may not have been reached at the SLC site, when the original source of contamination within the fracture water has ceased, the direction of diffusion will be from the contaminated

[3] Estimates of recharge (the portion of rainfall that percolates down to the water table) for free draining site are between 150 $\mathrm{mm\ y^{-1}}$ and 350 $\mathrm{mm\ y^{-1}}$ compared to approximately 60 $\mathrm{mm\ y^{-1}}$ for the site with predominant cover of hardstanding.

matrix water to the less contaminated fracture water, which will act to prolong the period of bromate contamination.

5.10.1.5 Seasonal mobilisation of porewater within the zone of water table fluctuation

Within the zone of water table fluctuation, also referred to as the seasonally unsaturated zone (SUZ), fractures are periodically filled and drained when the water table fluctuates. Due to the low permeability of the Chalk matrix, the matrix remains saturated. Diffusive exchange between fracture water and matrix water occurs when the fractures are saturated. This may provide a seasonal source (or sink) to groundwater in the saturated putty chalk.

This process may explain the concentration of bromate and bromide within the SUZ. During periods of high groundwater levels, diffusion is likely to have occurred between contaminated groundwater and uncontaminated porewater in the SUZ. Periodic repetition of this process results in the accumulation of contamination within porewater of the SUZ. At a later stage of groundwater plume evolution, or if initially high concentrations are present in porewater (*e.g.* from leaching of contamination from above), diffusive exchange between contaminated porewater and less contaminated groundwater would occur seasonally, proving a seasonal source of bromate to groundwater.

5.11 Source terms for bromide and bromate release from the source site

In order to encompass the range of possible scenarios for bromate release to groundwater beneath the source site, three source term scenarios are developed within this chapter. They are summmarised below:

- **Scenario A - 'Catastrophic Release'** This scenario envisages a sudden, large, release of bromide and bromate to the unsaturated zone at some point in the operational history of the factory.
- **Scenario B - 'Steady Seepage'** This scenario envisages a steady discharge of bromide and bromate to the unsaturated zone during the operational lifetime of the factory.
- **Scenario C - 'Direct Release'** This scenario envisages a direct release of bromate to the saturated zone (by-passing the unsaturated zone) for a period of time over the operational history of the factory.

The three conceptual scenarios for bromate input to, and release from, the 'source zone' are quantified in the following sections, using estimates of bromide and bromate mass in the unsaturated and saturated zone of the source site (Section 5.7.2) to constrain the range of possible source histories.

5.11.1 General equations

Scenarios A and B are described by the following equations, which are derived in Figure 5.35. For all scenarios, time $t = 0$ is taken as 1955, the start of the operation lifetime of the factory.

The distribution coefficient, K_d, relates the amount of solute sorbed to sediment (measured as the soil concentration, C_S, in $\mathrm{mg\ kg^{-1}}$) to the amount of solute in solution (measured as the leachate

concentration, C_L, in $\mathrm{mg\,l^{-1}}$):

$$K_d = \frac{C_S}{C_L} \tag{5.3}$$

At time t, the total mass in the unsaturated zone, $M(t)$, is represented by the equation:

$$M(t) = M_0 \exp^{-Kt} + \frac{S-R}{K}(1 - \exp^{-Kt}) \tag{5.4}$$

Where S is the rate of 'seepage' of mass to the unsaturated zone, R is the rate of mass removal from the unsaturated zone (by excavation, remediation *etc.*), both of which are assumed to be constant over defined time periods, and K is a constant defined as:

$$K = \frac{1000r}{D\rho K_d} \tag{5.5}$$

where r is the infiltration rate or recharge rate, D is the thickness of the unsaturated zone, ρ is the bulk density of soil within the unsaturated zone, and K_d is the distribution coefficient.

The rate of leaching of contaminant from the unsaturated zone, $L(t)$, is represented as:

$$L(t) = KM(t) = KM_0 \exp^{-Kt} + (S-R)(1 - \exp^{-Kt}) \tag{5.6}$$

The total mass of contaminant leached from the unsaturated zone between time T_1 and T_2 is then given by:

$$M_L(t) = \int_{T_1}^{T_2} L(t)dt \tag{5.7}$$

The leached concentration, C_L, in $\mathrm{mg\,l^{-1}}$ is then given by

$$C_L(t) = \frac{L(t)}{1000rA\theta_m} \tag{5.8}$$

where θ_m is the mobile porosity (the effective porosity) and A is the site area open to infiltration.

5.11.2 Constraints

The source term in bounded by the following constraints:

- **Condition 1** – the mass in the unsaturated zone at the end of 1983 should correspond to the observed mass estimate for the unsaturated zone in 1984/1985;
- **Condition 2** – the total mass input up until 1983 should be at least the observed mass estimate for the *saturated* zone in 1984/1985;
- **Condition 3** – the mass in the unsaturated zone in 2000/2001 should correspond to the observed mass estimate for the unsaturated zone in 2000/2001;
- **Condition 4** – the total mass input up until 2008 should be at least the amount of mass estimated to have been removed by Hatfield and other abstractions between 1981 and 2008.

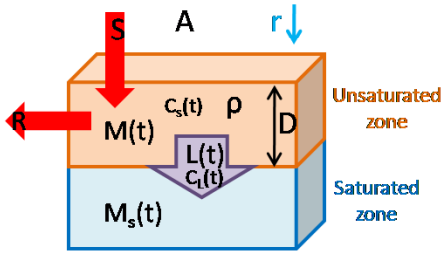

M(t)	Mass of bromide/bromate in unsaturated zone [kg]
L(t)	Rate of leaching of bromide/bromate from unsaturated zone [kg]
$C_s(t)$	Concentration of bromide/bromate in soil of unsaturated zone [mg kg^{-1}]
$C_L(t)$	Concentration of bromide/bromate in leachate from unsaturated zone [mg kg^{-1}]
K_d	Distribution coefficient [l kg^{-1}]
D	Thickness of unsaturated zone [m]
A	Site area [m^2]
r	Infiltration/recharge rate [mm y^{-1}]
ρ	Unsaturated zone soil bulk density [kg m^{-3}]
R	Rate of removal of bromide/bromate [kg y^{-1}]
S	Rate of addition of bromide/bromate [kg y^{-1}]
$M_s(t)$	Total mass of bromide/bromate in saturated zone [kg]

$$C_s = \frac{M(t)}{AD\rho} \times 10^6 \qquad C_L = \frac{L(t)}{rA} \times 10^3$$

$$K_d = \frac{C_s}{C_L} = \frac{rM(t)}{\rho DL(t)} \times 10^3$$

$$L(t) = \frac{1000r}{\rho DK_d} M(t) = K\,M(t) \qquad \text{where } K = \frac{1000r}{\rho DK_d} \qquad \text{Equation (1)}$$

Change in mass in unsaturated zone, ΔM, over time step Δt:

$$\Delta M = M_{t+\Delta t} - M_t = (M_t - L_t\Delta t - R\Delta t + S\Delta t) - M_t = S\Delta t - R\Delta t - L_t\Delta t$$

$$\Delta M = S\Delta t - R\Delta t - K\,M_t\Delta t$$

$$\int_{M=M_o}^{M=M_t} \frac{1}{K\,M_t - S + R}\,\mathrm{dM} = \int_{t=0}^{t=t} -1\,\mathrm{dt}$$

$$\frac{1}{K}\ln\left(\frac{K\,M_t - S + R}{K\,M_o - S + R}\right) = -t$$

$$M_t = M_o e^{-Kt} + \frac{(S-R)}{K}(1 - e^{-Kt}) \qquad \text{Equation (2)}$$

$$L_t = KM_t = KM_o e^{-Kt} + (S-R)(1 - e^{-Kt}) \qquad \text{Equation (3)}$$

Figure 5.35: Derivation of equations for mass of bromide/bromate in the unsaturated zone and the rate of input of bromide/bromate from the unsaturated zone to the saturated zone.

5.11.3 Bromide mass between 1985 and 2001

Conditions 1 and 3 are used to constrain the general equations for bromide between 1985 and 2001, where estimates for the total mass of bromide in the saturated zone (Section 5.7.2) are available based on results of site investigation in 1984/1985 and 2000/2001. For the purposes of calculations, the mass estimates are taken to be at the beginning of 1985 and the beginning of 2001 ($t = 30$ years and $t = 46$ years respectively).

Scenario A (Section 5.11.4) and Scenario B (Section 5.11.5), the recharge rate between 1984 and 1987 is assumed to be 500 $\mathrm{mm\ year^{-1}}$ corresponding to the 'recharge pulse' period when the site cover was removed and the site left to drain freely. From 1987 onwards, when the site is covered with housing and hardstanding, the recharge rate is assumed to be the lower rate of 290 $\mathrm{mm\ year^{-1}}$. In 1986, a quantity of bromate (for which there is an estimate in Section 5.7.1) was removed from the site by excavation of material from the unsaturated zone.

The leachate test results (Section 5.6.5) suggest a K_d for bromide of approximately 12 $\mathrm{l\ kg^{-1}}$. However, this value suggests too much partitioning for reasonable values of infiltration rate, and equation 5.4 cannot be fit to the observed mass estimates in 1985 and 2001 (Figure 5.36). In order to fit the observed mass results, a value of K_d of 0.20 $\mathrm{l\ kg^{-1}}$ is required (Figure 5.36). Therefore a K_d of 0.20 $\mathrm{l\ kg^{-1}}$ is used subsequently for calculating the source term for bromide.

For Scenario A (Section 5.11.4) and Scenario B (Section 5.11.5) assume that the pattern of bromate release from the source zone corresponds to the pattern of bromide release. The bromate mass is estimated from the bromide source term by the relationship observed in 2000 and 2001 (Figure 5.22):

Bromate conc. ($\mathrm{mg\ kg^{-1}}$) = 0.36 $\times$ Bromide conc. ($\mathrm{mg\ kg^{-1}}$) + 32.1 ($\mathrm{mg\ kg^{-1}}$)

In order to fit the observed bromate mass results, a value of K_d of 0.23 $\mathrm{l\ kg^{-1}}$ is required (Figure 5.36). Therefore a K_d of 0.23 $\mathrm{l\ kg^{-1}}$ is used subsequently for calculating the source term for bromate.

The source terms for Scenario A and Scenario B from 1984 onwards are illustrated in Figure 5.37 as bromide and bromate concentrations released to the saturated zone from 1984 onwards.

5.11.4 Scenario A: Catastrophic Leak + Recharge Pulse

The 'catastrophic release' scenario is represented by postulating a rapid, large release of bromide/bromate approximately midway through the factory operational lifetime (1965). No additional mass is released to the unsaturated zone. The pattern of bromate release is assumed to mirror the pattern of bromide release from the source zone. The mass of bromide/bromate in the unsaturated zone is subject to leaching by infiltrating water recharging the saturated zone. Recharge rates are assumed to be 290 $\mathrm{mm\ year^{-1}}$, corresponding to the estimated value with a cover of buildings and hardstanding. From 1984, the scenario proceeds as described in Section 5.11.3 and Figure 5.37.

Equation 5.4 is used to calculate the mass of bromide in 1965 of 11,140,000 kg (Figure 5.38), and the mass of bromate in 1965 of 221,600 kg (Figure 5.39). The 'catastrophic' release rate is therefore

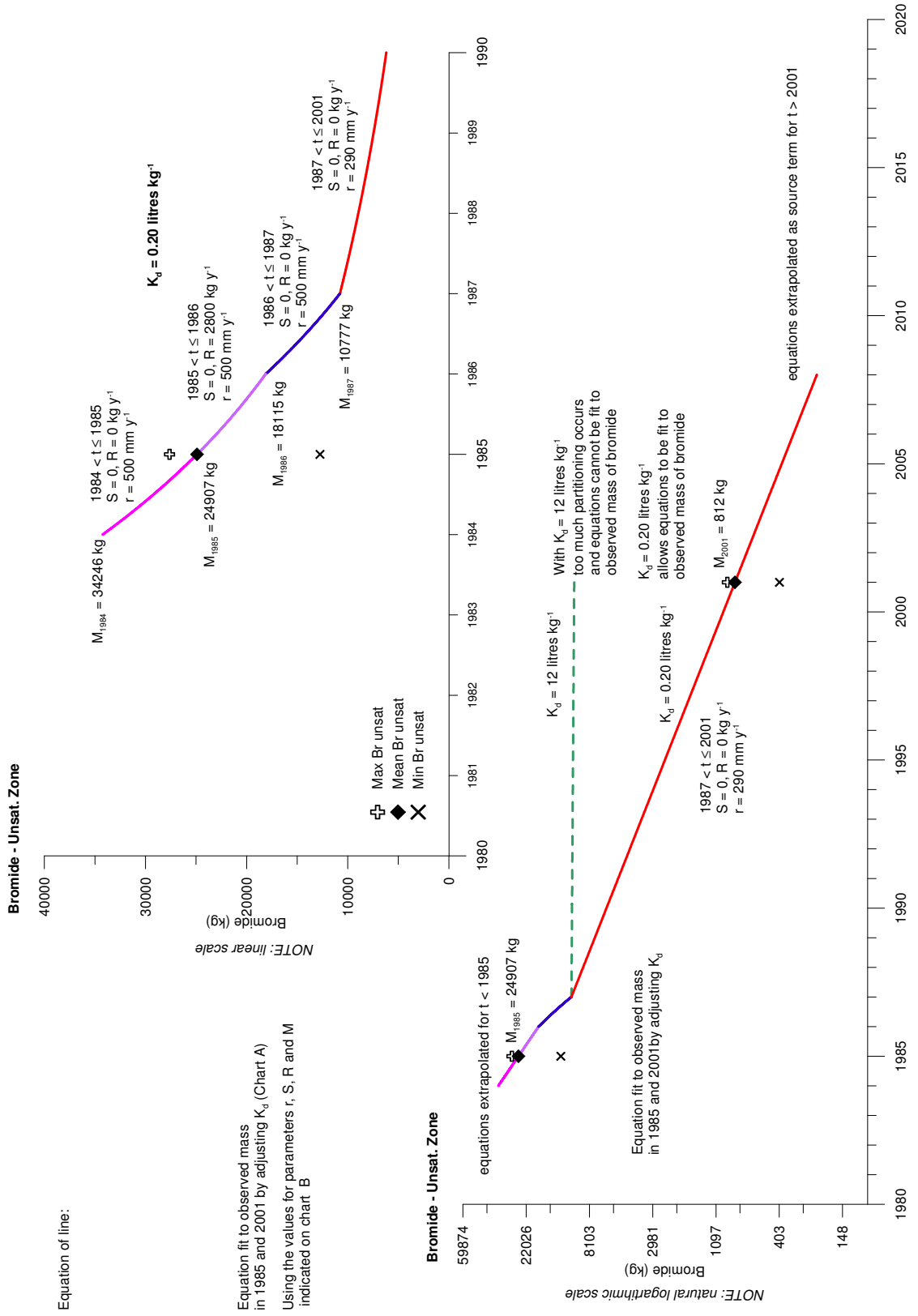

Figure 5.36: Equations for bromide mass, fit to observed values from 1985 and 2001. Parameters are defined in Figure 5.11.1

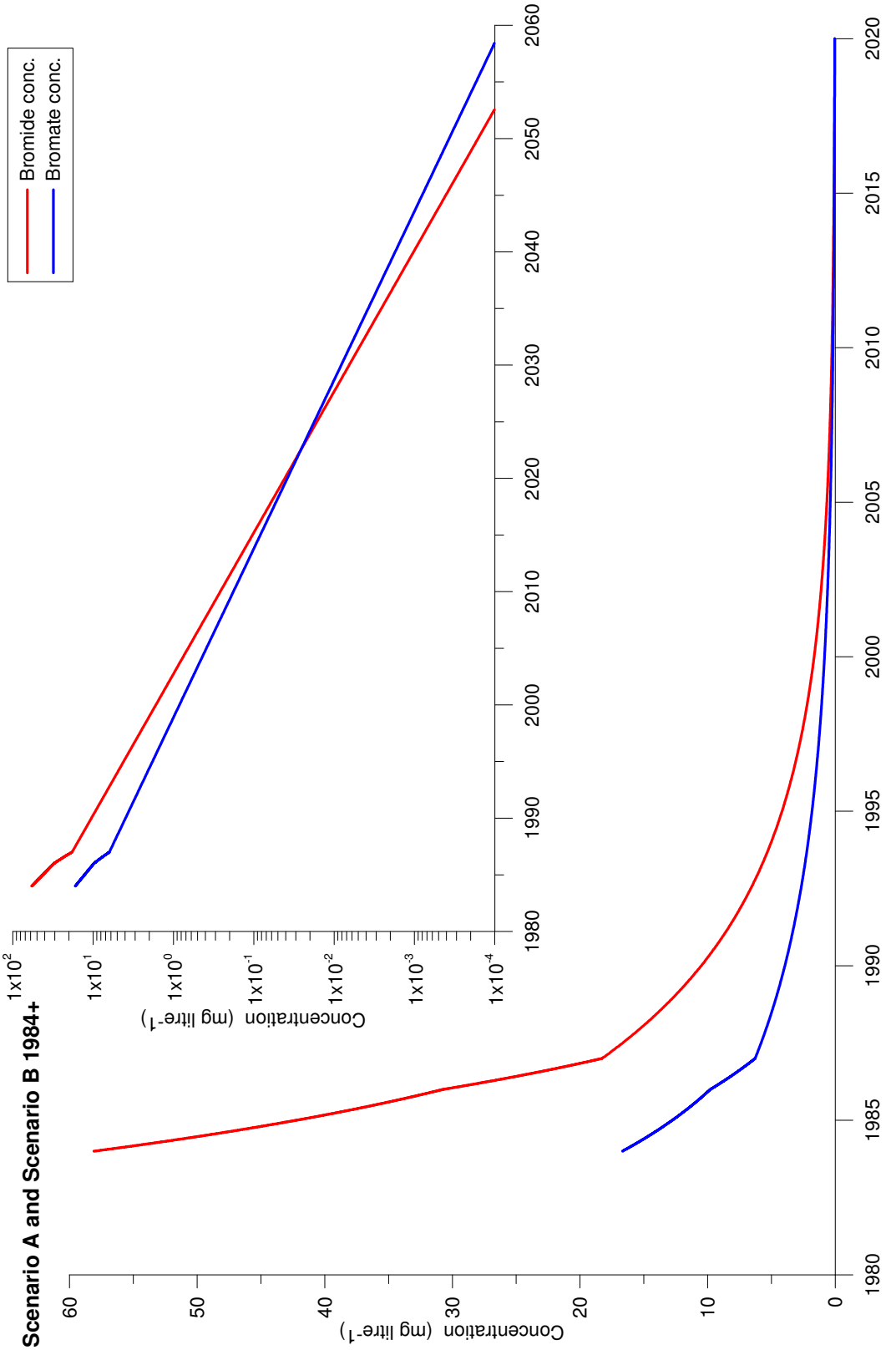

Figure 5.37: Bromide and bromate concentrations for Scenario A and Scenario B from 1984 into the future.

taken as 11,140,000 kg of bromide and 221,600 kg of bromate input over the year of 1965. Table 5.5 summarises how the source term relates to the four conditions in Section 5.11.2. Scenario A is illustrated as a source term in Figure 5.40.

5.11.5 Scenario B: Steady Seepage + Recharge Pulse

The scenario is represented by contaminant input (at a low rate) prior to the recharge pulse in 1984, and then a rapid increase in input rate coinciding with recharge pulse. The pattern of bromate release is assumed to mirror the pattern of bromide release from the source zone.

The 'steady seepage + recharge pulse' scenario is represented by postulating a constant rate of contaminant release to the unsaturated zone during the operational lifetime of the factory. The mass of bromide/bromate in the unsaturated zone is subject to leaching by infiltrating water recharging the saturated zone. Recharge rates are assumed to be 290 $\mathrm{mm\ year^{-1}}$, corresponding to the estimated value with a cover of buildings and hardstanding. From 1984, the scenario proceeds as described in Section 5.11.3 and Figure 5.37.

Equation 5.4 is used to calculate the rate of seepage of bromide between 1955 and 1984 as 6355 $\mathrm{kg\ y^{-1}}$ of bromide (Figure 5.38), 1837 $\mathrm{kg\ y^{-1}}$ of bromate (Figure 5.39). Table 5.5 summarises how the source term relates to the four conditions in Section 5.11.2. Scenario B is illustrated as a source term in Figure 5.40.

Table 5.5: Mass predicted by source history scenarios A and B compared to observed mass constraints. Condition 4 is based on an estimate by Buckle (2002) of the mass removed at Hatfield and Essendon between 1981 and 2000.

BROMIDE		**Observed**	Scenario A		Scenario B	
		kg	kg	% of observed	kg	% of observed
Condition 1	Mass in unsat. Zone 1985 = observed mass in unsat. Zone 1985	**2.49E+04**	2.49E+04	100%	2.49E+04	100%
Condition 2	Mass leached between 1955 and 1984 > observed mass in sat. Zone 1985	**1.79E+04**	1.11E+06	6189%	1.50E+05	836%
Condition 3	Mass in unsat. Zone 2001 = observed mass in unsat. Zone 2001	**8.12E+02**	8.12E+02	100%	8.12E+02	100%
Condition 4	Total mass leached up to 2008 > mass removed by abstractions 1981-2008	**2.23E+04**	1.14E+06	5125%	1.84E+05	824%

BROMATE		**Observed***	Scenario A		Scenario B	
		kg	kg	% of observed	kg	% of observed
Condition 1	Mass in unsat. Zone 1985 = observed mass in unsat. Zone 1985	**9.00E+03**	9.00E+03	100%	9.00E+03	100%
Condition 2	Mass leached between 1955 and 1984 > observed mass in sat. Zone 1985	**6.49E+03**	1.27E+05	1956%	3.28E+04	506%
Condition 3	Mass in unsat. Zone 2001 = observed mass in unsat. Zone 2001	**5.08E+02**	5.08E+02	100%	5.08E+02	100%
Condition 4	Total mass leached up to 2008 > mass removed by abstractions 1981-2008	**8.84E+03**	1.38E+05	2127%	4.39E+04	497%
		* Bromate concentrations prior to 2000 are estimated based on bromide concentrations.				

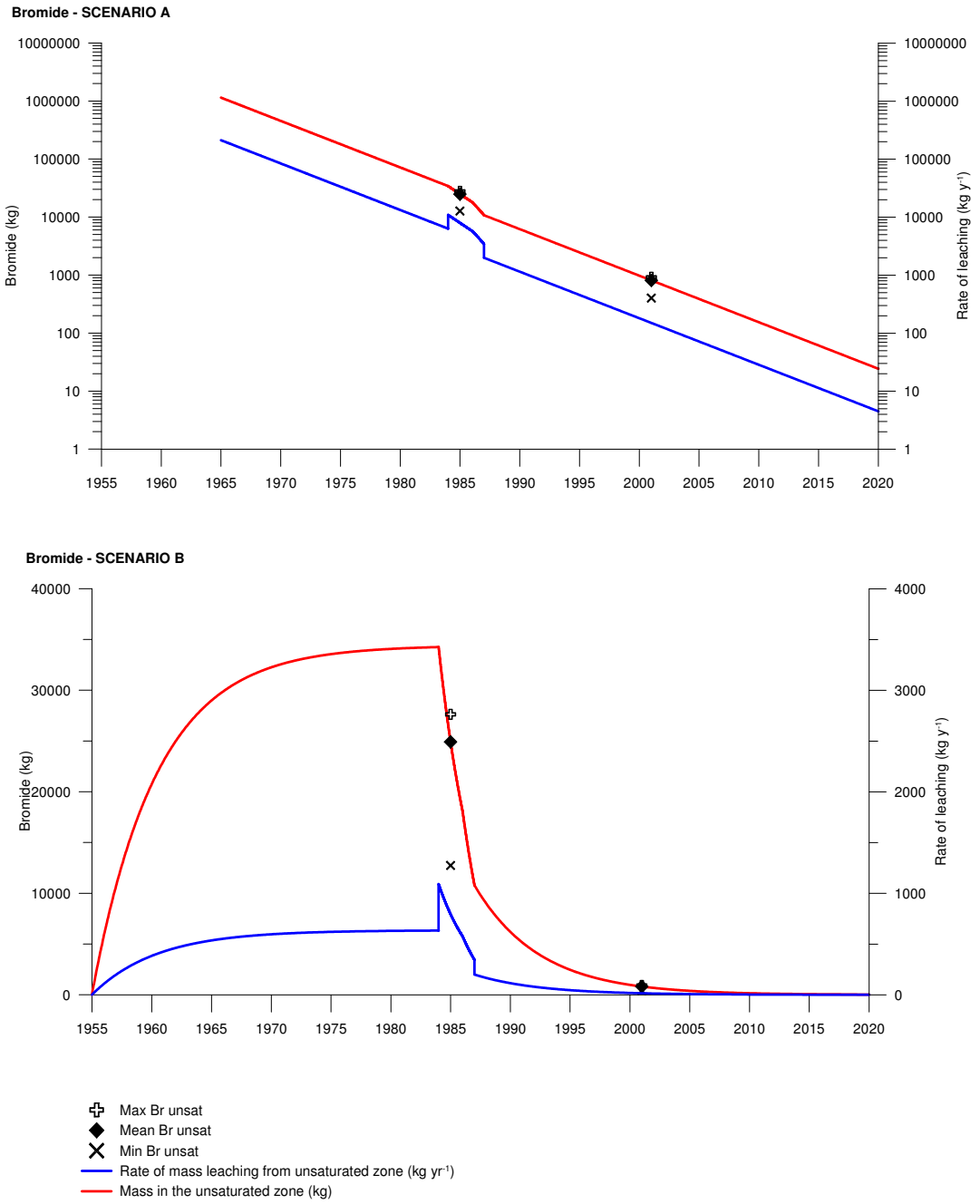

Figure 5.38: Bromide source history for Scenarios A and B.

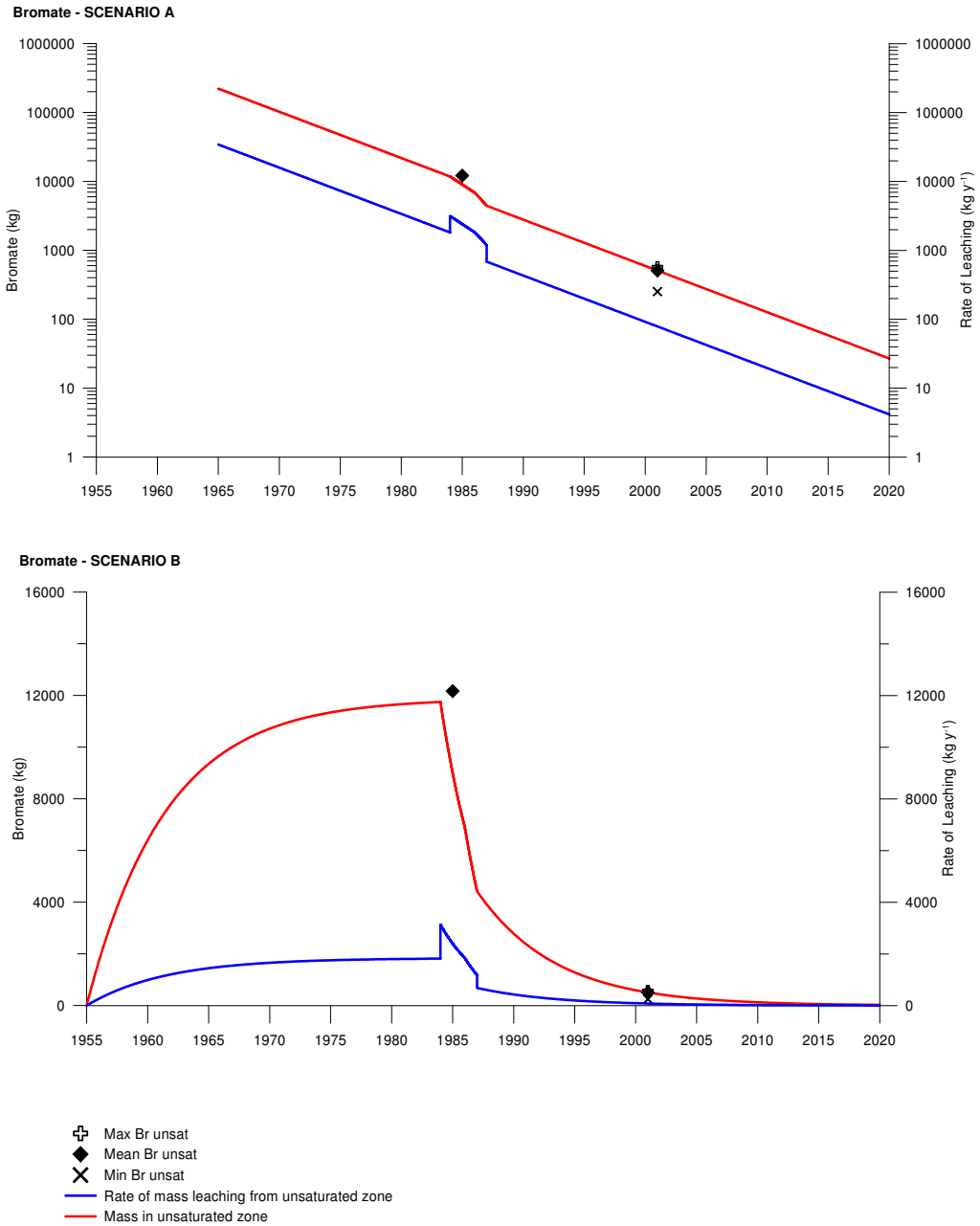

Figure 5.39: Bromide source history for Scenarios A and B.

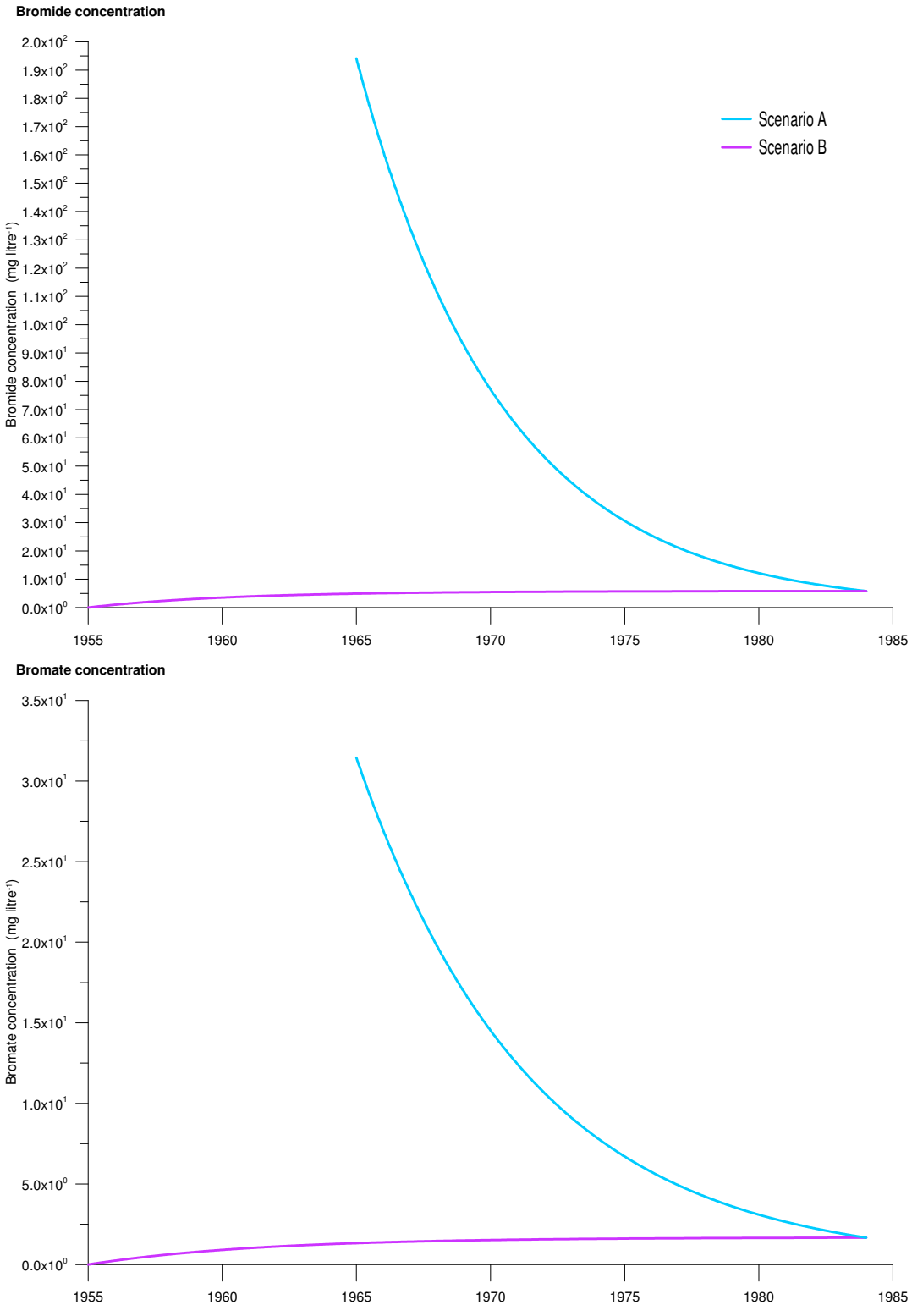

Figure 5.40: Bromide and bromate concentrations for Scenario A and Scenario B between 1955 and 1984. After 1984 concentrations proceed as in Figure 5.37.

5.11.6 Scenario C - Late stage Seepage + Recharge Pulse

Scenario C assumes that the pattern of bromate release differs from the pattern of bromide release from the source zone. However, due to the absence of observed bromate concentrations in soil or groundwater prior to 2001, it is difficult to constrain the source term; conditions 1 and 2 cannot be applied.

Scenario C assumes that the results from 1983 investigation that indicated bromate concentrations below detection limits, were representative of bromate concentrations in the shallow unsaturated zone of the site. Therefore, bromate input must have occurred directly to the saturated zone, by-passing the shallow soils, to result in the elevated bromate concentrations observed from 2000 in the saturated zone porewater and groundwater.

Scenario C is represented by postulating a constant flux of bromate to the saturated zone for a period of the operational lifetime of the factory. The mass flux, and the time period over which this occurs, are constrained by the observed porewater and groundwater concentrations at the source zone from 2000 to 2008. Bromate concentrations are simulated from the input at the top of the saturated putty chalk to the base of the putty Chalk, at which point they are assumed to represent the groundwater and porewater concentrations measured at the monitoring locations at the source zone (Locations **219**, **221** and **222**. The simulation set-up is described in Section 5.12. The source term is varied until a reasonable fit to the observed concentrations is achieved (Figure 5.41). The selected source term is a steady concentration of 3000 $\mathrm{mg\ l^{-1}}$ of bromate between 1955 and 1960.

5.11.7 Bromate flux in 2001

Using equation 5.6, and the observed mass of bromide in the unsaturated zone of 508 kg in 2001, the bromate flux from the unsaturated zone to the saturated zone is calculated as 78 $\mathrm{kg\ y^{-1}}$ in 2001 for Scenario A and Scenario B. This value is at least an order of magnitude lower than the estimated mass flux based on interpolations of observed groundwater concentrations (Section 5.8). This suggests that there is a source of bromate mass, additional to the bromate mass leaching from the unsaturated zone, that is contributing to the mass transported off-site in groundwater. This could indicate that there were inputs of bromate direct to the saturated zone (by-passing the unsaturated zone) that are not represented by source history scenarios A and B. Source scenario C attempts to capture this possibility. Using simulated concentrations at the base of the unsaturated zone for Scenario C in 2001, the bromate mass flux in groundwater is approximately 3 $\mathrm{kg\ d^{-1}}$ to 13 $\mathrm{kg\ d^{-1}}$ (1095 $\mathrm{kg\ y^{-1}}$ to 4745 $\mathrm{kg\ y^{-1}}$), which is of a similar magnitude to the estimates based on observed concentrations in 2001 to 2003 (Section 5.8).

5.12 Verifying source terms with observed down-gradient concentrations

The **DP1-D** (Dual Porosity in 1-Dimension) modelling code is a semi-analytical solute transport code developed by John Barker, based on Barker (1982). The code simulates one-dimensional transport through a double-porosity medium with a specified input concentration and a constant flow regime. The outputs are the solute concentration in the fractures and the average matrix porewater solute concentration for a specified set of times and distance from the input point. The code is written in Fortran and has been

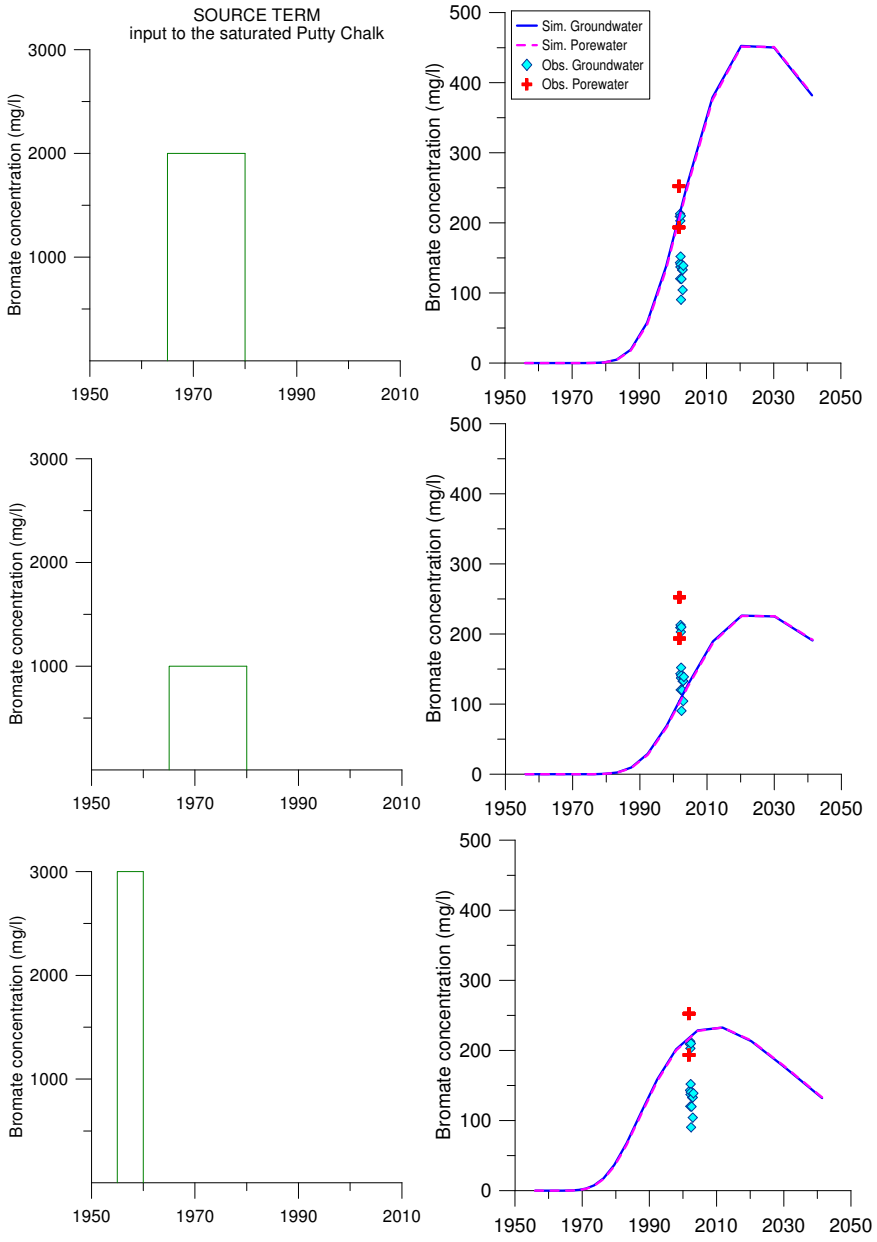

Figure 5.41: Bromate source history for Scenario C.

implanted in Excel. The spreadsheet accesses the code, held in a dynamic link library, via Visual Basic.

In order to evaluate the potential for the **DP1-D** code was used to simulate bromide and bromate concentrations down-gradient along a one-dimensional flow line from the source zone. The simulated results were compared to observed concentrations at three locations with bromide monitoring data available for 1983-1987 and 2000-2008, and bromate data for 2000-2008 only.

The parameters selected (Figure 5.42; Sections 5.12.1 to 5.12.6) were chosen as best available estimates from investigation data (*i.e.* the model was not calibrated to produce the observed concentrations.)

The conceptual model for bromate and bromide release to groundwater beneath the site considers the 'putty chalk' to represent a low permeability layer between the base of the unsaturated zone, and groundwater migrating off-site in the 'blocky chalk'. Groundwater flow is therefore assumed to be essentially vertical within the putty chalk layer. Groundwater flow is simulated vertically through the putty chalk layer to the saturated blocky chalk below the site, and then groundwater is simulated horizontally along a groundwater flowline (Figure 5.42).

5.12.1 Fracture Spacing $2b$

There is little available local information for fracture spacing in the region of the source site and $1\ \mathrm{km}$ down-gradient. However, geophysical logging by Three Valleys Water in the Hatfield area indicates flowing fracture separations of approximately $1.00\ \mathrm{m}$ to $1.40\ \mathrm{m}$. This is comparable to the values reviewed in Section 2.7.3.3 for unweathered Chalk. Therefore, a fracture spacing ($2b$) of $1.0\ \mathrm{m}$ is used for the 'blocky chalk'.

For the weathered 'putty chalk', the fracture spacing is considered likely to be less than the unweathered 'blocky chalk'. The values reviewed in Section 2.7.3.3 suggest a value of $0.10\ \mathrm{m}$ for fracture spacing ($2b$) in the Putty Chalk.

5.12.2 Fracture Aperture a

Based on the review of data from the literature (Section 2.7.3.3), a representative fracture aperture of $10^{-3}\ \mathrm{m}$ is used for the 'blocky chalk'.

This is likely to be significantly less for the Putty Chalk. Atkins (2002) estimated fracture apertures for the Putty Chalk of $10^{-6}\ \mathrm{m}$ based on the hydraulic conductivity, K, values calculated from measured putty chalk matrix porosities (2.7.3.1)and the relationship:

$$K = \frac{\rho g a^2}{12\mu}$$

where ρ is the fluid density, μ is the fluid viscosity, and g is the acceleration due to gravity.

5.12.3 Fracture Porosity θ_m

The mobile (or fracture) porosity, θ_m, for slab geometry with fracture aperture a and block thickness $2b$, is given by equation 5.9:

$$\theta_m = \frac{a}{2b + a} \tag{5.9}$$

Using the values for a and b in sections 5.12.2 and 5.12.1, the mobile porosity θ_m is estimated as 1.0×10^{-5} for the putty chalk and 1.0×10^{-3} for the blocky chalk.

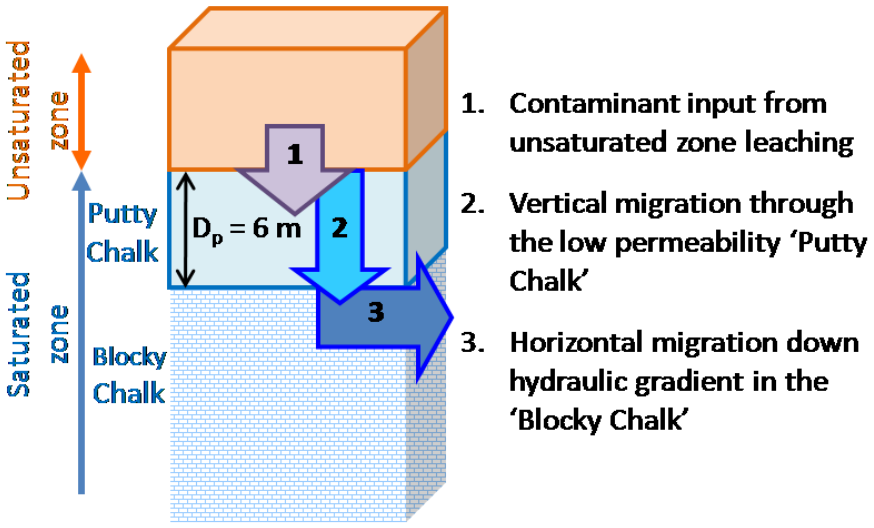

		Putty Chalk	Blocky Chalk	unit
fracture aperture	a	1.00E-06	1.00E-03	m
fracture spacing	2b	0.10	1.00	m
mobile porosity	θ_m	1.00E-05	1.00E-03	
immobile porosity	θ_{im}	0.38	0.38	
mobile velocity	v	9	900	m day^{-1}

Figure 5.42: Conceptual model for off-site verification simulations

5.12.4 Matrix Porosity Φ

During the 2001 site investigation (Atkins, 2002), 15 samples of Chalk from the saturated zone were tested. Results ranged between 0.308 and 0.457, with an average of 0.380. For the blocky chalk, a representative value for the Chalk in the area is 0.388 (Section 2.6). This value for Φ is used for both the saturated putty chalk and the saturated blocky chalk.

For a slab geometry, with fracture aperture a block thickness $2b$, this matrix porosity, Φ, this equates to an immobile porosity, θ_{im}, of 0.38, from equation 5.10:

$$\theta_{im} = \frac{2b\Phi}{2b + a} \tag{5.10}$$

Therefore, the immobile porosity θ_{im} is estimated as 0.38 for the putty chalk and 0.38 for the blocky chalk.

5.12.5 Fracture Velocity

Groundwater velocity, v, was calculated from the darcy velocities, q, determined from the single borehole dilution testing at Nashe's Farm and Harefield House (Section 3.6) and the mobile porosity value estimated above.

The darcy velocities ranged from 0.5 to 3.0 $\mathrm{m\ day^{-1}}$, with average of 1.0 $\mathrm{m\ day^{-1}}$ (Nashe's Farm), and 0.3 to 1.3 $\mathrm{m\ day^{-1}}$, with average of 0.8 $\mathrm{m\ day^{-1}}$ (Harefield House).

For the blocky chalk, with an effective porosity of 1.0×10^{-3}, this results in fracture velocities ranging from 300 to 3000 $\mathrm{m\ day^{-1}}$, with an average of 900 $\mathrm{m\ day^{-1}}$.

For the putty chalk, hydraulic conductivity is estimated to be around 10^{-4} to 10^{-2} $\mathrm{m\ day^{-1}}$, compared to 10^{0} to 10^{1} $\mathrm{m\ day^{-1}}$ for the blocky chalk aquifer. Therefore, the hydraulic conductivity for the putty chalk is approximately 10^{2} to 10^{4} times less than for the 'blocky Chalk'.

Additionally, the vertical hydraulic conductivity is likely to be around 10 % of the horizontal conductivity. This results in an estimated vertical darcy velocity in the putty chalk of 10^{4} times less than the hydraulic conductivity in the blocky chalk. Therefore, the vertical darcy velocity in the putty chalk is estimated as an average of 9.0×10^{-5} $\mathrm{m\ day^{-1}}$. With an effective porosity of 1.0×10^{-5}, this results in fracture velocities ranging from 3 to 30 $\mathrm{m\ day^{-1}}$, with an average of 9 $\mathrm{m\ day^{-1}}$.

5.12.6 Effective Diffusion Coefficient D_E

The effective diffusion coefficient for bromide and bromate is taken as 8.64×10^{-6} $\mathrm{m^2\ day^{-1}}$ (Section 2.9.4.1).

5.12.7 Simulation Results

5.12.7.1 Scenario A

For Scenario A, simulated bromide groundwater concentrations show good agreement with the observed bromide concentrations at monitoring locations **225**, **028** and **019** (Figure 5.43), although the simulated concentrations for 1983 to 1985 are at the lower limit of the observed concentrations. Observed porewater bromide concentrations are only available for location **225**; simulated porewater concentrations are at the lower limit of observed porewater concentrations.

Simulated bromate concentrations groundwater show good agreement with the observed bromate concentrations at monitoring location **225** and **028** (Figure 5.44), but simulated concentrations at location **019** are at the lower limit of the the observed concentrations.

5.12.7.2 Scenario B

For Scenrio B, simulated bromide concentrations (Figure 5.45) and bromate concentrations (Figure 5.46) are generally lower than observed concentrations by approximately one order of magnitude.

5.12.7.3 Scenario C

Simulated bromate concentrations for Scenario C (Figure 5.47) show good agreement with the observed bromide concentrations at all three of the monitoring locations.

5.12.7.4 Discussion of simulation results

The simulated groundwater and porewater concentrations at locations **225**, **028** and **019** for scenario A, B and C indicate that observed concentrations (1983 to 1985 and 2000 to 2008) are on the rising limb of bromide and bromate concentrations.

There is some indication in the bromide groundwater monitoring results (Section 5.6.3) that bromide concentrations increased between 1985 and 2001 at locations **225**, **028** and **019**. However, the large scatter in the observed monitoring data due to seasonal variations makes trends difficult to discern (See Chapter 4). It is therefore very difficult to be certain about which point on the simulated concentration versus time curve the current observations represent, and hence how successful the source terms and the model are in simulating bromate evolution close to the site.

Saturated zone chalk porewater bromide concentrations are available from location **225** in 2001 and in 1985 from location **B1-[85]**, which was at a similar location. The large range of both porewater and groundwater concentrations in both 1985 and 2001 make it difficult to decide on a representative figure for each, and therefore to determine the relative magnitude of porewater and groundwater concentrations. A mean porewater concentration and a mean groundwater concentration would indicate higher porewater bromide concentrations than bromide groundwater concentrations in 2001. This would imply, contrary to the simulated 'rising limb', that concentrations in 2001 were on the falling limb (Figure 5.48). However, the reverse is indicated in 1985; mean groundwater concentrations are higher than mean porewater bromide concentrations.

If the results of these two boreholes can be considered representative of the same location, then porewater bromate concentrations do show an increase between 1985 and 2001. The very large range of the groundwater concentration in 1985 makes it difficult to determine whether (mobile) groundwater concentrations have increased or decreased. An increase in bromide porewater concentrations between 1985 and 2001 would imply observed concentrations to be on the rising limb.

5.13 Summary and conclusions

Three source term scenarios have been developed which attempt to represent the range of possible bromide and bromate source histories. Scenario A ('catastrophic release') and Scenario B ('steady seepage') assume that bromide and bromate have had similar histories and that the main process contributing to

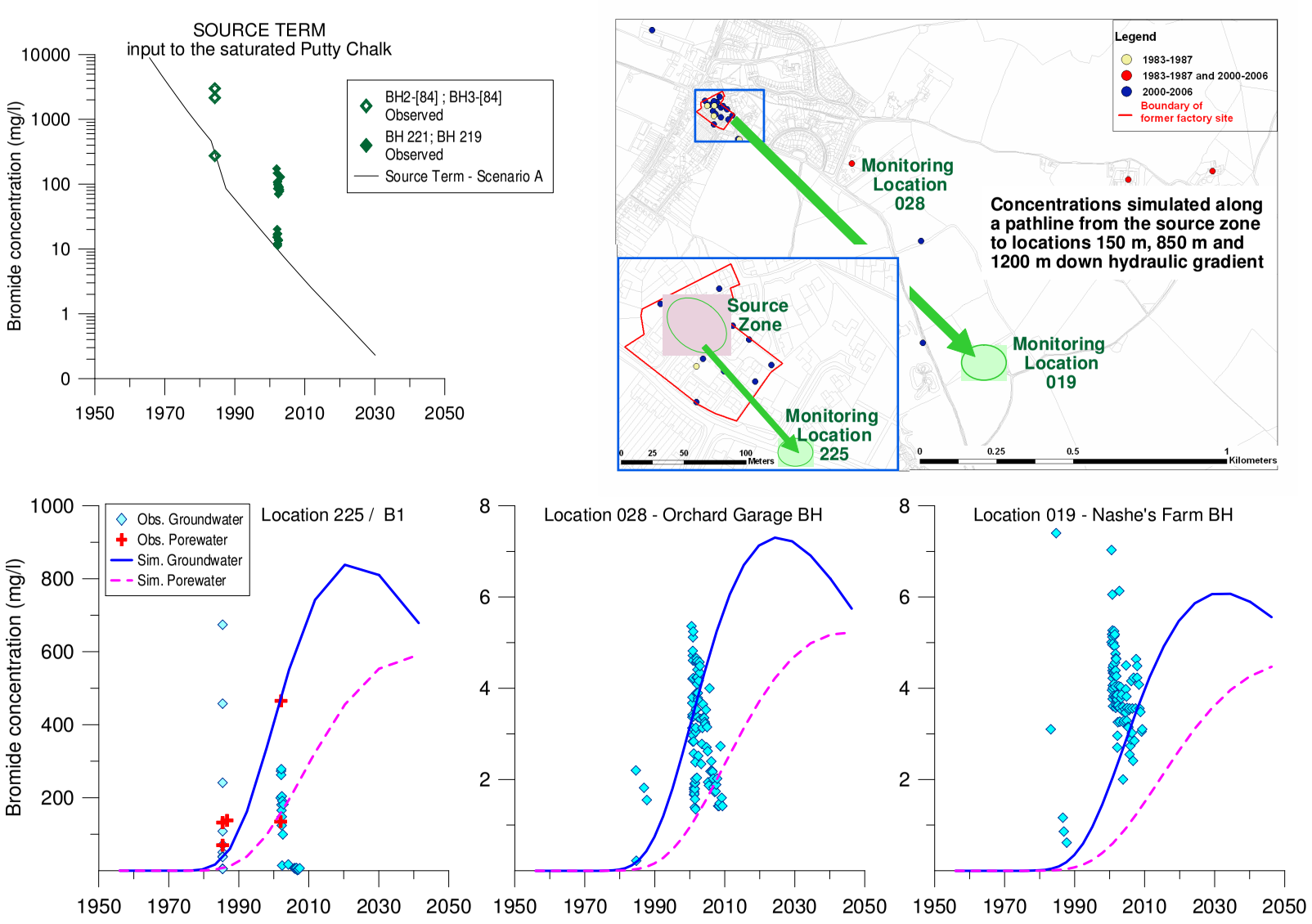

Figure 5.43: Comparison of simulated bromide concentrations for source history Scenario A and observed concentrations at three monitoring locations.

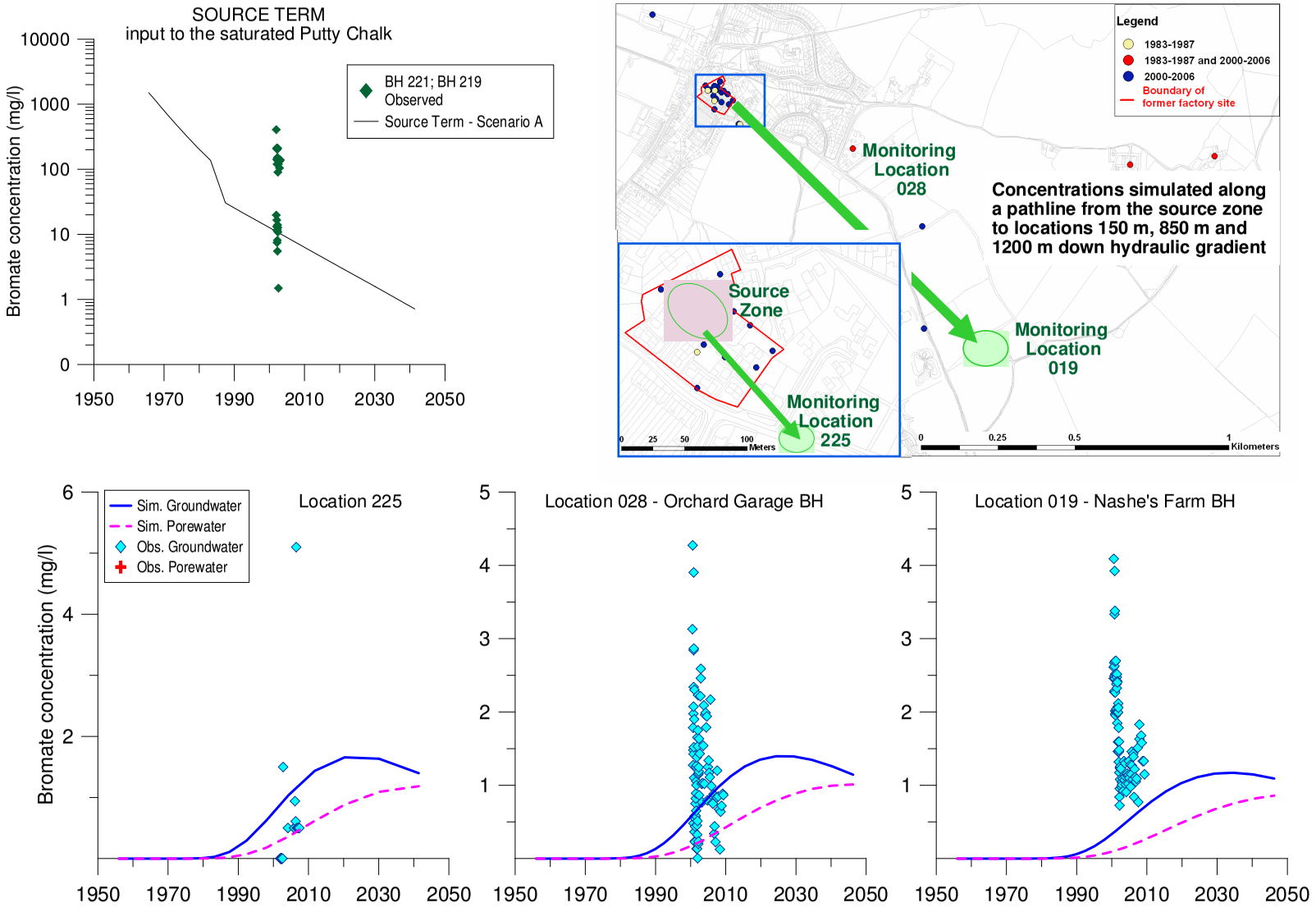

Figure 5.44: Comparison of simulated bromate concentrations for source history Scenario A and observed concentrations at three monitoring locations.

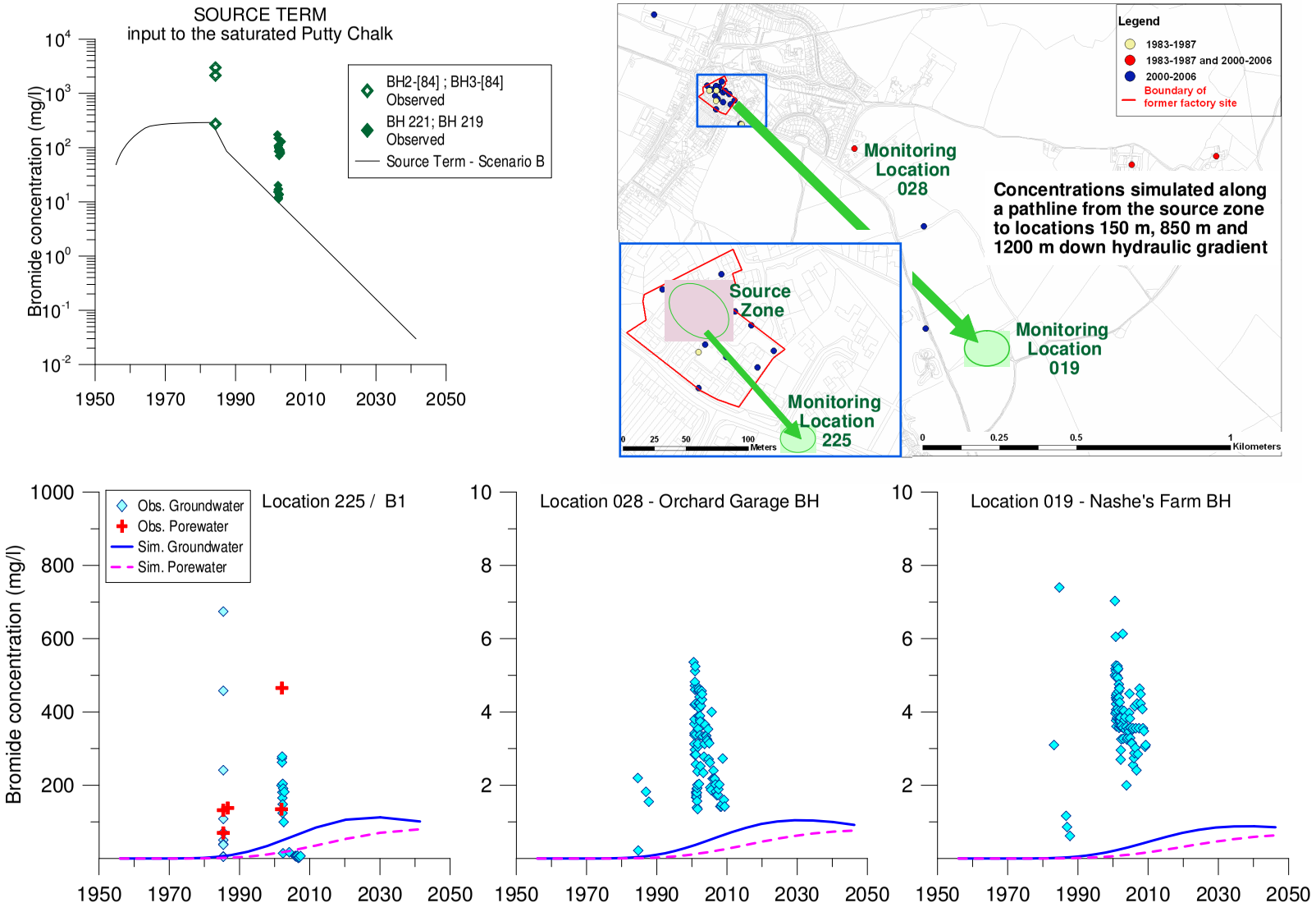

Figure 5.45: Comparison of simulated bromide concentrations for source history Scenario B and observed concentrations at three monitoring locations.

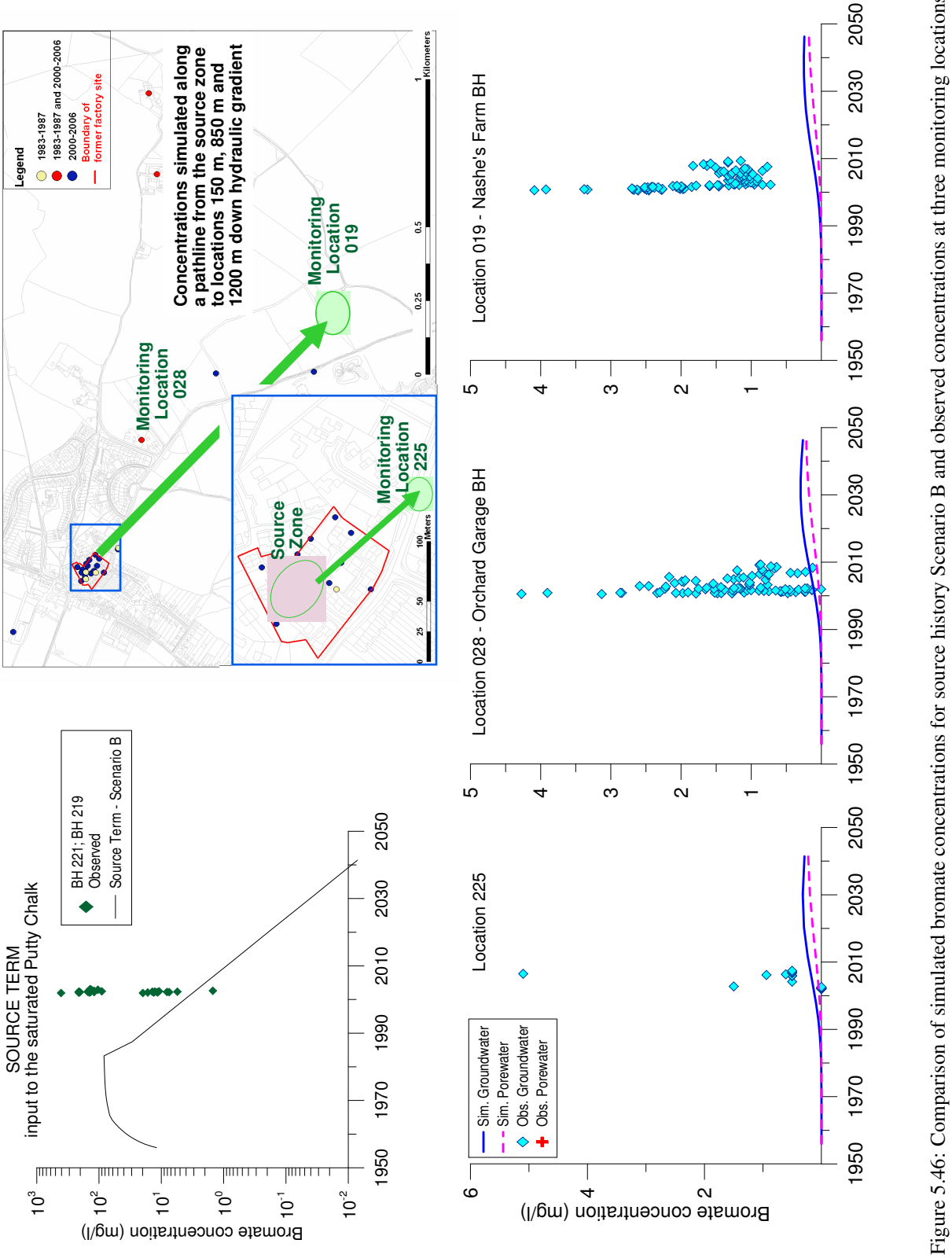

Figure 5.46: Comparison of simulated bromate concentrations for source history Scenario B and observed concentrations at three monitoring locations.

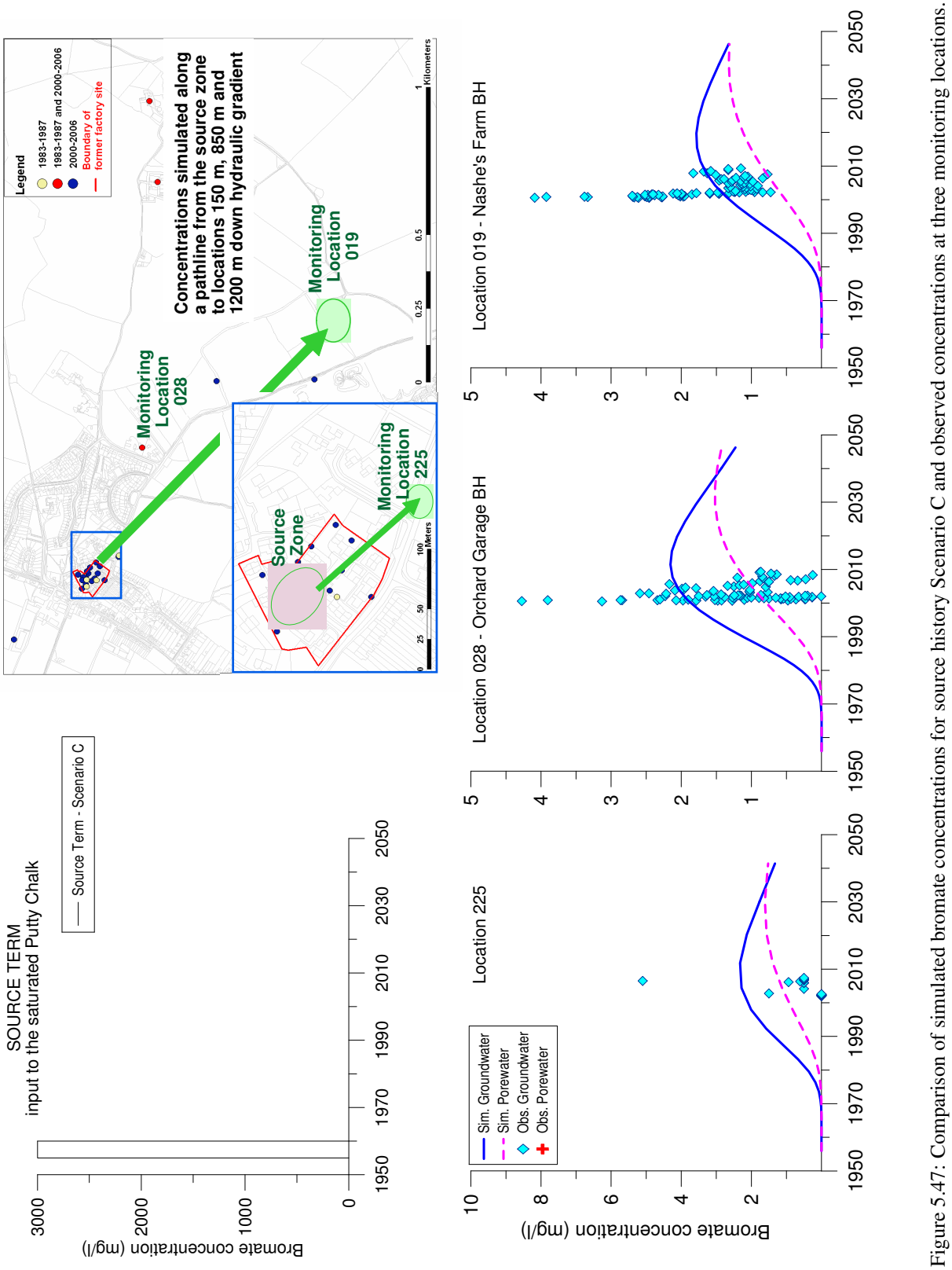

Figure 5.47: Comparison of simulated bromate concentrations for source history Scenario C and observed concentrations at three monitoring locations.

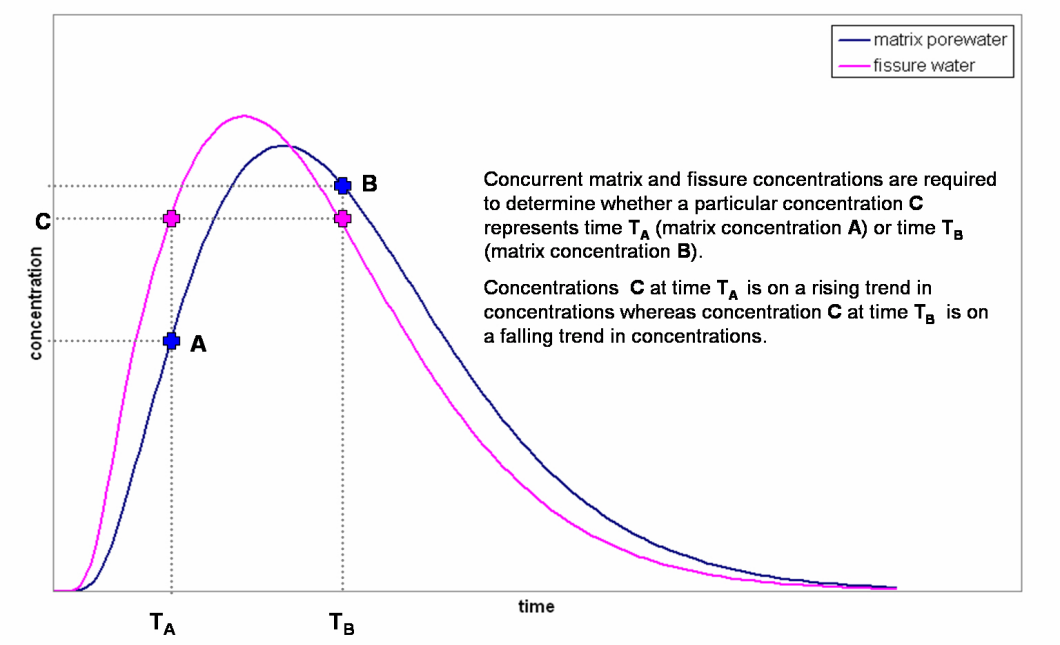

Figure 5.48: Concurrent matrix and fissure concentrations are required to determine at which point along the concentration-time graph a particular fissure concentration represents.

contaminant input to the saturated zone beneath the site is the leaching of bromide and bromate mass from the *un*saturated zone. The scenarios are constrained by estimates of the observed mass of bromide and bromate in 1985 and 2001. Scenario C ('direct release') assumes that bromate is released direct to the saturated zone, by-passing the unsaturated zone. Scenario C is constrained by the observed groundwater concentrations at the source site in 2001.

The one-dimensional double-porosity transport code, DP1-D, has been used to simulate concentrations in groundwater down-gradient of the source site. Simulated concentrations using the source term scenarios A and C show relatively good agreement with observed groundwater concentrations at locations 150 m, 500 m and 1000 m down-gradient of the source site. However, the relatively short period of time for which monitoring data are available, combined with the large seasonal variations in concentrations, means that the trends are difficult to discern, and robust conclusions cannot be made as to whether or not the simulations are representative of the observed data.

Chapter 6

Multiple Analytical Pathways Approach

6.1 Chapter Objectives

The objectives of this chapter are:

- To review the previous modelling approaches that have been implemented for bromate and/or bromide contamination in Hertfordshire;
- To develop an analytical network modelling approach to allow representation of Fickian double-porosity diffusion and to integrate karstic transport pathways within the network; and
- To use this model to provide predictions for the likely long-term evolution of bromate concentrations at key output locations.

6.2 Previous modelling approaches for Bromide and Bromate in the Chalk

6.2.1 Early model assessments

A series of modelling studies for the migration of inorganic *bromide* were undertaken in 1984 and 1985 prior to the redevelopment of the St Leonard's Court site (Chemfix, 1984, 1985b,d). The studies resulted in a significant underestimate of the extent of migration.

The modelling exercises were based on the two-dimensional advection-dispersion equation with point-source contamination estimated from limited field data. Two conditions were considered: firstly that the site was immediately redeveloped with predominantly impermeable hardcover and secondly that the site was left fallow and open to infiltration. The reports concluded that, if the site was immediately redeveloped with predominantly impermeable cover, the bromide plume of concentrations above 100 $\mu\mathrm{g\,l^{-1}}$ would be limited to a plume some 250 $\mathrm{m} \times 100\ \mathrm{m}$ in size in a direction 11 degrees south of east, and was unlikely to affect abstraction boreholes. If the site remained fallow, there was some risk of contamination of boreholes within the Sandridge area. The modelling was criticised by the Environment Agency (Thomas, 2000) for neglecting the influence of higher transmissivity along the dry valley in Sandridge, which would have indicated a more southerly flow direction, and for not considering the impacts of fissure flow within the Chalk. There were also some issues with the conceptualisation of the

source term which have been discussed in Section 5.9, and indicate that the mass input to the aquifer is likely to have been considerably underestimated by the Chemfix modelling.

6.2.2 Pollutant Linkage Assessment using CONSIM

Atkins (2002) used the **CONSIM** modelling package to demonstrate that the bromate concentrations measured in the unsaturated zone soils during the site investigation at the St Leonard's Court site were, through leaching, providing an on-going source of bromate pollution above the drinking water standards to the saturated Chalk aquifer beneath the site. Their conceptualisation of the source has been discussed in Chapter 5.

6.2.3 One-dimensional analytical model DP1D

Atkins (2004) used the **DP1-D** (Dual Porosity in 1-Dimension) code developed by John Barker (*e.g.* Barker (2005)) to simulate bromate concentrations along three flow lines:

- Orchard Garage (Location **028**) to Hatfield P.S. (Location **001**)
- Orchard Garage (Location **028**) to Essendon P.S. (Location **143**)
- Hatfield P.S. (Location **001**) to Hoddesdon P.S. (Location **300**)

The model parameters were derived from literature data, and site-specific data where available, and are reasonably consistent with the likely parameters for the Chalk aquifer in the region reviewed in Chapter 2. A constant source term was assumed from 1970 to 2000 of 1000 μg l^{-1} at Orchard Garage and 100 μg l^{-1} at Hatfield. Between 2000 and 2004, monitoring data at Orchard Garage and Hatfield respectively were used to represent the source terms. From 2004 into the future constant source terms of 1000 μg l^{-1} at Orchard Garage and 244 μg l^{-1} at Hatfield were assumed.

The simulated bromate concentrations at Hatfield P.S. and Essendon P.S. corresponded well to the 'average' observed bromate concentration trends. Simulated concentrations at Hoddesdon corresponded reasonably well to the 'average' observed bromate concentration trends. The simulations did not capture the seasonal variation evident in observed bromate concentrations due to the non-seasonality of the model, the relatively constant source-term, and the smoothing effect of the double-porosity diffusive exchange. All scenarios indicated increasing concentrations over time. This rising trend was interpreted by Atkins (2004) as suggesting that the 'plume' is not in steady state, *i.e.* fracture and matrix concentrations had not yet reached equilibrium at any of these locations.

6.2.4 Dispersion modelling

Since the **DP1-D** modelling does not account for mechanical dispersion, Atkins (2004) used a steady-state two-dimensional solution to the advection-dispersion equation derived by Bear (1972). A constant source injection was assumed. The dispersion modelling assumed a direct travel path from the north Hatfield area (*e.g.* Park Street, Location **265**) to the NNR source at Hoddesdon, and calculated concentrations at NNR locations which would be expected assuming dispersion from a the direct travel path. The calculated concentrations were compared to the observed concentrations at these locations. Atkins (2004) concluded that concentrations at Amwell Hill, Amwell Marsh, Broxbourne and Turnford were

significantly higher than would be expected purely from the effects of dispersion, with the results for Turnford and Amwell Hill in particular suggesting that a further mechanism of contaminant transport, such as separate direct flow pathways leading to these wells, was important.

6.2.5 Catchment-scale distributed flow modelling using MODFLOW and MT3D

A series of modelling studies have been undertaken using the **MODFLOW** suite of codes (MacDonald and Harbaugh, 1984; Harbaugh et al., 2000) coupled with the mass transport in three dimensions (**MT3D**) code (Zheng, 1990; Zheng and Wang, 1999). The first major modelling study was initiated as a joint project between the Environment Agency and Vivendi Water Partnership (now TVW). This single layer model model, known as the Bromate Groundwater Flow Model (BGFM), described in Buckle (2002, 2003), was developed as a subset of the Upper Lee and Mimram Model (ULMM) (Entec, 2002), a regional scale groundwater resource model for the Chiltern Hills. The BGFM was unable to reproduce observed groundwater flows within the Vale of St Albans immediately down-gradient of Sandridge, and this resulted in inadequate representation of the 'plume' geometry within the Vale of St Albans leading to modelled breakthrough of bromate at Roestock P.S. (where it is not currently observed) and a significant underestimate of concentrations at Essendon P.S. These deficiencies could not be improved by additional calibration and the use of the model was subsequently suspended pending a review of the conceptual understanding Buckle (2003).

The second major **MODFLOW/MT3D** catchment-scale flow and transport model, the Northern New River (NNR) model (Atkins, 2005), was developed by Atkins for Thames Water (TWUL) with the aim to model bromate transport to the Lee Valley. The NNR model was developed by extending the ULMM of Entec (2002) to the south and west to include the Lee Valley. Calibration of the flow model was improved relative to the BGFM and the relative spatial distributions of groundwater levels better reflected that of observed data, although a number of deficiencies remained. In particular, calibration of water levels close to source was poor, and as a result the simulated hydraulic gradient was steeper than observed. Also, water levels at North Mymms were simulated to be higher, and the mound to extend over a larger area, than observed. Bromate transport was modelled using **MT3D-MS** (Zheng, 1990; Zheng and Wang, 1999), a multiple species version of **MT3D** which is can be used to approximate double-porosity exchange though a first order exchange coefficient (but see the discussion of its deficiencies in Section 6.2.6). Using a constant source term of 5000 $\mu g\, l^{-1}$, the shape and magnitude of the apparent bromate 'plume' was well replicated by the model between Sandridge and Essendon P.S., but the model significantly underestimates the further migration of bromate to the NNR well field. Calibration attempts by varying the mass transfer coefficient, dispersivity and effective porosity and source concentrations were able to increase migration toward the NNR well field, however this was at the expense of either the model stability or of the modelled plume geometry resulting in a much wider plume than observed.

Therefore, the modelling exercises described above were not be able to duplicate the migration of bromate to the NNR wells via the Hertfordshire karst system. Cook (2010) notes that although the role of the karst in the transport of bromate was acknowledged in the conceptual understanding underpinning

the models (Buckle, 2002), the representation of the karst system within the model is limited, probably due to deficiencies in the conceptual model and inadequate data to properly parameterise the system at that time. Cook (2010) used his new conceptualisation of the Hertfordshire karst flow system, along with hydrodynamic parameters determined by catchment-scale tracer testing, and the single borehole dilution tests described in this thesis (Section 3.6.1), to develop a suite of new models incorporating representations of the karst flow system.

Initially, Cook (2010) developed a steady-state subset **MODFLOW** model of the NNR model to allow faster execution times, simpler initial calibration to long-term heads and flows and improved model stability. The 200 m by 200 m grid of the NNR model was retained. The model uses an EPM approach, and incorporates a karst zone along palaeogene boundary which is represented as a zone of high hydraulic conductivities, between one and a few cells wide. The karst zone also extends westwards into the Vale of St. Albans. The model was used to simulate flowlines (using **MODPATH**) for the 2008 bacteriophage tracer tests, and parameters calibrated to achieve good representation of all three tracer breakthroughs based on the advective transport routes indicated by **MODPATH** flowlines.

Cook (2010) then converted the calibrated steady-state flow and transport model to a transient flow and transport model. The transient flow model was found, for the majority of locations, to replicate the magnitude of head variation and also the seasonal behaviour and trends relatively well. The transport model (using MT3D-MS) was run for three source scenarios (see discussion of source terms in Section 6.2.5.1), as well as constant concentration source of 5000 $\mu\mathrm{g\ l^{-1}}$ for comparison with the NNR model of Atkins (2005). Cook (2010) found that the simulations showed closer agreement with travel time of the recharge pulse mass input and observed data at receptors if the westward extension of the karst EPM into the Vale of St Albans was removed. With karst in the Vale of St. Albans, weakly postulated on the basis of the tracer tests, the timing of simulated peak concentrations precedes that of all observations. However, with the karst zone removed, simulated concentrations are lower, and travel times slower, due to additional dispersion and double-porosity attenuation.

Simulations using the constant concentration source of 5000 $\mu\mathrm{g\ l^{-1}}$ were able to closely replicate observed bromate concentrations to Hatfield in magnitude and spatial distribution. Simulations using the previous estimates (now superseded) of the three source term scenarios (Section 6.2.5.1) resulted in concentrations that were universally lower than observed. Cook (2010) concluded that these source terms were too low and increased them by a factor of three. The revised source term Scenario B was found to result in relatively good spatial and temporal representation of bromate concentrations compared to observed data. The situation as modelled by the revised source term of Cook (2010) suggests that current levels of bromate in the aquifer are the result of the passage of the 1983-1987 high concentration recharge pulse from the source zone.

The model produces a relatively stable 'plume' in the Vale of St Albans area after approximately 10 years of bromate input. Breakthrough to the Lee Valley occurs shortly afterwards due to the rapid transport within the karst system, and is strongly seasonal. The model predicts that bromate concentrations in excess of the drinking water standards persist within the Vale of St Albans for the modelling period

(*i.e.* at least up until 2050). For locations in the Lea Valley, dilution in the karst system acts to reduce concentrations significantly to less than drinking water standards once the high mass flux associated with the 1983-1987 recharge pulse has declined. However periodic seasonal pulses of a around 1 $\mu g\, l^{-1}$ occur at locations in the Lee Valley for the remainder of the modelling period. These pulses are strongly influenced by karstic seasonal dilution.

Cook (2010) lists the main areas of uncertainty that limit the effectiveness and confidence in the **MODFLOW/MT3DMS** predictive modelling using the currently available data:

- The description of the source term and its implementation in the model;
- A limited period of observation data in relation to the likely duration of the bromate contamination and with respect to the timing of the breakthroughs;
- Uncertainty with respect to the extent to which the chalk matrix has become contaminated and detailed parameterisation of that process;
- Deficiencies in the model representation of both dual porosity and karstic transport and the transfers between them.

6.2.5.1 Source Term comparison

The source terms used by Cook (2010) are superseded versions of the source terms developed in Chapter 5. Figure 6.1 illustrates how these superseded source terms relate to the current versions in this thesis. Between 1955 and 2008 superseded Scenario A represents a cumulative mass input to the saturated zone beneath the source site of 22900 kg of bromate and superseded Scenario B a cumulative mass input of 21000 kg of bromate compared to cumulative mass inputs of 138000 kg and 43900 kg for the current Scenario A and Scenario B respectively. For comparison, a constant concentration source term of 5000 $\mu g\, l^{-1}$ between 1970 and 2008 represents a cumulative mass input to the saturated zone beneath the source site of approximately 139000 kg of bromate.

6.2.6 Weaknesses of MODFLOW and MT3D

The **MODFLOW** suite of codes (Harbaugh et al., 2000) were originally developed to model Darcian flows in porous granular aquifers such as the extensive glacial sand and gravel aquifers of the United States. In order to model fractures or karstified rocks, an EPM approach must be adopted.

The solute transport code **MT3D-MS** (Mass Transport in 3-Dimensions Multi-Species) (Zheng and Wang, 1999) uses the groundwater flow files from **MODFLOW** as the basis for solute transport calculations. The multi-species version of **MT3D** has capability for dual-domain mass transfer to represent double-porosity diffusive exchange. The code allows solute transfer between mobile and immobile domains controlled by a first order mass transfer coefficient. The governing equations (without explicit consideration of sorption) can be expressed as a statement of mass conservation for the mobile domain

$$\theta_m \frac{\partial C_m}{\partial t} = -q\frac{\partial C_m}{\partial x} + \theta_m D_{im}\frac{\partial^2 C_m}{\partial x^2} - \zeta\left(C_m - C_{im}\right) \tag{6.1}$$

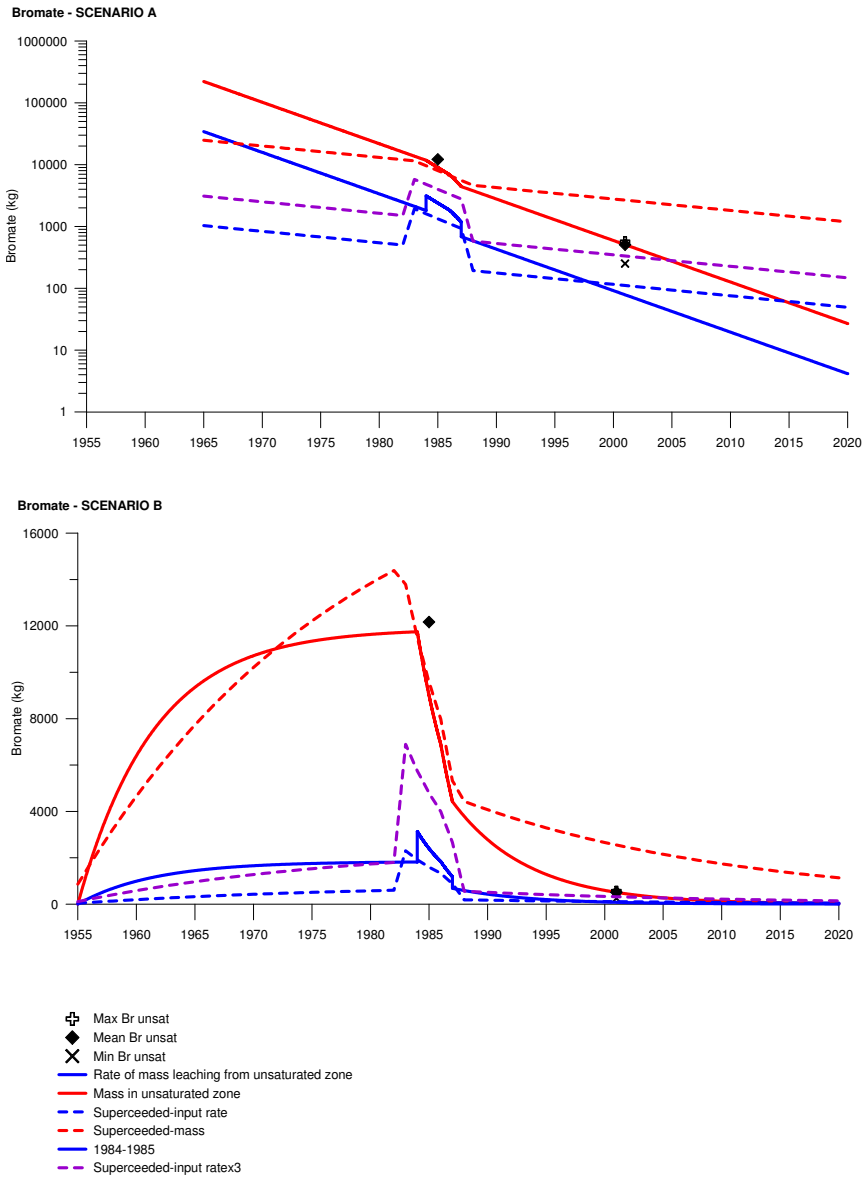

Figure 6.1: Comparison of the superseded versions of the the source terms used by Cook (2010) to the current versions in this thesis.

and as a statement mass conservation for the immobile domain

$$\theta_{im} \frac{\partial C_{im}}{\partial t} = \zeta \left(C_m - C_{im} \right) \tag{6.2}$$

Where C_m and C_{im} are the concentrations in the mobile and immobile domains respectively, θ_m and θ_{im} are the porosity of the mobile and immobile domain respectively, q is the darcy flux, and ζ is the first-order mass transfer coefficient.

The first order mass transfer coefficient approach is only an approximation to the diffusion process, which is more accurately represented by a Fickian approach (as used in **DP1D** and **MAP** codes). The predictions made by the mass transfer approach and Fickian diffusion converge as a steady-state condition between fracture and matrix porewater solute concentration is attained (Barker, 1985b). At early times the **MT3D-MS** approach will over-estimate solute concentration in fracture water by underestimating the diffusive flux into the immobile matrix porewater domain. The rate of transfer from the mobile to immobile domain is too slow as it does not account for the infinitely steep concentration gradient that initially exists at the mobile/immobile interface. The mass transfer approach will therefore predict a solute 'plume' to have moved further than that modelled using the Fickian exchange approach.

When the concentration gradient is reversed and the the movement of solute is from the immobile to the mobile domain, the reverse will be the case such that the rate of transfer of solute back into the mobile groundwater in the fracture system predicted by a first order mass transfer coefficient will be slower than predicted by a Fickian approach. Consequently the mass transfer approach will underestimate the fracture water solute concentrations.

Compounding this deficiency of a mass transfer approach, the **MT3D-MS** code of Zheng and Wang (1999) does not allow back-diffusion from the immobile matrix domain to the mobile fissure water domain. Therefore the persistence of contamination will be considerably underestimated as the secondary source of contaminant is effectively 'lost' into a matrix sink.

An indication of whether the system is likely to approach a steady-state within the time frame of interest can be given by calculating the time for diffusion across a matrix block (Barker, 1993). If the system is likely to achieve a steady state within the time frame for which predictions are required then it is reasonable to model it using a mass transfer coefficient approach. However, if accurate predictions are required for early or late times, a Fickian approach is recommended. Based on typical parameters for the chalk west in the Vale of St Albans, $t_{cb} = 2.89 \times 10^4$ days ≈ 79 years (Appendix F). For the karst system east of Hatfield, t_{cb} ranges from 9×10^4 to 4×10^5 days, or approximately 250 to 1100 years (Appendix F). Therefore, the mass transfer approach is not likely to be valid for bromate in Hertfordshire.

Furthermore, as noted by Cook (2010), an equivalent porous media model cannot represent simultaneously the conduit and fracture systems: model cells must either be an EPM of the karst conduits or an EPM of the non-karstic fissured aquifer system. The best replication of Vale of St Albans transport in MODFLOW and MT3D-MS is achieved using a non-karst double-porosity approximation. Conversely, the majority of transport east of Hatfield is represented by an EPM representing karst transport. The role of double-porosity diffusive exchange within the fracture system east of Hatfield is not simulated.

6.3 Development of a Multiple Analytical Pathways Approach

6.3.1 DP1-D

The **DP1-D** solute transport code has been introduced in Section 5.12. The DP1D model has been used by Watson (2004) to model chloride contamination in the Chalk of the Tilmanstone Valley in Kent. The simulations successfully reproduced the observed porewater and fracture water profiles at two times, separated by 25 years. Forward modelling indicated that the double porosity diffusion extends the duration of contamination in the catchment by several decades. The concentrations in the mobile zone simulated by the **DP1-D** model were compared to concentrations modelled by a three-dimensional numerical model using **MODFLOW** and **MT3DMS** and compared well, except for early and late times in the contamination evolution. Karst conduit flow was not however considered to be a significant feature at Tilmanstone.

6.3.2 Multiple Analytical Pathways (MAP) model

Barker (2001) developed the 'Multiple Analytical Pathways' (**MAP**) model to simulate long-term nitrate concentrations in the saturated zone where the effects of double-porosity diffusion were important. The model was used by Williams et al. (2003) to evaluate the effects of changes in soil water concentration associated with changes in land use as a result of the Nitrate Sensitive Area Scheme on groundwater nitrate concentrations at Public Water Supply boreholes and spring sources in the Oolitic Limestone of Oxfordshire and the Sherwood Sandstone of North Yorkshire. Model output was compared with observed concentrations, and the parameters (travel times in the unsaturated zone, aquifer kinematic porosity and aquifer type) adjusted to give a calibrated model which was then used to predict future concentrations over long time periods.

The MAP approach models flow and transport along a series of 'streamtubes' which represent flow lines from recharge areas at the ground surface through to output features, such as wells, where the concentration predictions are required. The flow system must be steady-state, and is modelled separately from the transport problem to determine the flow lines. Williams et al. (2003) developed a steady-state **MODFLOW** (Harbaugh et al., 2000) groundwater flow model and used the **MODPATH** (Pollock, 1989) particle tracking program to determine the 'streamtubes', *i.e.* the travel distances and travel times from the water table to various abstraction locations.

Contaminant transport along streamtubes is modelled analytically to provide solutions to a wide range of transport processes, including Fickian double-porosity diffusive exchange. The form of the analytical solutions that have been adopted is that of Laplace transforms (Barker, 1982), and implementation of the method is based on numerical inversion of the Laplace transform solutions. Figure 6.2 illustrates the approach, and Figure 6.3, the mathematical basis.

One advantage of this methodology is that the number of parameters which are varied during the calibration process is small. This means that predictions of future concentrations are likely to be well constrained (Barker, 2001). Another advantage is that only concentrations at the times and points of interest need be computed, so that times can be increased on a logarithmic scale to permit accurate prediction over very long time-scales typical of double-porosity systems, whilst keeping the method

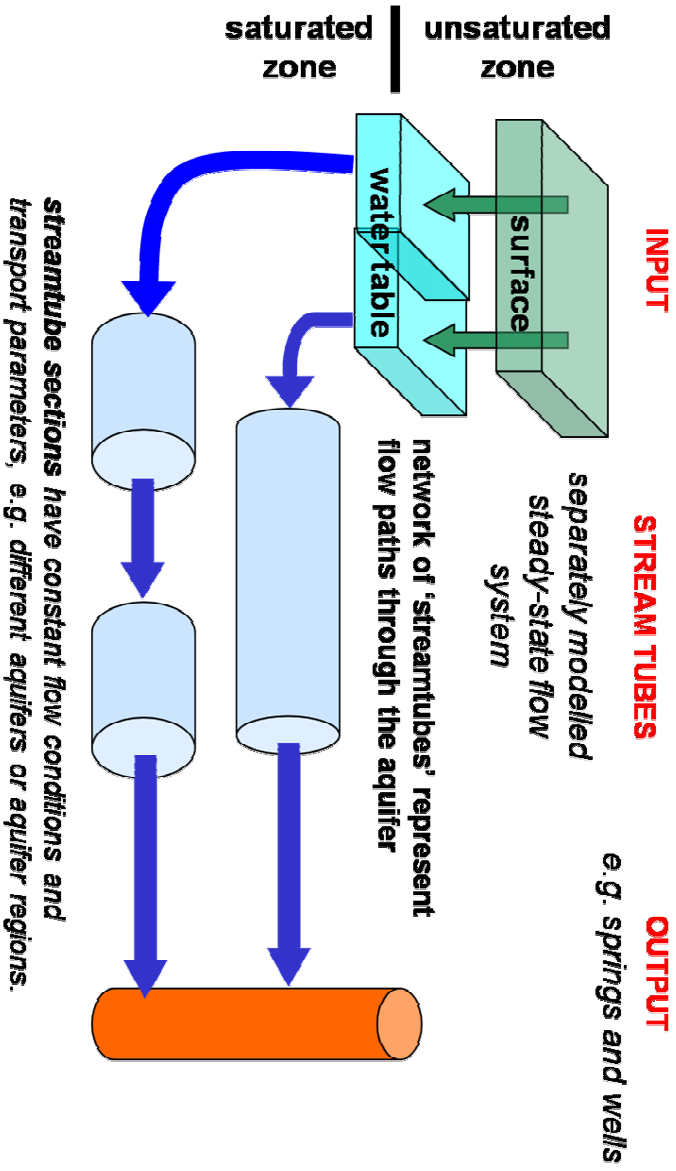

Figure 6.2: Conceptual and mathematical basis for the Multiple Analytical Pathways of Barker (2001).

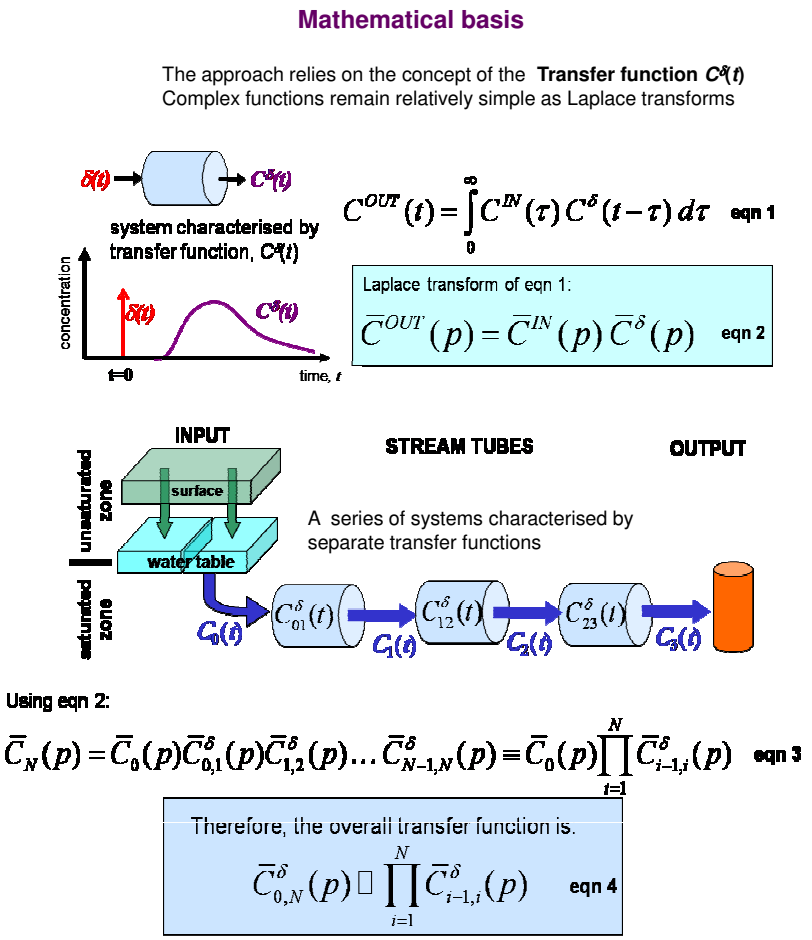

The concentration at a point of interest is evaluated by numerical inversion of the Laplace transform of the product of the cumulative transfer function and the input function.

A clear advantage is that only concentrations at points and times of interest need be computed. E.g. times can be increased on a logarithmic scale when studying long-term behaviour of dual-porosity systems.

Figure 6.3: Conceptual and mathematical basis for the Multiple Analytical Pathways of Barker (2001).

computationally fast. A disadvantage of the methodology is than no account can be made of variations in abstraction volumes, because this is a steady-state model that specifies equilibrium flow pathways from the water table to the abstractions. The necessary assumption that the transport equations are linear restrict the type of systems that can be modelled. For example, when sorption is important, only the linear isotherm is amenable to simulation with **MAP**.

The **MAP** model used by Williams et al. (2003) did not permit branching or joining streamtubes (although in principle, branching or joining networks of streamtubes are possible provided each junction is characterised by a simple additive relation between the streamtube concentrations and fluxes). In addition, the model was not coded to give matrix concentrations as an output.

6.3.3 GoldSim Contaminant Transport Model

The simulation model **GoldSim** (developed by GoldSim Technology Group) uses an approach akin to the MAP approach to simulate flow and transport along 'pipe pathways'. **GoldSim** is a highly graphical, object orientated computer program for carrying out dynamic, probabilistic simulations. The Contaminant Transport Module is an extension which allows simulation of the release, transport and fate of mass within environmental systems (GoldsimTechnologyGroup, 2007). A contaminant transport model is constructed by defining multiple transport pathways and linking them together into an interconnected network. Transport pathways can be used to simulate horizontal transport in aquifers, and specifically 'pipe pathways' can be used to simulate a broad range of advectively-dominated transport processes involving one-dimensional advection, longitudinal dispersion, retardation, decay and ingrowth, and exchanges with immobile storage zones (*e.g.* matrix diffusion). The transport equations are solved analytically using a Laplace transform approach based on Barten (1996) and Barker (1985a). Double-porosity diffusion can be represented by *matrix diffusion zones*. Solutes diffuse from the mobile zone into a surrounding porous immobile zone. The diffusive process is one-dimensional and orthogonal to the flow direction, and according to Fick's laws. Matrix diffusion zones can have one of three possible geometries: slab, sphere or slot.

The **GoldSim** model provides simulation output as a time series of concentration or mass flux leaving the pipe pathway within the mobile zone. The model is not currently coded to provide output for concentration or mass within the immobile zone. However, a crude approximation can be made by using a series of linked 'cells' (see explanation in Appendix E).

6.3.4 Comparison of DP1D, MAP and GoldSim

In order to explore the functionality of **GoldSim** and validate its predictions against the **MAP** model and the **DP1D** model, the input and output files from one of the Nitrate Sensitive Areas (NSA) case studies described in Williams et al. (2003) and Silgram et al. (2005) were obtained and the streamtubes from the **MAP** model were reproduced in **GoldSim**. The case study was the Old Chalford NSA: a small (81 km^2) catchment with a series of spring sources in the Oolitic Limestone in Oxfordshire.

The validation (Appendix E) indicated that mobile (fissure) concentrations simulated by the **MAP** model and **GoldSim CT** model were almost identical both with and without simulation of double-porosity diffusion, the apparent differences being a result of the mandatory 10 % minumum dispersion

in **GoldSim**. However, the immobile (matrix) concentrations simulated by the 'diffusion cells' approximation in **GoldSim** did not compare well to the average immobile (matrix) concentrations simulated for a similar scenario in **DP1D**.

The conclusion from this exercise was that neither **MAP** or **GoldSim** were currently appropriate for the aims of the modelling for Hertfordshire bromate contamination as they are unable to provide predictions for matrix porewater concentrations, which could be used in the future to validate the model predictions for long-term fissure water concentrations.

6.4 Analytical Network Model

To allow the branching and joining necessary to represent the Hertfordshire karst system, and the double-porosity diffusive exchange to be simulated as both mobile (fissure) concentrations and immobile (matrix porewater) concentrations, Prof. John Barker developed a network model (J. A. Barker, *pers. comm.*).

The network is defined by 'branches' connecting up-stream and down-stream 'nodes'. Branches represent flow lines through the saturated zone. A number of branches may enter and/or leave each node, allowing branching and joining to be represented. Flow and transport is simulated along the network.

The model is run in Microsoft Excel, with the code written in Visual Basic.

6.4.1 Mathematical Basis

As with the MAP model, the transport equations are modelled analytically using Laplace transforms, and the solution implemented via numerical inversion of the Laplace transform solutions.

6.4.2 Node Input - the Source Function

The model allows considerable flexibility with the 'source function', *i.e.* the concentration input at a node. The source function is specified by sets of:

- the node number;
- any two times;
- the concentrations at those times; and
- the type of behaviour (constant, linear or exponential) between those times.

6.4.3 Node and Branch description

Branches are defined between an up-stream node and down-stream node. The transport processes represented are double-porosity diffusive exchange between immobile matrix water and mobile fracture water, and dispersion in the fracture network.

Branches are characterised by the following parameters:

- the volumetric groundwater flux along the branch, Q;
- the groundwater travel time along the branch, t_a;
- the characteristic time for diffusion across a matrix block, t_{cb};

- the porosity ratio, σ;
- the geometry of the matrix blocks (currently only a slab geometry is modelled by the code);
- the dispersivity to path length ratio, $\alpha \div x$.

6.4.4 Node and Branch Output

The following solute concentrations are output at specified times:

- c_n - the solute concentration in the fractures at the node;
- c_f - the solute concentration in the fractures at the downstream end of a branch;
- c_m - the average solute concentration in the matrix at the downstream end of a branch;
- c_{fav} - the average concentration in the fractures over whole branch;
- c_{mav} - the average concentration in the matrix over whole branch;
- c_{tav} - the porosity weighted average concentration for fractures and matrix.

Where branches converge at a node, the resulting solute concentration, c_n, is given by the sum of the concentrations, c_f, at the end of each of these branches weighted according to the volumetric groundwater fluxes through each.

6.5 A Network Model for Hertfordshire

6.5.1 Selection of Nodes and Branches

The network is chosen to connect key output locations within the study area that have been interpreted to be connected by flowlines. The nodes and branches forming the network are illustrated in Figure 6.4. Only the karstic connections that were indicated by the tracer tests are included as branches to Arkley Hole Spring and Lynchmill Spring, although in reality there are likely to be additional pathways to these output springs. The MODPATH flowlines from the model by Cook (2010) were used as an indication of the existence of flowlines between the source site in Sandridge and locations down-hydraulic-gradient. However, the travel times and fluxes indicated by the flow lines were not explicitly used because the distributed model averages parameters over large grid squares, and as such it was considered that the parameters were not representative of the travel times along the branches, especially along karstic branches.

6.5.2 Parameters for 'double-porosity' branches

The parameter ranges for each branch are indicated in Appendix F.

6.5.2.1 Diffusion Coefficient, D_{im}

The effective diffusion coefficient for bromide and bromate is taken as $8.64 \times 10^{-6}\ \mathrm{m^2\ day^{-1}}$ which is equivalent to $1.00 \times 10^{-10}\ \mathrm{m^2\ s^{-1}}$ (Section 2.9.4.1).

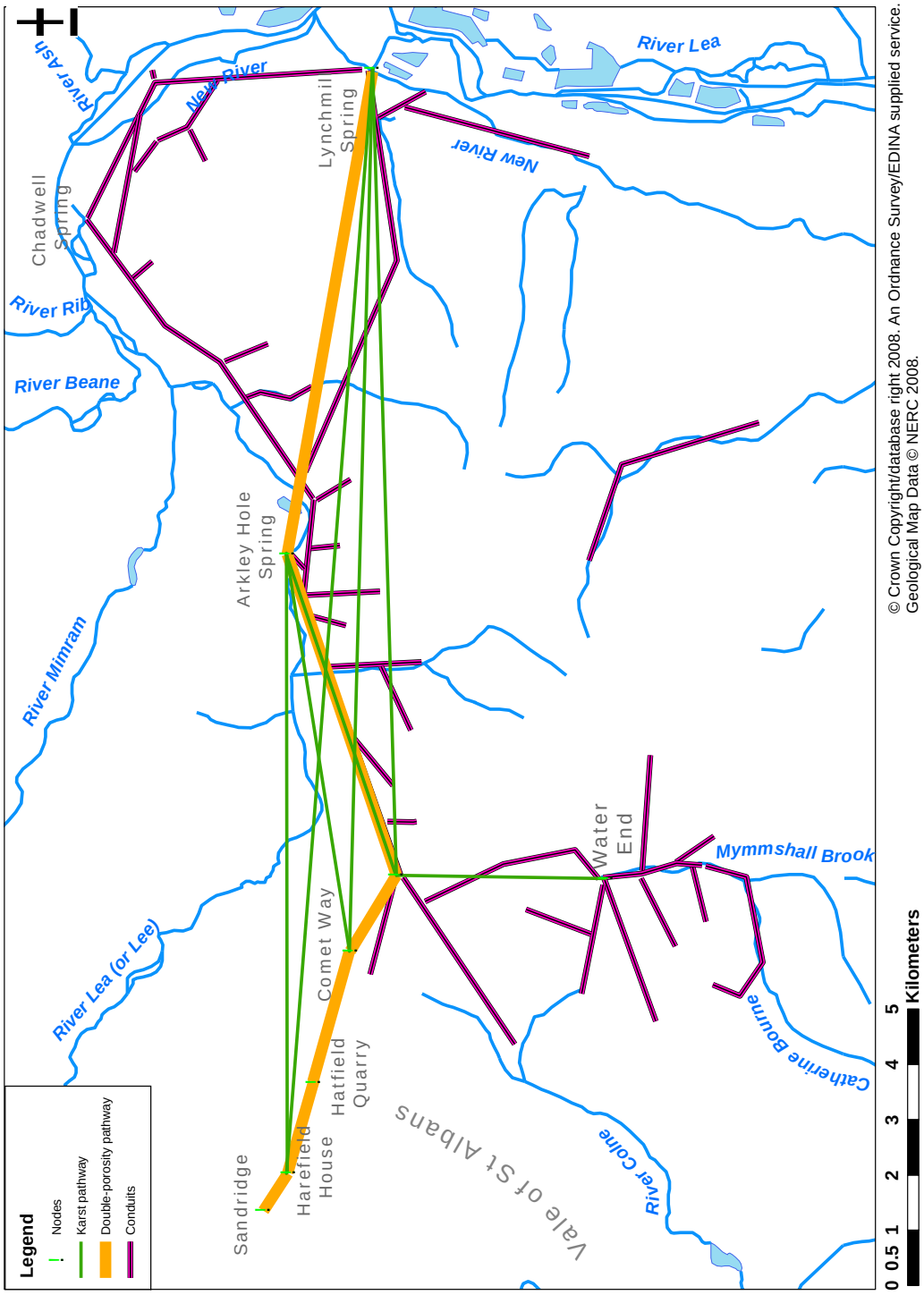

Figure 6.4: Nodes and branches represented in the Network Model for Hertfordshire. Note that branches are shown schematically as straight-line connectors and are not intended to indicate the precise geographical route.

6.5.2.2 Matrix Porosity Φ

For the blocky chalk, a representative value for the Chalk in the area is 0.388 (Section 2.6), with a standard deviation of 0.058. Therefore, the range of values is taken to be 0.27 to 0.50, with a mean of 0.39.

6.5.2.3 Sandridge to Comet Way, via Harefield House and Hatfield Quarry

For Sandridge to Hatfield, the parameters were estimated from a combination of typical values from the literature and values obtained from fieldwork in the area.

The parameters a (fracture aperture) and b (half block thickness) determine the value of σ, and along with D_{im}, the value of t_{cb} (sections 5.12.1 to 5.12.3). Based on the review of data from the literature (Section 2.7.3.3), a representative fracture aperture a of 10^{-3} m is used for the Chalk between Sandridge and the Hatfield area. It is considered that there is a large uncertainty associated with this parameter, and therefore, for the purposes of uncertainty estimation, the range is taken to be from an order of magnitude lower to an order of magnitude higher.

There is little available local information for fracture spacing in the region of the source site and 1 km down-gradient. However, geophysical logging undertaken by TVW in the Hatfield area indicates flowing fracture separations of approximately 1.00 m to 1.40 m. This is comparable to the flowing fracture spacing observed from the single borehole dilution testing (Appendix D). These values fall at the upper end of the range of the literature values for unweathered Chalk reviewed in Section 2.7.3.3. Although, as noted in the review, these values relate to observed discontinuities, and may not relate to the presence of hydraulically significant (flowing) *fissures*. The values relating to the spacing of flowing horizons tend to have larger spacings. Therefore, for the purposes of uncertainty analysis, the range of block sizes ($2b$) is taken to be from 0.50 to 1.50 m, with a mean of 1.00 m.

The darcy flux, q, was taken from the results of the borehole dilution testing at Nashe's Farm, Harefield House, and Comet Way (Section 3.6.1). This was converted to a velocity, v, using the mobile porosity determined from a and b. This was then converted to a travel time t_a for the path length. The darcy fluxes ranged from 0.5 to 3.0 m day^{-1}, with average of 1.0 m day^{-1} (Nashe's Farm), and 0.3 to 1.3 m day^{-1}, with average of 0.8 m day^{-1} (Harefield House). At Comet Way, darcy flux was almost an order of magnitude higher: ranging from 4.5 to 14.5 m day^{-1}, with average of 8.0 m day^{-1}. Therefore, for the branch Sandridge to Harefield House, and from Harefield House to Hatfield Quarry, q was taken to be 0.3 m day^{-1} to 3.0 m day^{-1}, with an average of 1.0 m day^{-1}. For the branch Hatfield Quarry to Comet Way q was taken to be 4.5 m day^{-1} to 14.5 m day^{-1}, with an average of 8.0 m day^{-1}.

The volumetric groundwater flux, Q, was determined from the recharge model used for the MODFLOW modelling by Atkins (2004) and Cook (2010), as indicated by the MODPATH flowline. For Sandridge to Hatfield, the recharge flux was 0.008 m day^{-1}, which over the site area of 7600 m^2 at SLC, results in a volumetric flux of 6.08 m^3 day^{-1}. The volumetric flux was assumed to remain constant along the flowline.

The value for dispersivity α was taken as 10 % of the path length, x.

6.5.2.4 Comet Way to 'conduit junction'

This branch was taken as a 1.59 km branch linking Comet Way BH to the main conduit network. The parameters used were the same as for the branch linking Hatfield Quarry and Comet Way.

6.5.2.5 'Conduit junction' to Arkley Hole Spring and Lynchmill Spring

It is postulated that flowlines characterised by double-porosity bromate transport continue from Comet Way (via the 'conduit junction') to Arkley Hole Spring and Lynchmill Spring. There is very little information to parameterise these pathways. Therefore, the parameters used between Hatfield Quarry to Comet Way and to the 'conduit junction' are used. These branches were taken as 5.71 km and 15.71 km respectively.

6.5.2.6 Worst case and best case scenarios

The range of parameters outlined in the sections above, are used to define a 'typical case', 'worst case' (highest peak bromate concentrations) and 'best case' (lowest peak bromate concentrations) by the combinations indicated in Table 6.1.

Table 6.1: Parameter combinations for 'best-case' (lowest peak bromate concentrations) and 'worst-case' (highest peak bromate concentrations) scenarios.

parameter	'worst case'	'best case'
a	min	max
b	max	min
θ_m	min	max
Φ	min	max
θ_{im}	min	max
σ	min	max
q	max	min
v	max	min

6.5.3 Parameters for karst branches

The parameters for each branch are given in Appendix F.

The parameters t_{cb}, σ, t_a, and $alpha \div x$ were obtained from Cook (2010), who fitted results from the tracer test breakthroughs from Water End to Arkley Hole Spring, Lynchmill Spring, and Turnford PS to the **DP-1D** model of Barker (2005). The DP-1D curves were fit to the observed data by adjusting two parameters: the volume to area ratio, b, and the ratio of the inner and outer radius of a concentric cylinder, ρ, using a least squares method. It should be noted that a number of combinations of b and ρ produce comparable fits and thus the solutions are non-unique. However, Cook (2010) found that all follow the same general form to give $t_a < t_{cf} \ll t_{cb}$.

The relative magnitudes of the characteristic times indicates that matrix diffusion is relatively insignificant in terms of the conduit transport although it does play some role in extending the tracer tail at

low concentrations.

Characteristic times are given in Table 6.2. The data for the breakthroughs from Harfield House and Comet Way boreholes were not considered robust enough to be fit to the **DP-1D** model. Therefore, the parameters t_{cb} and σ for the branches from Harefield House and Comet Way to Arkley Hole and Lynchmill spring were taken to be the same as those from Water End to Arkley Hole and Lynchmill springs. The values for t_a were taken from the travel times determined by Cook (2010) for these connections.

Table 6.2: Parameters derived from fitting the DP-1D model (Barker, 2005) to tracer breakthrough curves from Water End injection (Cook, 2010). Characteristic times are in hours.

Pathway	t_a	t_{cf}	t_{cb}
Essendon PS	6.21×10^1	2.26×10^5	8.43×10^6
Arkley Hole Spring	6.75×10^1	2.90×10^4	1.05×10^7
Lynchmill Spring	1.05×10^2	6.00×10^3	2.17×10^6
Turnford PS	1.46×10^2	2.08×10^3	7.49×10^5

Groundwater fluxes along the pathways were estimated from the tracer mass recovery data from the tracer tests. Cook (2010) estimated the *pro rata* flow rate to each location based on the average gauged flow to Water End swallow holes of 10756.8 $\mathrm{m}^3\ \mathrm{day}^{-1}$. The recovery percentage compared the recovered mass to the amount available to recover at that time assuming literature derived values for phage inactivation. The groundwater fluxes for the branches from Comet Way and Harefield House were estimated by multiplying the recovery percentage for these connections by the groundwater flux from the boreholes as estimated by the results from the single borehole dilution testing (Section 3.6.1.

For the branch Water End to Arkley Hole and Water End to Lynchmill Spring, the relative flux was estimated by reference to the water balance by Cook (2010). Allogenic recharge accounted for 23.7 % of flow and groundwater inflow for 14.4 %. Therefore, the flux in the karst system coming from Water End was taken to be 165 % (23.7 % ÷ 14.4 %) of the flux along the flow line from SLC (*i.e.* 9.8 $\mathrm{m}^3\ \mathrm{day}^{-1}$) and based on the tracer recovery data, this is apportioned as 7.2 $\mathrm{m}^3\ \mathrm{day}^{-1}$ and 2.6 $\mathrm{m}^3\ \mathrm{day}^{-1}$ to Arkley Hole and Lynchmill respectively.

The value for $\alpha \div x$ was taken as 0.1 % for the branches from Water End, and 1.0 % for the branches to the west of the main conduit network based from Harefield House and Comet Way.

6.6 Network Model for Hertfordshire - Results of initial simulations

Simulated bromate (Figure 6.5 to Figure 6.9) and bromide (Figures 6.10 to 6.12) concentrations using the network model described above, with the source term scenarios defined in Section 5.11, show reasonable agreement with observed concentrations. A constant concentration source term of 5000 $\mu\mathrm{g}\ \mathrm{l}^{-1}$ bromate between 1970 and 2050 was also simulated for comparison with Cook (2010) and

In general, Scenario B results in simulated bromate and bromide concentrations well below ob-

served concentrations between 2000 and 2008. For Harefield House, the observed bromate concentrations span the simulated bromate concentrations for Scenario A and Scenario C. For Hatfield Quarry and Comet Way, Scenario C passes through the cluster of observed bromate concentrations, and simulated concentrations for Scenario A are at the lower limits of observed bromate concentrations. For bromide, the simulated concentrations for Scenario A pass through the cluster of observations at Harefield House, Hatfield Quarry and Comet Way (although the simulated concentration 'front' appears to occur 5-10 years late at Hatfield Quarry), and simulated concentrations for Scenario B are well below observed concentrations at all locations.

The 5000 μg l^{-1} constant concentration source term takes longer to reach peak concentrations, which are also higher than for the other three source scenarios. The constant concentration source term predicts bromate concentrations lower than observed between 2000 and 2008. This is in contrast to Atkins (2005) and Cook (2010) who found that the same constant concentration source term gave good agreement with the observed concentrations between 2000 and 2008, and is probably due to the increased travel time from the source site to the monitoring locations introduced by the representation of vertical migration through a low permeability 'putty chalk' layer at the source site in the modelling in this thesis.

The general form of the predictions is a bell-shaped curve, with an extended 'tail' at later times as a result of the diffusion from matrix water back into the mobile water. The predicted peak bromate concentrations occur first for Scenario C, then for Scenario A, and last for Scenario B which shows a much lower and broader peak.

The importance of double-porosity diffusion in maintaining an elevated 'tail' can be clearly seen by comparing the simulated fissure and matrix concentrations at the end of each branch. For Scenario A, matrix and fracture concentrations attain diffusive equilibrium at 2060, 2080 and 2085 for Harefield House, Hatfield Quarry and Comet Way respectively. For Scenario C, matrix and fracture concentrations attain diffusive equilibrium at 2045, 2065 and 2070 for Harefield House, Hatfield Quarry and Comet Way respectively. After this time, bromate within the matrix provides a secondary source of contamination which acts to maintain elevated concentrations in the fissures for a prolonged period of time.

At Harefield House, simulated node concentrations remain above 10 μg l^{-1} until 2225 for Scenarios A and C and 2175 for Scenario B. At Hatfield Quarry, simulated node concentrations remain above 10 μg l^{-1} until 2325 for Scenarios A and C and 2250 for Scenario B. At Comet Way, simulated node concentrations remain above 10 μg l^{-1} until 2310 for Scenarios A and C and 2230 for Scenario B.

The 'worst-case' and 'best-case' scenarios (as illustrated for Scenario C in Figure 6.13) affect the timing, magnitude and sharpness of the peak bromate concentration. Compared to the'typical-case' Scenario, 'worst-case' scenarios have a narrower, higher concentration peak which occurs earlier, and 'best-case' scenarios have a broader, lower concentration peak which occurs later. The relative difference between the magnitude and timing of predicted concentrations for best, worst and typical scenarios increases as the distance from the source site increases. The differences in the magnitude and duration of the bromate concentration peaks are due to the extent of diffusive exchange that occurs between fissure and matrix. The most bromate mass diffuses into the immobile matrix porewater from the mobile fissure

water for the 'best-case' set of parameters. This attenuates the rise of bromate concentrations in the fissures, but the back-diffusion from the matrix porewater to the fissures slows the falling limb of the concentration peak.

For the spring concentrations, simulated bromate and bromide concentrations are significantly lower (by around an order of magnitude) than observed concentrations. The concentrations at the spring nodes, reflect the contributions from the four branches joining the spring node (Figure 6.8 and Figure 6.9), along with the appropriate dilution at the node to represent water flux from flow lines that do not contain bromate. The double-porosity branch contributes bromate concentrations in a broad peak; maximum concentrations occur later (between 2050 and 2100) and are maintained for a longer duration, than peak bromate concentrations provided by the karstic branches. The karstic branches from Harefield House and Comet Way transport bromate at high concentrations within the fissures to the Arkley Hole and Lynchmill Spring, while the karstic branch from the 'karst junction' to the springs, transports lower concentrations, although the relative flux is much higher. Simulated matrix concentrations at the end of the karst branches shows that double-porosity diffusion between matrix and fissure concentrations does have a significant effect in attenuating bromate concentrations. However, substantially more diffusion of bromate occurs along the double-porosity branch.

6.7 Discussion and conclusions

The network modelling approach developed in this chapter has been successful in providing a representation of double-porosity effects on the catchment-scale migration of bromate contamination. Model simulations, using a selection of what are considered to be typical parameters for the Hertfordshire Chalk, and the range of source terms developed earlier in this thesis, simulate bromate and bromide concentrations of the order of magnitude of those observed at locations within the Vale of St Albans, west of the Palaeogene feather edge where the main karst system.

However, in comparison to the long time-scales predicted to be relevant to the evolution of bromate within the double-porosity Chalk aquifer, observations are available over a very short period of time, generally for a maximum of eight years between 2000 and 2008, and for significantly less than this at a number of locations. The seasonal variations within the observed monitoring data also makes trends difficult to discern (See Chapter 4). It is therefore very difficult to be certain about which point on the simulated concentration versus time curve the current observations represent, and hence how successful the model is in simulating bromate evolution. The only way of becoming more certain as to the simulated curves are representing concentrations at the correct point in evolution, is to have a longer series of monitoring data that would identify a clearer rising or falling trend, and to have data for porewater bromate concentrations which would identify at which point along the curve a particular observation represents.

No additional calibration was undertaken on the results because it is considered that the available observed monitoring data are insufficient to be able to undertake a robust calibration. Over the timescale for which elevated bromate concentrations are predicted by the model simulations, the observed data are available over a very short timescale. It is therefore potentially possible to fit the curve to observations

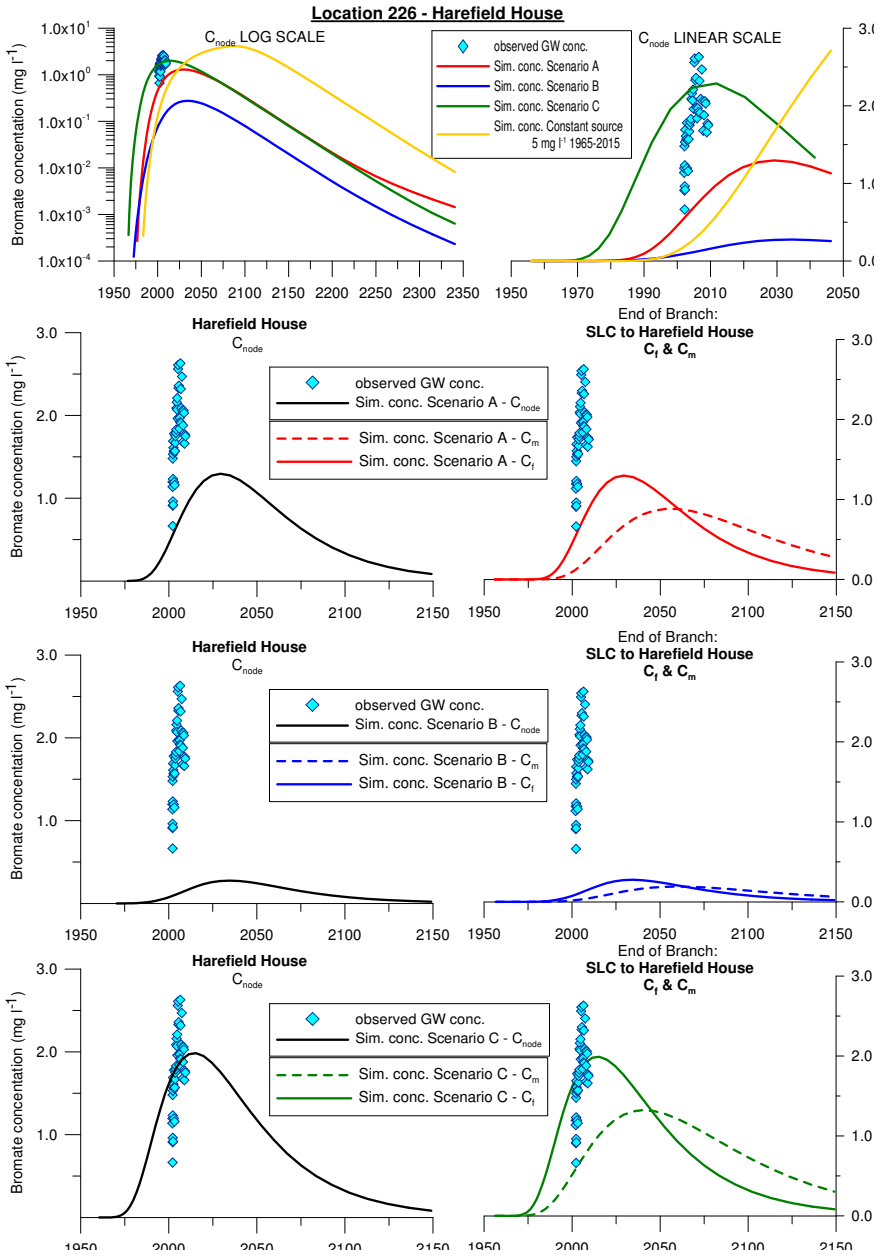

Figure 6.5: Simulated bromate concentrations at Harefield House using source terms for Scenario A, B and C (Section 5.11), and a constant concentration source term of 5000 μg l^{-1}.

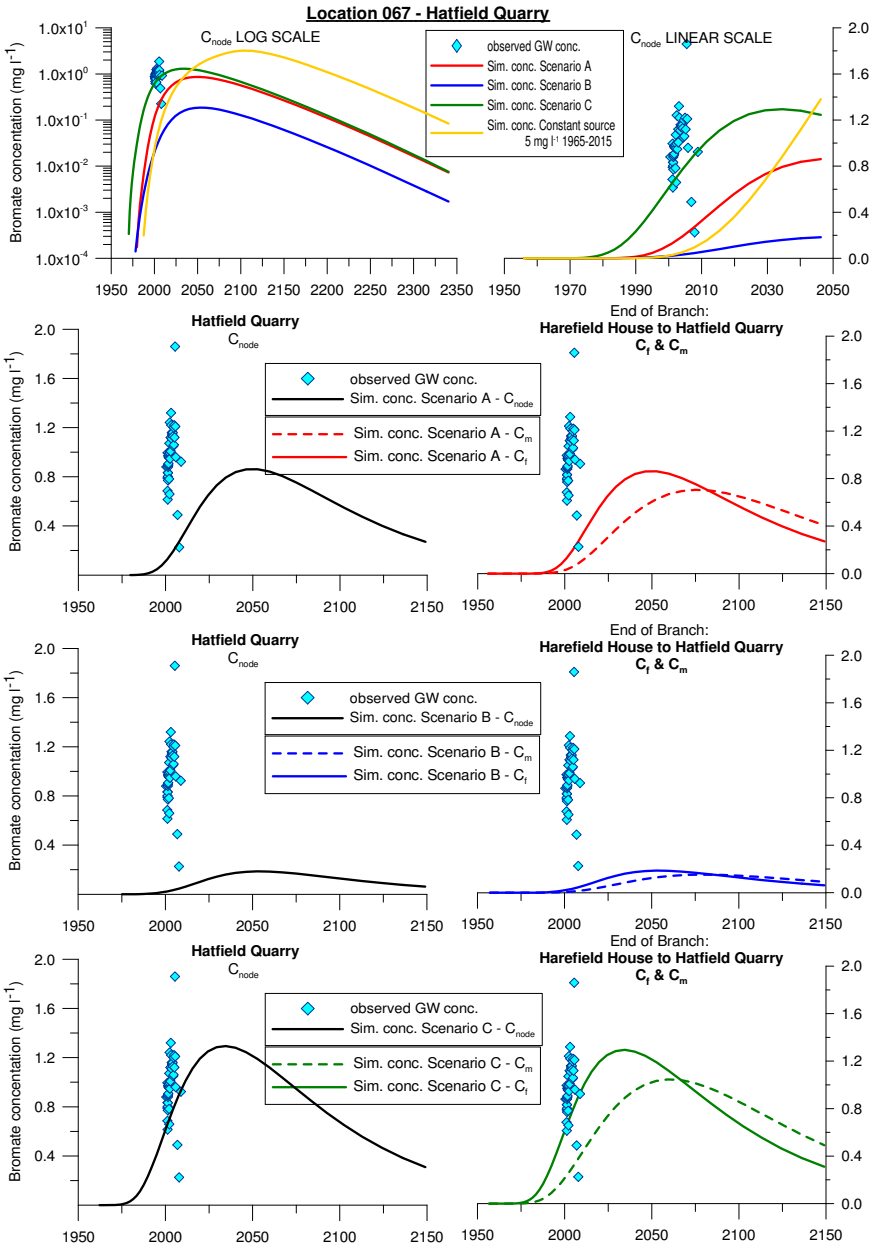

Figure 6.6: Simulated bromate concentrations at Hatfield Quarry using source terms for Scenario A, B and C (Section 5.11), and a constant concentration source term of 5000 μg l^{-1}.

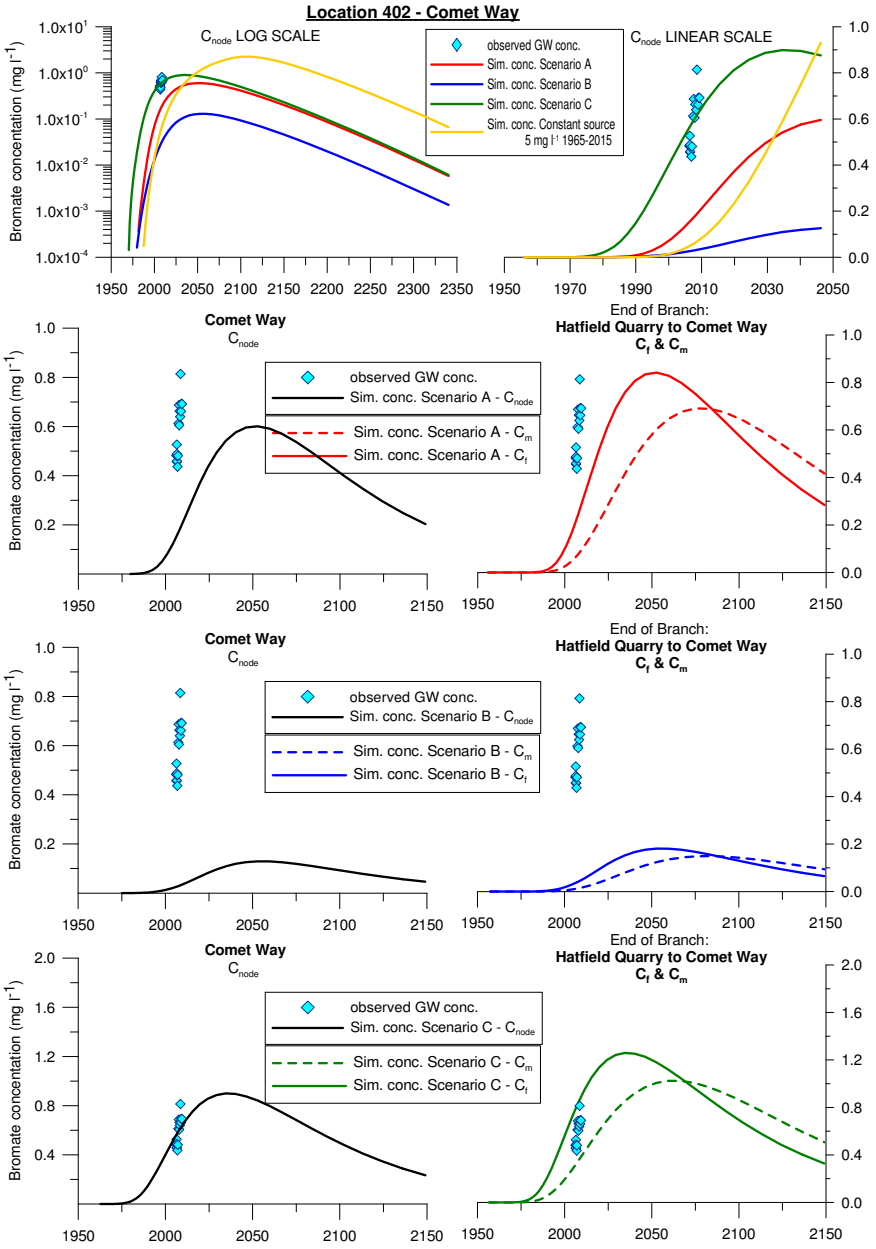

Figure 6.7: Simulated bromate concentrations at Comet Way using source terms for Scenario A, B and C (Section 5.11), and a constant concentration source term of 5000 $\mu g\, l^{-1}$.

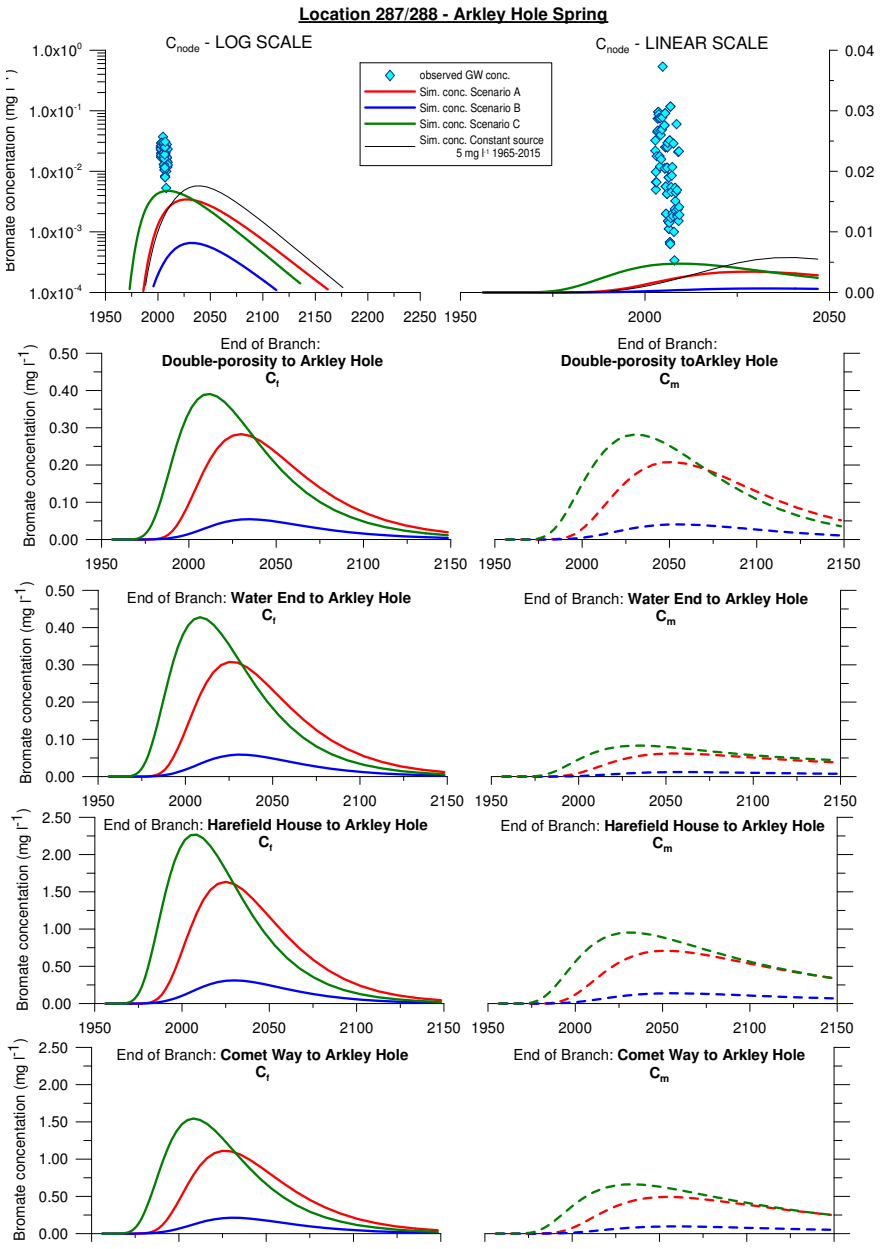

Figure 6.8: Simulated bromate concentrations at Arkley Hole Spring node, and at the end of contributing branches, using source terms for Scenario A, B and C (Section 5.11), and a constant concentration source term of 5000 μg l^{-1}.

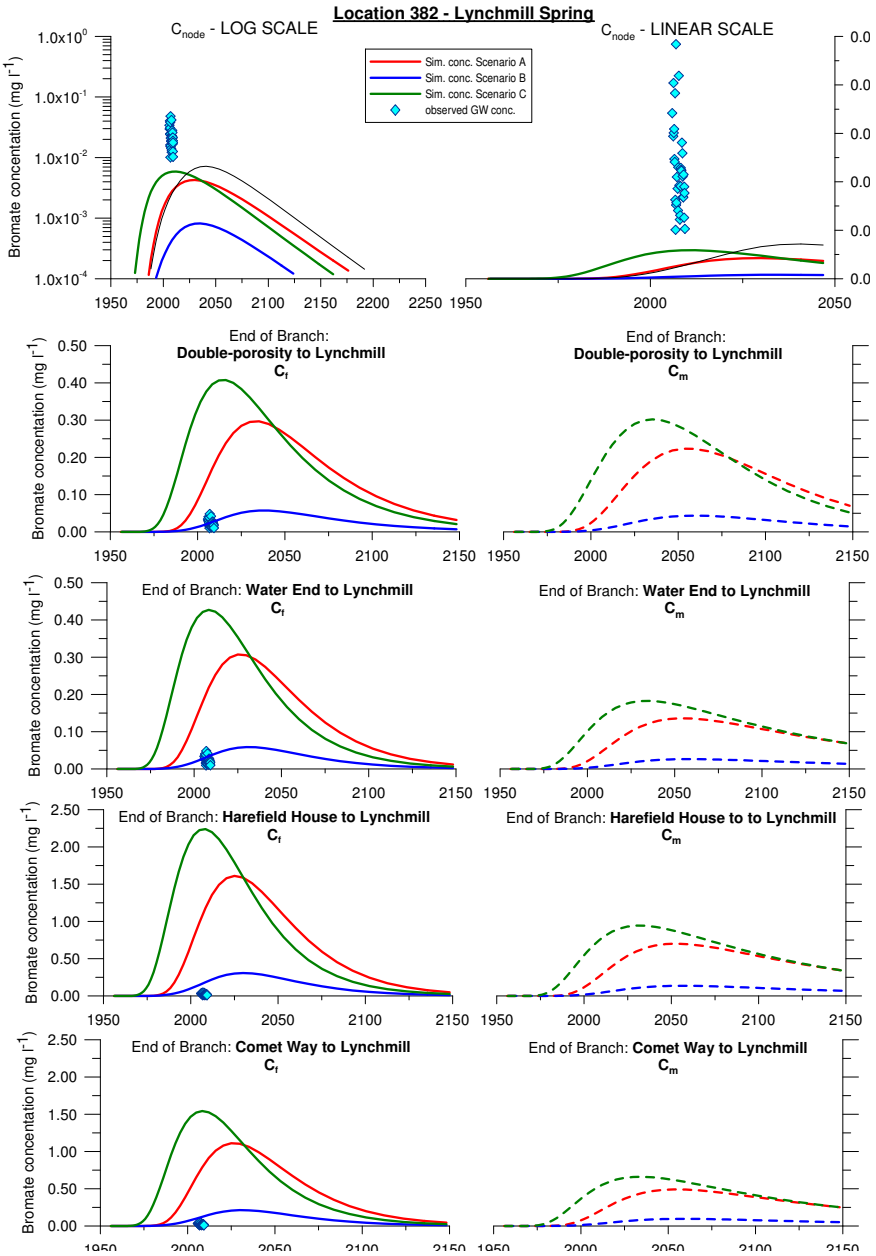

Figure 6.9: Simulated bromate concentrations at Lynchmill Spring node, and at the end of contributing branches, using source terms for Scenario A, B and C (Section 5.11), and a constant concentration source term of 5000 μg l^{-1}.

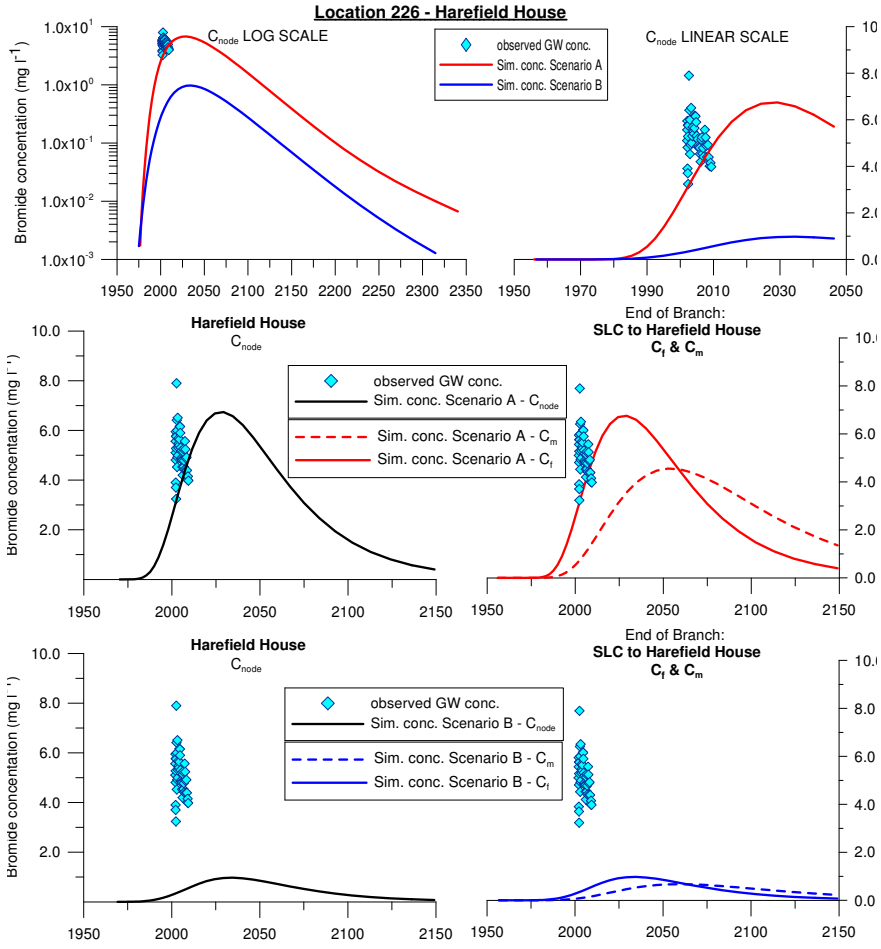

Figure 6.10: Simulated bromide concentrations at Harefield House using source terms for Scenario A and B.

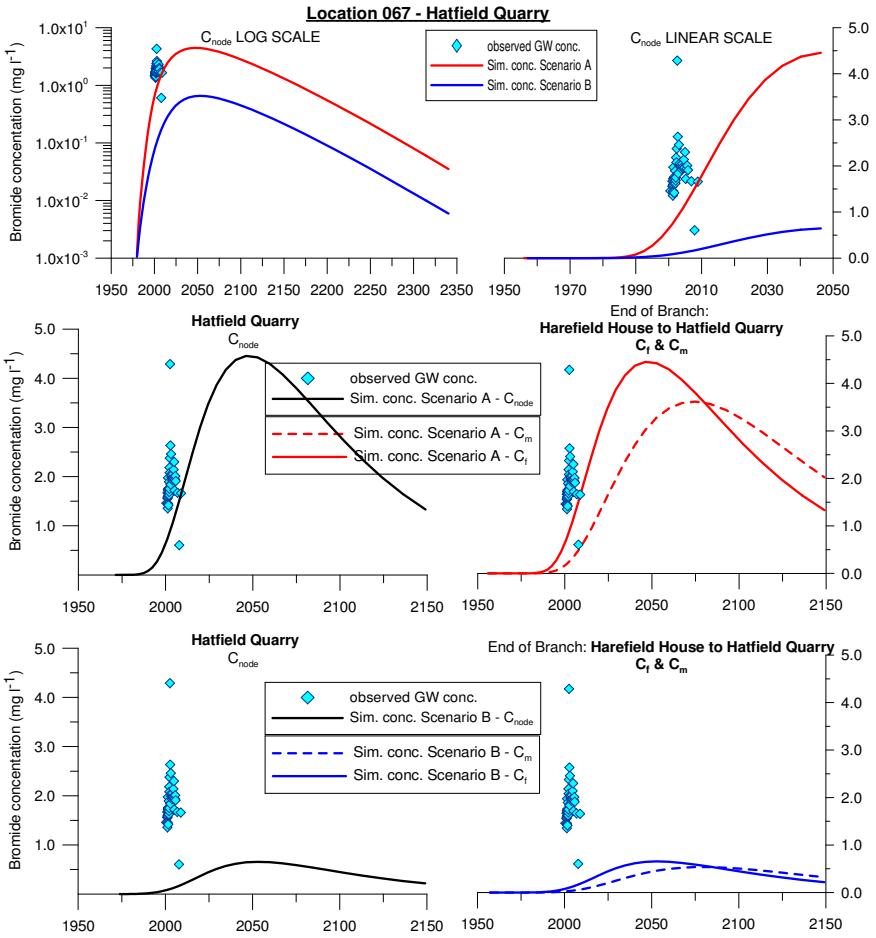

Figure 6.11: Simulated bromide concentrations at Hatfield Quarry using source terms for Scenario A and B.

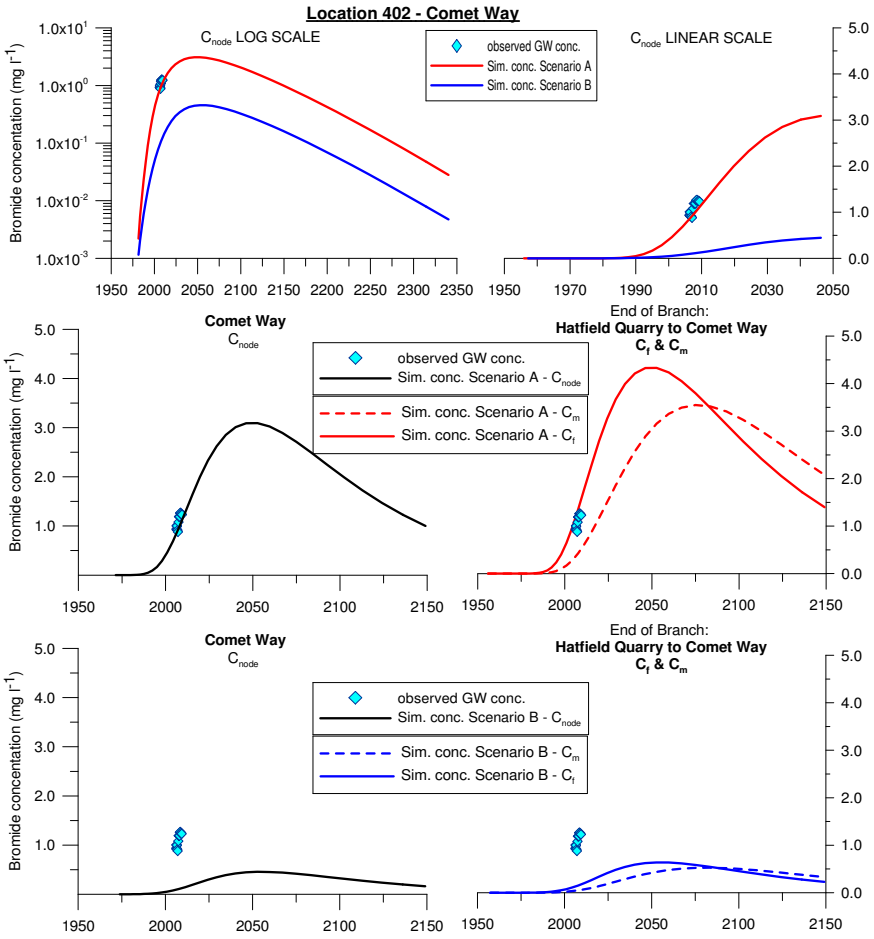

Figure 6.12: Simulated bromide concentrations at Comet Way using source terms for Scenario A and B.

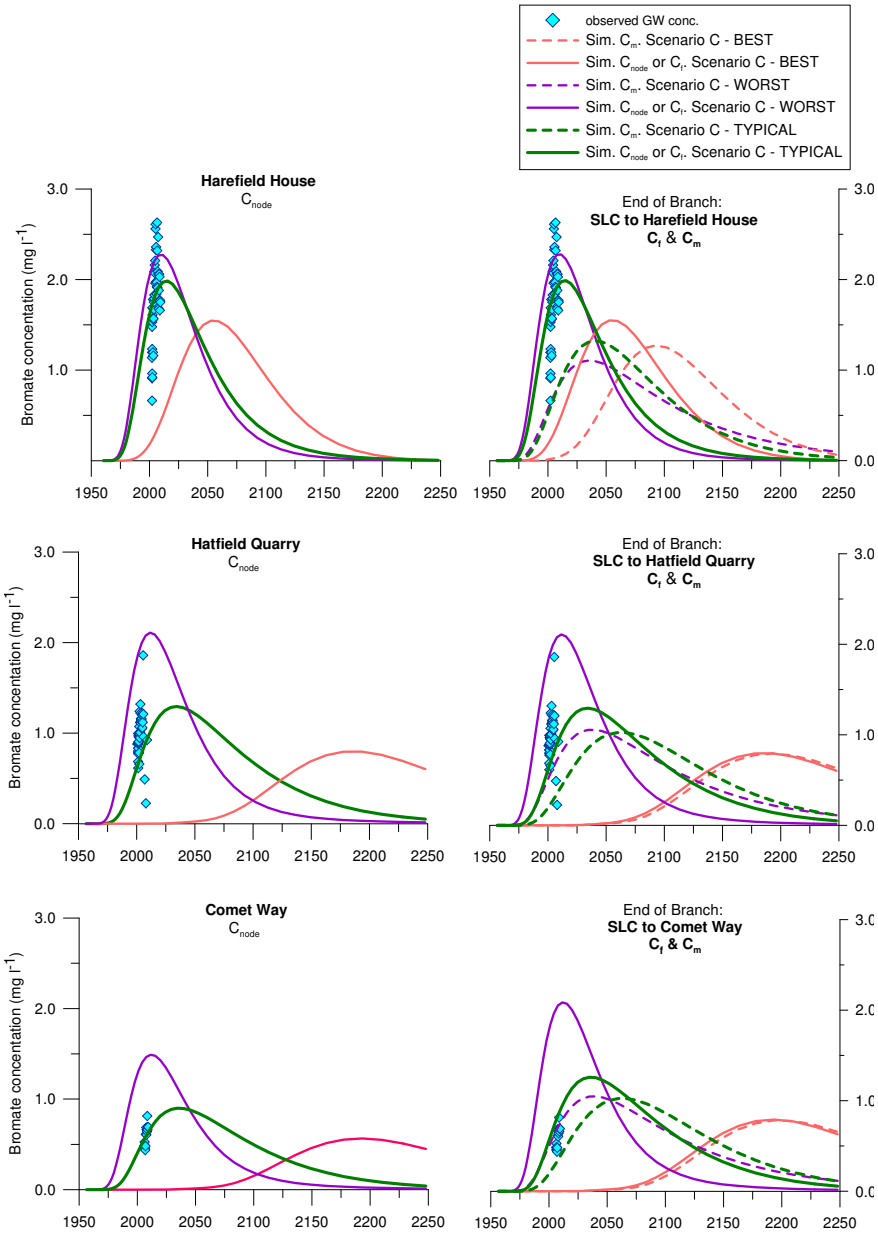

Figure 6.13: Simulated bromate concentrations for Scenario C at Harefield House, Hatfield Quarry, and Comet Way using ‘best-case’, ‘typical-case’ and ‘worst-case’ parameters.

in a number of ways: the point of time in the contaminant evolution which is represented by the observations is not evident. A longer period of monitoring data would be necessary to identify trends which could allow the curve to be calibrated with more certainty. Furthermore, observations of a particular *fissure* concentration can represent one of two points on the simulated curve (Figure 6.14). Concurrent observations of *matrix porewater* concentrations are required to identify which point in the evolution such a fissure concentration represents.

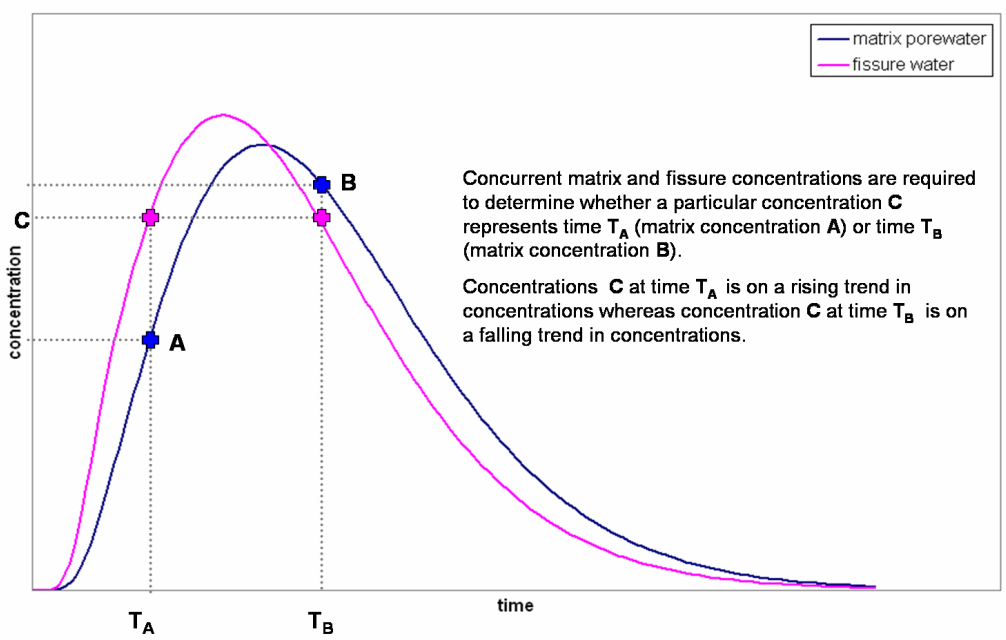

Figure 6.14: Concurrent matrix and fissure concentrations are required to determine at which point along the concentration-time graph a particular fissure concentration represents.

The network model has been less successful in representing concentrations at locations to the east of the Palaeogene escarpment, where the karst flow system is believed to have a dominant effect on the migration of bromate contamination across the catchment. This could be due to the uncertainty in the relative fluxes of the karst system. More extensive tracer testing and flow gauging could help to reduce this uncertainty.

The representation of the karst branches within the network model is a very simplistic approximation to the likely reality. The karst branches represented are only those that were identified by tracer testing, but in reality there are likely to be additional connections. Also, very limited interaction between karst branches and double-porosity branches is simulated by this model: the flow pathway between the Hatfield Area and Arkley Hole and Lynchmill Spring is represented by either a single karst branch or a single double-porosity branch. Further work could experiment with more extensive branching and joining between karst branches and double-porosity branches.

The Network model represents a one-dimensional steady-state flow regime between nodes. Therefore, unlike numerical models such as MODFLOW and MT3D, the network model model output does not capture seasonal variations in concentrations, nor incorporate transient flow conditions such as those

introduced by changes in abstraction regimes.

Despite the uncertainties in the foregoing discussion, the network model has been successful in highlighting the long-term effects of double-porosity nature of the chalk on the catchment-scale evolution of bromate, which previous models of models of bromate in Hertfordshire have neglected. The timescale of the catchment bromate contamination in Hertfordshire is similar to that of extensive chloride pollution of the Chalk of the Tilmanstone valley in Kent from coalfield brines. Watson (2004) used a one-dimensional semi-analytical model (DP1D), incorporating Fickian diffusion between matrix water and fracture water, was used to simulate chloride migration and was able to reproduce the observed porewater and fracture water profiles. Forward modelling indicated that the double porosity diffusion extends the duration of contamination in the catchment by several decades. (Watson, 2004; Burgess et al., 2005). The long-term effects of the double-porosity nature of the Chalk is relevant to catchment-scale Nitrate (NO_3^-) pollution in the Chalk (*e.g.* Williams et al. 2003; Silgram et al. 2005), and potentially other aquifers which possess double-porosity characteristics, as it highlights the timescales over which land management changes will take effect.

The double-porosity diffusion significantly extends the duration of elevated levels of contamination by providing a secondary source of bromate. Concentrations are predicted to remain above regulatory limits in the Vale of St Albans for around 200 years. The persistence of bromate within the Hertfordshire Chalk aquifer for such long time scales has enormous financial implications for water resources engineering: current treatment processes and scavenge pumping management measures may cease to be sustainable, and finding alternative sources of water supply may become increasingly necessary. There remains substantial uncertainty in the predicted time-series of bromate concentrations, and this could be addressed by further sensitivity analyses and calibration as further monitoring data become available. Nevertheless, the persistence of bromate for decades to centuries is the best available estimate at the current time, and should be considered in management strategies in Hertfordshire.

Chapter 7

Conclusions

This chapter considers the contributions of the analysis and interpretation of data and the modelling work presented in Chapters 3, 4, 5 and 6 in meeting the aims and objectives of the research outlined in Chapter 1. For convenience, the research objectives are repeated and discussed in sections 7.1.1, 7.1.2 to 7.1.3.

7.1 Fulfillment of research aims and objectives

The overall aim for the EngD research presented in this thesis is:

> *To develop greater understanding of the processes controlling the spatial distribution and temporal evolution of bromate contamination within the Hertfordshire Chalk aquifer, including bromate release from the source zone, and to use this as the basis of predictive models incorporating the effects of double-porosity diffusion on the long-term evolution of bromate.*

The research presented in this thesis has fulfilled this overall aim by developing a refined conceptual model of bromate transport within the catchment and interpreting the spatial distribution of bromate in light of this conceptual understanding, by conceptualising and quantifying a range of source history scenarios for bromate input to the aquifer, and by using these advancements in understanding as a basis for developing a network model that demonstrates the influences of double-porosity diffusion on the long-term evolution of bromate at a catchment-scale.

7.1.1 Evolution of bromate contamination

Objectives:

- *To develop a conceptual model for groundwater flow and contaminant transport in the Hertfordshire Chalk aquifer system by review of existing data and interpretation of additional tracer testing and geophysical testing;*
- *To use the available information and monitoring data to describe the spatial distribution and temporal evolution of bromate across the catchment, and to interpret this in association with the conceptual model of the flow and transport system.*

The detailed analysis of bromate and bromide monitoring data presented in Chapter 4 has revealed that bromate concentrations are affected by influences including recharge (soil moisture deficit, rainfall),

water level, and abstractions. These relationships, integrated with the observations of the geology, hydrogeology and hydrology of the area affected by the bromate contamination, have been used to refine the conceptual model of groundwater flow and transport of bromate within the catchment Chapter 3. The conceptualisation supports double-porosity dominated transport of bromate within the Vale of St. Albans area, which maintains a highly attenuated, relatively stable contaminant distribution west of Hatfield. To the east of Hatfield, a significant karst network related to the position of the Palaeogene overlap of the Chalk influences bromate trasport, dispersing bromate over large distances toward the northern and middle Lea Valley. The revised conceptual understanding provides the basis for modelling approaches applied to predict long-term, large-scale transport of bromate within the Hertfordshire Chalk (section 7.1.3), and has allowed a new interpretation of the spatial distribution and evolution of bromate and bromide within the catchment to be developed between 2000 and 2008.

However, the interpretation of the spatial and temporal evolution of bromate and bromide within the catchment is hampered by a number of inadequacies in the available monitoring data: trends are difficult to discern because monitoring data is available for a relatively short period of time, monitoring frequency varies considerably between locations and varies over time at individual locations, and there are strong seasonal influences. Data are generally for (non depth-specific) pumped groundwater samples so that vertical distribution of bromate contamination cannot be investigated, nor can the matrix porewater concentrations be diagnosed. This is a severe limitation of the monitoring and investigation programme, effectively preventing proper consideration of diffusive retardation of bromate which the thesis shows may prolong the occurrence of bromate contamination by 200 years.

7.1.2 The source

Objectives:

- *To describe and quantify the distribution of bromate at the source site through collation and description of site investigation and monitoring data;*
- *To develop alternative conceptual scenarios for bromate release to groundwater and quantify these as 'source terms';*
- *To use the available monitoring data to constrain the potential source terms.*

In Chapter 5, the available site investigation data was assessed and interpreted to estimate the quantity of bromate and bromide present on site in the unsaturated and saturated zone soils and groundwater prior to the redevelopment of the site in the mid 1980s and subsequent to the discovery of bromate contamination in early 2000s. These estimates have been used to constrain three source term scenarios for bromate input to the aquifer beneath the site. There are many uncertainties associated with an incomplete knowledge of the history of the site, and the three source scenarios attempt to capture the range of possible bromide and bromate source histories. This rigorous analysis of the source zone provides a significant improvement in the characterisation of the bromate 'source term' compared to previous representations, particularly the constant concentrations source terms used by Buckle (2003) and Atkins

(2005). Nevertheless, it is recognised that due to the relative scarcity of data, these scenarios still represent crude estimates of the reality.

The one-dimensional double-porosity transport code, DP1D (Barker, 2005), has been used to simulate concentrations in groundwater down-gradient of the source site. Simulated concentrations using two of the source term scenarios show relatively good agreement with observed groundwater concentrations at locations 150 m, 500 m and 1000 m down-gradient of the source site. Either a 'catastrophic release' of bromide/bromate to the unsaturated zone followed by leaching to groundwater beneath the site, or a 'direct release' of bromate to the saturated zone, sometime between 1960 and 1970, result in the closest fit to observed data. Porewater concentrations are not available for locations down-gradient of the source site. The lack of porewater concentrations and the relatively short period of time for which groundwater monitoring data (fissure concentrations) are available, combined with the large seasonal variations in concentrations, means that the trends are difficult to discern, and robust conclusions cannot be made as to whether or not the simulations are representative of the actual release scenarios.

7.1.3 Catchment-scale modelling of bromate transport

Objectives:

- *To develop analytical network modelling of contaminant transport to allow representation of Fickian double-porosity diffusion and to integrate karstic transport pathways within the network;*
- *To use this model to produce predictions for the likely bromate concentrations at key output locations over the long-term.*

A novel analytical network model to represent the Hertfordshire Chalk catchment has been developed in Chapter 6, using code written by Prof. John Barker. The network model simulates Fickian double-porosity diffusive exchange along interconnecting flow-lines, while allowing karstic branches to be incorporated into the network. The model was parameterised by a combination of values found within the literature, and the results of the single borehole dilution testing and catchment-scale natural gradient tracer testing.

The network model, using the range of source terms developed in Chapter 5, has been successful in simulating bromate and bromide concentrations of the order of magnitude of those observed at locations within the Vale of St. Albans, west of the main karst system. The network model highlights the long-term effects of double-porosity nature of the chalk on the catchment-scale evolution of bromate. The double-porosity diffusion significantly extends the duration of elevated levels of contamination by providing a secondary source of bromate: bromate concentrations within the Vale of St. Albans are predicted to remain above regulatory limits for around 200 years.

The network model has been less successful in representing concentrations at locations to the east of the Palaeogene escarpment, where the karst flow system is believed to have a dominant effect on the migration of bromate contamination across the catchment. This is largely due to the uncertainty in the relative fluxes of the karst system. The representation of the karst branches within the network model is a very simplistic approximation to the likely reality. The karst branches represented are only those that

were identified by tracer testing, and very limited interaction between karst branches and double-porosity branches is simulated by this model. Further work could experiment with more extensive branching of the karst network and closer interaction between karst branches and double-porosity branches.

The Network model represents a one-dimensional steady-state flow regime between nodes. Therefore, unlike numerical models such as MODFLOW and MT3D, the network model model output does not capture seasonal variations in concentrations, nor incorporate transient flow conditions such as those introduced by changes in abstraction regimes. However, the analytical network model has a number of advantages over the numerical models. In particular, the analytical model is computationally fast over long time-scales, taking seconds to minutes to run compared to days to weeks for the catchment MODFLOW and MT3D-MS models (Atkins, 2005; Cook, 2010). Also, for the analytical network model, the number of parameters which are varied during the calibration process is small compared to a distributed parameter numerical model. No additional calibration was undertaken on the results within this thesis due to insufficient monitoring data. Without measured bromate concentrations in porewater and longer time-series of bromate concentrations in fissure water becoming available, no effective calibration will be possible.

7.2 Recommendations for further work

The ability to validate the conceptualisations and modelling representations of bromate transport in the Hertfordshire Chalk is dependent on the available of representative observation data. Although a bromate monitoring programme has been underway since mid 2000, in comparison to the long time-scales predicted to be relevant to the evolution of bromate within the double-porosity Chalk aquifer, observations are available over a very short period of time: generally for a maximum of eight years between 2000 and 2008, and for significantly less than this at a number of locations. The seasonal variations within the observed monitoring data also makes trends difficult to discern. Furthermore, the vast majority of the data relate to bromate concentrations withi the mobile *fissure* water; concurrent bromate concentrations in the immobile *matrix porewater* are absent except in close proximity to the source site. Both concentrations in the fissure water and matrix porewater are necessary to fully characterise a system influenced by double-porosity exchange and establish the extent of disequilibrium between fissures and matrix.

It is therefore considered essential that a number of cored investigatory boreholes are drilled across the bromate affected area, and particularly in the the Vale of St. Albans area between the source site and the Hatfield. These boreholes should be sampled for matrix porewater and fissure water. Samples should be taken at specific depths to provide information about the vertical extent of contamination.

It would be informative to run the MODFLOW/MT3D-MS model of Cook (2010) as a steady-state simulation, with the source terms used in this thesis, to directly compare simulated concentrations at the locations also included in the Hertfordshire network model, with the results simulated by the network model. This would allow the impacts of using a first order mass transfer coefficient to represent double-porosity as opposed to representing it as a Fickian diffusion process to be assessed.

Bibliography

Allen, D. J., Brewerton, L. J., Coleby, L. M., Gibbs, B. R., Lewis, M. A., MacDonald, A. M., Wagstaff, S. J. and Williams, A. T. (1997), The physical properties of major aquifers in England and Wales. British Geological Survey Technical Report WD/97/34, Technical Report, British Geological Survey.

Atkins (2002), St. Leonard's Court, Sandridge, St. Albans. Environmental Site Investigation and Quantitative Pollutant Linkage Assessment., Technical Report, Atkins Ltd.

Atkins (2004), Bromate Contamination in the Lee Valley. Phase 1: Data Collation and Conceptualisation., Technical Report, Atkins Limited.

Atkins (2005), Bromate Contamination in the Lee Valley Phase 2: Modelling Report., Technical Report, Atkins Limited.

Atkins (2006), Bromate Monitoring Data Review, Technical Report, Atkins Limited.

Atkinson, T. C. and Smith, D. I. (1974), Rapid groundwater flow in fissures in the chalk: an example from south Hampshire, *Quarterly Journal of Engineering Geology and Hydrogeology* **7**(2), 197–205.

Atkinson, T. and Smart, P. (1981), Artificial Tracers in Hydrology, *in A Survey of British Hydrology*, Royal Society, London, pp.173–190.

Banks, D., Davies, C. and Davies, W. (1995), The Chalk as a karstic aquifer: evidence from a tracer test at Stanford Dingley, Berkshire, UK, *Quarterly Journal of Engineering Geology and Hydrogeology* **28**(Supplement$_1$), $S31 - -38$.

Barker, J. A. (1982), Laplace transform solutions for solute transport in fissured aquifers, *Advances in Water Resources* **5**(2), 98–104.

Barker, J. A. (1985a), Block-Geometry Functions Characterizing Transport in Densely Fissured Media, *Journal of Hydrology* **77**(1-4), 263–279.

Barker, J. A. (1985b), Modelling the effects of matrix diffusion on transport in densely fissured media., *in Hydrogeology in the Service of Man. Memoirs of the 18th Congress of the International Association fo Hydrogeologists.*, Vol. XVIII, International Association of Hydrogeologists, Cambridge, pp.250–269.

Barker, J. A. (1991), Transport in fractured rock, *Applied groundwater hydrology* pp.199–216.

Barker, J. A. (1993), Modelling of flow and transport in the chalk, *in* R. A. Downing, M. Price and G. P. Jones (eds.), *The Hydrogeology of the Chalk of North-West Europe*, Clarendon Press, Oxford, pp.35–38.

Barker, J. A. (2001), Mathemetical basis for the MAP model., Technical Report.

Barker, J. A. (2005), DP1D-Link Description of the code and issues. Version 6., Technical Report.

Barker, J. A. and Foster, S. S. D. (1981), A Diffusion Exchange Model for Solute Movement in Fissured Porous Rock, *Quarterly Journal of Engineering Geology* **14**(1), 17–24.

Barker, J. A., Wright, T. and Fretwell, B. (2000), A pulsed-velocity method of solute transport modelling., *in* A. Dassargues (ed.), *Tracers and Modelling in Hydrogeology, Proceedings of the TraM'2000 Conference*, Vol. International Association of Hydrological Sciences Publication 262, IAHS Press, Liege, Belgium, p.297302.

Barten, W. (1996), Linear response concept combining advection and limited rock matrix diffusion in a fracture network transport model, *Water Resources Research* **32**(11), 3285–3296.

Bear, J. (1972), *Dynamics of Fluids in Porous Media.*, Elsevier, New York.

Bibby, R. (1981), Mass treansport studies in dual porosity media., *Water Resources Research* **17**, 1075–1081.

Bloomfield, J. (1996), Characterisation of hydrogeologically significant fracture distributions in the Chalk: An example from the Upper Chalk of southern England, *Journal of Hydrology* **184**(3-4), 355–379.

Bloomfield, J. P., Brewerton, L. J. and Allen, D. J. (1995), Regional trends in matrix porosity and dry density of the chalk of England, *Quarterly Journal of Engineering Geology* **28**, S131–S142.

Bloomfield, J. P., Farrant, A. R. and Cunningham, J. (2004), Structural Interpretation of the Chalk of the Hertford District based on Slope Aspect Mapping (Draft). BGS Report Ref. CR/04/XXC, Technical Report Ref. CR/04/XXC, British Geological Survey.

Board, W. R. (1972), The Hydrogeology of the London Basin, Technical Report, Water Resources Board.

Bristow, R., Mortimore, R. and Wood, C. (1997), Lithostratigraphy for mapping the Chalk of southern England, *Proceedings of the Geologists Association* **108**, 293–315.

Buckle, D. (2002), Bromate Groundwater Flow Study. Phase 1 (Conceptual Understanding) Report. Undertaken on behalf of the Environment Agency and Three Valleys Water., Technical Report, Vivendi Water Partnership.

Buckle, D. (2003), Bromate Groundwater Flow Study. Phase 2 Interim (Modelling) Report. Undertaken on behalf of the Environment Agency and Three Valleys Water., Technical Report, Vivendi Water Partnership.

Burgess, W., Barker, J., Watson, S. and Fretwell, B. (2005), Contaminant retardation by double porosity diffusive exchange in the Chalk: implications for monitoring., *in Bringing Groundwater Quality Research to the Watershed scale. Proceedings of the 4th International Groundwater Quality Conference..*, IAH, Waterloo, Canada.

Butler, R., Godley, A., Lytton, L. and Cartmell, E. (2005), Bromate environmental contamination: Review of impact and possible treatment, *Critical Reviews in Environmental Science and Technology* **35**(3), 193–217.

Chatfield, C. (2004.), *The Analysis of Time Series: An Introduction.*, sixth edition edition, Chapman and Hall/CRC.

Chemfix (1984), Sandridge site bromide modelling exercise, Technical Report.

Chemfix (1985a), Evaluation of the results from the borehole situated 120m down dip from the Sandridge site., Technical Report.

Chemfix (1985b), Field report for drilling of borehole C1 at House Lane, Sandridge on 21/22 January 1985, Technical Report.

Chemfix (1985c), Report of the second phase of the field investigation at the Sandridge site, Technical Report.

Chemfix (1985d), Report on the further modelling studies for the Sandridge site., Technical Report.

CL:AIRE (2002), Site characterisation in support of monitored natural attenuation of fuel hydrocarbons and MTBE in a chalk aquifer in southern England., *in Case study bulletin CSB1.*, Contaminated Land: Applications in Real Environments (CL:AIRE).

Cook, S. J. (2010), The hydrogeology of bromate contamination in the Hertfordshire Chalk: Incorporating Karst in Predictive Models., EngD, University College London.

Cushman, J. H. (1990), An Introduction to Hierarchical Porous Media, *in* J. H. Cushman (ed.), *Dynamics of Fluids in Hierarchical Porous Media*, Academic Press Ltd, London, pp.1–6.

de Marsily, G. (1986), *Quantitative Hydrogeology : Groundwater Hydrology for Engineers*, Academic Press, Orlando FL.

Domenico, P. and Schwartz, W. (1998), *Physical and Chemical Hydrogeology.*, second edition edition, Wiley.

EA (2005), Part IIA of the Rnvironmental Protection Act 1990. Decision Document for St Leonard's Court., Technical Report, Environment Agency.

Edmunds, W. M. (1996), Bromine geochemistry of British groundwaters, *Mineralogical Magazine* **60**(399), 275–284.

Edmunds, W. M., Cook, J. M., Kinniburgh, D. G., Miles, D. L. and Trafford, J. M. (1989), Trace-element occurrence in British groundwaters., Technical Report BGS Research Report SD/89/3, British Geological Survey.

Edwards, A. J., Hobbs, S. L. and Smart, P. L. (1991), Effects of quarry dewatering on a karstified limestone aquifer: A case study from the Mendip Hills, England., *in Third Conference on Hydrogeology, Ecology, Monitoring, and Management of Ground Water in Karst Terranes.*, National Water Well Association, pp.77–92.

Entec (2000), River Mimram and Upper Lee Water Resources Sustainability Study Groundwater Model. Phase 1 Report: Data Collation and Formulation of Conceptual Model. Undertaken on behalf of the Environment Agency., Technical Report, Entec.

Entec (2002), River Mimram and Upper Lee Water Resources Sustainability Study Groundwater Model. Phase 2 Model Development and Refinement. Undertaken on behalf of the Environment Agency., Technical Report, Entec.

Fitzpatrick, C. M. (2007), Hatfield Pumping Test. Interim Report for TVW and TWUL for the period July 2005 to December 2006., Technical Report, University College London.

Ford, D. C. and Williams, P. (2007), *Karst hydrogeology and geomorphology*, John Wiley, Chichester.

Foster, S. S. D. (1975), The Chalk groundwater tritium anomaly – A possible explanation, *Journal of Hydrology* **25**(1-2), 159–165.

Foster, S. S. D. and Milton, V. A. (1974), The permeability and storage of an unconfined chalk aquifer, *Hydrological Sciences Bulletin* **19**, 485–500.

Gale, A., Hancock, J., Bristow, R., Mortimore, R. and Wood, C. (1999), 'Lithostratigraphy for mapping the Chalk of southern England' by Bristow et al. (1997): discussion, *Proceedings of the Geologists Association* **110**, 65–72.

GoldsimTechnologyGroup (2007), GoldSim Contaminant Transport Module. User Guide, Technical Report, GoldsimTechnologyGroup.

Goudie, A. (1990), *The Landforms of England and Wales*, Basil Blackwell, Oxford.

Grisak, G. E. and Pickens, J. F. (1980), Solute Transport through Fractured Media .1. The Effect of Matrix Diffusion, *Water Resources Research* **16**(4), 719–730.

Grisak, G. E. and Pickens, J. F. (1981), An Analytical Solution for Solute Transport through Fractured Media with Matrix Diffusion, *Journal of Hydrology* **52**(1-2), 47–57.

Hancock, J. M. (1975), The petrology of the Chalk, *Proceedings of the Geologists' Association* **86**(4), 499–535.

Harbaugh, A. W., Banta, E. R., Hill, M. and McDonald, M. (2000), MODFLOW-2000, The U.S. Geological Survey modular ground-water modelUser Guide to modularization concepts and the ground-water flow process., Technical Report, U.S. Geological Survey,.

Harold, C. H. H. (1937), Thirty-second Annual Report on the results of the chemcial and bacteriological examination of the London waters for the twelve months ended 31st December 1937., Technical Report, Metropolitan Water Board.

Headworth, H. (1972), The analysis of natural groundwater fluctuations in the chalk of Hampshire., *Journal of the Institute of Water Engineers* **26**, 107–124.

Headworth, H. G. (1978), Hydrogeological characteristics of artesian boreholes in the Chalk of Hampshire, *Quarterly Journal of Engineering Geology and Hydrogeology* **11**(2), 139–144.

Headworth, H. G., Keating, T. and Packman, M. J. (1982), Evidence for a shallow highly-permeable zone in the Chalk of Hampshire, U.K, *Journal of Hydrology* **55**(1-4), 93–112.

Helsel, D. and Hirsch, R. (1993), *Statistical Methods in Water Resources*, Elsevier.

Hijnen, W., Voogt, R., Veenendaal, H. and van der Jagt, H. (1995), Bromate reduction by denitrifying bacteria., *Applied Environmental Microbiology* **61**, 239.

Hill, D. (1984), Diffusion coefficients of nitrate, chloride, sulphate and water in cracked and uncracked Chalk., *Journal of Soil Science* **35**, 27–33.

Hydrotechnica (1988), Northern New River Wellfield Pump Testing. Final Report., Technical Report, Hydrotechnica.

Ineson, J. (1962), A hydrogeological study of the permeability of Chalk, *Journal of the Institution of Water Engineers* **16**, 449–463.

Kachi, S. (1987), Tracer studies in the Chalk aquifer near Cambridge., PhD thesis, University of East Anglia.

Klinck, B. A., Hopson, P. M., Lewis, M. A., MacDonald, D. M., Inglethorpe, S. D. J., Entwisle, D. C., Harrington, J. F. and Williams, L. (1998), The hydrogeological behaviour of the clay-with-flints in southern England. British Geological Survey Technical Report, WE/97/5., Technical Report, British Geological Survey.

Komex (2000), Site Investigation at St Leonards Court, Sandridge, St Albans., Technical Report 50598, Komex.

Kruithof, J. and Meijers, R. (1995), Bromate formation by ozonation ans advanced oxidation and potential options in drinking water treatment., *Water Supply* **13**, 93.

Lewin, K., Bradshaw, K., Blakey, N., Turrell, J., Hennings, S. and Fleming, R. (1994), Leaching Tests for Assessment of Contaminated Land: Interim NRA Guidance. National Rivers Authority RD Note 301 ., Technical Report, National Rivers Authority.

MacDonald, A., Brewerton, L. and Allen, D. (1998), Evidence for rapid groundwater flow and karst type behaviour in the Chalk of Southern England., *in* N. Robins (ed.), *Groundwater Pollution, Aquifer Recharge and Vulnerability, Geological Society of London Special Publication No. 130*, pp.95–106.

MacDonald, A. M. and Allen, D. J. (2001), Aquifer properties of the Chalk of England, *Quarterly Journal of Engineering Geology and Hydrogeology* **34**(4), 371–384.

MacDonald, M. G. and Harbaugh, A. W. (1984), A modular three-dimensional finite-difference groundwater flow model., Technical Report, U.S. Geological Survey.

Mathias, S. A., Butler, A. P., Jackson, B. M. and Wheater, H. S. (2006), Transient simulations of flow and transport in the Chalk unsaturated zone, *Journal of Hydrology* **330**(1-2), 10–28.

Mathias, S. A., Butler, A. P., McIntyre, N. and Wheater, H. S. (2005), The significance of flow in the matrix of the Chalk unsaturated zone, *Journal of Hydrology* **310**(1-4), 62–77.

Maurice, L. D., Atkinson, T. C., Barker, J. A., Bloomfield, J. P., Farrant, A. R. and Williams, A. T. (2006), Karstic behaviour of groundwater in the English Chalk, *Journal of Hydrology* **330**(1-2), 63–70.

Mortimore, R. N. (1993), Chalk water and engineering geology., *in* R. A. Downing, M. Price and G. P. Jones (eds.), *The Hydrogeology of the Chalk of North-West Europe*, Clarendon Press, Oxford, pp.67–92.

Mortimore, R., Pomerol, B. and Foord, R. J. (1990), Engineering stratigraphy and paeleogeography for the chalk of the Anglo-Paris Basin, *in Proceedings of the International Chalk Symposium 1989*, Thomas Telford.

Oakes, D. (1977), The movement of water and solutes through the unsaturated zone of the Chalk of the United Kingdom., *in 3rd International Hydrology Symposium*, Fort Collins, Colorado State University, pp.447–459.

Ogata, A. and Banks, R. B. (1961), A solution of the differential equation of longitudinal dispersion in porous media., *United States Geological Survey Professional Paper* **411-A**.

Pollock, D. W. (1989), Documentation of computer programs to compute and display pathlines using resultsd form the U.S. Geological survey modular three-dimensional finite-difference ground-water model., Technical Report, U.S. Geological Survey.

Price, M. (1987), Fluid flow in the Chalk of England, *in* J. C. Goff and B. P. J. Williams (eds.), *Fluid Flow in Sedimentary Basins and Aquifers. Geological Society of London Special Publication 34*, pp.141–156.

Price, M., Atkinson, T. C., Barker, J. A., Wheeler, D. and Monkhouse, R. A. (1992), A Tracer Study of the Danger Posed to A Chalk Aquifer by Contaminated Highway Run-Off, *Proceedings of the Institution of Civil Engineers-Water Maritime and Energy* **96**(1), 9–18.

Price, M., Atkinson, T. C., Wheerler, D., Barker, J. A. and Monkhouse, R. A. (1989), The Movement of Groundwater in the Chalk Aquifer near Bricket Wood, Hertfordshire, and its Possible Pollution by Drainage from the M25 Motorway. British Geological Survey Report WD/89/3., Technical Report, British Geological Survey.

Price, M., Bird, M. J. and Foster, S. S. D. (1976), Chalk pore-size measurements and their significance, *Water Services* **80**(968), 596–600.

Price, M., Downing, R. A. and Edmunds, W. M. (1993), The Chalk as an aquifer, *in* R. A. Downing, M. Price and G. P. Jones (eds.), *The Hydrogeology of the Chalk of North-West Europe*, pp.35–58.

Price, M., Low, R. G. and McCann, C. (2000), Mechanisms of water storage and flow in the unsaturated zone of the Chalk aquifer, *Journal of Hydrology* **233**(1-4), 54–71.

Price, M., Morris, B. and Robertson, A. (1982), A study of intergranular and fissure permeability in Chalk and Permian aquifers, using double-packer injection testing, *Journal of Hydrology* **54**(4), 401–423.

Rawson, P. F., Allen, P. M. and Gale, A. S. (2001), The Chalk Group - a revised lithostratigraphy., *Geoscientist* **11**, 21.

Roberts, M. (2001), The Sandridge/Hatfield Bromate Pollution Investigation, Technical Report, Environment Agency.

Rouleau, A. and Gale, J. E. (1985), Statistical characterisation of the fracture system in the Stripa Granite, Sweden, *Int. J. Rock Mech. Min. Sci. Geomech. Abstr.* **22**, 353–367.

Shand, P., Tyler-Whittle, R., Besien, T., Peach, D. W., Lawrence, A. R. and Lewis, H. O. (2003), Baseline Report Series: 6. The Chalk of the Colne and Lee river catchments, Technical Report British Geological Survey Commissioned Report CR/03/069N. Environment Agency National Groundwater Contaminated Land Centre Technical Report NC/99/74/6, British Geological Survey and Environment Agency.

Silgram, M., Williams, A., Waring, R., Neumann, I., Hughes, A., Mansour, M. and Besien, T. (2005), Effectiveness of the nitrate sensitive areas scheme in reducing groundwater concentrations in England, *Quarterly Journal of Engineering Geology and Hydrogeology* **38**, 117–127.

Smith, D., Wearn, P., Richards, H. and Rowe, P. (1970), Water movement in the unsaturated zone of high and low permeabilitystrata using natural tritium., *in Isotope Hydrology*, Atomic Energy Agency, Vienna, pp.73–87.

Snow, D. T. (1968), Rock fracture spacing, opening and porosities, *Journal of the Soil and Foundations Division, Proceedings of the American Society of Civil Engineers* **94**, 19.

STATS (1983a), Interim report on site investigation, ref 83/3105., Technical Report, St Albans Testing Services.

STATS (1983b), Second report on site investigation, ref 83/3105A, Technical Report, St Albans Testing Services.

STATS (1983c), Third report on site investigation, ref 83/3105C, Technical Report, St Albans Testing Services.

STATS (1984), Report on further site investigations. ref AM/3554, Technical Report, St Albans Testing Services.

Thomas, J. (2000), Note on the 1984 and 1985 modelling studies., Technical Report, Environment Agency.

Walsh, P. and Ockenden, A. (1982), Hydrogeological observations at the Water End swallow hole complex, North Mimms, Hertfordshire., *Transactions of the British Cave Research Association.* **9**, 184–194.

Ward, R. S. (1989), Artificial tracer and natural 222Rn studies of the East Anglian Chalk aquifer., PhD thesis, University of East Anglia, Norwich.

Ward, R. S., Williams, A. T., Barker, J. A., Brewerton, L. J. and Gale, I. N. (1998), Groundwater tracer tests: a review and guidelines for their use in British aquifers. RD Technical Report W160, Technical Report, Environment Agency. NOT IN FILE.

Watson, S. J. (2004), Solute transport and hydrodynamic characteristics in the Chalk aquifer at Tilmanstone, Kent, PhD, University College London.

White, W. B. (2003), Conceptual models for karstic aquifers., *Speleogenesis and Evolution of Karst Aquifers* **1**(1), 1–6.

Whittaker, H. (1921), Water Supply of Buckinghamshire and Hertfordshire. Geological Survey Memoirs., Technical Report, British Geological Survey.

Williams, A., Barker, J. A., Silgram, M., Mansour, M., Neumann, I. and Hughes, A. (2003), The use of flow modelling to assess the impact of agricultural control measures on abstracted groundwater quality., *in MODFLOW and More. Understanding through Modelling.*, pp.446–450.

Williams, A., Bloomfield, J., Griffiths, K. and Butler, A. (2006), Characterising the vertical variations in hydraulic conductivity within the Chalk aquifer, *Journal of Hydrology* **330**(1-2), 53–62.

Williams, R. (1987), Frost weathered mantles on the Chalk., *in* J. Boardman (ed.), *Periglacial processes and landforms in Britain and Ireland*, Cambridge University Press, Cambridge, pp.127–133.

Woods, M. A. (2003), The Stratigraphy of the Chalk Group of the Hertford District: a preliminary study for Veolia Water Partnership. BGS Report Ref.CR/03/216, Technical Report Ref.CR/03/216, British Geological Survey.

Woods, M. A. (2006), UK Chalk Group stratigraphy (Cenomanian-Santonian) determined from borehole geophysical logs, *Quarterly Journal of Engineering Geology and Hydrogeology* **39**, 83–96.

Woods, M. A. and Aldiss, D. T. (2004), The stratigraphy of the Chalk Group of the Berkshire Downs, *Proceedings of the Geologists Association* **115**, 249–265.

Worthington, S. . (2003), A comprehensive strategy for understanding flow in carbonate aquifers., *Speleogenesis and Evolution of Karst Aquifers* **1**(1), 1–8.

Worthington, S., Ford, D. C., Beddows, P. A. and Dreybrodt, W. (2000), Porosity and permeability enhancement in unconfined aquifers as a result of solution., *in* A. Klimchouk, D. C. Ford and A. N. Palmer (eds.), *Speleogenesis: Evolution of karst aquifers.*, National Speleological Society, Huntsville, Alabama, pp.463–472.

Younger, P. L. (1989), Devensian Periglacial Influences on the Development of Spatially-Variable Permeability in the Chalk of Southeast England, *Quarterly Journal of Engineering Geology* **22**(4), 343–354.

Younger, P. L. and Elliot, T. (1995), Chalk fracture system characteristics: implications for flow and solute transport, *Quarterly Journal of Engineering Geology and Hydrogeology* **28**(Supplement$_1$), $S39 - -50$.

Zheng, C. (1990), MT3D: A modular three-dimensional transport model for simulation of advection, dispersion, and chemical reactions of contaminants in groundwater systems. Report to the U.S. Environmental Porectection Agency., Technical Report.

Zheng, C. and Wang, P. P. (1999), MT3DMS: A modular three-dimensional multispecies transport model for simulation of advection, dispersion, and chemical reactions of contaminants in groundwater systems; documentation and users guide. Contract Report SERDP-99-1., Technical Report, U.S. Army Engineer Research and Development Center.

Appendix A

Chronology of key events

Appendix A

Chronology of key events

This chronology of key events in the history of bromate contamination in Hertfordshire has been compiled based on information obtained from the Jon Newton at the Environment Agency, Rob Sage at VWTV and Philip Bishop at TWUL.

1955 Planning permission granted for use of the site for the manufacture of specified chemicals.

1955–1980 The site occupied by Steetly Chemical Works and operated for the production of bromine-based chemicals, including bromate.

1982 The works are decommissioned.

1983 Crest Nicholson Residential Ltd (Crest) purchase the factory site and adjoining land.

1984 Crest are granted planning permission for 30 houses and commence demolition and clearance of buildings and hardstanding from the site.

1983–1985 Intrusive investigations on behalf of Crest. The site is found to be contaminated with organic bromide compounds. The potential for bromide pollution of groundwater is recognised and assessed by consultants to Crest.

1985–1986 Crest granted increased planning permission for 66 houses on the site. Approval requires the removal of contaminated soil to minimum of 1 m depth across the entire site. Excavations completed by August 1986.

1986–1987 Construction of the residential development St Leonard's Court (SLC) begins in November 1986 and is completed by October 1987.

1998–1999 VWTV detect bromate at Essendon PWS at concentrations of 10.8 $\mu g\ l^{-1}$ in December 1999. The EA are informed.

2000 VWTV detect bromate concentrations of $\sim$100 $\mu g\ l^{-1}$, well in excess of the future drinking water standard of 10 $\mu g\ l^{-1}$, at Hatfield PWS. The EA are informed and abstractions for public supply are ceased. A sampling programme is undertaken that identifies St Leonard's Court as the source of the contamination. St Albans District council (SADC) commission intrusive investigations at

the SLC site. The bromate groundwater monitoring programme begins to establish the extent and migration of the contamination.

2002 The monitoring network is expanded and special investigations of surface waters are commenced, including the Ellenbrook and the River Colne. SLC is designated as 'Contaminated Land' based upon the 'significant pollutant linkage' between bromate and bromide in the unsaturated zone and groundwater in the underlying Chalk aquifer. The site is adopted as a 'special site' by the Environment Agency (EA). The EA begin consultation and investigation as to the determination of the 'appropriate persons'.

2003–2004 Bromate concentrations continue to increase at Essendon PWS and the NNR wells, threatening available water resources for pulic supply.

2005 Pumping trial is commenced at Hatfield PWS to assess the possibility of scavenge pumping to protect down-gradient sources at Essendon PWS and the NNR wells. The EA issue a remediation notice to two appropriate persons: Redland Minerals Ltd for the Bromate contamination, and Crest Nicholson Residential Ltd for the Bromide contamination. Both parties appeal.

2007 Appeals to the remediation notice are heard by public inquiry. Scavenge pumping of the Hatfield source is promoted as an interim remediation measure and is incorporated in the Inspectors Remediation Notice. An abstraction license is granted by the EA to VWTV for up to 9 Ml/d for the purposes of groundwater remediation only.

2009 Decision is reached by the Secretary of State to uphold a modified remediation notice against Redland Minerals Ltd and against Crest Nicholson Residential Ltd. Both parties apply for judicial review.

2010 The judicial review case is dismissed.

Appendix B

Business Case for the research

Appendix B

Business Case for the research

The bromate contamination plume represents a major threat to the long-term quality of a number of strategic public water supply sources, and also many private supply sources. The main driver for the research conducted so far, and the funding for the additional research, is the impact of the bromate contamination on water quality and resource availability.

Bromate concentrations above the regulatory standard for drinking water of 10 $\mu g\ l^{-1}$ bromate (UK Water Supply (Water Quality) Regulations 2000) are exceeded, or close to exceedence in major PWS sources operated by both VWP and TWUL. Elevated bromate concentrations in PWS sources are resulting in significant cost ($\sim$£2million since May 2000) to the Water Companies. These costs include:

- The loss of large 9ML/d source since May 2000 when Hatfield Bishops Rise was taken out of supply;
- The cost of blending at Essendon. The future use of Essendon may be restricted depending on future blending arrangements.
- The cost of extra treatment required from the NNR sources/River Lee at Hornsey WTW.

The impact on water resources has lead Veolia Water Partnership (VWP) to plan to install two alternative sources outside of the plume area. These boreholes are likely to replace Hatfield and Essendon by December 2008. The total cost of the relocation amounts to $\sim$£8 million. Additional bromate mitigation and treatment measures are being considered by TWUL to safeguard the continued use of the NNR sources, which will entail further expenditure. The costs of these impacts of the bromate contamination are being largely borne by the water companies (and ultimately the customers). Although the Contaminated Land regime being enforced by the Environment Agency may result in the identified 'polluter' being liable for costs, this process in likely to take many years and the outcome is uncertain.

Water companies are particularly concerned that the future movement of the plume may affect additional large PWS sources. In order to evaluate the most appropriate strategies for the current and future management of groundwater quality, it is essential that additional research focusing on bromate behaviour and movement in the aquifer is undertaken. This will allow the water companies and the Environment Agency to refine their understanding of the contamination within the aquifer and to make predictions as to the future evolution of the plume.

For example, a better understanding of the nature of groundwater flow in the area, will help to characterise and quantify the effect of pumping the Hatfield borehole has on concentrations at other key locations (particularly Essendon and NNR sources). This will allow the feasibility of using scavenge pumping as a means of controlling concentrations at these sources to be evaluated.

Appendix C

Hatfield Pumping Trial statistical analyses

Essendon bromate versus Hatfield abstraction

Regression Analysis: Bromate (ug/L) versus T

The regression equation is
Bromate as BrO3 (ug/l) = 30.1 - 1.43 H(T)

335 cases used, 945 cases contain missing values

Predictor	Coef	SE Coef	T	P
Constant	30.0819	0.6198	48.54	0.000
H(T)	-1.4257	0.1253	-11.38	0.000

S = 5.93134 R-Sq = 28.0% R-Sq(adj) = 27.8%

Analysis of Variance

Source	DF	SS	MS	F	P
Regression	1	4555.7	4555.7	129.49	0.000
Residual Error	333	11715.2	35.2		
Total	334	16270.9			

Regression Analysis: Bromate as BrO3 (ug/l) versus H(T-1)

The regression equation is
Bromate as BrO3 (ug/l) = 29.9 - 1.44 H(T-1)

335 cases used, 945 cases contain missing values

Predictor	Coef	SE Coef	T	P
Constant	29.8580	0.5608	53.24	0.000
H(T-1)	-1.4417	0.1155	-12.48	0.000

S = 5.76994 R-Sq = 31.9% R-Sq(adj) = 31.7%

Analysis of Variance

Source	DF	SS	MS	F	P
Regression	1	5184.6	5184.6	155.73	0.000
Residual Error	333	11086.3	33.3		
Total	334	16270.9			

Regression Analysis: Bromate as BrO3 (ug/l) versus H(T-2)

The regression equation is
Bromate as BrO3 (ug/l) = 30.5 - 1.58 H(T-2)

335 cases used, 945 cases contain missing values

Predictor	Coef	SE Coef	T	P
Constant	30.4704	0.5382	56.62	0.000
H(T-2)	-1.5824	0.1104	-14.33	0.000

S = 5.49730 R-Sq = 38.2% R-Sq(adj) = 38.0%

Analysis of Variance

Source	DF	SS	MS	F	P
Regression	1	6207.5	6207.5	205.41	0.000
Residual Error	333	10063.4	30.2		
Total	334	16270.9			

Regression Analysis: Bromate as BrO3 (ug/l) versus H(T-3)

The regression equation is
Bromate as BrO3 (ug/l) = 30.0 - 1.41 H(T-3)

335 cases used, 945 cases contain missing values

Predictor	Coef	SE Coef	T	P
Constant	30.0122	0.5830	51.48	0.000
H(T-3)	-1.4105	0.1160	-12.16	0.000

S = 5.81719 R-Sq = 30.7% R-Sq(adj) = 30.5%

Analysis of Variance

Source	DF	SS	MS	F	P
Regression	1	5002.3	5002.3	147.82	0.000
Residual Error	333	11268.6	33.8		
Total	334	16270.9			

Regression Analysis: Bromate as BrO3 (ug/l) versus H(T-4)

The regression equation is
Bromate as BrO3 (ug/l) = 29.8 - 1.31 H(T-4)

335 cases used, 945 cases contain missing values

Predictor	Coef	SE Coef	T	P
Constant	29.8401	0.6273	47.57	0.000
H(T-4)	-1.3084	0.1211	-10.80	0.000

S = 6.01551 R-Sq = 25.9% R-Sq(adj) = 25.7%

Analysis of Variance

Source	DF	SS	MS	F	P
Regression	1	4220.9	4220.9	116.64	0.000
Residual Error	333	12050.1	36.2		
Total	334	16270.9			

Regression Analysis: Bromate as BrO3 (ug/l) versus H(T-5)

The regression equation is
Bromate as BrO3 (ug/l) = 29.8 - 1.28 H(T-5)

334 cases used, 946 cases contain missing values

```
Predictor     Coef  SE Coef      T      P
Constant   29.7661   0.6775  43.94  0.000
H(T-5)     -1.2757   0.1308  -9.76  0.000


S = 6.11821   R-Sq = 22.3%   R-Sq(adj) = 22.0%


Analysis of Variance

Source           DF       SS      MS      F      P
Regression        1   3562.6  3562.6  95.17  0.000
Residual Error  332  12427.6    37.4
Total           333  15990.2
```

Regression Analysis: Bromate as BrO3 (ug/l) versus H(T-6)

```
The regression equation is
Bromate as BrO3 (ug/l) = 28.7 - 1.09 H(T-6)


333 cases used, 947 cases contain missing values


Predictor     Coef  SE Coef      T      P
Constant   28.6746   0.6490  44.19  0.000
H(T-6)     -1.0912   0.1281  -8.52  0.000


S = 6.26975   R-Sq = 18.0%   R-Sq(adj) = 17.7%


Analysis of Variance

Source           DF       SS      MS      F      P
Regression        1   2851.0  2851.0  72.53  0.000
Residual Error  331  13011.5    39.3
Total           332  15862.6
```

Regression Analysis: Bromate as BrO3 (ug/l) versus H(T-7)

```
The regression equation is
Bromate as BrO3 (ug/l) = 28.4 - 1.08 H(T-7)


333 cases used, 947 cases contain missing values


Predictor     Coef  SE Coef      T      P
Constant   28.4450   0.6316  45.04  0.000
H(T-7)     -1.0846   0.1288  -8.42  0.000


S = 6.28231   R-Sq = 17.6%   R-Sq(adj) = 17.4%


Analysis of Variance

Source           DF       SS      MS      F      P
Regression        1   2798.9  2798.9  70.92  0.000
Residual Error  331  13063.7    39.5
Total           332  15862.6
```

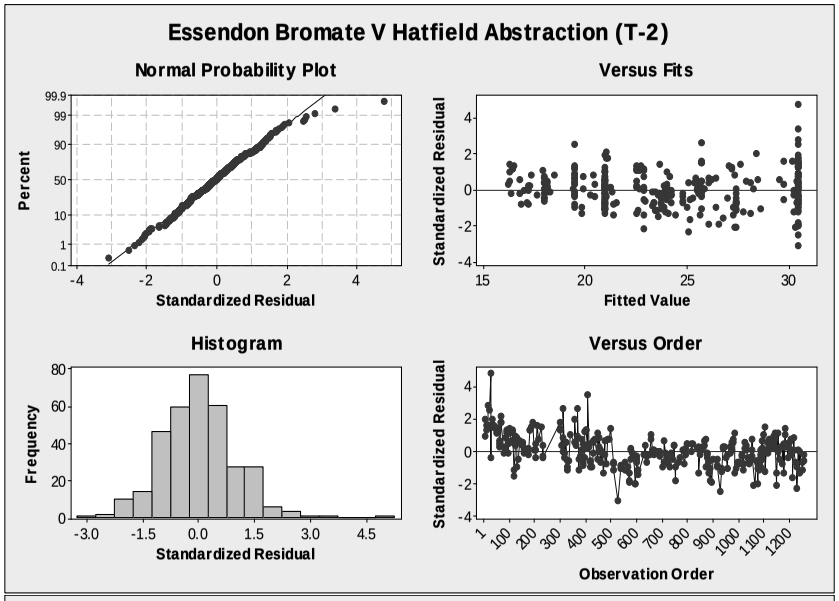

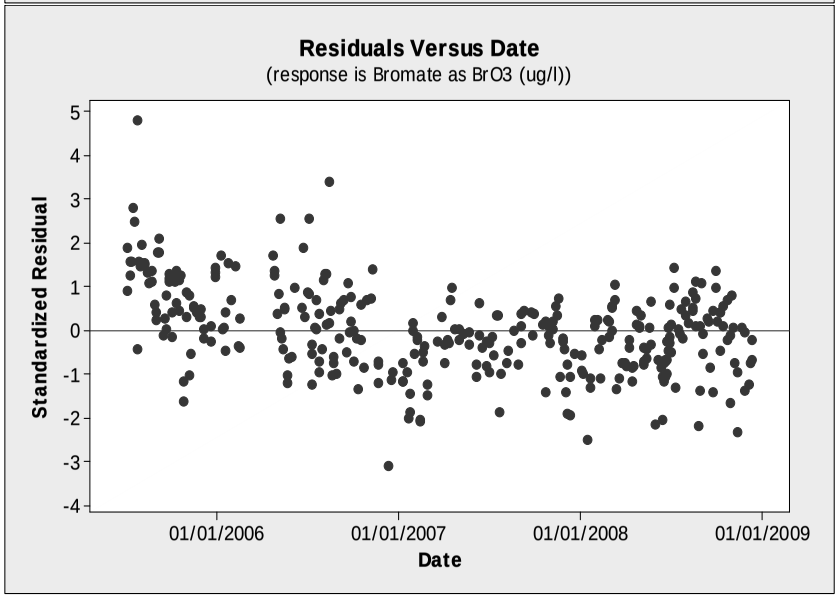

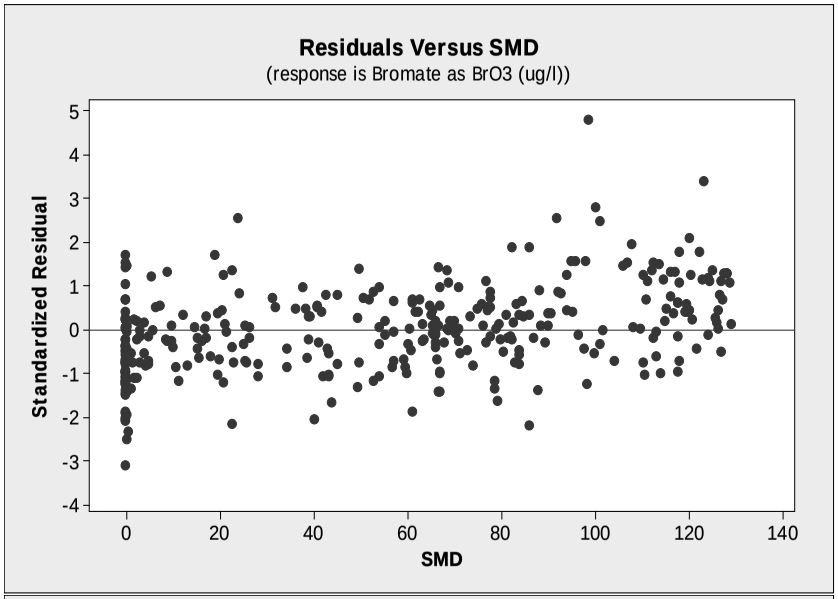
Residuals Versus SMD
(response is Bromate as BrO3 (ug/l))
Standardized Residual
SMD

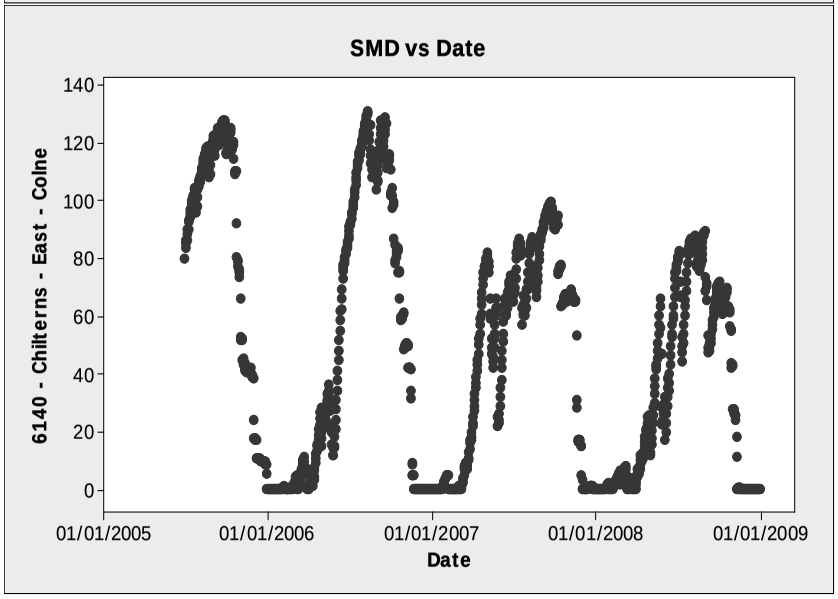
SMD vs Date
6140 - Chilterns - East - Colne
Date

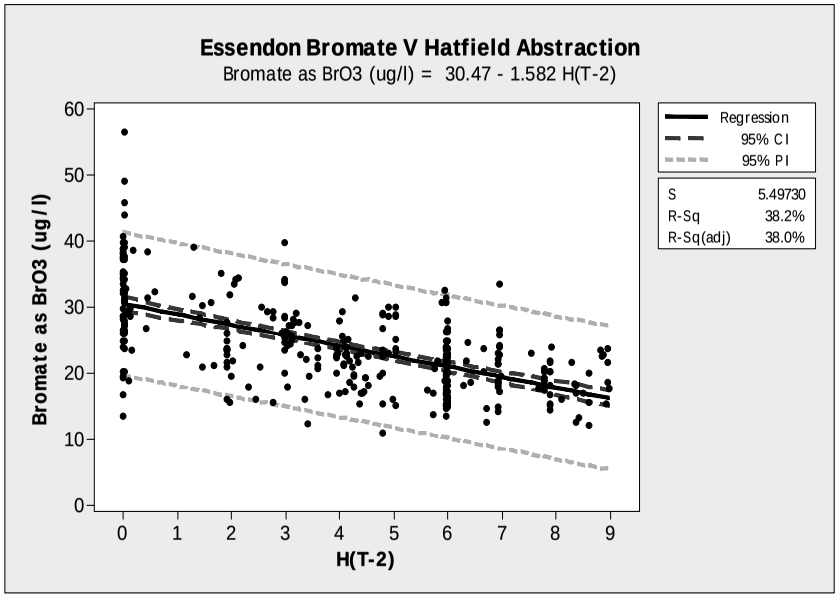
Essendon Bromate V Hatfield Abstraction
Bromate as BrO3 (ug/l) = 30.47 - 1.582 H(T-2)
Regression
95% CI
95% PI
S 5.49730
R-Sq 38.2%
R-Sq(adj) 38.0%
Bromate as BrO3 (ug/l)
H(T-2)

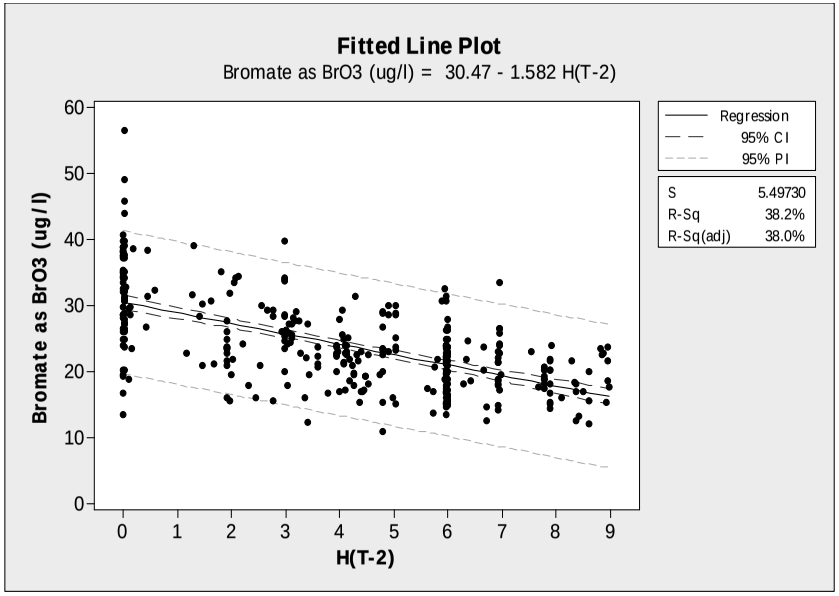
Fitted Line Plot
Bromate as BrO3 (ug/l) = 30.47 - 1.582 H(T-2)
Regression
95% CI
95% PI
S 5.49730
R-Sq 38.2%
R-Sq(adj) 38.0%
Bromate as BrO3 (ug/l)
H(T-2)

Regression Analysis: Bromate as BrO3 (ug/l) versus H(T-2), SMD - 6140

The regression equation is
Bromate as BrO3 (ug/l) = 27.8 - 1.66 H(T-2) + 0.0543 SMD - 6140

335 cases used, 945 cases contain missing values

Predictor	Coef	SE Coef	T	P
Constant	27.7737	0.5847	47.50	0.000
H(T-2)	-1.6599	0.1008	-16.47	0.000
SMD - 6140	0.054310	0.006448	8.42	0.000

S = 4.99745 R-Sq = 49.0% R-Sq(adj) = 48.7%

Analysis of Variance

Source	DF	SS	MS	F	P
Regression	2	7979.4	3989.7	159.75	0.000
Residual Error	332	8291.5	25.0		
Total	334	16270.9			

Source	DF	Seq SS
H(T-2)	1	6207.5
SMD - 6140	1	1771.9

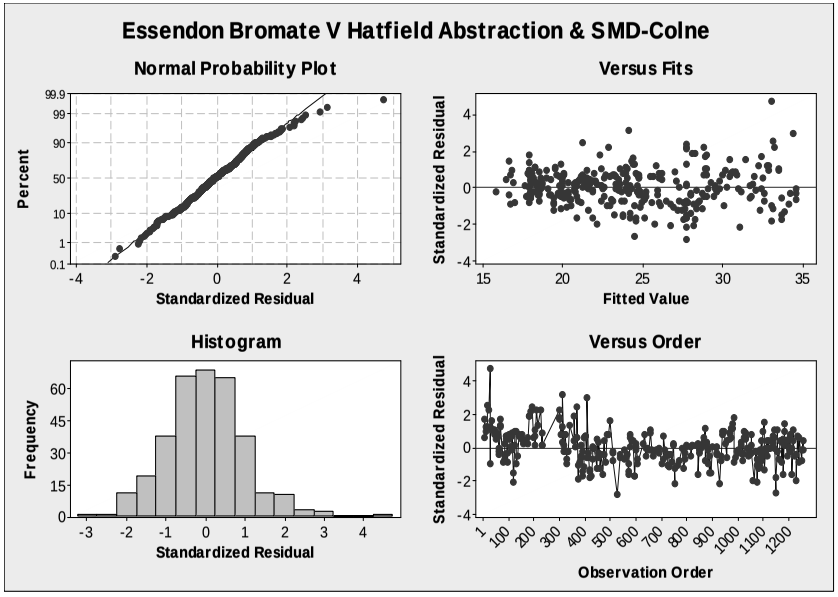

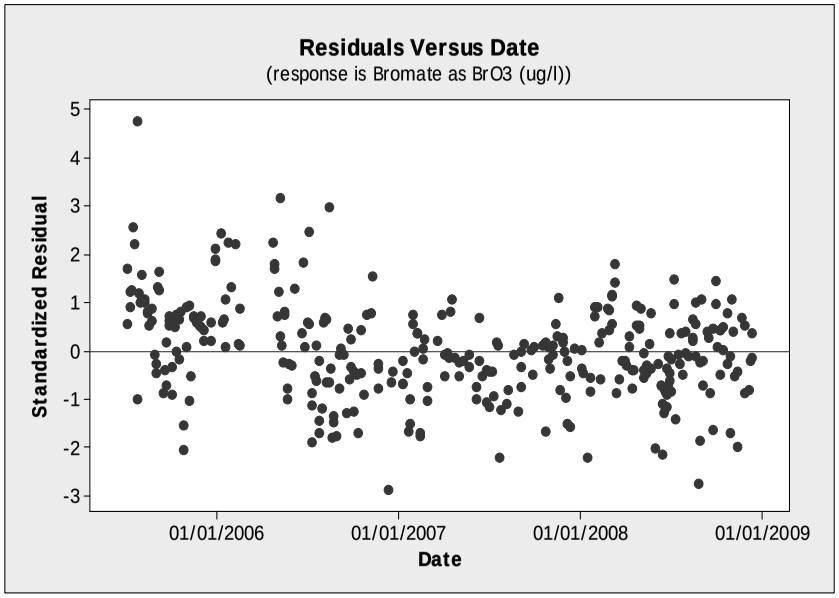

Amwell Hill bromate versus Hatfield abstraction

Regression Analysis: Bromate as BrO3 (ug/l) versus H(T)

The regression equation is
Bromate as BrO3 (ug/l) = 9.81 - 0.246 H(T)

140 cases used, 1140 cases contain missing values

Predictor	Coef	SE Coef	T	P
Constant	9.8098	0.7629	12.86	0.000
H(T)	-0.2463	0.1530	-1.61	0.110

S = 5.04930 R-Sq = 1.8% R-Sq(adj) = 1.1%

Analysis of Variance

Source	DF	SS	MS	F	P
Regression	1	66.10	66.10	2.59	0.110
Residual Error	138	3518.36	25.50		
Total	139	3584.46			

Regression Analysis: Bromate as BrO3 (ug/l) versus H(T-1)

The regression equation is
Bromate as BrO3 (ug/l) = 9.65 - 0.226 H(T-1)

140 cases used, 1140 cases contain missing values

Predictor	Coef	SE Coef	T	P
Constant	9.6549	0.7078	13.64	0.000
H(T-1)	-0.2262	0.1479	-1.53	0.128

S = 5.05383 R-Sq = 1.7% R-Sq(adj) = 1.0%

Analysis of Variance

Source	DF	SS	MS	F	P
Regression	1	59.78	59.78	2.34	0.128
Residual Error	138	3524.69	25.54		
Total	139	3584.46			

Regression Analysis: Bromate as BrO3 (ug/l) versus H(T-2)

The regression equation is
Bromate as BrO3 (ug/l) = 9.58 - 0.194 H(T-2)

138 cases used, 1142 cases contain missing values

Predictor	Coef	SE Coef	T	P
Constant	9.5796	0.6867	13.95	0.000
H(T-2)	-0.1943	0.1462	-1.33	0.186

S = 5.04850 R-Sq = 1.3% R-Sq(adj) = 0.6%

Analysis of Variance

Source	DF	SS	MS	F	P
Regression	1	45.04	45.04	1.77	0.186
Residual Error	136	3466.27	25.49		
Total	137	3511.32			

Regression Analysis: Bromate as BrO3 (ug/l) versus H(T-3)

The regression equation is
Bromate as BrO3 (ug/l) = 9.70 - 0.192 H(T-3)

137 cases used, 1143 cases contain missing values

Predictor	Coef	SE Coef	T	P
Constant	9.6970	0.7308	13.27	0.000
H(T-3)	-0.1923	0.1478	-1.30	0.196

S = 5.01945 R-Sq = 1.2% R-Sq(adj) = 0.5%

Analysis of Variance

Source	DF	SS	MS	F	P
Regression	1	42.64	42.64	1.69	0.196
Residual Error	135	3401.30	25.19		
Total	136	3443.94			

Regression Analysis: Bromate as BrO3 (ug/l) versus H(T-4)

The regression equation is
Bromate as BrO3 (ug/l) = 10.2 - 0.263 H(T-4)

135 cases used, 1145 cases contain missing values

Predictor	Coef	SE Coef	T	P
Constant	10.1753	0.7859	12.95	0.000
H(T-4)	-0.2632	0.1485	-1.77	0.079

S = 4.97687 R-Sq = 2.3% R-Sq(adj) = 1.6%

Analysis of Variance

Source	DF	SS	MS	F	P
Regression	1	77.86	77.86	3.14	0.079
Residual Error	133	3294.31	24.77		
Total	134	3372.17			

Regression Analysis: Bromate as BrO3 (ug/l) versus H(T-5)

The regression equation is

Bromate as BrO3 (ug/l) = 10.6 - 0.332 H(T-5)

132 cases used, 1148 cases contain missing values

Predictor	Coef	SE Coef	T	P
Constant	10.5789	0.7819	13.53	0.000
H(T-5)	-0.3325	0.1514	-2.20	0.030

S = 4.91246 R-Sq = 3.6% R-Sq(adj) = 2.8%

Analysis of Variance

Source	DF	SS	MS	F	P
Regression	1	116.44	116.44	4.82	0.030
Residual Error	130	3137.19	24.13		
Total	131	3253.63			

Regression Analysis: Bromate as BrO3 (ug/l) versus H(T-6)

The regression equation is
Bromate as BrO3 (ug/l) = 10.5 - 0.311 H(T-6)

130 cases used, 1150 cases contain missing values

Predictor	Coef	SE Coef	T	P
Constant	10.5225	0.7461	14.10	0.000
H(T-6)	-0.3107	0.1502	-2.07	0.041

S = 4.86986 R-Sq = 3.2% R-Sq(adj) = 2.5%

Analysis of Variance

Source	DF	SS	MS	F	P
Regression	1	101.44	101.44	4.28	0.041
Residual Error	128	3035.59	23.72		
Total	129	3137.03			

Regression Analysis: Bromate as BrO3 (ug/l) versus H(T-7)

The regression equation is
Bromate as BrO3 (ug/l) = 10.0 - 0.166 H(T-7)

128 cases used, 1152 cases contain missing values

Predictor	Coef	SE Coef	T	P
Constant	10.0003	0.7198	13.89	0.000
H(T-7)	-0.1658	0.1537	-1.08	0.283

S = 4.86991 R-Sq = 0.9% R-Sq(adj) = 0.1%

Analysis of Variance

Source	DF	SS	MS	F	P
Regression	1	27.61	27.61	1.16	0.283
Residual Error	126	2988.22	23.72		
Total	127	3015.83			

Residual Plots for Bromate as BrO3 (ug/l)

Residuals from Bromate as BrO3 (ug/l) vs Date

Residuals from Bromate as BrO3 (ug/l) vs 6600 - Lee Chalk

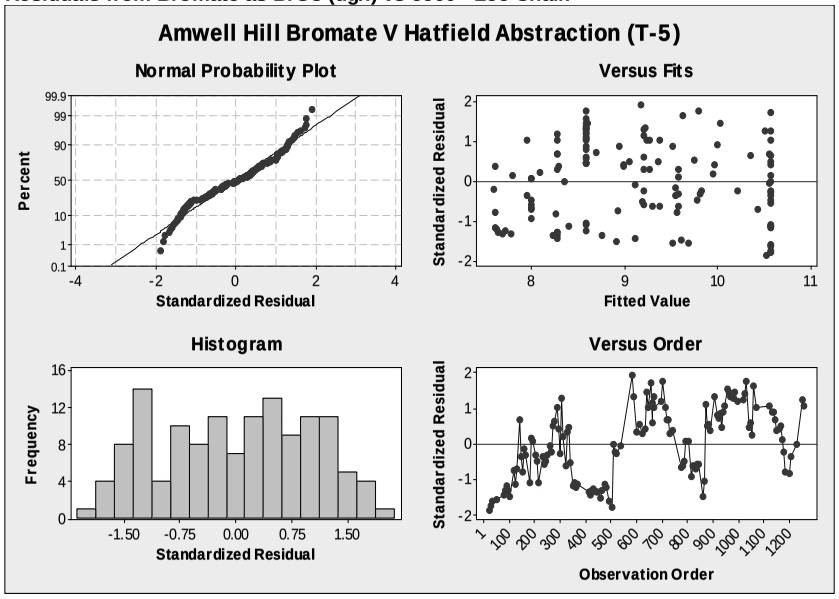

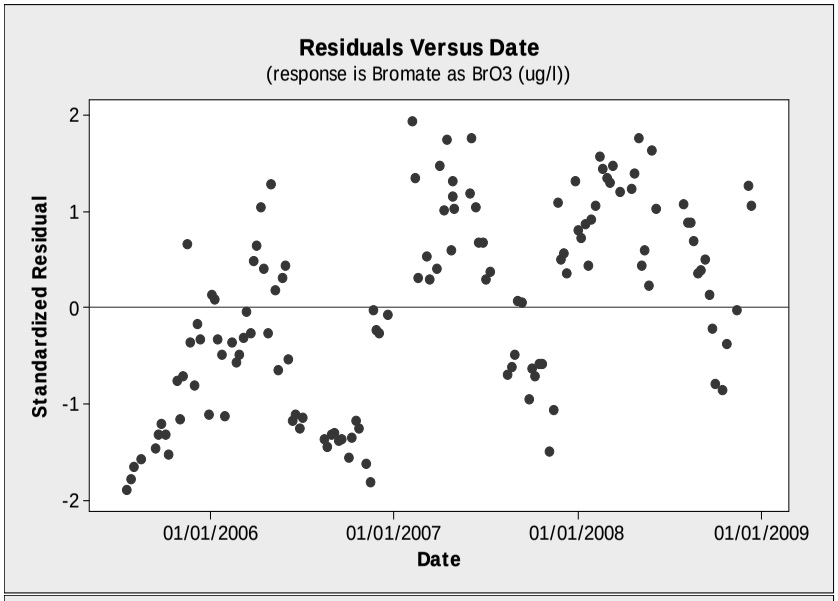

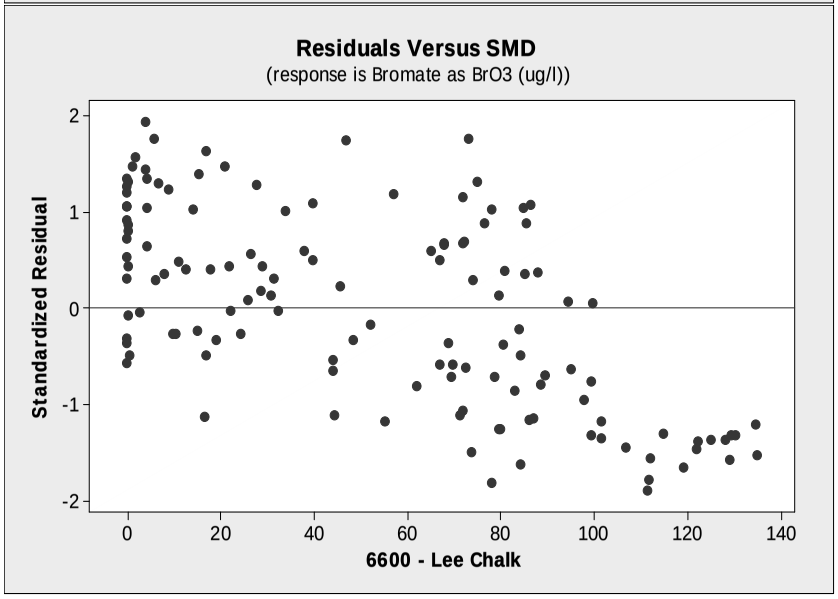

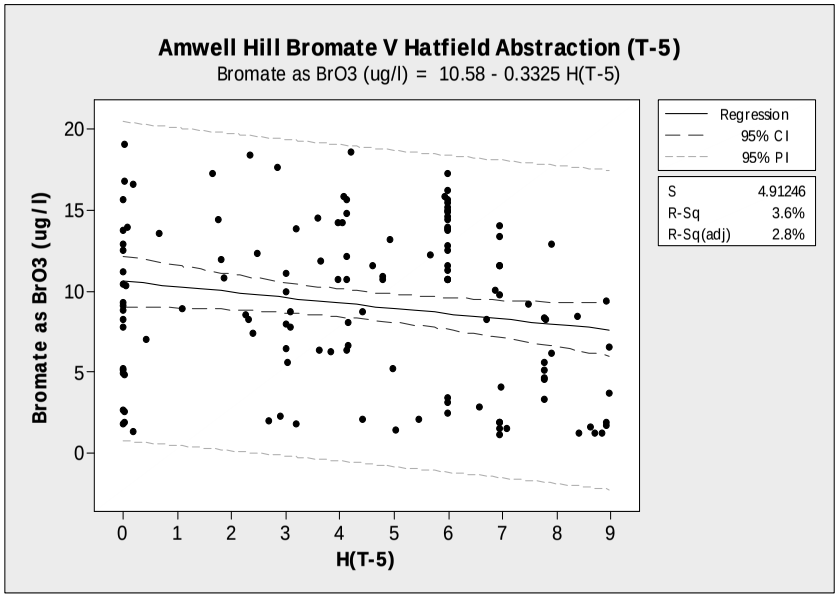

Regression Analysis: Log(BrO3) versus H(T-5)

The regression equation is
Log(BrO3) = 0.971 - 0.0255 H(T-5)

132 cases used, 1148 cases contain missing values

Predictor	Coef	SE Coef	T	P
Constant	0.97134	0.05276	18.41	0.000
H(T-5)	-0.02553	0.01021	-2.50	0.014

S = 0.331481 R-Sq = 4.6% R-Sq(adj) = 3.9%

Analysis of Variance

Source	DF	SS	MS	F	P
Regression	1	0.6864	0.6864	6.25	0.014
Residual Error	130	14.2844	0.1099		
Total	131	14.9708			

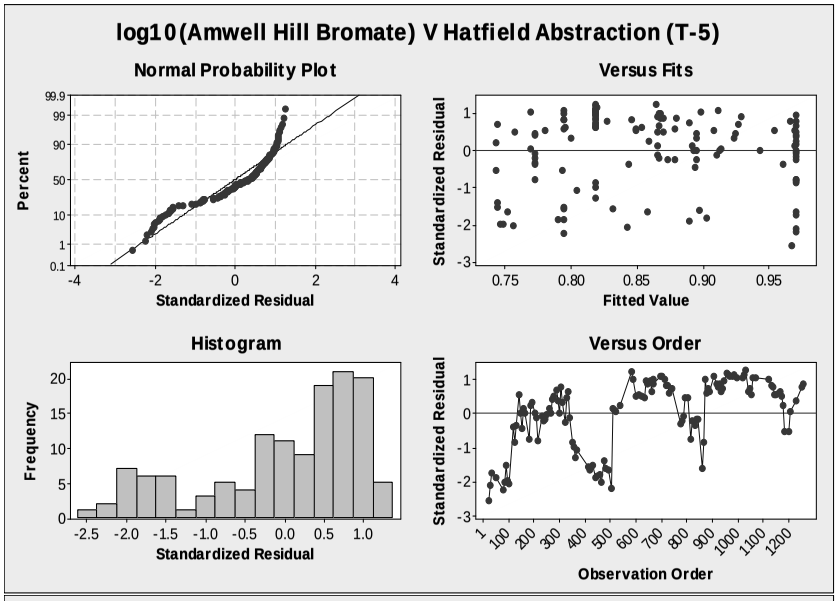

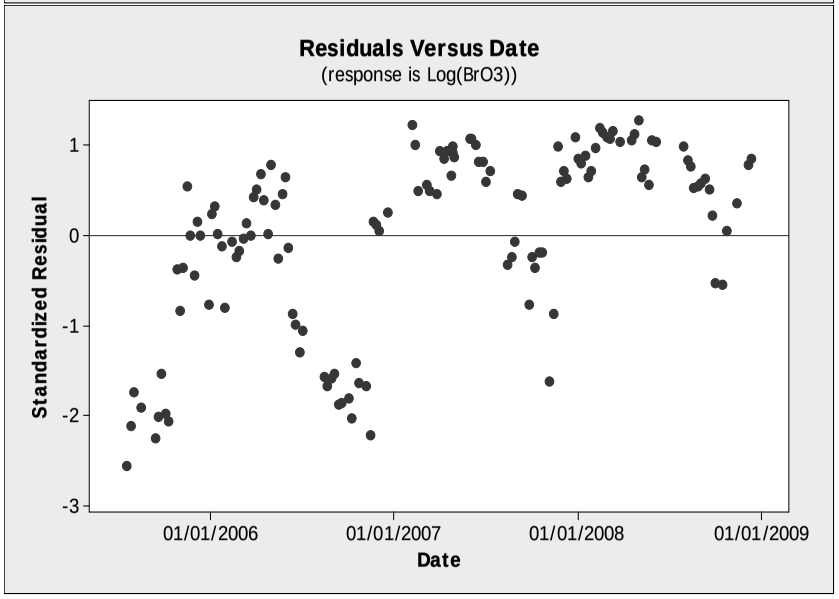

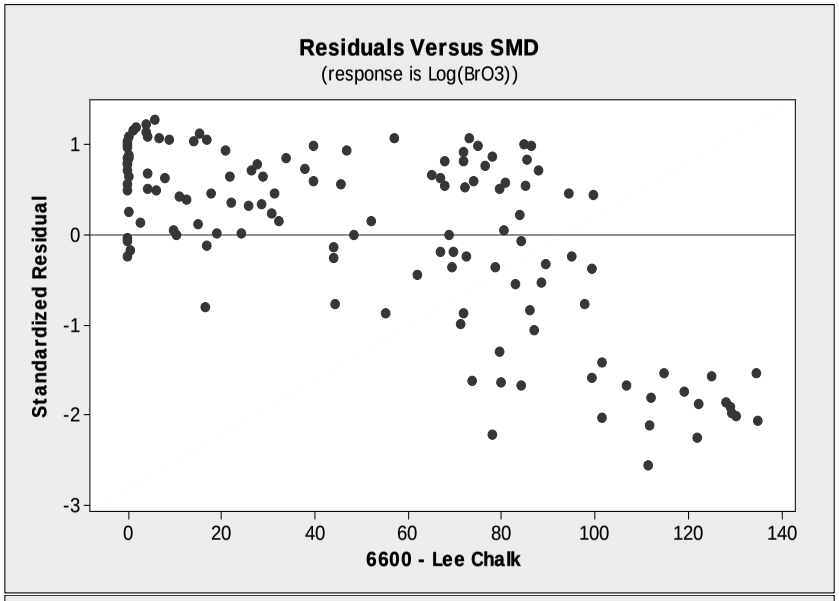

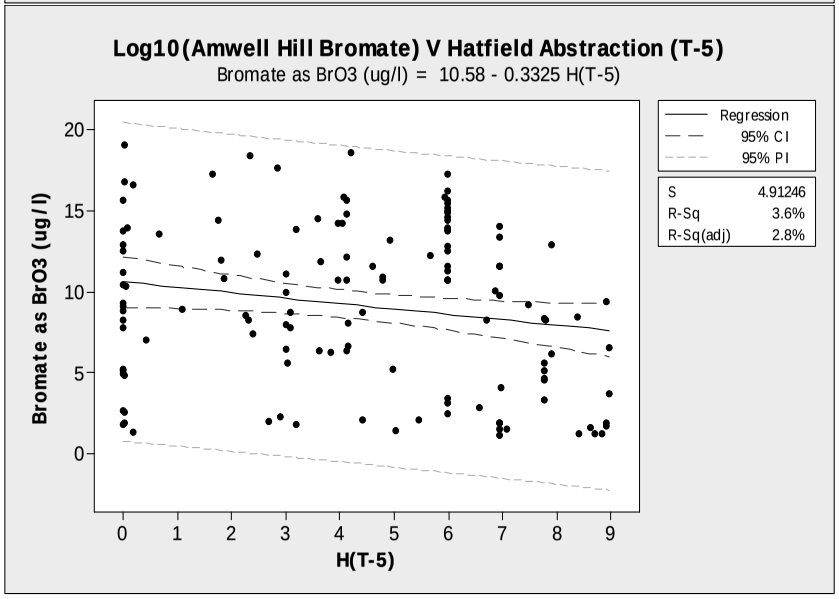

Fitted Line: Bromate as BrO3 (ug/l) versus H(T-5)

Regression Analysis: Log(BrO3) versus H(T-5), 6600 - Lee Chalk

The regression equation is
Log(BrO3) = 1.17 + 0.00429 H(T-5) - 0.00617 6600 - Lee Chalk

132 cases used, 1148 cases contain missing values

Predictor	Coef	SE Coef	T	P
Constant	1.16628	0.03976	29.34	0.000
H(T-5)	0.004287	0.007452	0.58	0.566
6600 - Lee Chalk	-0.0061678	0.0005116	-12.06	0.000

S = 0.228179 R-Sq = 55.1% R-Sq(adj) = 54.4%

Analysis of Variance

Source	DF	SS	MS	F	P
Regression	2	8.2543	4.1272	79.27	0.000
Residual Error	129	6.7165	0.0521		
Total	131	14.9708			

Source	DF	Seq SS
H(T-5)	1	0.6864
6600 - Lee Chalk	1	7.5679

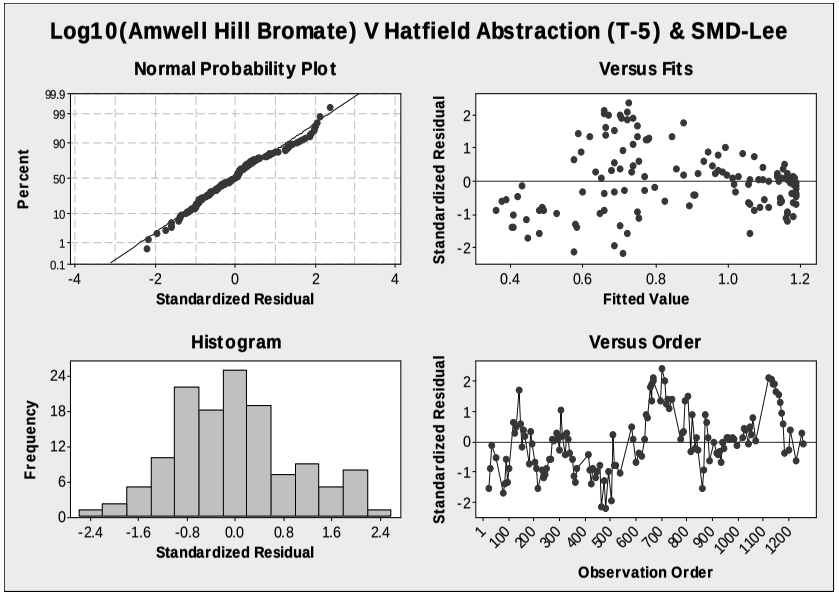

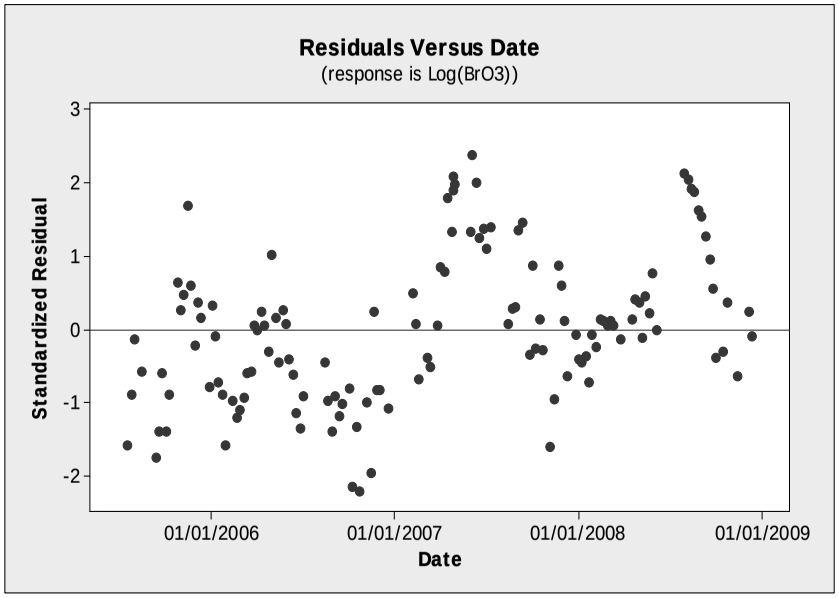

Hoddesdon bromate versus Hatfield abstraction

Regression Analysis: Bromate as BrO3 (ug/l) versus H(T)

The regression equation is
Bromate as BrO3 (ug/l) = 30.1 - 1.50 H(T)

163 cases used, 1117 cases contain missing values

Predictor	Coef	SE Coef	T	P
Constant	30.092	1.430	21.05	0.000
H(T)	-1.4977	0.2935	-5.10	0.000

S = 9.96038 R-Sq = 13.9% R-Sq(adj) = 13.4%

Analysis of Variance

Source	DF	SS	MS	F	P
Regression	1	2584.1	2584.1	26.05	0.000
Residual Error	161	15972.7	99.2		
Total	162	18556.7			

Regression Analysis: Bromate as BrO3 (ug/l) versus H(T-1)

The regression equation is
Bromate as BrO3 (ug/l) = 28.9 - 1.30 H(T-1)

163 cases used, 1117 cases contain missing values

Predictor	Coef	SE Coef	T	P
Constant	28.858	1.340	21.53	0.000
H(T-1)	-1.3023	0.2885	-4.51	0.000

S = 10.1149 R-Sq = 11.2% R-Sq(adj) = 10.7%

Analysis of Variance

Source	DF	SS	MS	F	P
Regression	1	2084.5	2084.5	20.37	0.000
Residual Error	161	16472.2	102.3		
Total	162	18556.7			

Regression Analysis: Bromate as BrO3 (ug/l) versus H(T-2)

The regression equation is
Bromate as BrO3 (ug/l) = 28.9 - 1.29 H(T-2)

161 cases used, 1119 cases contain missing values

Predictor	Coef	SE Coef	T	P
Constant	28.900	1.281	22.57	0.000
H(T-2)	-1.2927	0.2762	-4.68	0.000

S = 9.96880 R-Sq = 12.1% R-Sq(adj) = 11.6%

Analysis of Variance

Source	DF	SS	MS	F	P
Regression	1	2177.1	2177.1	21.91	0.000
Residual Error	159	15800.9	99.4		
Total	160	17978.0			

Regression Analysis: Bromate as BrO3 (ug/l) versus H(T-3)

The regression equation is
Bromate as BrO3 (ug/l) = 30.6 - 1.54 H(T-3)

159 cases used, 1121 cases contain missing values

Predictor	Coef	SE Coef	T	P
Constant	30.595	1.352	22.63	0.000
H(T-3)	-1.5435	0.2744	-5.63	0.000

S = 9.63218 R-Sq = 16.8% R-Sq(adj) = 16.2%

Analysis of Variance

Source	DF	SS	MS	F	P
Regression	1	2936.4	2936.4	31.65	0.000
Residual Error	157	14566.3	92.8		
Total	158	17502.6			

Regression Analysis: Bromate as BrO3 (ug/l) versus H(T-4)

The regression equation is
Bromate as BrO3 (ug/l) = 32.9 - 1.90 H(T-4)

157 cases used, 1123 cases contain missing values

Predictor	Coef	SE Coef	T	P
Constant	32.913	1.401	23.49	0.000
H(T-4)	-1.8999	0.2673	-7.11	0.000

S = 9.16736 R-Sq = 24.6% R-Sq(adj) = 24.1%

Analysis of Variance

Source	DF	SS	MS	F	P
Regression	1	4245.5	4245.5	50.52	0.000
Residual Error	155	13026.3	84.0		
Total	156	17271.8			

Regression Analysis: Bromate as BrO3 (ug/l) versus H(T-5)

The regression equation is
Bromate as BrO3 (ug/l) = 31.9 - 1.78 H(T-5)

155 cases used, 1125 cases contain missing values

Predictor	Coef	SE Coef	T	P
Constant	31.891	1.358	23.48	0.000
H(T-5)	-1.7775	0.2702	-6.58	0.000

S = 9.23033 R-Sq = 22.1% R-Sq(adj) = 21.5%

Analysis of Variance

Source	DF	SS	MS	F	P
Regression	1	3688.3	3688.3	43.29	0.000
Residual Error	153	13035.5	85.2		
Total	154	16723.7			

Regression Analysis: Bromate as BrO3 (ug/l) versus H(T-6)

The regression equation is
Bromate as BrO3 (ug/l) = 31.5 - 1.72 H(T-6)

153 cases used, 1127 cases contain missing values

Predictor	Coef	SE Coef	T	P
Constant	31.456	1.314	23.94	0.000
H(T-6)	-1.7190	0.2686	-6.40	0.000

S = 9.25704 R-Sq = 21.3% R-Sq(adj) = 20.8%

Analysis of Variance

Source	DF	SS	MS	F	P
Regression	1	3508.8	3508.8	40.95	0.000
Residual Error	151	12939.6	85.7		
Total	152	16448.5			

Regression Analysis: Bromate as BrO3 (ug/l) versus H(T-7)

The regression equation is
Bromate as BrO3 (ug/l) = 31.7 - 1.73 H(T-7)

151 cases used, 1129 cases contain missing values

Predictor	Coef	SE Coef	T	P
Constant	31.699	1.351	23.46	0.000
H(T-7)	-1.7299	0.2768	-6.25	0.000

S = 9.27060 R-Sq = 20.8% R-Sq(adj) = 20.2%

Analysis of Variance

Source	DF	SS	MS	F	P
Regression	1	3355.4	3355.4	39.04	0.000
Residual Error	149	12805.7	85.9		
Total	150	16161.1			

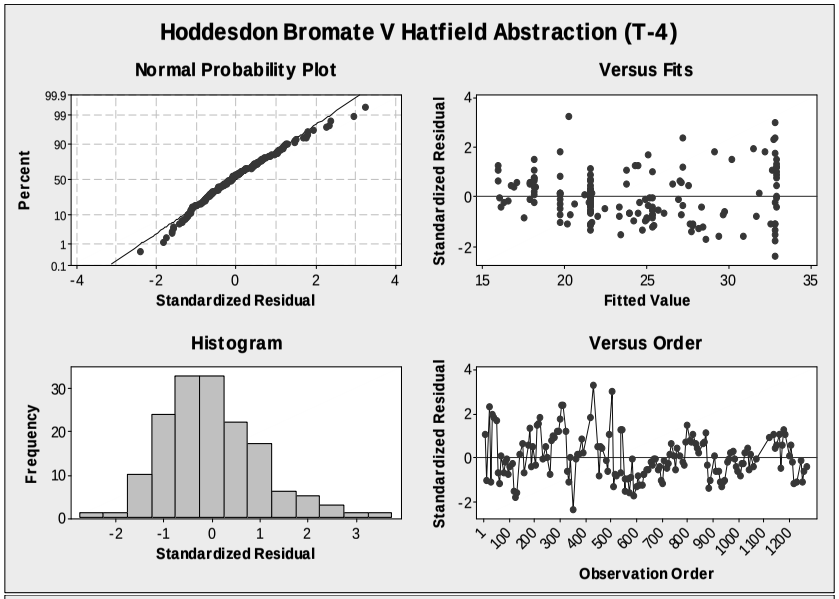

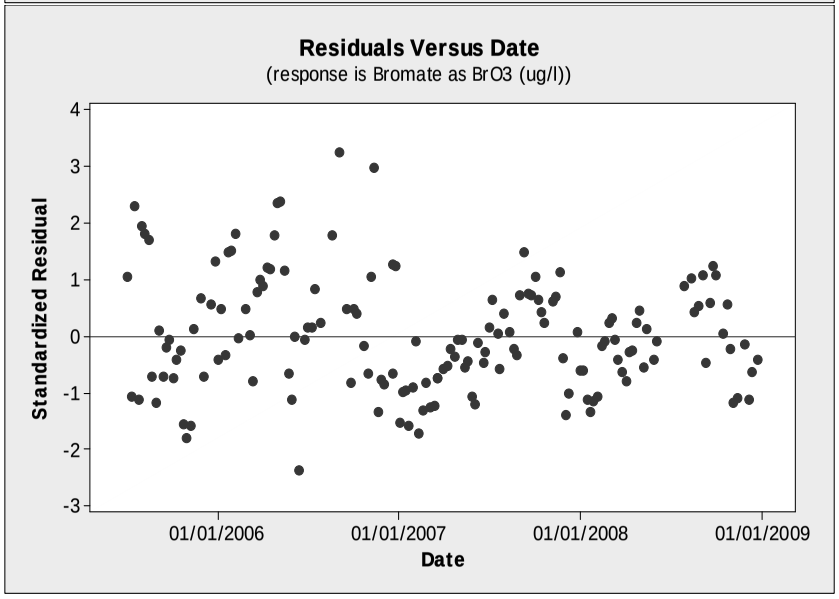

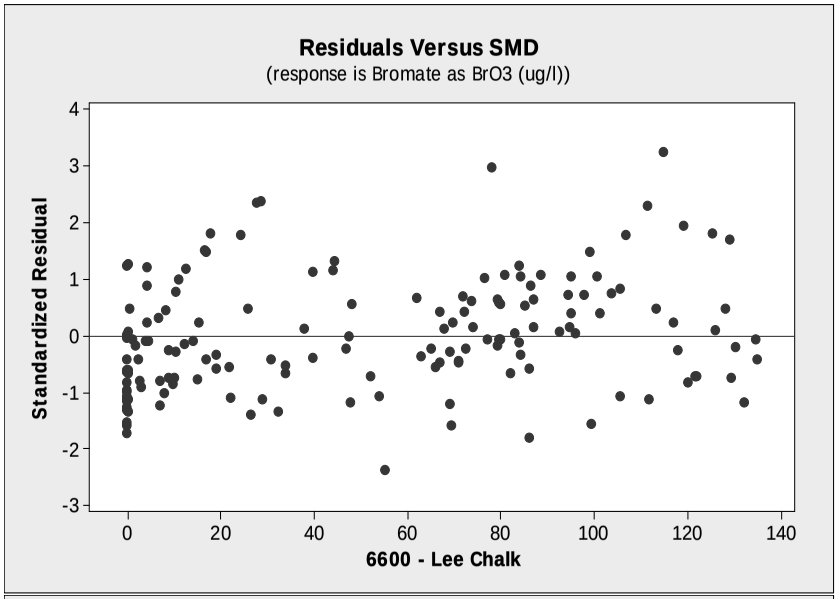

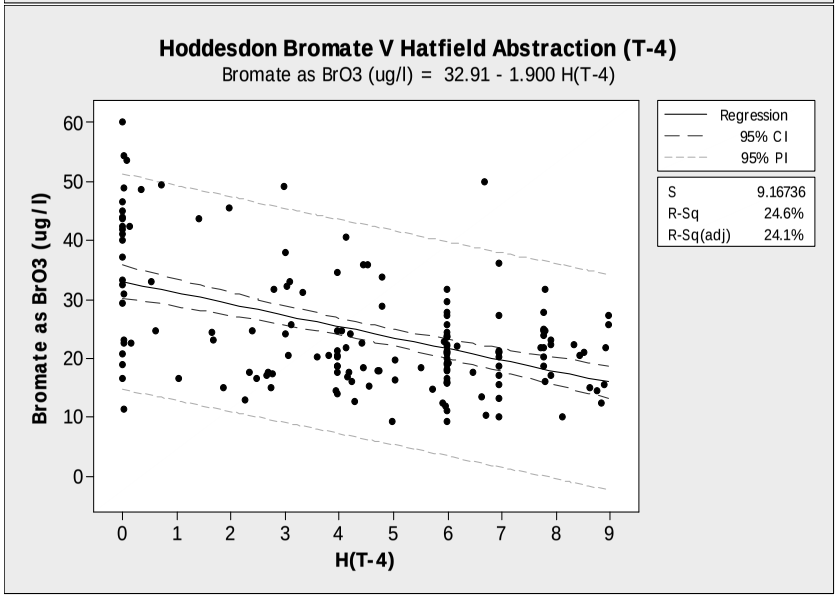

Regression Analysis: Log(BrO3) versus H(T-4)

The regression equation is
Log(BrO3) = 1.48 - 0.0288 H(T-4)

157 cases used, 1123 cases contain missing values

Predictor	Coef	SE Coef	T	P
Constant	1.48051	0.02381	62.19	0.000
H(T-4)	-0.028756	0.004541	-6.33	0.000

S = 0.155743 R-Sq = 20.6% R-Sq(adj) = 20.0%

Analysis of Variance

Source	DF	SS	MS	F	P
Regression	1	0.97253	0.97253	40.09	0.000
Residual Error	155	3.75967	0.02426		
Total	156	4.73220			

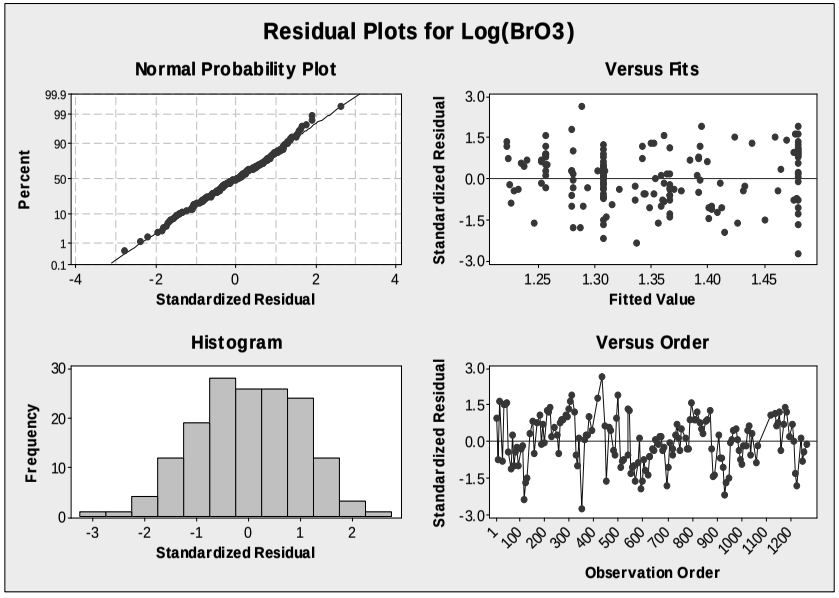

Regression Analysis: Bromate as BrO3 versus H(T-4), 6600 - Lee Chalk

The regression equation is
Bromate as BrO3 (ug/l) = 31.1 - 2.19 H(T-4) + 0.0602 6600 - Lee Chalk

157 cases used, 1123 cases contain missing values

Predictor	Coef	SE Coef	T	P
Constant	31.082	1.450	21.43	0.000

```
H(T-4)           -2.1915   0.2712  -8.08  0.000
6600 - Lee Chalk  0.06018  0.01717   3.51  0.001


S = 8.85068   R-Sq = 30.2%   R-Sq(adj) = 29.2%


Analysis of Variance

Source           DF       SS      MS      F      P
Regression        2   5208.3  2604.1  33.24  0.000
Residual Error  154  12063.5    78.3
Total           156  17271.8


Source           DF  Seq SS
H(T-4)            1  4245.5
6600 - Lee Chalk  1   962.7
```

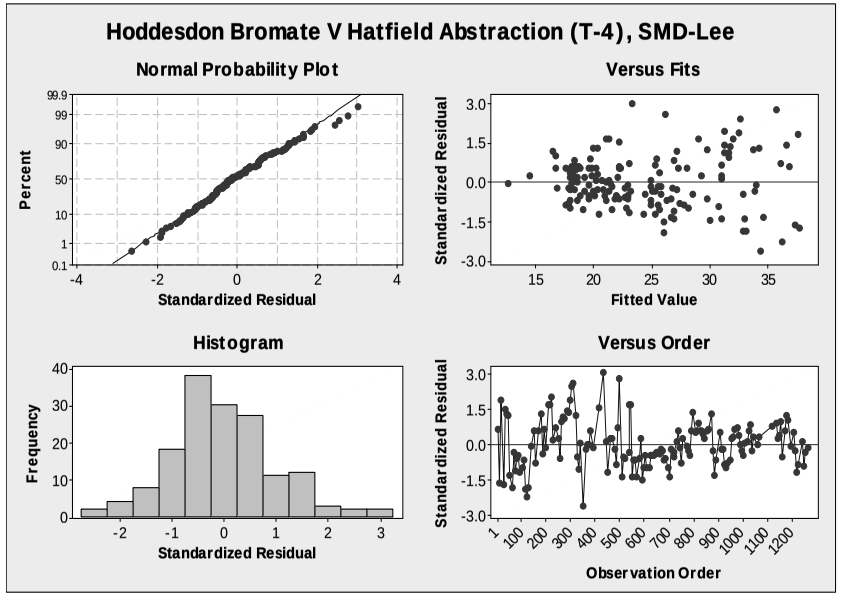

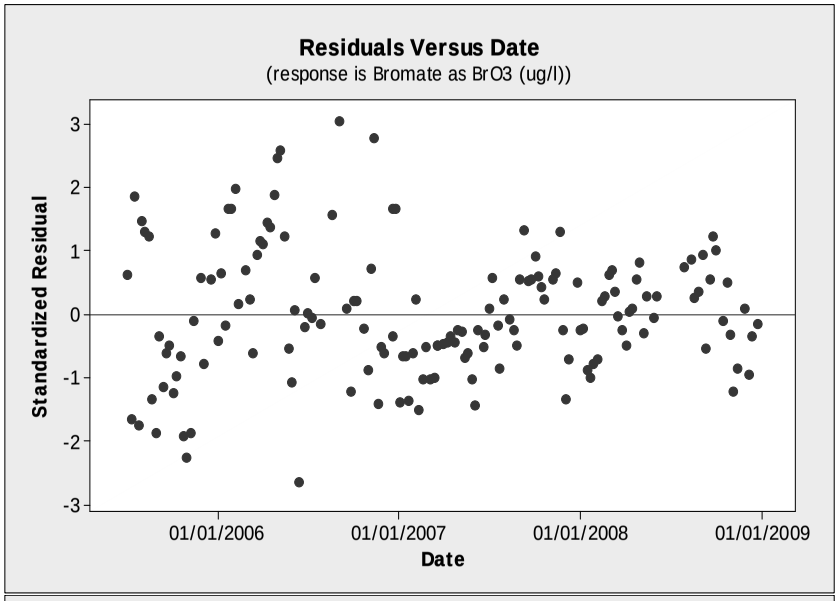

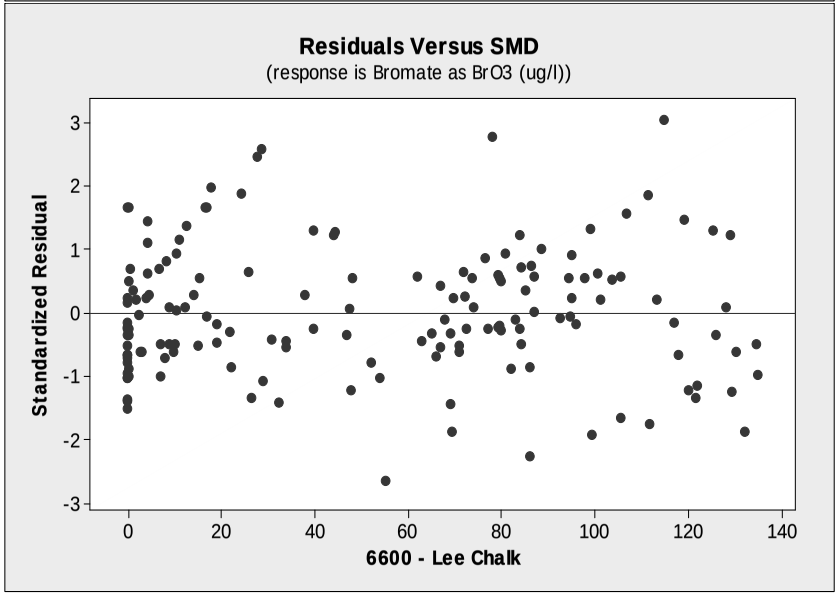

Regression Analysis: Bromate as BrO3 (ug/l) versus H(T)

The regression equation is
Bromate as BrO3 (ug/l) = 20.1 - 0.599 H(T)

167 cases used, 1113 cases contain missing values

Predictor	Coef	SE Coef	T	P
Constant	20.107	1.115	18.03	0.000
H(T)	-0.5987	0.2260	-2.65	0.009

S = 7.85914 R-Sq = 4.1% R-Sq(adj) = 3.5%

Analysis of Variance

Source	DF	SS	MS	F	P
Regression	1	433.50	433.50	7.02	0.009
Residual Error	165	10191.39	61.77		
Total	166	10624.89			

Regression Analysis: Bromate as BrO3 (ug/l) versus H(T-1)

The regression equation is
Bromate as BrO3 (ug/l) = 20.0 - 0.614 H(T-1)

167 cases used, 1113 cases contain missing values

Predictor	Coef	SE Coef	T	P
Constant	20.002	1.042	19.19	0.000
H(T-1)	-0.6138	0.2193	-2.80	0.006

S = 7.84057 R-Sq = 4.5% R-Sq(adj) = 4.0%

Analysis of Variance

Source	DF	SS	MS	F	P
Regression	1	481.60	481.60	7.83	0.006
Residual Error	165	10143.29	61.47		
Total	166	10624.89			

Regression Analysis: Bromate as BrO3 (ug/l) versus H(T-2)

The regression equation is
Bromate as BrO3 (ug/l) = 19.7 - 0.558 H(T-2)

166 cases used, 1114 cases contain missing values

Predictor	Coef	SE Coef	T	P
Constant	19.7126	0.9846	20.02	0.000
H(T-2)	-0.5575	0.2112	-2.64	0.009

S = 7.86399 R-Sq = 4.1% R-Sq(adj) = 3.5%

Analysis of Variance

Source	DF	SS	MS	F	P
Regression	1	430.95	430.95	6.97	0.009
Residual Error	164	10142.15	61.84		
Total	165	10573.10			

Regression Analysis: Bromate as BrO3 (ug/l) versus H(T-3)

The regression equation is
Bromate as BrO3 (ug/l) = 19.4 - 0.417 H(T-3)

165 cases used, 1115 cases contain missing values

Predictor	Coef	SE Coef	T	P
Constant	19.407	1.090	17.80	0.000
H(T-3)	-0.4167	0.2211	-1.88	0.061

S = 7.94870 R-Sq = 2.1% R-Sq(adj) = 1.5%

Analysis of Variance

Source	DF	SS	MS	F	P
Regression	1	224.34	224.34	3.55	0.061
Residual Error	163	10298.64	63.18		
Total	164	10522.98			

Regression Analysis: Bromate as BrO3 (ug/l) versus H(T-4)

The regression equation is
Bromate as BrO3 (ug/l) = 20.9 - 0.672 H(T-4)

163 cases used, 1117 cases contain missing values

Predictor	Coef	SE Coef	T	P
Constant	20.879	1.156	18.05	0.000
H(T-4)	-0.6717	0.2178	-3.08	0.002

S = 7.76930 R-Sq = 5.6% R-Sq(adj) = 5.0%

Analysis of Variance

Source	DF	SS	MS	F	P
Regression	1	573.85	573.85	9.51	0.002
Residual Error	161	9718.28	60.36		
Total	162	10292.13			

Regression Analysis: Bromate as BrO3 (ug/l) versus H(T-5)

The regression equation is

Bromate as BrO3 (ug/l) = 21.4 - 0.802 H(T-5)

161 cases used, 1119 cases contain missing values

Predictor	Coef	SE Coef	T	P
Constant	21.401	1.168	18.32	0.000
H(T-5)	-0.8018	0.2238	-3.58	0.000

S = 7.73725 R-Sq = 7.5% R-Sq(adj) = 6.9%

Analysis of Variance

Source	DF	SS	MS	F	P
Regression	1	768.65	768.65	12.84	0.000
Residual Error	159	9518.54	59.87		
Total	160	10287.19			

Regression Analysis: Bromate as BrO3 (ug/l) versus H(T-6)

The regression equation is
Bromate as BrO3 (ug/l) = 21.1 - 0.755 H(T-6)

159 cases used, 1121 cases contain missing values

Predictor	Coef	SE Coef	T	P
Constant	21.121	1.160	18.20	0.000
H(T-6)	-0.7553	0.2291	-3.30	0.001

S = 7.79163 R-Sq = 6.5% R-Sq(adj) = 5.9%

Analysis of Variance

Source	DF	SS	MS	F	P
Regression	1	659.74	659.74	10.87	0.001
Residual Error	157	9531.39	60.71		
Total	158	10191.13			

Regression Analysis: Bromate as BrO3 (ug/l) versus H(T-7)

The regression equation is
Bromate as BrO3 (ug/l) = 21.5 - 0.861 H(T-7)

157 cases used, 1123 cases contain missing values

Predictor	Coef	SE Coef	T	P
Constant	21.456	1.111	19.32	0.000
H(T-7)	-0.8609	0.2270	-3.79	0.000

S = 7.72186 R-Sq = 8.5% R-Sq(adj) = 7.9%

Analysis of Variance

Source	DF	SS	MS	F	P
Regression	1	857.65	857.65	14.38	0.000
Residual Error	155	9242.21	59.63		
Total	156	10099.85			

Regression Analysis: Bromate as BrO3 (ug/l) versus H(T-8)

The regression equation is
Bromate as BrO3 (ug/l) = 21.1 - 0.898 H(T-8)

166 cases used, 1114 cases contain missing values

Predictor	Coef	SE Coef	T	P
Constant	21.110	1.034	20.41	0.000
H(T-8)	-0.8979	0.2174	-4.13	0.000

S = 7.65848 R-Sq = 9.4% R-Sq(adj) = 8.9%

Analysis of Variance

Source	DF	SS	MS	F	P
Regression	1	1000.2	1000.2	17.05	0.000
Residual Error	164	9619.0	58.7		
Total	165	10619.2			

Regression Analysis: Bromate as BrO3 (ug/l) versus H(T-9)

The regression equation is
Bromate as BrO3 (ug/l) = 20.4 - 0.734 H(T-9)

166 cases used, 1114 cases contain missing values

Predictor	Coef	SE Coef	T	P
Constant	20.4131	0.9986	20.44	0.000
H(T-9)	-0.7342	0.2090	-3.51	0.001

S = 7.76026 R-Sq = 7.0% R-Sq(adj) = 6.4%

Analysis of Variance

Source	DF	SS	MS	F	P
Regression	1	742.84	742.84	12.34	0.001
Residual Error	164	9876.34	60.22		
Total	165	10619.18			

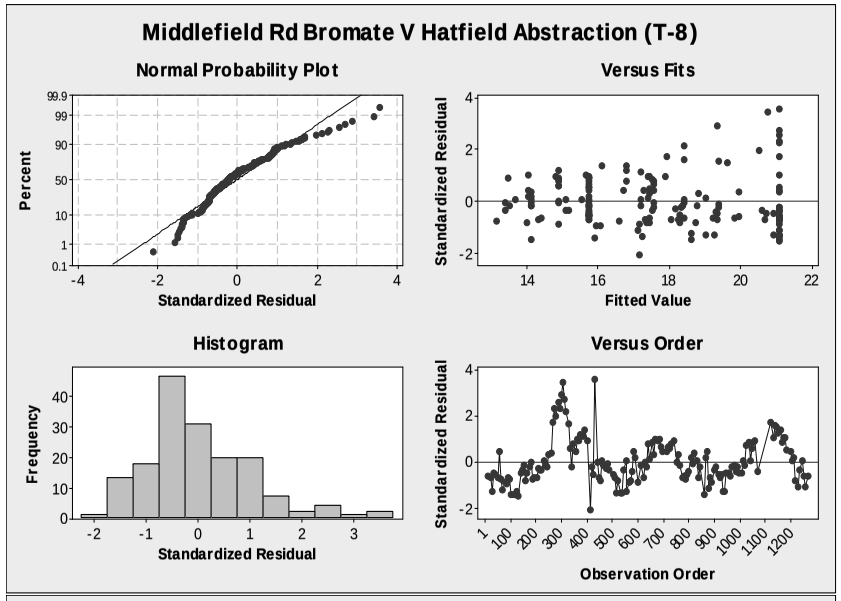

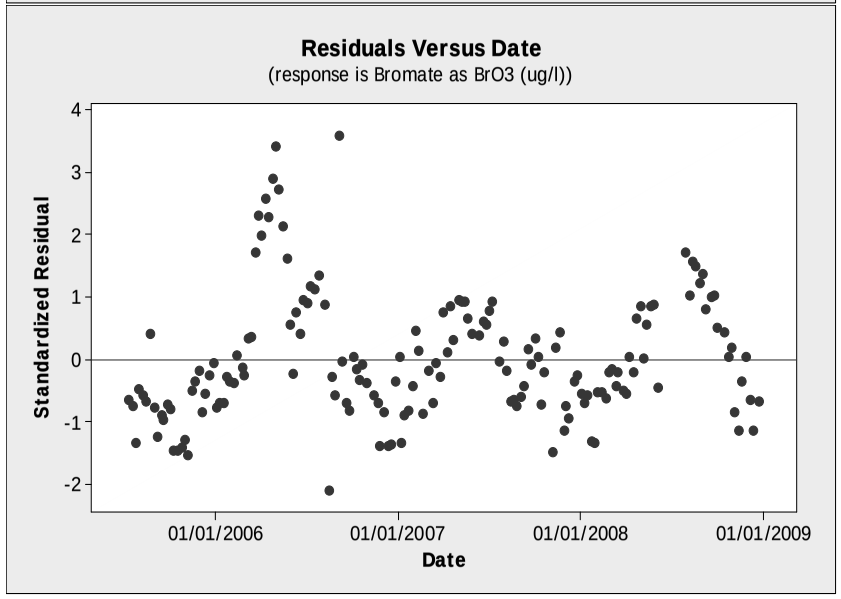

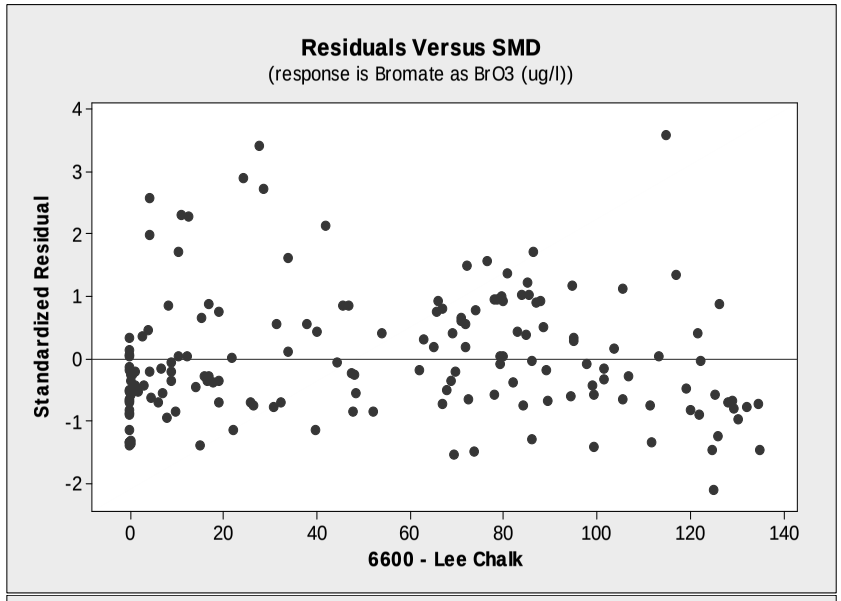

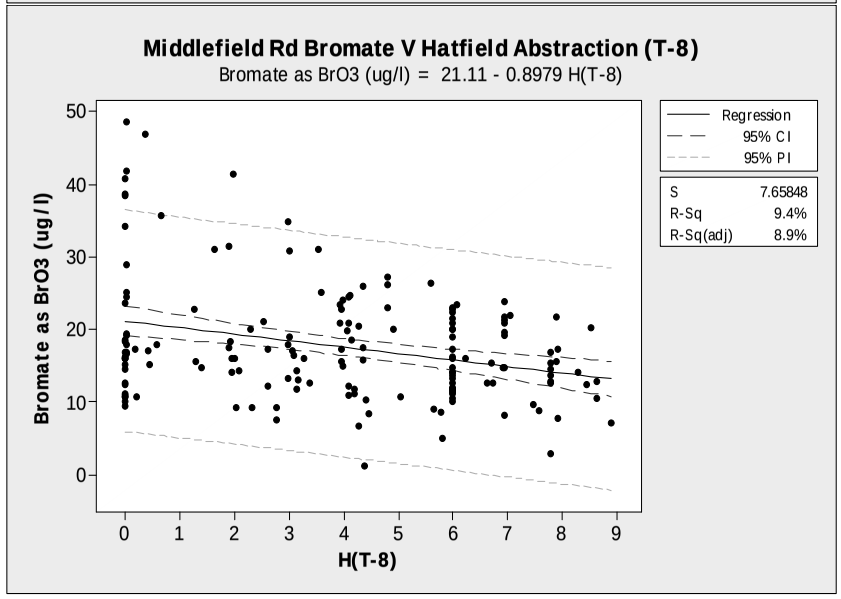

Regression Analysis: Log(BrO3) versus H(T)

Regression Analysis: Log(BrO3) versus H(T-8)

The regression equation is
Log(BrO3) = 1.28 - 0.0200 H(T-8)

166 cases used, 1114 cases contain missing values

Predictor	Coef	SE Coef	T	P
Constant	1.28012	0.02699	47.43	0.000
H(T-8)	-0.020048	0.005675	-3.53	0.001

S = 0.199886 R-Sq = 7.1% R-Sq(adj) = 6.5%

Analysis of Variance

Source	DF	SS	MS	F	P
Regression	1	0.49866	0.49866	12.48	0.001
Residual Error	164	6.55252	0.03995		
Total	165	7.05119			

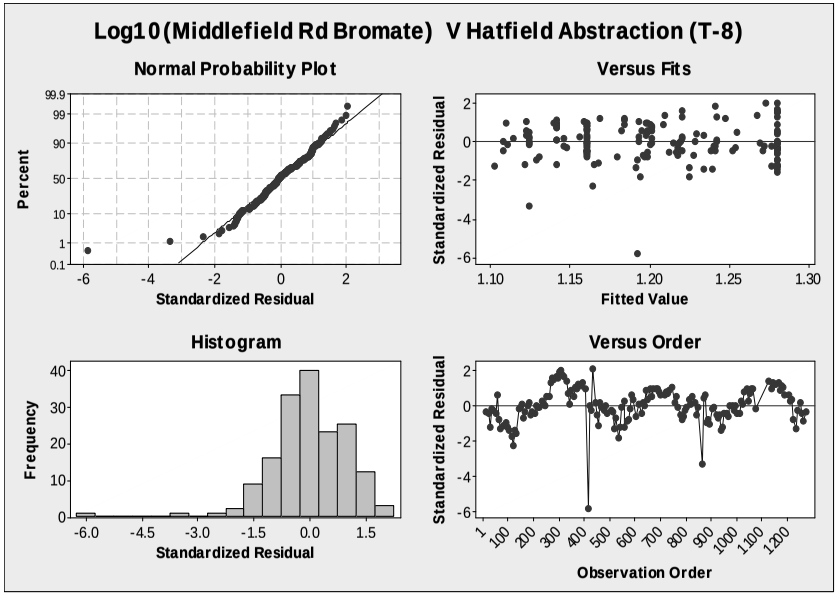

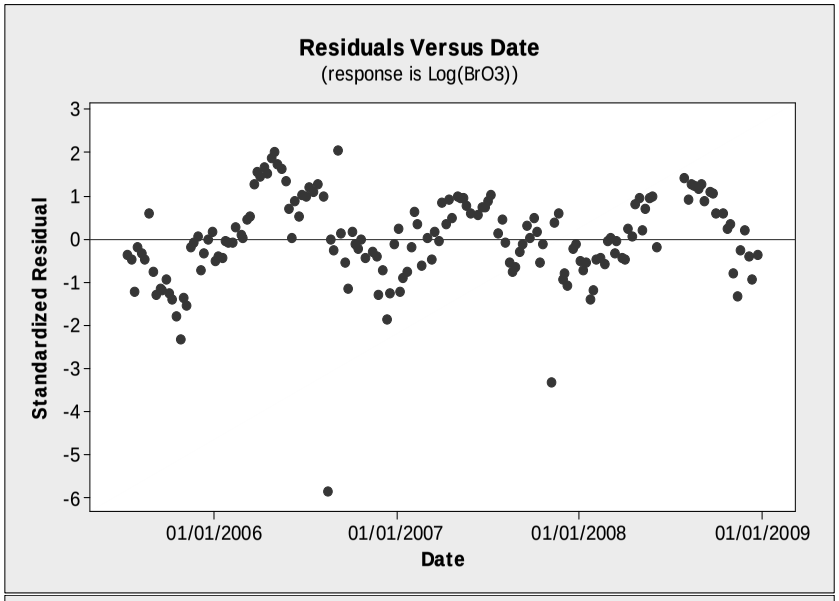

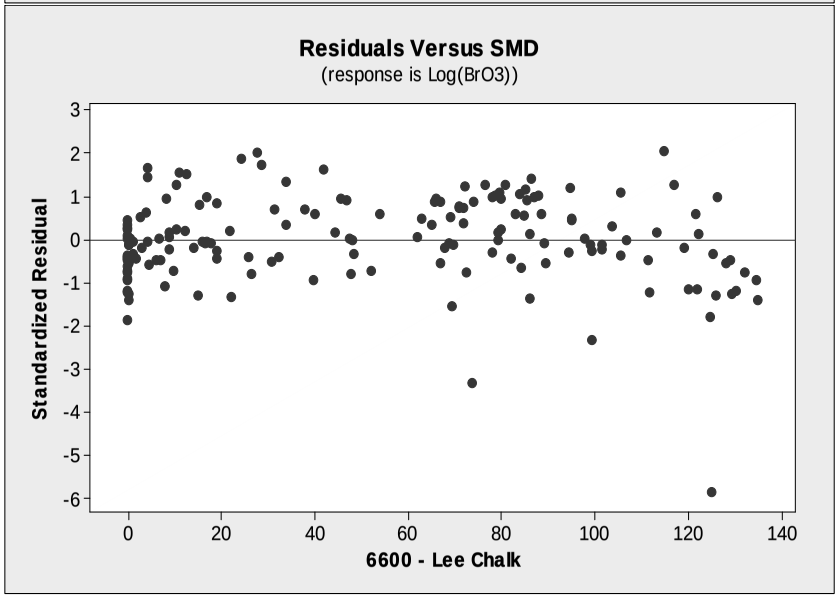

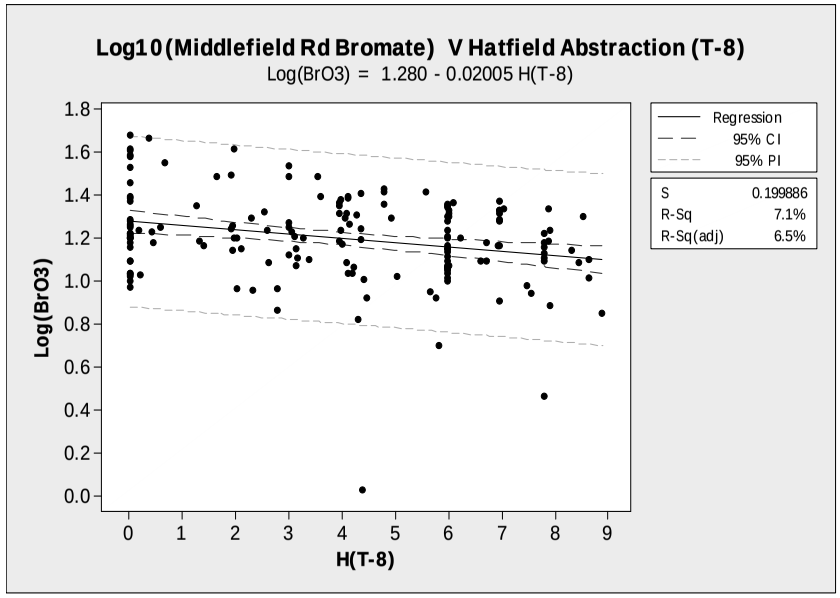

Regression Analysis: Log(BrO3) versus H(T-8), 6600 - Lee Chalk

The regression equation is
Log(BrO3) = 1.29 - 0.0191 H(T-8) - 0.000323 6600 - Lee Chalk

166 cases used, 1114 cases contain missing values

Predictor	Coef	SE Coef	T	P
Constant	1.29369	0.03101	41.72	0.000
H(T-8)	-0.019106	0.005776	-3.31	0.001
6600 - Lee Chalk	-0.0003230	0.0003625	-0.89	0.374

S = 0.200012 R-Sq = 7.5% R-Sq(adj) = 6.4%

Analysis of Variance

Source	DF	SS	MS	F	P
Regression	2	0.53042	0.26521	6.63	0.002
Residual Error	163	6.52077	0.04000		
Total	165	7.05119			

Source	DF	Seq SS
H(T-8)	1	0.49866
6600 - Lee Chalk	1	0.03176

Unusual Observations

Obs	H(T-8)	Log(BrO3)	Fit	SE Fit	Residual	St Resid
119	5.82	0.7005	1.1505	0.0240	-0.4500	-2.27R
412	4.39	0.0273	1.1694	0.0300	-1.1421	-5.78R
432	0.01	1.6854	1.2564	0.0377	0.4289	2.18R
860	7.80	0.4624	1.1209	0.0273	-0.6585	-3.32R

R denotes an observation with a large standardized residual.

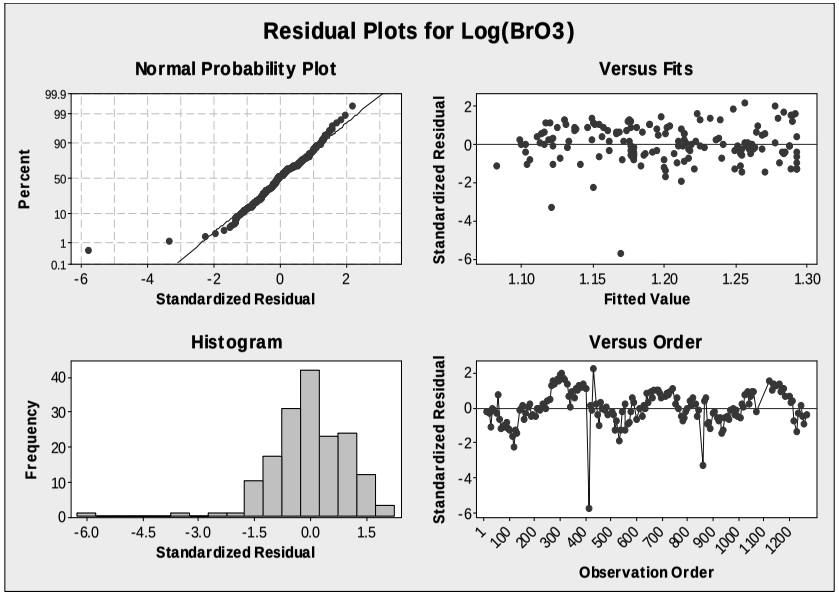

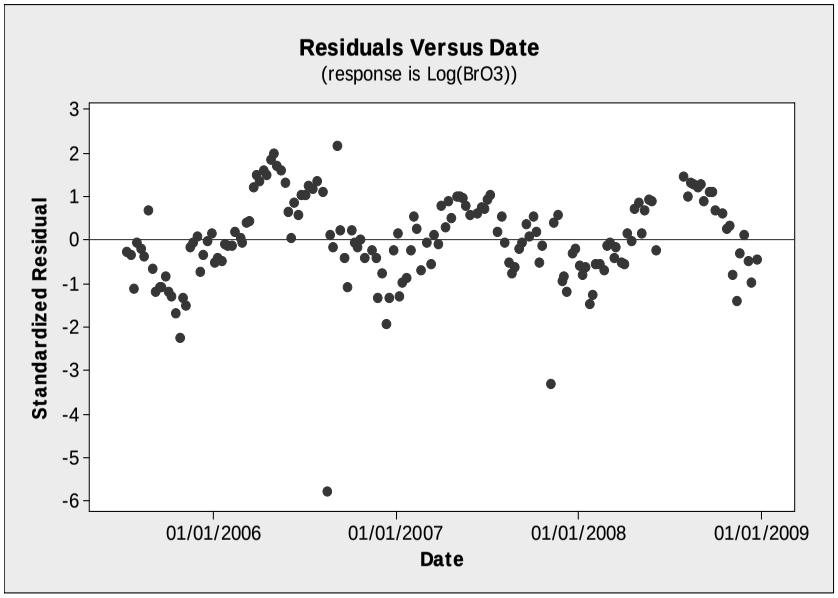
Residuals Versus Date
(response is Log(BrO3))
Standardized Residual
3
2
1
0
-1
-2
-3
-4
-5
-6
01/01/2006
01/01/2007
01/01/2008
01/01/2009
Date

Rye Common versus Hatfield abstraction

Regression Analysis: Bromate as BrO3 (ug/l) versus H(T)

The regression equation is
Bromate as BrO3 (ug/l) = 9.48 - 0.062 H(T)

162 cases used, 1118 cases contain missing values

Predictor	Coef	SE Coef	T	P
Constant	9.4817	0.9441	10.04	0.000
H(T)	-0.0619	0.1917	-0.32	0.747

S = 6.65172 R-Sq = 0.1% R-Sq(adj) = 0.0%

Analysis of Variance

Source	DF	SS	MS	F	P
Regression	1	4.60	4.60	0.10	0.747
Residual Error	160	7079.26	44.25		
Total	161	7083.87			

Regression Analysis: Bromate as BrO3 (ug/l) versus H(T-1)

The regression equation is
Bromate as BrO3 (ug/l) = 9.92 - 0.182 H(T-1)

162 cases used, 1118 cases contain missing values

Predictor	Coef	SE Coef	T	P
Constant	9.9169	0.8838	11.22	0.000
H(T-1)	-0.1817	0.1883	-0.96	0.336

S = 6.63461 R-Sq = 0.6% R-Sq(adj) = 0.0%

Analysis of Variance

Source	DF	SS	MS	F	P
Regression	1	40.99	40.99	0.93	0.336
Residual Error	160	7042.88	44.02		
Total	161	7083.87			

Regression Analysis: Bromate as BrO3 (ug/l) versus H(T-2)

The regression equation is
Bromate as BrO3 (ug/l) = 9.71 - 0.133 H(T-2)

162 cases used, 1118 cases contain missing values

Predictor	Coef	SE Coef	T	P
Constant	9.7070	0.8341	11.64	0.000
H(T-2)	-0.1332	0.1810	-0.74	0.463

S = 6.64265 R-Sq = 0.3% R-Sq(adj) = 0.0%

Analysis of Variance

Source	DF	SS	MS	F	P
Regression	1	23.91	23.91	0.54	0.463
Residual Error	160	7059.96	44.12		
Total	161	7083.87			

Regression Analysis: Bromate as BrO3 (ug/l) versus H(T-3)

The regression equation is
Bromate as BrO3 (ug/l) = 9.60 - 0.092 H(T-3)

162 cases used, 1118 cases contain missing values

Predictor	Coef	SE Coef	T	P
Constant	9.5952	0.9208	10.42	0.000
H(T-3)	-0.0919	0.1898	-0.48	0.629

S = 6.64902 R-Sq = 0.1% R-Sq(adj) = 0.0%

Analysis of Variance

Source	DF	SS	MS	F	P
Regression	1	10.36	10.36	0.23	0.629
Residual Error	160	7073.51	44.21		
Total	161	7083.87			

Regression Analysis: Bromate as BrO3 (ug/l) versus H(T-4)

The regression equation is
Bromate as BrO3 (ug/l) = 10.2 - 0.212 H(T-4)

162 cases used, 1118 cases contain missing values

Predictor	Coef	SE Coef	T	P
Constant	10.1653	0.9752	10.42	0.000
H(T-4)	-0.2124	0.1869	-1.14	0.257

S = 6.62719 R-Sq = 0.8% R-Sq(adj) = 0.2%

Analysis of Variance

Source	DF	SS	MS	F	P
Regression	1	56.73	56.73	1.29	0.257
Residual Error	160	7027.13	43.92		
Total	161	7083.87			

Regression Analysis: Bromate as BrO3 (ug/l) versus H(T-5)

The regression equation is
Bromate as BrO3 (ug/l) = 10.5 - 0.289 H(T-5)

161 cases used, 1119 cases contain missing values

Predictor	Coef	SE Coef	T	P
Constant	10.5022	0.9737	10.79	0.000
H(T-5)	-0.2887	0.1899	-1.52	0.130

S = 6.61969 R-Sq = 1.4% R-Sq(adj) = 0.8%

Analysis of Variance

Source	DF	SS	MS	F	P
Regression	1	101.31	101.31	2.31	0.130
Residual Error	159	6967.44	43.82		
Total	160	7068.74			

Regression Analysis: Bromate as BrO3 (ug/l) versus H(T-6)

The regression equation is
Bromate as BrO3 (ug/l) = 10.3 - 0.269 H(T-6)

161 cases used, 1119 cases contain missing values

Predictor	Coef	SE Coef	T	P
Constant	10.3476	0.9314	11.11	0.000
H(T-6)	-0.2688	0.1893	-1.42	0.157

S = 6.62574 R-Sq = 1.3% R-Sq(adj) = 0.6%

Analysis of Variance

Source	DF	SS	MS	F	P
Regression	1	88.57	88.57	2.02	0.157
Residual Error	159	6980.18	43.90		
Total	160	7068.74			

Regression Analysis: Bromate as BrO3 (ug/l) versus H(T-7)

The regression equation is
Bromate as BrO3 (ug/l) = 11.0 - 0.435 H(T-7)

161 cases used, 1119 cases contain missing values

Predictor	Coef	SE Coef	T	P
Constant	11.0406	0.9371	11.78	0.000
H(T-7)	-0.4355	0.1903	-2.29	0.023

S = 6.56048 R-Sq = 3.2% R-Sq(adj) = 2.6%

Analysis of Variance

Source	DF	SS	MS	F	P
Regression	1	225.39	225.39	5.24	0.023
Residual Error	159	6843.35	43.04		
Total	160	7068.74			

Regression Analysis: Bromate as BrO3 (ug/l) versus H(T-8)

The regression equation is
Bromate as BrO3 (ug/l) = 10.7 - 0.388 H(T-8)

161 cases used, 1119 cases contain missing values

Predictor	Coef	SE Coef	T	P
Constant	10.7462	0.9074	11.84	0.000
H(T-8)	-0.3884	0.1935	-2.01	0.046

S = 6.58474 R-Sq = 2.5% R-Sq(adj) = 1.9%

Analysis of Variance

Source	DF	SS	MS	F	P
Regression	1	174.70	174.70	4.03	0.046
Residual Error	159	6894.04	43.36		
Total	160	7068.74			

Regression Analysis: Bromate as BrO3 (ug/l) versus H(T-9)

The regression equation is
Bromate as BrO3 (ug/l) = 10.1 - 0.226 H(T-9)

161 cases used, 1119 cases contain missing values

Predictor	Coef	SE Coef	T	P
Constant	10.1108	0.8765	11.54	0.000
H(T-9)	-0.2256	0.1848	-1.22	0.224

S = 6.63661 R-Sq = 0.9% R-Sq(adj) = 0.3%

Analysis of Variance

Source	DF	SS	MS	F	P
Regression	1	65.65	65.65	1.49	0.224
Residual Error	159	7003.09	44.04		
Total	160	7068.74			

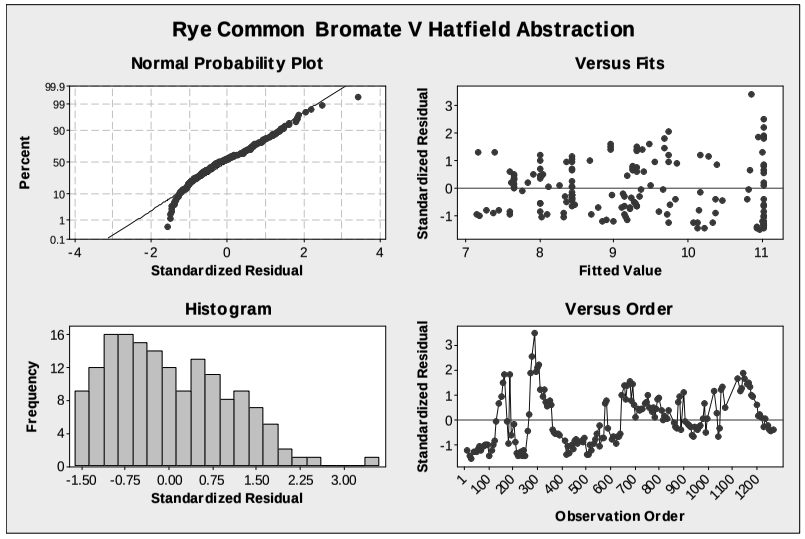

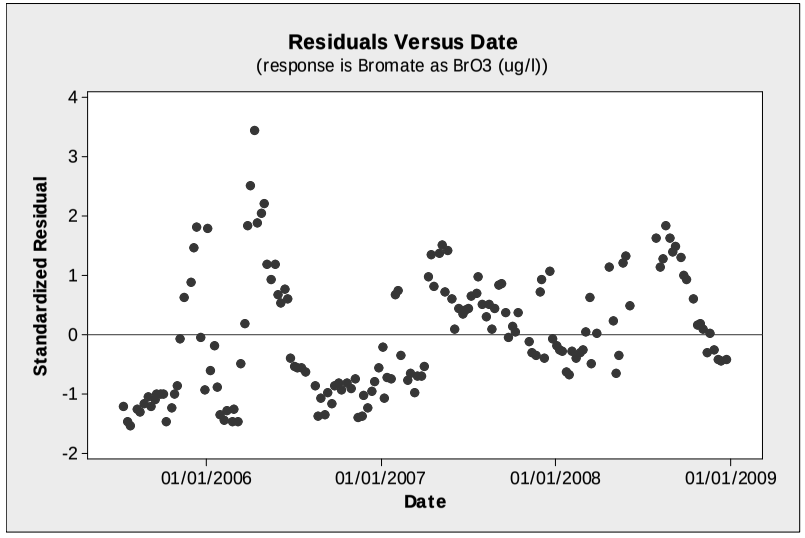

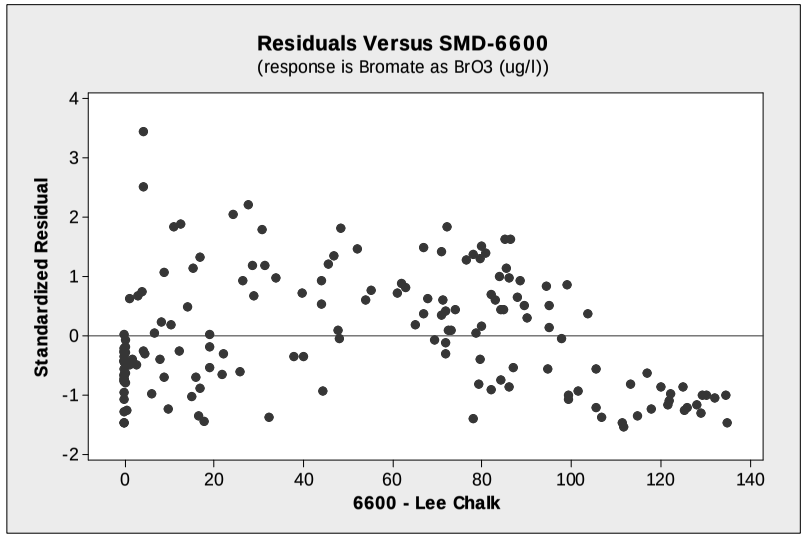

Regression Analysis: Log(BrO3) versus H(T-7)

The regression equation is
Log(BrO3) = 0.867 - 0.0122 H(T-7)

161 cases used, 1119 cases contain missing values

Predictor	Coef	SE Coef	T	P
Constant	0.86739	0.05813	14.92	0.000
H(T-7)	-0.01220	0.01180	-1.03	0.303

S = 0.406946 R-Sq = 0.7% R-Sq(adj) = 0.0%

Analysis of Variance

Source	DF	SS	MS	F	P
Regression	1	0.1769	0.1769	1.07	0.303
Residual Error	159	26.3312	0.1656		
Total	160	26.5081			

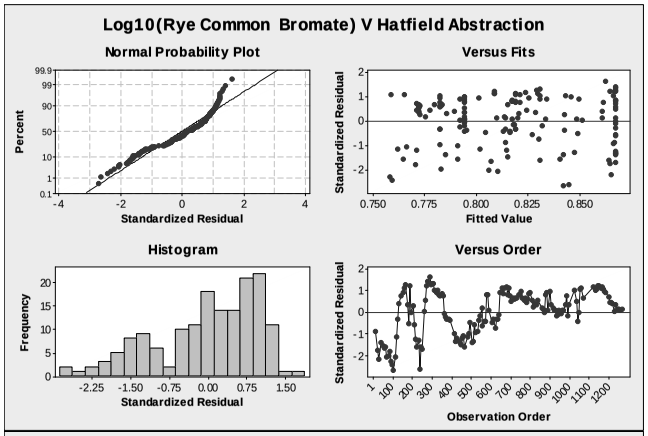

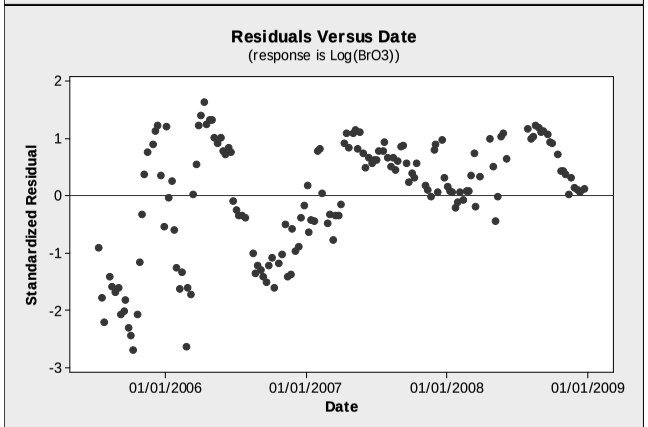

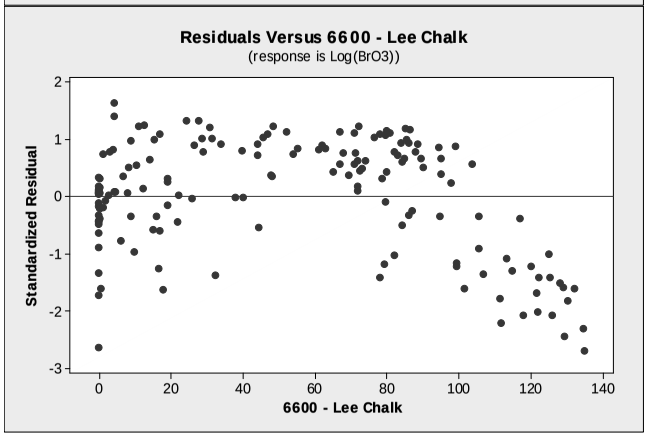

Regression Analysis: Bromate as BrO3 versus H(T-7), 6600 - Lee Chalk

The regression equation is
Bromate as BrO3 (ug/l) = 11.8 - 0.350 H(T-7) - 0.0206 6600 - Lee Chalk

161 cases used, 1119 cases contain missing values

Predictor	Coef	SE Coef	T	P
Constant	11.786	1.034	11.40	0.000
H(T-7)	-0.3499	0.1961	-1.78	0.076
6600 - Lee Chalk	-0.02063	0.01239	-1.66	0.098

S = 6.52423 R-Sq = 4.9% R-Sq(adj) = 3.7%

Analysis of Variance

Source	DF	SS	MS	F	P
Regression	2	343.38	171.69	4.03	0.020
Residual Error	158	6725.37	42.57		
Total	160	7068.74			

Source	DF	Seq SS
H(T-7)	1	225.39
6600 - Lee Chalk	1	117.98

Unusual Observations

Obs	H(T-7)	Bromate as BrO3 (ug/l)	Fit	SE Fit	Residual	St Resid
278	0.00	27.300	11.699	1.012	15.601	2.42R
286	0.41	33.200	11.554	0.963	21.646	3.35R
307	0.01	25.406	11.210	0.936	14.196	2.20R

R denotes an observation with a large standardized residual.

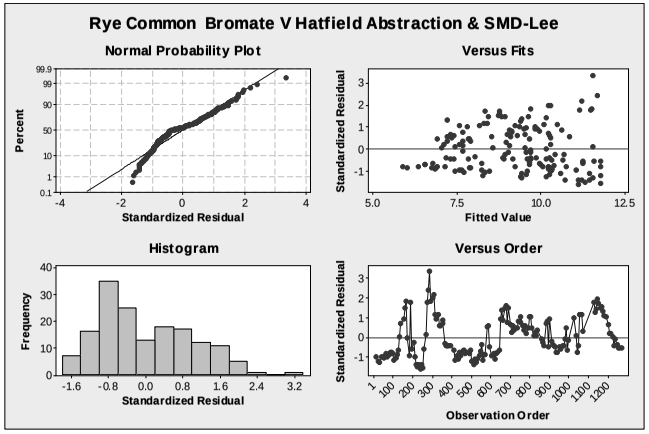

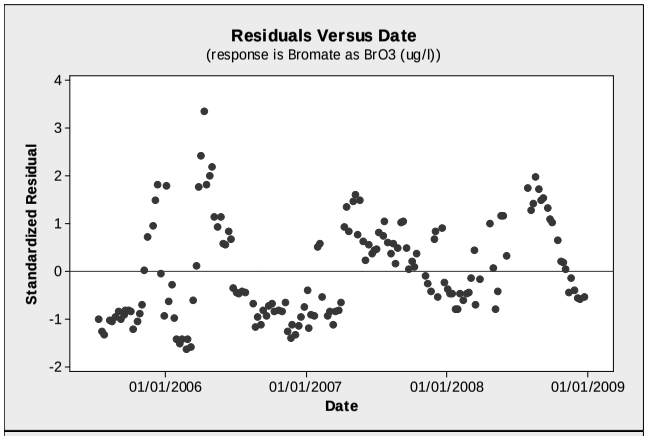

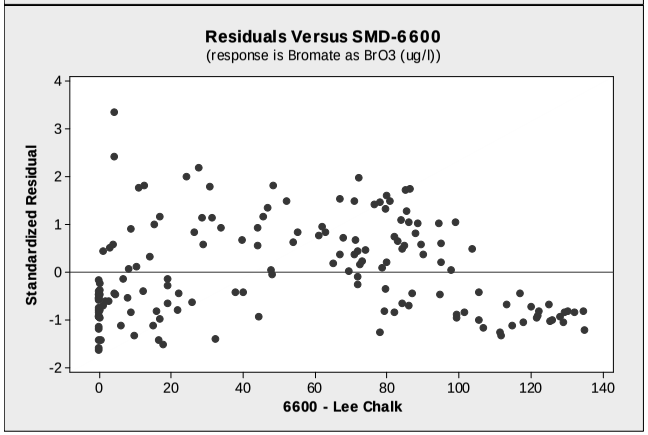

Turnford bromate versus Hatfield abstraction

Regression Analysis: Bromate as BrO3 (ug/l) versus H(T)

The regression equation is
Bromate as BrO3 (ug/l) = 21.0 - 1.04 H(T)

164 cases used, 1116 cases contain missing values

Predictor	Coef	SE Coef	T	P
Constant	21.041	1.279	16.45	0.000
H(T)	-1.0437	0.2567	-4.07	0.000

S = 8.92022 R-Sq = 9.3% R-Sq(adj) = 8.7%

Analysis of Variance

Source	DF	SS	MS	F	P
Regression	1	1315.0	1315.0	16.53	0.000
Residual Error	162	12890.4	79.6		
Total	163	14205.4			

Unusual Observations

Obs	H(T)	Bromate as BrO3 (ug/l)	Fit	SE Fit	Residual	St Resid
5	0.03	40.813	21.010	1.272	19.803	2.24R
12	0.23	39.123	20.801	1.230	18.322	2.07R
286	0.00	43.500	21.041	1.279	22.459	2.54R
300	0.01	40.816	21.030	1.277	19.786	2.24R
307	1.84	45.790	19.121	0.919	26.669	3.01R
319	2.99	37.711	17.920	0.760	19.791	2.23R
495	0.00	0.600	21.038	1.278	-20.438	-2.32R
1146	4.80	34.400	16.035	0.714	18.365	2.07R

R denotes an observation with a large standardized residual.

Regression Analysis: Bromate as BrO3 (ug/l) versus H(T-1)

The regression equation is
Bromate as BrO3 (ug/l) = 20.4 - 0.975 H(T-1)

164 cases used, 1116 cases contain missing values

Predictor	Coef	SE Coef	T	P
Constant	20.435	1.190	17.18	0.000
H(T-1)	-0.9752	0.2501	-3.90	0.000

S = 8.95332 R-Sq = 8.6% R-Sq(adj) = 8.0%

Analysis of Variance

Source	DF	SS	MS	F	P
Regression	1	1219.1	1219.1	15.21	0.000
Residual Error	162	12986.2	80.2		
Total	163	14205.4			

Unusual Observations

Obs	H(T-1)	Bromate as BrO3 (ug/l)	Fit	SE Fit	Residual	St Resid
5	0.00	40.813	20.435	1.190	20.378	2.30R
12	0.44	39.123	20.005	1.103	19.118	2.15R
271	0.65	38.100	19.801	1.062	18.299	2.06R
286	0.00	43.500	20.435	1.190	23.065	2.60R
300	0.37	40.816	20.074	1.116	20.742	2.33R
307	1.98	45.790	18.504	0.841	27.286	3.06R
319	3.00	37.711	17.509	0.731	20.202	2.26R
495	0.00	0.600	20.431	1.189	-19.831	-2.23R
1146	4.80	34.400	15.758	0.738	18.642	2.09R

R denotes an observation with a large standardized residual.

Regression Analysis: Bromate as BrO3 (ug/l) versus H(T-2)

The regression equation is
Bromate as BrO3 (ug/l) = 19.8 - 0.867 H(T-2)

164 cases used, 1116 cases contain missing values

Predictor	Coef	SE Coef	T	P
Constant	19.849	1.138	17.44	0.000
H(T-2)	-0.8673	0.2447	-3.54	0.001

S = 9.02099 R-Sq = 7.2% R-Sq(adj) = 6.6%

Analysis of Variance

Source	DF	SS	MS	F	P
Regression	1	1022.1	1022.1	12.56	0.001
Residual Error	162	13183.3	81.4		
Total	163	14205.4			

Unusual Observations

Obs	H(T-2)	Bromate as BrO3 (ug/l)	Fit	SE Fit	Residual	St Resid
5	0.00	40.813	19.849	1.138	20.964	2.34R
12	0.01	39.123	19.840	1.136	19.283	2.15R
271	0.00	38.100	19.849	1.138	18.251	2.04R
286	0.00	43.500	19.849	1.138	23.651	2.64R
300	0.01	40.816	19.840	1.136	20.976	2.34R
307	0.01	45.790	19.840	1.136	25.950	2.90R
319	3.00	37.711	17.247	0.722	20.464	2.28R
495	0.00	0.600	19.846	1.138	-19.246	-2.15R
1146	4.79	34.400	15.691	0.758	18.709	2.08R

R denotes an observation with a large standardized residual.

Regression Analysis: Bromate as BrO3 (ug/l) versus H(T-3)

The regression equation is
Bromate as BrO3 (ug/l) = 20.2 - 0.882 H(T-3)

164 cases used, 1116 cases contain missing values

Predictor	Coef	SE Coef	T	P
Constant	20.172	1.184	17.04	0.000
H(T-3)	-0.8819	0.2407	-3.66	0.000

S = 8.99859 R-Sq = 7.7% R-Sq(adj) = 7.1%

Analysis of Variance

Source	DF	SS	MS	F	P
Regression	1	1087.5	1087.5	13.43	0.000
Residual Error	162	13117.9	81.0		
Total	163	14205.4			

Unusual Observations

Obs	H(T-3)	Bromate as BrO3 (ug/l)	Fit	SE Fit	Residual	St Resid
5	0.01	40.813	20.163	1.182	20.650	2.31R
12	0.00	39.123	20.172	1.184	18.951	2.12R
271	0.01	38.100	20.163	1.182	17.937	2.01R
286	0.00	43.500	20.172	1.184	23.328	2.62R
300	0.01	40.816	20.163	1.182	20.653	2.32R
307	0.01	45.790	20.163	1.182	25.627	2.87R
319	3.00	37.711	17.526	0.740	20.185	2.25R
495	0.00	0.600	20.169	1.183	-19.569	-2.19R
1146	4.79	34.400	15.946	0.731	18.454	2.06R

R denotes an observation with a large standardized residual.

Regression Analysis: Bromate as BrO3 (ug/l) versus H(T-4)

The regression equation is
Bromate as BrO3 (ug/l) = 22.1 - 1.24 H(T-4)

164 cases used, 1116 cases contain missing values

Predictor	Coef	SE Coef	T	P
Constant	22.115	1.265	17.49	0.000
H(T-4)	-1.2359	0.2426	-5.09	0.000

S = 8.69378 R-Sq = 13.8% R-Sq(adj) = 13.3%

Analysis of Variance

Source	DF	SS	MS	F	P
Regression	1	1961.1	1961.1	25.95	0.000
Residual Error	162	12244.2	75.6		
Total	163	14205.4			

Unusual Observations

Obs	H(T-4)	Bromate as BrO3

Obs	H(T-4)	(ug/l)	Fit	SE Fit	Residual	St Resid
5	0.12	40.813	21.967	1.240	18.846	2.19R
286	0.00	43.500	22.115	1.265	21.385	2.49R
300	0.01	40.816	22.103	1.263	18.713	2.18R
307	0.01	45.790	22.103	1.263	23.687	2.75R
319	3.00	37.711	18.408	0.759	19.303	2.23R
495	0.00	0.600	22.111	1.264	-21.511	-2.50R
530	0.00	4.026	22.111	1.264	-18.085	-2.10R
1133	5.04	33.300	15.892	0.696	17.408	2.01R
1146	4.79	34.400	16.192	0.686	18.208	2.10R

R denotes an observation with a large standardized residual.

Regression Analysis: Bromate as BrO3 (ug/l) versus H(T-5)

The regression equation is
Bromate as BrO3 (ug/l) = 21.7 - 1.19 H(T-5)

163 cases used, 1117 cases contain missing values

Predictor	Coef	SE Coef	T	P
Constant	21.684	1.245	17.42	0.000
H(T-5)	-1.1898	0.2420	-4.92	0.000

S = 8.57627 R-Sq = 13.1% R-Sq(adj) = 12.5%

Analysis of Variance

Source	DF	SS	MS	F	P
Regression	1	1777.5	1777.5	24.17	0.000
Residual Error	161	11841.9	73.6		
Total	162	13619.4			

Unusual Observations

Obs	H(T-5)	Bromate as BrO3 (ug/l)	Fit	SE Fit	Residual	St Resid
12	0.02	39.123	21.660	1.241	17.463	2.06R
286	0.00	43.500	21.684	1.245	21.816	2.57R
300	1.09	40.816	20.387	1.032	20.429	2.40R
307	0.01	45.790	21.672	1.243	24.118	2.84R
319	2.99	37.711	18.127	0.746	19.584	2.29R
495	0.00	0.600	21.679	1.244	-21.079	-2.48R
1133	4.92	33.300	15.826	0.687	17.474	2.04R

R denotes an observation with a large standardized residual.

Regression Analysis: Bromate as BrO3 (ug/l) versus H(T-6)

The regression equation is
Bromate as BrO3 (ug/l) = 20.8 - 1.02 H(T-6)

163 cases used, 1117 cases contain missing values

Predictor	Coef	SE Coef	T	P
Constant	20.847	1.260	16.55	0.000
H(T-6)	-1.0213	0.2502	-4.08	0.000

S = 8.75548 R-Sq = 9.4% R-Sq(adj) = 8.8%

Analysis of Variance

Source	DF	SS	MS	F	P
Regression	1	1277.4	1277.4	16.66	0.000
Residual Error	161	12342.0	76.7		
Total	162	13619.4			

Unusual Observations

Obs	H(T-6)	Bromate as BrO3 (ug/l)	Fit	SE Fit	Residual	St Resid
12	0.02	39.123	20.827	1.256	18.296	2.11R
286	0.00	43.500	20.847	1.260	22.653	2.61R
300	3.00	40.816	17.784	0.751	23.032	2.64R
307	0.01	45.790	20.837	1.258	24.953	2.88R
319	2.99	37.711	17.794	0.752	19.917	2.28R
495	0.01	0.600	20.841	1.259	-20.241	-2.34R

R denotes an observation with a large standardized residual.

Regression Analysis: Bromate as BrO3 (ug/l) versus H(T-7)

The regression equation is
Bromate as BrO3 (ug/l) = 21.3 - 1.15 H(T-7)

163 cases used, 1117 cases contain missing values

Predictor	Coef	SE Coef	T	P
Constant	21.315	1.261	16.90	0.000
H(T-7)	-1.1460	0.2547	-4.50	0.000

S = 8.66839 R-Sq = 11.2% R-Sq(adj) = 10.6%

Analysis of Variance

Source	DF	SS	MS	F	P
Regression	1	1521.7	1521.7	20.25	0.000
Residual Error	161	12097.7	75.1		
Total	162	13619.4			

Unusual Observations

Obs	H(T-7)	Bromate as BrO3 (ug/l)	Fit	SE Fit	Residual	St Resid
12	0.03	39.123	21.280	1.255	17.843	2.08R
286	0.41	43.500	20.845	1.174	22.655	2.64R
300	3.00	40.816	17.877	0.742	22.939	2.66R
307	0.01	45.790	21.303	1.259	24.487	2.86R
319	3.00	37.711	17.877	0.742	19.834	2.30R

R denotes an observation with a large standardized residual.

Regression Analysis: Bromate as BrO3 (ug/l) versus H(T-8)

The regression equation is
Bromate as BrO3 (ug/l) = 20.3 - 0.978 H(T-8)

163 cases used, 1117 cases contain missing values

Predictor	Coef	SE Coef	T	P
Constant	20.296	1.176	17.26	0.000
H(T-8)	-0.9783	0.2479	-3.95	0.000

S = 8.78231 R-Sq = 8.8% R-Sq(adj) = 8.3%

Analysis of Variance

Source	DF	SS	MS	F	P
Regression	1	1201.6	1201.6	15.58	0.000
Residual Error	161	12417.8	77.1		
Total	162	13619.4			

Unusual Observations

Obs	H(T-8)	Bromate as BrO3 (ug/l)	Fit	SE Fit	Residual	St Resid
12	0.00	39.123	20.296	1.176	18.827	2.16R
229	3.00	36.686	17.361	0.719	19.325	2.21R
271	0.00	38.100	20.296	1.176	17.804	2.05R
278	0.65	37.600	19.660	1.049	17.940	2.06R
286	0.00	43.500	20.296	1.176	23.204	2.67R
300	1.97	40.816	18.368	0.830	22.448	2.57R
307	0.37	45.790	19.934	1.103	25.856	2.97R
319	2.99	37.711	17.370	0.720	20.341	2.32R

R denotes an observation with a large standardized residual.

Regression Analysis: Bromate as BrO3 (ug/l) versus H(T-9)

The regression equation is
Bromate as BrO3 (ug/l) = 20.2 - 0.961 H(T-9)

163 cases used, 1117 cases contain missing values

Predictor	Coef	SE Coef	T	P
Constant	20.243	1.142	17.73	0.000
H(T-9)	-0.9610	0.2364	-4.07	0.000

S = 8.75886 R-Sq = 9.3% R-Sq(adj) = 8.7%

Analysis of Variance

Source	DF	SS	MS	F	P
Regression	1	1267.9	1267.9	16.53	0.000
Residual Error	161	12351.5	76.7		
Total	162	13619.4			

Unusual Observations

Obs	H(T-9)	Bromate as BrO3 (ug/l)	Fit	SE Fit	Residual	St Resid
12	0.00	39.123	20.243	1.142	18.880	2.17R
229	1.99	36.686	18.330	0.816	18.356	2.10R
271	0.00	38.100	20.243	1.142	17.857	2.06R
286	0.00	43.500	20.243	1.142	23.257	2.68R
300	0.01	40.816	20.233	1.140	20.583	2.37R
307	0.01	45.790	20.233	1.140	25.557	2.94R
319	3.00	37.711	17.360	0.716	20.351	2.33R
495	0.01	0.600	20.235	1.140	-19.635	-2.26R
1139	5.04	33.800	15.402	0.740	18.398	2.11R

R denotes an observation with a large standardized residual.

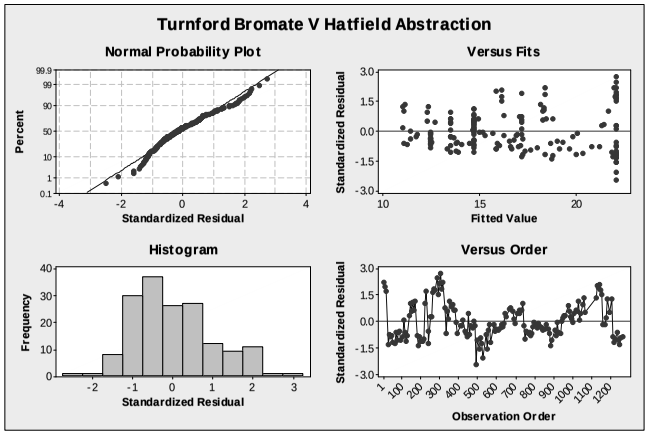

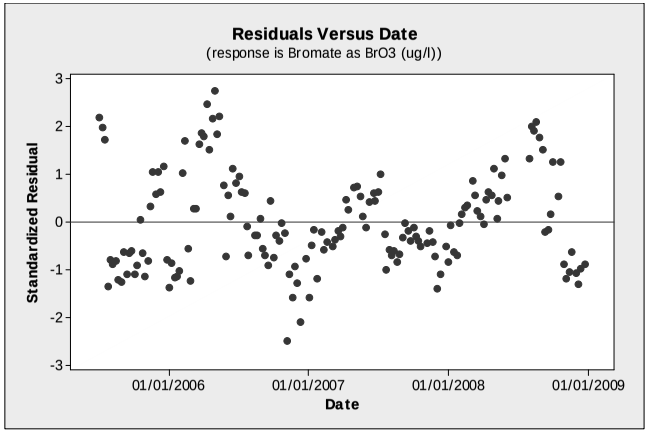

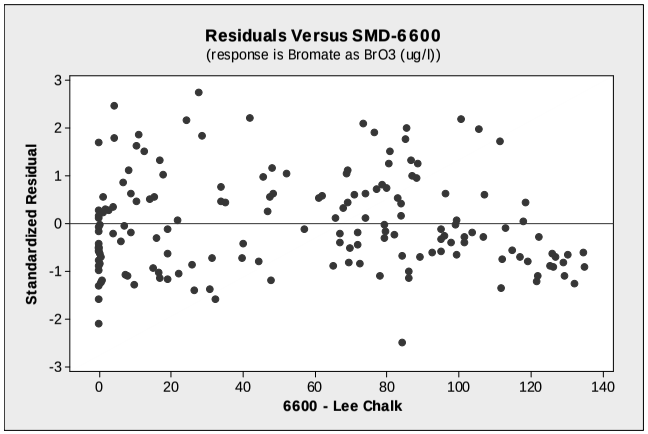

Regression Analysis: Log(BrO3) versus H(T-4)

The regression equation is
Log(BrO3) = 1.26 - 0.0244 H(T-4)

164 cases used, 1116 cases contain missing values

Predictor	Coef	SE Coef	T	P
Constant	1.26135	0.03632	34.73	0.000
H(T-4)	-0.024447	0.006967	-3.51	0.001

S = 0.249658 R-Sq = 7.1% R-Sq(adj) = 6.5%

Analysis of Variance

Source	DF	SS	MS	F	P
Regression	1	0.76735	0.76735	12.31	0.001
Residual Error	162	10.09733	0.06233		
Total	163	10.86468			

Unusual Observations

Obs	H(T-4)	Log(BrO3)	Fit	SE Fit	Residual	St Resid
495	0.00	-0.2218	1.2613	0.0363	-1.4831	-6.00R
530	0.00	0.6049	1.2613	0.0363	-0.6564	-2.66R

R denotes an observation with a large standardized residual.

Regression Analysis: Bromate as BrO3 versus H(T-4), 6600 - Lee Chalk

The regression equation is
Bromate as BrO3 (ug/l) = 22.4 - 1.19 H(T-4) - 0.0094 6600 - Lee Chalk

164 cases used, 1116 cases contain missing values

Predictor	Coef	SE Coef	T	P
Constant	22.413	1.374	16.31	0.000
H(T-4)	-1.1862	0.2588	-4.58	0.000
6600 - Lee Chalk	-0.00937	0.01673	-0.56	0.576

S = 8.71226 R-Sq = 14.0% R-Sq(adj) = 12.9%

Analysis of Variance

Source	DF	SS	MS	F	P
Regression	2	1984.89	992.45	13.08	0.000
Residual Error	161	12220.46	75.90		
Total	163	14205.35			

Source	DF	Seq SS
H(T-4)	1	1961.10
6600 - Lee Chalk	1	23.79

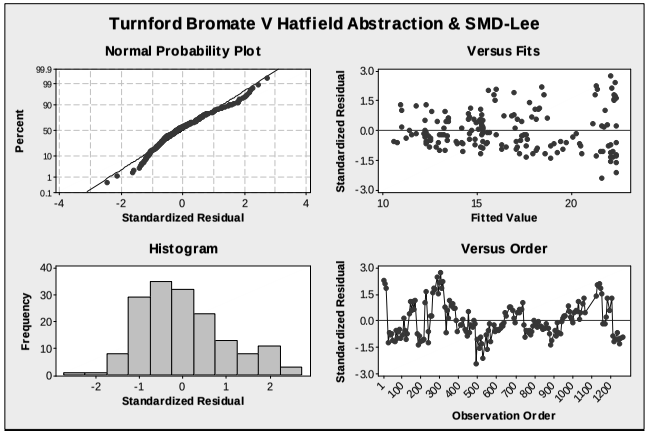

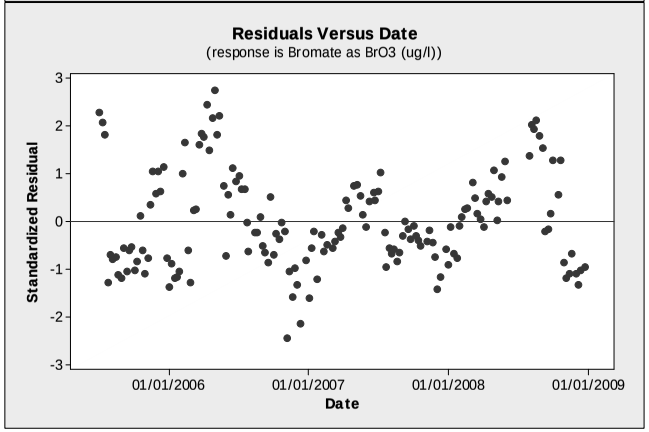

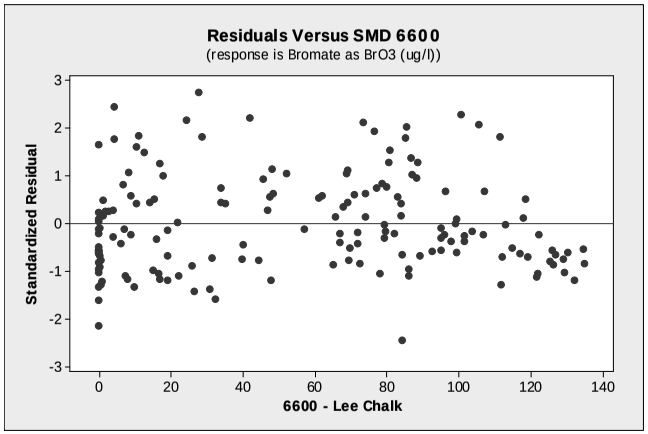

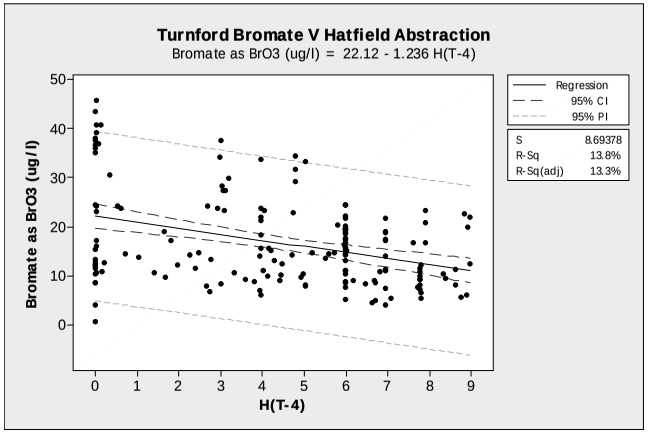

Broxbourne bromate versus Hatfield abstraction
Fitted Line: Bromate as BrO3 (ug/l) versus H(T)

Regression Analysis: Bromate as BrO3 (ug/l) versus H(T)

The regression equation is
Bromate as BrO3 (ug/l) = 25.0 - 1.46 H(T)

141 cases used, 1139 cases contain missing values

Predictor	Coef	SE Coef	T	P
Constant	25.024	1.186	21.10	0.000
H(T)	-1.4599	0.2415	-6.04	0.000

S = 7.59608 R-Sq = 20.8% R-Sq(adj) = 20.2%

Analysis of Variance

Source	DF	SS	MS	F	P
Regression	1	2107.6	2107.6	36.53	0.000
Residual Error	139	8020.4	57.7		
Total	140	10128.0			

Unusual Observations

Obs	H(T)	Bromate as BrO3 (ug/l)	Fit	SE Fit	Residual	St Resid
12	0.23	40.651	24.689	1.139	15.962	2.13R
19	0.20	41.973	24.732	1.145	17.241	2.30R
286	0.00	42.700	25.024	1.186	17.676	2.36R
307	1.84	47.352	22.338	0.846	25.014	3.31R
313	2.99	36.112	20.659	0.697	15.453	2.04R
403	5.81	0.665	16.542	0.757	-15.877	-2.10R
530	0.00	5.911	25.021	1.185	-19.110	-2.55R
571	2.01	6.900	22.096	0.821	-15.196	-2.01R

R denotes an observation with a large standardized residual.

Regression Analysis: Bromate as BrO3 (ug/l) versus H(T-1)

The regression equation is
Bromate as BrO3 (ug/l) = 23.5 - 1.15 H(T-1)

141 cases used, 1139 cases contain missing values

Predictor	Coef	SE Coef	T	P
Constant	23.456	1.144	20.50	0.000
H(T-1)	-1.1542	0.2405	-4.80	0.000

S = 7.90584 R-Sq = 14.2% R-Sq(adj) = 13.6%

Analysis of Variance

Source	DF	SS	MS	F	P

```
Regression        1   1440.2  1440.2  23.04  0.000
Residual Error  139   8687.8    62.5
Total           140  10128.0


Unusual Observations

            Bromate
            as BrO3
Obs  H(T-1)   (ug/l)     Fit  SE Fit  Residual  St Resid
 12    0.44   40.651  22.949   1.060    17.702      2.26R
 19    0.17   41.973  23.260   1.111    18.713      2.39R
 40    2.99   36.335  20.005   0.699    16.330      2.07R
271    0.65   39.300  22.706   1.021    16.594      2.12R
286    0.00   42.700  23.456   1.144    19.244      2.46R
300    0.37   39.185  23.029   1.073    16.156      2.06R
307    1.98   47.352  21.171   0.806    26.181      3.33R
313    3.00   36.112  19.994   0.698    16.118      2.05R
400    5.15    0.897  17.512   0.733   -16.615     -2.11R
530    0.00    5.911  23.454   1.144   -17.543     -2.24R
571    0.00    6.900  23.454   1.144   -16.554     -2.12R

R denotes an observation with a large standardized residual.
```

Regression Analysis: Bromate as BrO3 (ug/l) versus H(T-2)

```
The regression equation is
Bromate as BrO3 (ug/l) = 23.4 - 1.20 H(T-2)


141 cases used, 1139 cases contain missing values


Predictor     Coef  SE Coef      T      P
Constant    23.420    1.059  22.11  0.000
H(T-2)     -1.1981   0.2251  -5.32  0.000


S = 7.77993   R-Sq = 16.9%   R-Sq(adj) = 16.3%


Analysis of Variance

Source           DF       SS      MS      F      P
Regression        1   1714.7  1714.7  28.33  0.000
Residual Error  139   8413.3    60.5
Total           140  10128.0


Unusual Observations

            Bromate
            as BrO3
Obs  H(T-2)   (ug/l)     Fit  SE Fit  Residual  St Resid
 12    0.01   40.651  23.408   1.058    17.243      2.24R
 19    0.01   41.973  23.408   1.058    18.565      2.41R
 40    3.00   36.335  19.826   0.674    16.509      2.13R
271    0.00   39.300  23.420   1.059    15.880      2.06R
286    0.00   42.700  23.420   1.059    19.280      2.50R
300    0.01   39.185  23.408   1.058    15.777      2.05R
307    0.01   47.352  23.408   1.058    23.944      3.11R
313    2.99   36.112  19.837   0.674    16.275      2.10R
530    0.00    5.911  23.418   1.059   -17.507     -2.27R
571    0.00    6.900  23.416   1.059   -16.516     -2.14R

R denotes an observation with a large standardized residual.
```

Regression Analysis: Bromate as BrO3 (ug/l) versus H(T-3)

```
The regression equation is
Bromate as BrO3 (ug/l) = 23.6 - 1.16 H(T-3)


141 cases used, 1139 cases contain missing values


Predictor     Coef  SE Coef      T      P
Constant    23.593    1.107  21.31  0.000
H(T-3)     -1.1563   0.2236  -5.17  0.000


S = 7.81728   R-Sq = 16.1%   R-Sq(adj) = 15.5%


Analysis of Variance

Source           DF       SS      MS      F      P
Regression        1   1633.7  1633.7  26.73  0.000
Residual Error  139   8494.3    61.1
Total           140  10128.0


Unusual Observations

            Bromate
            as BrO3
Obs  H(T-3)   (ug/l)     Fit  SE Fit  Residual  St Resid
 12    0.00   40.651  23.593   1.107    17.058      2.20R
 19    0.01   41.973  23.582   1.106    18.391      2.38R
 40    2.99   36.335  20.136   0.695    16.199      2.08R
271    0.01   39.300  23.582   1.106    15.718      2.03R
286    0.00   42.700  23.593   1.107    19.107      2.47R
300    0.01   39.185  23.582   1.106    15.603      2.02R
307    0.01   47.352  23.582   1.106    23.770      3.07R
313    3.00   36.112  20.124   0.694    15.988      2.05R
417    4.63   34.924  18.240   0.674    16.684      2.14R
530    0.00    5.911  23.591   1.107   -17.680     -2.28R
571    0.00    6.900  23.590   1.107   -16.690     -2.16R

R denotes an observation with a large standardized residual.
```

Regression Analysis: Bromate as BrO3 (ug/l) versus H(T-4)

```
The regression equation is
Bromate as BrO3 (ug/l) = 25.0 - 1.39 H(T-4)


141 cases used, 1139 cases contain missing values


Predictor     Coef  SE Coef      T      P
Constant    25.036    1.170  21.40  0.000
H(T-4)     -1.3929   0.2261  -6.16  0.000


S = 7.56504   R-Sq = 21.5%   R-Sq(adj) = 20.9%


Analysis of Variance

Source           DF       SS      MS      F      P
```

Regression	1	2173.0	2173.0	37.97	0.000
Residual Error	139	7954.9	57.2		
Total	140	10128.0			

Unusual Observations

Obs	H(T-4)	Bromate as BrO3 (ug/l)	Fit	SE Fit	Residual	St Resid
12	0.02	40.651	25.008	1.166	15.643	2.09R
19	0.08	41.973	24.924	1.155	17.049	2.28R
286	0.00	42.700	25.036	1.170	17.664	2.36R
307	0.01	47.352	25.022	1.168	22.330	2.99R
313	2.99	36.112	20.871	0.706	15.241	2.02R
403	5.15	0.665	17.862	0.663	-17.197	-2.28R
417	6.96	34.924	15.341	0.870	19.583	2.61R
530	0.00	5.911	25.031	1.169	-19.120	-2.56R
571	1.86	6.900	22.449	0.849	-15.549	-2.07R

R denotes an observation with a large standardized residual.

Regression Analysis: Bromate as BrO3 (ug/l) versus H(T-5)

The regression equation is
Bromate as BrO3 (ug/l) = 25.6 - 1.53 H(T-5)

140 cases used, 1140 cases contain missing values

Predictor	Coef	SE Coef	T	P
Constant	25.570	1.139	22.45	0.000
H(T-5)	-1.5311	0.2191	-6.99	0.000

S = 7.22703 R-Sq = 26.1% R-Sq(adj) = 25.6%

Analysis of Variance

Source	DF	SS	MS	F	P
Regression	1	2550.1	2550.1	48.82	0.000
Residual Error	138	7207.7	52.2		
Total	139	9757.8			

Unusual Observations

Obs	H(T-5)	Bromate as BrO3 (ug/l)	Fit	SE Fit	Residual	St Resid
12	0.02	40.651	25.540	1.135	15.111	2.12R
19	0.17	41.973	25.310	1.108	16.663	2.33R
124	0.00	11.098	25.567	1.139	-14.469	-2.03R
286	0.00	42.700	25.570	1.139	17.130	2.40R
300	1.09	39.185	23.902	0.946	15.283	2.13R
307	0.01	47.352	25.555	1.137	21.797	3.05R
417	4.43	34.924	18.788	0.611	16.136	2.24R
530	1.33	5.911	23.528	0.906	-17.617	-2.46R

R denotes an observation with a large standardized residual.

Regression Analysis: Bromate as BrO3 (ug/l) versus H(T-6)

The regression equation is
Bromate as BrO3 (ug/l) = 24.7 - 1.40 H(T-6)

140 cases used, 1140 cases contain missing values

Predictor	Coef	SE Coef	T	P
Constant	24.723	1.157	21.36	0.000
H(T-6)	-1.3998	0.2312	-6.05	0.000

S = 7.47451 R-Sq = 21.0% R-Sq(adj) = 20.4%

Analysis of Variance

Source	DF	SS	MS	F	P
Regression	1	2047.9	2047.9	36.66	0.000
Residual Error	138	7709.8	55.9		
Total	139	9757.8			

Unusual Observations

Obs	H(T-6)	Bromate as BrO3 (ug/l)	Fit	SE Fit	Residual	St Resid
12	0.02	40.651	24.695	1.153	15.956	2.16R
19	0.06	41.973	24.639	1.146	17.334	2.35R
286	0.00	42.700	24.723	1.157	17.977	2.43R
300	3.00	39.185	20.523	0.689	18.662	2.51R
307	0.01	47.352	24.709	1.155	22.643	3.07R
400	3.60	0.897	19.683	0.646	-18.786	-2.52R
522	0.06	9.200	24.636	1.145	-15.436	-2.09R

R denotes an observation with a large standardized residual.

Regression Analysis: Bromate as BrO3 (ug/l) versus H(T-7)

The regression equation is
Bromate as BrO3 (ug/l) = 24.1 - 1.30 H(T-7)

140 cases used, 1140 cases contain missing values

Predictor	Coef	SE Coef	T	P
Constant	24.132	1.183	20.39	0.000
H(T-7)	-1.3009	0.2441	-5.33	0.000

S = 7.65760 R-Sq = 17.1% R-Sq(adj) = 16.5%

Analysis of Variance

Source	DF	SS	MS	F	P
Regression	1	1665.6	1665.6	28.40	0.000
Residual Error	138	8092.2	58.6		
Total	139	9757.8			

Unusual Observations

Obs	H(T-7)	Bromate

Obs	H(T-7)	Bromate as BrO3 (ug/l)	Fit	SE Fit	Residual	St Resid
12	0.03	40.651	24.093	1.177	16.558	2.19R
19	0.23	41.973	23.833	1.137	18.140	2.40R
271	0.20	39.300	23.872	1.143	15.428	2.04R
286	0.41	42.700	23.599	1.101	19.101	2.52R
300	3.00	39.185	20.230	0.697	18.955	2.49R
307	0.01	47.352	24.119	1.181	23.233	3.07R
400	5.41	0.897	17.094	0.726	-16.197	-2.12R
558	0.00	7.800	24.130	1.183	-16.330	-2.16R

R denotes an observation with a large standardized residual.

Regression Analysis: Bromate as BrO3 (ug/l) versus H(T-8)

The regression equation is
Bromate as BrO3 (ug/l) = 23.6 - 1.25 H(T-8)

140 cases used, 1140 cases contain missing values

Predictor	Coef	SE Coef	T	P
Constant	23.634	1.119	21.12	0.000
H(T-8)	-1.2457	0.2375	-5.24	0.000

S = 7.67845 R-Sq = 16.6% R-Sq(adj) = 16.0%

Analysis of Variance

Source	DF	SS	MS	F	P
Regression	1	1621.5	1621.5	27.50	0.000
Residual Error	138	8136.3	59.0		
Total	139	9757.8			

Unusual Observations

Obs	H(T-8)	Bromate as BrO3 (ug/l)	Fit	SE Fit	Residual	St Resid
12	0.00	40.651	23.634	1.119	17.017	2.24R
19	0.44	41.973	23.086	1.036	18.887	2.48R
229	3.00	35.822	19.897	0.679	15.925	2.08R
271	0.00	39.300	23.634	1.119	15.666	2.06R
286	0.00	42.700	23.634	1.119	19.066	2.51R
300	1.97	39.185	21.180	0.786	18.005	2.36R
307	0.37	47.352	23.173	1.049	24.179	3.18R
558	0.00	7.800	23.631	1.119	-15.831	-2.08R

R denotes an observation with a large standardized residual.

Regression Analysis: Bromate as BrO3 (ug/l) versus H(T-9)

The regression equation is
Bromate as BrO3 (ug/l) = 23.8 - 1.28 H(T-9)

140 cases used, 1140 cases contain missing values

Predictor	Coef	SE Coef	T	P
Constant	23.780	1.073	22.17	0.000
H(T-9)	-1.2799	0.2238	-5.72	0.000

S = 7.56065 R-Sq = 19.2% R-Sq(adj) = 18.6%

Analysis of Variance

Source	DF	SS	MS	F	P
Regression	1	1869.2	1869.2	32.70	0.000
Residual Error	138	7888.6	57.2		
Total	139	9757.8			

Unusual Observations

Obs	H(T-9)	Bromate as BrO3 (ug/l)	Fit	SE Fit	Residual	St Resid
12	0.00	40.651	23.780	1.073	16.871	2.25R
19	0.01	41.973	23.768	1.071	18.205	2.43R
271	0.00	39.300	23.780	1.073	15.520	2.07R
286	0.00	42.700	23.780	1.073	18.920	2.53R
300	0.01	39.185	23.768	1.071	15.417	2.06R
307	0.01	47.352	23.768	1.071	23.584	3.15R
400	3.88	0.897	18.815	0.639	-17.918	-2.38R
403	3.60	0.665	19.173	0.641	-18.508	-2.46R
445	0.01	8.547	23.768	1.071	-15.221	-2.03R
538	0.00	8.600	23.777	1.072	-15.177	-2.03R
558	0.00	7.800	23.777	1.072	-15.977	-2.13R

R denotes an observation with a large standardized residual.

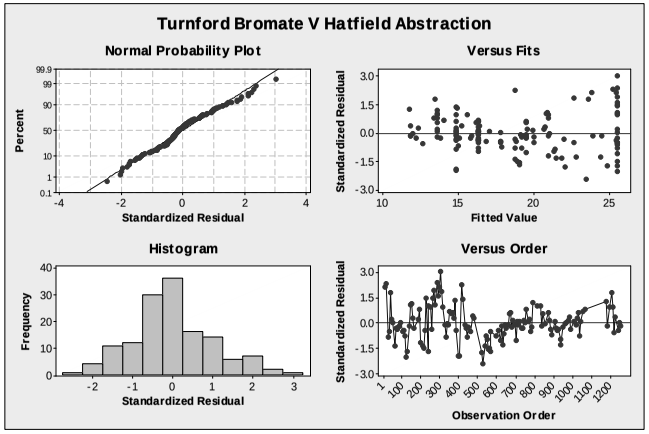

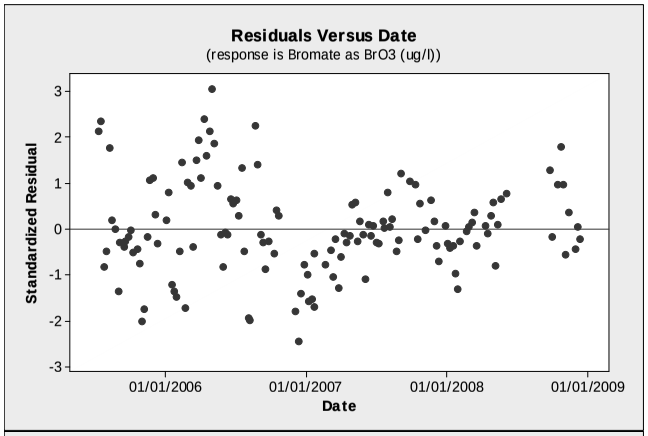

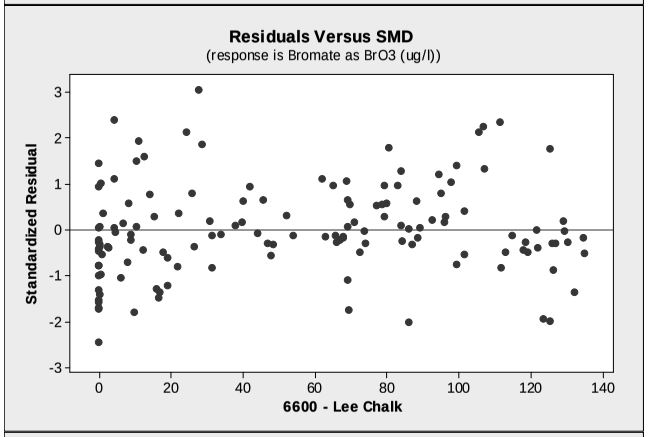

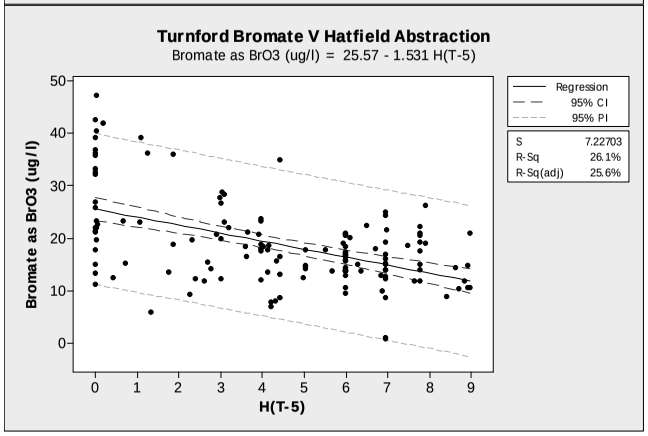

Regression Analysis: Bromate as BrO3 versus H(T-5), 6600 - Lee Chalk

The regression equation is
Bromate as BrO3 (ug/l) = 25.0 - 1.65 H(T-5) + 0.0203 6600 - Lee Chalk

140 cases used, 1140 cases contain missing values

Predictor	Coef	SE Coef	T	P
Constant	24.997	1.209	20.67	0.000
H(T-5)	-1.6493	0.2347	-7.03	0.000
6600 - Lee Chalk	0.02030	0.01473	1.38	0.170

S = 7.20359 R-Sq = 27.1% R-Sq(adj) = 26.1%

Analysis of Variance

Source	DF	SS	MS	F	P
Regression	2	2648.6	1324.3	25.52	0.000
Residual Error	137	7109.2	51.9		
Total	139	9757.8			

Source	DF	Seq SS
H(T-5)	1	2550.1
6600 - Lee Chalk	1	98.6

Unusual Observations

Obs	H(T-5)	Bromate as BrO3 (ug/l)	Fit	SE Fit	Residual	St Resid
19	0.17	41.973	26.982	1.641	14.991	2.14R
98	0.00	*	27.670	1.902	*	* X
99	0.00	*	27.695	1.916	*	* X
108	0.00	*	27.616	1.871	*	* X
124	0.00	11.098	26.741	1.419	-15.643	-2.21R
286	0.00	42.700	25.084	1.189	17.616	2.48R
300	1.09	39.185	23.694	0.955	15.491	2.17R
307	0.01	47.352	25.544	1.134	21.808	3.07R
400	6.96	0.897	16.024	1.155	-15.127	-2.13R
403	6.96	0.665	16.064	1.176	-15.399	-2.17R
417	4.43	34.924	19.858	0.987	15.066	2.11R
530	1.33	5.911	22.797	1.047	-16.886	-2.37R

R denotes an observation with a large standardized residual.
X denotes an observation whose X value gives it large leverage.

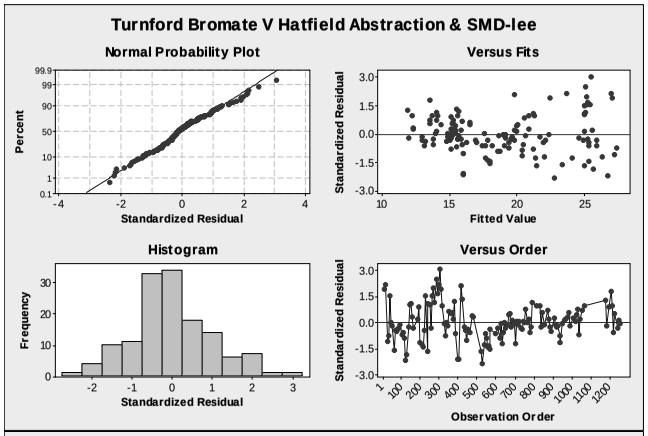

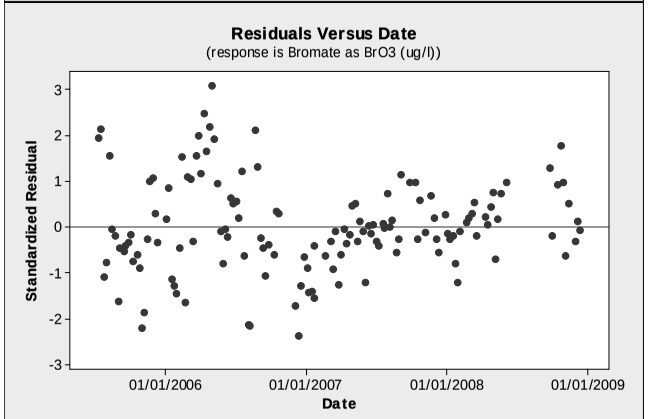

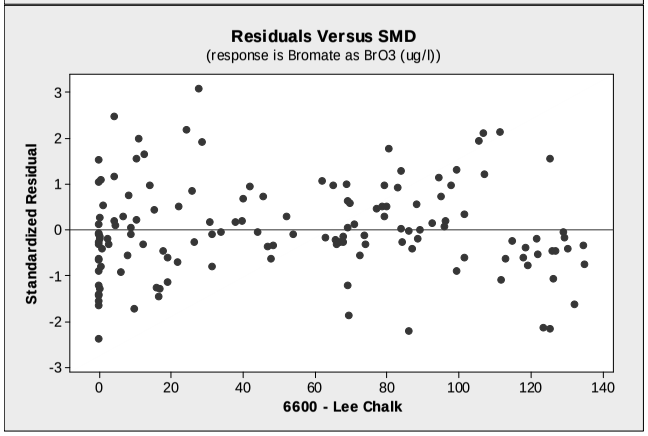

Amwell Marsh bromate versus Hatfield abstraction

Regression Analysis: Bromate as BrO3 (ug/l) versus H(T)

The regression equation is
Bromate as BrO3 (ug/l) = 13.9 - 0.582 H(T)

185 cases used, 1095 cases contain missing values

Predictor	Coef	SE Coef	T	P
Constant	13.9156	0.5481	25.39	0.000
H(T)	-0.5823	0.1147	-5.08	0.000

S = 4.12680 R-Sq = 12.3% R-Sq(adj) = 11.9%

Analysis of Variance

Source	DF	SS	MS	F	P
Regression	1	438.71	438.71	25.76	0.000
Residual Error	183	3116.57	17.03		
Total	184	3555.28			

Regression Analysis: Bromate as BrO3 (ug/l) versus H(T-1)

The regression equation is
Bromate as BrO3 (ug/l) = 13.6 - 0.523 H(T-1)

185 cases used, 1095 cases contain missing values

Predictor	Coef	SE Coef	T	P
Constant	13.5558	0.5222	25.96	0.000
H(T-1)	-0.5233	0.1131	-4.63	0.000

S = 4.17033 R-Sq = 10.5% R-Sq(adj) = 10.0%

Analysis of Variance

Source	DF	SS	MS	F	P
Regression	1	372.61	372.61	21.42	0.000
Residual Error	183	3182.67	17.39		
Total	184	3555.28			

Regression Analysis: Bromate as BrO3 (ug/l) versus H(T-2)

The regression equation is
Bromate as BrO3 (ug/l) = 13.2 - 0.467 H(T-2)

185 cases used, 1095 cases contain missing values

Predictor	Coef	SE Coef	T	P
Constant	13.2494	0.4969	26.66	0.000
H(T-2)	-0.4672	0.1101	-4.24	0.000

S = 4.20568   R-Sq = 9.0%   R-Sq(adj) = 8.5%

Analysis of Variance

Source	DF	SS	MS	F	P
Regression	1	318.43	318.43	18.00	0.000
Residual Error	183	3236.86	17.69		
Total	184	3555.28			

Regression Analysis: Bromate as BrO3 (ug/l) versus H(T-3)

The regression equation is
Bromate as BrO3 (ug/l) = 13.9 - 0.584 H(T-3)

185 cases used, 1095 cases contain missing values

Predictor	Coef	SE Coef	T	P
Constant	13.8630	0.5152	26.91	0.000
H(T-3)	-0.5836	0.1078	-5.41	0.000

S = 4.09212   R-Sq = 13.8%   R-Sq(adj) = 13.3%

Analysis of Variance

Source	DF	SS	MS	F	P
Regression	1	490.86	490.86	29.31	0.000
Residual Error	183	3064.42	16.75		
Total	184	3555.28			

Regression Analysis: Bromate as BrO3 (ug/l) versus H(T-4)

The regression equation is
Bromate as BrO3 (ug/l) = 14.7 - 0.736 H(T-4)

185 cases used, 1095 cases contain missing values

Predictor	Coef	SE Coef	T	P
Constant	14.7466	0.5310	27.77	0.000
H(T-4)	-0.7362	0.1044	-7.05	0.000

S = 3.90887   R-Sq = 21.4%   R-Sq(adj) = 20.9%

Analysis of Variance

Source	DF	SS	MS	F	P
Regression	1	759.18	759.18	49.69	0.000
Residual Error	183	2796.10	15.28		
Total	184	3555.28			

Regression Analysis: Bromate as BrO3 (ug/l) versus H(T-5)

The regression equation is
Bromate as BrO3 (ug/l) = 14.8 - 0.761 H(T-5)

184 cases used, 1096 cases contain missing values

Predictor	Coef	SE Coef	T	P
Constant	14.7941	0.5351	27.65	0.000
H(T-5)	-0.7611	0.1073	-7.09	0.000

S = 3.91184   R-Sq = 21.7%   R-Sq(adj) = 21.2%

Analysis of Variance

Source	DF	SS	MS	F	P
Regression	1	770.07	770.07	50.32	0.000
Residual Error	182	2785.05	15.30		
Total	183	3555.13			

Regression Analysis: Bromate as BrO3 (ug/l) versus H(T-6)

The regression equation is
Bromate as BrO3 (ug/l) = 14.3 - 0.680 H(T-6)

184 cases used, 1096 cases contain missing values

Predictor	Coef	SE Coef	T	P
Constant	14.3209	0.5288	27.08	0.000
H(T-6)	-0.6804	0.1095	-6.22	0.000

S = 4.01414   R-Sq = 17.5%   R-Sq(adj) = 17.1%

Analysis of Variance

Source	DF	SS	MS	F	P
Regression	1	622.50	622.50	38.63	0.000
Residual Error	182	2932.62	16.11		
Total	183	3555.13			

Regression Analysis: Bromate as BrO3 (ug/l) versus H(T-7)

The regression equation is
Bromate as BrO3 (ug/l) = 14.3 - 0.686 H(T-7)

184 cases used, 1096 cases contain missing values

Predictor	Coef	SE Coef	T	P
Constant	14.2658	0.5244	27.21	0.000
H(T-7)	-0.6859	0.1112	-6.17	0.000

S = 4.01934   R-Sq = 17.3%   R-Sq(adj) = 16.8%

Analysis of Variance

Source	DF	SS	MS	F	P
Regression	1	614.90	614.90	38.06	0.000
Residual Error	182	2940.22	16.16		
Total	183	3555.13			

Regression Analysis: Bromate as BrO3 (ug/l) versus H(T-8)

The regression equation is
Bromate as BrO3 (ug/l) = 13.9 - 0.620 H(T-8)

184 cases used, 1096 cases contain missing values

Predictor	Coef	SE Coef	T	P
Constant	13.8845	0.5215	26.62	0.000
H(T-8)	-0.6197	0.1151	-5.39	0.000

S = 4.10470 R-Sq = 13.7% R-Sq(adj) = 13.3%

Analysis of Variance

Source	DF	SS	MS	F	P
Regression	1	488.69	488.69	29.00	0.000
Residual Error	182	3066.44	16.85		
Total	183	3555.13			

Regression Analysis: Bromate as BrO3 (ug/l) versus H(T-9)

The regression equation is
Bromate as BrO3 (ug/l) = 13.6 - 0.531 H(T-9)

184 cases used, 1096 cases contain missing values

Predictor	Coef	SE Coef	T	P
Constant	13.5639	0.5094	26.63	0.000
H(T-9)	-0.5313	0.1098	-4.84	0.000

S = 4.16036 R-Sq = 11.4% R-Sq(adj) = 10.9%

Analysis of Variance

Source	DF	SS	MS	F	P
Regression	1	404.96	404.96	23.40	0.000
Residual Error	182	3150.17	17.31		
Total	183	3555.13			

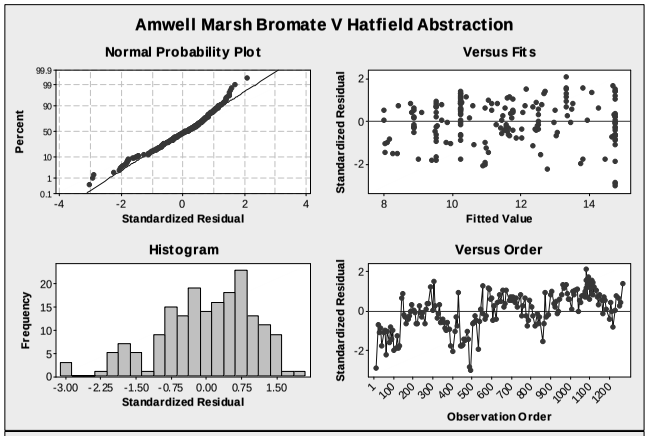

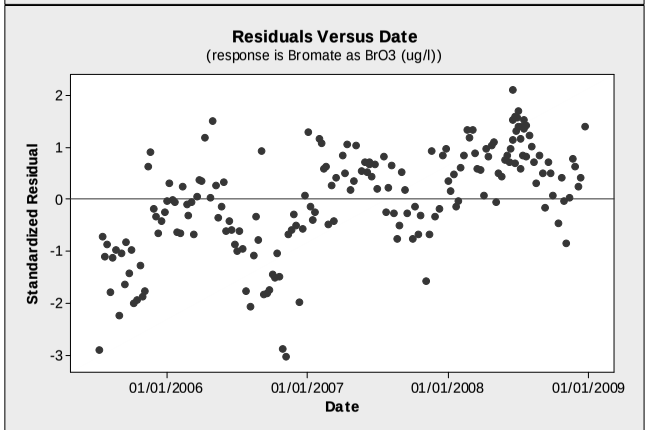

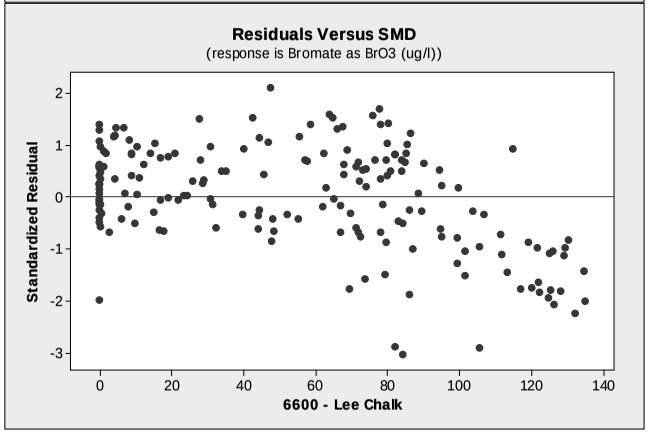

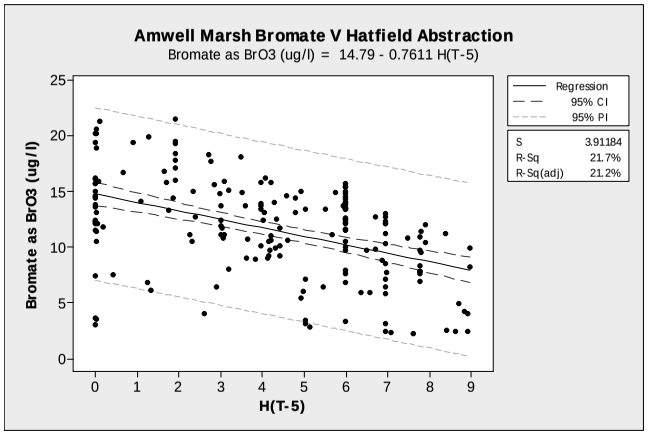

Regression Analysis: Log(BrO3) versus H(T-5)

The regression equation is
Log(BrO3) = 1.16 - 0.0327 H(T-5)

184 cases used, 1096 cases contain missing values

Predictor	Coef	SE Coef	T	P
Constant	1.15814	0.02736	42.33	0.000
H(T-5)	-0.032743	0.005485	-5.97	0.000

S = 0.200004 R-Sq = 16.4% R-Sq(adj) = 15.9%

Analysis of Variance

Source	DF	SS	MS	F	P
Regression	1	1.4252	1.4252	35.63	0.000
Residual Error	182	7.2803	0.0400		
Total	183	8.7055			

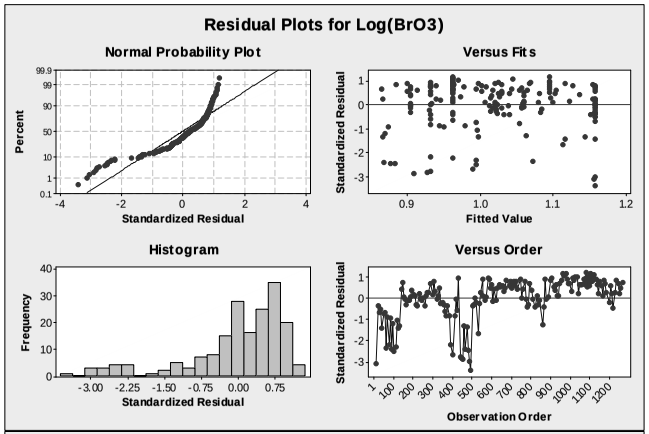

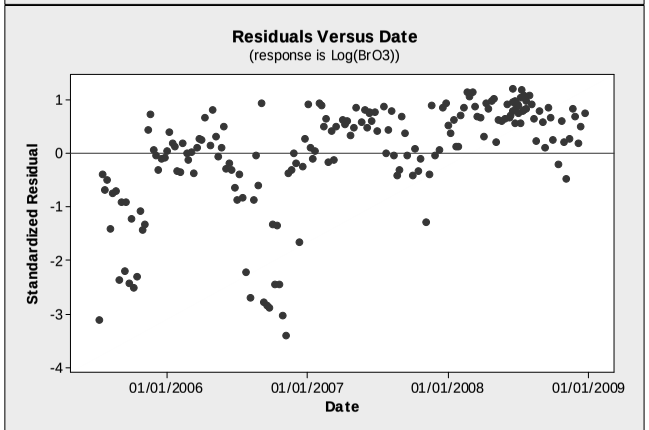

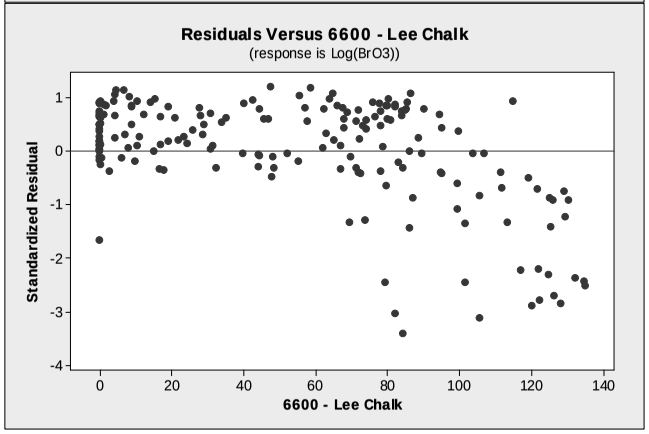

Regression Analysis: Bromate as BrO3 versus H(T-5), 6600 - Lee Chalk

The regression equation is
Bromate as BrO3 (ug/l) = 16.5 - 0.567 H(T-5) - 0.0463 6600 - Lee Chalk

184 cases used, 1096 cases contain missing values

Predictor	Coef	SE Coef	T	P
Constant	16.4972	0.5259	31.37	0.000
H(T-5)	-0.56654	0.09821	-5.77	0.000
6600 - Lee Chalk	-0.046287	0.006332	-7.31	0.000

S = 3.44667 R-Sq = 39.5% R-Sq(adj) = 38.9%

Analysis of Variance

Source	DF	SS	MS	F	P
Regression	2	1404.93	702.46	59.13	0.000
Residual Error	181	2150.20	11.88		
Total	183	3555.13			

Source	DF	Seq SS
H(T-5)	1	770.07
6600 - Lee Chalk	1	634.85

Residual Plots for Bromate as BrO3 (ug/l)

Residuals from Bromate as BrO3 (ug/l) vs Date

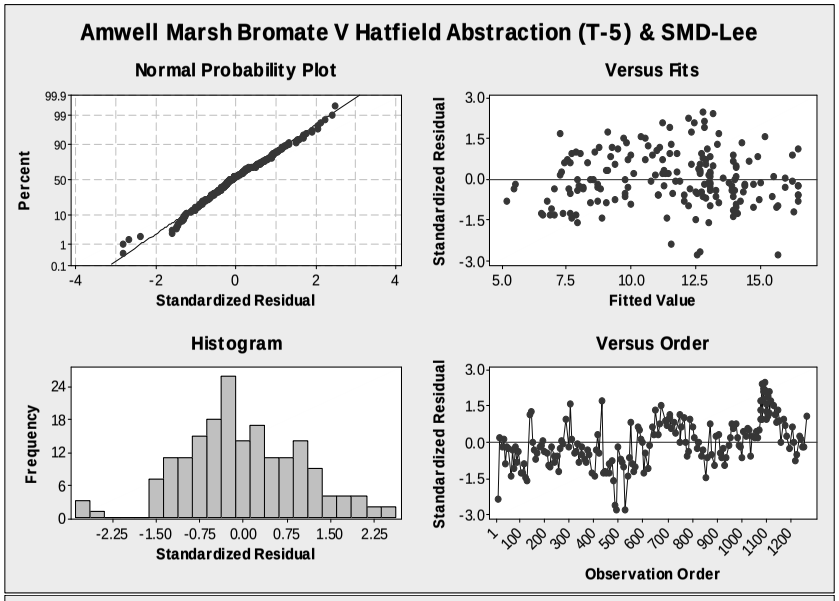

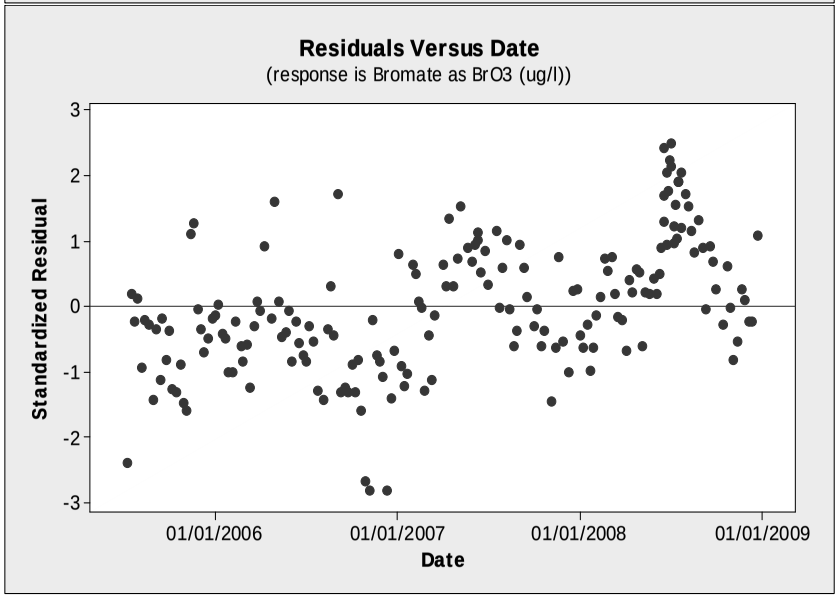

Hatfield bromate versus Hatfield abstraction

Regression Analysis: Bromate as BrO3 (ug/l) versus H(T)

The regression equation is
Bromate as BrO3 (ug/l) = 347 - 11.4 H(T)

509 cases used, 771 cases contain missing values

Predictor	Coef	SE Coef	T	P
Constant	346.696	4.538	76.39	0.000
H(T)	-11.4384	0.7956	-14.38	0.000

S = 40.6581 R-Sq = 29.0% R-Sq(adj) = 28.8%

Analysis of Variance

Source	DF	SS	MS	F	P
Regression	1	341709	341709	206.71	0.000
Residual Error	507	838112	1653		
Total	508	1179822			

Regression Analysis: Bromate as BrO3 (ug/l) versus H(T-1)

The regression equation is
Bromate as BrO3 (ug/l) = 336 - 10.2 H(T-1)

508 cases used, 772 cases contain missing values

Predictor	Coef	SE Coef	T	P
Constant	336.382	4.039	83.28	0.000
H(T-1)	-10.1684	0.7372	-13.79	0.000

S = 41.0422 R-Sq = 27.3% R-Sq(adj) = 27.2%

Analysis of Variance

Source	DF	SS	MS	F	P
Regression	1	320518	320518	190.28	0.000
Residual Error	506	852337	1684		
Total	507	1172855			

Regression Analysis: Bromate as BrO3 (ug/l) versus H(T-2)

The regression equation is
Bromate as BrO3 (ug/l) = 326 - 8.60 H(T-2)

506 cases used, 774 cases contain missing values

Predictor	Coef	SE Coef	T	P
Constant	326.356	3.783	86.28	0.000
H(T-2)	-8.5973	0.7075	-12.15	0.000

S = 42.3414 R-Sq = 22.7% R-Sq(adj) = 22.5%

Analysis of Variance

Source	DF	SS	MS	F	P
Regression	1	264752	264752	147.68	0.000
Residual Error	504	903568	1793		
Total	505	1168321			

Regression Analysis: Bromate as BrO3 (ug/l) versus H(T-3)

The regression equation is
Bromate as BrO3 (ug/l) = 322 - 7.69 H(T-3)

504 cases used, 776 cases contain missing values

Predictor	Coef	SE Coef	T	P
Constant	321.597	3.808	84.46	0.000
H(T-3)	-7.6940	0.7199	-10.69	0.000

S = 43.5241 R-Sq = 18.5% R-Sq(adj) = 18.4%

Analysis of Variance

Source	DF	SS	MS	F	P
Regression	1	216388	216388	114.23	0.000
Residual Error	502	950964	1894		
Total	503	1167353			

Regression Analysis: Bromate as BrO3 (ug/l) versus H(T-4)

The regression equation is
Bromate as BrO3 (ug/l) = 317 - 6.67 H(T-4)

504 cases used, 776 cases contain missing values

Predictor	Coef	SE Coef	T	P
Constant	317.162	3.893	81.47	0.000
H(T-4)	-6.6668	0.7293	-9.14	0.000

S = 44.6489 R-Sq = 14.3% R-Sq(adj) = 14.1%

Analysis of Variance

Source	DF	SS	MS	F	P
Regression	1	166603	166603	83.57	0.000
Residual Error	502	1000749	1994		
Total	503	1167353			

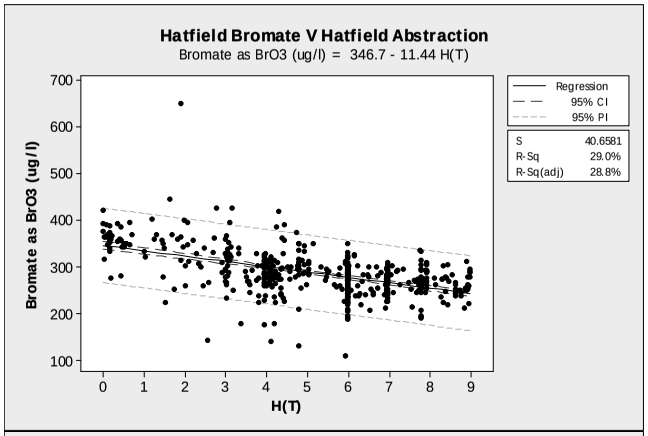

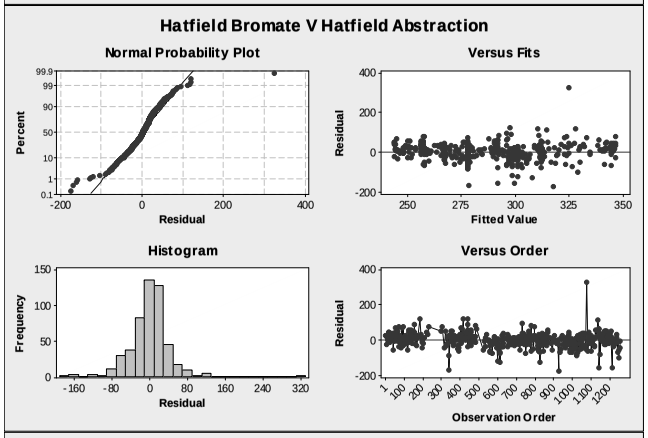

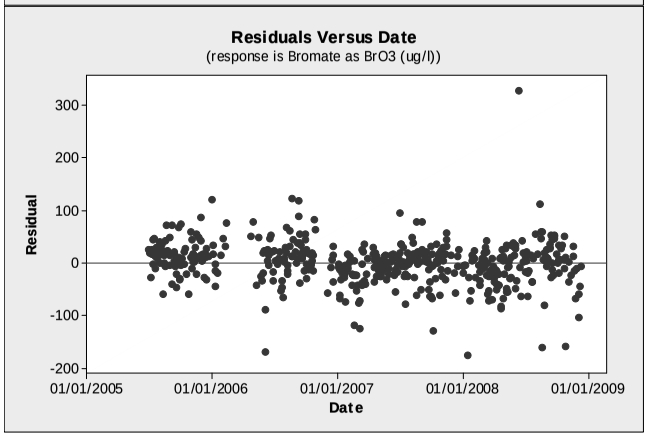

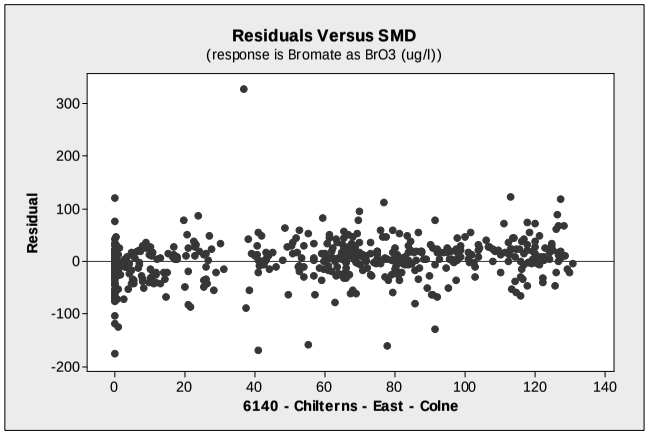

Regression Analysis: Bromate as BrO3 versus H(T), 6140 - Chilterns

The regression equation is
Bromate as BrO3 (ug/l) = 338 - 12.5 H(T) + 0.245 6140 - Chilterns - East - Colne

509 cases used, 771 cases contain missing values

Predictor	Coef	SE Coef	T	P
Constant	338.259	4.644	72.85	0.000
H(T)	-12.5002	0.7939	-15.75	0.000
6140 - Chilterns - East - Colne	0.24523	0.04290	5.72	0.000

S = 39.4447 R-Sq = 33.3% R-Sq(adj) = 33.0%

Analysis of Variance

Source	DF	SS	MS	F	P
Regression	2	392546	196273	126.15	0.000
Residual Error	506	787276	1556		
Total	508	1179822			

Residual Plots for Bromate as BrO3 (ug/l)

Residuals from Bromate as BrO3 (ug/l) vs Date

Residuals from Bromate as BrO3 (ug/l) vs 6140 - Chilterns - East - Colne

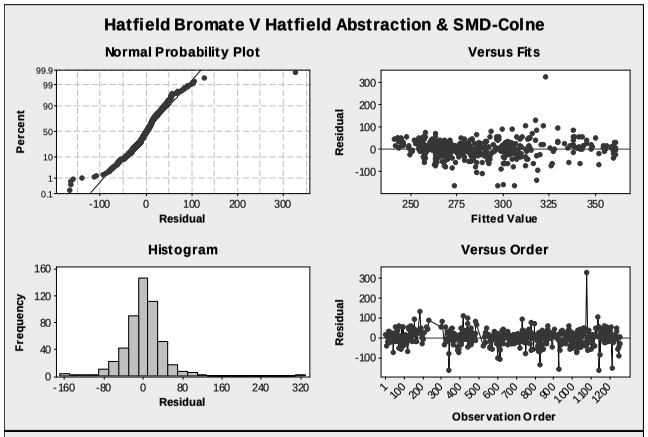

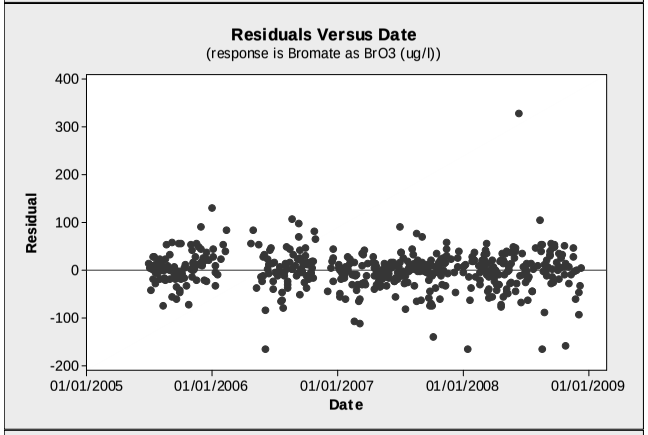

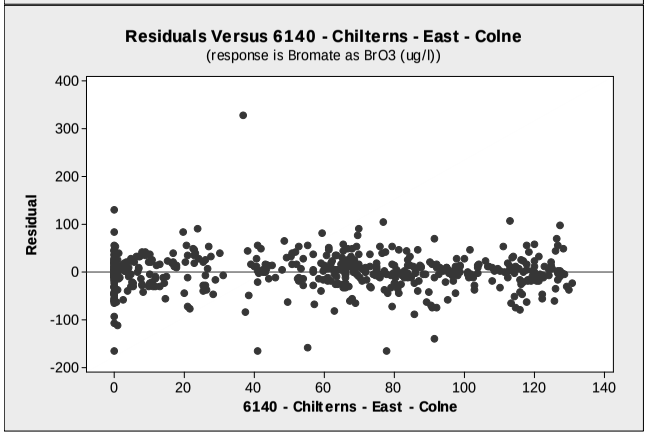

Chadwell Spring versus Hatfield abstraction

Regression Analysis: Bromate as BrO3 (ug/l) versus H(T)

The regression equation is
Bromate as BrO3 (ug/l) = 1.58 - 0.0996 H(T)

141 cases used, 1139 cases contain missing values

Predictor	Coef	SE Coef	T	P
Constant	1.5843	0.1394	11.37	0.000
H(T)	-0.09963	0.02872	-3.47	0.001

S = 0.871765 R-Sq = 8.0% R-Sq(adj) = 7.3%

Analysis of Variance

Source	DF	SS	MS	F	P
Regression	1	9.1432	9.1432	12.03	0.001
Residual Error	139	105.6365	0.7600		
Total	140	114.7797			

Unusual Observations

Obs	H(T)	Bromate as BrO3 (ug/l)	Fit	SE Fit	Residual	St Resid
292	1.97	3.3000	1.3881	0.0960	1.9119	2.21R
607	4.35	3.2000	1.1505	0.0737	2.0495	2.36R
614	3.04	3.7000	1.2817	0.0798	2.4183	2.79R
621	3.96	3.2000	1.1901	0.0736	2.0099	2.31R
627	3.96	3.0000	1.1901	0.0736	1.8099	2.08R
943	6.00	3.2000	0.9870	0.0910	2.2130	2.55R
950	5.99	3.5000	0.9872	0.0910	2.5128	2.90R
965	5.99	3.3000	0.9871	0.0910	2.3129	2.67R
1008	5.99	3.5000	0.9875	0.0909	2.5125	2.90R
1014	3.99	3.4000	1.1868	0.0735	2.2132	2.55R

R denotes an observation with a large standardized residual.

Regression Analysis: Bromate as BrO3 (ug/l) versus H(T-1)

The regression equation is
Bromate as BrO3 (ug/l) = 1.51 - 0.0861 H(T-1)

141 cases used, 1139 cases contain missing values

Predictor	Coef	SE Coef	T	P
Constant	1.5104	0.1328	11.38	0.000
H(T-1)	-0.08607	0.02814	-3.06	0.003

S = 0.879593 R-Sq = 6.3% R-Sq(adj) = 5.6%

Analysis of Variance

Source	DF	SS	MS	F	P
Regression	1	7.2375	7.2375	9.35	0.003
Residual Error	139	107.5421	0.7737		
Total	140	114.7797			

Regression Analysis: Bromate as BrO3 (ug/l) versus H(T-2)

The regression equation is
Bromate as BrO3 (ug/l) = 1.45 - 0.0745 H(T-2)

141 cases used, 1139 cases contain missing values

Predictor	Coef	SE Coef	T	P
Constant	1.4469	0.1254	11.54	0.000
H(T-2)	-0.07451	0.02747	-2.71	0.008

S = 0.885578 R-Sq = 5.0% R-Sq(adj) = 4.3%

Analysis of Variance

Source	DF	SS	MS	F	P
Regression	1	5.7692	5.7692	7.36	0.008
Residual Error	139	109.0105	0.7842		
Total	140	114.7797			

Regression Analysis: Bromate as BrO3 (ug/l) versus H(T-3)

The regression equation is
Bromate as BrO3 (ug/l) = 1.53 - 0.0891 H(T-3)

141 cases used, 1139 cases contain missing values

Predictor	Coef	SE Coef	T	P
Constant	1.5287	0.1340	11.41	0.000
H(T-3)	-0.08913	0.02804	-3.18	0.002

S = 0.877371 R-Sq = 6.8% R-Sq(adj) = 6.1%

Analysis of Variance

Source	DF	SS	MS	F	P
Regression	1	7.7802	7.7802	10.11	0.002
Residual Error	139	106.9995	0.7698		
Total	140	114.7797			

Regression Analysis: Bromate as BrO3 (ug/l) versus H(T-4)

The regression equation is
Bromate as BrO3 (ug/l) = 1.63 - 0.105 H(T-4)

141 cases used, 1139 cases contain missing values

Predictor	Coef	SE Coef	T	P
Constant	1.6317	0.1402	11.64	0.000
H(T-4)	-0.10451	0.02732	-3.83	0.000

S = 0.864349 R-Sq = 9.5% R-Sq(adj) = 8.9%

Analysis of Variance

Source	DF	SS	MS	F	P
Regression	1	10.933	10.933	14.63	0.000
Residual Error	139	103.847	0.747		
Total	140	114.780			

Regression Analysis: Bromate as BrO3 (ug/l) versus H(T-5)

The regression equation is
Bromate as BrO3 (ug/l) = 1.70 - 0.119 H(T-5)

140 cases used, 1140 cases contain missing values

Predictor	Coef	SE Coef	T	P
Constant	1.6991	0.1438	11.82	0.000
H(T-5)	-0.11918	0.02829	-4.21	0.000

S = 0.857985 R-Sq = 11.4% R-Sq(adj) = 10.8%

Analysis of Variance

Source	DF	SS	MS	F	P
Regression	1	13.063	13.063	17.75	0.000
Residual Error	138	101.587	0.736		
Total	139	114.650			

Regression Analysis: Bromate as BrO3 (ug/l) versus H(T-6)

The regression equation is
Bromate as BrO3 (ug/l) = 1.68 - 0.119 H(T-6)

140 cases used, 1140 cases contain missing values

Predictor	Coef	SE Coef	T	P
Constant	1.6839	0.1383	12.18	0.000
H(T-6)	-0.11936	0.02769	-4.31	0.000

S = 0.855697 R-Sq = 11.9% R-Sq(adj) = 11.2%

Analysis of Variance

Source	DF	SS	MS	F	P
Regression	1	13.604	13.604	18.58	0.000
Residual Error	138	101.046	0.732		
Total	139	114.650			

Regression Analysis: Bromate as BrO3 (ug/l) versus H(T-7)

The regression equation is

Bromate as BrO3 (ug/l) = 1.60 - 0.104 H(T-7)

140 cases used, 1140 cases contain missing values

Predictor	Coef	SE Coef	T	P
Constant	1.5990	0.1382	11.57	0.000
H(T-7)	-0.10402	0.02876	-3.62	0.000

S = 0.871130 R-Sq = 8.7% R-Sq(adj) = 8.0%

Analysis of Variance

Source	DF	SS	MS	F	P
Regression	1	9.9265	9.9265	13.08	0.000
Residual Error	138	104.7238	0.7589		
Total	139	114.6503			

Regression Analysis: Bromate as BrO3 (ug/l) versus H(T-8)

The regression equation is
Bromate as BrO3 (ug/l) = 1.65 - 0.119 H(T-8)

140 cases used, 1140 cases contain missing values

Predictor	Coef	SE Coef	T	P
Constant	1.6474	0.1373	12.00	0.000
H(T-8)	-0.11877	0.02932	-4.05	0.000

S = 0.861689 R-Sq = 10.6% R-Sq(adj) = 10.0%

Analysis of Variance

Source	DF	SS	MS	F	P
Regression	1	12.184	12.184	16.41	0.000
Residual Error	138	102.466	0.743		
Total	139	114.650			

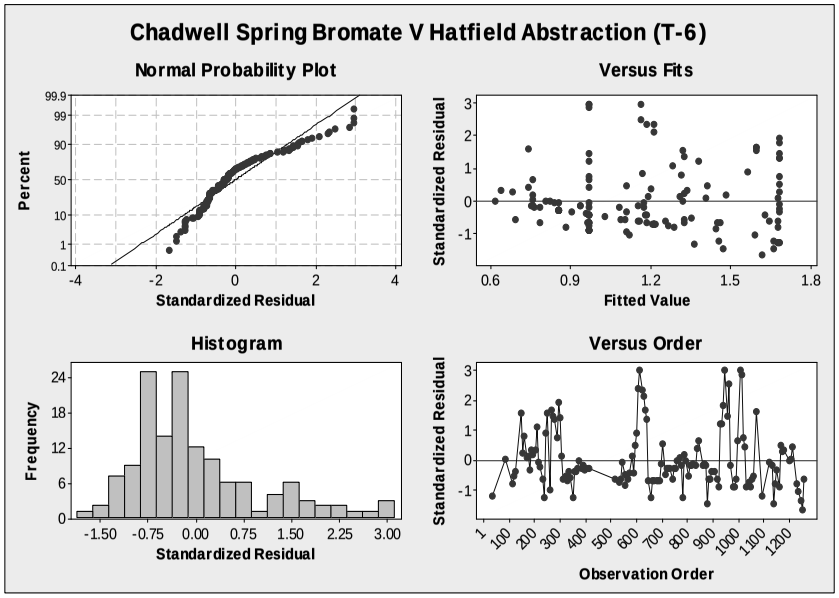

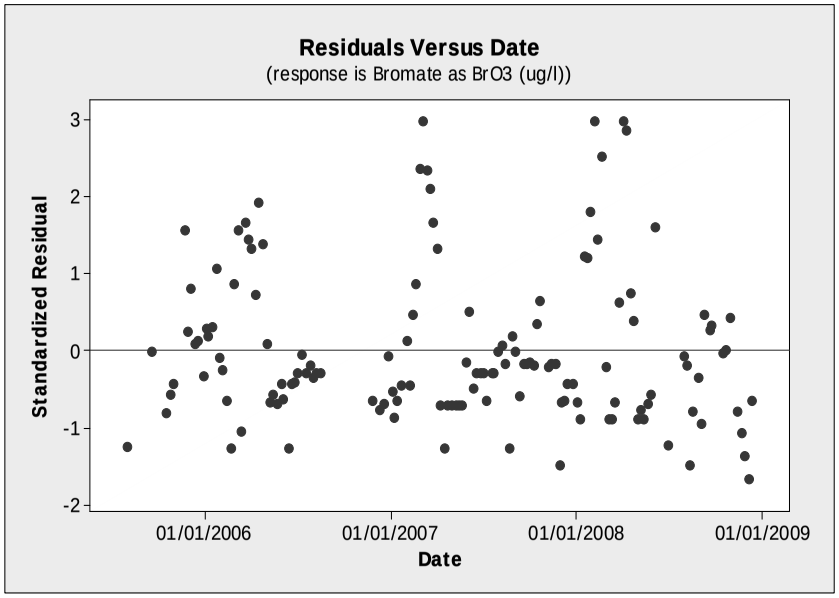

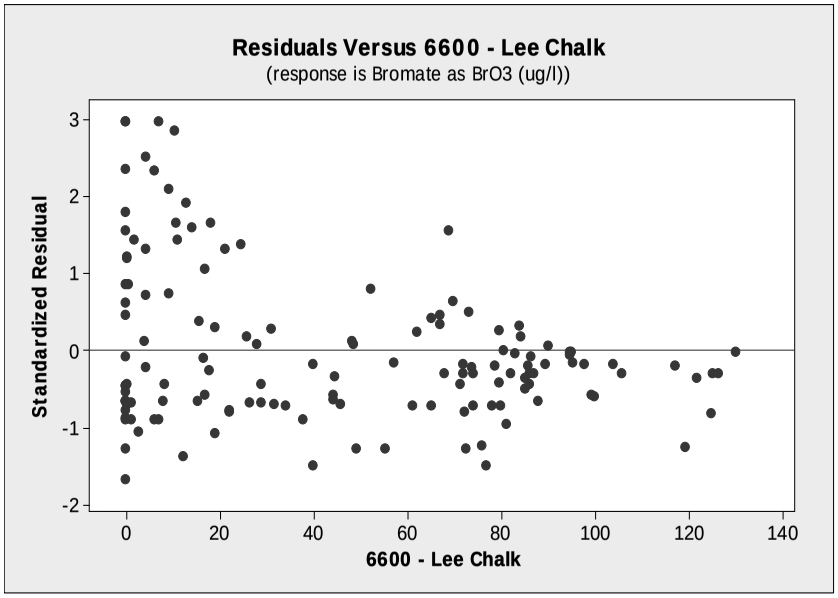

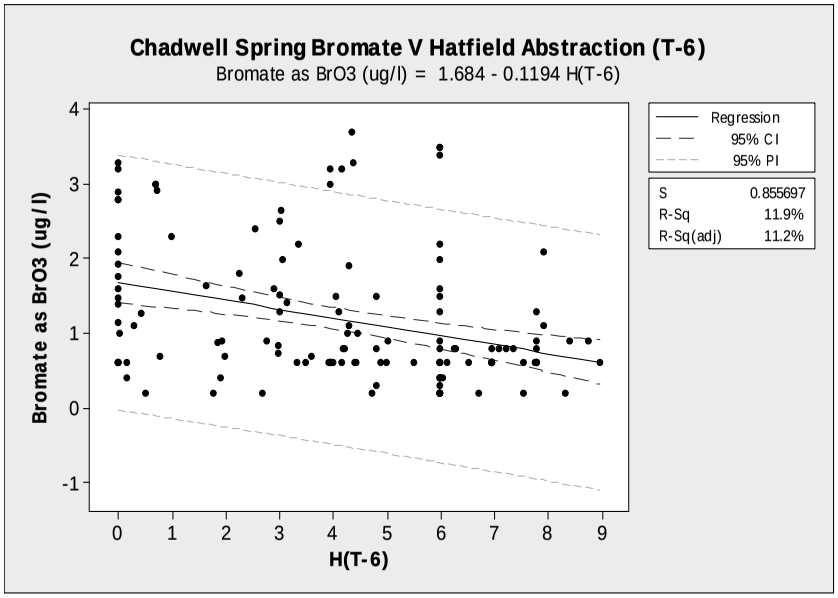

Regression Analysis: log10(Bromate) versus H(T-6)

The regression equation is
log10(Bromate) = 0.135 - 0.0438 H(T-6)

140 cases used, 1140 cases contain missing values

Predictor	Coef	SE Coef	T	P
Constant	0.13503	0.05058	2.67	0.009
H(T-6)	-0.04383	0.01013	-4.33	0.000

S = 0.313056 R-Sq = 11.9% R-Sq(adj) = 11.3%

Analysis of Variance

Source	DF	SS	MS	F	P
Regression	1	1.8348	1.8348	18.72	0.000
Residual Error	138	13.5246	0.0980		
Total	139	15.3593			

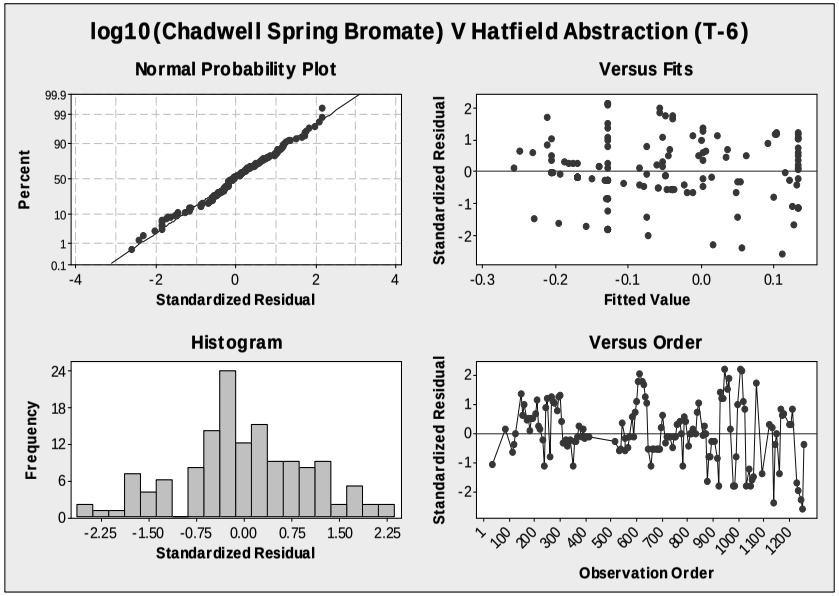

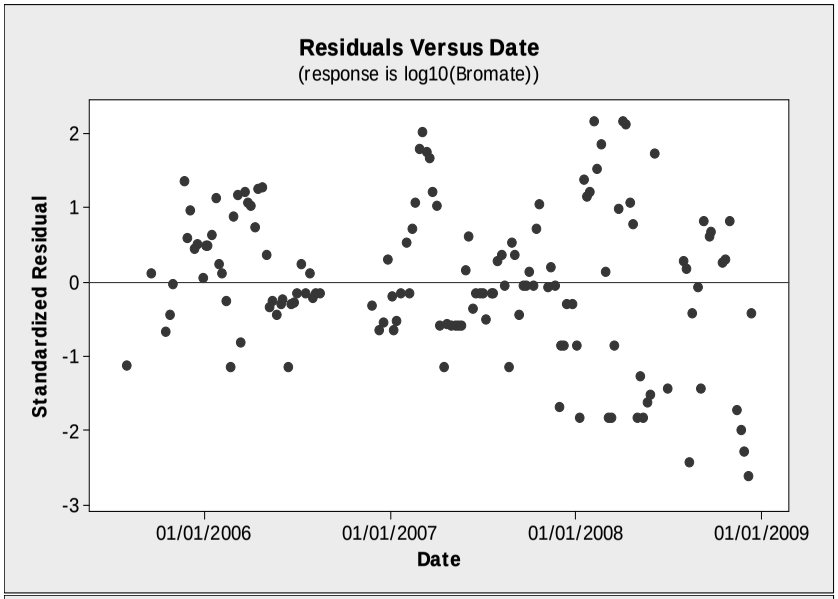

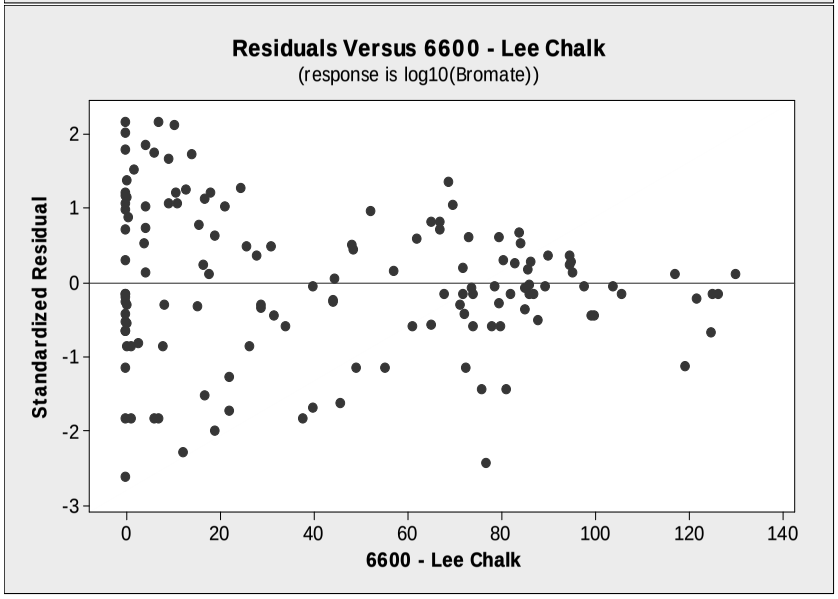

Regression Analysis: log10(Bromate) versus H(T-6), 6600 - Lee Chalk

The regression equation is
log10(Bromate) = 0.165 - 0.0374 H(T-6) - 0.00130 6600 - Lee Chalk

140 cases used, 1140 cases contain missing values

Predictor	Coef	SE Coef	T	P
Constant	0.16476	0.05279	3.12	0.002
H(T-6)	-0.03742	0.01065	-3.51	0.001
6600 - Lee Chalk	-0.0012969	0.0007160	-1.81	0.072

S = 0.310501 R-Sq = 14.0% R-Sq(adj) = 12.7%

Analysis of Variance

Source	DF	SS	MS	F	P
Regression	2	2.1510	1.0755	11.16	0.000
Residual Error	137	13.2083	0.0964		
Total	139	15.3593			

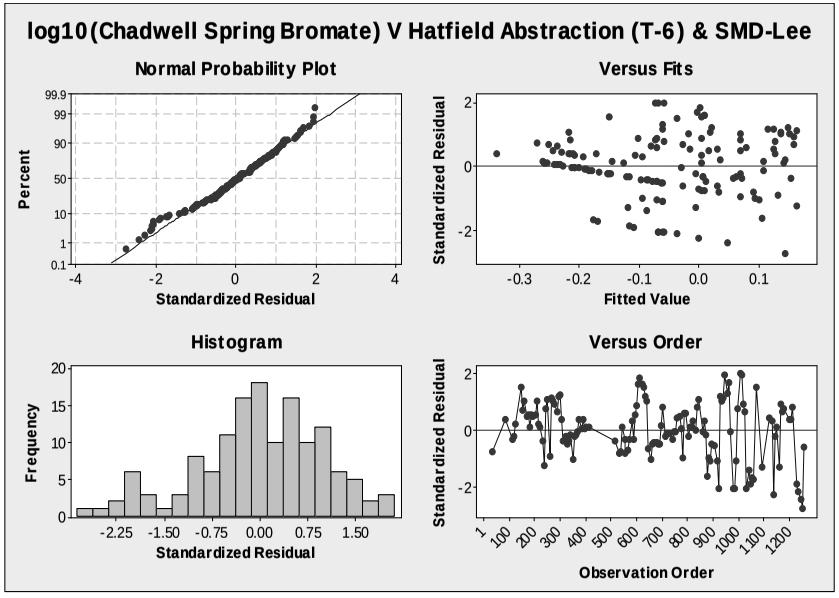

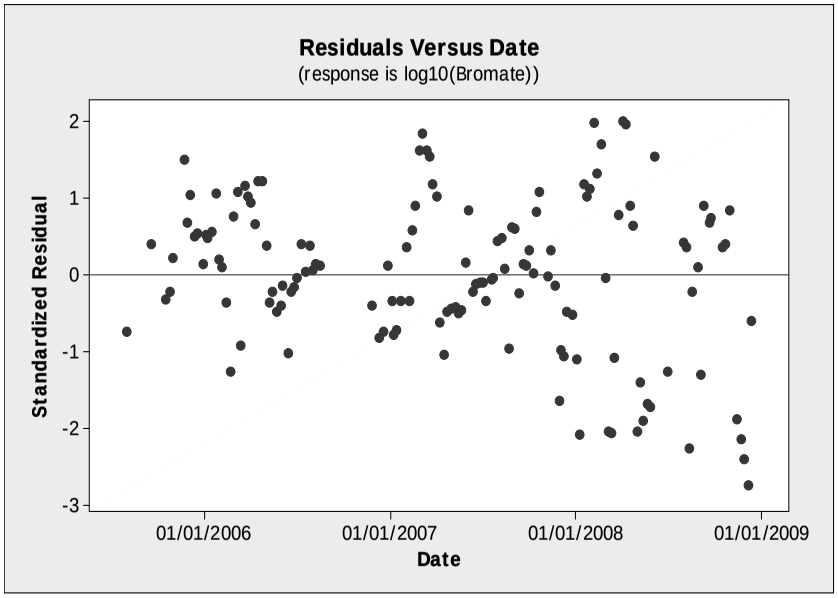
Residuals Versus Date
(response is log10(Bromate))
Standardized Residual
2
1
0
-1
-2
-3
01/01/2006
01/01/2007
01/01/2008
01/01/2009
Date

Appendix D

Single Borehole Dilution Testing

Appendix D

Single Borehole Dilution Testing

D.1 Introduction

A series of single borehole dilution tests (SBDT) within existing boreholes in the Hertfordshire Chalk were undertaken during 2008. These single borehole dilution tests were undertaken in conjunction with a programme of point-to-point Natural Gradient Tracer Testing using Bacteriophage which are described by Cook (2010).

D.2 Objectives

The objectives were:

- To determine the hydraulically active horizons within the selected boreholes in order to guide injection strategies for the natural gradient point-to-point tracer testing;
- To use uniform injection SBDTs to obtain a direct measurement of horizontal specific discharge (Darcy velocity);
- To use point injection SBDTs to determine vertical flow rates within the boreholes;

The scope of works comprised:

- Single borehole dilution testing
- Geophysical logging (Temperature & Conductivity, Gamma & Caliper, Formation Resistivity and Impellor Flowmeter)
- Down-hole CCTV

Four boreholes were identified as suitable based on criteria outlined by Maurice (2009):

1. Nashe's Farm Borehole (location **019**)
2. Comet Way Borehole (location **402**)
3. Harefield House Borehole (location **226**)
4. Hatfield Business Park Borehole (location **002**)

The location at Hatfield Business Park was not tested due to difficulties in obtaining permission.

D.3 Methodology

The field methodology followed Ward et al. (1998) and Maurice (2009). To summarise, a concentrated solution of table salt (sodium chloride) was injected as a tracer into the water column via a weighted hosepipe. For uniform injections, tracer solution was injected throughout the full length of water column; for point injections, tracer solution was added at a specific interval. A Solinst Levelogger LTC probe was used to measure the electrical conductance profile before and after injection to monitor the dilution of the salt within the water column to background concentrations over time. The probe measured depth below the water table using a pressure transducer. Corrections were made for changes in atmospheric pressure, and temperature adjustment periods.

A proforma and groundwater risk assessment was submitted to the Environment Agency for approval in November 2007.

D.4 Results and Interpretation

Maurice (2009) used a simple model to simulate the EC profiles produced by different types of flowing features, and the results from this are used in the interpreation of the EC profiles below.

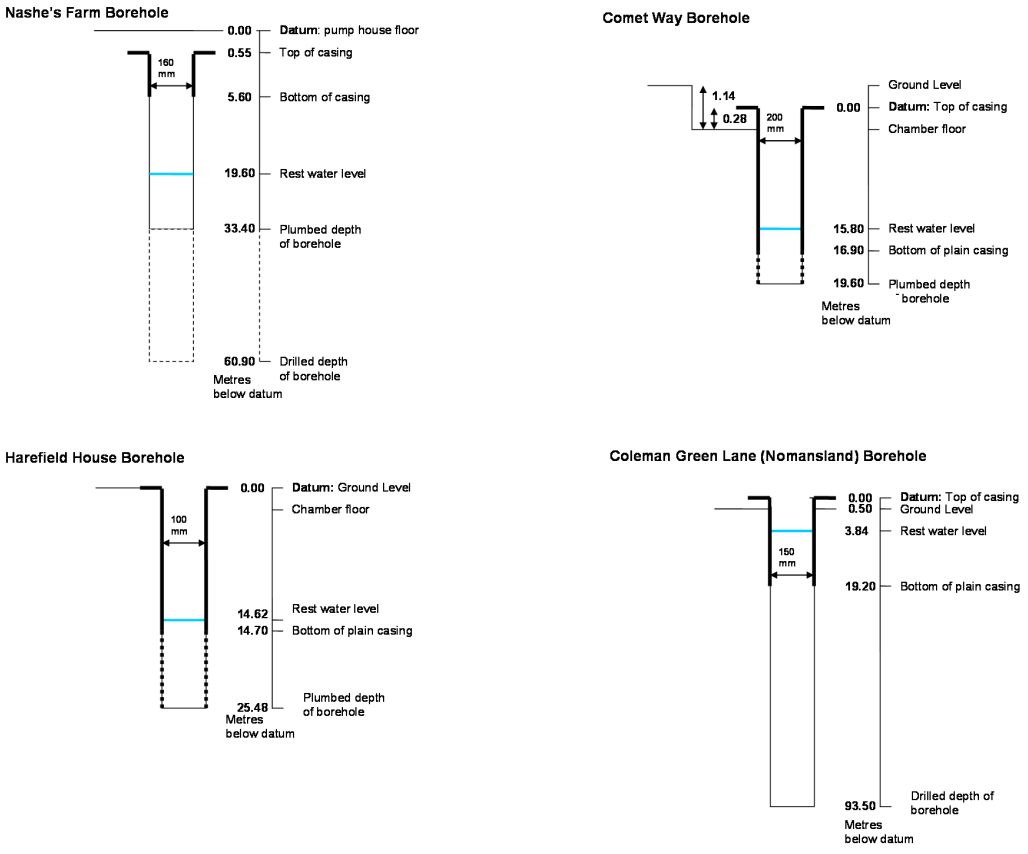

Figure D.1: Borehole construction details for the boreholes used for the single borehole dilution testing.

D.4.1 Nashe's Farm BH

The borehole construction and water level details are shown schematically in Figure D.1.

D.4.1.1 Geophysical testing

The results from the Geophysical testing are detailed in the memo from Jessica Randle (2008). The results pertinent to the dilution testing are summarised below:

- The calliper trace indicates that the open hole section of the borehole has a variable diameter, with some fractures/fissures widening to 300 mm. In particular there are increases in borehole diameter between 20.5 and 22.5 m below datum (bD) and between 24.5 and 25.5 m bD.

- The impellor flow logs detected some upward flow within the borehole between 23.3 m bD and 24.8 m bD.

D.4.1.2 Tracer efflux times

The electrical conductance (EC) profile for the uniform injection (Figure D.2) shows that the tracer is diluted to background concentrations by 21 hours after injection, and has declined to $\sim$10 % of the initial concentration by 6 hours 13 minutes after injection. Extrapolation of the graph of summed tracer concentration indicates that the tracer concentrations are likely to have diluted to background concentrations by $\sim$10 hours.

D.4.1.3 EC profile interpretation - Uniform Injection

Assuming a uniform column of tracer immediately after injection, the initial profile indicates that rapid dilution occurred in the top section of the profile (20.0 to 22.5 m bD), mid water column (24.5 to 26.0 m bD) and bottom part of the profile (30.0 to 31.5 m bD) before the initial log was run (Figure D.2). Subsequent profiles show gradual dilution of tracer throughout the borehole column, with profiles becoming near vertical after 2 hours 50 minutes and dilution apparently continuing at a more uniform, slower rate.

The horizons at 20.0-22.5 m bD and 24.5-26.0 m bD correspond to depths of increased borehole diameter (Section D.4.1.1). The reduced tracer concentrations ('troughs') at these horizons compared to tracer concentrations in the rest of the borehole column can therefore be explained (at least in part) by increased dilution due to increased borehole diameter. For an increase in diameter from 200 mm to 240 mm between 24.5 and 26.0 m bD, the dilution factor is 1.44, which would reduce EC from 2.2 $\mathrm{mS\ cm^{-1}}$ to 1.5 $\mathrm{mS\ cm^{-1}}$. For an increase in diameter from 200 mm to 300 mm between 20.0 and 22.5 m bD, the dilution factor is 2.25, which would reduce EC from 2.2 $\mathrm{mS\ cm^{-1}}$ to 1.0 $\mathrm{mS\ cm^{-1}}$. These dilutions are larger than those measured, but this could be due to incomplete mixing. The rapid dilution at these concentration 'trough' locations could also be a result of inflow or crossflow from fractures/fissures at these horizons (Maurice, 2009). The concentration 'trough' at 24.5-26.0 m bD appears to become less prominent with time, which would be consistent with dilution as a result of increased diameter. In contrast, the 'trough' at 30.0-31.5 m bD persists, which could indicate a flowing feature at this location.

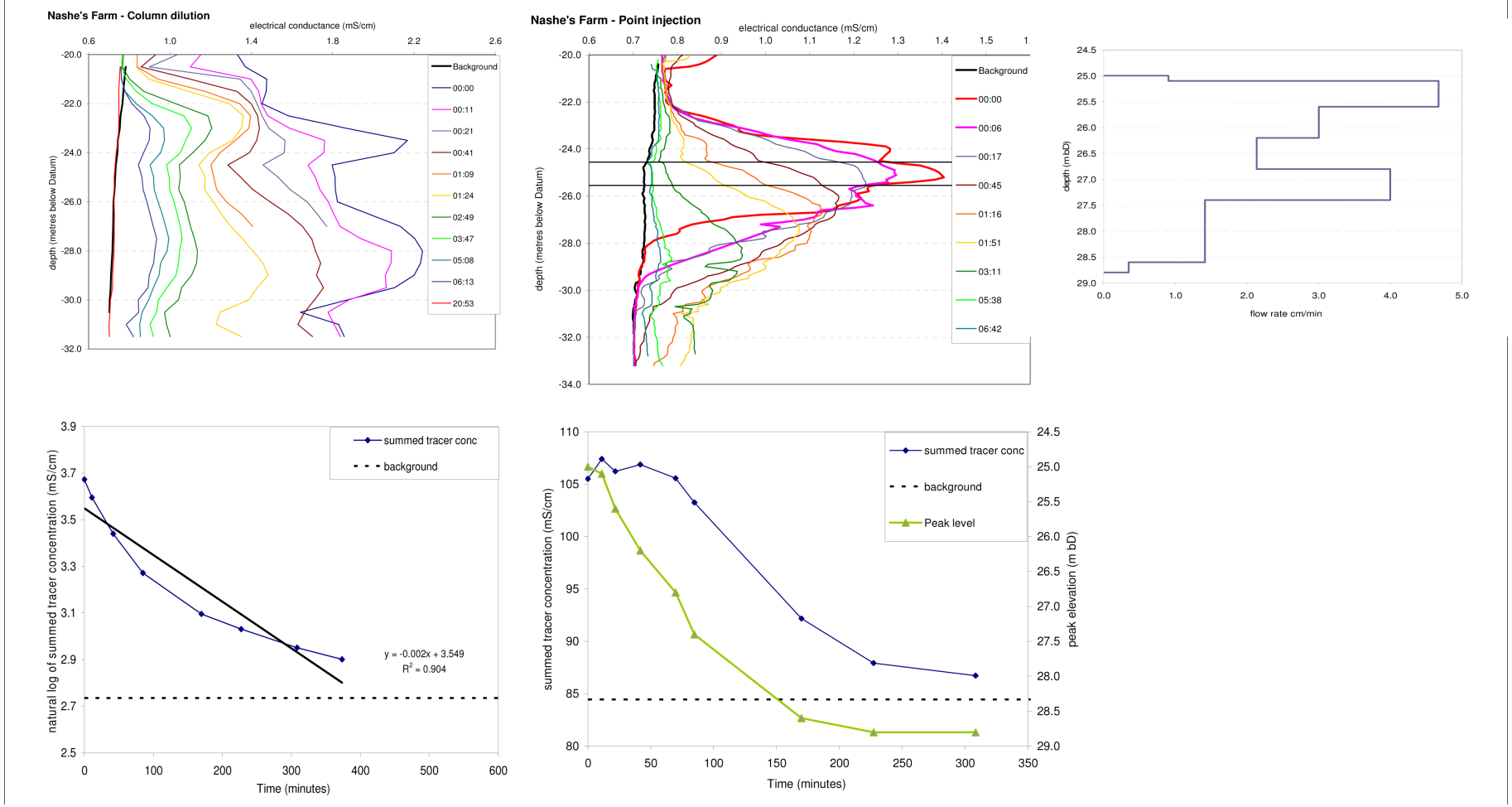

Figure D.2: Electrical Conductance profile for uniform injection (column dilution) SBDT and point injection SBDT at Nashe's Farm BH. Tracer was injected between 24.5 and 25.5 m bD for the point injection. Vertical flow rate is based on the vertical position of the point injection concentration peak.

The sharp boundary between 24.5 and 22.0 m bD in the initial (t=0:00) profile appears to move up the borehole to ∼21.0 m bD by the profile at 11 minutes, where it then remains. This is consistent with upward flow recorded by the impellor flow meter between 23.3 m bD and 24.8 m bD (section **??**). Apart from this, there do not appear to be any definite features on the uniform injection EC profile which indicate vertical flow within the borehole (Maurice, 2009).

D.4.1.4 EC profile interpretation - Point Injection

In order to investigate the flow behaviour in the mid section of the profile, a pulse of tracer was injected to between 5.86 and 4.86 below the water table (24.55 and 25.55 m bD). The EC profile immediately after injection shows a relatively broad concentration peak (EC above background between approximately 22.5 and 27.5 m bD), with a sharper concentration spike between 24.5 and 25.5 m bD (Figure D.2). Subsequent profiles show that the tracer peak moves down the borehole (vertical flow) until it reaches between 28.0 and 29.5 m bD, after which the peak flattens out and concentrations decrease towards background levels.

Summed tracer concentrations for the point injection indicate a low rate of mass loss over the first 100 minutes as the peak moves between 25.0 and 26.8 m bD. There is then significant mass loss between 100 and 300 minutes as the peak moves between 26.8 and 28.8 m bD. Vertical flow rates show a reduction in flow rate below ∼27.5 m bD, which reduces to zero at ∼28.5 m bD. There also appears to be a decrease in flow rate at ∼26.5 m bD. These observations could indicate outflow (or crossflow with net outflow) at these horizons (Maurice, 2009).

D.4.2 Comet Way BH

The borehole construction and water level details are shown schematically in Figure D.1.

D.4.2.1 Geophysical testing

The results from the Geophysical testing are detailed in Jessica Randle (2008). The tests were limited due to the small amount of water in the borehole and poor verticality of the boreole. The results pertinent to the dilution testing are summarised below:

- The impeller flowmeter logs detected a slight downward flow within the borehole from 17.0mbD, in the slotted section of casing.

D.4.2.2 Tracer efflux times

The electrical conductance (EC) profile for the uniform injection (Figure D.3) shows that the tracer is diluted to background concentrations by 1 hour after injection in the section with slotted casing, and by 2 hours in the section of plain casing.

D.4.2.3 EC profile interpretation - Uniform Injection

Due to a misinterpretation of borehole construction information, tracer was added to the full 3.8 m of water column (between 15.9 and 19.8mbD), including the section of water column within the plain casing.

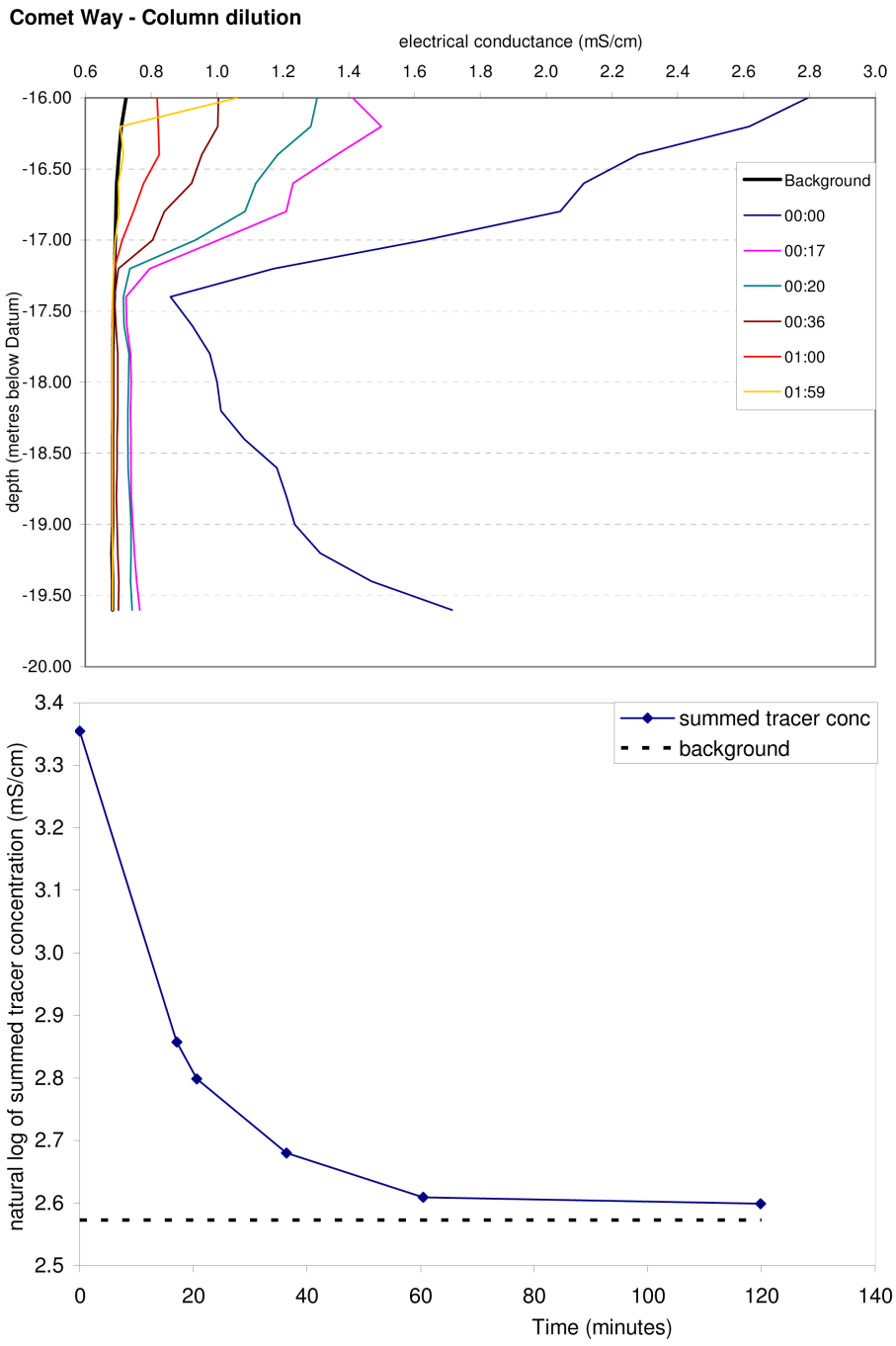

Figure D.3: Electrical Conductance profile for uniform injection (column dilution) SBDT at Comet Way BH.

Assuming a uniform column of tracer immediately after injection, the initial profile indicates that rapid dilution occurred in the slotted casing (below 16.9 m bD), particularly between 17.0 and 19.0 m bD, before the initial log was run. The subsequent profiles (17 minutes to 2 hours) are near vertical in the cased section and indicate dilution continuing at a more uniform, slower rate.

The tracer in the section of plain casing (between 15.9 and 16.9 m bD) also gradually dilutes to background concentrations, which implies that the tracer moves downwards into the slotted casing section. This concurs with the downward flow detected by the impellor flow meter from 17.0 m bD. However, since the profiles do not show a tracer front moving down the borehole, this vertical flow appears to happen rapidly in relation to horizontal flow out of the borehole.

D.4.3 Harefield House BH

The borehole construction and water level details are shown schematically in Figure D.1.

D.4.3.1 Geophysical testing

Geophysical test results are not available for Harefield House Borehole as the borehole diameter was too small to accommodate the equipment.

D.4.3.2 Tracer efflux times

The electrical conductance (EC) profile for the uniform injection (Figure D.4) shows that the tracer is diluted to background concentrations over the majority of the profile by 4 hours 4 minutes after injection. Elevated concentrations remain in the bottom section of the borehole below 25.5 m bD. Extrapolation of the graph of summed tracer concentration indicates that the tracer concentrations are likely to have diluted to background concentrations by ∼1800 minutes (∼30 hours).

D.4.3.3 EC profile interpretation - Uniform Injection

Tracer solution was only placed in the section of borehole with slotted casing, with fresh water in the cased section. Assuming a uniform column of tracer immediately after injection, the initial profile indicates that rapid dilution occurred in the upper section of the profile (16-21.5 m bD), before the initial log was run. Subsequent profiles show gradual dilution along the length of the borehole. Summed concentrations indicate rapid exponential mass loss until 41 minutes after injection. Total mass remains almost constant until 1490 minutes (24 hours 50 minutes), after which it decreases approximately exponentially to background concentrations.

D.4.3.4 EC profile interpretation - Point Injection

In order to investigate the flow behaviour in the mid section of the profile, a pulse of tracer was injected at 22.9 m bD (Point injection 1) and a separate pulse was injected at 19.5 m bD (Point injection 2).

Point Injection 1 (22.9 m bD)

The EC profile immediately after injection shows elevated concentrations between ∼21.5 and ∼25.0 m bD in addition to the high concentrations seen at the bottom of the borehole in the background profile and subsequent profiles. Subsequent profiles show that the tracer front moves up the borehole (vertical flow) until it reaches ∼17.0 m bD at 26 minutes. The summed tracer concentrations

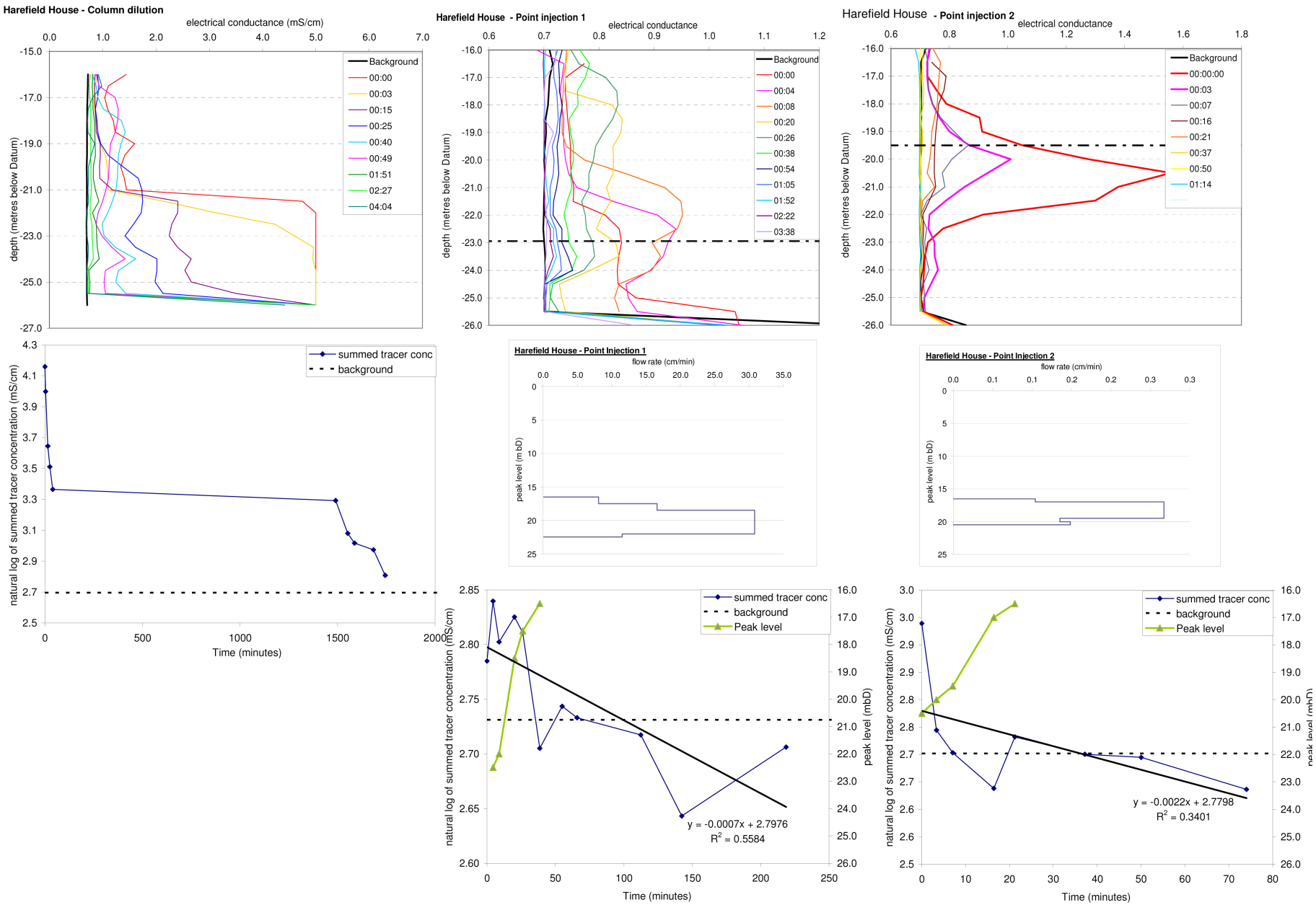

Figure D.4: Electrical Conductance profile for uniform injection (column dilution) SBDT and point injection SBDT at Harefield House BH. Two point injections were carried out: one with tracer injected at 22.9 m bD and a separate one with tracer injected at 19.5 m bD. Vertical flow rate is based on the vertical position of the point injection concentration peak.

indicate that the mass appears to increase from the initial profile until the profile at 26 minutes. There do not appear to be any consistent 'nick points' which would indicate outflow horizons over the section of vertical flow.

Point injection 2 (19.5 m bD)

The EC profile immediately after injection shows elevated concentrations between $\sim$81.5 and $\sim$22.5 m bD, with a relatively sharp peak at $\sim$20.5 m bD. Subsequent profiles show that the tracer peak moves up the borehole (vertical flow) as it dilutes, until it returns to background concentrations by 37 minutes. There do not appear to be any consistent 'nick points' which would indicate outflow horizons over the section of vertical flow. Summed tracer concentrations for point injection 2indicate mass loss over the first 16 minutes as the peak moves between $\sim$20.5 and $\sim$17.0 m bD. Summed concentrations hover around background concentrations for the remainder of the dilution until 74 minutes.

D.5 Calculation of horizontal specific discharge (Darcy Velocity)

The results for the

D.5.1 Methodology

Methodology is outlined in Figure D.5

D.5.2 Results

Plots of $\ln \frac{C_t - C_b}{C_0 - C_b}$ for Nashe's Farm, Harefield House, and Comet Way are included.

Assumptions:

- The concentrations within the borehole remains uniform and equal to the concentration leaving the borehole;
- The concentration at time zero is instantaneously raised to ci;
- Water enters the borehole from an aquifer thickness equal to the screened or open length of the borehole - i.e. there is not vertical flow in the aquifer
- Water upstream of the borehole is at a uniform background concentration of cb; and
- The flow is steady state.

If these assumptions above are met, then the change in tracer mass in the borehole over a time interval Δt will be equal to the mass fluxes into and out of the borehole(Ward et al., 1998):

$$\pi R^2 L_{sat} \Delta C = q L_{scrn} \alpha D (c_b - c) \Delta t \tag{1}$$

where:

R	borehole radius
L_{sat}	saturated depth of borehole
ΔC	change in borehole concentration
q	Darcy velocity in the aquifer
L_{scrn}	open length of the borehole
α	ratio of the width of the aquifer contributing flow to the borehole to the borehole diameter (see figure)
D	borehole diameter ($2R$)
c_b	background aquifer concentration of tracer (often zero)

The above equation can be integrated from time zero (borehole concentration c_i) to any given time t (borehole concentration $c(t)$):

$$\pi R^2 L_{sat} \int_{c_i}^{c} \frac{dc'}{c_b - c'} = q L_{scrn} \alpha D \int_0^t dt' \tag{2}$$

which becomes

$$\pi R^2 L_{sat} \ln\left(\frac{c_b - c}{c_b - c_i}\right) = q L_{scrn} \alpha D t \tag{3}$$

Rearranging to make q the subject

$$q = \frac{\pi R^2 L_{sat}}{\alpha D t L_{scrn}} \ln\left(\frac{c_b - c}{c_b - c_i}\right) \tag{4}$$

The value of α can be anywhere in the range 0 to 8 (Klotz er al 1972), although where there is no gravel pack,

$$\alpha = 2$$

is usually sufficient.

Assuming $L_{sat} = L_{scrn}$, and since $D = 2R$, then

$$q = \frac{\pi R}{4t} \ln\left(\frac{c_b - c}{c_b - c_i}\right) \tag{5}$$

which can be arranged as

$$\ln\left(\frac{c - c_b}{c_i - c_b}\right) = -\frac{4qt}{\pi R} \tag{6}$$

Therfore, if field results are ploted as $\ln\left(\frac{c-c_b}{c_i-c_b}\right)$ against t, then the gradient m of the straight line graph $y = mx + c$ is given by $\frac{4q}{\pi R}$, and hence

$$q = \frac{\pi R m}{4} \tag{7}$$

Once the darcy velocity is determined from equation above, further parameters can be obtained from the following relationships:

$$q = -Ki \tag{8}$$

$$v = q/n_e \tag{9}$$

Figure D.5: Methodology for determination of specific discharge (darcy velocity) from the results of the Single Borehole Dilution Tests.

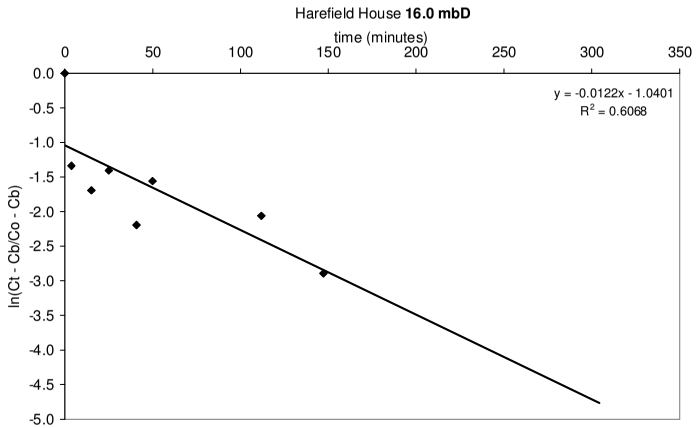
Harefield House **16.0 mbD**
time (minutes)
ln(Ct - Cb/Co - Cb)
y = -0.0122x - 1.0401
R² = 0.6068

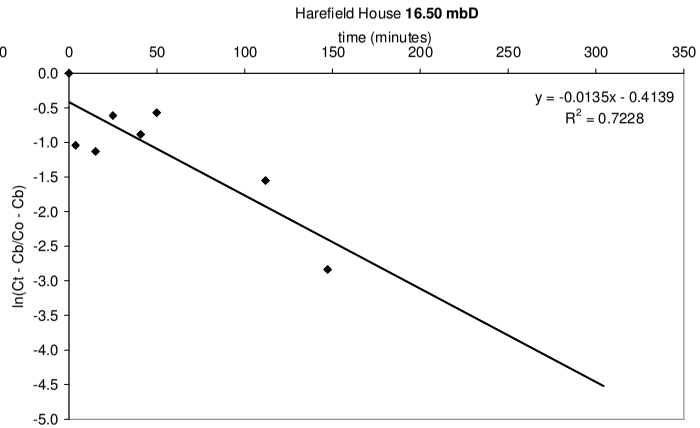
Harefield House **16.50 mbD**
time (minutes)
ln(Ct - Cb/Co - Cb)
y = -0.0135x - 0.4139
R² = 0.7228

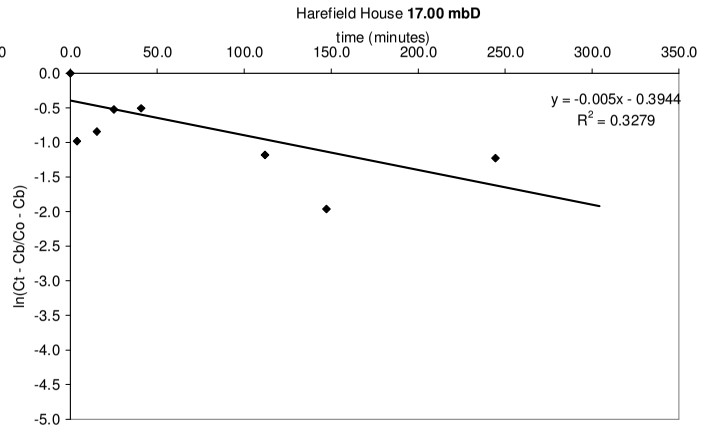
Harefield House **17.00 mbD**
time (minutes)
ln(Ct - Cb/Co - Cb)
y = -0.005x - 0.3944
R² = 0.3279

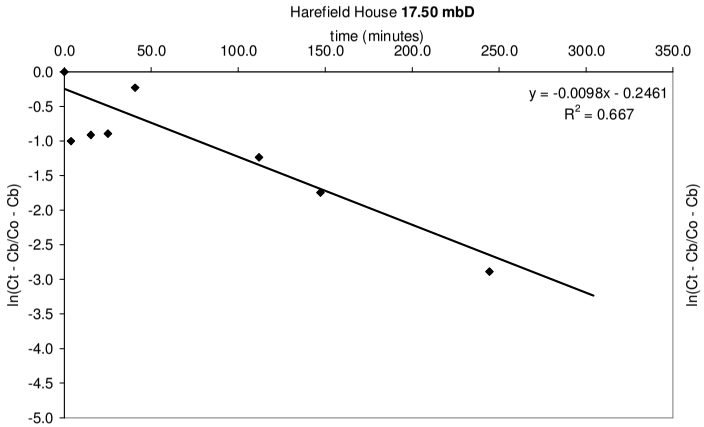
Harefield House **17.50 mbD**
time (minutes)
ln(Ct - Cb/Co - Cb)
y = -0.0098x - 0.2461
R² = 0.667

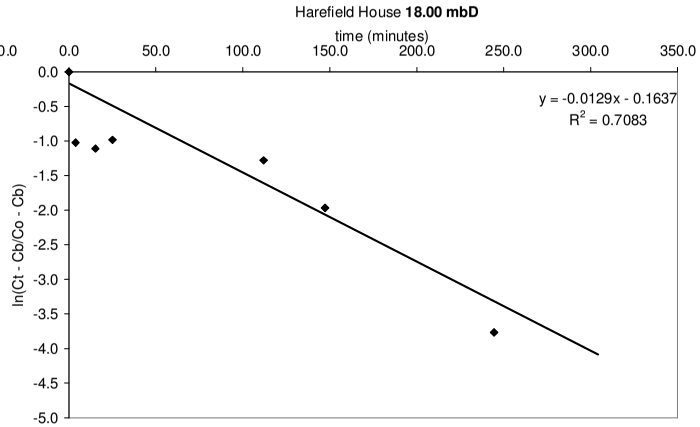
Harefield House **18.00 mbD**
time (minutes)
ln(Ct - Cb/Co - Cb)
y = -0.0129x - 0.1637
R² = 0.7083

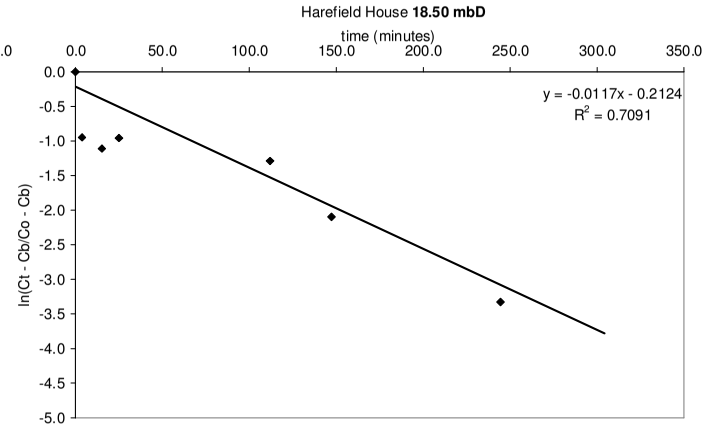
Harefield House **18.50 mbD**
time (minutes)
ln(Ct - Cb/Co - Cb)
y = -0.0117x - 0.2124
R² = 0.7091

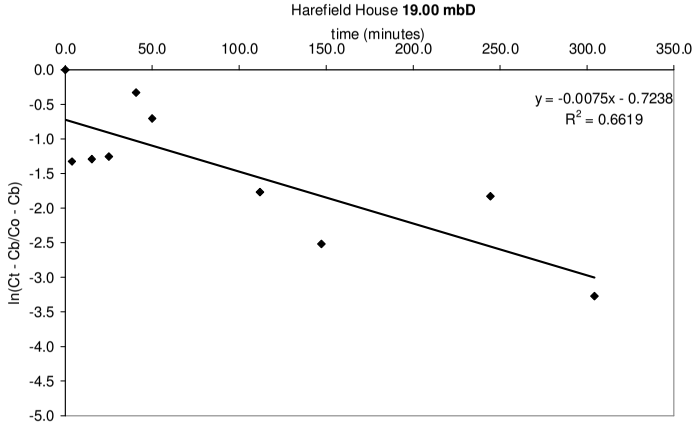
Harefield House **19.00 mbD**
time (minutes)
ln(Ct - Cb/Co - Cb)
y = -0.0075x - 0.7238
R² = 0.6619

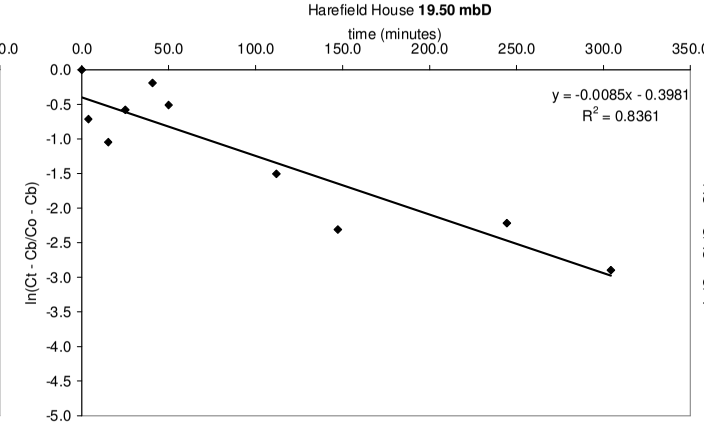
Harefield House **19.50 mbD**
time (minutes)
ln(Ct - Cb/Co - Cb)
y = -0.0085x - 0.3981
R² = 0.8361

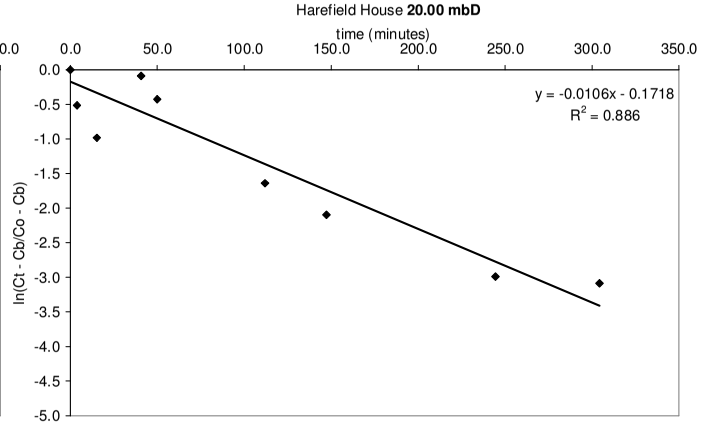
Harefield House **20.00 mbD**
time (minutes)
ln(Ct - Cb/Co - Cb)
y = -0.0106x - 0.1718
R² = 0.886

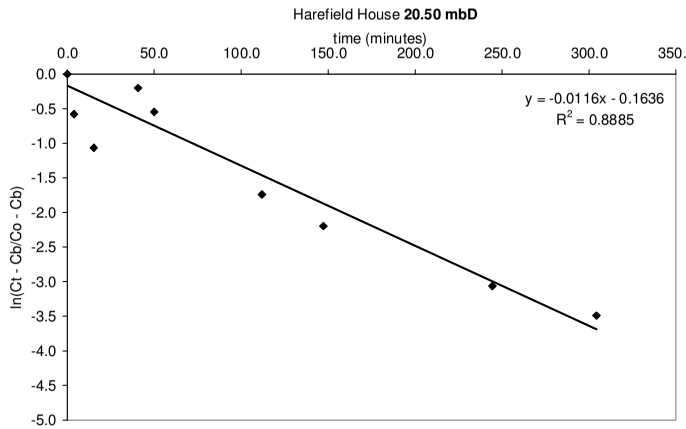
Harefield House **20.50 mbD**
time (minutes)
ln(Ct - Cb/Co - Cb)
y = -0.0116x - 0.1636
R2 = 0.8885

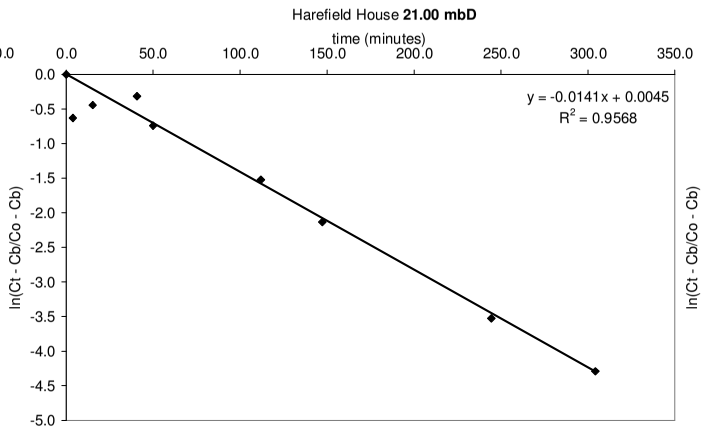
Harefield House **21.00 mbD**
time (minutes)
ln(Ct - Cb/Co - Cb)
y = -0.0141x + 0.0045
R2 = 0.9568

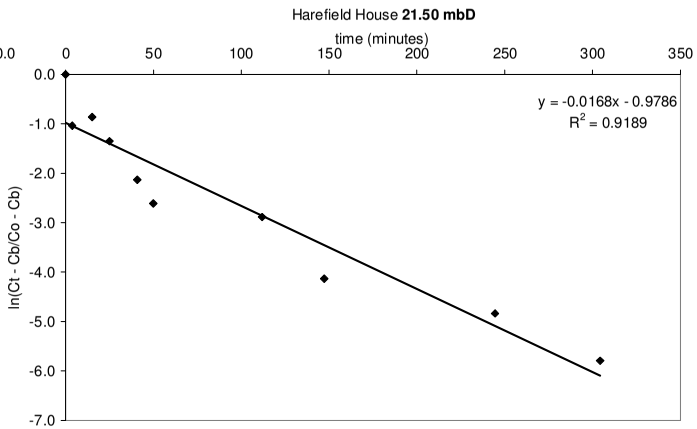
Harefield House **21.50 mbD**
time (minutes)
ln(Ct - Cb/Co - Cb)
y = -0.0168x - 0.9786
R2 = 0.9189

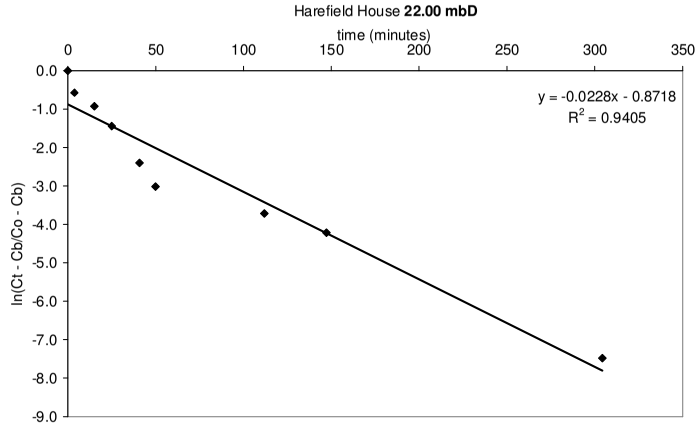
Harefield House **22.00 mbD**
time (minutes)
ln(Ct - Cb/Co - Cb)
y = -0.0228x - 0.8718
R2 = 0.9405

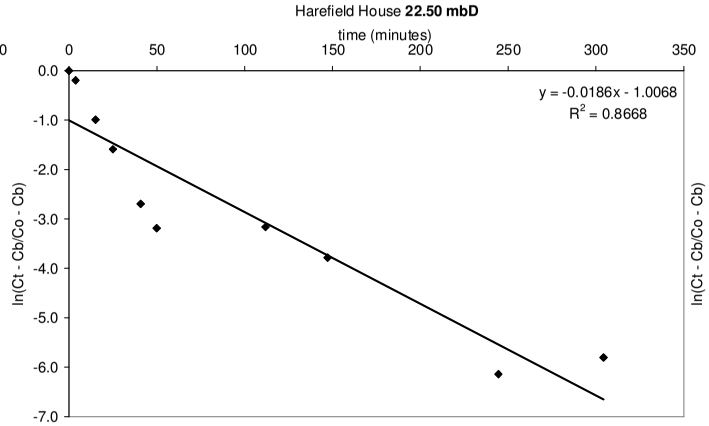
Harefield House **22.50 mbD**
time (minutes)
ln(Ct - Cb/Co - Cb)
y = -0.0186x - 1.0068
R2 = 0.8668

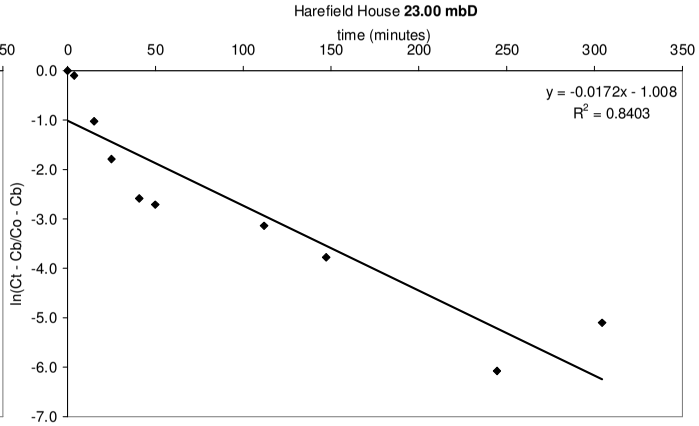
Harefield House **23.00 mbD**
time (minutes)
ln(Ct - Cb/Co - Cb)
y = -0.0172x - 1.008
R2 = 0.8403

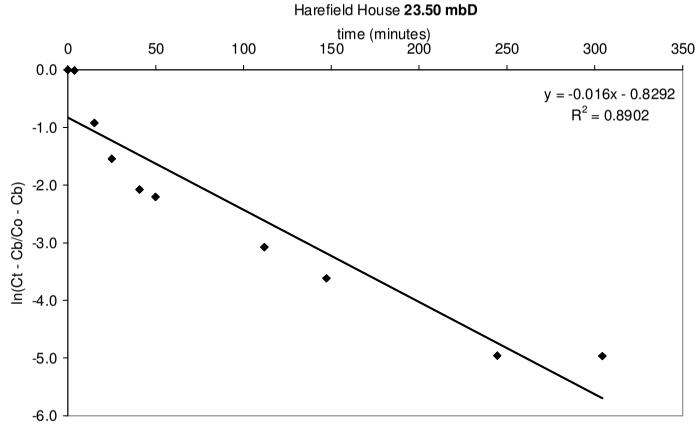
Harefield House **23.50 mbD**
time (minutes)
ln(Ct - Cb/Co - Cb)
y = -0.016x - 0.8292
R2 = 0.8902

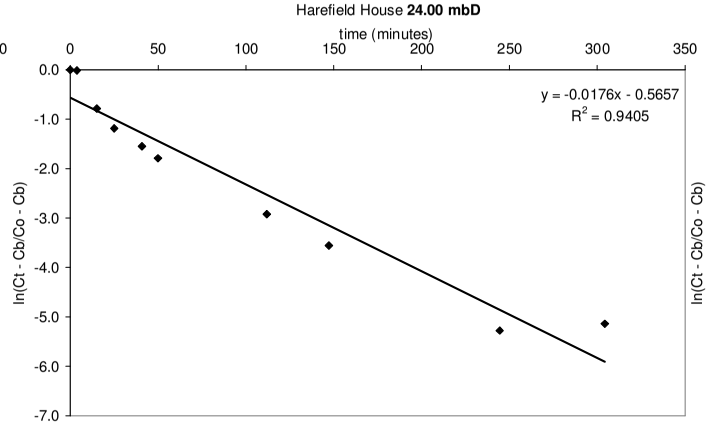
Harefield House **24.00 mbD**
time (minutes)
ln(Ct - Cb/Co - Cb)
y = -0.0176x - 0.5657
R2 = 0.9405

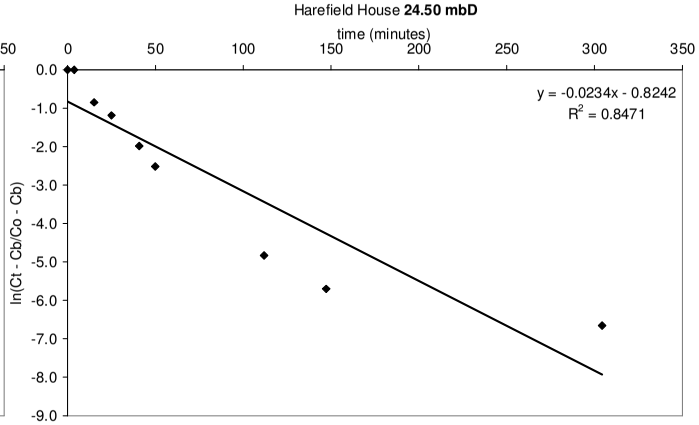
Harefield House **24.50 mbD**
time (minutes)
ln(Ct - Cb/Co - Cb)
y = -0.0234x - 0.8242
R2 = 0.8471

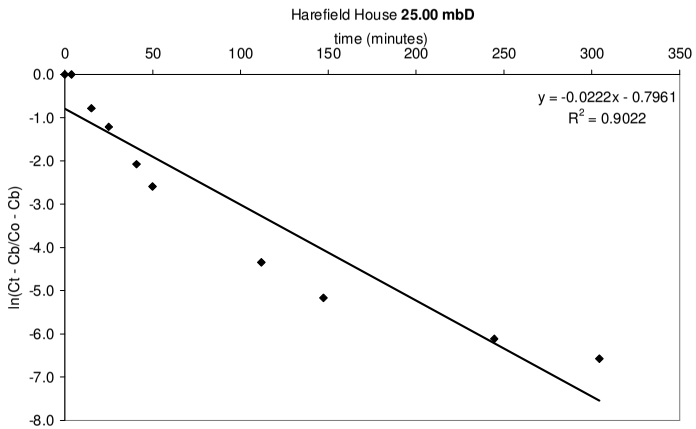
Harefield House **25.00 mbD**
time (minutes)
0
50
100
150
200
250
300
350
0.0
-1.0
-2.0
-3.0
-4.0
-5.0
-6.0
-7.0
-8.0
ln(Ct - Cb/Co - Cb)
y = -0.0222x - 0.7961
R2 = 0.9022

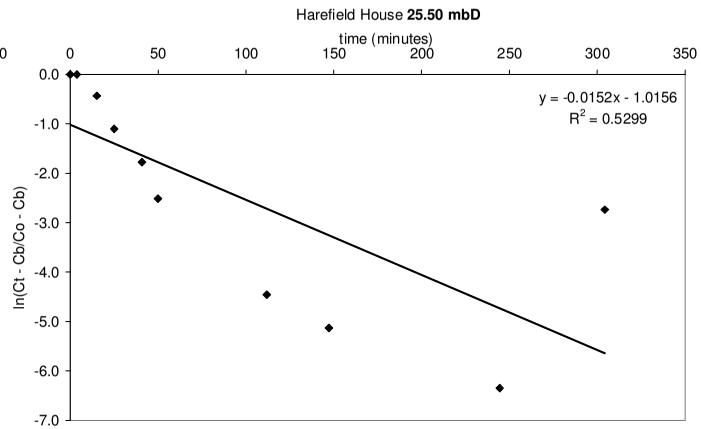
Harefield House **25.50 mbD**
time (minutes)
0
50
100
150
200
250
300
350
0.0
-1.0
-2.0
-3.0
-4.0
-5.0
-6.0
-7.0
ln(Ct - Cb/Co - Cb)
y = -0.0152x - 1.0156
R2 = 0.5299

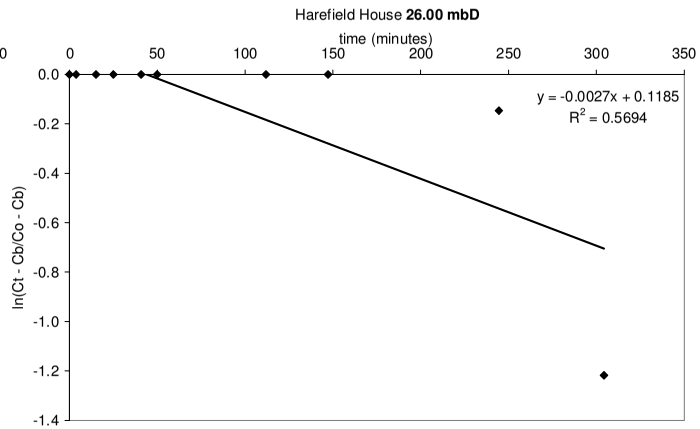
Harefield House **26.00 mbD**
time (minutes)
0
50
100
150
200
250
300
350
0.0
-0.2
-0.4
-0.6
-0.8
-1.0
-1.2
-1.4
ln(Ct - Cb/Co - Cb)
y = -0.0027x + 0.1185
R2 = 0.5694

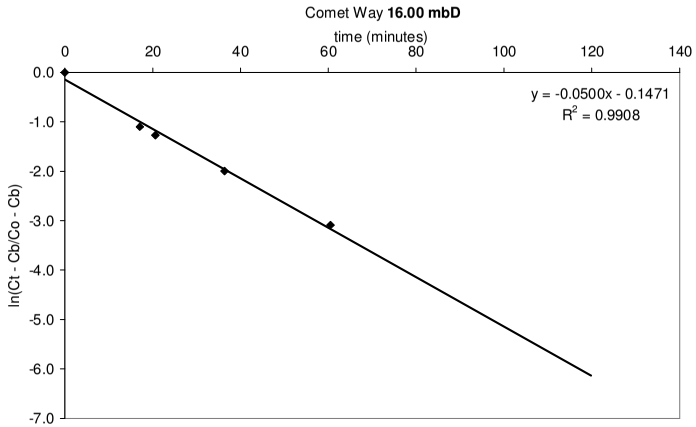
Comet Way **16.00 mbD**
time (minutes)
y = -0.0500x - 0.1471
R^2 = 0.9908
ln(Ct - Cb/Co - Cb)

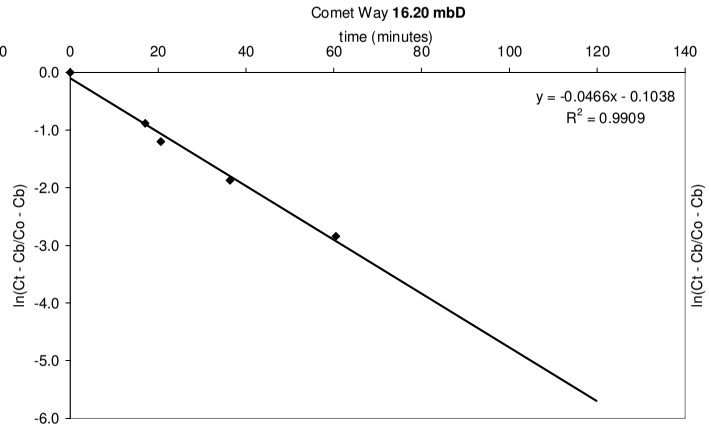
Comet Way **16.20 mbD**
time (minutes)
y = -0.0466x - 0.1038
R^2 = 0.9909
ln(Ct - Cb/Co - Cb)

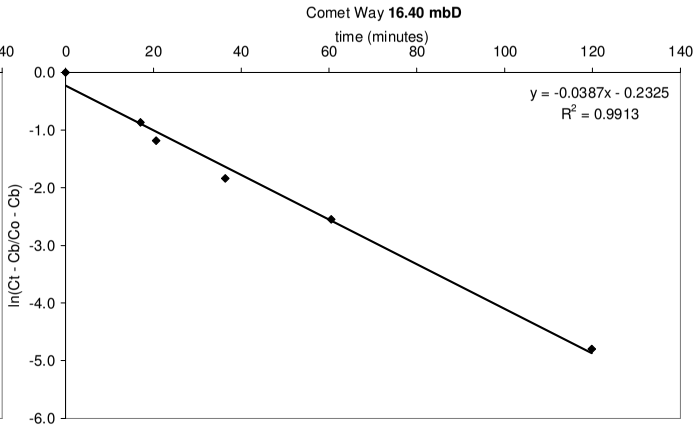
Comet Way **16.40 mbD**
time (minutes)
y = -0.0387x - 0.2325
R^2 = 0.9913
ln(Ct - Cb/Co - Cb)

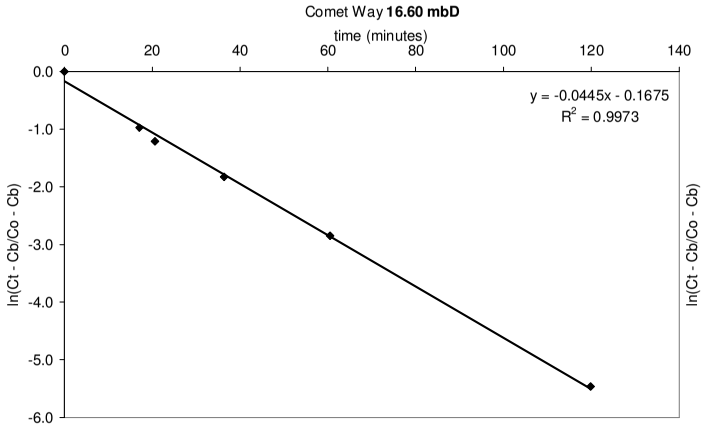
Comet Way **16.60 mbD**
time (minutes)
y = -0.0445x - 0.1675
R^2 = 0.9973
ln(Ct - Cb/Co - Cb)

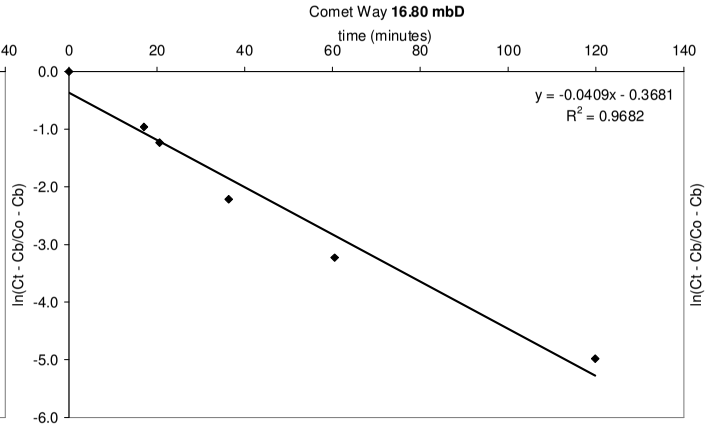
Comet Way **16.80 mbD**
time (minutes)
y = -0.0409x - 0.3681
R^2 = 0.9682
ln(Ct - Cb/Co - Cb)

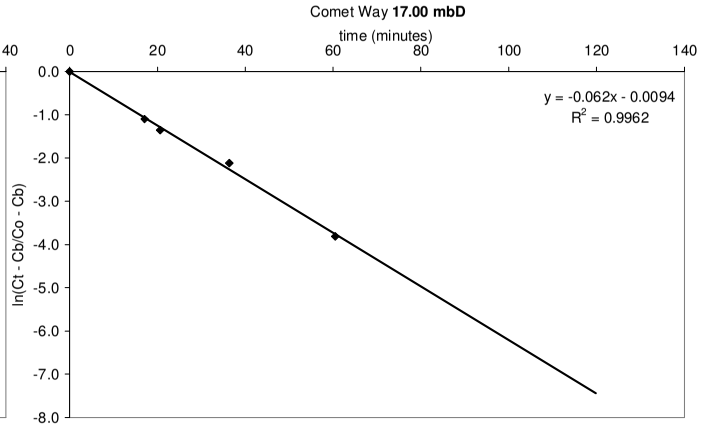
Comet Way **17.00 mbD**
time (minutes)
y = -0.062x - 0.0094
R^2 = 0.9962
ln(Ct - Cb/Co - Cb)

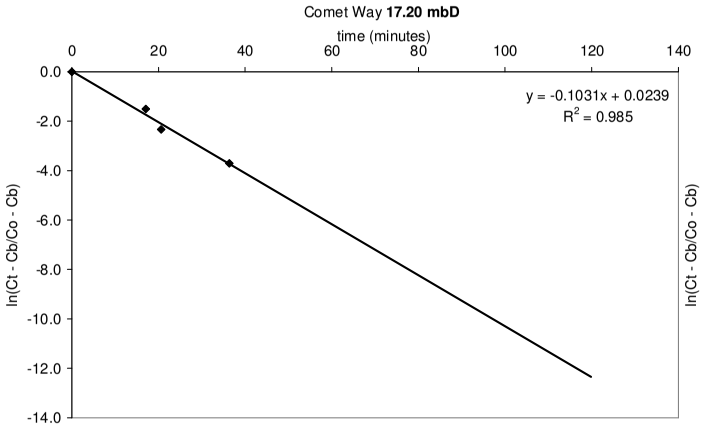
Comet Way **17.20 mbD**
time (minutes)
y = -0.1031x + 0.0239
R^2 = 0.985
ln(Ct - Cb/Co - Cb)

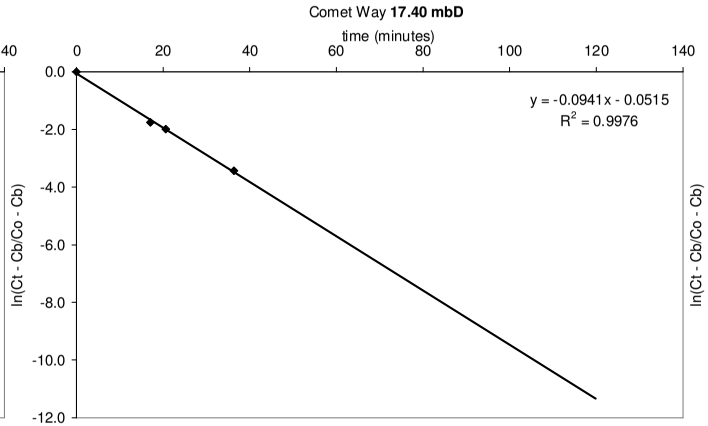
Comet Way **17.40 mbD**
time (minutes)
y = -0.0941x - 0.0515
R^2 = 0.9976
ln(Ct - Cb/Co - Cb)

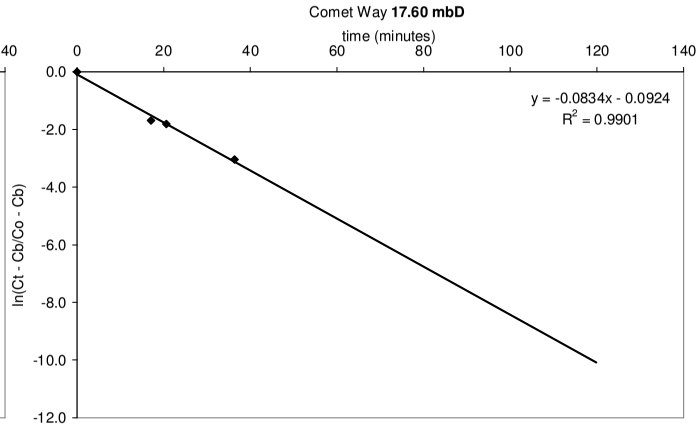
Comet Way **17.60 mbD**
time (minutes)
y = -0.0834x - 0.0924
R^2 = 0.9901
ln(Ct - Cb/Co - Cb)

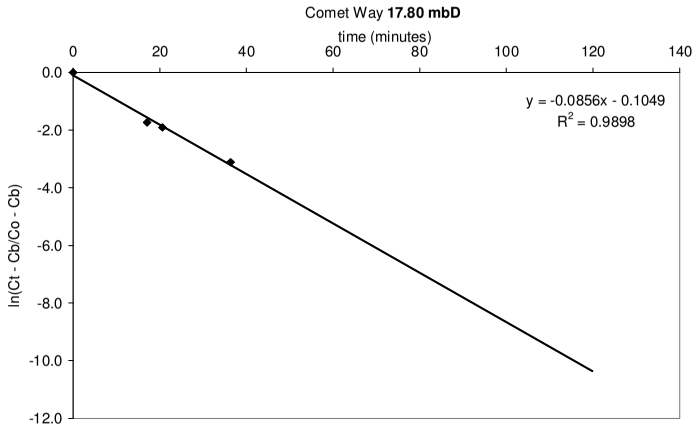
Comet Way **17.80 mbD**
time (minutes)
ln(Ct - Cb/Co - Cb)
y = -0.0856x - 0.1049
R² = 0.9898

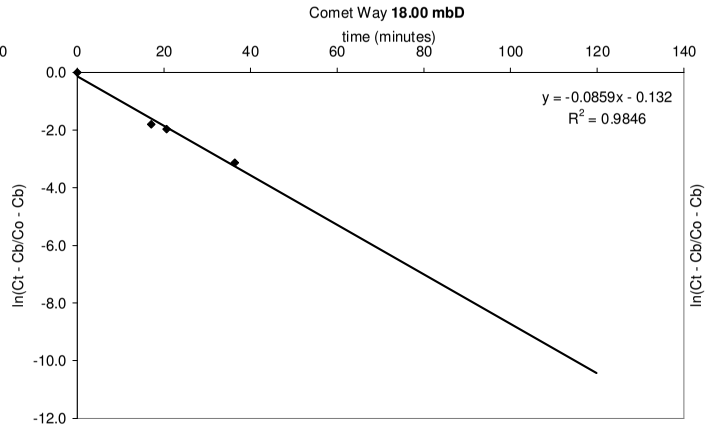
Comet Way **18.00 mbD**
time (minutes)
ln(Ct - Cb/Co - Cb)
y = -0.0859x - 0.132
R² = 0.9846

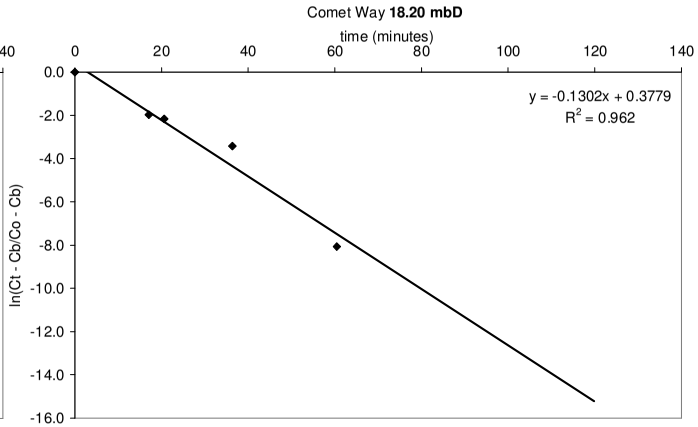
Comet Way **18.20 mbD**
time (minutes)
ln(Ct - Cb/Co - Cb)
y = -0.1302x + 0.3779
R² = 0.962

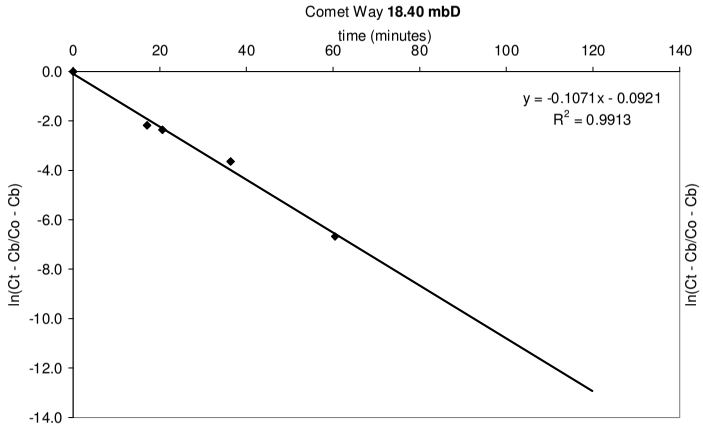
Comet Way **18.40 mbD**
time (minutes)
ln(Ct - Cb/Co - Cb)
y = -0.1071x - 0.0921
R² = 0.9913

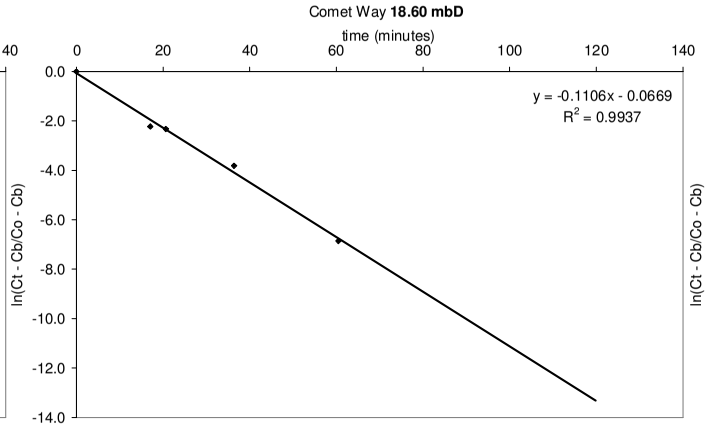
Comet Way **18.60 mbD**
time (minutes)
ln(Ct - Cb/Co - Cb)
y = -0.1106x - 0.0669
R² = 0.9937

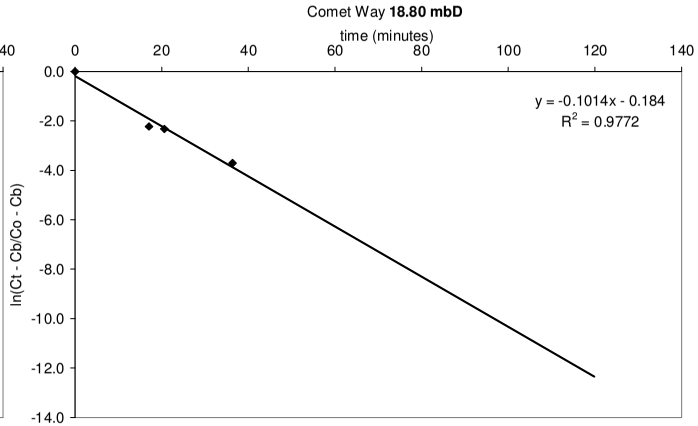
Comet Way **18.80 mbD**
time (minutes)
ln(Ct - Cb/Co - Cb)
y = -0.1014x - 0.184
R² = 0.9772

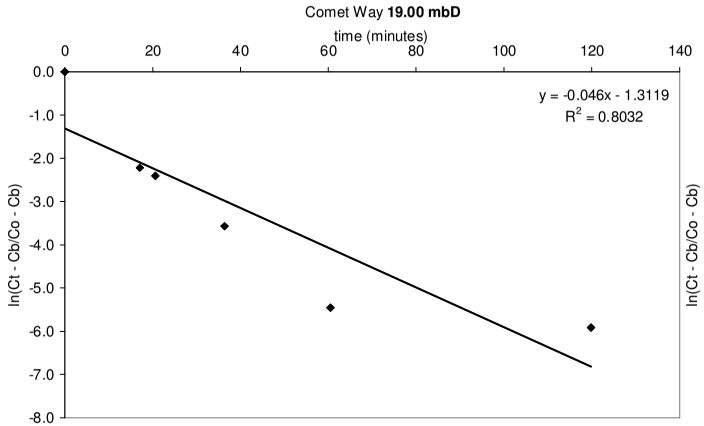
Comet Way **19.00 mbD**
time (minutes)
ln(Ct - Cb/Co - Cb)
y = -0.046x - 1.3119
R² = 0.8032

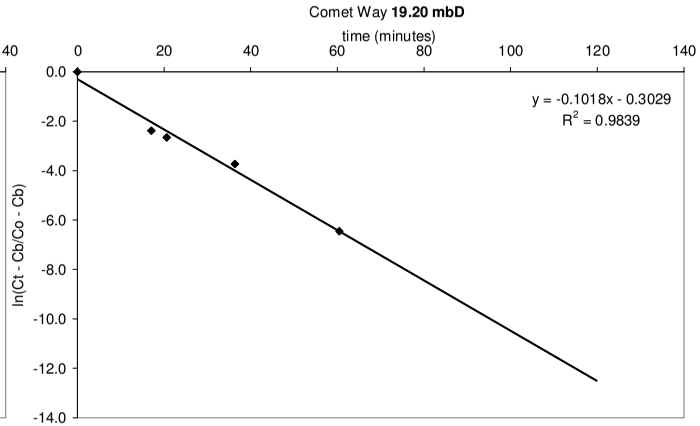
Comet Way **19.20 mbD**
time (minutes)
ln(Ct - Cb/Co - Cb)
y = -0.1018x - 0.3029
R² = 0.9839

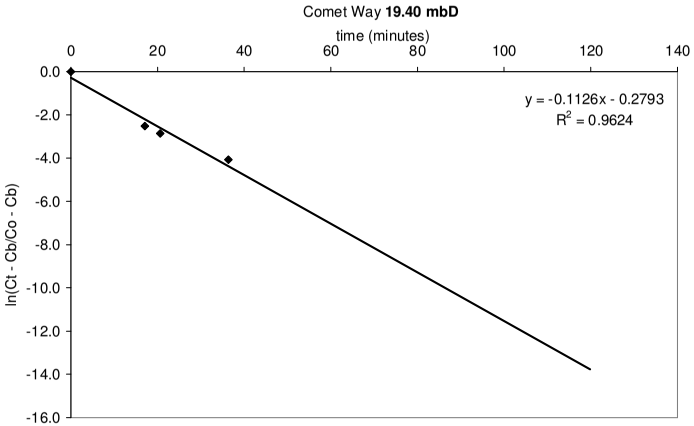
Comet Way **19.40 mbD**
time (minutes)
ln(Ct - Cb/Co - Cb)
y = -0.1126x - 0.2793
R² = 0.9624

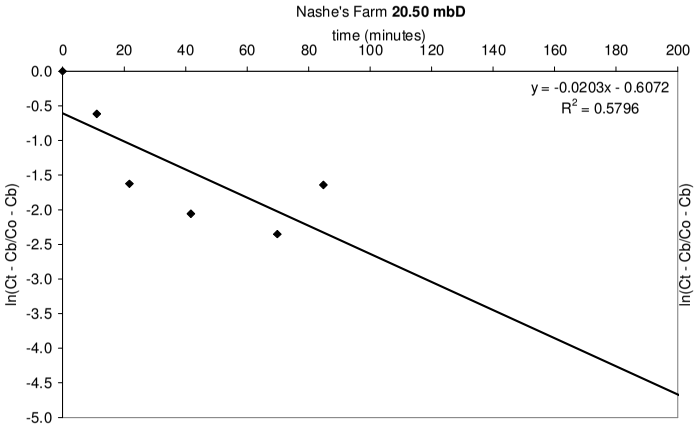
Nashe's Farm **20.50 mbD**
time (minutes)
ln(Ct - Cb/Co - Cb)
y = -0.0203x - 0.6072
R2 = 0.5796

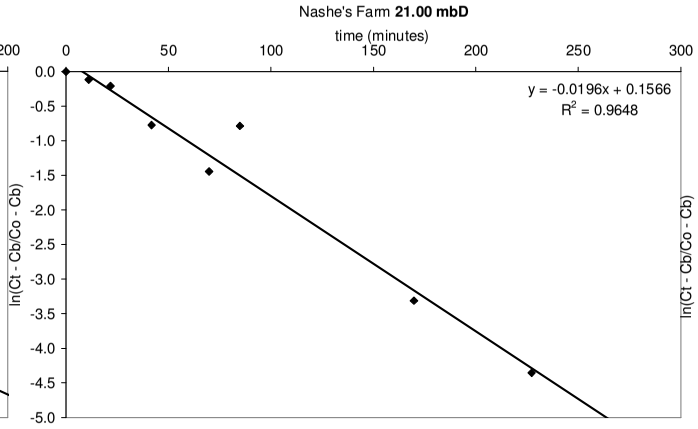
Nashe's Farm **21.00 mbD**
time (minutes)
ln(Ct - Cb/Co - Cb)
y = -0.0196x + 0.1566
R2 = 0.9648

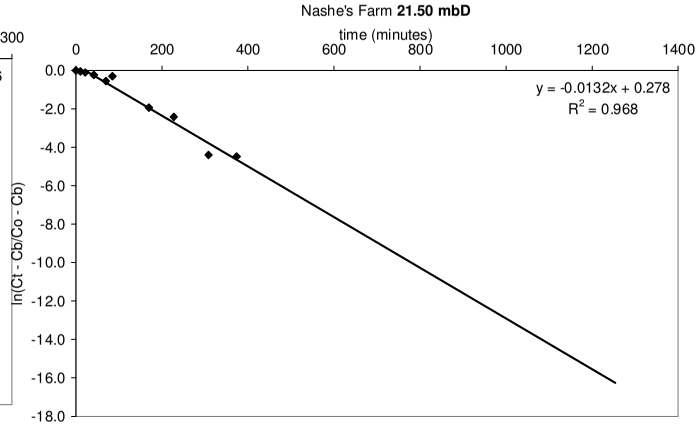
Nashe's Farm **21.50 mbD**
time (minutes)
ln(Ct - Cb/Co - Cb)
y = -0.0132x + 0.278
R2 = 0.968

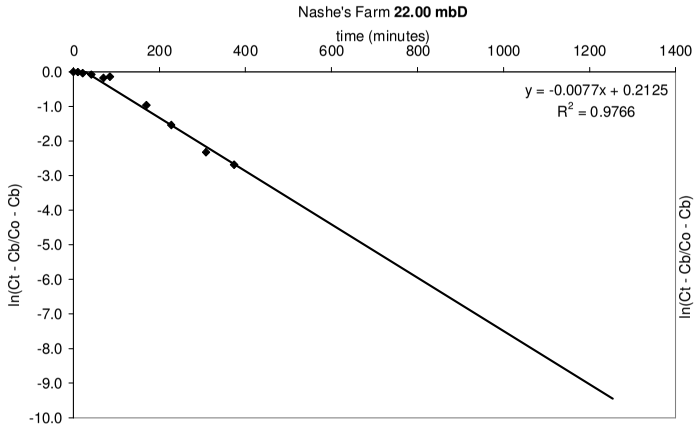
Nashe's Farm **22.00 mbD**
time (minutes)
ln(Ct - Cb/Co - Cb)
y = -0.0077x + 0.2125
R2 = 0.9766

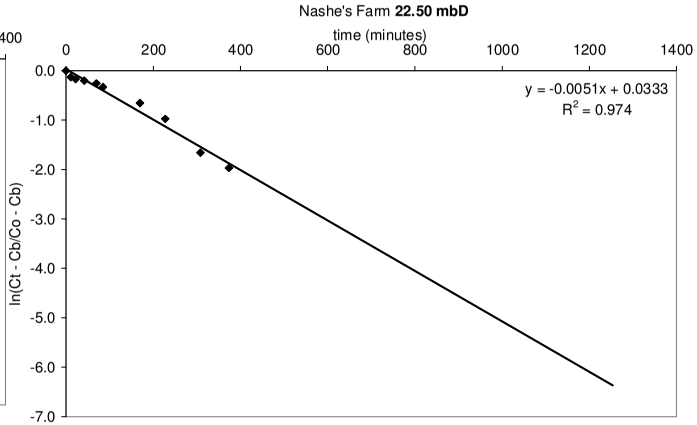
Nashe's Farm **22.50 mbD**
time (minutes)
ln(Ct - Cb/Co - Cb)
y = -0.0051x + 0.0333
R2 = 0.974

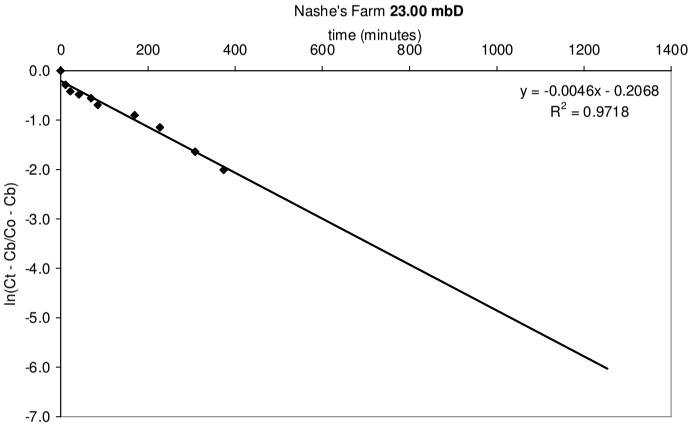
Nashe's Farm **23.00 mbD**
time (minutes)
ln(Ct - Cb/Co - Cb)
y = -0.0046x - 0.2068
R2 = 0.9718

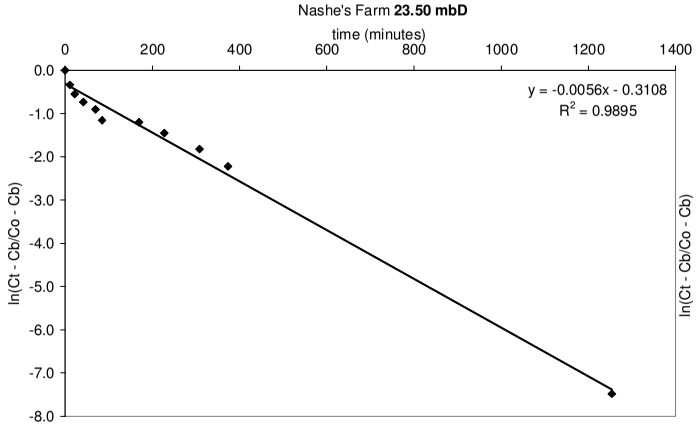
Nashe's Farm **23.50 mbD**
time (minutes)
ln(Ct - Cb/Co - Cb)
y = -0.0056x - 0.3108
R2 = 0.9895

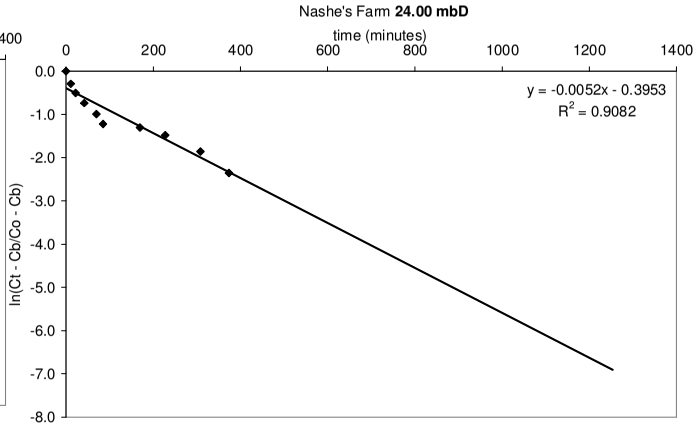
Nashe's Farm **24.00 mbD**
time (minutes)
ln(Ct - Cb/Co - Cb)
y = -0.0052x - 0.3953
R2 = 0.9082

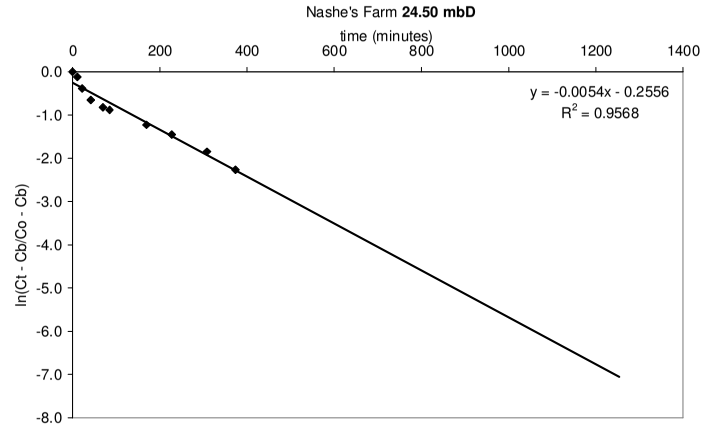
Nashe's Farm **24.50 mbD**
time (minutes)
ln(Ct - Cb/Co - Cb)
y = -0.0054x - 0.2556
R2 = 0.9568

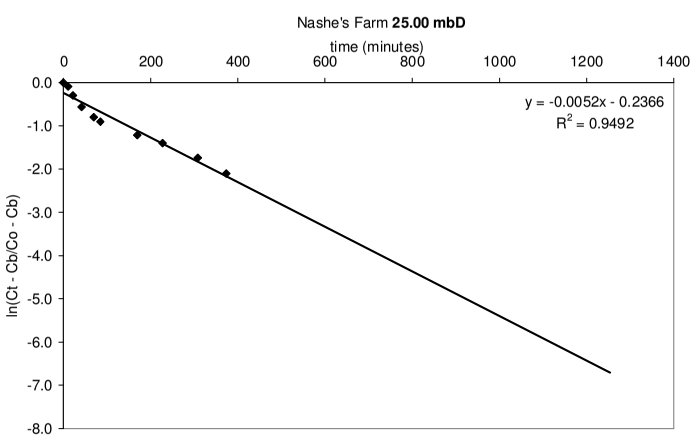
Nashe's Farm **25.00 mbD**
time (minutes)
ln(Ct - Cb/Co - Cb)
y = -0.0052x - 0.2366
R2 = 0.9492

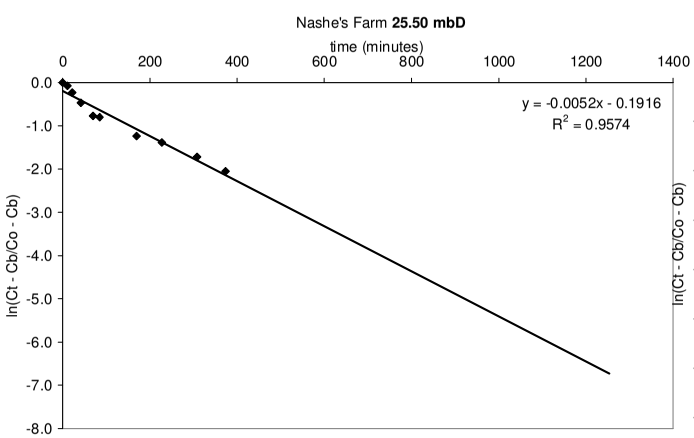
Nashe's Farm **25.50 mbD**
time (minutes)
ln(Ct - Cb/Co - Cb)
y = -0.0052x - 0.1916
R2 = 0.9574

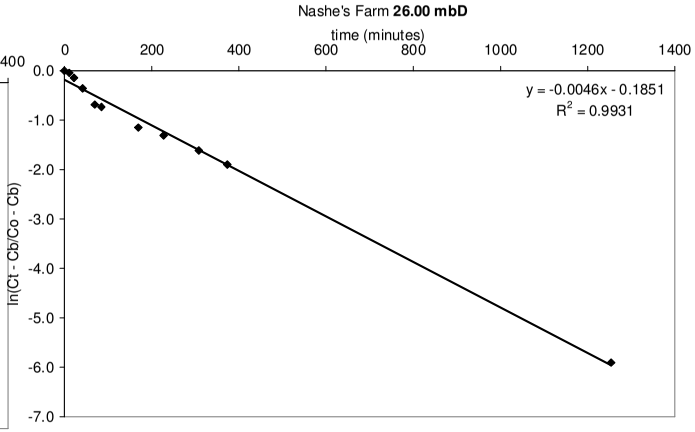
Nashe's Farm **26.00 mbD**
time (minutes)
ln(Ct - Cb/Co - Cb)
y = -0.0046x - 0.1851
R2 = 0.9931

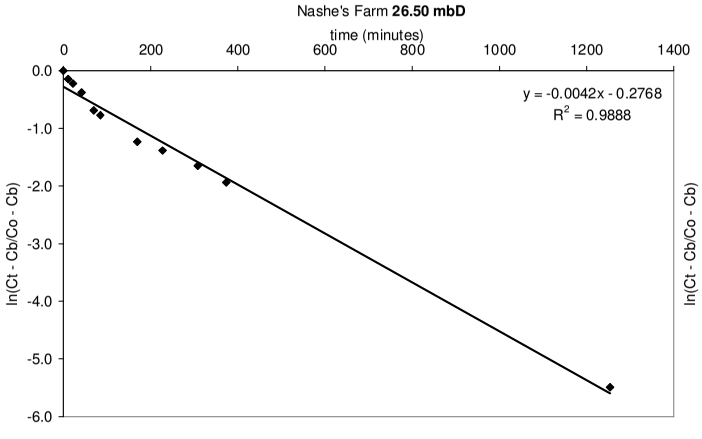
Nashe's Farm **26.50 mbD**
time (minutes)
ln(Ct - Cb/Co - Cb)
y = -0.0042x - 0.2768
R2 = 0.9888

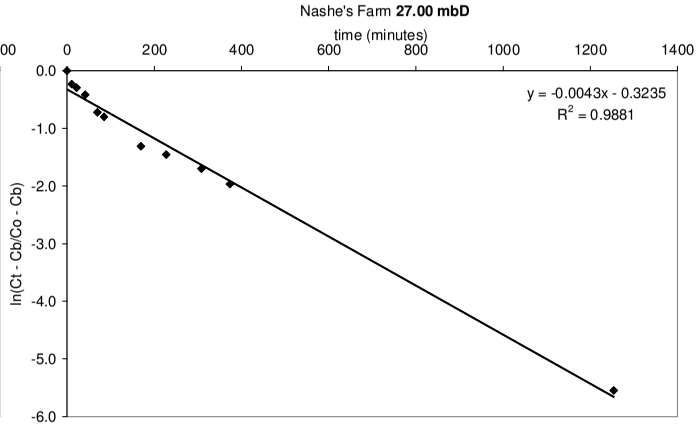
Nashe's Farm **27.00 mbD**
time (minutes)
ln(Ct - Cb/Co - Cb)
y = -0.0043x - 0.3235
R2 = 0.9881

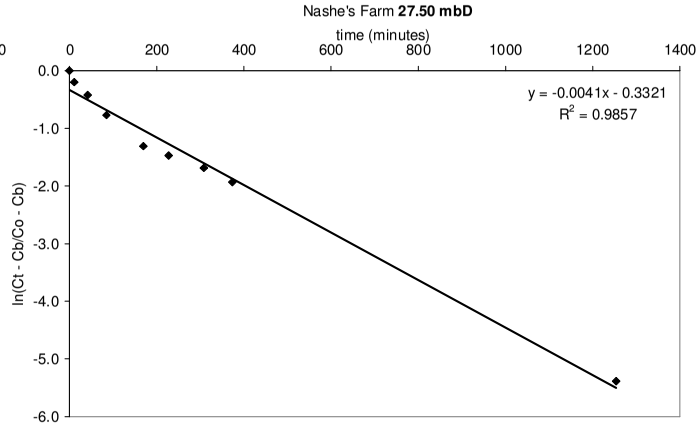
Nashe's Farm **27.50 mbD**
time (minutes)
ln(Ct - Cb/Co - Cb)
y = -0.0041x - 0.3321
R2 = 0.9857

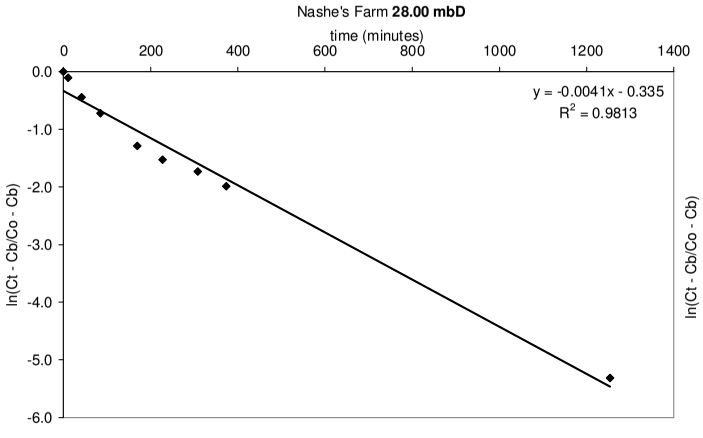
Nashe's Farm **28.00 mbD**
time (minutes)
ln(Ct - Cb/Co - Cb)
y = -0.0041x - 0.335
R2 = 0.9813

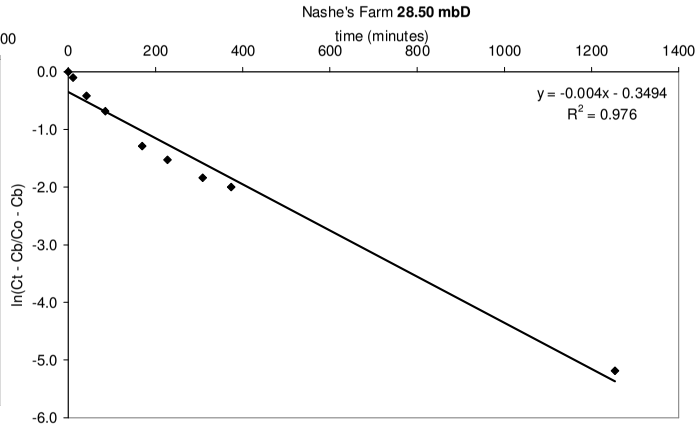
Nashe's Farm **28.50 mbD**
time (minutes)
ln(Ct - Cb/Co - Cb)
y = -0.004x - 0.3494
R2 = 0.976

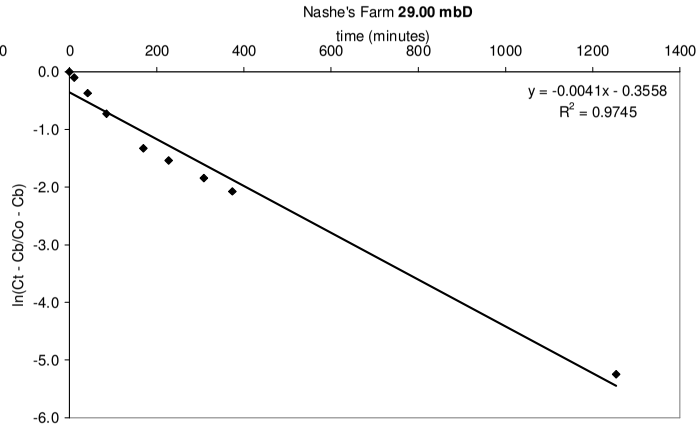
Nashe's Farm **29.00 mbD**
time (minutes)
ln(Ct - Cb/Co - Cb)
y = -0.0041x - 0.3558
R2 = 0.9745

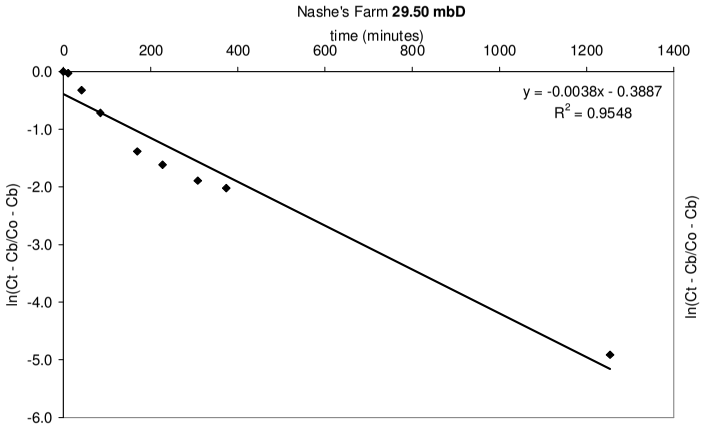
Nashe's Farm **29.50 mbD**
time (minutes)
0
200
400
600
800
1000
1200
1400
0.0
-1.0
-2.0
-3.0
-4.0
-5.0
-6.0
ln(Ct - Cb/Co - Cb)
y = -0.0038x - 0.3887
R2 = 0.9548

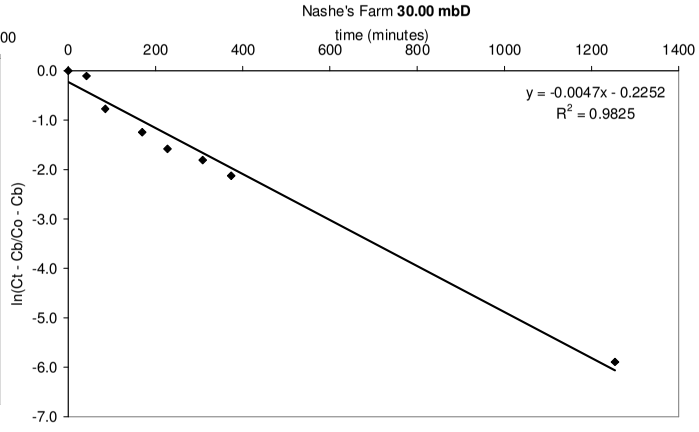
Nashe's Farm **30.00 mbD**
time (minutes)
0
200
400
600
800
1000
1200
1400
0.0
-1.0
-2.0
-3.0
-4.0
-5.0
-6.0
-7.0
ln(Ct - Cb/Co - Cb)
y = -0.0047x - 0.2252
R2 = 0.9825

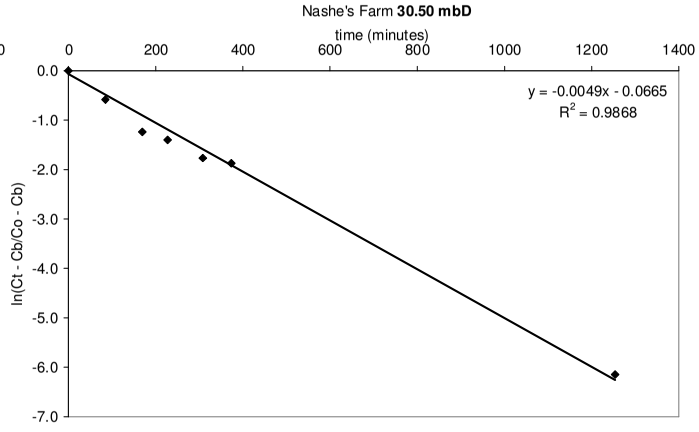
Nashe's Farm **30.50 mbD**
time (minutes)
0
200
400
600
800
1000
1200
1400
0.0
-1.0
-2.0
-3.0
-4.0
-5.0
-6.0
-7.0
ln(Ct - Cb/Co - Cb)
y = -0.0049x - 0.0665
R2 = 0.9868

THREE VALLEYS WATER

Memorandum

Date: 12/02/08

To:	Ciara Fitzpatrick Simon Cook	UCL
From:	Jessica Randle	TVW Water Resources
CC:	Rob Sage	TVW Water Resources

Re: Comet Way BH5 Downhole Inspection

Dear Ciara/Simon

Please find below a summary of the downhole inspection undertaken in Borehole No. 5 at Comet Way, Hatfield, conducted on Tuesday 29th January.

Figure 1: Borehole Headworks

Figure 2: Borehole Chamber

Geophysical Logging

Figure 3 displays the fully processed composite log of the geophysical tools ran during the survey. The fluid temperature and conductivity sonde was not used during the inspection as there was only 3.8m of water in the borehole. The tool itself is over two and a half metres long. The borehole is cased to total depth, therefore the formation resistivity tool could not be run. During logging, the legs on the caliper sonde did not open. This is likely to be due to the poor verticality seen in the borehole.

The filtered gamma log displays a count rate of 80 counts per second (CPS) until 2.8mbD, suggesting a clay rich soil or made ground overlying the Chalk. Beneath here, the rate decreases to 19CPS, suggesting a lithological boundary with the Chalk. At 12.7mbD, the count rate is seen to increase again to a maximum of 50CPS before falling when the water level is encountered, which is to be expected as the gamma reading is attenuated when measured in water. The final two metres of the profile displays a constant value of 11CPS.

The impeller flowmeter logs detected a slight downward flow within the borehole from 17.0mbD, in the slotted section of casing. Flow horizons, if present, are indicated by changes in the impeller rotation rate and time per revolution that are not associated with changes in the cable speed.

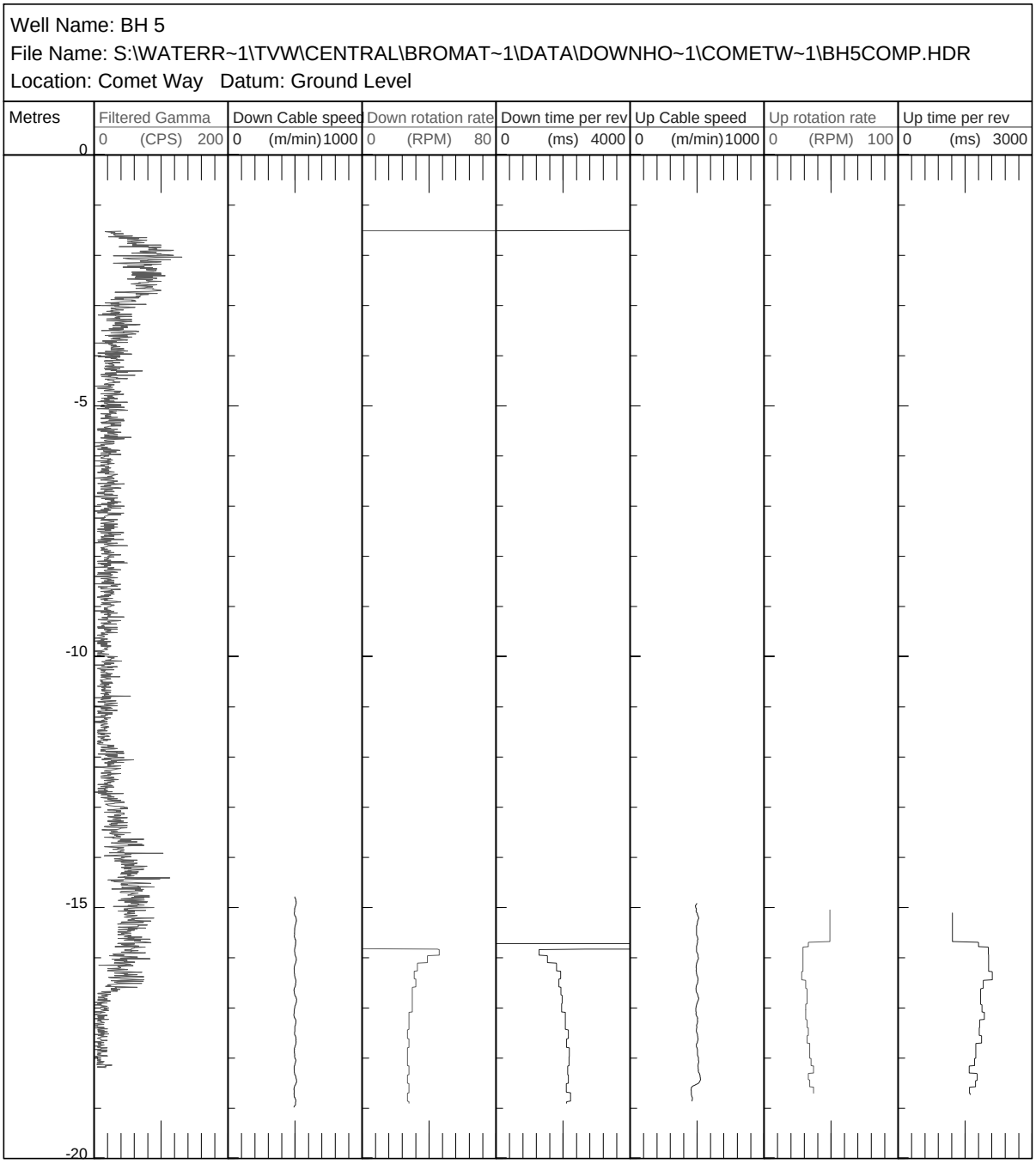

Figure 3: Comet Way Borehole No. 5 Composite Geophysical Log

CCTV Inspection

A summary of the features seen during the CCTV inspection is shown in Table 1.

Depth (mbD)	Features
0	Top of Casing
1.2	Plain steel casing, in good condition
2.4	Casing joint, poor contact between sections, overhang present
8.1	Casing joint, poor contact between sections, overhang present
14.0	Casing joint, poor contact between sections, overhang present CCTV camera knocks against the sides of the borehole. Beneath this depth, borehole is off vertical
15.8	Rest Water Level, surface is dirty, water underneath is clear
16.9	Casing is slotted. Slots are clean, horizontal and arranged in three columns. Off white Chalk is visible through the slots
19.4	Beer can is present in the borehole. Estimated base of borehole is at 19.6mbD. Base is even and covered with sediment

Table 1. Summary of CCTV Inspection Findings for Borehole No. 5

Regards

Jessica Randle

Water Resources

(01923) 814249/ #4249

THREE VALLEYS WATER

Memorandum

Date: 12/02/08

To:	Ciara Fitzpatrick Simon Cook	UCL
From:	Jessica Randle	TVW Water Resources
CC:	Rob Sage Maria Teneke	TVW Water Resources
Re:	Nashes Farm Downhole Inspection	

Dear Ciara/Simon

Please find below a summary of the downhole inspection undertaken at Nashes Farm, conducted on Monday 4th February.

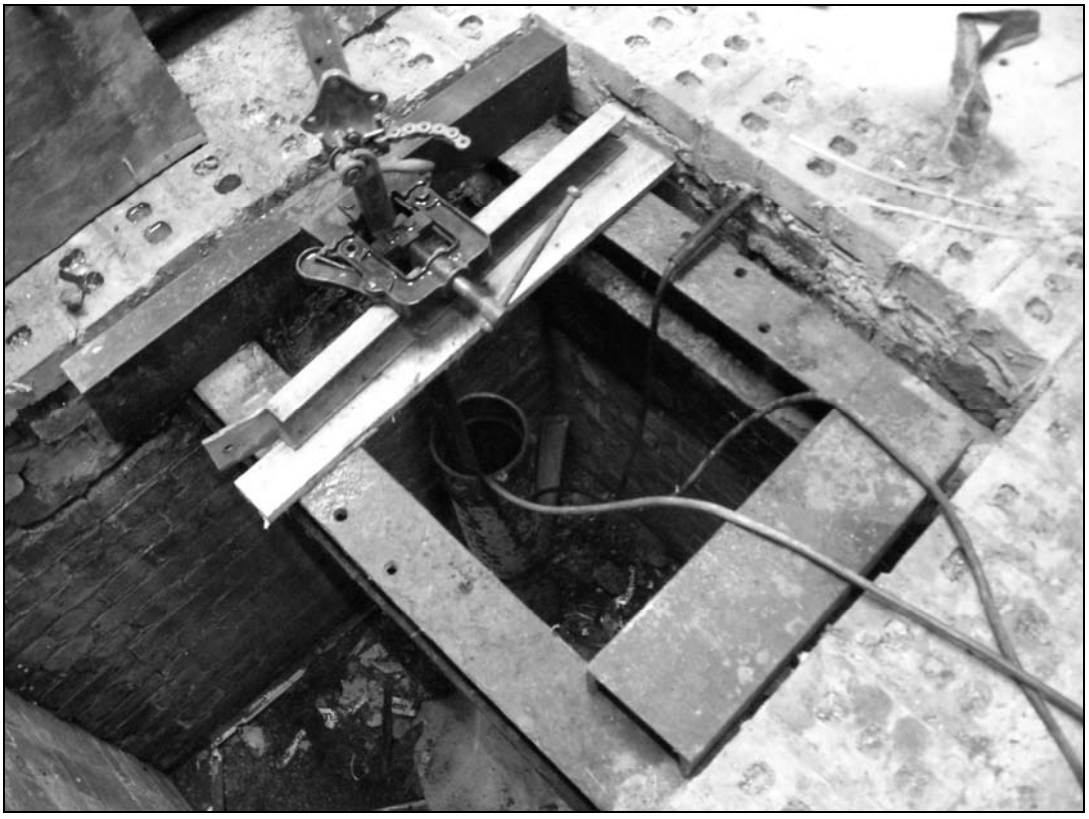

Figure 1: Borehole Headworks

Figure 2: Borehole Chamber

Geophysical Logging

Figure 3 shows the geophysical logs produced by the fluid temperature and conductivity sondes run in the borehole. During logging, the depth scale did not record properly, although all other parameters are ok. Note the top of the log is at 19.6mbD and the base of the log is at 32mbD, giving a 12.4m section. Figure 4 displays the fully processed composite log of the remaining geophysical tools ran during the survey.

The fluid temperature profile displays 11.2°C at the rest water level (RWL), which is encountered at 19.6mbD and remains constant until the base of the log. Sudden changes in the geothermal gradient may be due to possible flow horizons. The differential temperature log indicates that no discernable fluctuations are evident within the borehole.

The fluid conductivity profile gradually decreases from 704μS/cm at the RWL to 644μS/cm at the base of the log. Again, changes in the profile may infer flow horizons. The differential conductivity log indicates no significant fluctuations relating to flow.

After initially high values reflecting the pumping house and surrounding made ground, the filtered gamma log displays a count rate of 2.7 counts per second (CPS) until 8.7mbD. Beneath here, the rate increases slightly to 3.6CPS. A decrease to 2.4CPS is observed from the rest water level (RWL) at 19.6mbD, which is to be expected as the gamma reading is attenuated when measured in water. This value is maintained until the base of the borehole. No obvious lithological boundaries are identifiable from the gamma profile.

The caliper trace confirms the internal diameter of the plain casing to be 160mm. The open hole section of the borehole appears well fractured and displays a variable diameter, with some fissures widening to 300mm.

The formation resistivity varies between a minimum of 38.5Ωm at 21.6mbD and 29.3Ωm at 23.5mbD. With only 10m of saturated open hole section, it is difficult to stratigraphically place where the borehole lies in terms of Chalk formations. There are no obvious marker horizons present and the resistivity trace is strongly linked to fluctuations with the caliper log. The shallow depth of the borehole, the well fissured nature of the open hole section and the presence of large sections of flint would suggest that the borehole comprises Upper Chalk. The sudden increase in resistivity at the bottom of the log is due to a test measurement carried out during logging to ensure the sonde is calibrated correctly.

The impeller flowmeter logs detected some upwards flow within the borehole between 23.3mbD and 24.8mbD. Flow horizons, if present, are indicated by changes in the impeller rotation rate and time per revolution that are not associated with changes in the cable speed.

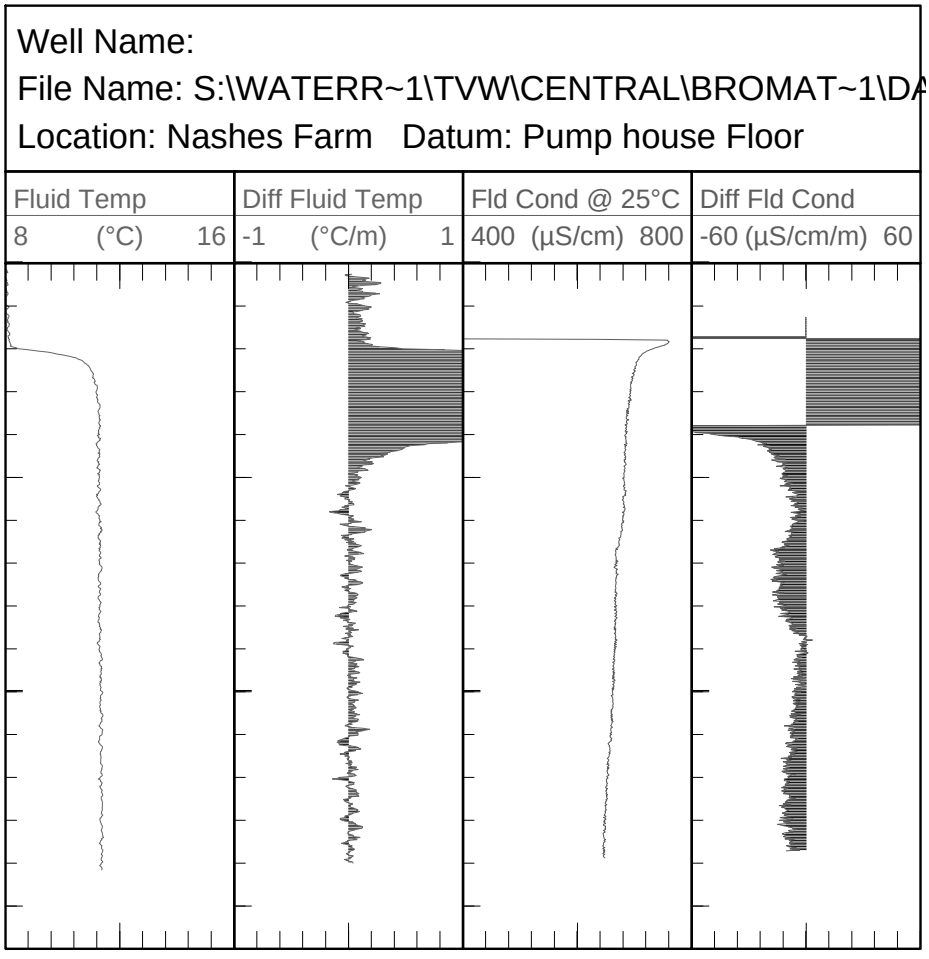

Figure 3: Nashes Farm Borehole TCDS Geophysical Log

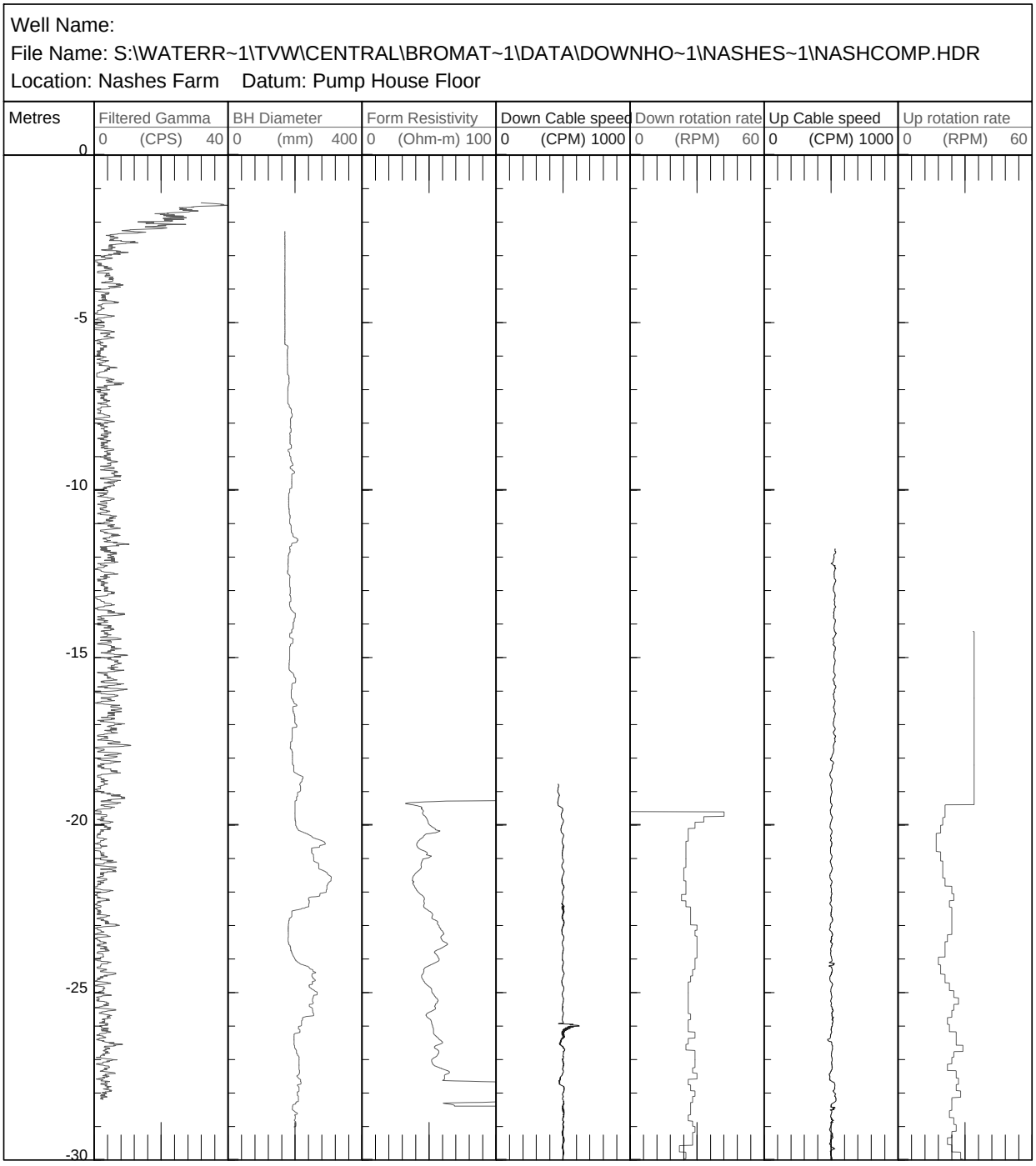

Figure 4: Nashes Farm Borehole Composite Geophysical Log

CCTV Inspection

A summary of the features seen during the CCTV inspection is shown in Table 1.

Depth (mbD)	Features
0	Pump House floor
1.2	Plain steel casing, slightly rusted, in reasonable condition
5.9	Base of casing Chalk is stained brown, smooth and stable

Depth (mbD)	Features
7.4	Borehole circumference appears irregular
8.0	Chalk opens out to one side, flints present
9.3	Borehole circumference appears irregular
11.6-12.3	Chalk surface becomes more rough
13.8	Chalk opens out to one side. Beneath here the Chalk is whiter
16.5	Chalk opens out to one side
17.3	CCTV camera gets stuck on a large piece of flint protruding from the side of the borehole
18.3	Borehole circumference appears irregular
19.5	Rest water level, water is reasonably clear
19.6	Chalk appears smooth
20.4	Borehole opens out and the circumference appears irregular
22.5	CCTV camera knocks against a ledge on the side of the borehole. Chalk beneath here is smooth
23.1-24.4	Large vertical groove appears to one side of the borehole
24.4	Borehole opens out, circumference becomes irregular
30.7	CCTV Camera gets stuck on the sides of the borehole, survey terminated
*Please note the borehole was plumbed to a depth of 32.70m	

Table 1. Summary of CCTV Inspection Findings for borehole

Regards

Jessica Randle

Water Resources

(01923) 814249/ #4249

Appendix E

MAP, GoldSim and DP1D comparison

Validation of GSIM-MAP-DP1D

1 Replication of Old Chalford Network

1.1 Comparison of complete streamtube set in MAP & GSIM

Based on the parameters given in the **MAP** input files received from Ann Williams, the complete streamtube set (a total of 103 streamtubes, with 5 output locations) was replicated in **GSIM**. Initially, the model was run without matrix diffusion zones. The parameters used for the MAP simulation including matrix diffusion were unavailable (I'm waiting to see if Ann can find these input files). Using best estimates of the parameters relating to matrix diffusion, the GSIM model was re-run including matrix diffusion zones.

1.1.1 Advection Only (no matrix diffusion)

Simulated **mobile** zone concentrations are identical (Figure 1), except the GSIM output is smoothed by the effect of mandatory dispersion in GSIM (minimum 10% of the path length).

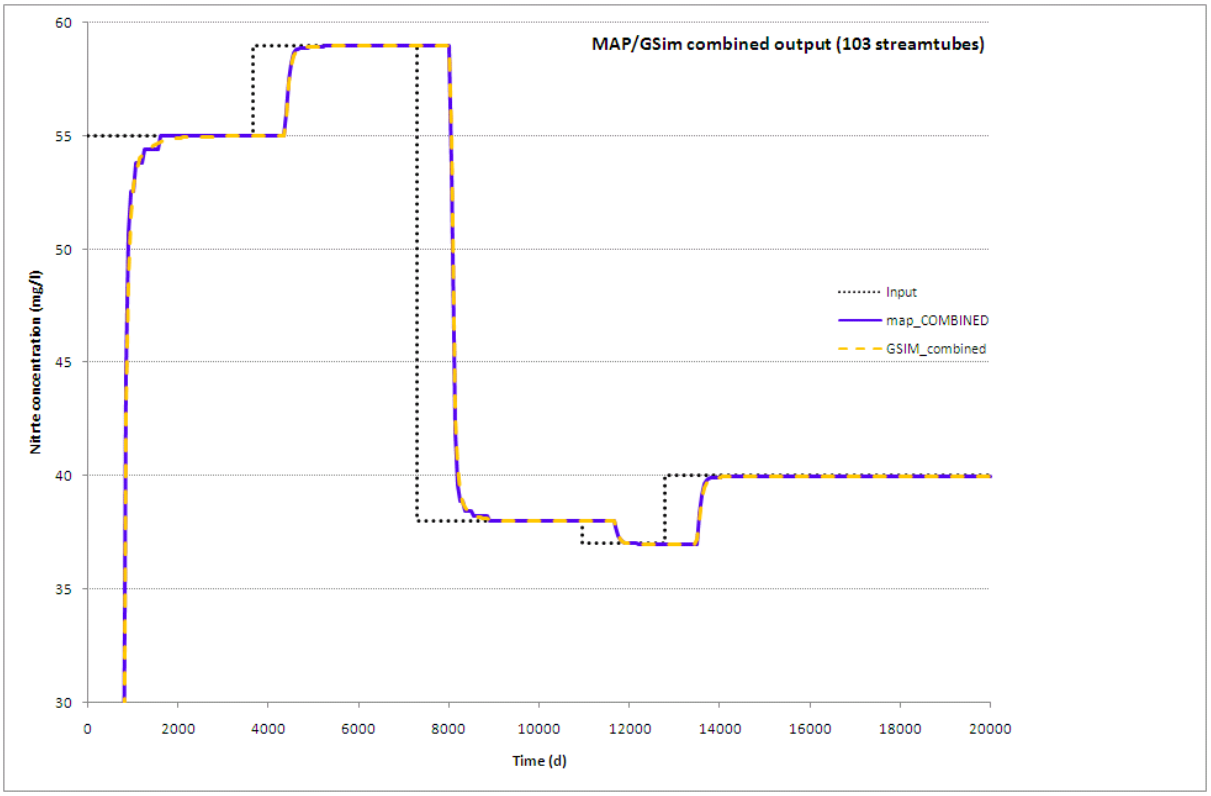

Figure 1: Comparison of simulated mobile zone concentrations (no matrix diffusion) using GSIM and MAP.

1.1.2 Advection + matrix diffusion

Simulated **mobile** zone concentrations from the MAP and GSIM models are very similar (Figure 2), with differences presumably a result of differences in parameter values for diffusion and matrix geometry.

Concentrations in the **immobile** zone were simulated using a 'diffusion cells' approach (see note below). Since MAP is not currently coded to give immobile zone concentrations, the simulated concentrations could not be validated against MAP.

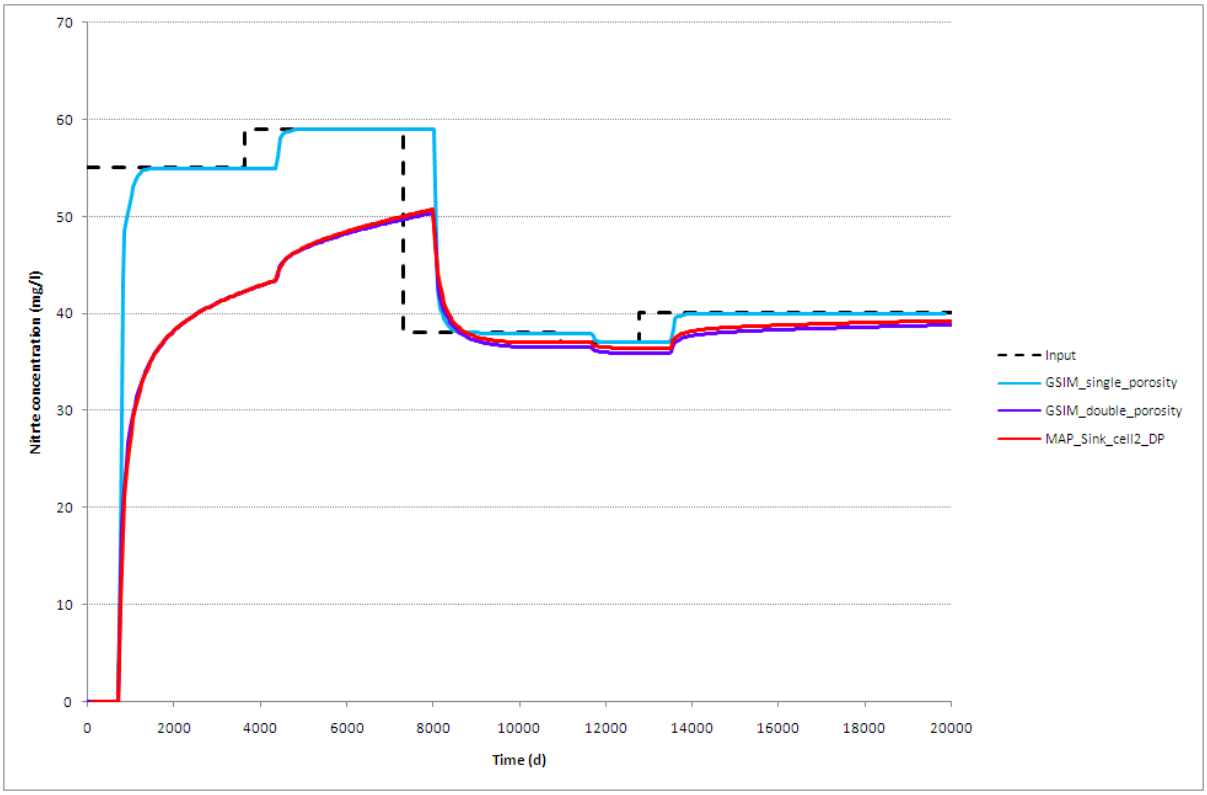

Figure 2: Comparison of simulated mobile zone concentrations with matrix diffusion using GSIM and MAP.

2 Immobile zone concentrations

2.1 Comparison of single pipe GSIM-DP1D

In order to compare average immobile zone concentrations, a single streamtube was modelled with both GSIM and DP1D.

The single streamtube modelled with DP1D is an average of the 9 streamtubes leading to the output 'Sink 2'. This was chosen so that an approximate comparison could be made between this GSIM/DP1D single streamtube and MAP output for Sink 2.

Despite using the same parameters in both simulations, simulated mobile and immobile zone concentrations are significantly different (Figure 3; Figure 4). . (Mobile zone concentrations remain very similar in GSIM and MAP outputs). In particular, the relative difference between mobile and immobile concentrations is larger in DP1D than in GSIM, indicating that more diffusion into the matrix is occurring in GSIM than in DP1D (Figure 4).

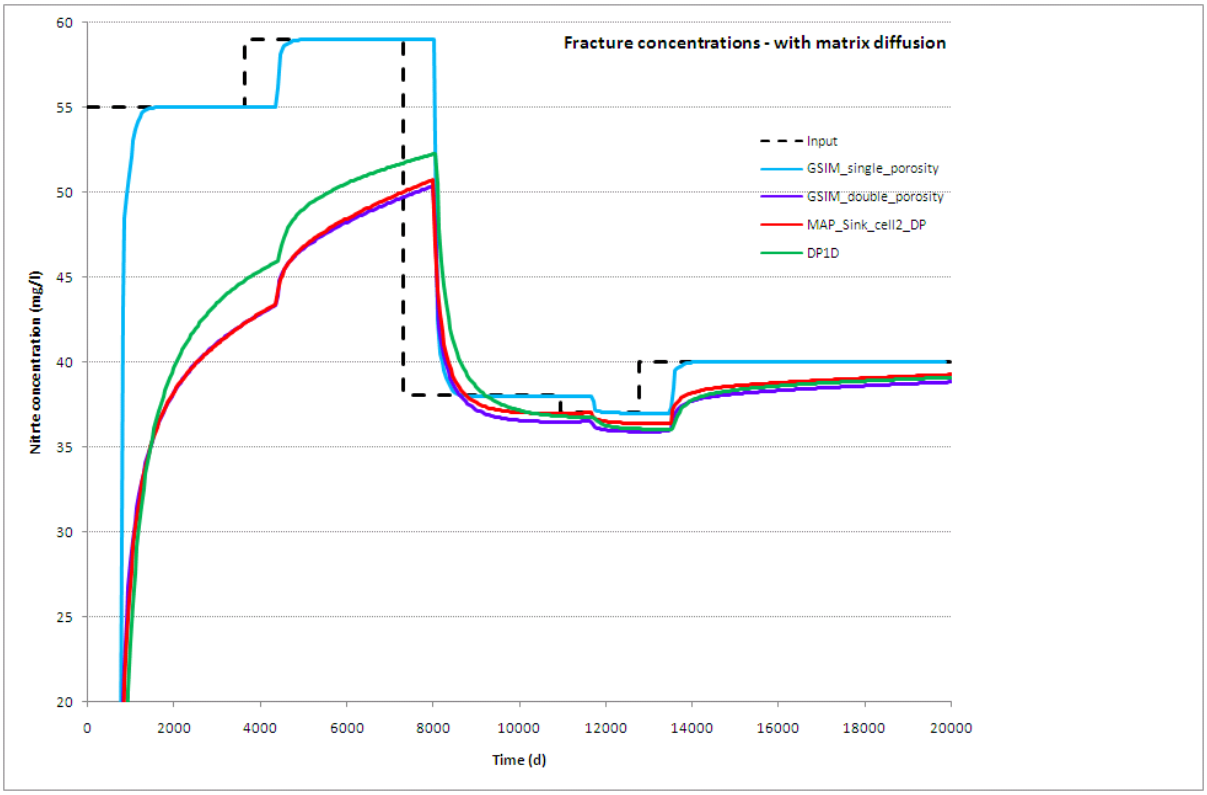

Figure 3: Comparison of mobile zone concentrations with matrix diffusion using GSIM and MAP & DP1D.

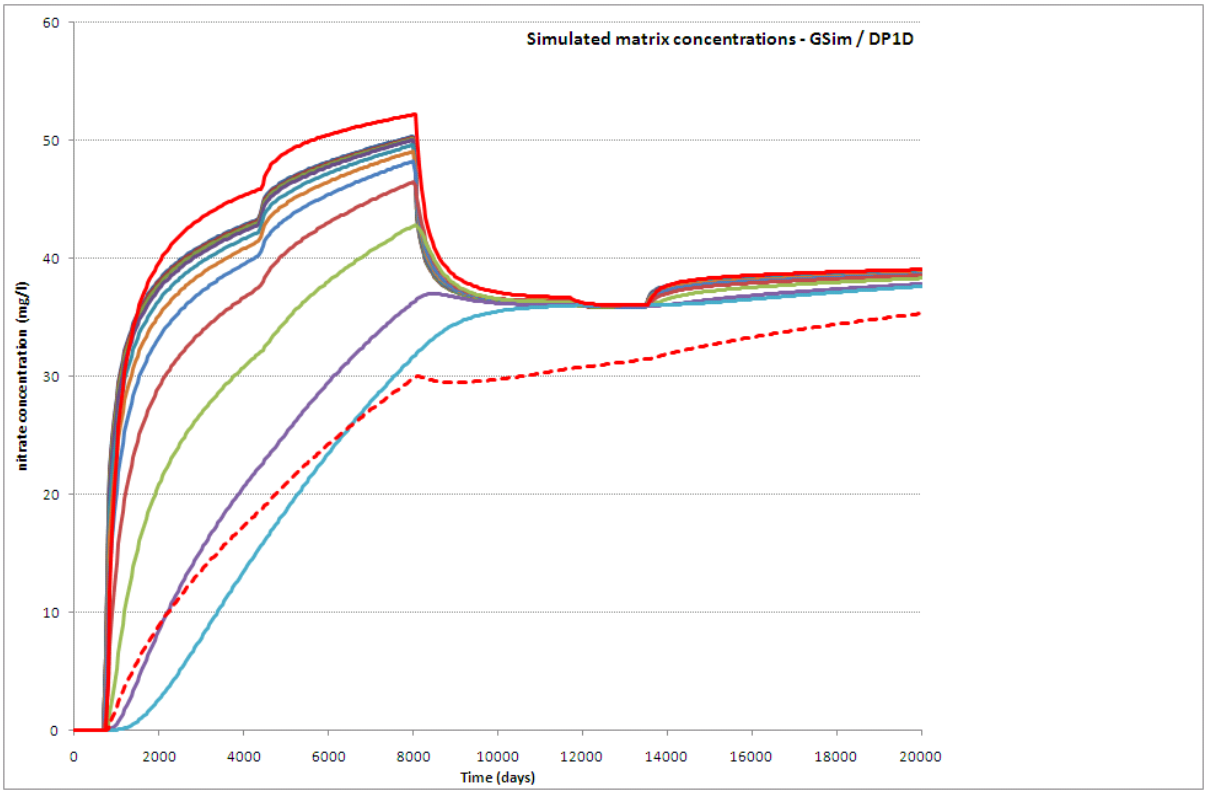

Figure 4: Comparison of mobile and immobile zone concentrations using GSIM, MAP & DP1D. Solid red line is DP1D mobile concentration, dashed red line is DP1D immobile concentration. Other lines represent GSIM immobile zone concentration at distances into the matrix block, until half block thickness.

Possible explanations that were considered are summarised below:

2.1.1 Differences in Block Geometry Functions (BGFs)

I have done my best to work through the maths of GSIM pipe pathways and I think that the BGFs for slab and sphere geometry are those in Barker (1985), which are presumable used in MAP and DP1D.

2.1.2 Differences in input boundary conditions

GSIM uses a mass balance boundary condition (mass flux) rather than a concentration boundary condition. To account for this, the parameter δ was set to $\delta=1$ in DP1D. This did not result in a significant improvement to the match between DP1D and GSIM outputs.

2.1.3 Fickian diffusion Vs Mass transfer

It is recognised that the 'diffusion cell' approach does not represent Fickian diffusion, but rather used a constant mass transfer coefficient. However, although this will lead to differences in predicted immobile concentrations by this method compared to a Fickian representation, particularly at early and late times, in GSIM this will not have an effect on mobile concentrations as along the streamtubes Fickian diffusion is simulated analytically (as in MAP). The 'diffusion cells' approach merely allows an estimate of immobile concentrations at a point in the absence of coding to give the analytically calculated immobile concentrations as an output.

2.1.4 Conclusions

Simulations with GSIM and MAP, using identical/best-estimate parameters, produce identical/similar output concentrations for mobile concentrations with and without inclusion of matrix diffusion. However, it is not possible to compare simulated immobile zone concentrations as neither model is coded to produce this as an output.

An approximation for immobile zone concentrations can be made by setting up a series of coupled 'diffusion cells' which are linked to the output mobile zone concentration. However, there is no MAP output to validate/verify this approach. When a single pathway is simulated with DP1D and GSIM, mobile and immobile zone concentrations are substantially different.

NOTE: 'Diffusion cells' approach to estimate matrix concentrations in GSIM

This approach is represented diagrammatically in Figure 5.

A series of GSIM 'cell pathways' (mixing cells) are generated to represent half a matrix block. The first cell contains water only, and its concentration is fixed to the output concentration from the pipe pathway (streamtube) mobile zone at that point. The rest of the cells contain saturated porous matrix material and represent thin slices of matrix moving from the fracture into the matrix block. Each matrix cell is coupled to the adjacent cells by a 'diffusive mass transfer link'. This link represents diffusive exchange of mass between immobile porewater in adjacent matrix cells, and is described using a constant mass transfer rate. The linked cells therefore form a finite difference network. Concentrations are calculated at each time step.

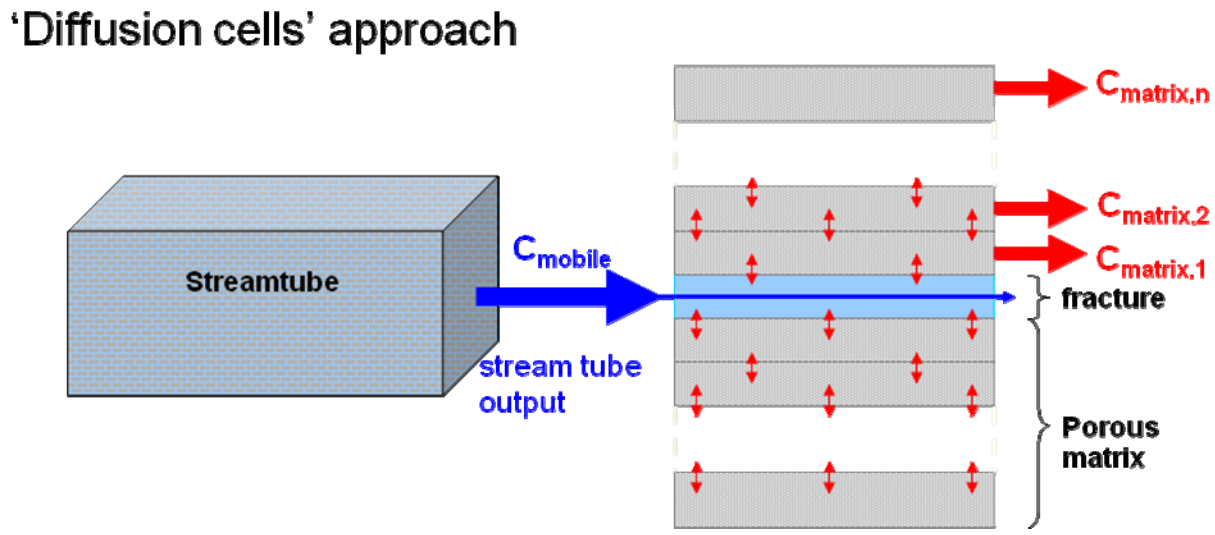

Figure 5: The 'diffusion cells' approach to estimate immobile concentrations in GSIM.

Diffusion Cell Set-up

Describe set-up

X1		
Fracture	Y1	0
Matrix	Y2	0.001
Matrix	Y3	0.003
Matrix	Y4	0.005
Matrix	Y5	0.01
Matrix	Y6	0.02
Matrix	Y7	0.03
Matrix	Y8	0.05
Matrix	Y9	0.1
Matrix	Y10	0.2
Matrix	Y11	0.4
Matrix	Y12	0.6

The numbers in the cells specify the Y-coordinate for the start of the corresponding cell element. In the last row the number specifies the Y-coordinate for the end of the last Cell.

Fracture cells contain water only

Matrix cells contain chalk with porosity and water within the pores.

The fracture cell has a 'specified concentration' boundary condition which is specified as the concentration output of the pipe element.

Cells are linked by a diffusive mass transfer links.

The diffusive flux f from pathway i to pathway j is computed as follows:

$f_{i \rightarrow j} = D(c_i - c_j)$

where D = diffusive conductance for the species in the mass flux link [L^3/T], ci and cj are dissolved concentration of the species in the medium (water) within cell i and cell j respectively.

Diffusive conductance terms are computed as follows:

$$D = \frac{A}{\frac{Li}{d*tpi*npi} + \frac{Lj}{d*tpj*npj}}$$

where Li and Lj are the diffusive lengths for the diffusive mass flux link in cell i and cell j (the default is distance from the centre of the cell to the edge or interface of the cell)

d is the diffusivity for species in water

tpi is the tortuosity for the porous medium in cell i

npi is the porosity for the porous medium in cell i

GoldSim calculates the effective diffusion coefficient for the pipe pathway as D_{im} = d*t*n.

I have set d, t and n to give a D_{im} of 1.74 x 10-10 m2/s, which is the value in DP1D, therefore n = 0.5, t = 0.7 and d = 0.50 x 10-9 **m2/s.**

Appendix F

Parameters for Hertfordshire Network Model

Appendix F

Parameters for Hertfordshire Network Model

Table F.1: Parameters used in the Hertfordshire Network Model

Double-porosity Branches		**Q (m^3/d)**	**t_a (hours)**	**t_{cb} (hours)**	**sigma**	**t_{cf} (hours)**	**alpha/x**
Sandridge to Harefield House	typical	6.08E+00	9.44E+00	2.89E+04	3.80E+02	2.00E-01	1.00E-01
	worst case	6.08E+00	1.89E-02	6.51E+04	4.05E+03	3.97E-03	1.00E-01
	best case	6.08E+00	5.56E+01	7.23E+03	2.50E+01	1.16E+01	1.00E-01
Harefield House to Hatfield Quarry	typical	6.08E+00	2.50E+01	2.89E+04	3.80E+02	2.00E-01	1.00E-01
	worst case	6.08E+00	5.00E-02	6.51E+04	4.05E+03	3.97E-03	1.00E-01
	best case	6.08E+00	1.47E+02	7.23E+03	2.50E+01	1.16E+01	1.00E-01
Hatfield Quarry to Comet Way	typical	6.08E+00	2.60E+00	2.89E+04	3.80E+02	2.00E-01	1.00E-01
	worst case	6.08E+00	9.56E-03	6.51E+04	4.05E+03	3.97E-03	1.00E-01
	best case	6.08E+00	9.06E+00	7.23E+03	2.50E+01	1.16E+01	1.00E-01
Comet Way to Join	typical	6.08E+00	1.99E+00	2.89E+04	3.80E+02	2.00E-01	1.00E-01
	worst case	6.08E+00	7.31E-03	6.51E+04	4.05E+03	3.97E-03	1.00E-01
	best case	6.08E+00	6.93E+00	7.23E+03	2.50E+01	1.16E+01	1.00E-01
Join to Arkley Hole (DP)	typical	6.08E+00	6.34E+01	2.89E+04	3.80E+02	2.00E-01	1.00E-01
	worst case	6.08E+00	1.27E-01	6.51E+04	4.05E+03	3.97E-03	1.00E-01
	best case	6.08E+00	3.73E+02	7.23E+03	2.50E+01	1.16E+01	1.00E-01
Arkley Hole to Lynchmill (DP)	typical	6.08E+00	1.74E+02	2.89E+04	3.80E+02	2.00E-01	1.00E-01
	worst case	6.08E+00	3.49E-01	6.51E+04	4.05E+03	3.97E-03	1.00E-01
	best case	6.08E+00	1.03E+03	7.23E+03	2.50E+01	1.16E+01	1.00E-01
Karst Branches		**Q (m^3/d)**	**t_a (hours)**	**t_{cb} (hours)**	**sigma**	**t_{cf} (hours)**	**alpha/x**
Join to Arkley Hole (Karst)		2.60E+00	1.65E+00	4.38E+05	1.90E+01	1209.125	0.001
Join to Lynchmill (Karst)		7.22E+00	3.12E+00	9.04E+04	1.90E+01	249.9371	0.001
Harefield House to Arkley Hole (Karst)		3.04E-03	2.30E+01	4.38E+05	1.90E+01	1209.125	0.01
Harefield House to Lynchmill (Karst)		1.31E-02	5.29E+01	9.04E+04	1.90E+01	249.9371	0.01
Comet Way to Arkley Hole (Karst)		8.23E-01	9.02E+00	4.38E+05	1.90E+01	1209.125	0.01
Comet Way to Lynchmill (Karst)		1.61E+00	9.02E+00	9.04E+04	1.90E+01	249.9371	0.01